

13th International Conference

Tunnel Safety and Ventilation

ITnA-Reports
Volume 109 | April 21-22, 2026
Series Editor: Christian Trapp
Editor: Michael Bacher

TUNNEL SAFETY AND VENTILATION
Graz, Austria • www.tunnel-graz.at

13th International Conference
TUNNEL SAFETY AND VENTILATION

April 21 – 22, 2026

Graz, Austria

ITnA-Reports, Vol. 109

Reports of the Institute of Thermodynamics
and Sustainable Propulsion Systems

Series Editor Univ.-Prof. Dr.-Ing. Christian Trapp

Editor Dipl.-Ing. Dr.techn. Michael Bacher
Cover Verlag der Technischen Universität Graz
Cover pictures (left to right) 1. Chalabala / Adobe Stock
2. Helmut Lunghammer
3. ITnA / TU Graz
4. Helmut Lunghammer
5. ÖBB / isochrom
6. (center) Sakarin Sawasdinaka / Shutterstock.com
Print Druckhaus Thalerhof GmbH

2026 Verlag der Technischen Universität Graz
Technikerstraße 4, 8010 Graz
verlag@tugraz.at
www.tugraz-verlag.at

Print:
ISBN 978-3-99161-087-8

E-Book:
ISBN 978-3-99161-088-5
DOI 10.3217/978-3-99161-087-8



This work is licensed under the Creative Commons

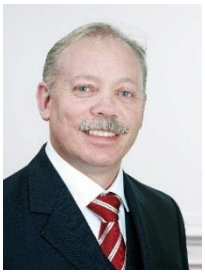
Attribution-ShareAlike 4.0 International (CC BY-SA 4.0) license.

https://creativecommons.org/licenses/by-sa/4.0/deed.en

This CC license does not apply to the cover, third party material
(attributed to other sources) and content noted otherwise.

SCIENTIFIC COMMITTEE

The Scientific Committee consists of leading experts in tunnel ventilation and safety from around the world, ensuring the highest level of scientific quality.



Rune Brandt, CH



Raphael Defert, CH



Ignacio Del Rey, ES



Daniel Fruhwirt, AT



Norris Harvey, US



Haukur Ingason, SE



Ingo Kaundinya, DE



Bernhard Kohl, AT



Antoine Mos, FR



Günter Rattei, AT



Conrad Stacey, AU



Peter Sturm, AT



Frédéric Waymel, FR



Alan Vardy, UK

ORGANIZING COMMITTEE

The Organizing Committee is endeavoring to provide an interesting and inspiring conference.

Michael Bacher
Daniel Fruhwirt
Elisabeth Holler

PREFACE

This conference proceedings brings together the contributions from the 13th International Conference on Tunnel Safety and Ventilation, which took place in Graz on April 21–22, 2026. The conference is an established meeting place for operators, users, technicians, researchers, and industry partners. The goal is to provide a structured forum for the exchange of information on the planning, construction, and equipment of road and rail tunnels, as well as for the continuous development of knowledge and practice. The contributions offer in-depth insights into key issues of tunnel safety and ventilation and make a concrete contribution to the sustainable and efficient development of the sector.

Special attention was given to cross-cutting topics that shape the state of the art and future directions. Sustainability and energy efficiency were examined from multiple angles, including low- and lean-tech approaches and concrete operational measures. Model-based predictive ventilation control demonstrates how energy demand can be reduced and emissions lowered.

Digitalization and automation were also in focus, addressing both the practical use of digital twins for road tunnels and secure, web-based supervisory control platforms. Advances in sensing and data fusion, as well as systematic condition assessment of tunnel equipment, form the foundation for proactive operations. The concept of smart tunnels in an Industry 5.0 context links dynamic risk analysis with enhanced resilience, while developments in risk analysis software support evidence-based decision-making.

In the field of ventilation, practice-oriented optimizations and fundamental findings were presented: optimization of main fans and associated drives, system upgrades in major road tunnels, acceptance criteria for longitudinal ventilation, and methods to enhance performance during the transient stages of fire events. Specific operational scenarios were addressed, such as control strategies for short, longitudinally ventilated tunnels under temporary bidirectional traffic, alongside phenomena like smoke recirculation at portals and pollutant dispersion at tunnel exits in urban street canyons. Foundational work on aerodynamics, such as the influence of cross-sectional geometry, air speeds near wall-mounted services, and train-induced aerodynamic loads, and on fire dynamics, including validation of flow resistance through full-scale fire tests and improved fidelity in simulations, strengthens both design and operational decision-making.

Safety under incident conditions was examined from multiple perspectives, including maintaining critical functions during widespread power outages and synthesizing lessons learned from numerous operating concepts in Swiss road tunnels. Cultural differences in road tunnel fire safety and the specific challenges of covered highways broaden the view on normative and context-dependent solutions. Empirical studies on human behavior in smoke, covering individual and group effects on movement, reaction, and evacuation, inform the design of escape

and rescue concepts. With new vehicle technologies advancing, several contributions considered risks and opportunities around automated driving in tunnels, thermal runaway in lithium-ion batteries, and the consequences of large electric vehicle fires, as well as heat transfer between ground and tunnel air and its implications for structural integrity and ventilation design. On the rail side, research conducted during the construction of large-scale projects, such as the Koralm Tunnel, provided valuable real-world insights.

The technical visit led to the new Wettmannstätten railway station and the ÖBB Asset Service Center (ASC). As decentralized hubs of ÖBB-Infrastruktur AG, the ASCs showcase maintenance, service, and fault rectification in practice; in incident response, they are often the first on site, ensuring the swift restoration of technical systems such as switches and signals. Insights into processes and technology underscore the importance of integrating planning, operation, and maintenance.

Our sincere thanks go to Austrian Federal Railways (ÖBB) for their support, to the exhibitors for presenting their products and engaging in intensive exchange, to all participants and last but not least the presenters for their dedicated contributions. We also thank everyone involved in ensuring the smooth running of the event. We hope that the contributions assembled here will provide impetus for future projects, research initiatives, and decisions, laying the foundation for reliable, evidence-based, and sustainable advancements.

Michael Bacher and Organizing Committee

TABLE OF CONTENTS

TUNNEL SAFETY AND VENTILATION
Graz, April 20–21, 2026

Preface

Keynote Speakers

Sustainability of tunnel operation: New approaches – a PIARC briefing note and collection of case studies **1**
René LIST[1], PIARC Technical Committee - Working Group[2]
1: ASFINAG, AT
2: PIARC - World Road Association

The Koralmtunnel as a real-world laboratory: Research work and findings during the construction of the Koralmtunnel **3**
Helmut STEINER[1], Michael BACHER[2], Daniel FRUHWIRT[2]
1: Austrian Federal Railways, AT
2: Graz University of Technology, Institute of Thermodynamics and Sustainable Propulsion Systems, AT

ASFINAG in case of a blackout – overview and measures **16**
Günter RATTEI, Alice MAHR-SAVERSCHEL
ASFINAG/SG PPK, AT

Session S1:

Safe tunnels for smart vehicles: Challenges and opportunities of automated driving in road tunnels **24**
Regina SCHMIDT[1], Harald KAMMERER[1], Georg MAYER[2], Markus HOFER[3], Oliver ZENDEL[3]
1: ILF Consulting Engineers Austria GmbH, AT
2: BUNG Ingenieure AG, DE
3: AIT Austria Institute of Technology GmbH, AT

Conformity bias influence on walking speed in a smoke-filled tunnel experiment
Miho SEIKE[1], Wenhao LI[2], Takao FUTAGAMI[3] **34**
1: University of Tsukuba, JP
2: Liaodong University, CN
3: Shinshu University, JP

Impact of group effects on the reaction and escape behaviour of users in road tunnels - results of realistic large group experiments **41**
Frank LEISMANN[1], Christian THIENERT[1], Markus JENKI[2], Robert WENIGHOFER[3], Anne LEHAN[4], David STÜHLER[2], David CZUDNOCHOWSKI[2], Stefan KAUFMANN[4], Robert GALLER[3]
1: STUVA e.V., DE
2: CSS – Centre for Security and Society, DE
3: Technical University of Leoben, AT
4: BASt, Federal Highway and Transport Research Institute, DE

Session S2:

Digital Twins for road tunnels – expectations meet reality **49**
Goetz VOLLMANN[1], Zuzan AZAD[1], Lisa VON ROESSING[2], Benedikt FALTIN[2],
Anne LEHAN[3], Marius NONO TAMO[3], Karl HANKE[4], Annika JODEHL[4]
1: Ruhr University Bochum, Institute for Tunnelling and Construction Management, DE
2: Ruhr University Bochum, Institute of Computing in Engineering, DE
3: BASt, Federal Highway and Transport Research Institute, DE
4: BUNG-Group, DE

R&D project tunnelsensorfusion **57**
Dietmar HARBAUER
ASFINAG Alpenstraßen GmbH, AT

Development of a systematic approach for evaluation of the condition of the tunnel equipment **67**
Anne LEHAN[1], Gerhard HUDECEK[2], Harald KAMMERER[3], Frank HEIM[4]
1: BASt, Federal Highway and Transport Research Institute, DE
2: ASFINAG Maut Service GmbH, AT
3: ILF Consulting Engineers Austria GmbH, AT
4: Die Autobahn GmbH des Bundes, DE

Session G2:

Methodology for the performance enhancement of longitudinal ventilation systems during transient stage of a fire **74**
Miguel DEL MORAL, Alexander GRATCH, Davide D'EUSTACCHIO,
Alvaro MENESES, Justo SUAREZ
Soler&Palau Ventilation Systems SLU, ES

Performance improvement of a hybrid ventilation system via predictive control **83**
Diego ANGELI[1], Paolo LEVONI[2], Pietro CINGI[3], Giovanni Sebastiano BAROZZI[4],
Paolo VERRAZ[5], Cedric PETITCOLIN[5]
1: DISMI - University of Modena and Reggio Emilia, IT
2: mimesis s.r.l., IT
3: EN&TECH - University of Modena and Reggio Emilia, IT
4: DIEF - University of Modena and Reggio Emilia, IT
5: TMB-GEIE, IT & FR

Enhancements of tunnel ventilation system for road tunnels adopting aerodynamic control & monitoring strategies **91**
Kelvin Ka Wing CHEUNG[1], Leo Lung CHAN[1], Anthony WAN[2], Hau Ming LEE[2]
1: AECOM Asia Company Limited, HK
2: BYME Engineering (Hong Kong) Limited, HK

Session S3:

Ventilation control optimisation for short longitudinally ventilated road tunnels in case of temporary bidirectional traffic operation **103**
Oliver HEGER, Gregor SCHMÖLZER
ILF Consulting Engineers Austria GmbH, AT

External smoke movement and its impact on station design – Guidance for ventilation layout **114**
Jolyon THOMPSON, Mark GILBEY
WSP UK Ltd., UK

Safety challenges of highway lids in the US **123**
Petr POSPISIL[1], Colin SANTANGELO[2], Bernd HAGENAH[1]
1: Tunnel Safety & Ventilation Consultant, US
2: HNTB Corporation, US

Cultural differences in road tunnel fire safety **137**
Conrad STACEY, Michael BEYER
Stacey Agnew Pty Ltd., AU

Session G3:

The best thing FEDRO has provided us within recent years! Experience from over 50 operational concepts for Swiss road tunnels **143**
Ralf WETZEL[1], Christian JÄGER[2]
1: ILF Beratende Ingenieure AG, CH
2: WSP Ingenieure AG, CH

Thrust comparison of conventional jet fans and fans with shaped silencers in an Italian road tunnel based on In-Situ measurements **152**
Fathi TARADA[2], Luca STANTERO[1], Pier BERTACCHE[1], Natalino DANIELE BOFFA[3], Francesco BEZZI[3], Natalino LUCATELLI[4]
1: Risk Design Engineering, IT
2: Mosen Ltd., UK
3: ANAS SpA, IT
4: De Cardenas Fans & Service SRL, IT

Optimization of the main fans and associated drives for the E4 Stockholm bypass **161**
Rune BRANDT[1,2], Peter STEVELINK[3]
1: HBI Haerter, CH
2: Trafikverket, SE
3: Zitron, NL

Experimental investigation of thermal runaway in lithium-ion batteries: Implications for tunnel safety and structural integrity **171**
Davide PAPURELLO[1,2], Luca MUSSO[1,2], Carlo BARBETTA[3], Romano BORCHIELLINI[1,2], Maciej SOBOTKA[3], Daniel FRUHWIRT[4]
1: Department of Energy, Politecnico di Torino, IT
2: Energy Center, Politecnico di Torino, IT
3: Systemair GmbH, DE /Systemair Srl, IT
4: Graz University of Technology, Institute of Thermodynamics and Sustainable Propulsion Systems, AT

Session S4:

Smart tunnel in industry 5.0: Improving road tunnel resilience by dynamic risk analysis **181**
Alessandro FOCARACCI[1], Francesca ZACCHEI[2], Luigi MARTIRANO[2]
1: Prometeoengineering.it S.r.l., IT
2: La Sapienza - University of Rome, IT

Acceptance criteria for design of longitudinal ventilation systems in road tunnels: Theoretical framework **190**
Matteo PACHERA, Ranjit CHAUDHARY, Jef VAN NEROM, Stefaan VERNIEUWE
Sweco, BE

State of the art and lines of development for the ARTU risk analysis software **204**
Rugiada SCOZZARI, Michele FRONTERRÈ
Cantene s.r.l, IT

Session G4:

Heat transmission between ground and tunnel air for different configurations and uses **213**
Juan Manuel SANZ SACRISTÁN
Sener Mobility SA, ES

Enhancement of the dispersion of pollutants near a tunnel ending in a street canyon, a CFD case study **224**
Gabriel REMION[1], Bruno VIDAL[1], Thierry KUBWIMANA[1], Marouane YAGHZAR[1], Antoine MOS[1], Romain BOISSAT[2], Edwige REVELAT[2], Alexis STEPANIAN[2]
1: CETU, FR
2: AtmoSud, FR

Smoke recirculation at road-tunnel portals **235**
Marco BETTELINI, Marco TOBLER, Raphaël DEFERT
Amberg Engineering Ltd., CH

Session S5:

Application of low-tech and lean-tech concepts to road tunnels for greater energy efficiency **244**
Tristan REGNIER, Olivier MARTINETTO, Florent GUIRAL
Egis, FR

Effects of contributing to decarbonization by model-based predictive ventilation control (MPVC) on expressways **253**
Hiroki UEDA[1], Atsushi ICHIKAWA[2], Minoru YUHARA[3], Masaki HIRO[1], Yuichiro FUJITA[1], Wataru TAKAHASHI[4], Alan VARDY[5]
1: Nippon Expressway Research Institute Company Limited, JP
2: East Nippon Expressway Company Limited, JP
3: AMEC Consultants Company Limited, JP
4: Central Nippon Highway Engineering Nagoya Company Limited, JP
5: University of Dundee, UK

Improving energy efficiency in road tunnels **262**
Lorenz KIRCHEBNER[1], Alexander WIERER[1], Christof SISTENICH[2], Michael BACHER[3], Marlene HINTERHOFER[3], Thomas MARCHER[4], Georg KAML[4]
1: crypta.sec conceptum GmbH, AT
2: BASt, Federal Highway and Transport Research Institute, DE
3: Graz University of Technology, Institute of Thermodynamics and Sustainable Propulsion Systems, AT
4: Graz University of Technology, Institute of Rock Mechanics and Tunnelling, AT

Session G5:

On smoke detection systems in road tunnels – a quantitative comparison **271**
Samuel GEHRIG[1], Simon FREY[2], Benjamin POLLINGER[1], Reto BUCHMANN[3], Bernard CRAUSAZ[4]
1: AFRY Switzerland AG, CH
2: HBI Haerter, CH
3: buntech GmbH, CH
4: Federal Roads Office FEDRO, CH

Ventilation system upgrade for Huguenot tunnel in South Africa **283**
Tiago MASSINGUE[1], Julia KEARNS[2]
1: The South African National Roads Agency SOC Ltd, ZA
2: SMEC South Africa (Pty) Ltd, ZA

Web-SCADA: A web-based supervisory control and data acquisition platform for road tunnel safety in Japan **291**
Leon DICKEL[1], Mathis RUFFIEUX[1], Jean ROUGE[1], Yen-Hung LAI[1], Masahide NAKAMURA[2], Alan VARDY[3]
1: Sohatsu Systems Laboratory Inc., JP
2: Kobe University, JP
3: University of Dundee, UK

Session S6:

Towards accurate tunnel fire simulations: Grid sensitivity and les model comparison in fire dynamics simulator **304**
Mahfuz SARWAR[1], K.A.M. MOINUDDIN[2]
1: Fire Rescue Victoria (FRV), Major Community Infrastructure Unit (MCIU), AU
2: Centre for Environmental Safety and Risk Engineering (CESARE), Victoria University, AU

On the flow resistance of tunnel fires – validation by full-scale fire tests **319**
Ingo RIESS[1], Rajdeep DEB[2], Alex WEBER[2]
1: Riess Ingenieur-GmbH, CH
2: OST Ostschweizer Fachhochschule, CH

Effect of road tunnel fitout on smoke control **328**
Michael BEYER, Conrad STACEY
Stacey Agnew Pty Ltd., AU

Session G6:

Consequences from large EV fires in tunnels - a DACH research activitiy **338**
Daniel FRUHWIRT[1], Alexander KORES[1], Robert GALLER[2], Robert WENIGHOFER[2], Bastiaan LOTTMAN[3], Simon FREY[4], Christian THIENERT[5], Frank LEISMANN[5], Christoph SCHNEIDER[6],
1: Graz University of Technology, Institute of Thermodynamics and Sustainable Propulsion Systems, AT
2: Technical University of Leoben, AT
3: ILF Consulting Engineers Austria GmbH, AT
4: HBI Haerter AG, CH
5: Studiengesellschaft für Tunnel und Verkehrsanlagen – STUVA – e. V., DE
6: WSP, CH

Modelling airborne brake wear particle transport in subway systems: A line-scale framework **346**
Rodrigo HERRERO, Carla SÁNCHEZ, Laura RODRÍGUEZ
Metro de Madrid (MdM), ES

From motion to understanding: How deep learning enhances automatic incident detection **359**
Emmanuel MARCHAND, Maciej SEKULA, Christophe COLOMBEL
Citilog, FR

Session S7:

Influence of the tunnel cross-section on tunnel aerodynamics **364**
Verena LANGNER, Andreas HUBER, Johannes RODLER,
Gruner GmbH Wien, AT

Air speeds near services on tunnel walls **374**
Mark GILBEY[1], Dami AJEWOLE[1], David SOPER[2], Mike JESSON[2], Ian STRUDWICK[3]
1: WSP Ltd, UK
2: University of Birmingham, UK
3: HS2 Ltd, UK

Train-induced aerodynamic loads acting on installations of Granitztal tunnel **384**
Michael REITERER
REVOTEC, AT

Reports of the institute of Thermodynamics and Sustainable Propulsion Systems **392**

SUSTAINABILITY OF TUNNEL OPERATION: NEW APPROACHES – A PIARC BRIEFING NOTE AND COLLECTION OF CASE STUDIES [1]

[1]René List, [2]PIARC Technical Committee, Working Group

[1]ASFINAG, AT
[2]PIARC - World Road Association

DOI 10.3217/978-3-99161-087-8-001 (CC BY-NC 4.0)
https://creativecommons.org/licenses/by/4.0/deed.de
This CC license does not apply to third party material (attributed to other sources) and content noted otherwise.

ABSTRACT

Sustainability means creating a new economic and social model that can respond to today's environmental challenges. Applied to road tunnels, this concept includes the environmental aspects of reducing energy consumption and emissions and minimizing impacts over the tunnel's full life cycle. The economic aspects of modern road tunnels focus on keeping costs under control over time, supporting innovation, and helping create local jobs. Ultimately, the social aspects, which are about making tunnels safe, accessible, and well-integrated into their urban surroundings must not be left out of consideration. In this context, road authorities and infrastructure managers are increasingly expected to promote energy efficiency and adopt sustainable methods for the construction and operation of public roads including road tunnels. A large part of the operational expenditure in this regard is related to the provision and consumption of electrical energy. Considering that road tunnels are complex and costly objects with a life cycle of typically more than 80 years, it becomes clear that a concept for sustainable and energy-efficient road tunnel operation is of great importance. The aim of this briefing note including a collection of case studies was therefore to gather, evaluate and comment on international expertise related to measures aiming at the design and operation of road tunnels in a more sustainable way.

Keywords: road tunnel, energy-efficiency, sustainability, life cycle, electrical-energy

1. INTRODUCTION

In the document "2025R03EN - A PIARC Briefing Note and Collection of Case Studies" [1] you will find several case studies written by experts from around the world that showcase different examples that are particularly suitable for providing an insight into the implementation of possible measures and their effects. While the case studies mainly focus on environmental and energy-related improvements, many of them also contain implicit benefits for social and economic sustainability, although such aspects have not been specifically analyzed in this document.

2. SUMMARY AND CONCLUSION

The added value of this briefing note consists of the description of approaches to the design and operation of road tunnels in terms of energy supply, energy demand, safety equipment used, life cycle-based design, impact of different operational phases, reporting and measurement of operational status and energy consumption. By referring to the state-of-the-art knowledge of international experts, this briefing note aims to give an insight into the latest developments regarding the topics covered and support decision makers, tunnel owners and managers, tunnel operators, designers, tunnel safety experts, safety officers and risk analysis specialists in the process of planning and deploying tunnel projects.

3. REFERENCES

[1] https://www.piarc.org/ressources/publications/source/4/1399cb2f-47231-2025R03EN-Sustainability-Tunnel-Operation-New-Approches-PIARC-Briefing-Note-Case-Studies.pdf

THE KORLM TUNNEL AS A REAL-WORLD LABORATORY: RESEARCH WORK AND FINDINGS DURING THE CONSTRUCTION OF THE KORALM TUNNEL

[1]Helmut Steiner, [2]Michael Bacher, [2]Daniel Fruhwirt

[1]Austrian Federal Railways, AT
[2]Graz University of Technology, AT

DOI 10.3217/978-3-99161-087-8-002 (CC BY-SA 4.0)
https://creativecommons.org/licenses/by/4.0/deed.de
This CC license does not apply to third party material (attributed to other sources) and content noted otherwise.

ABSTRACT

The Koralm Tunnel (KAT) was used as a real-world laboratory during the mechanical equipment phase and commissioning in order to investigate a range of operational, safety-related, and aerodynamic phenomena under realistic high-speed railway conditions. A series of coordinated experimental and measurement campaigns were conducted to generate data relevant for tunnel design validation, system commissioning, and future tunnel projects.

Dust exposure levels were investigated during high-speed train movements to assess occupational safety conditions and to evaluate particle transport mechanisms within the tunnel system. Based on these measurements, the service life of ventilation and technical room filters was determined under representative operating conditions. Pressure loads induced by train passages were measured both in the tunnel and within adjacent technical rooms, providing insight into transient pressure propagation and structural loading of technical installations.

The behaviour of pantographs during high-speed operation investigated using CFD simulations in order to determine the contact force between the pantograph head and the fixed catenary. The aim is to use this information to prevent arcing and burn marks on the the fixed catenary. In parallel, wall friction was determined using pressure and velocity measurements, contributing to an improved understanding of resistance effects relevant for ventilation design and energy demand. Aerodynamic processes in the cross passages and the unterground evacuation and rescue point (EVRP) were investigated to evaluate airflow patterns and pressure interactions under train-induced flow conditions.

In addition, meteorological pressure differences between the tunnel portals were recorded and analysed to quantify their influence on longitudinal airflow and pressure balance within the tunnel system. The results provide valuable experimental data for validating numerical models, supporting commissioning activities, and improving the design and operation of future long railway tunnels subjected to high-speed traffic.

Keywords: High-speed railway tunnels; Tunnel aerodynamics; Pressure loads; Dust exposure; Commissioning measurements

1. INTRODUCTION

Long railway tunnels designed for high-speed traffic represent highly complex aerodynamic systems in which train-induced flows, ventilation concepts, structural constraints, and operational safety requirements interact under transient conditions. While numerical simulations provide essential tools for design and planning, full-scale measurements under real operating conditions remain rare. Such measurements are, however, indispensable for validating design assumptions, improving model accuracy, and understanding coupled physical phenomena that cannot be fully captured by theoretical approaches alone.

The commissioning phase of the Koralm Tunnel offered a unique opportunity to use the tunnel as a real-world laboratory. During this phase, the mechanical equipment was already installed and high-speed train movements could be performed under controlled conditions, enabling comprehensive experimental investigations within a fully functional tunnel environment. This setting allowed the observation of aerodynamic, operational, and safety-relevant effects at full scale and under realistic boundary conditions, which are typically inaccessible once regular rail operation begins.

Within this framework, a series of coordinated measurement campaigns was carried out to address key questions related to occupational safety, aerodynamic behaviour, ventilation performance, and the interaction between train movement and tunnel infrastructure. The investigations focused not only on phenomena within the tunnel but also on their impact on adjacent technical rooms, emergency ventilation systems, and the overall pressure balance of the tunnel.

The data obtained from these experiments serve multiple purposes. They support the validation of numerical models used in tunnel design, contribute to the optimisation of ventilation and safety concepts, and provide practical insights for the commissioning of technical equipment. Furthermore, the findings offer valuable reference data for future long railway tunnel projects exposed to high-speed traffic, where comparable full-scale experimental evidence is typically unavailable.

2. KORALM BAHN, KORALM TUNNEL

The so called ‘Southern Corridor’, which includes the Koralm railway (*Koralm Bahn,* KAB), is part of the about 4’600 km long Baltic Sea –Adriatic Sea Corridor (BSAS) of the Trans European Transport Network (TEN–T). It represents the eastern transalpine north-south link and connects the ports and regions in the north (Baltic Sea, Baltic region, Poland) with Central Europe and the ports and regions in the upper Adriatic area.

The KAB, with a length of about 130 km, connects the Austrian federal regions Styria and Carinthia, and their capital cities Graz and Klagenfurt. The key element of this new route is the Koralm Tunnel (KAT) with a length of 32.9 km and a maximum rock overlying of about 1’200 m. The two single-track rail tunnels are connected via cross-passages every 500 m. These serve as escape routes and also contain the necessary equipment for tunnel operation. An underground Evacuation and Rescue Point (EVRP), approximately 1 km in length, is located between the two tubes near the center of the tunnel.

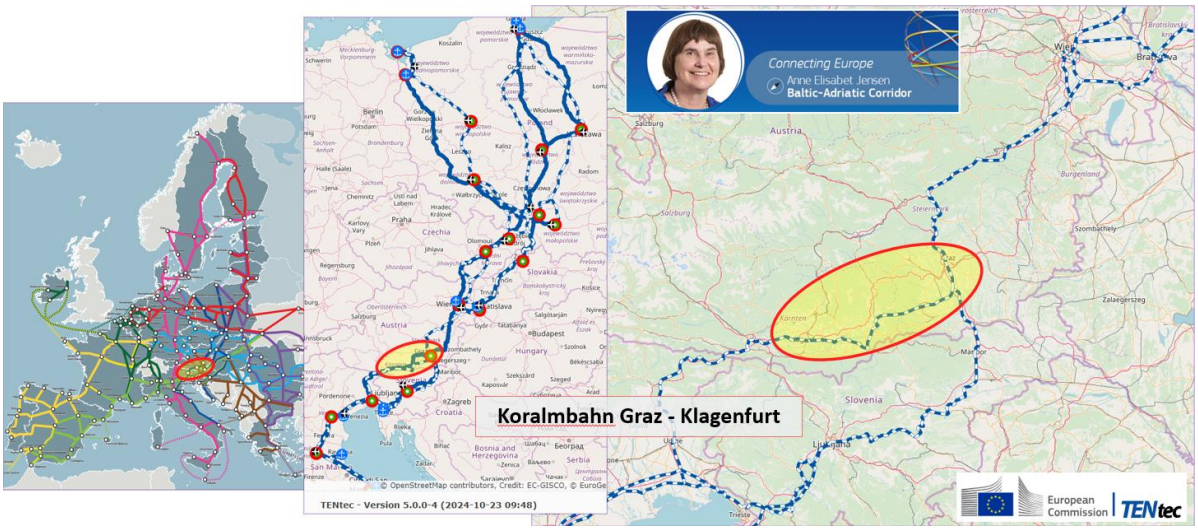


Figure 1: Baltic Sea -Adriatic Sead Transport Corridor [EU / ÖBB]

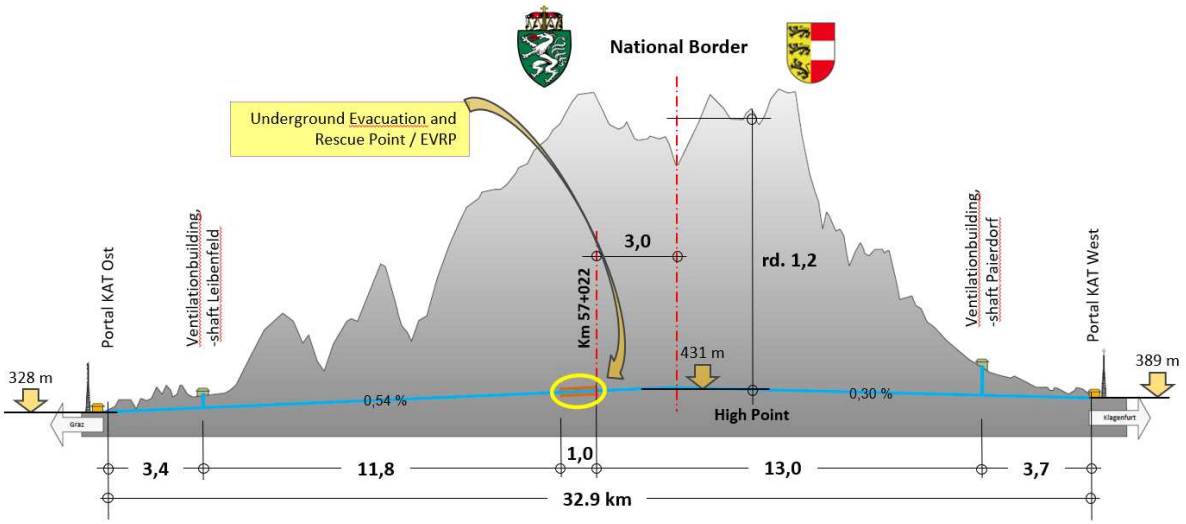


Figure 2: Koralm Tunnel - overview longitudinal section [ÖBB]

3. SURFACE ROUGHNESS

In the aerodynamic design of ventilation systems for railway tunnels, values taken from literature are commonly used to estimate the surface or friction coefficient [1] [2] [3]. This approach is based on the relationship between the Reynolds number and the friction coefficient, as flow losses are strongly influenced by the flow regime and the condition of the tunnel wall. In railway tunnels, the Reynolds number, depending on tunnel cross-section and flow velocity, typically ranges from approximately 4.5×10^5 to 1.5×10^8 [1], [2]. Under these conditions, the flow is always fully turbulent, and wall roughness has a major influence on the friction coefficient.

For an exact determination of the friction coefficient, the average roughness height of the tunnel surface would be required. In practice, however, this information is usually not available. Therefore, empirical values from the literature are often applied. Depending on the quality of the concrete surface and the presence of installations, roughness coefficients are typically assumed to range from λ=0.013 to λ=0.025 [4]. A commonly used reference value for a tunnel tube with minor obstacles is approximately λ=0.015 [4].

During the commissioning phase of the Koralm Tunnel, dedicated measurements were carried out to experimentally determine the actual surface friction coefficient. Over a measurement length of 500 m, the loss of pressure was recorded at a mean flow velocity of 6.2 m/s. To determine the air density, air temperature and air pressure were measured during the test using a Testo 400 device. The loss of pressure was measured using a 500 m long plastic tube connected to a high-precision differential pressure sensor manufactured by Halstrup-Walcher (measurement range 250 Pa ± 0,5% FS). The flow velocity was determined contact-free using an ultrasonic flow measurement device, which measures velocity along a defined measurement path (measurement accuracy ±0.2 m/s). In the measurement section, the tunnel is constructed using segmental lining in the form of precast concrete segments (see **Figure 3**).



Figure 3: Finish of the tunnel surface

Using this measurement setup, an average tunnel friction coefficient of $\boldsymbol{\lambda}$**=0.0158** was determined. This value includes not only the concrete tunnel surface but also typical tunnel installations such as the fixed catenary, handrails, and leaky feeder communication cable, small signs (20 cm × 20 cm), thus providing a realistic parameter for aerodynamic design.

4. METEOROLOGICAL PORTAL PRESSURE DIFFERENCE

Another key parameter in the design of ventilation systems for long railway tunnels is the consideration of meteorological influences. Especially in tunnels with significant overburden, very different weather systems can prevail simultaneously at the two portals. These differences can lead to considerable portal pressure differences, which strongly influence the longitudinal airflow within the tunnel. Pure wind effects are of secondary importance in such cases, as the resulting wind pressures can be up to one order of magnitude smaller than the portal pressure differences.

For a reliable determination of these portal pressure differences, highly accurate absolute pressure sensors are required. The measurement accuracy should be in the range of approximately ±5 Pa. Conventional meteorological absolute pressure sensors, however, often provide accuracies of only about ±50 Pa and are therefore of limited suitability for this purpose.

During the planning phase, site-specific measurement data are often not available. In practice, data from nearby meteorological stations are therefore commonly used. In addition, it must be defined in advance which percentile of the measured portal pressure differences is relevant for the dimensioning of the ventilation system. In Austria, for example, the 95th and 98th percentiles of hourly mean values are frequently applied for road tunnels [5].

In the design of the ventilation system for the Koralm Tunnel, absolute pressure, air temperature, and relative humidity were taken into account. For this purpose, five-year time series from meteorological stations operated by Geosphere Austria located near the tunnel portals were used (approximately 3 km in straight-line distance from the eastern portal and about 4.5 km from the western portal). Based on the measured absolute pressures, portal pressure differences were calculated, taking into account the respective installation heights of the sensors, and the 95th percentile relevant for ventilation design was derived.

Since these stations are not located directly at the tunnel portals, and since the absolute pressure sensors used have limited measurement accuracy, a one-year direct measurement campaign of the absolute pressures was conducted at the portals from October 2024 to October 2025. These measurements with highly accurate absolute pressure sensors were subsequently compared with the data from the meteorological stations of Geosphere Austria in order to assess and validate the reliability of the previously used data basis and to evaluate the differences between the two measurement methods.

Table 1: Percentile comparison between directly measured portal differential pressure using high-precision absolute pressure sensors (left) and meteorological measurements from further away using standard absolute pressure sensors (right).

portal differential pressure measurement			**meteorological measurement**		
percentile	pressure on the east portal	pressure on the west portal	percentile	pressure on the east portal	pressure on the west portal
	[Pa]	[Pa]		[Pa]	[Pa]
100	331	518	100	356	531
95	112	220	95	131	192
90	86	168	90	106	136
85	65	135	85	89	103
80	50	113	80	73	81
50	0	28	50	2	0

The one-year absolute pressure measurements carried out directly at the portals using high-precision sensors clearly show that the assumptions made for the ventilation design are adequate. In comparison, the data from more distant meteorological stations equipped with standard absolute pressure sensors exhibit significant deviations. In some cases, the actual portal pressure differences are considerably overestimated, while in others they are underestimated.

However, these parameters are essential for the safe and energy-efficient operation of the ventilation system. It is therefore recommended to conduct meteorological measurements with high-accuracy absolute pressure sensors in the immediate vicinity of the tunnel portals as early as possible, ideally before the planning phase begins.

5. DUST GENERATION

A particularly interesting aspect is dust exposure during the commissioning phase. At this time, there is still a lot of work left to be done in the tunnel. At the same time, so-called stepwise high-speed test movements are frequently conducted. These movements generate strong air movements that can resuspend dust and thereby significantly increase PM concentrations. The limit values relevant to workplaces are particularly interesting in this context. ([6], [7], [8]):

Substance	Limit type	Value	Unit
Fine quartz (<2.5µm)	8 hours	0.1	mg/m³

Several studies on dust exposure in railway tunnels already exist (e.g. [9] [10] [11]). However, their primary objective was to determine emissions from rail traffic. These studies do not provide information on 8 hours workplace concentrations.

Air quality during the commissioning phase is of special interest, as completion works inside the tunnel are conducted at this time. At the same time, so-called stepwise high-speed test movements are often conducted during this phase. These train activities generate a strong air flow, which leads to resuspension of dust and thereby higher PM levels. A few studies about PM exposure in railway tunnels and emission from railways have been conducted. These mainly refer to tunnels that have been in operation for many years. Stepwise high-speed test movements are an essential part of the commissioning process of railway tunnels, particularly on high-speed lines. Their purpose is to verify the interaction between the train, the fixed catenary or conductor rail, the tunnel geometry, and the aerodynamic boundary conditions under real operating conditions. Stepwise high-speed test movements refer to the gradual increase of train speed up to the intended operating speed, with measurements and observations carried out at each speed level.

To investigate PM levels in the Koralm Tunnel, dust measurements were carried out over a period of one month in a tunnel section located approximately 6 km from the western portal. A particle analyser was used to record the particle mass concentration and particle size distribution with high temporal resolution. The instrument operates based on the light-scattering principle, in which particles are assigned to defined size classes. An internal algorithm is then used to calculate particle volume and particle mass. For this purpose, the analyser applies a particle density corresponding to a typical environmental aerosol. Since the actual particle density of the tunnel aerosol during the commissioning phase is still strongly influenced by construction activities and, in addition, emissions from passing trains contain a higher proportion of heavy metals, the default particle density needs to be corrected. For this reason, a cascade impactor was employed, which allowed for parallel sampling of PM10, PM2.5, and PM1 fractions on filters. By weighing the filter samples before and after the tests, the actual particle mass of aforementioned PM fractions could be determined and a correction factor for the online measurement could be derived.

Figure 4 and **Figure 5** illustrate the PM levels (1-minute average values) during a single train pass at the beginning of the measurement period. From these measurements, an 8-hour average value was subsequently calculated in order to allow comparison with the corresponding limit value. In addition, one measurement day with several trains passing in short intervals was evaluated, and the 8-hour average was also determined for this case. **Figure 4** shows the results of the dust measurement on 7 May 2025. A Railjet passed through the tunnel at 250 km/h. No further train movements were scheduled for the rest of the day. During this movement, PM10 concentrations of approximately 9,730 µg/m³ were recorded. The PM2.5 peak-concentrations reached 1,450 µg/m³, and the maximum PM1 was 240 µg/m³. It took roughly 5 hours to again reach the background concentrations. In contrast, **Figure 5** shows the dust measurement from 12 May 2025. The Railjet travelled through the tunnel at only about 50 km/h. Again, no further train movements took place for the remaining day. Slightly higher PM10 peak values were measured than during the 250 km/h movement, with a maximum of approximately 9,980 µg/m³. PM2.5 concentrations ranged between 4 and 1,360 µg/m³, and PM1 values between 3 and 201 µg/m³. Background levels were reached after approximately 3.5 hours.

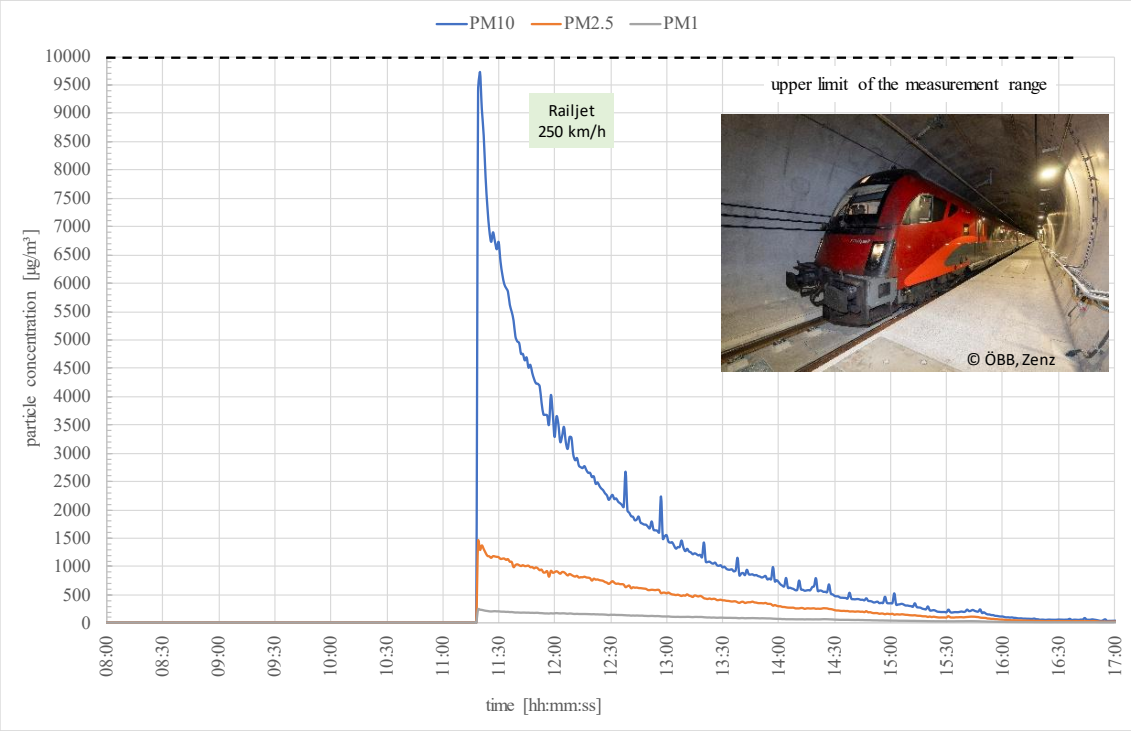


Figure 4: PM1, PM2,5 and PM10 concentration on 07.05.2025 – Railjet v=250km/h

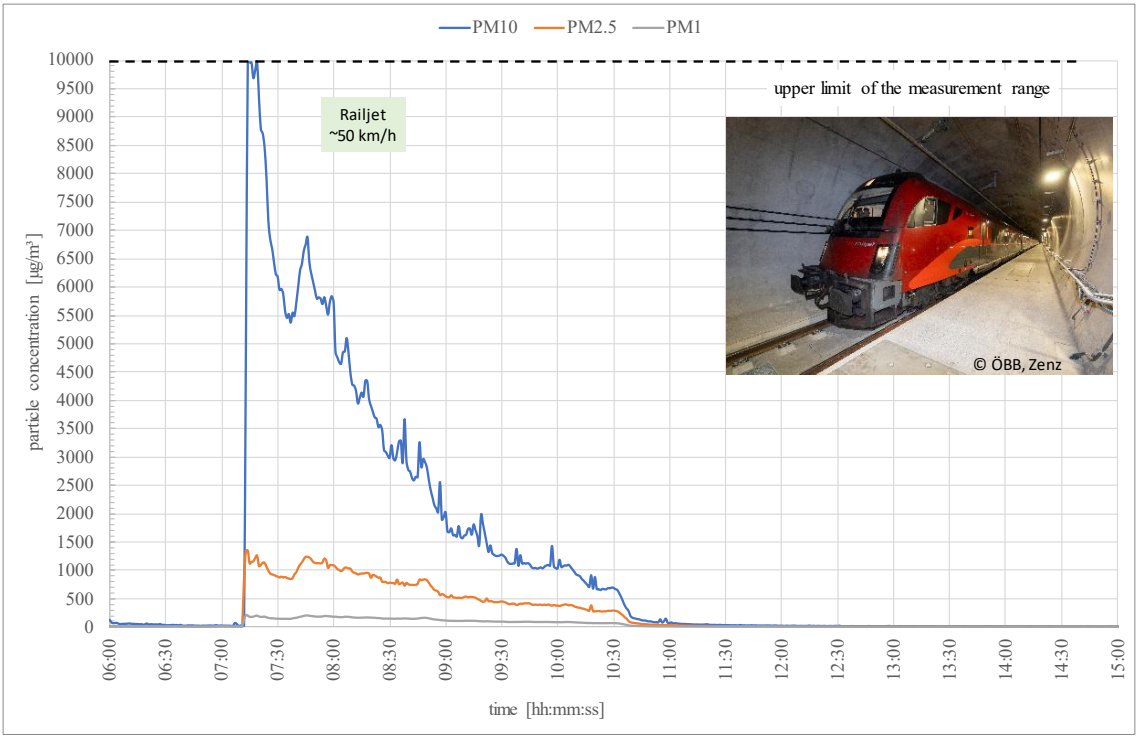


Figure 5: PM1, PM2,5 and PM10 concentration on 12.05.2025 – Railjet v~50km/h

For a final comparison, a measurement day at the end of the campaign was selected, during which six trains passed the test location. The train movements were scheduled in intervals of roughly one and a half hours. The train speed varied between 160 km/h and 230 km/h. **Figure 6** shows the results of the dust measurement on 10 June 2025. The Railjet passed through the tunnel in short time intervals at speeds of 160 km/h, 180 km/h, 200 km/h, and 230 km/h. The peak PM concentrations were 8,085 µg/m³ (PM10), 1,110 µg/m³ (PM2.5) and 201 µg/m³ (PM1). After the last train pass, background levels were reached again after five hours.

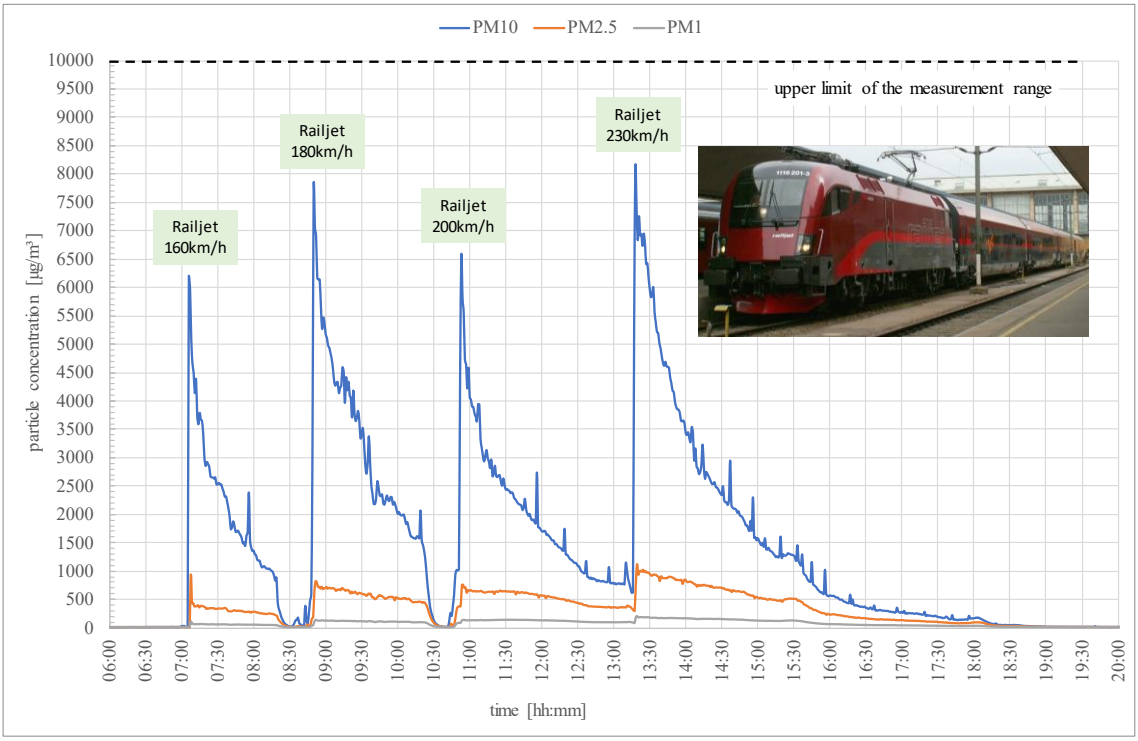


Figure 6: PM1, PM2,5 and PM10 concentration on 10.06.2025 – Railjet v=160km/h, v=180km/h, v=200km/h, v=230km/h

To assess dust exposure with respect to the 8-hour limit value, the corresponding time-weighted averages for PM10 were calculated for the three measurement days presented and compared with the respective limit value. To calculate the average value for the 8-hour period, the calculation was started immediately when the maximum peak began to rise.

measurement day	**Limit type**	**Value**	**Unit**
07.05.2025	8 hours	0.28	mg/m³
12.05.2025	8 hours	0,30	mg/m³
10.06.2025	8 hours	0.50	mg/m³

Based on the results of the dust investigation, it can be concluded that appropriate protective measures must be provided for persons present in the tunnel during train operations in the commissioning phase (e.g., wearing FFP3 respiratory masks, reducing the duration of stay, etc.). However, access to the railway tunnel is usually not permitted while trains are running. Assuming that work can only be carried out several hours after the trains have passed, the dust problem is mitigated accordingly.

6. FILTER SERVICE LIFE

The Koralm Tunnel has a total of 69 technical cross passages, arranged at intervals of 500 m. These cross passages contain the technical equipment required for tunnel operation, organized into five different room categories like the telecommunication room. The telecommunication room is particularly critical, as a maximum room temperature of 22 °C must be maintained there. To ensure this temperature, cooling of the telecommunication room is necessary. On the one hand this is due to the high rock temperature, which ranges from about 16 °C near the portals to approximately 31 °C in the sections with the highest rock coverage, and, on the other hand, to the considerable heat dissipation from the electronic components required for safe tunnel operation. In the central sections of the tunnel with large coverage and correspondingly high rock temperatures, the telecommunication rooms are therefore cooled

using standard air-conditioning systems. In cooler sections of the tunnel (a total of 29 cross passages), the telecommunication rooms are cooled using air taken from cooler one of the two tunnel tubes. The tunnel air is filtered and used to cool the electronic equipment. The warmed air is then discharged back into the tunnel. To ensure the required cooling performance, the airflow rate must be at least 1.1 m³/s. Air filtration is done through a coarse (ISO 16890, Coarse 90%) and a fine dust (ISO 16890, ePM10 80%) filter

The coarse and fine dust filters are the main components influencing the airflow rate of the cooling fans. As dust loading of the filters increases, the overall system resistance rises and the operating point of the fan shifts. The maximum acceptable total pressure loss for coarse and fine dust filters should not exceed 470 Pa. The permissible change in flow rate within the system, together with the fan operating point, the fan characteristic curve, and the total system pressure, determine the allowable increase in resistance of the two filters.

For planning service intervals of the coarse and fine dust filters, it was necessary to determine reference values for filter service life. For this purpose, in-situ investigations were initiated. The objective was to record and analyse the temporal behaviour of dust loading on a specific coarse and fine dust filter during continuous operation with high train frequency. The collected data were used to support statements about the accumulation patterns of dust on the filters and to estimate the approximate filter service life. The configuration of the test setup essentially corresponded to the air-cooling system used in the Koralm Tunnel (see **Figure 7**).

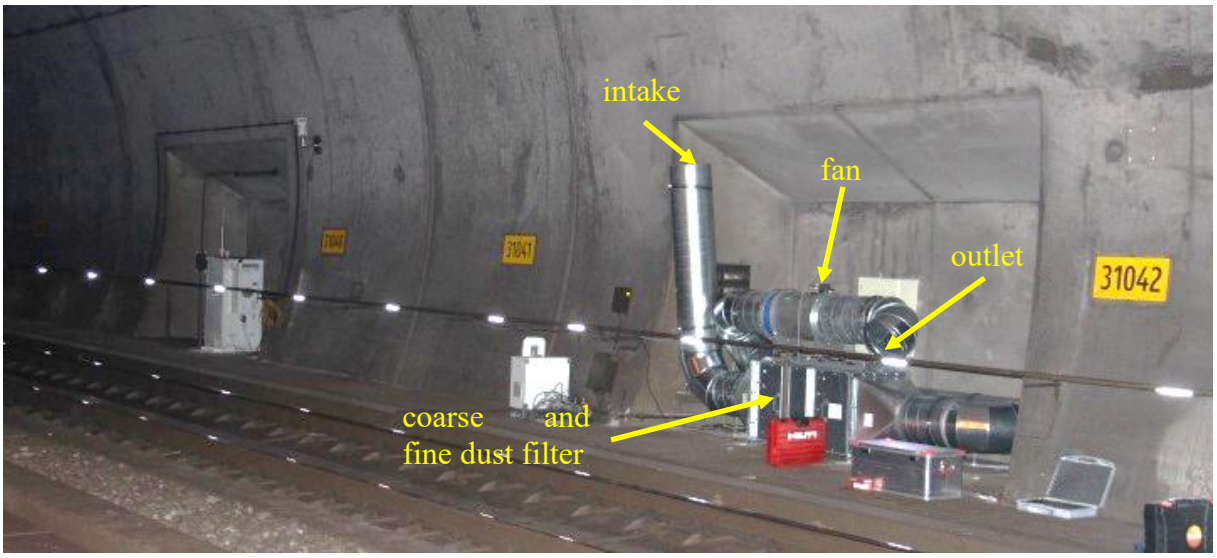


Figure 7: Test setup in tunnel Münster [12]

About the measurement period, the airflow rate of the fan decreased from an initial value of about 1.6 m³/s to approximately 0.9 m³/s. The critical point, defined as the airflow dropping below 1.1 m³/s (minimum volume flow for cooling), was reached approximately 42 days after the start of the measurement. At this time, the pressure loss of the coarse dust filter was about 140 Pa, the pressure loss of the fine dust filter was about 206 Pa, and the total pressure loss approximately 350 Pa. The results of the test are shown in **Figure 8**.

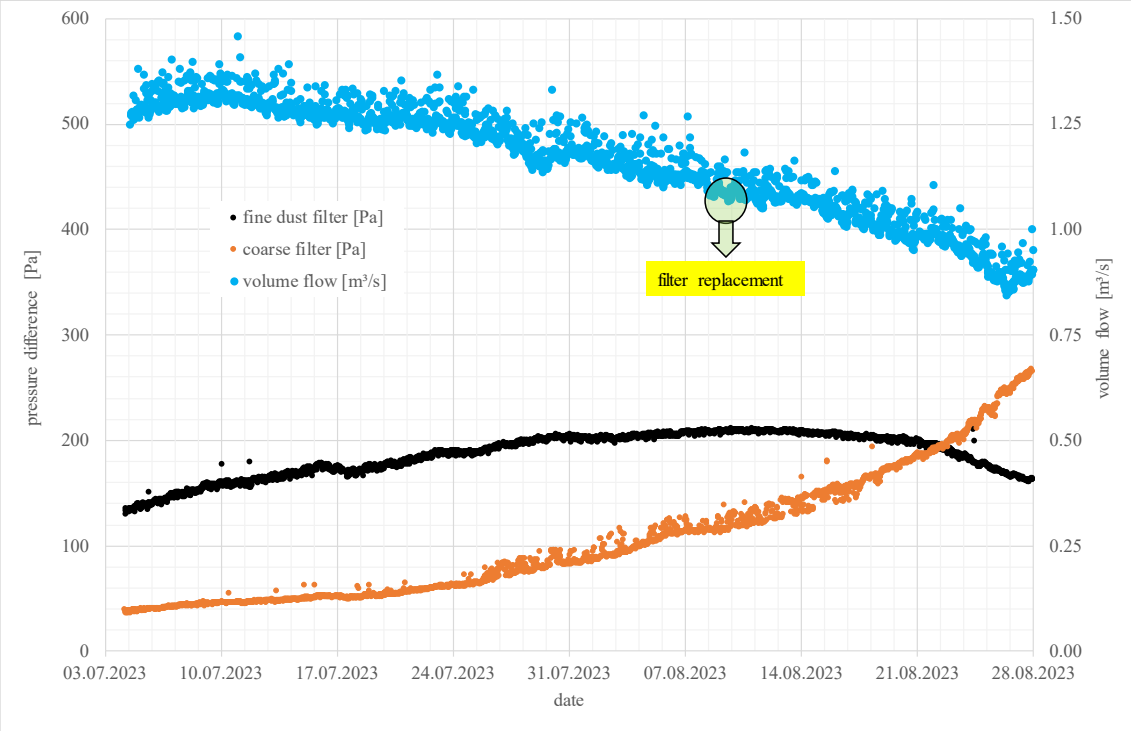


Figure 8: Temporal development of filter pressure losses and airflow rate**.**

During the test period, the average measured daily PM10 concentration was about 53 µg/m³ (daily mean value), with values ranging between 80 µg/m³ and 360 µg/m³.

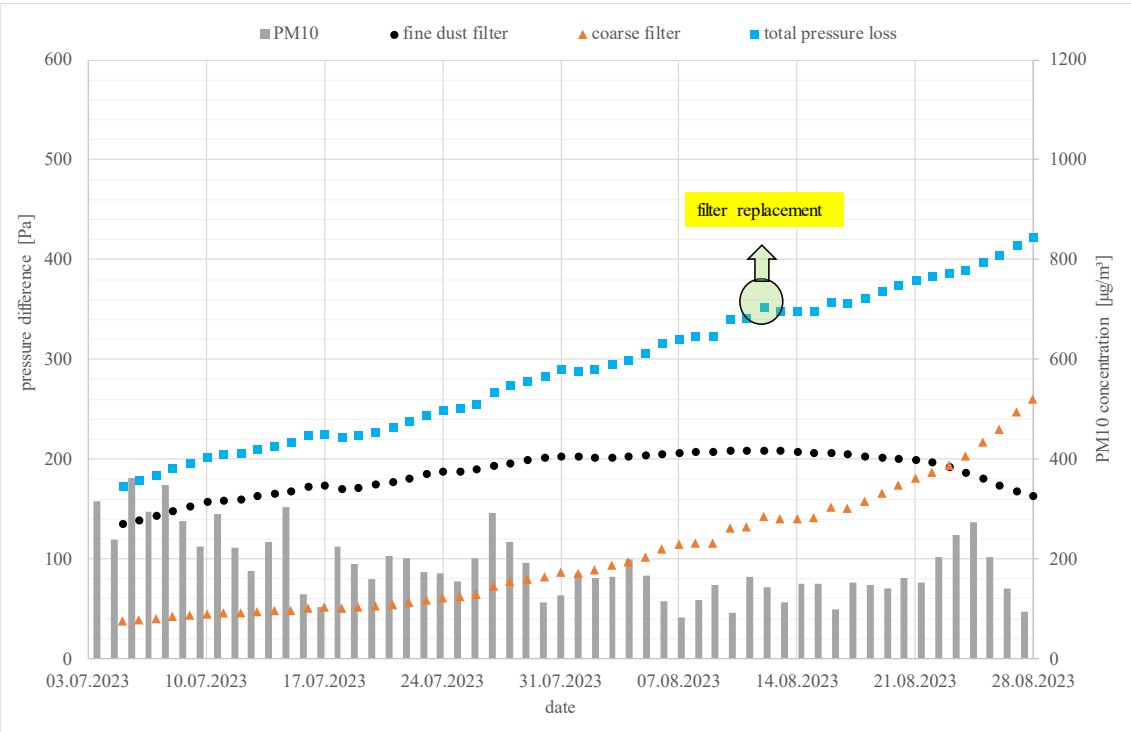


Figure 9: Temporal development (daily average values) of the pressure losses across the coarse and fine dust filters and the PM10 concentration in the tunnel air – operation at 50 Hz.

7. PRESSURE LOADS CAUSED BY TRAIN PASSAGES

Train-induced dynamic pressure loads generated by entering or passing trains in railway tunnels represent a significant aerodynamic stress on tunnel structures and their technical installations. Particularly in long tunnel structures, these transient pressure loads can lead to complex pressure profiles that affect both the main tunnel cross-section and connected structures such as cross passages, technical rooms, and ventilation structures. As part of a detailed measurement campaign, dynamic pressure loads were recorded in the KAT in both tunnel tubes, in front of cross passages CP56 and CP63, as well as within the cross passages. The objective of the measurement campaign was to systematically record and quantify the pressure loads occurring during the stepwise high-speed test movements in the tunnel itself and their propagation into the corridor of the CP, the telecommunications room (TC) and into the low-voltage (LV). Ultra-stable piezoresistive miniature absolute pressure sensors were used for the pressure measurements. This calibrated and temperature-compensated sensors provided highly accurate and stable absolute pressure readings over a wide temperature range. The characteristic parameters of the pressure sensor are listed below.

Measuring range	0 to 15 psi
Compensated temperature range	-20 °C to +85 °C
Operating temperature range	-40 °C to +125 °C

Figure 10 shows the locations and labelling of the monitoring points for CP56 and in both tunnel tubes. In both tunnel tubes, two pressure sensors were installed directly in front of the cross passage. One absolute pressure sensor was mounted on the inner lining of the tunnel (MP24/25), and the second on the wall panel on the side facing the tunnel (MP13/16). These two monitoring points allowed for recording the initial pressure signature of the passing train. To capture the propagation of the pressure waves into the telecommunication room and into the escape route, five additional pressure sensors were installed in the telecommunication room (MP43), the adjacent the low-voltage (MP49) room and the escape route (MP12/35/45).

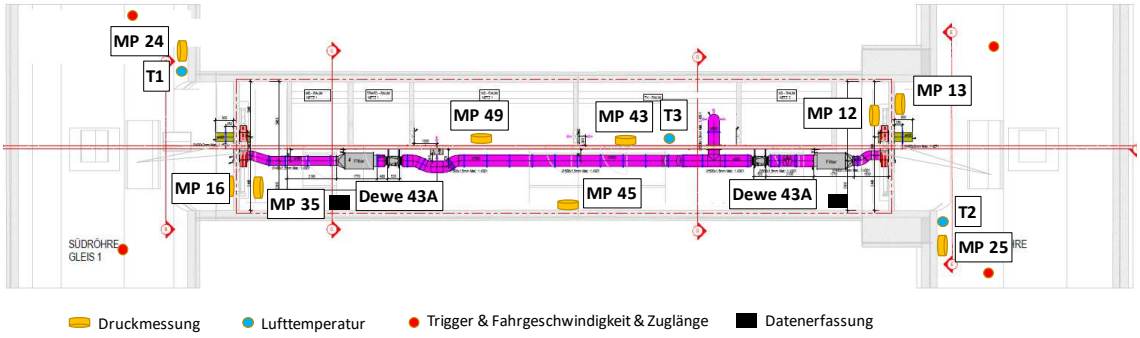


Figure 10: Measurement setup CP56

During the measurement campaign, a wide variety of trains passed through the Koralmtunnel. However, detailed information regarding train type and train length was not available. An evaluation of the train speeds shows that most train movements occurred at approximately 160 km/h. These movements fall within the speed class of 150 km/h to 175 km/h. **Figure 11** provides an overview of the defined speed classes.

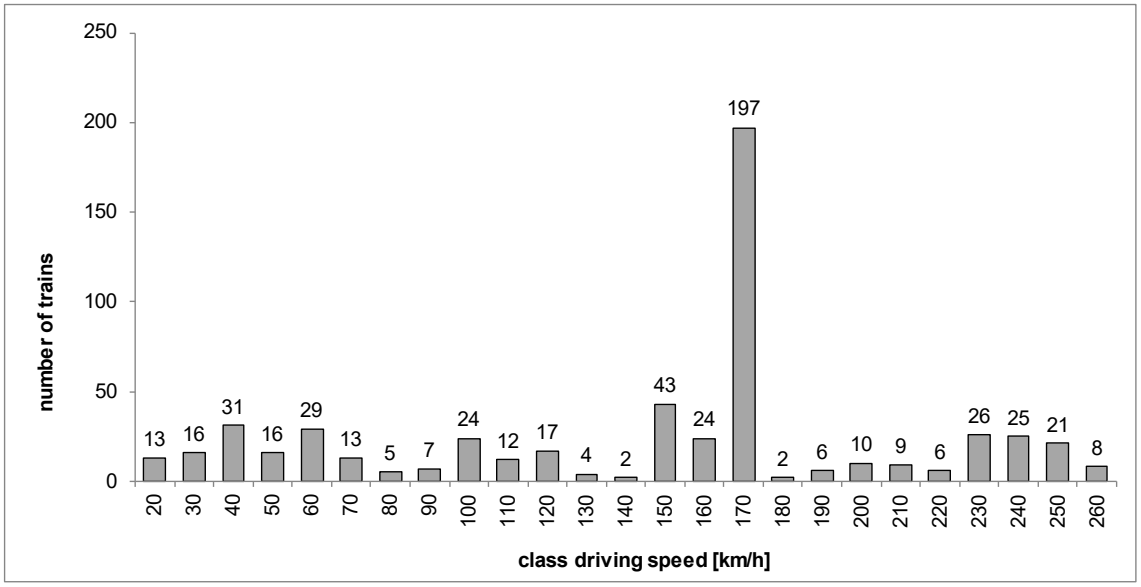


Figure 11: Train speed classification.

Figure 12 presents a summary of all measured maximum pressure loads (over- and underpressure) in the two tunnels, independent of the direction of movement. The figure also includes mathematical functions for the different monitoring points and pressure load ranges. A separate evaluation is required because the measuring points are located in cross-sections with different clear cross-sectional areas (CP56 track 1 = 42,66 m², CP56 track 2 = 51,2 m² and CP63 track 1 = 51,26 m², CP63 track 2 = 48,58 m). Dynamic pressure generally increases quadratically with train speed. Applying this relationship to the pressure loads induced by pressure waves shows very good agreement with the measurement data. At the same time, it becomes evident that the measured values exhibit considerable scatter, which is likely related to the aerodynamic shape and length of the rolling stock, as well as the direction of movement (distance between the portals and the respective measuring point).

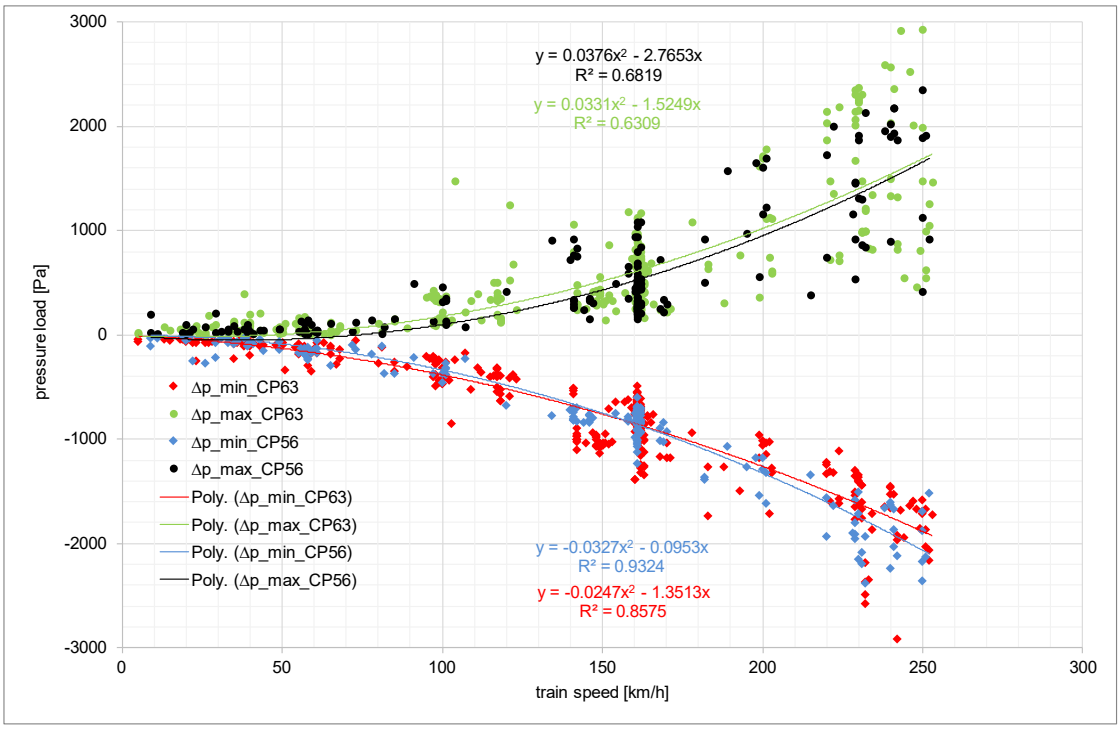


Figure 12: Pressure load based on all train movements at measuring points CP56 and CP63 in both tunnels.

8. SUMMARY

In particular, the commissioning test runs at the KAT were deliberately used to conduct in-situ experimental programs addressing a variety of research questions. Within the framework of these investigations, valuable practical experience was gained and relevant measurement results were obtained. The insights derived from these studies can be applied to future projects involving high-speed and long railway tunnels. The long-term objective is to further optimize the environmentally friendly and highly efficient railway system and to support its successful and innovative development in the future.

9. REFERENCES

[1] Donald S. Miller, *Internal Flow Systems*. Brookside: Miller Innovations, 2008.
[2] Springer-Verlag GmbH, *VDI-Wärmeatlas*. Berlin, Heidelberg: Springer Berlin Heidelberg, 2013. Accessed: Jan. 10 2022.
[3] D. Surek and S. Stempin, *Technische Strömungsmechanik*. Wiesbaden: Springer Fachmedien Wiesbaden, 2014.
[4] Walter Pokorny, Hans-Heinrich Weiss, Ingo Krönke, "Theoretische und praktische Untersuchungen zur Lüftung von Straßentunneln," Wien Heft 171, 1981.
[5] Forschungsgesellschaft Straße - Schiene - Verkehr, Ed., "Tunnelausrüstung Belüftung Grundlagen: RVS 09.02.31," Jun. 2014.
[6] *Änderung der Grenzwerteverordnung, der Verordnung über die Gesundheitsüberwachung am Arbeitsplatz, der Bohrarbeitenverordnung sowie der Verordnung über Beschäftigungsverbote und -beschränkungen für Jugendliche, Anhang I/2025*, 2025.
[7] *Baulüftung im Untertagebau: SIA 196*, SN 531196:1998, Schweizerische Normen-Vereinigung, Nov. 1998.
[8] *Directive 2022/431 amending Directive 2004/37/EC on the protection of workers from the risks related to exposure to carcinogens or mutagens at work*, 2022.
[9] DZSF, *Größenspezifische und räumliche Verteilung von verkehrsbedingten Abrieben und partikulären Emissionen.* Accessed: Oct. 12 2022. [Online]. Available: https://www.dzsf.bund.de/SharedDocs/Standardartikel/DZSF/Projekte/Projekt_44_Abriebe_Emissionen.html
[10] Fruhwirt D., "Endbericht - Staubmessungen Burgstallertunnel V1.0," Final Report, Institute of Thermodynamics and Sustainable Propulsion Systems - Graz University of Technology, Graz I-15/22/DFr V&U I-20/04/647, 2022.
[11] Ehrbar, *Staub löst im Gotthard-Tunnel Fehlalarme aus.* Accessed: Jan. 12 2023.
[12] Fruhwirt, D.; Bacher, M., Steiner. H.; EXPERIENCES FROM FIVE YEARS OF PM MONITORING IN RAILWAY TUNNELS OF AUSTRIAN FEDERAL RAILWAYS (ÖBB); 12th International Conference Tunnels Safety and Ventilation, Graz, 2024

ASFINAG IN CASE OF A BLACKOUT – OVERVIEW AND MEASURES

Günter Rattei, Alice Mahr-Saverschel

ASFINAG/SG PPK, AT

DOI 10.3217/978-3-99161-087-8-003 (CC BY-NC 4.0)
https://creativecommons.org/licenses/by/4.0/deed.de
This CC license does not apply to third party material (attributed to other sources) and content noted otherwise.

ABSTRACT

ASFINAG is part of critical infrastructure and must be prepared for a blackout. A detailed emergency plan and over 70 concepts ensure safe and quick emergency operations, maintain communication, and keep roads open to guarantee security and stability during the crisis.

Keywords: Blackout, critical infrastructure, emergency plan, maintain communication

1. INTRODUCTION

ASFINAG (Autobahnen- und Schnellstraßen-Finanzierungs-Aktiengesellschaft) is the Austrian company responsible for planning, construction, maintenance, operation, and financing of the motorway and expressway network. The company currently manages a network of **2,266 km** of motorways and expressways. In addition, it operates **171 tunnels**, 92 of which are longer than 500 meters and fall under the **Road Tunnel Safety Act (STSG).** The entire network is monitored through **nine traffic management centers**. The infrastructure also includes **59 rest areas, 43 highway maintenance depots**, and **six toll stations**. In total, ASFINAG employs around **2,967 people** across Austria.

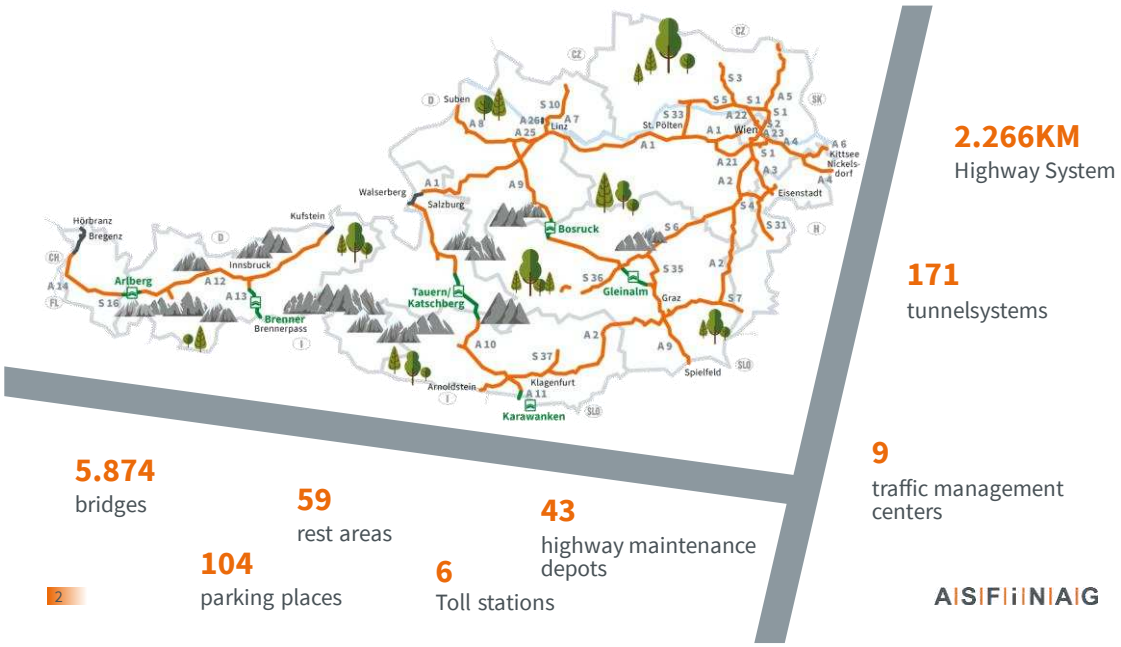


Figure 1: Overview of the ASFINAG Network

With **416 kilometers of tunnels**, which represents about 18.4% of the total network length of 2,266 kilometers, ASFINAG operates one of the most important tunnel networks in Europe.

2. PREPARATION FOR A BLACKOUT

2.1. Critical infrastructure

Critical infrastructure refers to organizations and facilities that are essential for the functioning of a state and society. They are responsible for basic services in areas such as energy, transport, communication, healthcare, and security. Important examples include hospitals.

A failure or serious disruption of these systems would have severe consequences: from long-lasting supply shortages and major disturbances of public order to extensive social and economic damage. The stability of these infrastructures is therefore crucial to ensure daily life, safety, and the economic performance of a country.

The **transport** sector provides **mobility** for people and goods and includes road, rail, air, and sea transport. This sector also includes ASFINAG, which is responsible for operating Austria's motorway and expressway network.

2.2. Ensuring Mobility During a Blackout

In the first step, it is important to clearly distinguish between the scenarios of power outage, energy shortage, and blackout. All these scenarios have been precisely defined within the company to ensure clear differentiation.

There is no uniform definition of the term "blackout" in Austria. However, the European Network of Transmission System Operators (ENTSO-E) provides a definition in its "System Operation Guideline" (SOGL, Regulation (EU) 2017/1485, Article 18, Paragraph 4):

A transmission system is considered to be in a blackout state if at least one of the following conditions is met:

- Loss of more than 50% of the load in the control area of the respective transmission system operator (TSO)
- Complete loss of voltage in the control area of the respective TSO for at least three minutes, requiring activation of system restoration plans

ASFINAG defines a blackout as a prolonged power outage (more than 12 hours) affecting at least all of Austria and large parts of Europe. Internally, a blackout is declared when two regional traffic management centers report an outage in their respective regions.

In addition to electricity, other infrastructures such as public transport, telecommunications, and logistics chains also fail immediately or with some delay.

To fully understand the impact of a blackout, it is necessary to consider the overall scenario, including the associated infrastructure failures and the time factor. In principle, a blackout is divided into three phases:



Figure 2: Overview of the ASFINAG Network

2.2.1. Key Responsibilities of ASFINAG in Standard Operations

ASFINAG uses about 128 GWh of electricity every year to carry out its core tasks. This is almost equal to Austria's total energy consumption for one day, making ASFINAG a major consumer nationwide.

This internal consumption includes all activities that ASFINAG performs on a daily basis. The core tasks are:

- Maintaining the infrastructure
- Building new roads and tunnels
- Operating toll systems
- Managing the network
- Financing the measures

In the cases of a blackout, these core tasks are reduced to **emergency operations**. This means that all tasks except "**managing the network**" are suspended. However, the entire road network remains open for individual traffic.

2.3. Emergency Plan & Emergency Operation Concepts

A blackout poses a serious risk to business operations. To be prepared and remain capable of acting in such a situation, ASFINAG has developed a structured emergency plan. The focus is on taking all necessary steps together to ensure safety, stability, and an orderly resumption of operations.

The blackout emergency plan aims to maintain stable emergency operations during a large-scale power outage, keep communication within the crisis organization running, and enable a controlled shutdown and restart of operations.

For all operational units at locations, offices, and construction sites, predefined procedures for blackout scenarios have been developed. In addition, specific emergency operation concepts have been created for the orderly suspension of construction sites. These concepts ensure a standardized approach in case of emergency and form part of ASFINAG's blackout emergency plan. In total, more than 70 emergency operation concepts have been prepared for sites and operational units.

These documents serve as the basis for being prepared for a potential blackout. For all operational units, clear specifications have been defined—from the number of required employees to duty schedules and concrete measures that must be implemented during emergency operations.

The emergency operation concepts apply from the moment a blackout is declared until it is officially ended by the ASFINAG crisis team.

In addition, checklists, forms for analog documentation, blackout entry procedures, maps, and instructions have been developed for each location. These structured checklists provide essential support for staff during a blackout.

Both preventive and immediate action checklists have been created. The checklists are adapted to the priorities of each location. Furthermore, the procedures for restarting operations have been clearly defined.

Emergency operation concepts have been prepared for the following operational units, among others:

- Highway Maintenance Depot (ABM)
  The main goal of the highway maintenance depot during a blackout is to keep the route operational as much as possible—at least one lane should remain open for all road users to ensure emergency operations and safety along the route. The emergency operation concept regulates the emergency operation of the motorway and expressway network, the minimum operating conditions during a blackout, and communication between ASFINAG's operational units and the crisis team.
- Traffic Management Center (VMZ)
  In the event of a blackout, the primary task of the traffic management center is to monitor the motorway and expressway network as effectively as possible, control tunnel and open-road facilities, and immediately alert internal and external emergency services about traffic disruptions (e.g., accidents). This ensures traffic safety and flow for road users during emergency operations.
- Maintenance (IH) / Operational Technology (BT)
  During a blackout, the main task of maintenance and operational technology is to keep the technical systems of tunnels and open-road facilities running to maintain the minimum operating conditions (e.g. LED guidance systems, 25% of lighting, Emergency call systems, Escape route signage and orientation lights…) of the motorway and expressway network. This ensures traffic safety and flow for road users during emergency operations.
- Main Toll Stations (HMS)
  In the event of a blackout, the primary task of the main toll station is to shut down the toll system in an orderly manner to maintain traffic flow in the toll area during the blackout. Toll collection will be suspended for the duration of the blackout.
- Construction Sites
  During a blackout, the main task of construction site managers (internal/external) is to secure the construction sites on the route with appropriate measures so that traffic flow and safety can be guaranteed for the duration of the blackout.

2.4. Communication During a Blackout

To ensure the maintenance of essential communication and data connections between the eight regional traffic management centers (VMZ), the VMZ Vienna-Inzersdorf, and the data center locations in Bruck/Leitha and Vienna-Inzersdorf during a blackout, ASFINAG has established a fail-safe communication network known as the ASFINAG Blackout (BO) Network.

In addition, extensions have been implemented to increase the reliability of the BO Network, ensuring availability for approximately seven days. For example, the regional VMZs in Klagenfurt and Plabutsch, as well as Bruck/Mur and the data center in Bruck/Leitha, have been interconnected within the BO Network. This interconnection creates a ring structure, which allows communication to continue even if individual connection paths fail, thereby improving resilience.

If the BO Network experiences a regional outage, a fallback option is available via the satellite internet uplink (Starlink). This ensures that communication between the St. Jakob site in the west and the Vienna-Inzersdorf site in the east remains possible when needed.

2.4.1. Information platform: Crisis Team

In the event of a blackout, functioning communication is of great importance. During such a situation, all normal communication channels (telephone, mobile phone, fax, email, internet) will no longer be available or will only work in a very limited way within a short time. To maintain communication with operational units, a “Vehicle Reporting System system” has been developed.

All information is collected by the crisis team and distributed from there using the available technical means. If all communication options fail, the Vehicle Reporting System system should be used whenever possible and reasonable. In this case, a clear picture of the local security situation must be available to avoid exposing the messenger to unnecessary risks. The decision on this lies with the crisis team, the regional traffic management centers (VMZ), and the highway maintenance depots (ABM).

The situation report serves as an exchange between the operational units and the crisis team. This report must be submitted at predefined time intervals. After a short processing period by the crisis team, the report is sent back to the operational units. The Vehicle Reporting System system is used for transmission. Feedback must be returned to the VMZ and handed over to the messenger for delivery to the respective locations.

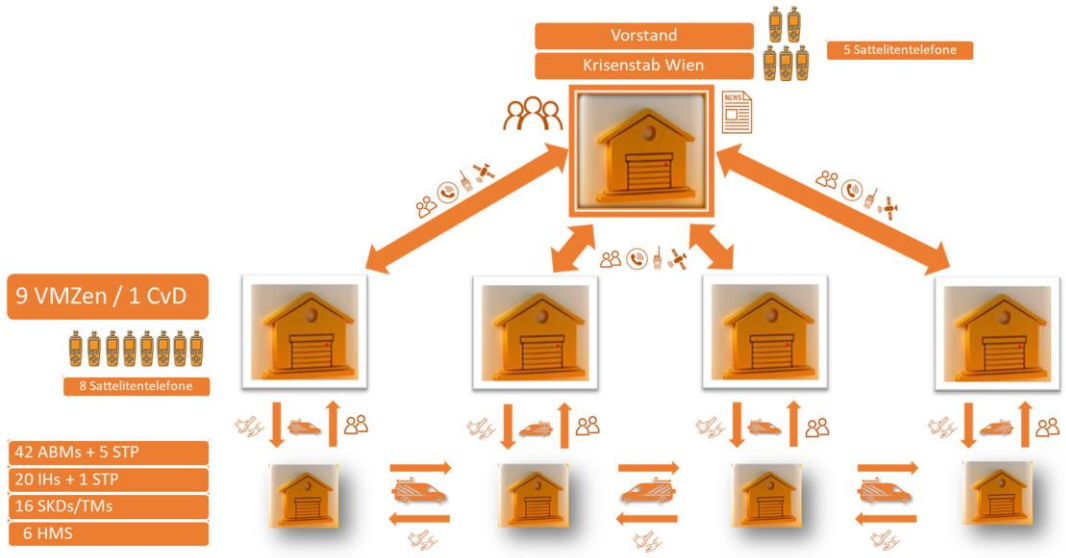


Figure 3: Communication Procedere between the

2.4.2. Vehicle Reporting System

Starting from the day after the blackout begins, the Vehicle Reporting System serves as the primary communication channel for operational units to deliver information about the current situation and to receive instructions.

Clear routes have been defined in advance for all units, determining the order of stations. At a specified time, a messenger collects the situation reports and delivers them directly to the next location, ensuring that the flow of information continues without delay.

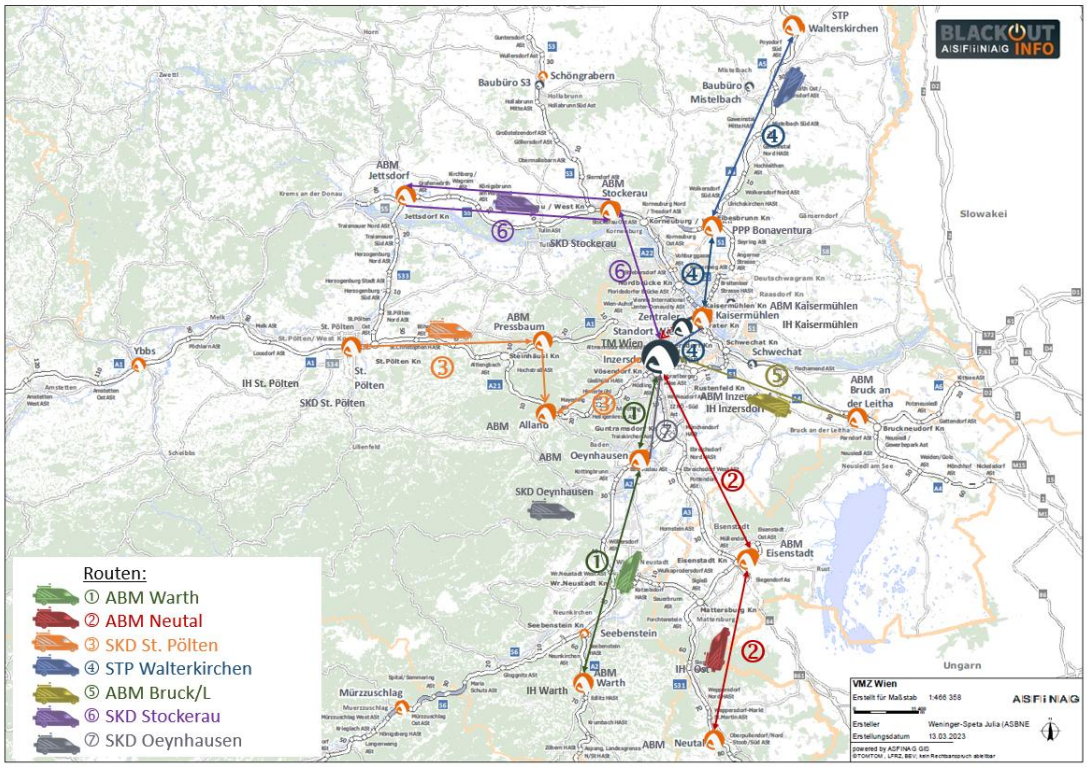


Figure 4: Example Region East of Austria

The transmission of daily reports follows a precisely coordinated schedule to ensure structured processing of possible measures. Without this clear timing, delays, bottlenecks, and coordination problems would occur within the crisis team.

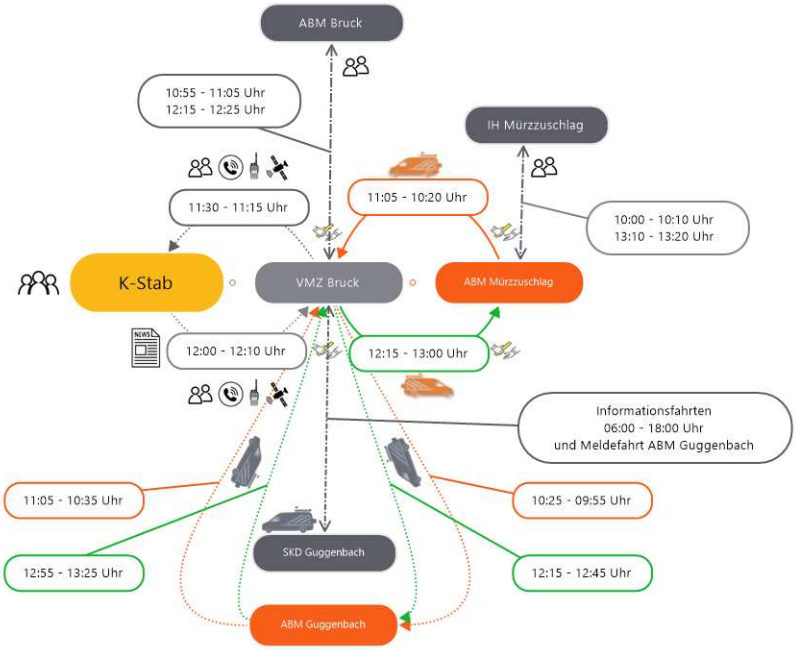


Figure 5: For example the Region around Bruck/Mur

The exact routes, handover times (start/end), handover locations (departure/arrival), handover method (in person/Vehicle Reporting System), and responsibilities (assigned to) are defined in specially adapted schedules for outbound and return trips for each location. All employees have been clearly instructed to strictly adhere to these times.

The Vehicle Reporting System system remains active until, after the restart, the crisis team announces the transition back to normal operations and the discontinuation of the reporting system.

2.5. Restart Planning System

The ASFINAG crisis team is responsible for the overall restart planning across ASFINAG and for the final termination of the blackout response. Once a secure power supply including communication is available, the ASFINAG crisis team will issue the clearance for restart to the Traffic Management Center (VMZ).

The VMZ must then independently resume its previously suspended activities step by step, reverse the immediate measures previously implemented in close cooperation with the technical maintenance team, and restore normal operations.

Special attention must be paid—across all systems (tunnels, variable message signs, rest areas, pumping stations, etc.)—to a controlled recommissioning process to avoid additional technical failures and damage to the facilities.

During recommissioning, priority must be given to critical route sections and those with high traffic volumes, tunnel systems with elevated risk levels, facilities in metropolitan areas (Vienna, Linz, Salzburg, Graz), and routes without diversion options (e.g., truck driving bans) before recommissioning rest areas, traffic control points, etc.

A prerequisite for starting the general recommissioning of outdoor facilities in tunnels and open areas is a stable control system, the ability for video surveillance, and communication

via radio and/or telephone with internal and external organizational units/emergency services. The crisis team will provide information on when these prerequisites are met.

In tunnel areas, the “Operational Conditions for Emergency Operation” will be lifted, and the facilities will, if necessary (e.g., system malfunctions; during spare part procurement, etc.), be operated based on the minimum operating conditions according to RVS 09.04.11 (Working Paper #32).

The transition of shift handover between the phases “Blackout” and “No Blackout” must be initiated by the responsible manager after recommissioning.

3. SUMMARY AND CONCLUSION

A blackout or large-scale power outage poses a major challenge for ASFINAG, as operations must be maintained in emergency mode for seven days. For this emergency operation, all necessary resources are provided to ensure operational capability. This includes the daily supply of food and drinks for key personnel and operational staff. Approximately 250 employees are required to maintain emergency operations.

The entire road network remains open for individual traffic. Tunnel facilities are operated in two groups: 24 high-priority tunnels are equipped with emergency generators to power safety-related systems. All other tunnels remain open, but only organizational measures apply. All tunnels operate with reduced speed limits.

A comprehensive communication system guarantees continuous information exchange between all relevant parties. This includes redundant channels and secure connections to ensure stable communication even during emergency operations.

SAFE TUNNELS FOR SMART VEHICLES: CHALLENGES AND OPPORTUNITIES OF AUTOMATED DRIVING IN ROAD TUNNELS

[1]Regina Schmidt, [1]Harald Kammerer, [2]Georg Mayer, [3]Markus Hofer, [3]Oliver Zendel

[1]ILF Consulting Engineers Austria GmbH, AT
[2]BUNG Ingenieure AG, DE
[3]AIT Austrian Institute of Technology GmbH, AT

DOI 10.3217/978-3-99161-087-8-004 (CC BY-SA 4.0)
https://creativecommons.org/licenses/by/4.0/deed.de
This CC license does not apply to third party material (attributed to other sources) and content noted otherwise.

ABSTRACT

The digitalization of traffic infrastructure is a key enabler for connected and automated driving. Automated vehicles will increasingly interact seamlessly with infrastructure, offering significant potential to reduce accidents and enhance both safety and road capacity. However, tunnels present unique challenges due to their specific safety requirements and the absence of Global Navigation Satellite System (GNSS) signals, which complicates accurate vehicle localization. Radio-based positioning systems also face issues such as multipath propagation caused by reflections in tunnel environments. Current solutions focus primarily on vehicle-based sensors, but these have limitations in tunnels. The research project AUDIT analyses localization by vehicle-based sensors as well as Cooperative Intelligent Transport Systems (C-ITS), which enable continuous bidirectional data exchange between vehicles and infrastructure. Safety impacts are assessed using systematic risk analysis methods, considering Society of Automotive Engineers (SAE) automation levels and mixed traffic scenarios. The project also discusses the effects on tunnel operations under both normal and emergency conditions from the operator's as well as tunnel user's perspective. Feasibility studies in Austrian and German tunnels will validate promising technologies for supporting automated driving in road tunnels. A dedicated test vehicle equipped with multiple sensors and communication modules collects comprehensive data to evaluate positioning accuracy and communication reliability. The findings will provide recommendations for sensor configurations, infrastructure adaptations, and operational protocols, including cost-benefit considerations. Ultimately, the project aims to provide actionable solutions for safe and efficient automated driving in tunnels, contributing to the development of unified standards and best practices for integrating automated vehicles into future transport systems.

Keywords: road tunnel, automated driving, C-ITS, tunnel safety, risk assessment, localization in tunnels

1. BACKGROUND AND MOTIVATION

The ongoing advancement of digitalizing traffic infrastructure is a crucial prerequisite for connected and automated driving. Automated vehicles will become an integral part of a system characterized by seamless interaction between vehicles and infrastructure. This development offers the potential to reduce accidents and significantly improve both traffic safety and road capacity [1].

Tunnels, due to their specific conditions, present a unique challenge that must be addressed from both the perspective of the vehicle and the infrastructure. Additionally, tunnels themselves have specific safety requirements due to additional risks in case of accidents or fires. Accurate positioning and localization of vehicles are crucial for automated driving. However, due to the lack of GNSS signal coverage in tunnels, this cannot be easily achieved. In Alpine regions as well as in big cities, the widespread presence of tunnels or urban canyons poses challenges for automated driving.

The research project "Artificial Intelligence for Improving the Safety of Tunnels and Tunnel Control Centers (KITT)" [2] has demonstrated that the collection of vehicle-generated data using C-ITS can improve preventive safety and the availability of road tunnels. However, this requires precise positioning and localization of vehicles within the tunnel. Current C-ITS modules utilize GNSS for this purpose. It was found that signal loss currently causes the On-Board Unit (OBU) installed in the vehicles to cease sending further C-ITS messages – even those for which the exact vehicle position is irrelevant. In order to fully utilize the advantages of C-ITS in road tunnels, further research is needed regarding the positioning and localization of vehicles within tunnel structures.

This paper describes the current findings and ongoing research within the project “Automated Driving in Road Tunnels (AUDIT)” with its main objective to identify the challenges related to automated driving in road tunnels, focusing on lessons learned from KITT, and to develop solution approaches. This involves evaluating the suitability and system limitations of localization and positioning systems currently used in vehicles, as well as communication technologies between vehicles and infrastructure. Infrastructure-related challenges and measures to support vehicle localization and communication in tunnels are also examined and assessed based on cost-benefit criteria.

This research is funded by the Austrian Research Promotion Agency (FFG) under the “DACH Transport Infrastructure Research Call 2024“ as part of a cross-border initiative for applied R&D services, supported by national public authorities in Austria and their representatives in Germany and Switzerland.

2. FUNDAMENTALS

2.1. Automated driving

Automated driving refers to the capability of a vehicle to operate and navigate without human input by using a combination of sensors, cameras, radar, Artificial Intelligence (AI), and Machine Learning (ML) algorithms. These systems allow the vehicle to perceive its environment, make decisions, and control driving functions such as steering, braking, and acceleration [3].

The degree of automation in a vehicle’s driving system can be described by the SAE Levels. They define six stages (Level 0 to 5), describing the transition from conventional driving to fully autonomous vehicles and regulating how driving tasks are distributed between human

and system. In Ref. [4] a seventh level, namely the L2+/++, is introduced. The six SAE-Levels named in [3] in combination with the intermediate level L2+/++ [4] are defined as follows:

- **Level 0 – no automation**: The human driver fully controls the vehicle and there are no automated driving functions, only warning systems may be present.
- **Level 1 – assisted driving**: Individual assistance systems such as cruise control or lane keeping assistant support the driver in specific tasks (longitudinal **or** lateral control). Full responsibility remains with the driver.
- **Level 2 – partial automation**: The vehicle takes over both longitudinal **and** lateral control under certain conditions (e.g., traffic jam assistant). The driver must monitor the system and be able to intervene at any time.
- **Level 2+/++ – advanced partial automation:** Navigation on autopilot. The driver must be able to immediately take full control whenever requested.
- **Level 3 – high automation**: The driver can temporarily hand over the driving task to the system and engage in other activities, as long as the vehicle operates within domain limits. The system independently recognizes its domain and prompts the driver to take over in good time.
- **Level 4 – full automation**: The vehicle drives completely autonomously in certain operational areas (e.g., highway, parking garage). The human becomes a passenger and does not need to intervene. If the system leaves its domain, it brings the vehicle to a safe state.
- **Level 5 – autonomous driving**: The vehicle takes over all driving tasks under all conditions, even in complex situations. There is no longer a driver, only passengers. Responsibility lies entirely with the system or manufacturer.

Automated vehicles can significantly increase traffic safety and efficiency. They reduce accidents, optimize traffic flow, and enable precise management of emergency situations. However, as the degree of automation increases, so do the requirements for sensors, communication, and positioning [1].

2.2. Vehicle-based sensor systems

Modern vehicles incorporate a diverse array of sensors designed to enhance driver assistance, safety and comfort. The following section examines the specific roles these in-vehicle sensors play in automated driving, with particular attention to their limitations within tunnel environments, [5].

Cameras are used to detect and classify objects, estimate distances, and recognize traffic lights, lane markings, and obstacles. However, their effectiveness is significantly reduced in adverse weather conditions such as rain or fog. In tunnels, varying light conditions as well as reflections from tunnel walls further impair camera performance, disqualifying their exclusive usage for vehicle localization in these environments.

The functionality of **Light Detection and Ranging-Systems** (**LiDAR-Systems)**, however, is more sophisticated in changing light conditions in tunnel environments due to the usage of laser beams to construct high-definition 3D maps of their surroundings. Yet, this systems are more expensive than cameras and have limited functionality in bad weather conditions such as rain or snowfall, [6].

Installed **Radar-Systems** are using long range radio waves for tracking objects and for measuring both their distance and velocity relative to its position. This system is independent of weather as well as light conditions. Radar information is used in technologies such as automatic cruise control, automatic emergency breaking or blind spot monitoring. However,

due to its large wavelength, the resolution is low and often contains noise leading to high uncertainties.

GNSS technology is a cornerstone for vehicle localization in the open, offering centimeter-level precision when enhanced with methods like real-time kinematics. However, in environments such as urban canyons and tunnels, GNSS signals are often obstructed or lost, resulting in unreliable positioning. When GNSS connectivity is interrupted, C-ITS messages are automatically deactivated, preventing C2X communication [7].

Inertial measurement units (IMUs), which include accelerometers and gyroscopes, track linear acceleration and rotational movements. Despite their high precision, IMUs accumulate small errors over time, making additional navigation systems necessary for accurate localization. Integrating GNSS data and employing AI-based error correction – through sensor fusion – significantly improves localization accuracy in road tunnels and urban canyons.

2.3. Connected driving

Apart from the above-mentioned vehicle-based sensor systems and the specification of their requirements and application possibilities, this project aims to additionally place a strong emphasis on C-ITS technology. The key to ensure safety, efficiency and environmental sustainability in the modern transport sector is communication – the communication among vehicles and the communication between vehicles and infrastructure. C-ITS is an initiative in this regard and enables communication in real time.

In vehicle-to-everything (V2X) and cellular-V2X (C-V2X) communication, access technologies such as ITS-G5, Long Term Evolution (LTE-V2X) and 5G new radio (5G NR-V2X) within the 5.9 GHz frequency band are used. In KITT [2] it was determined, that in road tunnels the infrastructure transmitters, the so-called Roadside Units (RSUs), must be installed approximately every 300 m to enable continuous monitoring.

RSUs in tunnels communicate event-based information, for example a breakdown, in real-time via Decentralized Environmental Notification Messages (DENM) while information about vehicle status or its exact position is continuously transmitted via Common Awareness Messages (CAM). All this information can be used to reduce accidents, optimize traffic flow, and enable precise management of emergency situations. However, one of the major findings of KITT was that, due to the absence of GNSS signals, currently installed C-ITS systems cease all functions and no massages are send or received. For this reason, C-ITS can currently not be used in tunnels. Either the infrastructure must provide a GNSS signal coverage or vehicle-side OBU systems have to be adapted.

2.4. Infrastructural localization systems

Ref. [8] identified ideal routes in the Swiss road network for future, initial test applications under real-world traffic conditions. The report highlighted the need to modernize tunnels to support automated vehicles, specifically mentioning optimizations in lighting conditions, accident detection systems, communication infrastructure, and road markings.

However, most tunnels are already equipped with modern **lighting systems** and well-maintained **road markings**. Installing **guidance systems** could further assist autonomous vehicle navigation in tunnels, provided that the markers remain clean and properly maintained for consistent operation. While tunnels are regularly cleaned and refurbished, the absence of vehicle-based standardizations leads to the situation that there are currently no established uniform requirements for optimal lighting conditions, the ideal condition of road markings or special uniform guidance systems necessary for automated driving. In the absence of

standardized guidelines or regulatory frameworks, it is reasonable to anticipate that no further installations or modifications will be made to the existing tunnel equipment.

The KITT research project found that missing GNSS signal currently is the main issue for stopping C-ITS communication. When the GNSS signal is lost, the OBU neither transmits nor receives information. Additionally, the GNSS signal cannot be used for localization purposes inside tunnel structures. The following section discusses several infrastructure-based technologies that are proposed to address the challenge of localization. The main emphasis lies on technologies that require minimal or no modifications to existing and currently installed vehicle equipment.

A cost-effective alternative to GNSS signals are **Bluetooth beacons** installed in tunnel structures [9], [10]. On vehicle side, a special Bluetooth receiving unit is needed. In measuring the received signal strength, the difference in signal time of arrival and its frequency as well as the angle of arrival, precise localization data can be determined. However, the beacons need to be positioned in optimal distances throughout the tunnel. Under ideal conditions, localization precision of 0.5 m to 1 m can be reached. However, due to signal reflection and signal interferences, precise localization may be impaired. Varying temperatures and humidity may additionally alter the correct functioning as well as shorten the lifespan of Bluetooth beacons.

For enhanced precision ranging from approximately 0.1 m to 0.3 m, **Ultra Wideband (UWB) beacons** [11]**,** [12] may be installed at intervals of less than 50 m within the tunnel, given their signal range of up to 50 m. The high accuracy of UWB systems stems from their ability to update positions nearly ten times per second and to utilize higher frequencies as well as greater bandwidths, thereby reducing susceptibility to interference from other communication systems. Nonetheless, UWBs are more expensive than Bluetooth beacons and have limited data transmission rates, restricting their capacity for large data transfers.

Other possible installations on infrastructure side are **GNSS repeaters** [13]. These are currently used in indoor environments where GNSS signals are otherwise unavailable. In order to facilitate this, an external antenna is positioned outside the structure to receive GNSS signals, which are then transmitted via coaxial cable to repeaters installed inside. However, for vehicle localization inside road tunnels, standard repeaters are insufficient: vehicle receivers may incorrectly interpret the location of the installed repeater inside the tunnel as that of the external antenna, thereby compromising position accuracy. Intelligent repeater systems attempt to resolve this issue by generating artificial GNSS signals that mimic real ones. By installing multiple GNSS repeaters throughout a tunnel, continuous GNSS signal coverage can be maintained. Nonetheless, localization accuracy remains lower than in open environments, and both installation and maintenance are costly and require frequent calibration to ensure reliable operation.

Nevertheless, the installation of intelligent GNSS repeater systems would offer two main benefits: enabling localization via GNSS signals and allowing current OBU to exchange information, which makes CIT-S communication feasible.

3. STAKEHOLDER EXPECTATIONS

In the beginning of the project, stakeholder interviews have been conducted and they revealed varying levels of awareness regarding the technical and organizational challenges associated with vehicle localization and communication in tunnel environments. Many stakeholders recognize the difficulties, and some are actively considering potential solutions. Automotive manufacturers generally consider the development of vehicle-side technology for C-ITS largely complete, noting that the next steps must come from the infrastructure side. However, opinions among infrastructure stakeholders are more heterogeneous. While there is consensus that both RSUs and OBUs are essential to enable C2X communication, it is widely acknowledged that GNSS-based OBUs do not function in tunnel environments due to the loss of satellite signal. Although the hardware costs for RSU installation in tunnel structures are considered manageable, stakeholders also point out that a comprehensive rollout is unlikely, given the significant effort required to process and manage the resulting amount of data.

Of particular interest during these discussions was the issue of responsibility. Regarding automated driving in tunnels, stakeholders agree that the responsibility for automated operations should not rest solely with tunnel operators. The anticipated benefits of automated driving include increased safety standards, improved efficiency, and greater system resilience. There is widespread agreement that responsibilities and costs must be clearly allocated: typically, tunnel and infrastructure operators are expected to finance tunnel equipment, while vehicle manufacturers are responsible for outfitting the vehicles. However, binding regulations are needed.

When questioned about operational changes, stakeholders generally see no need for dedicated lanes or tunnel tubes specially for automated vehicles. They stress that safe operation of automated vehicles in tunnels requires precise localization, uninterrupted communication, and robust data security. In order to meet this high safety standards, redundancy across different systems is considered essential. However, there is currently little initiative from the infrastructure side to address communication deficiencies, as there is a lack of standardized regulations and certifications with verifiable performance. Explicit guidelines on interface definitions are lacking, and binding regulations have not been established.

These issues must be resolved to ensure the successful and safe integration of automated and connected vehicle technologies in tunnel infrastructures.

4. OPPORTUNITIES FOR TUNNEL USERS AND OPERATORS

The AUDIT research project offers substantial and multifaceted benefits for a wide range of stakeholders, including tunnel operators, infrastructure owners, vehicle manufacturers, emergency services, and society at large. By enabling automated and connected driving in road tunnels, the project aims to fundamentally **improve traffic quality**. Automated vehicles, supported by advanced C-ITS, can travel with reduced gaps and more consistent speeds, which not only increases the overall capacity of existing road infrastructure but also helps to minimize congestion and bottlenecks. The integration of real-time data exchange between vehicles and infrastructure allows for more dynamic and effective traffic management, resulting in smoother traffic flow, shorter travel times, and a more reliable transportation system.

Furthermore, enhanced reliability and fewer disruptions also **increase the availability and resilience of tunnels**, which is crucial for maintaining the performance of the entire road network, especially on heavily trafficked routes with limited alternatives. For operators, this

means fewer interruptions and potential losses in toll revenue, supporting the financial sustainability of infrastructure management.

In addition, optimized traffic flow not only **reduces travel times** but also **lowers emissions and noise pollution**, contributing to environmental sustainability. The inclusive nature of the technologies developed within AUDIT ensure that people with limited driving abilities can safely navigate through tunnels, supporting broader access to mobility. Overall, the project advances sustainable transportation solutions by integrating cutting-edge vehicle technologies, improving safety, efficiency, and accessibility for all road users.

However, the main focus will be on the impact on **tunnel safety**. Tunnels are critical infrastructure elements with high safety requirements, and human error remains a leading cause of accidents in these environments. Automated vehicles can significantly reduce the risk of accidents by minimizing mistakes related to distraction, excessive speed, or insufficient distance between vehicles, [14]. The project leverages C-ITS to provide additional layers of safety, such as enhanced monitoring, early warnings about hazardous situations like accidents, construction zones, or traffic jams, and precise information for emergency responders. This not only protects tunnel users but also supports rescue operations by delivering accurate details about incident locations and the people or vehicles involved, especially in complex scenarios like tunnel fires.

The safety impacts will be assessed using **systematic risk assessment methods**, considering how automated driving – across SAE Levels 0 to 4 – affects safety in road tunnels. A set of relevant incident scenarios such as breakdowns, collisions, fires or wrong-way drivers, are analysed with both current and future fleet compositions with varying shares of automated vehicles. Safety goals – including traffic safety, but also flow optimization, energy efficiency, emission reduction, cost savings, mobility and inclusion, as well as user comfort – are systematically linked to scenarios and measures. Real-time data streams from connected vehicles are incorporated to enhance risk analysis and support dynamic adaptation of tunnel operations and emergency procedures. The analysis is conducted from both user and operator perspectives – in regular and emergency situations.

5. FEASIBILITY STUDY

At the end of the project feasibility studies will be conducted in real tunnel structures with the objective to perform an experimental validation and evaluation of sensor and localization technologies for automated driving in road tunnels. The aim is to establish the practical feasibility of reliable vehicle positioning and communication under real-world conditions. Representative test tunnels were selected: the Rosenstein tunnel (Stuttgart) in Germany and the Alpine Semmering and Steinhaus tunnels in Austria. A dedicated test vehicle (see Figure 1) is equipped with a diverse array of different sensor types and but also varying sensor quality. This includes multiple LiDAR units, high-resolution cameras, radar, GNSS, IMUs, and C-ITS communication modules.



Figure 1: Test vehicle equipped with various sensors [5]

Measurement runs will be conducted in both directions through the tunnels by forming a closed loop. Particular attention will be focused to the loss of GNSS signals upon tunnel entry and the subsequent performance of alternative localization methods such as LiDAR-IMU fusion and trajectory estimation based on Simultaneous Localization and Mapping (SLAM). The collected data will be rigorously analyzed, including comparisons with ground truth reference models obtained from high-precision laser scans, to quantify positioning accuracy, drift, and the effectiveness of loop closure techniques.

Furthermore, C-ITS measurements will be evaluated for signal quality and reliability, with additional tests planned to investigate V2X-Locate [15] capabilities and the integration of vehicle specific Controlled Area Network / On Board Diagnostic bus data (CAN/OBD2) for enhanced vehicle state awareness. The work plan also encompasses the assessment of sensor artifacts, infrastructure influences, and the operational robustness of communication systems, with iterative refinement based on feedback from consortium partners and technology providers.

The ultimate goal is to derive actionable recommendations for sensor configurations, infrastructure adaptations, and operational protocols that support safe and efficient automated driving in tunnel environments. This includes the development of digital twin models for scenario simulation, the calibration of risk and performance metrics, and the documentation of findings for both scientific dissemination and practical implementation.

6. SUMMARY AND CONCLUSION

Tunnels are central structures in the European road network. They are subject to strict safety requirements, which have been further tightened following major fire incidents. Their importance is growing as the expansion of above-ground transport routes increasingly face resistance. The future transport system will be shaped by connected, intelligent, and automated vehicles that enable cooperative mobility through interaction with infrastructure. Highly automated vehicles (SAE Level 4 and 5) can communicate directly with the traffic management to optimize traffic flow and increase route capacity.

KITT was the first project to investigate how sensor-based and C-ITS-based data can be used for real-time assessment of safety related events in tunnels. Soon it became clear that tunnels interrupt continuous GNSS signal coverage. The lack of precise positioning leads to pausing

of communication modules in C-ITS-enabled vehicles, resulting in no further messages being sent. The challenges of positioning and communication in tunnels have so far been scarcely examined and require further innovative approaches.

The AUDIT project represents a pioneering effort in advancing automated and connected driving within road tunnels, a domain that poses distinct technical and safety challenges. AUDIT places strong emphasis on the functionality of vehicle-based sensors in tunnel structures as well as on C-ITS, which facilitates real-time data exchange between vehicles and infrastructure. AUDIT also explores advanced wireless positioning techniques to overcome the limitations of GNSS signals in tunnels, taking into account the complex radio channel characteristics caused by reflections and signal fading. While simulated GNSS systems are available, their impact on C-ITS communication in tunnels remains largely untested in the DACH region.

Looking into the future, the insights and technologies generated by AUDIT will play a crucial role in enhancing safety and operational efficiency in tunnels and other critical infrastructure. The project's outcomes are expected to pave the way for more resilient, intelligent, and sustainable mobility solutions, fostering the development of unified standards and best practices for automated driving in complex environments. As automated and connected vehicles become increasingly prevalent, the work initiated by AUDIT will help ensure that tunnels are not only safe but also fully integrated into the future of intelligent transportation systems.

7. REFERENCES

[1] European Commission, „On the road to automated mobility: An EU strategy for mobility of the future," 2018.

[2] DE-Bundesministerium für Bildung und Forschung (BMBF), „Künstliche Intelligenz zur Verbesserung der Sicherheit von Tunneln und Tunnelleitzentralen (KITT)," 2021.

[3] SAE International, „J3016; Taxonomy and Definitions for Terms Related to Driving Automation Systems for On-Road Motor Vehicles," 2018.

[4] World Economic Forum, „Austonomous Vehicles: Timeline and Roadmap Ahead," White Paper, 2025.

[5] AIT, Bung, ILF, „Automtisiertes Fahren im Straßentunnel AUDIT - vorläufiger Ergebnisbericht," 2025.

[6] Zendel, O., Huemer, J., Murschitz, M., Dominguez, G. F., & Lobe, A., „Joint Camera and LiDAR Risk Analysis," Proceedings of the IEEE/CVF Conference on Computer Vision and Pattern Recognition (pp. 88-97), 2023.

[7] European Telecommunications Standards Institute (ETSI), „ETSI EN 302 890-2: Intelligent Transport Systems (ITS), Facilities Layer function; Part 2: Position and Time management (PoTi)," 2020. [Online]. Available: https://www.etsi.org/deliver/etsi_en/302800_302899/30289002/02.01.01_20/en_30289002v020101a.pdf.

[8] van Linn, A.; Schneider, R.; Kouvelas, A.; Makridis, M.; Genser, A., „Automatisiertens Fahren im Strassentunnel - Chancen, Risiken und ideale Strecken," 2023.

[9] Brož, J., Tichý, T., Prokeš, R., Štencek, A., & Šmerda, T. , „Proximity approach to bluetooth low energy-based localization in tunnels," Sustainability, 15(4), 3659. , 2023.

[10] J. Broz and T. Tichy, „Road Tunnel Positioning: Enabling Location-Based Services in GNSS-Denied Environments," IEEE Access, vol. 12, pp. 156694-156701, 2024.

[11] Konsyse, „UWB: Pros and Cons of Ultra-Wideband Technology," 2025. [Online]. Available: https://www.konsyse.com/articles/uwb-pros-and-cons-of-ultra-wideband-technology/.

[12] X. Liu, Q. Liu, Y. Chen. K. Ren and D. Zhu, „Tunnel localization for construction workers based on UWB and IMU," 2025.

[13] W. Fink, „ AUCON - GPS Systems for signal Distribution," [Online].

Available:https://www.gps-repeater.com/wp-content/uploads/2018/05/gnss_retransmission_system_2012.pdf.

[14] Wang, L., Zhong, H., Ma, W., Abdel-Aty, M., & Park, J. , „How many crashes can connected vehicle and automated vehicle technologies prevent: A meta-analysis," Accident Analysis & Prevention, 136, 105299, 2020.

[15] Cohda Wireless, „Cohda Wireless V2X-LocateE vs GNSS in undercover Car-park," 2025. [Online]. Available: https://cohdawireless.com/v2x-locate/.

CONFORMITY BIAS INFLUENCE ON WALKING SPEED IN A SMOKE-FILLED TUNNEL EXPERIMENT

[1]Miho Seike, [2]Wenhao Li, [3]Takao Futagami

[1]*University of Tsukuba, JP*
[2]*Liaodong University, CN*
[3]*Shinshu University, JP*

DOI 10.3217/978-3-99161-087-8-005 (CC BY-SA 4.0)
https://creativecommons.org/licenses/by/4.0/deed.de
This CC license does not apply to third party material (attributed to other sources) and content noted otherwise.

ABSTRACT

The influence of information from people—referred to as conformity bias in this study—during an actual evacuation owing to a tunnel fire has not been clarified, despite the high number of people present in the same area during such an event. Therefore, in this study, we conducted an experiment focusing on the peoples' behavior upon seeing another evacuee moving in the wrong direction.

The test was conducted using a full-scale road tunnel (50 m in length and 6 m in width) in the Fukushima robot test field. We simulated a darkened environment caused by smoke. The smoke was a mixture of water and glycol, ensuring it was non-irritant and non-toxic. Many tunnels in Asia, including Japan, have not installed a guide light function other than the guide board. Obstacles were set-up in the form of a small truck and van. The participants were not informed that a person moving in the wrong direction (staff member) would pass them along the way. Walking speed was calculated based on the speed before the participant encountered the staff member and after the encounter. The participants were made up of 20 men (average age of 42.6 years). The speeds of 12 participants (60%) decreased after the staff member had passed them.

Keywords: Tunnel, smoke, human behaviour, risk analysis, fire.

1. INTRODUCTION

During actual evacuations due to tunnel fires, a significant number of individuals are often present in the same vicinity. The presence of others can provide reassurance to evacuees, which can have both positive and negative implications for the efficiency of the evacuation process. Helbing et al. [1] identified nine characteristics of escape panic, one of which is the tendency for individuals to exhibit group behavior, meaning they often mimic the actions of others. This behavior is considered a response to unexpected dangerous events. Nilsson et al. [2] and Abe [3] reported that observing fellow evacuees can induce conformity behavior, characterized by fleeing simply because others are doing so. Synchronicity, as defined by Jung [4], refers to a causal coincidence that holds significant meaning for the individual experiencing it. Hanson and Klimo [5] posited that synchronicity is a goal-oriented phenomenon that occurs independently of an individual's conscious control, emphasizing the recognition of personal experiences and meaningful coincidences. Planer [6] asserted that synchronicity is unpredictable and cannot be the result of intention, underscoring the profound connection between an individual's mind and external events.

Classical conformity is a form of social influence wherein an individual modifies their behavior or attitudes in response to the actions, attitudes, or expectations of others, including adherence to perceived group norms. The seminal studies on classical conformity by Muzafer Sherif and Solomon Asch illustrate the significant impact of social pressure. Conformity can exert both beneficial and detrimental effects on leadership. Specifically, within leadership contexts, conformity can facilitate decision-making and enhance group cohesion, yet the pressure to conform may also lead to distorted thinking. In an experiment concerning tunnel fires, Nilsson et al. [2] discovered through full-scale evacuation experiments that individuals tend to evacuate upon observing others doing so, and that the actions of individuals influence the behavior of others. However, a pertinent question arises: if individuals observe someone acting contrary to what they believe is correct, how will they respond? The influence of information conveyed by individuals—termed conformity bias in this study—remains unclear. Consequently, this study conducted an experiment focusing on the behavior of individuals after observing another evacuee moving in the wrong direction.

2. EXPERIMENTAL SET-UP

In this study, experiments were conducted at the Fukushima robot test field (Figure 1). The tunnel dimensions were 50 m in length, 6 m in width, and 6 m in height. Consistent with previous studies [7–12], we utilized artificial smoke that was non-irritating and non-toxic, generated from a mixture of water and glycol. Ten smoke generators (PORTA SMOKE PS-2005; Dainichi, Japan) were strategically placed within the tunnel at intervals of 15 m, with a fan positioned in front of each generator to facilitate smoke diffusion. The diffusion state was visually inspected, and smoke density measurements were verified by the experimental staff prior to each experiment. The extinction coefficient (smoke density (Cs)) was quantified using four laser sensors (LV-NH100; Keyence, Japan), as outlined in previous studies [7–12]. Smoke density measurements were recorded at coordinates (x, y) = (10.5, −3.8), (26.8, 3.8), (35.5, 3.8), and (45.6, 3.8) at a height of 1.5 m (refer to Figure 2). The target Cs value was 1.0 m^{-1}.



Figure 1: Experiment conducted in a full-scale tunnel

The study comprised 20 male participants, ranging in age from 23 to 64 years, with a mean age of 42.6 years. Participants were instructed to don a safety vest, mask, helmet, and a wearable camera (Panasonic HX-A100). Additionally, each participant was provided with an Apple iPod (series 6) equipped with a flashlight function to simulate the illumination of a smartphone. Informed consent for participation in the study was obtained through a paper-based form, which received approval from the Ethics Committee (Ethical Committee for Epidemiology of Hiroshima University, E2021-2457).

3. SCENARIO AND HYPOTEHSYS SETTING

In this study, we deliberately introduced individuals moving in the opposite direction to that which evacuees perceived as correct, with the aim of creating uncertainty in directional information and examining the consequent changes in speed. This experiment involved participants who had no prior experience of evacuating in complete darkness filled with smoke, as would occur in a tunnel fire. It was hypothesized that encountering individuals moving in what was perceived as the "wrong" direction in an unfamiliar environment would induce psychological disturbance.

Figure 2 illustrates the experimental procedure. Initially, subjects moved from the starting point to the goal. They were instructed to reach the goal, press a button, and then return to the starting point, without being informed that staff members would be passing by along the route. The dotted lines represent the walking path of the staff members. The staff, attired identically to the evacuees, commenced walking just before the evacuee reached the van, moving at approximately 1.3 m/s, and consistently passed alongside the evacuee at a distance of about 1.0–1.5 meters. In instances where evacuees evacuated while touching the van, the staff passed by next to them. In this paper, observing individuals moving in the opposite direction is defined as the conformity bias, and the effect of this was investigated. Based on these scenarios, the following hypothesis was established: Hypothesis: Individuals moving in the opposite direction increase the uncertainty of directional information.

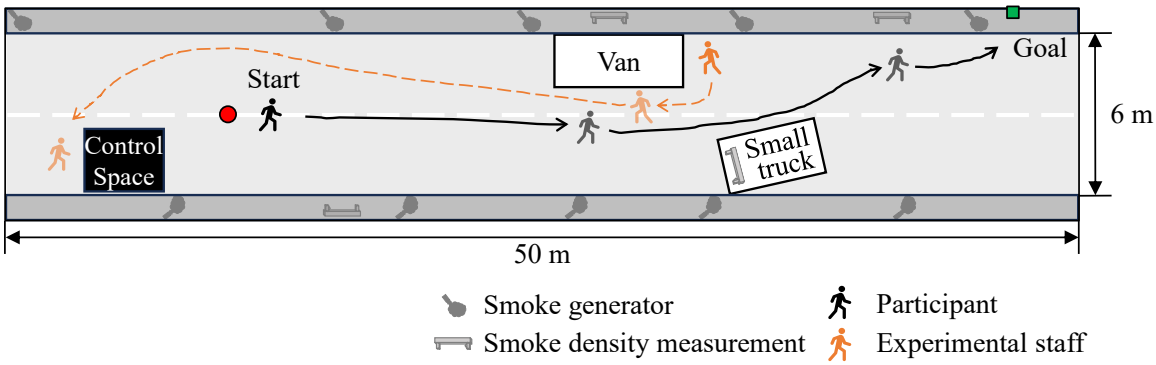


Figure 2: Experimental set-up and participant route
(vertical axis denotes width and horizontal axis denotes tunnel length)

4. RESULTS

Figure 3 illustrates the average walking speeds recorded before and after participants encountered the staff member, revealing a reduction of approximately 0.1 m/s. A summary of these walking speed results is presented in Table 1. T-tests conducted for each group indicated a statistically significant difference in walking speeds before and after the encounter at the 5% significance level. Figure 4 presents a scatter plot of walking speeds before and after the encounter with the staff member. The black dashed line represents a gradient of 1, serving to confirm any increase or decrease in speed, while the red solid and dashed lines denote the regression line and the 95% confidence intervals (2.5% and 97.5%), respectively. Data points situated above this line signify an increase in speed. Of the 20 participants, eight exhibited an increase in speed, whereas the remaining 12 demonstrated a decrease. Participants were categorized into 'speed increase' and 'speed decrease' groups, and significant differences were assessed before and after the encounter using t-tests. The initial speed of the 'speed decrease'

group was the highest at 0.82 m/s, which decreased by 0.22 m/s to 0.60 m/s after the encounter. This speed was also greater than that of the 'speed increase' group. The 'speed increase' group initially reduced their speed to 0.40 m/s, followed by an increase of 0.08 m/s. Although a significant difference between the 'speed increase' and 'speed decrease' groups was observed at the 0.1% level prior to the encounter, no significant difference was detected post-encounter. Furthermore, within both the 'speed increase' and 'speed decrease' groups, significant differences in speed before and after the encounter were observed at the 5% and 0.1% levels, respectively.

Figure 5 and Table 2 illustrate the heart rate (HR) measurements recorded before and after the interaction with the staff member. The mean HR exhibited a reduction of approximately 0.7 bpm; however, no statistically significant difference was detected between the pre- and post-encounter HR values. Additionally, Figure 6 depicts the relationship between HR and speed ratios before and after the encounter. It is noteworthy that, when comparing the current HR findings with the exercise-induced HR formula at a walking speed of 1.33 m/s as provided by Bassey et al. [13]—which is calculated based on an individual's height and weight—16 out of the 20 participants in this study demonstrated a higher HR than those reported by Bassey et al. [13]. Consequently, the observed HR changes in participants are unlikely to be attributed to physical exertion and are more plausibly linked to psychological factors. Pearson correlation analysis yielded a correlation coefficient of 0.52 (p-value = 0.019), signifying a significant result at the 5% significance level. Furthermore, an increase in speed was observed concomitant with an increase in the HR ratio.

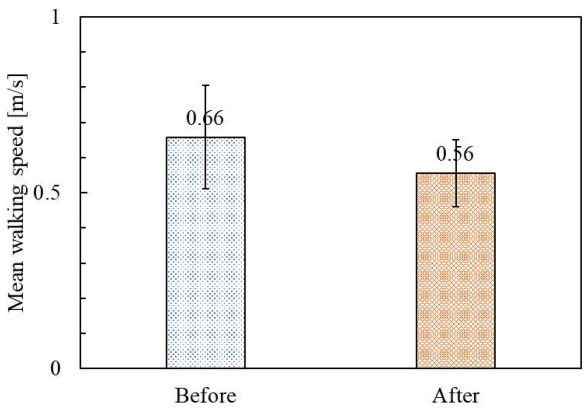


Figure 3: Mean walking speed (before and after)

Table 1: Walking speed (before and after)

	Before	After
Mean	0.66	0.56
Min	0.23	0.32
Max	1.59	1.27
Standard deviation	0.31	0.20
95%CI	0.15	0.10
p-value	0.017	
t-value (a two-tailed)	2.093	

5. DISCUSSION

The findings align with the hypothesized influence of social conformity-related processes on walking behavior in contexts of directional ambiguity. Contrary to inducing uniform behavioral alignment, the presence of counter-directional walkers prompted varied motor responses. Notably, 60% of participants exhibited a statistically significant reduction in walking speed. A significant correlation between speed ratio and HR ratio was also identified, indicating a link between motor adjustment and physiological arousal. Crucially, the observed

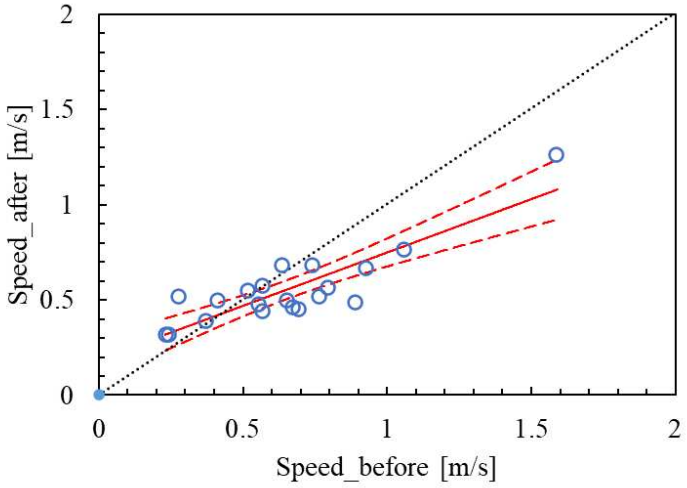


Figure 4: Scatter plot of walking speed (before and after)
Pearson correlation 0.87 ($p = 8.34 \times 10^{-7}$)

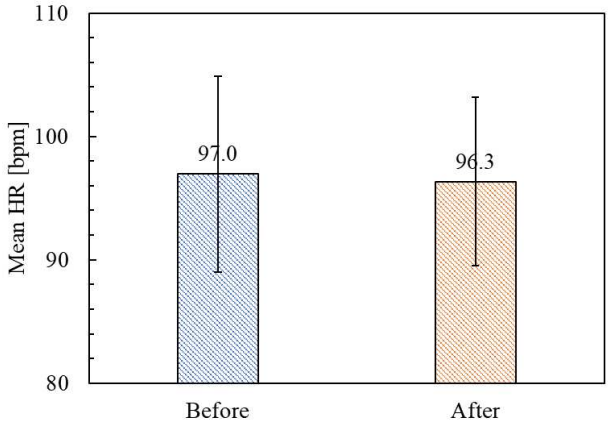


Figure 5: Mean heart rate (HR; before and after)

Table 2: HR (before and after)

	Before	After
Mean	97.0	96.3
Min	49.8	58.0
Max	128.3	119.2
Standard deviation	17.0	14.6
95%CI	7.94	6.84
p-value	0.621	

decrease in walking speed does not signify complete behavioral conformity, such as directional reversal, but rather reflects cautious modulation in response to socially induced directional ambiguity. The bidirectional pattern of speed change suggests that while directional ambiguity heightened arousal, it did not result in uniform behavioral outcomes. This divergence can be interpreted through Gray's Reinforcement Sensitivity Theory, which

suggests that individuals vary in their engagement of inhibitory and activation systems [14] when faced with ambiguity or conflict. In such scenarios, stronger inhibitory engagement may lead to cautious deceleration, whereas activation-oriented tendencies may promote urgency-driven acceleration. Nonetheless, these interpretations should be regarded as preliminary, given that dispositional sensitivity systems were not directly assessed and the sample was limited to 20 male participants. Future research incorporating personality measures and more diverse samples is essential to elucidate the mechanisms underlying these heterogeneous responses.

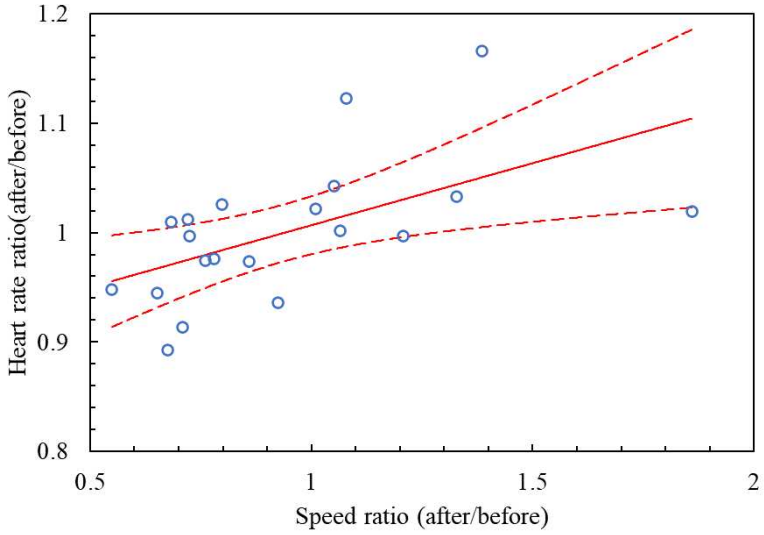


Figure 6: Relationship between the speed ratio and HR ratio
Pearson correlation 0.52 (p = 0.019)

6. REFERENCES

[1] Helbing, D., Farkas, I., Vicsek, T., 2000. Simulating dynamical features of escape panic. Nature, 407(6803), 487–490.

[2] Nilsson, D., Johansson, M., Frantzich, H., 2009. Evacuation experiment in a road tunnel: A study of human behaviour and technical installations. Fire Safety Journal, 44(4), 458–468.

[3] Abe, K., 1982. Fire and evacuation in a huge building. Accident Prevention Journal, 130, 21–27 (in Japanese).

[4] Jung, C. G., 1969. The psychology of the transference. Princeton University Press.

[5] Hanson, D., Klimo, J., 1998. Toward a phenomenology of synchronicity. In Phenomenological inquiry in psychology: Existential and transpersonal dimensions (pp. 281–307). Boston, MA: Springer US.

[6] Planer, R. J., 2023. Cooperative breeding and the evolutionary origins of shared intentionality. Philosophy, Theory, and Practice in Biology. 15(0).

[7] Seike, M., Kawabata, N., Hasegawa, M., 2016. Experiments of evacuation speed in smoke-filled tunnel. Tunnelling and Underground Space Technology, 53, 61–67.

[8] Seike, M., Kawabata, N., Hasegawa, M., 2017. Evacuation speed in full-scale darkened tunnel filled with smoke. Fire Safety Journal, 91, 901–907.

[9] Seike, M., Lu, Y. C., Kawabata, N., Hasegawa, M., 2021. Emergency evacuation speed distributions in smoke-filled tunnels. Tunnelling and Underground Space Technology, 112, 103934.

[10] Seike, M., Kawabata, N., Hasegawa, M., 2023. Walking speed under emergency situation in smoke-filled tunnel with obstacles. Tunnelling and Underground Space Technology, 133, 104939.

[11] Li, W., Seike, M., Fujiwara, A., Chikaraishi, M., 2024. Structural equation modeling of negative emotion and walking behavior by smoke-filled model-scale tunnel experiments. Safety Science, 171, 106394.

[12] Li, W., Seike, M., Fujiwara, A., Chikaraishi, M., 2024. Negative emotion degree in smoke filled tunnel evacuation. Tunnelling and Underground Space Technology, 153, 106010.

[13] Bassey, E. J., Macdonald, I. A., Patrick, J. M., 1982. Factors affecting the heart rate during self-paced walking. European Journal of Applied Physiology and Occupational Physiology, 48(1), 105–115.

[14] Gray, J., A., 1970. The psychophysiological basis of introversion-extraversion, Behaviour Research and Therapy, 8(3)., 249-266.

IMPACT OF GROUP EFFECTS ON THE REACTION AND ESCAPE BEHAVIOUR OF USERS IN ROAD TUNNELS - RESULTS OF REALISTIC LARGE GROUP EXPERIMENTS

[1]Frank Leismann, [1]Christian Thienert, [2]Markus Jenki, [3]Robert Wenighofer, [4]Anne Lehan, [2]David Stühler, [2]David Czudnochowski, [4]Stefan Kaufmann, [3]Robert Galler

[1]STUVA e.V., DE
[2]CSS – Centre for Security and Society, DE
[3]Technical University of Leoben, AT
[4]BASt, Federal Highway and Transport Research Institute, DE

DOI 10.3217/978-3-99161-087-8-006 (CC BY-SA 4.0)
https://creativecommons.org/licenses/by/4.0/deed.de
This CC license does not apply to third party material (attributed to other sources) and content noted otherwise.

ABSTRACT

The German Federal Highway and Transport Research Institute (BASt) initiated a research project that systematically investigated the influence of group effects on escape behaviour during self-rescue in road tunnels. As previous studies had shown that collective decision-making can delay the self-rescue process compared to a "single-person decision", large-group tests were conducted.

The study took place in a highly realistic road tunnel environment at the "Zentrum am Berg (ZaB)" in Austria involving a total of 5 large group tests (73 test persons and 47 vehicles), as well as 7 individual reference tests of single drivers. The scenario considered was a vehicle collision leading to a lorry fire in a bi-directional traffic setting, which was realistically simulated by using gas burners and smoke. Participants drove into the tunnel in their own cars without any prior knowledge of what to expect. Their perceptions, decisions and behaviour upon first recognising the accident site, approaching it, getting out of the vehicle, finding their way in the tunnel and escaping were documented in detail via "on-scene" interviews in the tunnel, follow-up interviews and video recordings. The tests were analysed from a sociological perspective in order to determine types of behaviour and critical situations. Further analysis from an engineering perspective was executed in order to obtain relevant parameters such as reaction and escape times.

The paper points out the most significant results from the large group tests focusing on quantitative parameters such as reaction times and evacuation speed. The numbers found are higher than the reference values for the single-person test. However, these results remain within the range of the values commonly used in risk analyses, meaning no specific adjustments to the current regulations are required. In addition, selected results from the behavioural analyses are presented briefly.

Keywords: Road-Tunnel, Self-Rescue Phase, Experiment, Group-Dynamic, Risk-Analysis, Human Behaviour

1. MOTIVATION AND OBJECTIVES

The evaluation of real events and previous studies provided evidence for the assumption that people often make collectively supported escape decisions in extreme situations. As the

influence of these group dynamic effects ("group effects") in the context of tunnel incidents had hardly been specifically investigated or quantified before, the German Federal Highway and Transport Research Institute (BASt) commissioned an interdisciplinary consortium of engineering and social sciences to conduct the research project "Analysis of Reaction and Escape Behaviour in Road Tunnels Considering Group Effects (FE 15.0703/2022/ERB)" in April 2023. The aim was to analyse sociological and engineering aspects in detail using realistic field trials with test participants This enables to check whether existing safety assessment procedures and the underlying regulations, which do not yet account for the effects of group dynamics on self-rescue, need to be adapted.

2. EXPERIMENT

2.1. Test Environment

As core-part of the project, trials with test subjects were carried out in the spring of 2024 at the "Zentrum am Berg" (ZaB) of the Montanuniversität Leoben (MUL) in Eisenerz, Styria, Austria. Built specifically for research and training purposes, this facility, corresponds to a real road tunnel in terms of dimensions and equipment. However, unlike tunnels with ongoing traffic, it allows for a flexible experimental environment without operational restrictions.



Figure 1: ZaB, north tube with road tunnel cross-section, perspective of the test participants approaching the accident scenario location, Source: STUVA

Along the designated route the test facility was equipped with original road signage for a speed limit of 50 km/h, indications of oncoming traffic tunnels, and no-overtaking signs. To allow the test subjects to get used to the situation, they drove along the route for as long as possible before reaching the accident site. The participants drove in their own vehicles in a loose convoy through a series of tunnels on the ZaB grounds. The first tunnel, consisting of the West tunnel tube and the South road tunnel, was about 715 metres long. The subjects then entered the second tunnel, which was designated as an oncoming traffic tunnel by signage and road markings. After about 270 metres, they reached a staged accident scenario.

2.2. Scenario

The accident scenario involved a truck fire in the opposite lane. The fire was simulated using gas burners and a cold smoke system to create defined and thus comparable fire, smoke, visibility, and ventilation conditions for all test runs. This also kept the danger to the test subjects very low. Obscured vision in the subject’s area was undesireble and had to be avoided as much as possible for safety reasons (risk of collision). In all test runs the fans were

controlled to move the non-hazardous, vaporised fog fluid as much as possible to the area behind the accident vehicle. Another truck and a car were positioned across the subjects' lane at the accident site in front of the burning truck mock-up, to act as an obstacle,



Figure 2: Truck mock-up, obstacles (cars and trucks), view opposite to direction of travel [1]

By the time the first test vehicle approached the accident site, there were already significant flames and smoke visible at the rear truck. The recognisability of the rear truck as a mock-up was hindered by the smoke. Due to the vehicle on the road, which was obviously involved in the accident with its hazard lights on, it was not possible to drive around or pass it. The test vehicles were forced to stop at a self-selected distance from the accident site. In the relevant area, there was a cross-passage with an emergency exit about 125 meters before the accident site and an emergency call niche about 20 meters before the fire site. Therefore, if they paid sufficient attention, the test subjects could see the burning truck, the emergency call niche, and the safe emergency exit. The driver and passenger doors of the two vehicles involved in the accident were open, making it clear that there were no injured or otherwise distressed people inside.

To standardise the test procedures, the "vehicle fire" operating program was started 60 seconds after the first vehicle came to a stop in front of the accident site. The jet fans in the test area were ramped up to 100% power accompanied by the corresponding noise. Simultaneously a pre-recorded loudspeaker announcement started, urging people to leave their vehicles. This voice announcement, characterised by a very clear and slow speech pattern, was played repeatedly with only short breaks of about 10 seconds.

2.3. Participants Trials

The core of the study consisted of test subject trials, including seven individual trials (as a reference) and five group trials. The test subjects were given only the most essential safety-related information. Communication between the subjects in advance was also prevented as far as possible. Test subjects were primarily recruited locally from communities around Eisenerz and Leoben through various digital and analogue channels. The aim was to recruit subjects from the "driving population"—that is, people who might actually find themselves in the situation under investigation—and to ensure representative age and gender distribution.

A total of seven individual trials and five group trials were conducted over two weekends in February and April 2024 with a total of 73 test subjects in 47 cars. The number of subjects in the group trials ranged from 12 to 14 people per trial run, distributed among seven to ten vehicles. This distribution aimed to replicate the different vehicle occupancy rates and

structures of passenger groups (co-workers, friends, families, and so on) during either holiday or commuter traffic.

2.4. Procedure

The trials were divided into three phases: briefing, carrying out, and debriefing. Upon arrival at the test site, participations were briefed on the requirements for taking part (not having consumed alcohol, holding a driver's license, giving consent to GDPR), provided safety instructions, and were given the opportunity to familiarise themselves with driving on the test site by taking a test drive through the first tunnel section.

During the test subject trials, the vehicles were lined up in a random order, and the fire simulation was started. After around 2 minutes of driving, the first vehicle in the second tunnel section came into view of the fire site for the first time and stopped at a self-selected distance from the accident scenario. Sixty seconds later, the fire ventilation started, and the repetitive loudspeaker announcements began.

Continuous video recording was conducted throughout the trial using fixed and mobile cameras to document the participants' behaviour – such as their interactions or escape behaviour – in detail and chronologically. Figure 3 shows the different perspectives of these images. The subjects' behaviour was not influenced, only recorded. This included how long they stayed in the car, when they left the vehicle, whether they stayed near the vehicle, whether and how they communicated with other road users, whether they sought out the emergency call booth and placed a call, and when and at what speed they began to flee. Once the test subjects had reached the tunnel portal or the smoke-free parallel tube via the emergency exit, an exercise observer informed them that the trial had ended.

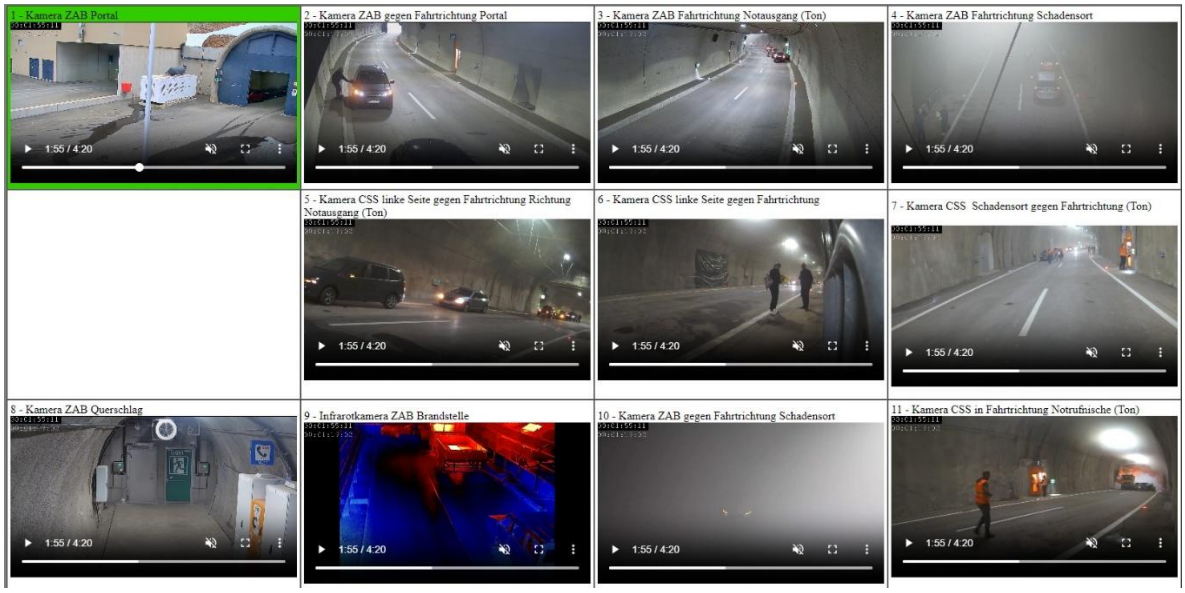


Figure 3: Synchronous display of camera views in the documentary [1]

The test subjects were interviewed in the tunnel immediately after the trials. The participants were asked to return to their vehicles. The occupants of the vehicles were asked about their perceptions, thoughts, decisions and alternative considerations, as well as their specific behaviour. The interviewers began the interview in the vehicle. The starting point for the descriptions was the entrance to the last section of the tunnel. A structured qualitative interview guide was used for this purpose. During the interview, the subjects' paths and stops were retraced together in the tunnel, and the interviews were recorded for analysis. Once back at the training building, a standardised survey was conducted using a questionnaire. Finally,

the participants were informed about the project's purpose and given the opportunity to ask questions.

3. EVALUATION

3.1. Sociological Evaluation

The sociological analysis of the observed group effects revealed a complex and multifaceted picture. to support analysis and evaluation, relevant behaviours were classified into four categories ranging from positive to ambivalent/problematic, critical to even fatal behaviours.

Individual experiments can be classified into a scheme with the dimensions 'manifest behaviour' and 'patterns of reasoning and decision-making', with the latter divided into the subdimensions 'professional' and 'situational'. Observed manifest behaviours included (A) stopping, not getting out of the vehicle and turning the vehicle around as a continuous sequence of actions. (B) Stopping and exploring/making emergency calls/escaping on foot, often as a multiple sequence. (C) Attempting to drive past the accident site. 'Professional' reasoning and decision-making patterns are comprehensive courses of action that are shaped by previous experience or prior knowledge. Situational uncertain decision-makers make decisions in the moment, often multiple times, and give ambivalent or vague reasons. Situational confident subjects can give clear reasons and show little uncertainty when reflecting afterwards, but they do not have a comprehensive predetermined course of action. Although only seven individual trials were conducted, almost all combinations could be observed, even professional reasoning that lead to critical, potentially fatal behaviours.

In order to capture group effects, the behaviour and decisions during the group trials was analysed at three levels: individual, immediate 'neighbourhood' (vehicle crews and vehicles directly in front of or behind) and larger groupings. At all three levels, the experiments revealed a surprising range of initial reactions to the scenario and stopping the cars, up to and including the final route choices in the tunnel. "Group effects" can be expected either in the orientation of individuals towards others, within groups or through the formation or dissolution of groups (grouping effects). To give an example: the empirical analysis showed that the orientation towards other people at an individual level could be mapped onto six types:

(A) Guiding others, no orientation towards others
(B0) No or little orientation towards others, own course of action enforced
(B1) Orientation towards others and own course of action equally important
(B2) Strong orientation towards others despite having a personal course of action
(B3) Orientation towards others because of a lack of own course of action
(C) Act only upon explicit request

Overall, positive effects predominated: problematic or critical behaviour of individuals could be corrected by group dynamics. The actions of other road users at the front of the row, such as exiting the vehicle or starting to flee, made driver at the back aware of the danger, prompting them to react even if they did not perceive any direct danger. Potentially fatal behaviour, such as attempts to turn the car around or return from safe areas to the smoke-filled tunnel, was also prevented in some experiments.

However, problematic and critical group effects also occurred. A striking example of this was the phenomenon of passivity as a group behavior. Whereby the inactivity of test subjects in front of a vehicle resulted in a lack of or delayed danger awareness among those behind them. In one trial one person's call to approach the danger zone could have had potentially fatal consequences for others. In another trial, a small group of people formed and decided

internally to conduct a search operation disregarding concerns within the group, thus exposing themselves to critical situations. In addition, ambivalent effects were identified, the impact of which depended heavily on the specific situation and the individuals involved. Many participants described their decisions as a conflict of objectives between saving themselves and saving others, whereby saving others could refer both to those directly affected by the accident and to the occupants of their own vehicle or people in the vicinity of their own vehicle or the "group" as a whole, i.e. all persons in the vehicles in the tunnel.

A detailed description of the complex relationships that could be traced based on the multilevel analysis can be found in the corresponding project report, Issue B 209 [1].

3.2. Quantitative Experimental Results

The goal of the quantitative engineering evaluation of the test subject trials was to derive reaction times and escape speeds from the (video) documentation of the escape behaviour. To this end, the individual escape paths and associated escape times of each subject were determined from the video recordings.

Reaction times were calculated as the sum of the time spent in the vehicle, any time spent exploring the situation, time taken to reach the emergency call niche, and the duration of placing a call. The individual behaviour of the test subjects and the paths they took were considered; not all subjects explored the situation, and only a few placed a call. Escape time was determined from the moment a person purposefully started moving towards a safe area until they reached it.

Figure 4 shows the statistical analysis of the time spent in the car—the time between stopping and leaving the vehicle—differentiated between individual and group trials. This included two individual drivers who turned their vehicles around, as the decision to become active and turn around is an escape decision in a broader sense. As a result, the median time spent in the vehicle was 24.5 seconds for individual trials and 44 seconds for group trials. The longer time spent in the vehicle during group trials is likely due to communication between the driver and passengers.

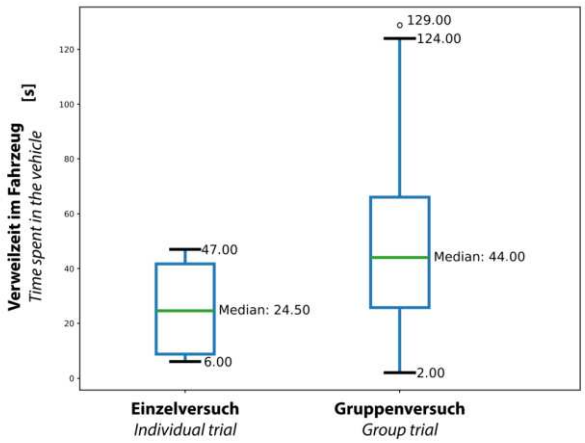


Figure 4: Time remained in the vehicle, differentiated between individual tests and group tests [1]

Figure 5 shows the statistical distribution of reaction times. In the individual trials, the median reaction time (for participants who did not place an emergency call) until they started to flee was 47 seconds. For people in the five group trials, this reaction time was significantly higher at 70 seconds. As with the time spent in the vehicle, this can be interpreted, as an indication that people in individual trials react faster because they do not wait for hints from others and do not spend time coordinating their approach.

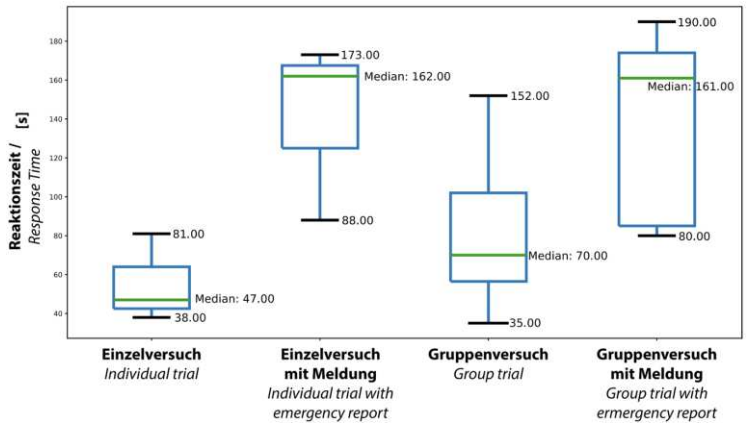


Figure 5: Statistical distribution of reaction times in individual and group trials [1]

In the individual trials the median escape speed of the test subjects was 1.27 metres per second. In the group trials, a slightly higher median speed of 1.43 metres per second was observed. This showed a considerable spread in individual speeds, which is attributable to different behaviors of the subjects, ranging from intensive communication during the escape to a running at a fast pace. These measured speed values generally align well with the assumptions used in common risk models for tunnel safety, such as the German model, which typically assumes an average escape speed of 1.3 meters per second. Furthermore, the empirical data underlines the general validity of the underlying escape model as a representative abstraction of human behavior within the risk assessment framework. Based on these results of the research project, there is no immediate need to fundamentally adapt the established methodology for the safety assessment of road tunnels in this respect.

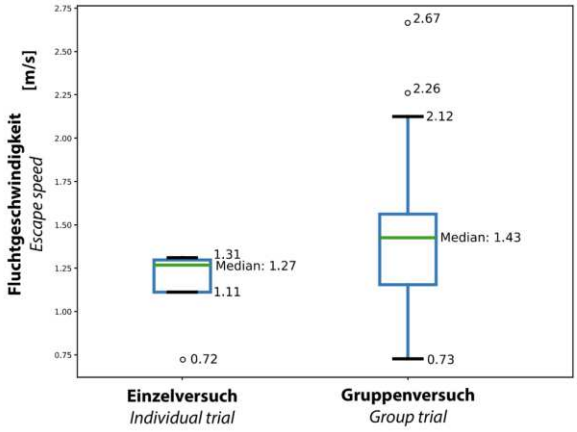


Figure 6: Statistical distribution of escape walking speed in individual and group experiments [1]

Table 1 summarises the parameters and shows that quantitatively, people in a group setting take a slightly longer to leave the vehicle and start fleeing but then seek a safe area at a faster walking speed. It should be noted that the result of the sociological analysis indicates a predominantly positive influence on self-rescue behaviour, but this cannot be reflected in the quantitative escape parameters. It is also worth noting that none of the individuals in the group trials remained sitting in the car.

Table 1: Overview of quantitative escape parameters comparing individual and group experiments

Parameter	Individual Trials	Group Trials
Median Time Spent in Vehicle	24.5 s	44.0 s
Median Reaction Time (without notification)	47.0 s	70. s
Median Escape Velocity	1.27 m/s	1.43 m/s

4. CONCLUSION AND OUTLOOK

The research project "Analysis of Reaction and Escape Behavior in Road Tunnels Considering Group Effects" has provided extensive insights into the influence of group dynamics on self-rescue in tunnel systems, based on sociological and engineering aspects. As part of the project, more than 70 test subjects were immersed in a highly realistic accident scenario with a fire in a road tunnel, and their behaviour during the self-rescue phase was analysed in detail. Numerous different behaviours were documented, and group effects were described.

However, when interpreting the results, it should be noted that the scenario still represented a relatively limited and ‘simple’ challenge in terms of tunnel length and accident scenario, the number of vehicles, the use of one lane only, the convoy length, path lengths, etc. These factors can be significantly more complex in other events. Restricting the test subjects to German speakers also represents a simplification.

The trials support the thesis that although group effects significantly expand the spectrum of escape behavior, they tend to improveself-rescue. However, negative grouping and group dynamic effects also occurred in the trials. It should be examined here whether and to what extent these can be addressed by safety concepts.

The engineering evaluation of the conducted trials, which determined the reaction times and resulting escape speeds for both group trials and individual reference persons, confirms the common assumptions of the basic parameters of risk models. Consequently, the results and data basis of the trials do not justifiy updating the regulations. However, due to the restriction to a single scenario and the limited total number of subjects, the transferability to general situations is limited.

Due to the extensive nature of the project’s fundamentals, results, and analyses, only a highly abbreviated form can be presented here. A detailed version can be found in the associated research report, which is part of the series "Reports of the Federal Highway and Transport Research Institute, Series B: Bridge and Civil Engineering" as Volume 209. This was published in April 2025 and is available for free download at: https://www.bast.de/DE/Publikationen/Berichte/unterreihe-b/2025-2023/b-209.html.

5. REFERENCES

[1] Analyse des Reaktions- und Fluchtverhaltens in Straßentunneln, Thienert, C.; Leismann, F.; Kaufmann, S. Jenki; R.; Galler, R.; Wenighofer, R.; Forschungsbericht in der Schriftenreihe „Berichte der Bundesanstalt für Straßen- und Verkehrswesen, Reihe B: Brücken- und Ingenieurbau“ der BASt, Band 209, Bergisch Gladbach, 2025

DIGITAL TWINS FOR ROAD TUNNELS – EXPECTATIONS MEET REALITY

[1]Goetz Vollmann, [1]Zuzan Azad, [2]Lisa Von Roessing, [2]Benedikt Faltin, [3]Anne Lehan, [3]Marius Nono Tamo, [4]Karl Hanke, [4]Annika Jodehl

[1]Ruhr University Bochum, Institute for Tunnelling and Construction Management, DE
[2] Ruhr University Bochum, Institute of Computing in Engineering, DE
[3]BASt, Federal Highway and Transport Research Institute, DE
[4]BUNG Group, DE

DOI 10.3217/978-3-99161-087-8-007 (CC BY-NC 4.0)
https://creativecommons.org/licenses/by/4.0/deed.de
This CC license does not apply to third party material (attributed to other sources) and content noted otherwise.

ABSTRACT

The German Ministry of transport (BMV) recently published a guideline that defines the basic features of Digital Twins (DT) in the course of the German federal road network and outlines their areas of application. While tunnels already require at least a partially digital environment, which is determined by existing regulations and their implementation, any type of DT must fit into these processes and regulative schemes. In doing so it will automatically redesign and redefine them in order to activate its full potential. That said, safety concerns are raised and need to be addressed. Moreover, the Kritis Regulation of the Federal Office of Information Security (BSI) categorises tunnel control centres as critical infrastructure facilities. Therefore, the number of processes that can be handed over to a DT is already limited due to security implications.

In the DIDYMOS project, the research partners are developing methods and processes for setting up DT for road tunnels, with the aim to implement them as a part of optimized operating approaches. In this context, the authors conducted extensive interviews with all stakeholder groups involved in tunnel operation. The results of the interviews show that, on the one hand, there is great curiosity about such approaches, but on the other hand, substantial concerns have been expressed as to whether tunnel operation needs to be redefined and reorganized if a DT is to be introduced into everyday operations. The interviews also address which tunnel operation tasks can or may be automated by DTs.

In this article, the authors present a summary of the interview results and highlight where stakeholder expectations and technical implementation concepts correlate or conflict with each other. Furthermore, preliminary dashboards of the developmental DT and how analyses can be carried out for the daily work are presented.

Keywords: Digital twin, road tunnel, tunnel operation, predictive maintenance, AI

1. INTRODUCTION

Digitalization has become an essential component of the construction industry, encompassing all phases of project development, including the initial planning phase, the construction phase, and the subsequent maintenance and operational phases. The German 'Masterplan BIM' guideline is primarily centered on the planning and construction phase [1]. In the meanwhile, there are no standards and guidelines on the implementation of digitalization and BIM in the operational phase. This can be primarily ascribed to the heterogeneity of the structures. Due to the necessity for a high level of technology in tunnels to ensure user safety, a large number

of digitized operating points already exist in these structures, while bridges and troughs still have comparatively less complex operating scenarios. This means that there is need of different approaches in the implementation of digital twins (DTs) as measure for maintenance and operation of the structures.

This issue is being addressed in the DIDYMOS project, which is funded by the BMV as part of the mFund funding initiative. For the first time, research is being conducted into the requirements and conditions for implementing DT-s for road tunnels. In the project methods for structural acquisition and digitization, as well as maintenance planning and operational optimization will be developed [2].

The following section primarily focuses on the framework conditions for the development of DTs, and presents the results of the expert interviews and discusses them in this context. However, the development of digital as-is models is only briefly described, with reference being made to parallel publications by the authors.

2. DIGITAL TWINS

2.1. Terms and conditions for developing DTs and DIDYMOS

Building Information Modeling (BIM) represents a collaborative methodology that enables the coordinated exchange and management of digital building information throughout the entire life cycle of a structure. At the core of BIM are digital building models that integrate geometric and semantic data.

However, these digital models, often referred to as BIM models, do not fully correspond to the definition of a DT [3]. Rather, DTs are an extension of such models, incorporating a continuous data link between the physical structure and its digital representation. This encompasses, in particular, the integration of real-time data, condition monitoring functions, and analysis and decision support systems that facilitate bidirectional data exchange between digital and physical objects [4]. A DT is thus composed of three primary components: a digital model, a physical equivalent, and the exchange of data between these two components. This data exchange can take place in several directions, i.e. from the digital model to its physical equivalent, vice versa, or in both directions in parallel [5].

A digital model of the structure is therefore a fundamental prerequisite for building a DT. If such a model is available, the model must be analyzed according to its lifecycle phase and assessed regarding its quality and level of detail. In particular, the model must be examined for its suitability as a foundation for DT. While verifying the existence of a model is usually straightforward, assessing its accuracy and completeness is considerably more complex.

In the case of existing tunnel structures, however, such models are often missing or outdated [6]. Consequently, reconstructing or updating digital representations of these assets from available tunnel documentation, such as drawings, reports, or point clouds, is a necessary first step. When performed manually, this process is highly time-consuming and laborious.

The DIDYMOS project addresses this challenge by developing methodologies for the (semi)automated generation of digital tunnel models using Artificial Intelligence (AI)-based techniques [7]. Different approaches are conceptualized based on the available data of the structures [8]. In addition, all partners are engaged in research related to the development of specific DTs and the implementation of specific use cases, utilizing AI-based analysis routines. Based on this foundation, some critical research questions arose:

- How can DT be integrated into tunnel operations given existing safety, regulatory, and stakeholder constraints?
- What technical and processual obstacles have to be tackled while implementing DT in tunnel operations?

For answering those questions and subsequently describing the accompanying use cases, it was imperative to undertake expert interviews. In doing so, it was possible to identify the needs and requirements for digital support in operation and maintenance, as well as to capture concerns regarding implementation and application.

2.2. Boundary condition for the development of DTs

The initial phase in developing a comprehensive concept for DTs was initiated by the BMV, which established a framework for the development of DTs [9]. This development must be in accordance with the normative regulations. The construction must comply with the requirements of ZTV-ING Part 7 [10], in conjunction with the parallel requirements of DIN 1076 [11] and RI-EBW-PRÜF [12]. This provides the framework for inspection and maintenance, including the evaluation of the structural integrity of the tunnel structure.

In accordance with the stipulations set out in the European Directive [13], a set of administrative and structural requirements were established within Germany for the operation of tunnels, with the objective of ensuring the safety level of such infrastructure. These were initially documented in RABT 2006 [14] and have since been transferred to RE-ING [15].

In addition, tunnel control centers are considered to be part of the federal critical infrastructure. This necessitates restrictions on the free availability of security-related data.

Furthermore, local conditions or individual operational philosophies may create framework conditions that can vary from one structure to another and must also be taken into account.

3. EXPERT INTERVIEWS

3.1. Interview results

As part of the expert interviews, a total of 14 experts (stakeholders) from various areas of tunnel operations were interviewed, including administrative authorities, tunnel managers, safety officers, and tunnel monitoring personnel. The aim was to identify which processes could be supported by an AI-based DT in tunnel operations. The interviews addressed the following thematic blocks:

1. General information
2. Processes and data
3. Forecasting
4. Data exchange / Visualization
5. Target Areas and Use Cases
6. Operational condition assessment and evaluation of tunnel ventilation system
7. Structural condition assessment and evaluation of tunnel linings
8. AI

Thematic blocks 1 and 2 provided an overview of relevant processes and data, as well as the experts' assessments regarding the use of the DT. In block 3, the experts explained the operational context in which they could imagine accessing forecasts in the course of decision-making. Block 4 focused on formulating requirements for the DT interface and visualization requirements. In block 5, specific use cases and target areas were described, which, from the experts' perspective, should be addressed by the DT. Blocks 6 and 7 focused on the selection and evaluation of Key Performance Indicators (KPIs) for both use cases mentioned above "Tunnel Ventilation" and "Tunnel Linings," which are examined in detail within the DIDYMOS project. Finally, Block 8 included discussions on experiences and requirements related to the use of AI in tunnel operations and maintenance. Excerpts from the results of this user requirements analysis are presented below. When recording user-specific requirements, the tunnel experts explained what additional information they would consider helpful when using DT. These are summarized in Table 1.

Table 1: Overview of expert/Stakeholder requirements for information displayed by a DT

Stakeholder requirements
Overview of structural and technical condition
Plant status and fault tracking
Cost development
Monitoring of structural damage
Statement on the completeness of data and documents
Statement on regulatory compliance information
Maintenance scheduling
Operational strategy
Traffic data
Condition of all tunnels at a glance

According to the experts, the DT of a tunnel should provide a comprehensive and up-to-date overview of the condition of the structure and its technical systems. Malfunctions and damages must be recorded, visualized, and tracked throughout the entire lifecycle of the structure. Cost development should also be represented transparently. Furthermore, experts emphasized the importance of a complete overview of all relevant data and documents via the DT. This refers to a centralized storage of all relevant information/data for the entire structure (single source of truth).

The DT should also provide information on the regulatory compliance of the structure and indicate when the next maintenance of specific equipment components is due. Information on operational strategies should be integrated, as well as traffic-related data that are crucial for improving traffic management and optimizing tunnel availability. Finally, the various DTs should be interconnected to enable a clear overview of the condition of all tunnels within the area of responsibility — ideally at a glance.

Additionally, the use of AI in tunnel operations and maintenance was discussed. Stakeholders outlined the potential and added value of AI from their perspective. These are presented in Table 2.

Table 2: Expert/Stakeholder perspectives on the Added Value of AI in tunnel operation and Maintenance

AI potentials and added value in tunnel operation and maintenance
Automated analysis of real-time and measurement data
Processing big data
Fast retrieval of desired information (Document Analysis)
Experience-based automated assessment (Lessons Learned)
Automated image and video analysis
Relief of personnel from specific tasks
Automated detection of anomalies and patterns through continuous monitoring
Automated generation of asset models
Enhancing damage identification processes
Automated suggestion generation for planning and renovation
Automated detection of incidents and traffic congestion

In summary, DTs offer numerous advantages for technical and organizational processes, according to the experts**.** A key benefit should be the high data quality enabled by continuous synchronization with the physical object, which makes precise analyses and supports decision-making possible. DTs can improve collaboration and reduce misunderstanding by visualizing and exchanging complex information. Another major advantage is the support of predictive maintenance: by analyzing real-time and historical data, potential failures can be identified early or prevented as far as possible, which increases operational safety and reduces costs.

3.2. Dashboard according to expert interview results

Following the results of the stakeholders' requirements of the DT, the project partners have developed concepts for several dashboards. These dashboards are still in the design phase. The provisional dashboards facilitate the visualization of the front-end layer of the digital twin, thereby displaying all the essential information regarding tunnel operation. As illustrated in Figure 1, the provisional dashboard represents one of the use cases that has been defined within the DIDYMOS project. The use case demonstrated is that of the structural condition assessment and evaluation of the tunnel’s inner lining.

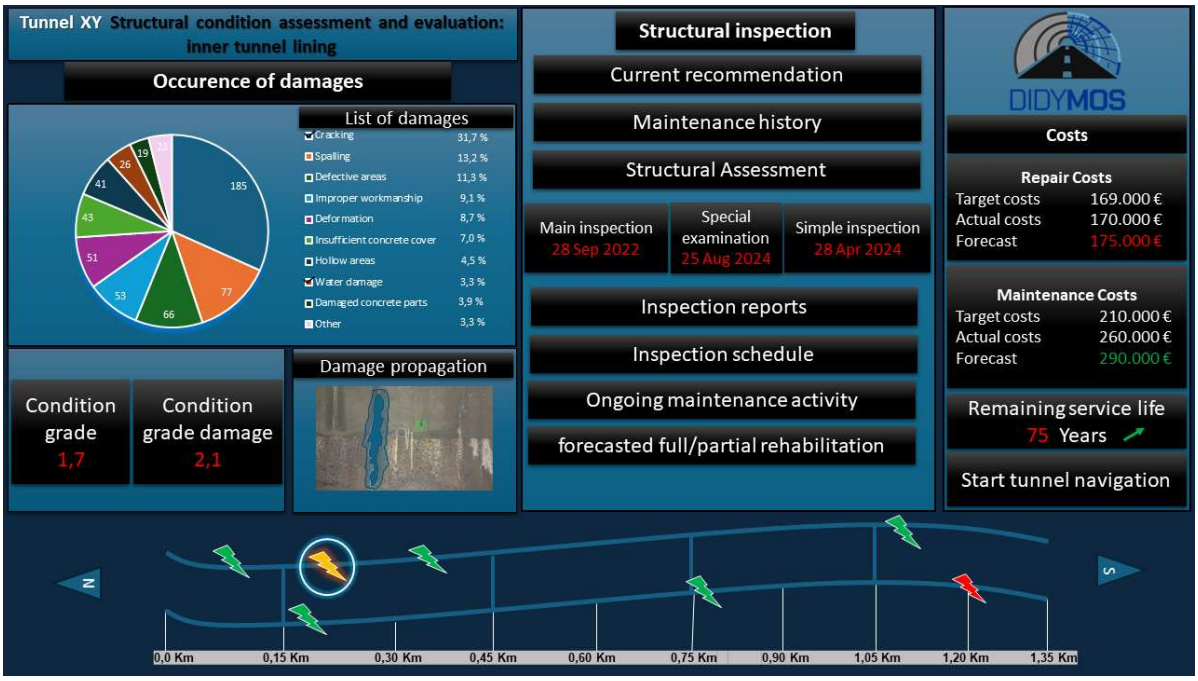


Figure 1: Provisional dashboard for the use case "structural condition assessment and evaluation of the tunnel inner lining" (Source: RUB TLB)

The provisional dashboard has been designed to incorporate as many of the requirements of the stakeholders as possible. The structural condition of the tunnel, the maintenance schedule and the inspection history are all displayed in a compact format and are easily locatable. The subsequent components are presented in order to illustrate the propagation of each documented damage, as well as the condition grade assigned to each individual damage. In addition, the requirement for cost development, encompassing its various cost categories, is presented. Moreover, the current vision entails the facilitation of navigation through a 3D model of the tunnel structure in its existing state. The navigation of the tunnel, including the location of all damage and the technical equipment information, can subsequently be located on an additional dashboard.

4. CHALLENGES IN THE IMPLEMENTATION OF DIGITAL TWINS

From the experts' perspective, despite the numerous advantages of a DT, there are several significant aspects that must be considered during development**.** For instance, the implementation and operation of a DT not only require specialized hardware and software, but also qualified personnel capable of deploying and maintaining. Moreover, there is a risk of excessive reliance on technology when decisions are made solely based on digital models. If the real-world situation is not sufficiently taken into account, this can lead to misjudgments. Therefore, the significance of high-quality data is paramount to the efficacy of a digital twin.

A further critical issue is the persuasion of those who are resistant to the adoption of digital technologies. According to stakeholders, many organizations have employees who are skeptical about new technologies or reject them outright. A meticulous and methodical change management process is imperative in fostering acceptance within this context. The potential dangers of generalization should not be underestimated either. It is important to note that a digital twin based on general assumptions and not adapted to the specific requirements of a structure may not be able to adequately reflect these special features. This may result in inaccurate assessments, especially when the decision-making or decision support for controlled processes is AI-based. As the volume of collected and analyzed data increases, so

does the risk of information overload. Without effective filtering and visualization methods to identify KPIs relevant to the specific application, it can become challenging to extract meaningful insights and make effective decisions.

A further key finding from the expert interviews conducted is that there is currently no uniform understanding of what a digital twin must achieve in the context of tunnel operation and what its specific design should look like. Having 16 federal states in Germany, each with a unique organizational structure, leads to a large heterogeneity. The challenges associated with developing a nationwide standard for DTs of tunnel structures is compounded by the heterogeneity of the software landscape and the varied responsibilities and administrative structures across different federal states. As is the case of BIM, this results in isolated solutions that are interoperable to a limited extend, thereby constraining the advantages to individual structures. Consequently, conducting a comprehensive network analysis, particularly in the context of forecasting life cycle costs and strategic maintenance planning, is impracticable under these conditions, despite this representing the optimal goal of development.

In addition to clarifying the terminology, it is imperative that there are clear administrative, legislative and technological framework conditions in place to enable standardized implementation. From an administrative perspective, there is a necessity for the coordination of responsibilities and the establishment of binding guidelines at both the federal and state levels. The objective of this coordination is to standardize data modelling, access rights and update cycles. In the context of legislation, the Federal Highways Act and associated administrative regulations would require amendments. Such adjustments are deemed necessary in order to incorporate the DT into operational processes.

5. SUMMARY AND CONCLUSIONS

DTs have a lot of potential to enhance the technical and economic efficiency of road tunnel structures, thereby increasing operational availability and ensuring user safety. However, it is imperative that standards are defined and established with utmost urgency to ensure the interoperability of conceptual approaches and to establish a uniform framework for the structures. Moreover, the development of isolated solutions from a network perspective is to be avoided. These principles are applicable not only in the context of tunnel structures but also in the context of other structures. The DT's working method offers a substantial added value that derives from the comprehensive, uniform digital data management at network level, and not primarily from the modeling of individual structures and the linking of existing information with a 3D model of the structure. Evidently, from a network standpoint, there is also rationale for integrating DT data concerning tunnel structures with those pertaining to bridge structures, retaining walls, and ancillary transport and drainage facilities. It is only on this basis that reliable and comparable statements can be made about the life cycle costs of the federal transportation network with overarching maintenance strategies and investment requirements. A DT, when used in conjunction with a dashboard for the front-end results, has the potential to engender substantial enhancements in the efficiency and operation of tunnel structures.

Acknowledgements:

This research was funded by the mFUND research programme of the Federal Ministry of Transport (BMV) (funding code: 01F2259A).

6. REFERENCES

[1] Federal Ministry of Transport. Masterplan BIM Federal Trunk Roads. Berlin, 2021.

[2] https://didymos.blogs.ruhr-uni-bochum.de/ (Last accessed 09.10.2025)

[3] Yu, G., Wang, Y., Mao, Z., Hu, M., Sugumaran, V., & Wang, Y. K. (2021). A digital twin-based decision analysis framework for operation and maintenance of tunnels. Tunnelling and underground space technology, 116, 104125.

[4] Diren, N. S., & Althen, S. (2023). Tunnel 4.0: managed digital twin for tunnel operations. In Expanding Underground-Knowledge and Passion to Make a Positive Impact on the World (pp. 2635-2642). CRC Press.

[5] Boje, C., Guerriero, A., Kubicki, S., & Rezgui, Y. (2020). Towards a semantic Construction Digital Twin: Directions for future research. Automation in construction, 114, 103179.

[6] Volk, R., Stengel, J., & Schultmann, F. (2014). Building Information Modeling (BIM) for existing buildings—Literature review and future needs. Automation in construction, 38, 109-127.

[7] Vollmann, G.; Azad, Z.; Lehan, A.; Tamo, M.; König, M.; Faltin, B. et al.: Digital twins for the predictive operation and maintenance of road tunnel structures and their safety equipment. In: Tunnelling into a Sustainable Future – Methods and Technologies. S. 4319–4326. DOI: 10.1201/9781003559047-550

[8] Phillip Schönfelder, Angelina Aziz, Benedikt Faltin, Markus König, Automating the retrospective generation of As-is BIM models using machine learning, Automation in Construction, Volume 152, 2023, 104937, ISSN 0926-5805, https://doi.org/10.1016/j.autcon.2023.104937

[9] Federal ministry of transport (BMV): digital twins for federal highways“, Framework document, Berlin, 2024

[10] Federal ministry of transport (BMV): Zusätzliche Technische Vertragsbedingungen und Richtlinien für Ingenieurbauten (ZTV-ING), Teil 7: Tunnelbau, Berlin, 2025

[11] Deutsches Institut for Normung e.V.: DIN 1076:1999 DE Ingenieurbauwerke im Zuge von Straßen und Wegen - Überwachung und Prüfung

[12] Bundesministerium für Verkehr (BMV): Richtlinie zur einheitlichen Erfassung, Bewertung, Aufzeichnung und Auswertung von Ergebnissen der Bauwerksprüfungen nach DIN 1076, Berlin, 2017

[13] European Commission (EC): Directive 2004/54/EC of the European Parliament and of the Council of 29 April 2004 on minimum safety requirements for tunnels in the Trans-European Road Network. Brussels, 2004

[14] Forschungsgesellschaft für Straßen- und Verkehrswesen (FGSV): Richtlinien für die Ausstattung und den Betrieb von Straßentunneln (RABT), Köln, 2006

[15] Bundesanstalt für Straßen- und Verkehrswesen (BASt): Richtlinien für den Entwurf, die konstruktive Ausbildung und Ausstattung von Ingenieurbauten (RE-ING), Bergisch Gladbach, 2025

R&D PROJECT TUNNEL SENSOR FUSION

Dietmar Harbauer

ASFINAG Alpenstraßen GmbH, AT

DOI 10.3217/978-3-99161-087-8-008 (CC BY-SA 4.0)
https://creativecommons.org/licenses/by/4.0/deed.de
This CC license does not apply to third party material (attributed to other sources) and content noted otherwise.

ABSTRACT

This paper describes the processes and results of an R&D project implemented by the author in the context of his work for ASFINAG.

Thanks to intelligent sensor data fusion it could be shown that the detection probability of events in road tunnels can be increased significantly while at the same time markedly reducing false positives.

The project was tested in three ASFINAG (Austrian Corporation for the Funding, Construction and Operation of the Country's High-Ranking Road Network) tunnels

1. BACKGROUND

As a result of the author's many years of membership in various working committees of "Österreichische(n) Forschungsgesellschaft Straße - Schiene - Verkehr FSV" (Austrian Research Society for Road, Rail and Traffic) as well as the fact that he had already had many years of experience with the operation of road tunnels at the time, the author recognised that the system architecture of operating and safety technology (Austrian acronym: BuS) in the tunnel systems harboured possible improvement potential. In principle, the sensor system architecture in road tunnels used to look as follows: [1]

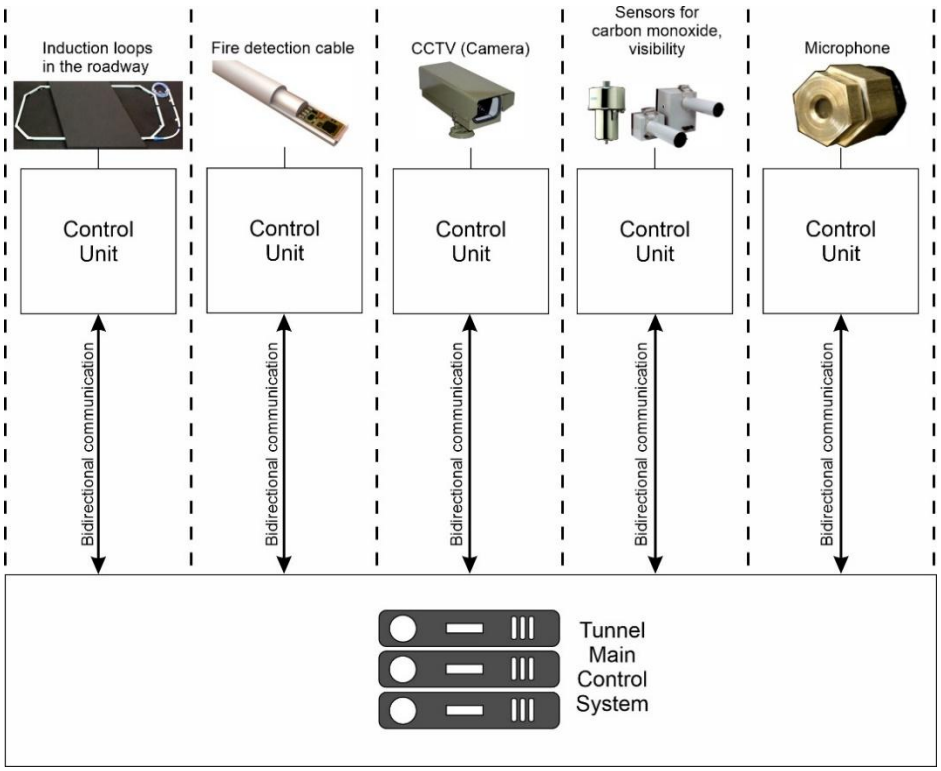


Figure 1: Principle of system architecture sensors in Austrian road tunnels

Every detection system is directly connected to the tunnel controls' central system (most often via a control unit) and is largely treated as independent from the adjacent systems. In reality, the technical realisation of the various sensor systems in Austrian road tunnels are vastly more complex. Especially data connection of the individual subsystems of a road tunnel's operating and safety equipment (BuS) and sensors is much more elaborate, meeting the current state of industrial standards. However, this doesn't change the parallel structure of the system architecture.

Each sensor works according to its technical/physical possibilities. This results in measuring errors whose deviation from the "correct" value vary. These measuring errors occasionally result in "false positives". The system architecture shown in Figure 1 has the disadvantage that systems' false positives add up and are transmitted to the SCADA system of the connected control centre. Following similar cases in the automotive industry, the author's idea was to combine various sensor systems' information on events in the tunnel to increase detection probability while lowering the rate of false positives. This idea led to the three-phase "Tunnel Sensor Fusion" R&D project [9]. The correct term is sensor data fusion. The principle is not new as it was used by NASA in its Apollo missions in the 1960s, back then using the Kalman filter to navigate its space ships ([2], Chapter 3.1, 3.1.1).

In the 1980s, the automotive industry started to use serially produced sensor data fusion to securely trigger certain systems in their vehicles [2]. Specifically to trigger airbags, [3], [4] and anti-lock brakes, [5]. Generally, one can describe sensor data fusion as follows: "Sensor fusion is defined as the process of combining signals acquired from various sensor sources to create a more valuable and precise output than that provided by individual sensors…." [6]

2. R&D PROJECT TUNNEL SENSOR FUSION

Due to the novelty and complexity of this undertaking, the tunnel sensor fusion project was divided into three phases stretching several years.

2.1. Phase I

Feasibility study to determine the basic principle of a fusion of various sensor families in a road tunnel. This phase was done offline, meaning that real event notifications from the data base of a tunnel in operation were copied and fed into test algorithms in the office.

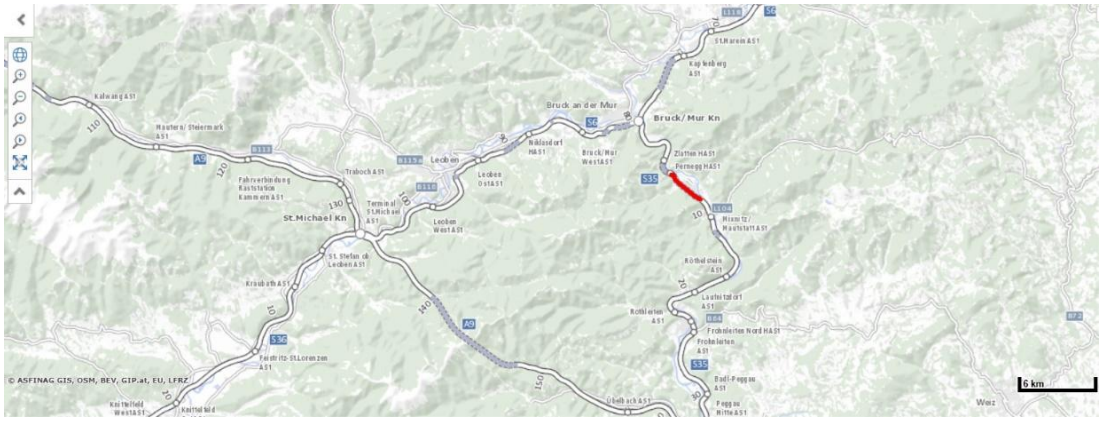


Figure 2: Screenshot ASFINAG GIS, S35 Expressway (Brucker Schnellstraße) with Kirchdorf Tunnel(red)

Kirchdorf Tunnel along the S35 Brucker Schnellstraße was chosen, specifically because it marked the first ASFINAG tunnel equipped with the then-new "Acoustic Tunnel Monitoring" (AKUT). [7]

Kirchdorf Tunnel is indicated in red in Figure 2. The tunnel has two tubes (one for every carriageway), is approx. 2.8 km long and was opened for traffic in May 2010. This tunnel's average daily traffic load in 2014 was approx. 16,400 vehicles.

At project start, no scope for the determination of the detection probability and simultaneous reduction in false positives had been defined. That's why the first, self-chosen task of the research consortium was an object-based data fusion (to model the tunnel). This, however, assumed that the installation position and physical/structural behaviour of every sensor ("sensor noise") had to be known exactly. Since this information was not available for the Kirchdorf Tunnel, the modelling approach was sidelined and the focus shifted to data fusion at property level (by means of machine learning). Basic information on artificial intelligence in general and machine learning in particular can be found in [8].

In preparation for tunnel sensor fusion, one important requirement is to create a "type of event/sensor" matrix as a first step. An extract of such a matrix for the Kirchdorf Tunnel is shown in the following.

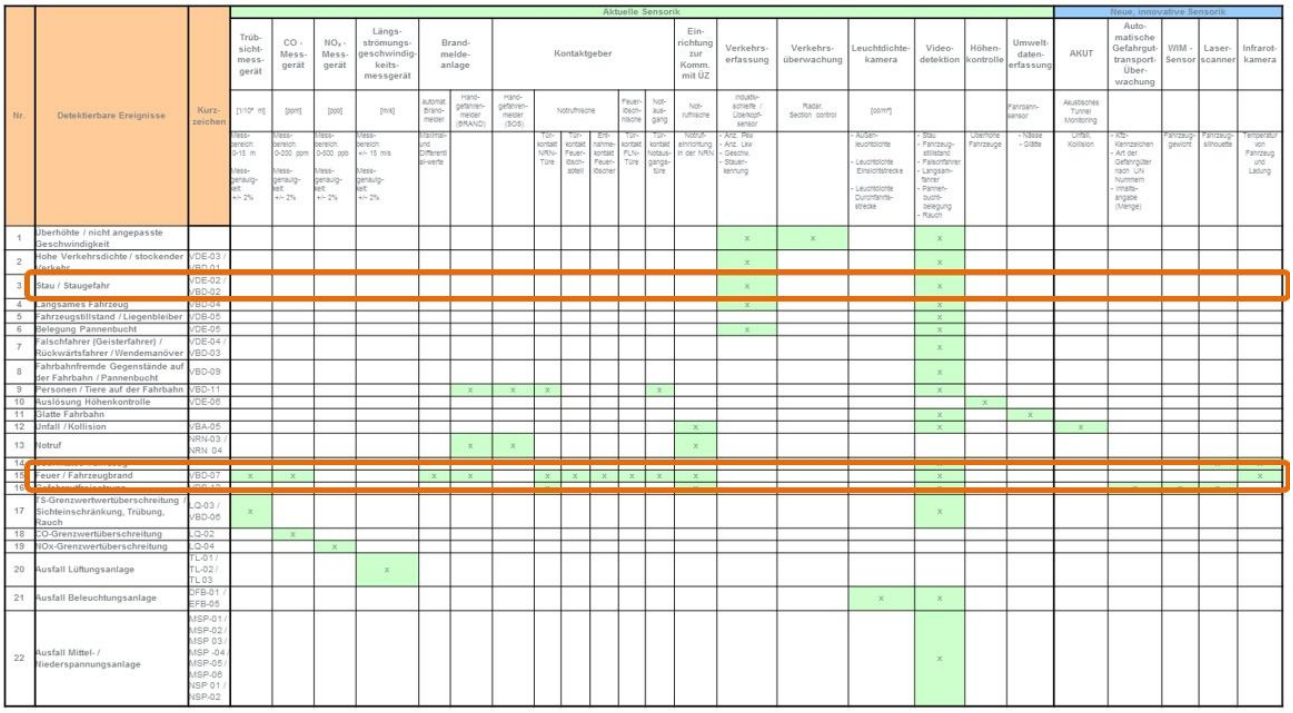


Figure 3: Extract from an event-sensor matrix for the Kirchdorf Tunnel



Figure 4: Event sensor-matrix zoom, Figure 3

Figure 3 shows possible events in a road tunnel from top to bottom and the sensor systems installed in the Kirchdorf Tunnel from left to right. An X in a cell means that the event listed in the row can be detected automatically by the respective sensor system in the Kirchdorf Tunnel. If a row contains more than one X this event can be detected by different sensor systems, meaning that all these various sensors can be combined using suitable algorithms. For a better view, the row containing the event type “fire / vehicle fire” was enlarged and displayed as Figure 4.

The general idea is in the assumption that one event type (e.g. drivers going the wrong way) in the tunnel is detected by several sensors belonging to various sensor families at various points in the tunnel. This results in the so-called feature vector. $x \in \mathbb{R}^n$:

$x = [\text{WrongWayDriverCounter, SlowVehicleCount, SmokeCount, StoppedCount}]^T$

In the feature vector, the viewed events are listed with one index number each. A feature vector of $x = [2,3,0,0]^T$, for instance, means that the involved sensor systems have detected the (same) wrong-way driver twice and a slow-moving vehicle three times in the same time window. The detection of slow-moving vehicles could originate from several, different vehicles and are most likely a secondary response to the wrong-way driver.

The detected feature vectors are then categorised using classification algorithms.

In the case of the wrong-way driver event type, the measurement results of the video detection and induction loop sensor families were combined using the sensor data fusion algorithm.

Training and test set for event type *Wrong-way driver*

Table 1: Overview of test data for the wrong-way driver event type

Set	**Number of Labels**	**True Positive Labels**	**False Positive Labels**
Total Set	169	166	3
Training Set	101	99	2
Test Set	68	67	1

The term label in Table 1 refers to the label assigned to a data set. Each data set was evaluated by a person and labelled accordingly based on the respective event video.

In machine learning, it is necessary to train the algorithm with (verified) test data. Table 1 shows the amount of data sets of the wrong-way driver event type that was used to train and test the respective algorithm.

A label contains:

- Time and date
- Class
- True positive or false positive

The assessment on the likelihood of event type X based on the present feature vector was carried out using widely available, tried and tested as well as documented classification algorithms. Various algorithms were tested to determine the best suited one. A description of the classifiers can be found in [9]. A comparison of the software-technical implementation of the classifier algorithms using "scikit-learn" can be seen in [10].

Table 2: Performance of different classifiers, wrong-way driver, Kirchdorf Tunnel

Classification algorithm	**Detection performance**
Nearest neighbour	0.985294117647
Linear Support Vector Machine (SVM)	0.985294117647
Linear Discriminant Analysis (LDA)	0.985294117647
Decision Tree	0.970588235294
Random Forest	0.970588235294
AdaBoost	0.985294117647
Radial Basis Function Kernel (RBF) SVM	0.985294117647
Naive Bayes	0.970588235294

The results of the probabilities for the wrong-way driver event type computed using various classifiers are shown in the right-hand column of Table 2. 1.0 equals 100% correct.

It is evident that several classifiers detect the wrong-way driver event type with a probability of > 98.5%

The approach within the project as well as all detailed events are listed in [11].

2.2. Phase II

Live system mounted in a road tunnel in operation; A (virtual) server on which various classifiers were tested was set up in parallel to the tunnel head server. See Table 3. The virtual server's software picked event notifications up from the tunnel head server, processed them in the sense of sensor fusion and entered the result into a data base together with the raw data from the individual sensor families for comparison. It did not interfere with the tunnel controls. Fears that the test system would be overloaded by the flood of data were unfounded.

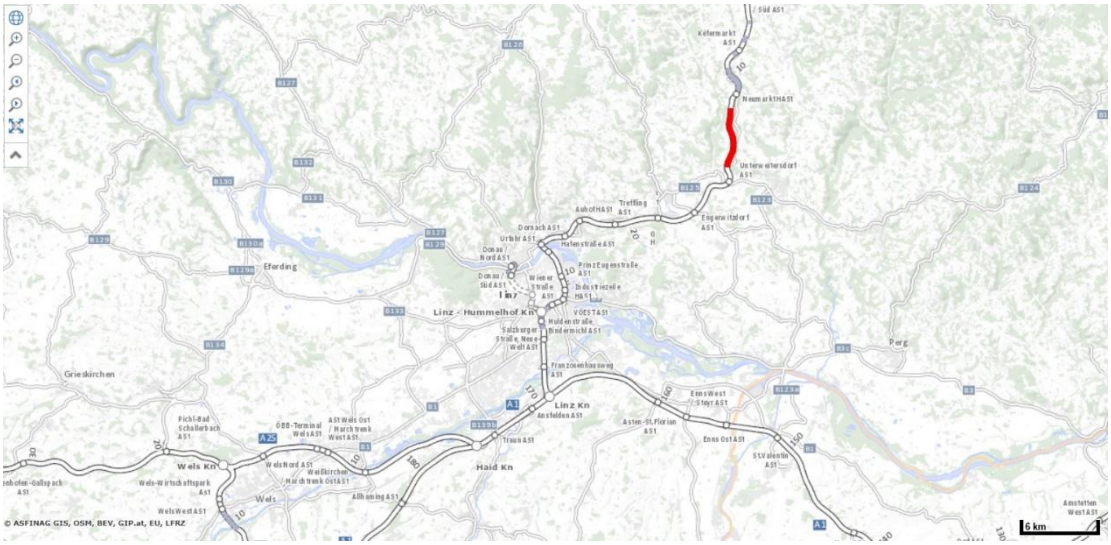


Figure 5: Screenshot ASFINAG GIS, S10 Expressway (Mühlviertler Schnellstraße) with Götschka Tunnel (red)

As a test object, the then-newest ASFINAG tunnel, the Götschka Tunnel along the S10 Mühlviertler Schnellstraße was chosen. The Götschka Tunnel is approx. 4.4km long, has two tubes (unidirectional traffic in each) and is equipped with combined ventilation (partially longitudinal, partially semi-transversal). Additionally, the Götschka Tunnel is equipped with "Acoustic Tunnel Monitoring" (AKUT). This fact was also relevant to the selection of this tunnel as a test object as this sensor type is also installed in the Kirchdorf Tunnel (Phase I), meaning that its configuration was very similar. In the project year of 2017, the average northbound traffic came in at approx. 18,000 vehicles, southbound at approx. 24,000 vehicles.

Results of sensor fusion using the example of the *wrong-way driver* event type.

Table 3: Performance of different classifiers, wrong-way driver, Götschka Tunnel

Classification algorithm	**Detection performance**
Nearest neighbour	0.848648648649
Linear SVM	0.848648648649
RBF SVM	0.816216216216
Decision Tree	0.816216216216

Random Forest	0.837837837838
AdaBoost	0.854054054054
Naive Bayes	0.383783783784
LDA	0.848648648649
dummyMostFrequClass	0.627027027027
dummyStratified	0.6
dummyUniformPrediction	0.540540540541

The results of the probabilities computed for the wrong-way driver event type based on various classifiers are shown in the right-hand column of Table 3. 1.0 equals 100% correct.

With the wrong-way driver event type the AdaBoost classifier reached its highest probability of > 85.4%.

Analysis and interpretation of Phases I and II

Both the Kirchdorf Tunnel and the Götschka Tunnel are tunnels of Risk Class III. This means that their equipment meets the same standard RVS requirements.

Nevertheless there are differences within the same classifiers which were tested for the wrong-way driver event type. Comparing the results of the classifiers in table 2 (Kirchdorf Tunnel) with the results of table 3 (Götschka Tunnel), it is evident that the results in the Götschka tunnel are consistently smaller for the same classifiers.

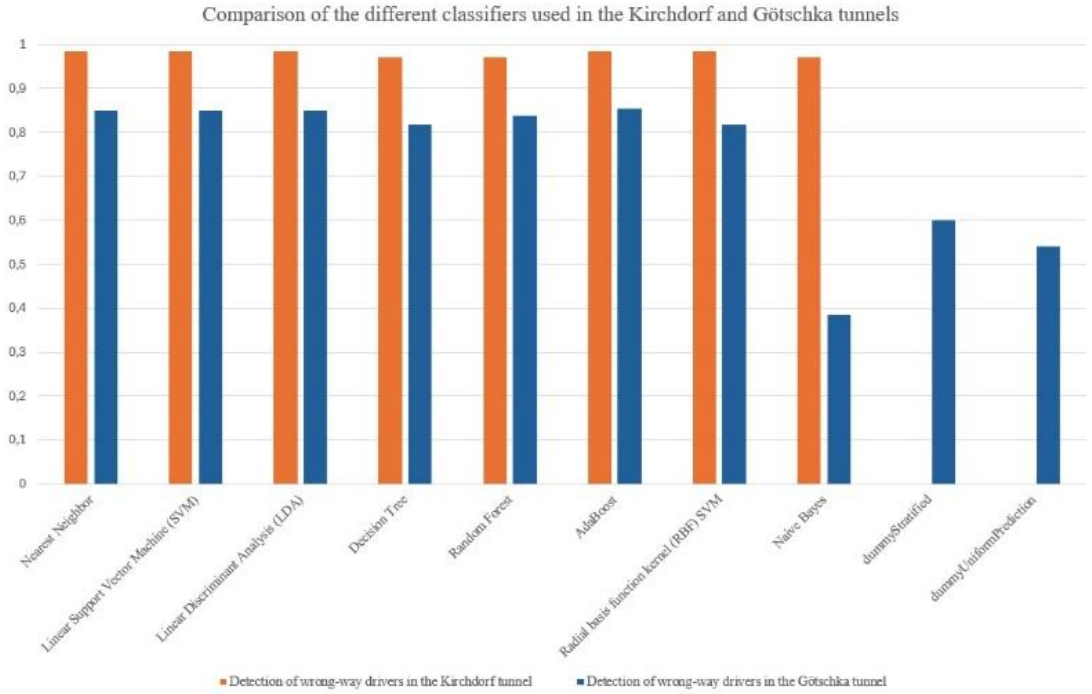


Figure 6: Diagram Comparison of the performance of different classifiers in the Kirchdorf / Götschka Tunnels

The differences in the performance of the algorithms were not looked at in detail in the framework of this project, but should be investigated in detail for all tunnels if one seeks to find a standard solution for the future. One possible explanation lies in the different tunnel cross-sections of the Prag-bound tube of the Götschka Tunnel which has three lanes instead of the two lanes of the Linz-bound / both tubes of the Kirchdorf Tunnel. One reason for this

could be that video detection, which contributes significantly to sensor data fusion, is (negatively) affected by the changes in tunnel geometry.

Both in Phase I and Phase II the AdaBoost classifier reached the highest detection probability.

2.3. Phase III

The aim of this project phase was to install a live system at an operational road tunnel and to present the results of the sensor data fusion in the responsible “regional traffic management centre” (rVMZ) of ASFINAG..

The focus of Phase III was less on checking the performance of classifiers / sensor fusion itself but more on making the results of sensor fusion available to the operators of the monitoring Regional Traffic Management Centre (rVMZ). The results of the sensor data fusion algorithm were displayed to the rVMZ's operators in addition to the conventional control technology (SCADA system). Using a specifically designed graphic interface, the operators were able to evaluate the correctness of the sensor data fusion algorithm once an event was processed. The system did not interfer with the tunnel controls or the rVMZ's control technology. The additional work for the operators in evaluating the results of the sensor fusion algorithm for its correctness yielded some highly valuable insights! The result: Many false positives were filtered out and all real alarms were displayed as such.

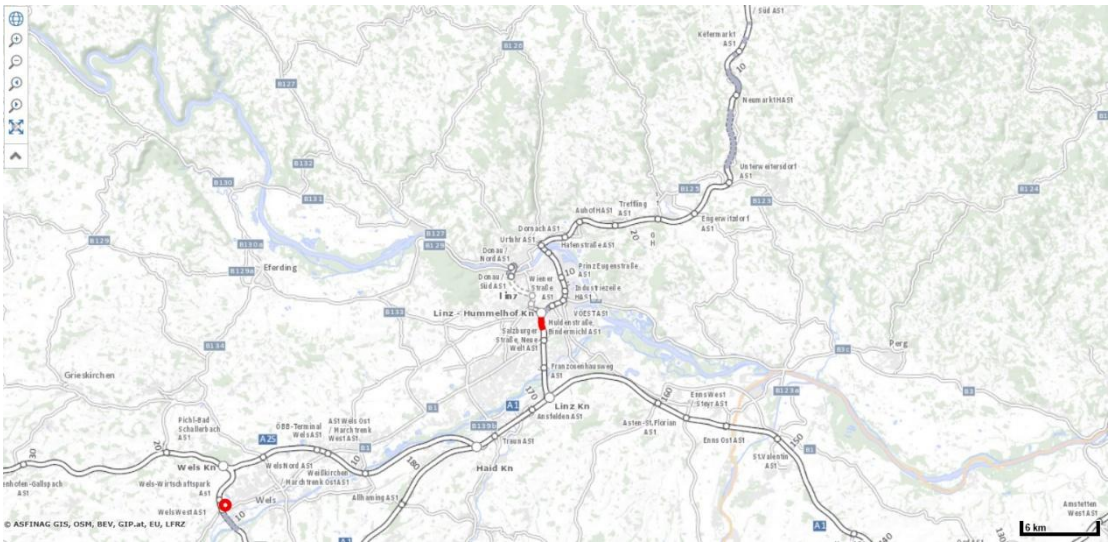


Figure 7: Screenshot ASFINAG GIS, A07 Highway (Mühlkreis Autobahn) with Bindermichl Tunnel (red)

The Bindermichl Tunnel along the A07 motorway (Mühlkreisautobahn) was chosen as a test object for Phase III. Many events occur in the Bindermichl Tunnel, which is very important for testing this novel system.

The Bindermichl Tunnel is an urban structure (rectangular cross-section) 1.06 kilometres long. It consists of two tubes with several lanes each as well as complex geometry with several accesses and exits. The tunnel has a north-south orientation and a daily average traffic volume of approx. 95,000 vehicles in the project year of 2023.

The Wels Regional Traffic Management Centre (rVMZ) is responsible for monitoring the tunnel.

Just like Phases I and II of the project, various classification algorithms were tested to determine the best-suited one.

The following classifiers were tested:

Table 4: Classification algorithms tested in the Bindermichl Tunnel

Nearest neighbour
K-Nearest neighbour
Logistic Regression
NG-Boost
XG-Boost
Decision Tree
Random Forest
Support Vector Machines

The analysis of the results data [12] showed that the NG-Boost classifier is best suited for this application.

“NGBoost generalizes gradient boosting to probabilistic regression by treating the parameters of the conditional distribution as targets for a multiparameter boosting algorithm. Furthermore, we show how the Natural Gradient is required to correct the training dynamics of our multiparameter boosting approach. NGBoost can be used with any base learner, any family of distributions with continuous parameters, and any scoring rule. NGBoost matches or exceeds the performance of existing methods for probabilistic prediction while offering additional benefits in flexibility, scalability, and usability.” [13]

The good result of the NGBoost algorithm confirms the performance of the Ada-Boost classifier in Phases I and II. It appears that the "boost" algorithm family is suited for the application of detecting events via tunnel sensor fusion.

Sensor data fusion results using the example of the *wrong-way driver* event type
Result of the (event video) evaluation by one person (data set "labelling", see Phase I) - all event types,
Test period 12.11.2023 to 11.01.2024

Table 5: Result evaluation by event videos, Bindermichl Tunnel

	Quantity
False events revealed by video analysis	648
True events revealed by video analysis	669
Total	1317

Algorithm results - all event types, test period 12.11.2023 to 11.01.2024

Table 6: Result of the algorithm, Bindermichl Tunnel

	Quantity
False events according to algorithm	648
True events according to algorithm	654
Exceptional special cases	15
Total	1317

In the test period of 12.11.2023 to 11.01.2024, the sensor fusion algorithm was able to compute 648 false positives as false in the Bindermichl Tunnel! All true alarms were correctly detected! The true alarms were displayed on the rVMZ test system's monitor and stored in a data base. Events detected as special cases were classified by a person based on event videos and showed certain deviations from common events. Example: Vehicle stopped on the hard shoulder - the

(usual) "stopped vehicle" event refers to a driving lane. Classified special cases: Reflection from wet roadway; snow on the roadway; stationary vehicles, triggered by the exit ramps. Although the special cases were identified and annotated by one person, they were not discussed further in this project.

3. SUMMARY AND CONCLUSION

The project showed that superpositioning the detection results of various sensor systems for one event type yields significant increases in detection probability while simultaneously lowering false positives. It is recommended to further pursue the principle of tunnel sensor fusion.
However, the following aspects should be investigated in follow-up projects:

- Test in tunnels with bidirectional traffic: All listed project phases were carried out in unidirectional tunnels (one tube per direction).
- Test which combination of sensor families suitable for an event type is optimal: Parameters of detection time, detection probability
- Direct access to the tunnel's subsystems. Collection of raw sensor data to prevent inadvertently neglecting the acknowledgement of past events (according to the system architecture for Austrian road tunnels)
- Consideration of roadway reflection
- Consideration of special tunnel geometries (access/exit ramps) and their effects on various event types
- Investigate the influence of tunnel geometries (number of lanes, round/rectangular cross-section, with/without false ceiling) on the important sensor family "automated video detection"
- Test how low the detection performance of individual sensor families may drop without negatively influencing the tunnel sensor fusion's overall performance
- What technologies are optimal for the individual sensor systems in making the best possible contribution to tunnel sensor fusion?
- Is it possible to optimate event detection time through (early) incorporation of unusual circumstances in the tunnel detected by tunnel sensor fusion?

One important insight is that the method shown here works in different tunnels that remain one-offs despite technical standardisation.
Classifiers from the family of boost algorithms appear to offer benefits over other classification algorithms for this application in terms of probability

4. REFERENCES

4.1. Literature

[1] Österreichische Forschungsgesellschaft Straße - Schiene - Verkehr (FSV) (2014): *RVS 09.02.22 Tunnel, Tunnelausrüstung, Betrieb und Sicherheit*; Vienna: FSV

[2] Kiebler, Jochen (2024): Lokalisierung und Fahrzustandsschätzung für eine voll-automatisierte elektrische Fahrzeugplattform,Wiesbaden, Germany: Springer Vieweg

[3] Kramer, Florian (2013): *Integrale Sicherheit von Kraftfahrzeugen*, Wiesbaden, Germany: Springer Vieweg

[4] Brand Andreas, Feser Michael, Happe Johannes, Schober Herbert (2011): *Ein Airbag-Steuergerät für mehr Fahrzeugsicherheit*, Bensheim, Germany, Tyco Electronics AMP GmbH

[5] Krey, Martin (2015): *Systemarchitektur und Signalverarbeitung für die Diagnose von magnetischen ABS-Sensoren*, Fakultät für Elektrotechnik, Helmut-Schmidt-Universität / Universität der Bundeswehr Hamburg

[6] ScienceDirect (2025): *Sensor Fusion (In subject area: Engineering)*, in sciencedirect.com,https://www.sciencedirect.com/topics/engineering/sensor-fusion, accessed on 2025-08-09
[7] Graf Franz, Rainer Harald, Rettenbacher Bernhard, Fišer Moritz (2011): *Akustisches Tunnelmonitoring – Verkehrsfreigabe für das weltweit erste System*, in: DAGA 2011, Düsseldorf
[8] S. Russell, P. Norvig, (2021): *Artificial Intelligence: A Modern Approach, Fourth Edition*, Hoboken: ISBN 9780134610993 (hardcover), Pearson Education, Inc. or its affiliates
[9] Yildirim, Soner; towards data science (2021): *15 Must-Know Machine Learning Algorithms*, https://towardsdatascience.com/15-must-know-machine-learning-algorithms-44faf6bc758e/ accessed on 2025-12-20
[10] scikit-learn developers (BSD License) (2007 - 2025): *Classifier comparison*, https://scikit-learn.org/stable/auto_examples/classification/plot_classifier_comparison.html accessed on 2025-12-20
[11] TB-Traxler GmbH (2014): Abschlussbericht „*Tunnelsicherheit durch intelligente Sensorfusion TSFu*“, Krems a.d. Donau; Published by Österreichische Forschungsförderungsgesellschaft mbH, Thematic Programmes, Verkehrsinfrastrukturforschung VIF2013, Vienna
[12] ECOexperts Automation GmbH (2025): *Tunnelsensorfusion Abschlussbericht*, Lebring, available at ASFINAG Alpenstraßen GmbH, Innsbruck
[13] Duan, Tony; Avati, Anand; Yi Ding, Daisy; Thai, Khanh K.; Basu, Sanjay; Ng, Andrew; Schuler, Alejandro; Stanford ML Group (2019-2020): *NGBoost: Natural Gradient Boosting for Probabilistic Prediction*, https://arxiv.org/abs/1910.03225 accessed on 2025-12-20

4.2. Figures

Figure 1: Principle of system architecture sensors in Austrian road tunnels
Figure 2: Screenshot ASFINAG GIS, Expressway S35 – Brucker Schnellstraße with Kirchdorf tunnel (red)
Figure 3: Extract from an event sensor matrix of the Kirchdorf tunnel
Figure 4: Zoom event sensor matrix, Figure 3
Figure 5: Screenshot ASFINAG GIS, Expressway S10 - Mühlviertler Schnellstraße with Götschka tunnel (red)
Figure 6: Diagram generated from table 4
Figure 7: Screenshot ASFINAG GIS, Highway A07 - Mühlkreis Autobahn with Bindermichl tunnel (red)

4.3. Tables

Table 1: Overview of test data for the wrong-way driver event type 60
Table 2: Performance of different classifiers, wrong-way driver, Kirchdorf Tunnel
Table 3: Performance of different classifiers, wrong-way driver, Götschka Tunnel
Table 4: Classification algorithms tested in the Bindermichl Tunnel
Table 5: Result evaluation by event videos, Bindermichl Tunnel
Table 6: Result of the algorithm, Bindermichl Tunnel

DEVELOPMENT OF A SYSTEMATIC APPROACH FOR EVALUATION OF THE CONDITION OF THE TUNNEL EQUIPMENT

[1]Anne Lehan, [2]Gerhard Hudecek, [3]Harald Kammerer, [4]Frank Heim

[1]BASt, Federal Highway and Transport Research Institute, DE
[2]ASFINAG Maut Service GmbH, AT
[3]ILF Consulting Engineers Austria GmbH, AT
[4]Die Autobahn des Bundes, DE

DOI 10.3217/978-3-99161-087-8-009 (CC BY-SA 4.0)
https://creativecommons.org/licenses/by/4.0/deed.de
This CC license does not apply to third party material (attributed to other sources) and content noted otherwise.

ABSTRACT

Road tunnels play a central role in ensuring the efficiency of the road transport network. Maintaining their availability and safety is therefore of great importance. To ensure this, the condition of the structures must be regularly recorded, documented and evaluated.

The structural inspection of road tunnels in the federal trunk road network in Germany is carried out according to a systematised procedure in accordance with DIN 1076, although the focus is primarily on the structural condition assessment. The question of the condition of the operational and safety-related tunnel equipment remains largely unanswered. This is recorded and summarised via regular maintenance and inspection. To date, it has not been summarised, e.g. by means of a condition mark as for the structure. In Austria, an evaluation methodology for operational equipment already exists, but it is to be updated based on experience gained from its application.

As part of a research project by the Federal Highway and Transport Research Institute, a system for assessing the condition of operational and safety equipment has therefore been developed. This provides a basis for forecasting the availability and necessary maintenance measures for the tunnel equipment in Germany and will thus be available in future as additional information alongside the condition rating for the structure.

For this purpose, practical evaluation criteria and an evaluation methodology were developed, and weighting approaches for the various equipment components were studied to take into account their relevance to tunnel safety. In addition, further parameters were defined to consider the importance of the tunnel in the road network for prioritization of measures.

This article presents the results of the study and highlights the challenges involved in developing and applying the system, the findings of the evaluation of the system on a specific structure, and the steps required to further refine the system for application.

Keywords: Condition mark, tunnel equipment, assessment method.

1. INTRODUCTION

The operational and safety equipment of road tunnels plays a central role in the availability and safety of the road transport network. While there is an established procedure for assessing the structural condition of tunnels in Germany in the form of DIN 1076 [1], there has been no comparable structured methodology for assessing tunnel equipment condition to date. The preparation of maintenance requirement forecasts is therefore based on the condition

assessment of the tunnel structure – the extensive renewal requirements for tunnel equipment have not been considered to date. Due to the scope of a tunnel's operational equipment, an underestimation of the maintenance costs for tunnel equipment and its cyclical renewal requirements can potentially lead to an incorrect underestimation of the follow-up costs [2].

The aim of the research project presented here [3] was therefore to develop an objective, comprehensible system for assessing the condition and predicting the availability of operational and safety-related tunnel equipment. The result is to be made available as additional information alongside the condition rating for the structure. This provides operators with a basis for deriving maintenance measures and strategies that better reflect the future funding requirements for maintenance demand forecasting.

The project was awarded to a consortium consisting of ILF and ASFINAG. ASFINAG's interest was mainly based on the fact that they had already been using a similar system for several years, but this system had weaknesses in the objectivity and systematics of the assessment areas, and participating in this project offered them the opportunity to update and further develop their methodology in accordance with RVS [4].

2. STRUCTURE OF THE TUNNEL EQUIPMENT

A structured classification of tunnel equipment is essential for systematic condition assessment and differentiated analysis of technical equipment. This two-stage classification is based on the specifications of RE-ING [5] and was further developed specifically during the course of the project. The aim was to create a uniform yet adaptable structure that both ensures comparability between different tunnel systems and considers the individual characteristics of road tunnels.

The functional blocks according to RE-ING Part 3 Section 3 provide a basic structure. Based on this, the functional blocks are subdivided according to the associated trades. The functional blocks represent higher-level operational functions such as lighting, ventilation or communication, while the trades, as the next smallest evaluation units, represent specific technical systems such as jet fans, emergency call systems or luminance measurements.

Table 1 shows the structure of tunnel equipment using the example of the ‘ventilation system’ functional block.

Table 1: Structuring the tunnel equipment into functional blocks and trades using the example ‘ventilation system’

functional block	trade
ventilation	Flow velocity measurement
	Jet fans
	Ventilation control
	Vibration measuring instruments
	Axial fans
	Ventilation flaps
	Ventilation of escape routes
	Fog measurement
	Wind measurement

The trade list usually contains around 80 trades and provides a good starting point for the majority of German road tunnels. Due to the individual nature of tunnels, minor adjustments may be necessary in practice. In addition, the assessment methodology always offers the

option of subdividing the trade list into even finer granularity if necessary (e.g. at the level of components or parts).
This approach enables a differentiated condition assessment at the functional level. At the same time, a flexible framework was deliberately created in the project in order to be able to map tunnel-specific equipment variants.

3. EVALUATION CRITERIA FOR TRADES

The core of the assessment methodology consists of five key assessment criteria, which are used to enable a differentiated and objective assessment of the technical condition of the individual trades. These criteria were defined based on literature research, expert interviews and practical experience and form the basis for determining the condition rating. Each criterion highlights a specific aspect of the performance of technical systems in tunnel operation. The five assessment criteria are defined as follows:

- The **functional condition** describes the ability of a component to reliably fulfil its intended function in tunnel operation. This assessment is based on functional tests, operational observations and, where applicable, measured values.
- The **substantial condition** assesses the physical condition of the components. This includes aspects such as corrosion, material fatigue, mechanical damage or electrical defects. The assessment is usually carried out visually or by means of simple measurement procedures as part of maintenance and inspection.
- The **susceptibility** of a component to failure is assessed based on historical failure data or empirical values. Both the frequency and the effects of failures are considered, thus allowing conclusions to be drawn about the reliability of a component.
- **Spare parts availability** describes whether sufficient spare parts are available or can be procured for a component. It considers both stock levels and the delivery capacity of manufacturers or suppliers.
- Finally, **support availability** assesses whether the necessary technical expertise is available to operate and maintain the trade throughout its life cycle. This includes both internal expertise and external support from manufacturers or service providers. For IT and software-based systems, the availability of updates and security patches is also considered.

For the practical application of this assessment logic, a structured assessment sheet was developed in the project, which serves as a central tool for carrying out the condition assessment (see Figure 1).

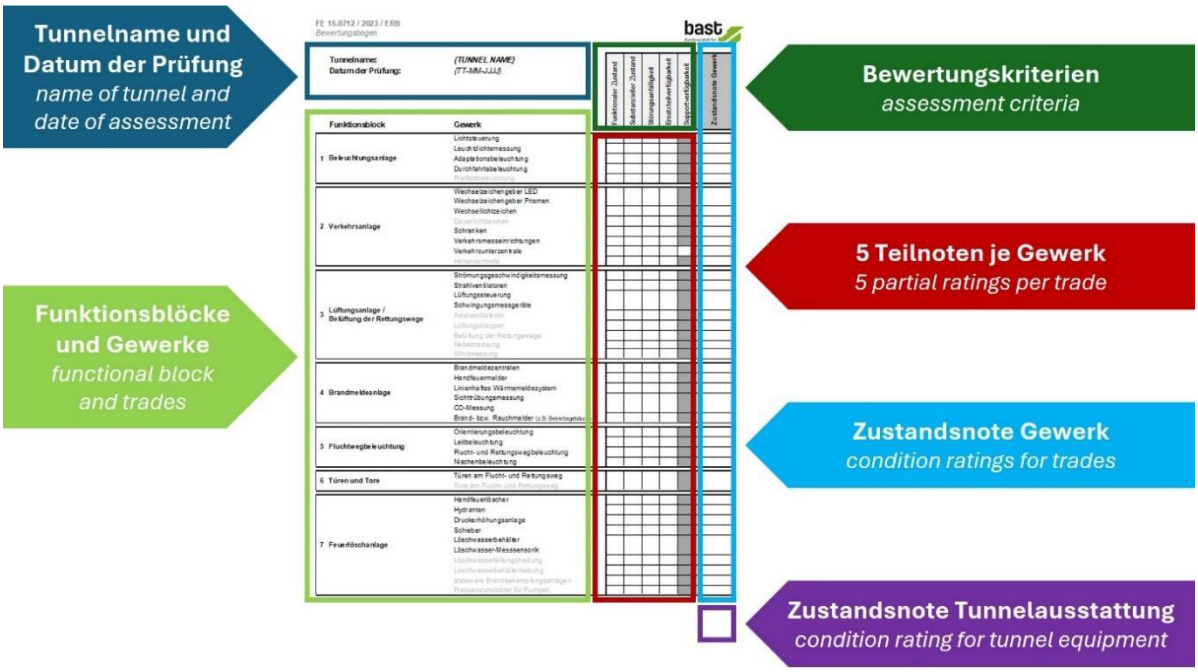


Figure 1: Overview of the contents of the evaluation form

The evaluation sheet is structured as an MS Excel file and contains a tabular overview of all functional blocks and the associated trades. For each trade, the five sub-scores for the evaluation criteria must be entered during the evaluation. The 'condition score for trades' and the 'condition score for tunnel equipment' are calculated automatically using predefined aggregation methods. In addition to the overview sheet, the evaluation form contains a template for an explanatory sheet that provides space for photographic documentation and textual comments. This increases the traceability of the evaluation and supports quality assurance.

4. GRADING OF THE EVALUATION CRITERIA

As part of the assessment methodology developed, a uniform five-point grading scale was introduced. The scale ranges from grade 1 ('very good') to grade 5 ('poor') and allows for a differentiated yet intuitive assessment of the condition of technical tunnel equipment. The choice of an odd-numbered scale with a neutral middle grade was made deliberately to enable a balanced assessment without having to force a positive or negative bias. A sixth level, as provided for in DIN 1076 with grade 6 ('unsatisfactory'), was not adopted, as such a poor condition in the area of tunnel equipment would usually be accompanied by an immediate suspension of operations and is therefore outside the scope of the methodology.

A specific grading system was developed for each of the five evaluation criteria. These grading systems consist of clearly defined descriptions for each sub-grade level and specific control questions that assist the user in evaluating the individual criteria. The control questions are formulated in such a way as to allow for the most objective and comprehensible classification possible. Depending on the criterion, logical links such as AND or OR conditions are used to adequately reflect the complexity of technical relationships. Where possible, the grading systems have been supplemented with practical examples.

Figure 2 shows a schematic representation of a rating system with control questions using the example of the evaluation criterion 'functional condition'.

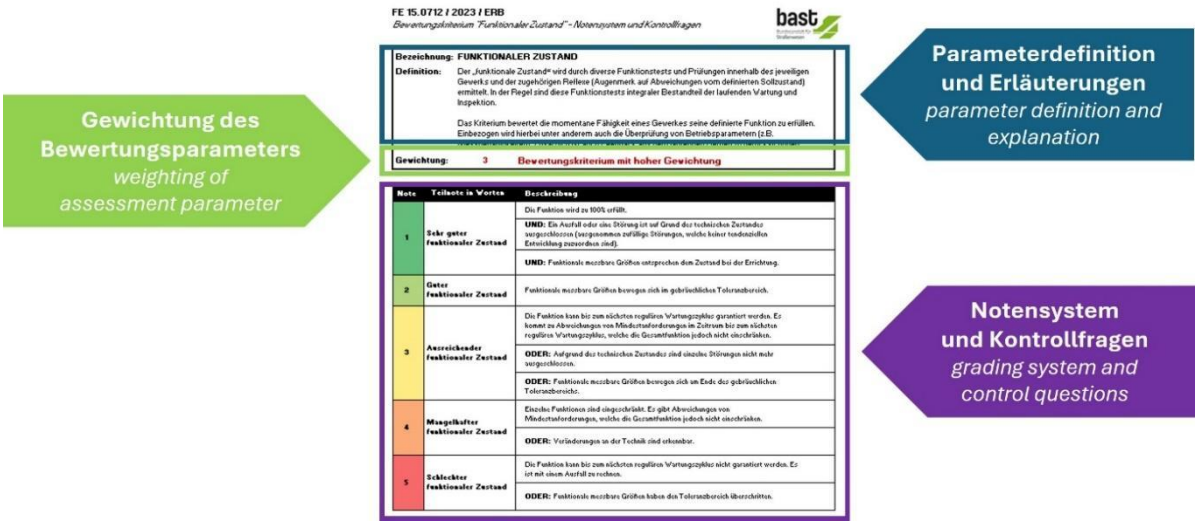


Figure 2: Presentation of the contents of the 'grading system with control questions' using the example of the assessment criterion 'functional condition' in the evaluation form

The five grading systems are an integral part of the evaluation sheet, which serves as a central tool for applying the methodology. In addition to the overview sheet for evaluating all trades (see Figure 1), the evaluation sheet for each evaluation criterion also includes the corresponding grading system with control questions for each sub-grade.

5. AGGREGATION OF CONDITION GRADES

Another important element of the assessment methodology is the aggregation of condition ratings, which is carried out both at the level of individual trades and for the entire tunnel equipment. This process is shown schematically in Figure 3.

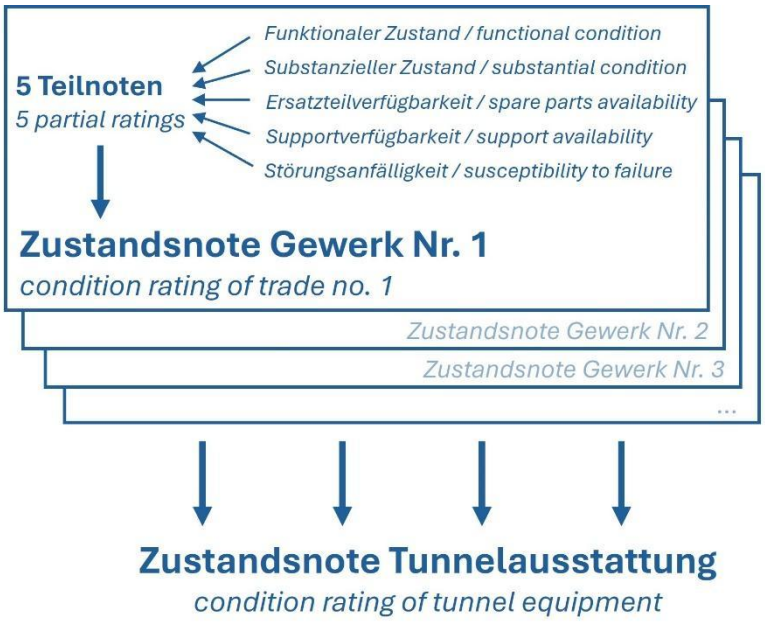


Figure 3: Schematic representation of the aggregation of the different condition marks

For each trade, a condition score is first calculated – the so-called ‘trade condition score’ – which combines the five evaluation criteria mentioned above. For this purpose, weightings for the individual criteria were determined in an expert workshop to reflect their respective relevance for safe and reliable tunnel operation. The functional condition is given the highest

weighting (3), followed by the substantial condition, susceptibility to failure and spare parts availability (2), while support availability is given the lowest weighting (1).

The weighted aggregation of these five evaluation criteria already results in a condensed, objective score after this step, which can be used both for short-term action planning and for strategic maintenance management. In practice, the ‘condition rate’ allows for the targeted prioritisation of maintenance and renewal measures, especially for components with a critical impact on operational safety. It can be used as a basis for decisions on adjusting maintenance intervals, planning replacement investments or initiating refurbishment measures.

In addition, the ‘condition rating for trades’ provides the basis for the overall assessment of the entire tunnel equipment and its consolidation into the so-called ‘condition rating for tunnel equipment’. Various methods were examined in the project for this aggregation, including simple averaging, weighted averages by functional blocks, and methods based on maximum values or median sets. The aim was to find a method that considers both the technical relevance of individual components and the heterogeneity of the tunnel facilities.

The ‘condition rating for tunnel equipment’ is available as an additional optional condition mark for road tunnels. It serves, for example, as an integral part of the overall assessment of tunnel equipment and can be used in aggregated form to derive long-term trends or to compare different tunnel facilities. In addition, it can serve as an indicator for budgeting in the context of resource requirement planning or to support transparent communication with supervisory authorities and internal stakeholders.

6. PRACTICAL APPLICATION

The assessment methodology developed in the project was specifically designed for practical application in operational practice and validated using a real German road tunnel. Particular emphasis was placed on ensuring that the methodology was not only theoretically sound, but also operationally feasible. The methodology was applied in collaboration with experts from tunnel operations, which provided practical feedback on the comprehensibility, manageability and informative value of the assessment logic. This feedback was directly incorporated into the optimisation of the methodology and led to a noticeable improvement in its practical applicability.

To facilitate practical application, a structured evaluation form has been developed as an MS Excel file, which will be available in future and will enable the evaluation of individual trades based on defined criteria and control questions.

The methodology was designed to be flexible and adaptable to different tunnel types and operator structures, thus enabling broad applicability and acceptance in the German federal highway network.

7. SUMMARY, CONCLUSION AND OUTLOOK

The project presented here makes a fundamental contribution to optimising the maintenance management of road tunnels by providing a structured and objectifiable methodology for recording and evaluating the condition of operational and safety-related tunnel equipment. While an established procedure exists for the structural substance in the form of DIN 1076, there has been no comparable approach for technical equipment to date, even though this contributes significantly to the availability and safety of tunnel facilities. The methodology developed is based on a clear structure of functional blocks and trades, a five-stage assessment logic with specific criteria, and a comprehensible aggregation of results. Validation in a real tunnel confirmed the practicability and relevance of the system but also showed that further

evaluations of additional structures are necessary with regard to the assessment scheme. This further development is necessary in order to test and apply the assessment system with different criteria (e.g. traffic type, lengths, level of equipment) and with regard to its robustness under different technical and organisational conditions. In particular, the aggregation methods for determining the overall condition assessment should be further validated and, if necessary, adapted.

In the long term, the plan is to provide a methodology at federal level that offers a uniform assessment basis for all tunnel facilities in the German federal highway network. In Austria, the results of the study will be used to improve the existing integrated asset management tools.

The results of the project provide a solid basis for maintenance planning decisions by enabling a more accurate representation of future funding requirements for maintenance demand forecasting and providing an improved planning basis for maintenance measures. In addition, the results make an important contribution to the digitalisation of transport infrastructure by digitally mapping the condition assessment process in a first step, thus laying the foundations for a digital way of working.

8. REFERENCES

[1] DIN 1076, Ingenieurbauwerke im Zuge von Straßen und Wegen, Überwachung und Prüfung, Ausgabe 1999-11.

[2] Lehan, A.; Thewes, M.: Einfluss der Nutzungsdauer auf die Lebenszykluskosten von Tunnelbauwerken, Tagungsband zum 9. BASt-Tunnelsymposium, Berichte der Bundesanstalt für Straßenwesen, BASt-Bericht B 157, abrufbar unter: https://www.bast.de/DE/Publikationen/Berichte/unterreihe-b/2022-2021/b-157.html

[3] Bundesanstalt für Straßen- und Verkehrswesen (BASt), Forschungsprojekt FE 15.0712 / 2023 /ERB: „Entwicklung einer Systematik zur Verfügbarkeitsbeurteilung der Tunnelausstattung“, noch nicht veröffentlicht.

[4] Österreichische Forschungsförderungsgesellschaft Straße – Schiene – Verkehr: Qualitätssicherung bauliche Erhaltung – Überwachung, Kontrolle und Prüfung von Kunstbauten – Straßentunnel – Betriebs- und Sicherheitseinrichtungen (RVS 13.03.41), 23.07.2014

[5] RE-ING Bundesministerium für Digitales und Verkehr, „Richtlinien für den Entwurf, die konstruktive Ausbildung und Ausstattung von Ingenieurbauten (RE-ING)“, März 2023

METHODOLOGY FOR THE PERFORMANCE ENHANCEMENT OF LONGITUDINAL VENTILATION SYSTEMS DURING TRANSIENT STAGE OF A FIRE

Miguel del Moral, Alexander Gratch, Davide D'Eustacchio, Álvaro Meneses, Justo Suarez

Soler&Palau Ventilation Systems SLU, ES

DOI 10.3217/978-3-99161-087-8-010 (CC BY-NC 4.0)
https://creativecommons.org/licenses/by/4.0/deed.de
This CC license does not apply to third party material (attributed to other sources) and content noted otherwise.

ABSTRACT

Ventilation systems in tunnels are designed for a maximum fire load. However, during the initial stages of a fire, the fire would not be completely developed and the activation of the system at maximum speed may disrupt smoke stratification, compromising occupants' evacuation.

This paper presents a methodology to assist designers in defining the optimal activation protocol for a longitudinal ventilation system, focusing on the response of the ventilation system during the transient stage of the fire. This methodology would aim to:

1. Enhance Available Safe Egress Time (ASET) over Required Safe Egress Time (RSET).
2. Assess the effectiveness and robustness of the ventilation system and its response in the design stages.
3. Help to define the safest procedures for the control centers, advising on how to operate the ventilation system depending on the real conditions in the event of a fire.

The methodology is presented in a case study, which is provided with a longitudinal ventilation system designed to achieve a specific air velocity for a given fire load. This methodology is not limited to a specific critical/confinement velocity model and a different formulation is also assessed in the process for comparison.

For the case study and the considered model, critical/confinement velocity is numerically estimated along time to serve as starting point in the process of defining the activation protocol for the ventilation system. This considers both sequential activation for jet fans and activation through variable speed drive.

Once the activation protocol is defined, the effectiveness of the response is assessed through Computational Fluid Dynamics (CFD) software, and the results are analyzed together with models for Required Safe Egress Time.

Keywords: Smoke control, critical velocity, CFD, ASET, transient-stage.

1. INTRODUCTION

Longitudinal ventilation systems are generally designed to overcome a certain critical or confinement velocity, and different models are available ([1], [2]). Both concepts, critical and confinement velocity, refer to the air inlet velocity necessary to effectively sweep downstream the smoke generated by a certain fire load (completely or allowing backlayering, respectively),

which would naturally provide for tenable conditions upstream but would inevitably disturb smoke stratification, affecting visibility and temperature after the fire. **Figure 1**, obtained from a real test, illustrates the fast destratification produced when jet fans are activated.



Figure 1: Smoke layer on a real test at TST. From left to right and up to down: an instant before the ventilation activation; 5 seconds after; 10 seconds after; 15 seconds after

The approach commonly used to prevent smoke stratification disruption consists of activating jet fans far away from the fire or, in some cases, even not activating any at all in the first stages, accepting smoke spread in all directions, and activating the ventilation only after a delay long enough to allow some time for occupants' evacuation. However, that time may not necessarily be enough to ensure all occupants' safe egress. Furthermore, while allowing smoke spread in both directions generally suffices to provide acceptable conditions at breathing height in the vicinity of the fire, after some meters the smoke layer tends to go to lower levels and, eventually, to cover the whole section of the tunnel, which is especially critical for occupants distant from the fire and with a reaction time much larger than those close to the fire. That strategy could also be particularly dangerous in sloped tunnels, where smoke would spread even faster in upward direction.

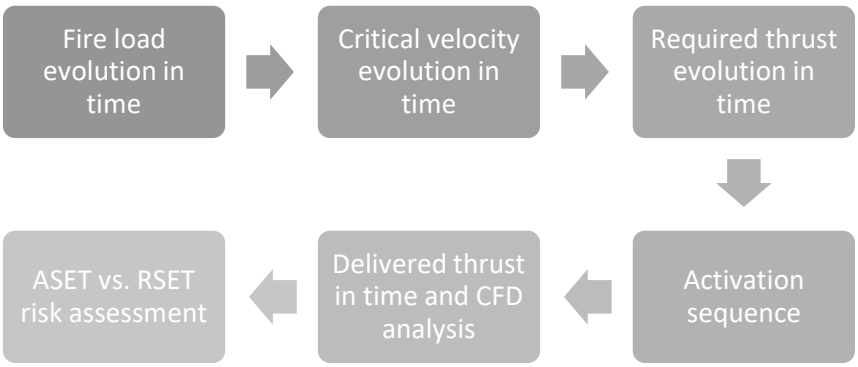


Figure 2: Methodology workflow.

That approach also transfers the responsibility of the proper activation of the system to the control center, which we can expect will be under great stress in the case of the fire, and would

have to deal with many more variables than the activation of the ventilation system. Although manual activation should always be available for control centers to properly adjust the response depending on the actual on-site conditions, relying solely on it also gives much more space for human mistakes.

Alternatively, this paper proposes a methodology (depicted in **Figure 2**) to assess the definition of a sequence of activation for the ventilation system, that would start at the very moment of the fire detection, and evaluate its risk implications for occupants.

The methodology is presented in a case study and estimates theoretically the required thrust at each moment depending on the growth type of the fire [3]. However, this methodology could also be used to implement automatized systems able to adapt the ventilation system response to the on-site real-time measurements related to the fire load, such as the temperature [4] or the air velocity in the inlet of the tunnel.

2. CASE STUDY

The methodology will be applied in a virtual unidirectional tunnel with a longitudinal ventilation system and the following characteristics:

Table 1: Characteristics of the case study tunnel

Parameter	Value
Width	12.8 m
Height	6.4 m
Length	600 m
Slope	0%
Lanes	2
Evacuation doors every	200 m (100 m of evacuation distance)
Rows of jet fans	7
Jet fans per row	2
Distance between rows	90 m
Lateral distance between jet fans	4 m
Jet fan thrust	809 N

The ventilation system was sized to provide tenable conditions (visibility and temperature levels compatible with life) upstream in case of a fire up to 50 MW while having slightly adverse wind conditions and dense traffic. Also, a 10% thrust redundancy was considered.

For simplicity purposes, a short tunnel with no slope was considered, although this methodology could be deemed especially useful in those cases. The simulation was carried out not considering the presence of cars, apart from the vehicle in flames, which would correspond to a large bus (50 MW). The presence of wind may have a significant impact in air velocity in short tunnels, but wind was not considered to allow a clear assessment of the methodology and the activation sequences analyzed. Consequently, the pressure drop inside the tunnel in the considered scenario is below the total pressure drop that the ventilation system would be able to overcome.

CFD simulations were carried out using FDS. Fire detection is considered to be produced by visual identification by the control center, at the beginning of the simulation. Fire growth is considered to start at the same instant for simplicity purposes.

3. METHODOLOGY

3.1. Analytical assessment: required thrust vs. delivered thrust

The methodology rests upon the concept of adapting the delivered thrust at each moment, adjusting the number of active fans and/or their speed using variable speed drive (VSD), to meet the thrust requirements of the tunnel in order to provide critical/confinement velocity upstream the fire, and consequently, sweeping the smoke in one direction (or delaying its upstream spread).

Critical velocity is estimated using the Thomas-Kennedy [1] and Beyer's models [2]:

$$V_c = K_1 K_g \left(\frac{gHQ}{\rho C_p A T_f} \right)^{1/3} \tag{1}$$

$$U_c = K_F \left(\frac{g L_n^3}{D_h^2} \frac{\Delta T_p}{T_a + \Delta T_p} \right)^{1/2} \tag{2}$$

Critical and confinement velocity would depend on the fire's heat release rate (HRR), which increases over time, typically following an αt^2 curve, with a growth coefficient determined by the fire development rate. To estimate the fire evolution, an ultra-fast fire (as defined by [3]) was considered for the case study.

Once the heat release rate at each point in time is defined, critical/confinement velocity is calculated for that moment, and the required upstream velocity can be plotted in time:

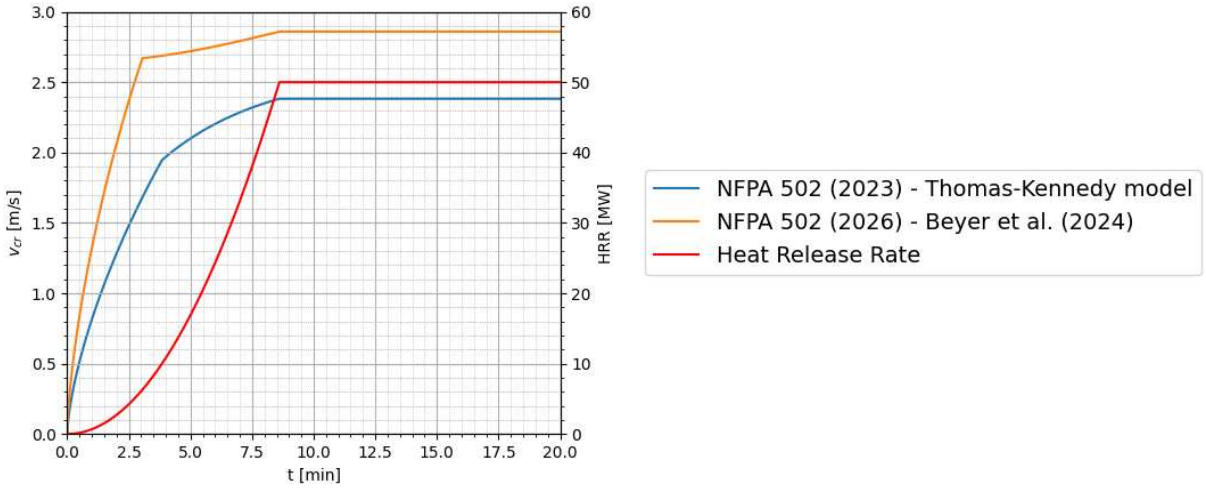


Figure 3: Required upstream velocity (critical or confinement) and HRR along time.

Different critical velocity models are plotted for information, but it is not the purpose of this paper to look into their differences. Also, the depicted methodology can be applied to both. Therefore, for practical purposes, the rest of the methodology is described using only Beyer's model for critical velocity.

For certain conditions (i.e. wind load and fire load and location) the confinement velocity would define the air profile in the tunnel, as well as the pressure drop between the inlet and the outlet. With this information, the required thrust could be easily calculated through momentum conservation. Following traditional PIARC's handbook formulation [5]:

$$F_{required} = \sum F_j = \left(\Delta p_{veh} + \Delta p_{tu} + \Delta p_{MT} + \Delta p_{fire} + \Delta p_{th} \right) \cdot A_T \tag{3}$$

Then, the real challenge arises: to deliver the required thrust at each point in time. This may be done with sequential activation of the jet fans and/or adjusting their speed. There are many possible combinations (see **Figure 4**), but a much smoother correlation can be achieved using both VSD and sequential activation. **Figure 5** shows one specific activation sequence (tagged as AS 4) considered for the case study, depicting each jet fan row's ramp-up time activation, referenced in percentual over its own maximum thrust capacity.

At this point a general remark is needed: meeting the required thrust with the delivered thrust would provide for tenable conditions upstream of the fire but would not necessarily avoid smoke destratification. For that purpose, lower air velocities may be required, depending on the case, hence delivered thrust will have to be, more often than not, below the required thrust.

There are available models to predict smoke destratification [6], however they were not assessed in the development of this paper (although the authors consider that they may be useful for further analysis).

Instead, CFD simulations were used to verify the performance of the considered activation sequences (defined in 3.2).

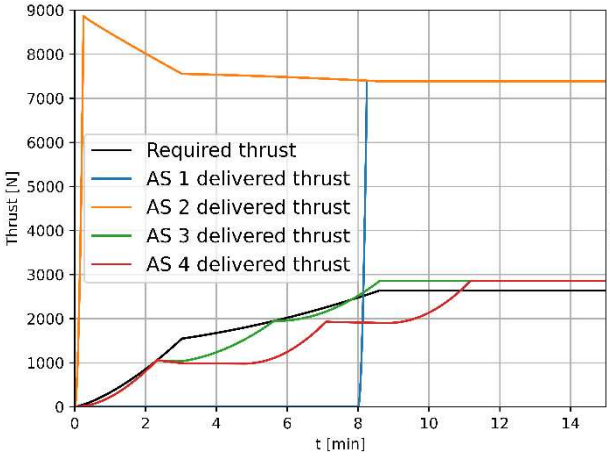


Figure 4: Required thrust vs. delivered thrust with different activation sequences.

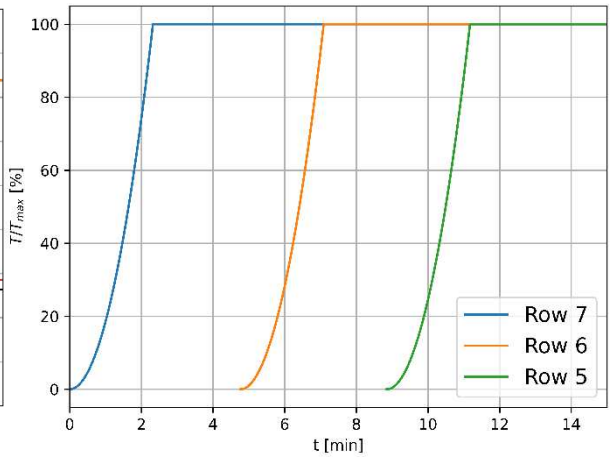


Figure 5: Activation Sequence 4, with percentual activation in time of each row of jet fans.

3.2. Numerical assessment: CFD simulation

For comparison purposes, four Activation Sequences (AS) are considered:

1. AS 1: the ventilation system remains off up to 480 s, when it is activated at high speed, all the fans at the same time.
2. AS 2: the ventilation system is activated at maximum speed upon fire detection.
3. AS 3: the ventilation system is activated sequentially and with VSD, aiming to provide closeness between the delivered thrust and the required thrust during transient stage.
4. AS 4: the ventilation system is activated sequentially and with VSD, delivering thrust below the required thrust during transient stage.

The CFD results for the different AS are show in **Figure 6**. Visibility at 1.8 m from the floor is shown, since it represents one of the critical indicators for tenability conditions for occupants' evacuation.

Note that AS 2 delivers a thrust much bigger than required thrust (see **Figure 4**). This is because the ventilation system was sized for a fire load higher than the one considered in the case study. The authors defined this intentionally to give proof that the bigger is not always the better: especially when a lot of thrust is available, a fast activation sequence may affect the occupants' visibility levels, hindering occupants' evacuation downstream the fire.

CFD results show that delaying the activation of the jet fans maximizes the time in which tenable conditions are provided downstream of the fire (right side of the tunnel). However, in unidirectional tunnels, occupants after the fire (right side of the tunnel) are generally the fastest ones to evacuate, since they usually can escape by driving. Results also show that after a certain time (around 420 s) the smoke layer goes down naturally in both directions, dropping visibility very quickly. This is especially dangerous upstream of the fire, where occupants would probably escape on foot and would take longer to react.

On the other hand, AS 3 and AS 4 can maintain clean conditions upstream permanently, but downstream visibility drops a bit sooner than in AS 1, so eventually, an ASET vs. RSET assessment is necessary to evaluate if the improvement in the upstream or downstream conditions can minimize the risk the occupants will be exposed to in the event of a fire.

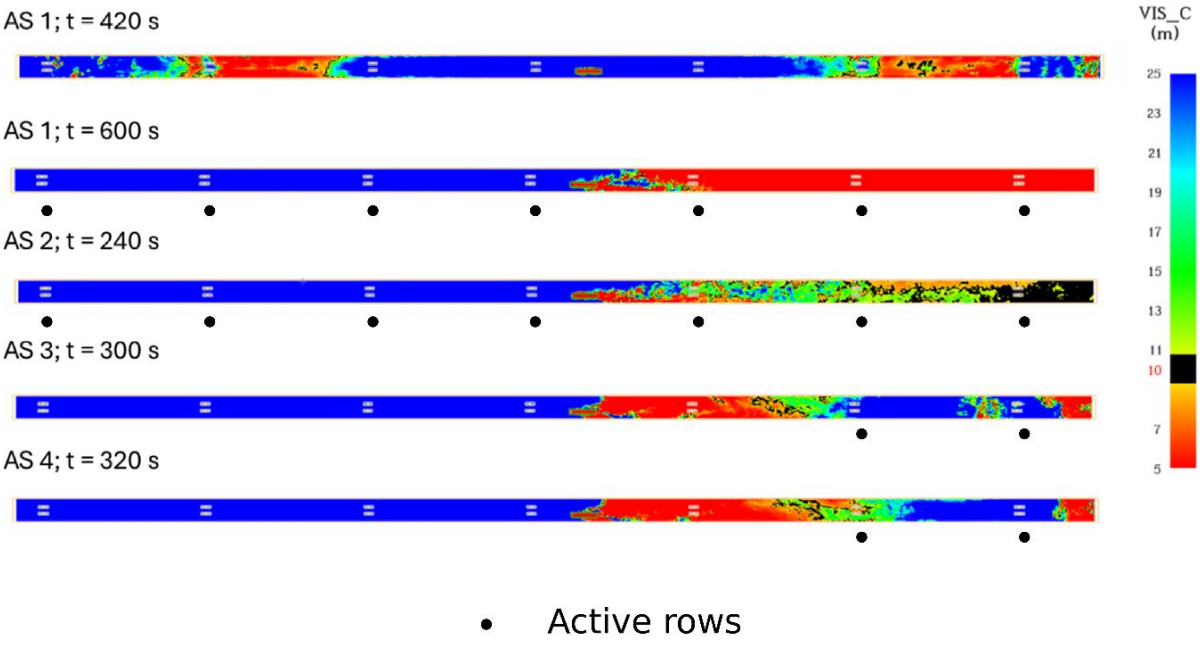


Figure 6: Visibility at 1.8 m from the floor on different moments, for the AS considered.

3.3. Risk assessment: ASET vs. RSET

For the Available Safe Egress Time (ASET) vs. Required Safe Egress Time (RSET) analysis, MARTE methodology [7][8] is considered.

The CFD results for each AS are simplified into a one-dimensional visibility profile, where the minimum visibility in the cross-section of the tunnel is saved over time. When visibility at some longitudinal point of the tunnel drops below 20 m, tenable conditions for the occupants are considered to be no longer provided.

This allows to plot when the conditions become unsafe at every point along the tunnel, which at the same time can be compared with the movement of the occupants in the tunnel and, consequently, assess how much time (and how many of them) spend in unsafe conditions.

For the occupants' movement estimation, a random occupant distribution is considered, with the following conditions:

- Walking pace: from 0.6 (people with reduced mobility) to 2 m/s (fast pace) before the fire. From 1 m/s (average walking speed) to 5 m/s (slow drive) after the fire.
- Reaction time: from 0 seconds (people after the fire already exiting by car the tunnel) to 5 minutes (people before and far away from the fire with a significant attachment feeling to the car).

Both unsafe conditions along time in the tunnel length and people movement are represented in **Figure 7** and **Figure 8**. Downstream of the fire, escape is considered to be carried out by car in dense traffic conditions. Evacuation routes are plotted as pointed vertical lines. Occupants' movement is also represented by lines, which appear continuous or dashed depending on whether they are located upstream or downstream of the fire, respectively. These lines become pointed once they cross an evacuation door (given that normally occupants should be able to escape through them).

These figures show that, with AS 1, occupants will be exposed to smoke inhalation especially upstream of the fire, where escape by foot is expected. Once the ventilation is activated, tenable conditions are recovered after a time that could be estimated with the following expression, where k is a coefficient greater than 1 and that would depend on each case:

$$t_{recovery} = k \cdot \frac{d_{fire-entry}}{V_{inlet}} \tag{4}$$

On the other hand, ASET vs RSET analysis for AS 4 shows permanently tenable conditions upstream the fire and a slight exposure downstream of the fire, for the occupants immediately after the vehicle in flames on their way to the exit.

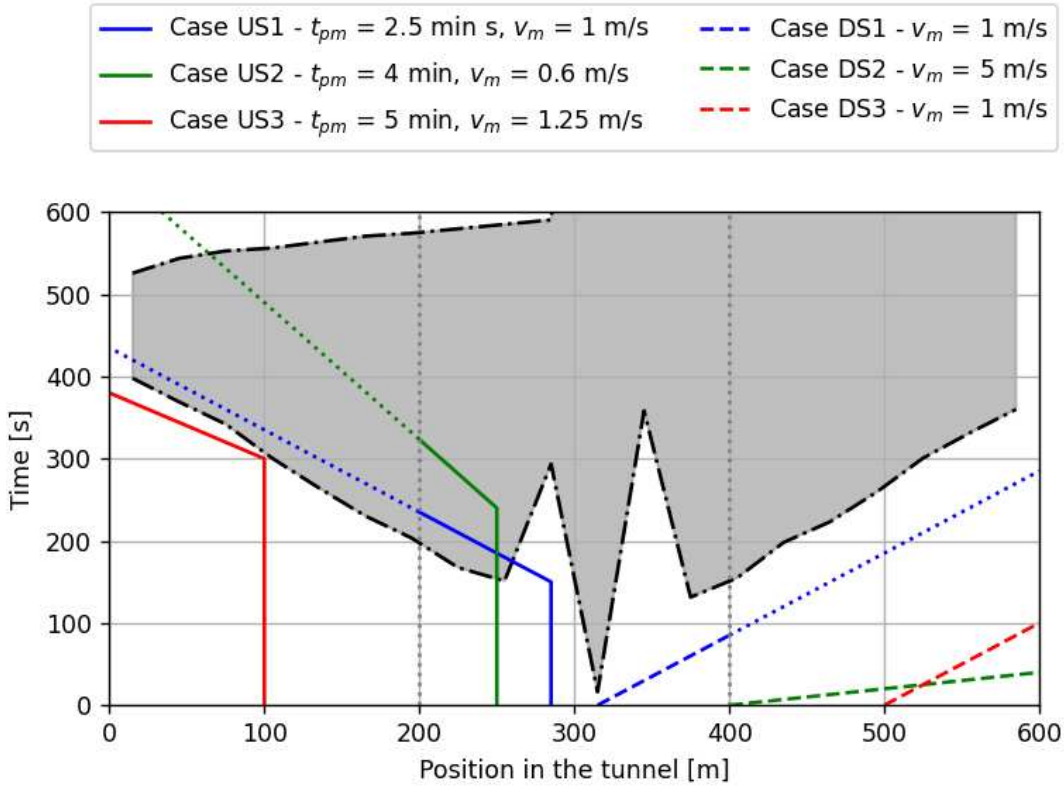


Figure 7: Tunnel conditions along time in the tunnel length and occupants' movement for AS 1

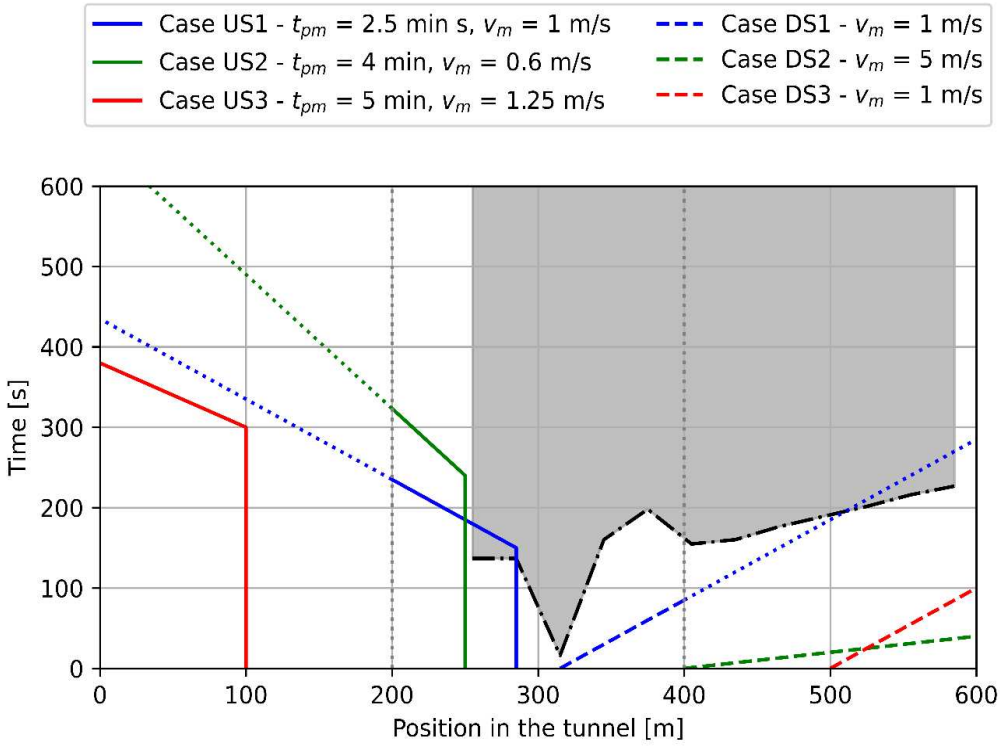


Figure 8: Tunnel conditions along time in the tunnel length and occupants' movement for AS 4

4. SUMMARY AND CONCLUSION

Delaying activation of the ventilation system (AS 1) in case of a fire in a unidirectional tunnel could lead to fatal results, especially for the occupants before the fire. A fast activation at maximum speed (AS 2), on the other hand, would provide good conditions before the fire but would worsen conditions after the fire, hindering vehicles and occupants' egress in that area. An automatic gradual response in which the ventilation is smoothly activated (AS 3 and AS 4) could optimize conditions upstream of the fire, maximizing the available time for the occupants before the fire while maintaining the available evacuation time downstream. It also avoids transferring the whole responsibility for the ventilation activation system to the control centers, giving them more tools to respond in the event of a fire and helping to prevent human mistakes. There are many options for this sequential activation, and some of them could even rely on on-site real-time data, adjusting the response depending on the actual fire load.

The methodology presented allows to mathematically determine, for a specific fire load model, the required thrust to reach critical velocity at each point in time and thus define a baseline to be met by the fans at every moment. The methodology does not address how to define the activation sequence but allows the consideration of any activation protocol. That activation protocol is then analyzed using CFD simulations to provide an ASET/RSET risk assessment, which eventually can lead to a risk comparison between different activation sequences.

The paper neither dives into proportional-integral (PI) forms of adjusting fan velocity on-site so measured air velocity meets a specific value, but rather on the tools to evaluate, at project stage, the performance of any specific activation sequence (which does not necessarily need to be PI) and their risk to occupants during the first stages of the fire, which may lead to compensation actions, like using information technologies to ensure safe occupant's egress (such as phone advice to enhance evacuation time and image recognition software to evaluate how many cars are still in the tunnel after the fire).

Although the methodology focuses on analysis purposes, the mathematical model presented could also be used to estimate the required thrust or critical velocity in a real fire scenario with on-site temperature readings. However, for that case, an additional physical model to translate those readings into Heat Release Rate (HRR) should be included. This could be interesting both for tunnels where there are no air velocity readings (and thus no PI is possible) and for those where there are velocity readings, in which case the mathematical model could help to set up a velocity instruction (which does not necessarily need to meet critical or confinement velocity, since this may lead to destratification of the smoke layer in early stages).

For the analyzed case study, the methodology proved to be useful in assessing the risk the occupants are exposed to, allowing a clear comparison of the risk implications between different activation sequences. This analysis also suggests that a smoother activation sequence, where the delivered thrust does not necessarily meet the required thrust (such as AS 4) may help to increase RSET than those which prioritize meeting the required thrust (such as AS 3). This also reflects the importance of the presented methodology to enhance activation sequence (and assess its risk) instead of relying on simpler alternatives for the control systems (such as PI) or those which focus on providing critical velocity in the early stages of the fire.

This methodology may be of special interest in sloped tunnels and tunnels where adverse conditions may be expected, given that those conditions may lead to a fast spread upstream the fire, hindering occupants' egress. It may also be of special interest to long tunnels or where large fast-growing fires may be expected (for example, large electric vehicles). The methodology, however, would be completely sterile when not accompanied by the necessary equipment to allow sequential activation, which is still common in many tunnels throughout Europe, some of them even of new construction.

5. REFERENCES

[1] NFPA 502, "Standard for Road Tunnels, Bridges and Other Limited Access Highways," The National Fire Protection Association, US, 2023.

[2] M. Beyer, C. Stacey, G. Brenn, "A Mixed Convection Model for Estimating the Critical Velocity to Prevent Smoke Backlayering in Tunnels", Fire Technology 61, 295–342, doi:10.1007/s10694-024-01607-8 US, 2025.

[3] NFPA 92, "Standard for Smoke Control Systems," The National Fire Protection Association, US, 2024.

[4] J. Bielawski, D. Luan, X. Zhang, W. Xie, X. Huang and W. Węgrzynski, "Distributed temperature sensor model for linear heat detection in tunnel fires," Tunneling and Underground Space Technology 167, Elsevier publishing, doi:10.1016/j.tust.2025.107092, US, 2025.

[5] PIARC, "AIPCR 2006.05.16.B: Ventilation", World Road Association, FR, 2006.

[6] Y. Guo, Z. Yuan, Y. Yuan, X. Cao, P. Zhao, "Numerical simulation of smoke stratification in tunnel fires under longitudinal velocities," Underground Space 6, 163-172, Elsevier publishing, doi:10.1016/j.undsp.2019.11.001, US, 2019.

[7] ATC, "Metodología de Análisis de Riesgos en Túneles de Carretera" Asociación Técnica de Carreteras, ES, 2024.

[8] PIARC, "2nd International Conference on Road Tunnel Operations and Safety, Volume II", ATC, 219-240, ES, 2022

PERFORMANCE IMPROVEMENT OF A HYBRID VENTILATION SYSTEM VIA PREDICTIVE CONTROL

[1]Diego Angeli, [2]Paolo Levoni, [3]Pietro Cingi, [4]Giovanni Sebastiano Barozzi, [5]Paolo Verraz, [5]Cedric Petitcolin

[1]DISMI - University of Modena and Reggio Emilia, IT
[2]mimesis s.r.l., IT
[3]EN&TECH - University of Modena and Reggio Emilia, IT
[4]DIEF - University of Modena and Reggio Emilia, IT
[5]TMB-GEIE, IT and FR

DOI 10.3217/978-3-99161-087-8-011 (CC BY-SA 4.0)
https://creativecommons.org/licenses/by/4.0/deed.de
This CC license does not apply to third party material (attributed to other sources) and content noted otherwise.

ABSTRACT

Accurate and responsive ventilation control is of primary importance in the airflow management in tunnels, especially in the case of fire events. This is even more critical in long single-tube, two-way road tunnels such as the Mont Blanc Tunnel, where the ventilation system is hybrid (longitudinal and transverse), and smoke must be confined and conveyed to suitable ceiling vents connected to an extraction shaft, while stratification must be kept as stable as possible. Jet fans are employed to realize the confinement, coupled with a PID controller which acts on the velocity excess in the position of the fire event, with the aim of nullifying it in the shortest possible time. The action of the controller is crucially subject to the action of several different factors: (i) the barometric pressure difference between portals, (ii) the accuracy and frequency of the reconstruction of pointwise velocity, and (iii) the delays related to the operation of the extraction system. All these factors, and especially the last one, can hinder the correct performance of the controller, by introducing perturbations leading the system to unwanted oscillatory behavior, potentially disrupting smoke stratifications and delaying smoke extraction and intervention of firefighting squads. To this aim, in this work we propose a novel approach based on predictive control, aimed at improving the performance of the Mont Blanc Tunnel ventilation system. The method is based on an a priori analysis of the ventilation transients and asymptotic conditions for a wide range of scenarios, using both field data and a 1D numerical model. Results of the analysis are then used to construct corrective factors for the PID input signal. The constants for the corrected PID are then optimized using a DOE approach. Preliminary numerical assessments indicate a significant improvement of the system response and a drastic reduction of oscillations.

Keywords: tunnel ventilation, predictive control, PID, 1D CFD model, airflow management.

1. INTRODUCTION

Ventilation control in road tunnels plays a fundamental role in ensuring operational efficiency and safety during emergency events such as fires. Long bi-directional tunnels such as the Mont Blanc Tunnel (11.6 km) pose further challenges, since they require a fine balance between longitudinal and transverse ventilation, to continuously feed fresh air across large distances while being able to manage and extract smoke at any location. The existing hybrid ventilation system of the TMB employs jet fans for confinement and extraction ducts for smoke removal [1-3]. The operation of jet fans is managed by a PID controller that reacts to sensor data in

real time. During a fire, the control system aims to establish a zero-velocity zone around the event to confine smoke spread.

Since the reopening of TMB in 2002, TMB-GEIE, the concessionary binational company of the infrastructure, has continuously refined its control logic to improve stability and responsiveness. However, systematic analyses of events occurred between 2015 and 2024, where the control logic was activated to manage and extract smoke, highlighted recurring non-conformities between the actual and target time to attain the zero-velocity conditions. In most cases, this occurred under specific combinations of barometric pressure difference (Δp) and event position (PM_{event}). The underlying issue was identified as the time delays between sensor readings, control actuation, and the activation transients of the extraction system. The durations of these transients are far from negligible, and their action significantly modifies the aeraulic conditions around PM_{event}. These conditions can cause transient sign inversions of the measured velocity, leading to counterproductive control actions.

Therefore, while keeping the basic operation of the control system unchanged, a corrective predictive modification was proposed, based on a pre-mapping of the effects of extraction on the velocity profile. This logic, which effectively constitutes predictive control [4-6], operates exclusively during the initial phase of event management and then gradually returns to the current PID logic after an appropriate time interval. The development of this control logic exploits the previous comprehensive physical and digital characterization of the TMB ventilation system operated through multi-point airflow measurements [1], continuous longitudinal profile acquisition [2], and a 1D numerical model [3]. In the following, the novel algorithm and its calibration are presented, alongside preliminary 1D CFD assessments.

2. METHODOLOGY

2.1. Current TMB Control Logic

The baseline TMB control algorithm reconstructs the longitudinal airflow velocity profile along the tunnel using an array of 20 ceiling anemometers [1]. The average velocity at the fire location, v_{event}, whose target value is zero, is fed into a PID controller that determines the number of jet fans to activate:

$$n_{fan}(t) = K_P v_{event}(t) + K_I \int_0^t v_{event}(t)dt + K_D \frac{dv_{event}(t)}{dt}$$

where n_{fan} is the number of jet fans to activate (positive or negative depending on the required direction of thrust), and K_P, K_I, K_D are the proportional, integral, and derivative gains, respectively. While efficient and robust, this logic reacts only to *current* measurements, while airflow perturbations induced by the system transient may invert v_{event}, temporarily driving the PID in the wrong direction. In fact, when the algorithm is triggered (at time t_1), the extraction system simultaneously ramps up to full capacity and the dampers in the event area open. As shown in Figure 1, these actions cause a rapid evolution of the longitudinal velocity profile during the initial phase of the event. Under normal ventilation mode, the longitudinal profile is monotonically increasing, since air is injected into the tunnel by the fresh-air system. When the extraction system is activated – i.e., air is removed from the tunnel – it introduces a decreasing segment in the velocity profile whose amplitude depends on the extraction rate. The final profile stabilizes only once the extraction system has reached steady-state operation (approximately 2–2.5 minutes). From a control standpoint, this means that the current logic is systematically delayed, as it corrects a condition that is rapidly evolving.

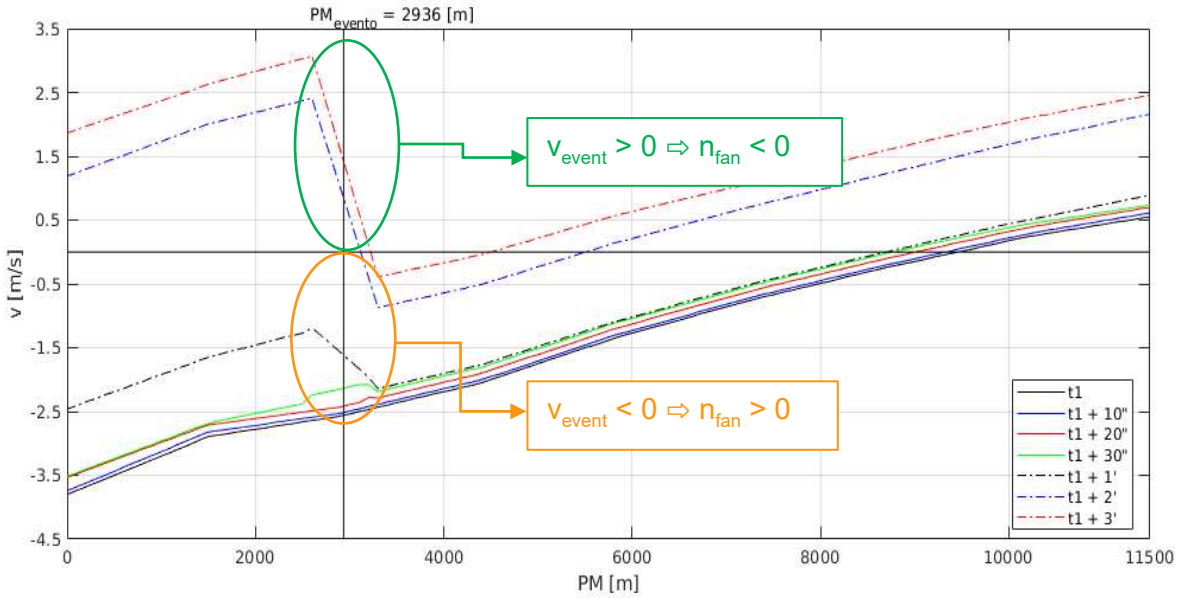


Figure 1: Evolution of the reconstructed TMB velocity profile during an event (starting at time t_1)

Although this characteristic is not always detrimental (in some cases, the delay helps stabilizing the zero-velocity point more quickly), in certain unfavorable combinations of Δp and PM_{event}, the extraction transient may even cause a sign reversal of the velocity at the event during the initial phase. Consequently, the initial corrective actions of the system may become counterproductive, delaying or hindering final stabilization. In practice, this manifests as early jet fan activations in the opposite direction of what is ultimately required for stable control (see again Figure 1). It is also important to note that velocity reversals near a fire or pollutant release can promote smoke destratification, which complicates rescue operations and increases risks for users.

2.2. Predictive Control Formulation

To overcome this limitation, a predictive term is introduced that estimates the future velocity using a correction matrix $\Delta v_{corr}(\Delta p, PM_{event})$ multiplied by a blending function f_b, derived from a first-order Hermite polynomial (Figure 2). The blending function ensures gradual transition from predictive to standard PID behavior over a blending time constant τ_b:

$$v_{pred} = v_{event} + \Delta v_{corr}(\Delta p, PM_{event}) \times f_b(t, \tau_b)$$

The correction matrix Δv_{corr} was pre-computed using the previously developed 1D CFD model of the TMB ventilation system described in [3].

The underlying idea originates from the observation that the extraction airflow rate – i.e., the alteration that extraction produces on the longitudinal velocity profile during the early phase of an event, as shown in Figure 1 – depends in general on both Δp and PM_{event}. As such, this effect can be pre-mapped, for example through field tests or CFD.

Values of Δv_{corr} were computed by simulating asymptotic scenarios for 31 values of Δp (from −750 to +750 Pa) and 17 evenly spaced event locations (5 m to 11 605 m), resulting in 527 scenarios. As shown in the plot of Figure 3, the general trend of the correction function confirms that extraction causes a measurable velocity rise or drop, depending primarily on the event location, while its variation with on Δp is minor.

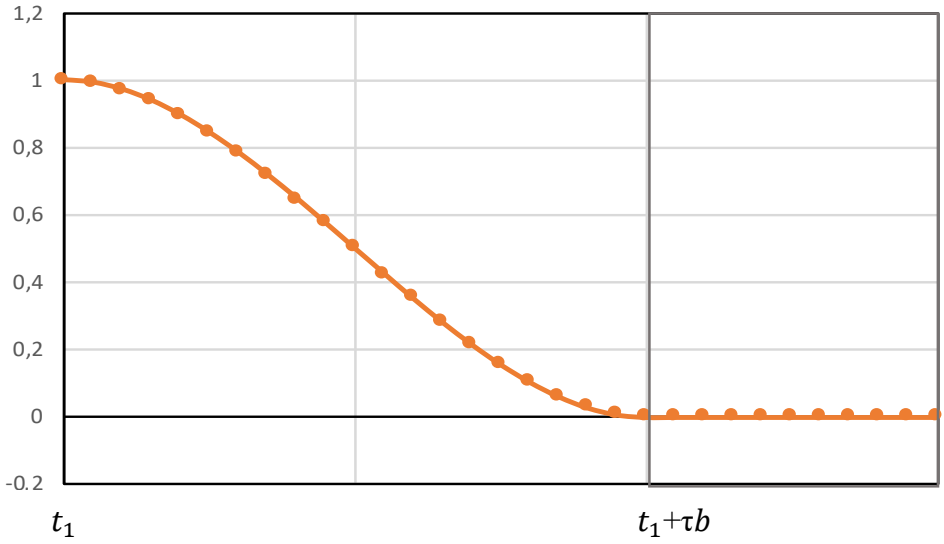


Figure 2: Predictive PID: smoothstep blending function $f_b(t, \tau_b)$.

The correction matrix Δv_{corr} was then used as a lookup table during subsequent calibration. Such format could also be conveniently implemented in the TMB control system.

The modified predictive PID law thus becomes:

$$\mathrm{n_{fan}(t)} = \mathrm{K_P} v_{pred}(\mathrm{t}) + \mathrm{K_I} \int_0^{\mathrm{t}} v_{pred}(\mathrm{t})\mathrm{dt} + \mathrm{K_D} \frac{\mathrm{d}v_{pred}(\mathrm{t})}{\mathrm{dt}}$$

This approach endows the controller with short-term predictive capability while preserving the computational simplicity of the velocity reconstruction algorithm and of the operational PID structure.

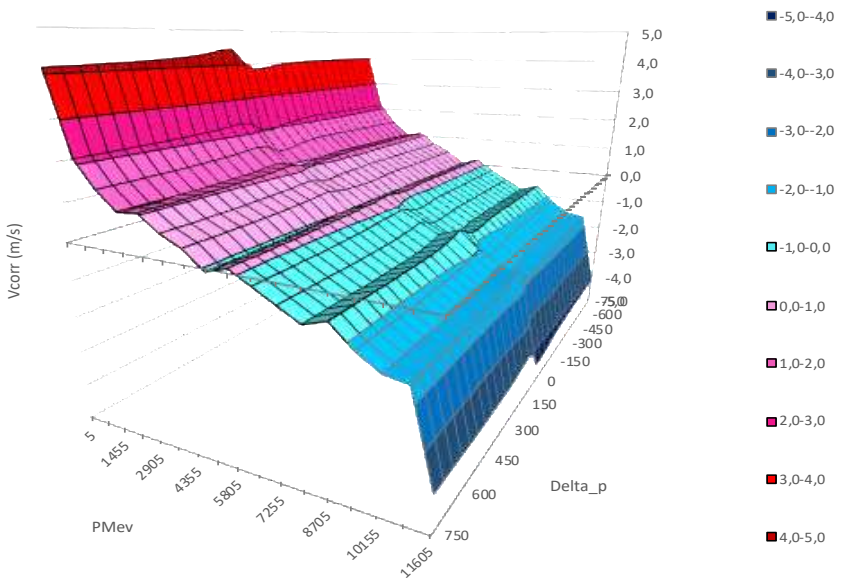


Figure 3: Predictive PID: correction matrix $\Delta v_{corr}(\Delta p, PM_{event})$.

2.3. Calibration

Compared to the current controller, the proposed modification introduces a new calibration parameter, τ_b, which extends the dimensionality of the parameter space from three (the PID gains (K_P, K_I, K_D) to four parameters: (K_P, K_I, K_D, τ_b). In this configuration, τ_b represents the temporal limit of the predictive correction, beyond which the standard control is fully restored. Meanwhile, the intensity of the correction gradually decreases according to the blending function f_b. Considering that the prescribed threshold for zero-velocity stabilization is 3 minutes, and that extraction stabilization typically occurs within 2–2.5 minutes, the range of τ_b was reasonably restricted between 90 and 150 seconds.

The calibration of the four parameters was carried out using a Design of Experiments (DOE) methodology. Three values of τ_b (90, 120, and 150 seconds) were tested, analyzing control performance over a matrix of (K_P, K_I) values, while K_D was kept constant and equal to the current coded value of the standard TMB controller, given that the derivative action is extremely sensitive to possible fluctuations of the measured field velocity, and that the current value already guarantees good stability.

A DOE campaign was executed to identify the optimal parameters (K_P, K_I, K_D, τ_b):

- $K_P \in$ [10, 20, 30, 40, 50]
- $K_I \in$ [0.07, 0.08, 0.09, 0.10, 0.11, 0.12]
- K_D = 1.38 (fixed)
- $\tau_b \in$ [90, 120, 150 s]

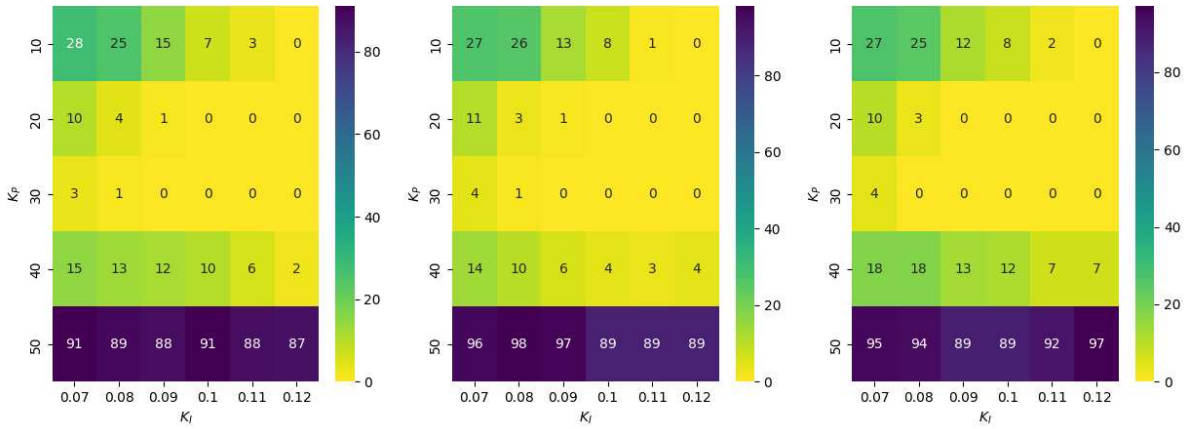
The ranges of (K_P, K_I) were chosen starting from the current values (10, 0.12) and increasing K_P to test higher responsiveness, while decreasing K_I to maintain stability. For each τ_b value, a total of 30 (K_P, K_I) combinations were simulated under 153 distinct conditions, representing all possible combinations of:

- 17 Δp-values: [−600, −450, −300, −250, −200, −150, −100, −50, 0, 50, 100, 150, 200, 250, 300, 450, 600 Pa],
- 9 PM_{event}-values: [725, 1450, 2900, 4350, 5800, 7250, 8700, 10150, 10875 m].

In particular, the Δp range between −300 and +300 Pa was investigated with a finer resolution, since most of the non-conforming cases occurred in this interval. For Δp values greater than 600 Pa or less than −600 Pa, the system performance depends almost exclusively on the installed jet fan power. The PM_{event} spacing was set equal to the length of the tunnel segments served by each fresh air fan [2], adding one intermediate point near each portal, where velocity control is generally more difficult. This yielded a total of 13770 simulations, providing a statistically robust basis for assessing the control performance.

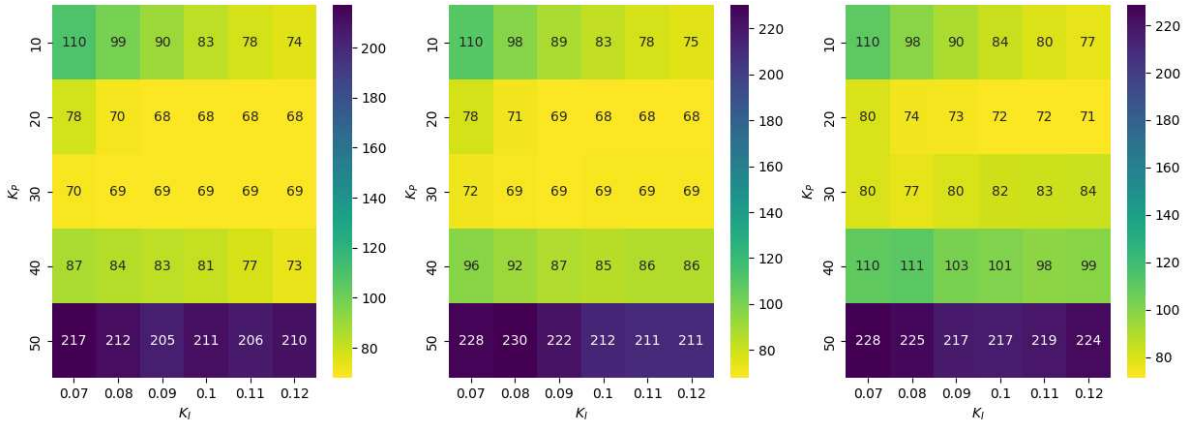
3. RESULTS AND DISCUSSION

Figure 4 shows three matrices (one for each τ_b value), indicating, for each (K_P, K_I) pair, the total number of cases in which velocity control proved non-compliant (i.e., cases where the event velocity did not fall within ±1 m/s in less than 3 minutes). For K_P = 20 and K_P = 30, more than one K_I-value produced fully compliant results. Values of K_P greater than 30, however, are characterized by excessive sensitivity and lead to numerous non-conformities, resulting from generally less stable control performance; therefore, such values were excluded from further consideration.



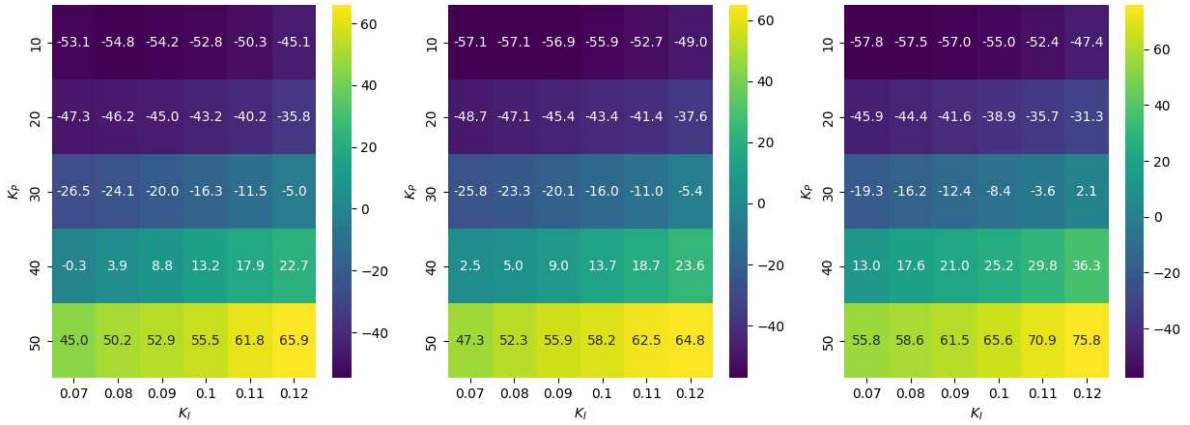
(a) (b) (c)

Figure 4: Cumulative number of non-conforming cases over the whole $(\Delta p, PM_{event})$ matrix used for calibration, and for (a) τ_b = 90 s, (b) τ_b = 120 s, (c) τ_b = 150 s.



(a) (b) (c)

Figure 5: Mean stabilization time over the whole $(\Delta p, PM_{event})$ matrix used for calibration, and for (a) τ_b = 90 s, (b) τ_b = 120 s, (c) τ_b = 150 s.



(a) (b) (c)

Figure 6: Cumulative velocity overshoot reduction over the whole $(\Delta p, PM_{event})$ matrix used for calibration, and for (a) τ_b = 90 s, (b) τ_b = 120 s, (c) τ_b = 150 s.

Two additional indicators were then analyzed to select the optimal configuration: the average time to reach the ±1 m/s threshold (Figure 5), and the cumulative reduction of velocity overshoot, that is, the maximum velocity values in the opposite direction of the jet fan thrust, compared with the current control logic (Figure 6). From the analysis of these indicators, it can be observed that:

- The value τ_b = 150 s results in slightly longer average time spans to reach the zero-velocity point, and these times are generally shorter for K_P = 20 and K_P = 30.
- For K_P = 30, the reduction of overshoot is smaller than in the cases with K_P = 20 and with the combination (K_P, K_I) = (10, 0.12) (representing the current parameter set).
- For K_P = 20, the greatest reduction of overshoot occurs for τ_b = 120 s and K_I = 0.1.
- The value τ_b = 120 s maximizes the reduction of velocity overshoots while at the same time limiting the average time to reach the zero-velocity point.
- The pair (K_P, K_I) = (20, 0.1) with τ_b = 120 s is overall the most favorable among those considered in the present analysis.
- The current pair (K_P, K_I) = (10, 0.12), if associated with the predictive logic, still ensures good performance.

Finally, Figure 7 presents two detailed comparisons between the current and the proposed control logic in terms of event velocity and algorithm output. In both cases, the parameter set (K_P, K_I, K_D, τ_b) = (20, 0.1, 120) was used for the predictive logic.

Figure 7a shows a case where the velocity at the start of the event is already within the prescribed threshold, but the extraction action causes an increase (overshoot) that the non-predictive PID counteracts only after a certain time. The predictive PID, on the other hand, by already accounting for the effect of extraction, mitigates this phenomenon and quickly reaches the desired stability conditions. Figure 7b instead shows a case where the extraction action associated with the non-predictive PID causes a sign change and a resulting overshoot. It can be noted that this phenomenon is almost eliminated by the predictive action of the proposed control logic.

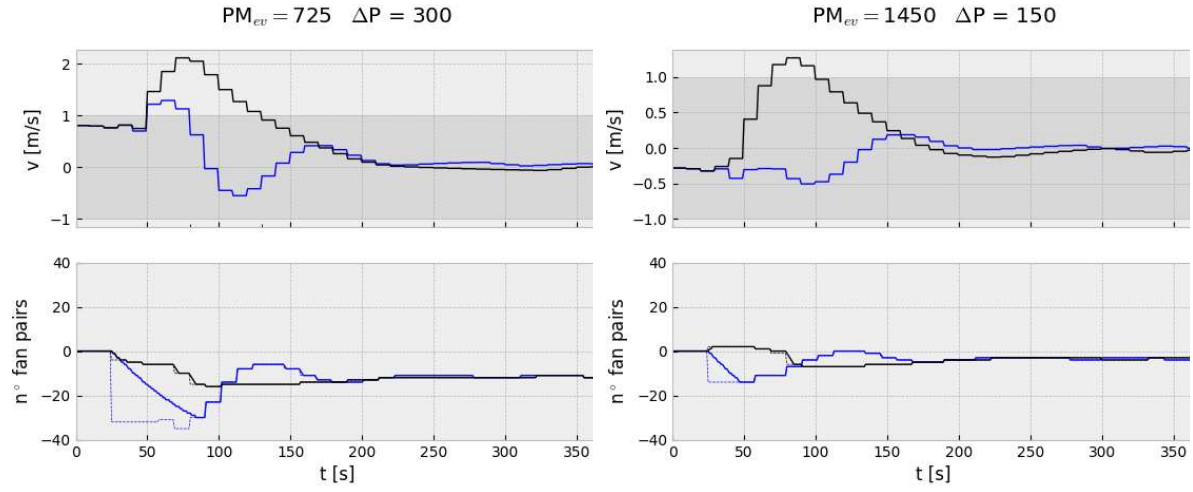


Figure 7: Comparison of the v_{event} and n_{fan} transients obtained with the current PID (black lines) and the predictive PID (blue lines) using the selected parameter combination (K_P, K_I, K_D, τ_b) = (20, 0.1, 120), for (a) $(\Delta p, PM_{event})$ = (300, 725) and (b) $(\Delta p, PM_{event})$ = (150, 1450). In the bottom graphs, dashed and solid lines indicate jet fan request (i.e. the controller output) and actual number of active jet fan pairs, respectively

4. SUMMARY AND CONCLUSION

A predictive extension of the TMB ventilation control algorithm, aimed at enhancing the overall performance and stability of the control system, was developed and calibrated. Such an extension consists in the introduction of a correction term added to the current measured velocity at the event location. This allows the system to estimate and feed into the PID controller the predicted velocity corresponding to the steady-state extraction regime. By doing so, the algorithm acquires predictive capabilities, which cannot be achieved through simple PID control. The correction term, interpolated from a precomputed matrix of values obtained via 1D CFD, is applied only during the initial phase of fire event management. Its influence is gradually reduced over time by a blending function, which governs the smooth transition from predictive to standard control.

An initial calibration of the predictive control parameters was conducted using a Design of Experiments (DOE) approach combined with 1D CFD analyses. A comprehensive matrix of scenarios was simulated to cover the entire operational range of the tunnel. The analysis theoretically confirmed the validity of the proposed approach, highlighting significant improvements in terms of control speed and stability. Specifically, the predictive modification allows for an increase in the proportional gain coefficient, resulting in a more responsive and precise control action.

While computationally lightweight, the method effectively introduces a model-informed feedforward correction. CFD-derived correlations embedded in the lookup matrix serve as a surrogate model of system dynamics, reducing the need for real-time estimation. The predictive controller thus offers a low-cost, high-impact enhancement for hybrid tunnel ventilation systems, demonstrating that integrating predictive elements into established control schemes can markedly improve tunnel safety and response performance. Future work will focus on field validation and potential coupling with real-time digital twin platforms for further adaptive optimization.

REFERENCES

[1] P. Levoni, D. Angeli, E. Stalio, E. Agnani, G.S. Barozzi, M. Cipollone, “Fluid-dynamic characterisation of the Mont Blanc tunnel by multi-point airflow measurements,” Tunnelling and Underground Space Technology 48 (2015) 110–122

[2] P. Levoni, D. Angeli, P. Cingi, G.S. Barozzi, M. Cipollone, “An integrated approach for the analysis and modeling of road tunnel ventilation. Part I: Continuous measurement of the longitudinal airflow profile,” Transportation Engineering 3 (2021) 100039.

[3] P. Cingi, D. Angeli, M. Cavazzuti, P. Levoni, E. Stalio, M. Cipollone, “An integrated approach for the analysis and modeling of road tunnel ventilation. Part II: Numerical model and its calibration,” Transportation Engineering 4 (2021) 100063.

[4] M. Casini, A. Giannitrapani, “Model Predictive Control for HVAC Systems: Applications to Tunnels and Large Enclosures,” Energy and Buildings 222 (2020) 110062.

[5] C. Poussot-Vassal et al., “Advanced control of ventilation in confined transport infrastructures,” Control Engineering Practice 86 (2019) 95–108.

[6] X. Zhao et al., “Predictive control of tunnel ventilation using CFD-assisted data-driven modeling,” Automation in Construction 129 (2021) 103809.

ENHANCEMENTS OF TUNNEL VENTILATION SYSTEM FOR ROAD TUNNELS ADOPTING AERODYNAMIC CONTROL & MONITORING STRATEGIES

[1]Kelvin KW Cheung, [1]Leo L Chan, [2]Anthony Wan, [2]Hau Ming Lee

[1]Building Engineering Group, AECOM Asia Company Ltd., HK
[2]BYME Engineering (Hong Kong) Ltd., HK

DOI 10.3217/978-3-99161-087-8-012 (CC BY-SA 4.0)
https://creativecommons.org/licenses/by/4.0/deed.de
This CC license does not apply to third party material (attributed to other sources) and content noted otherwise.

ABSTRACT

Control of tunnel air quality during normal operation and control of smoke under fire emergency are two essential functions of tunnel ventilation system for road tunnels. Effectiveness of these two functions depends on many tunnel design elements such as tunnel alignment, cross-sectional geometry, traffic operations, location of ventilation shafts/plants, control strategy for ventilation and smoke in tunnel, etc. Semi-transverse ventilation strategy is a widely adopted scheme in many vehicular road tunnels worldwide due to its many advantages, in particular its comparative balanced effectiveness between performance of normal ventilation and that of emergency smoke control, over other schemes. There are several major aspects that can be further enhanced to provide a more cost-effective and safer tunnel environment for tunnel users. The paper aims to firstly identify the critical elements affecting the performance of tunnel ventilation system and to illustrate their potential implications to ventilation and smoke control. Secondly, study of feasible technical resolutions to cope with these effects are then introduced and supplemented with some practical examples of ventilation schemes for illustration. Moreover, further review using computer simulation analyses is also conducted for verification of the system performance from aerodynamic and thermodynamic points of view. Furthermore, the system design and implementation with real-time automatic system control and monitoring on relevant tunnel environmental elements are then illustrated including air quality monitoring system, airflow velocity, fire detection system, fire alarm system and associated mechanical/ electrical system design elements. Potential application of Internet-of-Things (IoT) and digital twin technologies for further enhancement of the system operation is also discussed. Last but not the least, the paper shares some case-studies including computer simulation analysis and testing results for tunnel projects to illustrate the practical implementation of these enhancements.

Keywords: Tunnel Ventilation, Smoke Control, Semi-transverse, Fire Safety, Automation, Simulation Analyses

1. INTRODUCTION

In many recent road tunnel projects worldwide, semi-transverse ventilation strategy is a widely adopted scheme due to its many advantages, in particular its comparative balanced performances between ventilation for tunnel air quality control under normal operation and smoke control under emergency operation during congestion and bi-directional traffic conditions respectively [4]. On the other hand, there are several critical elements and design concerns that may affect operational effectiveness and efficiency of this tunnel ventilation

scheme. These include tunnel alignment and geometry, traffic operations, control strategy for both ventilation and smoke management in tunnel, etc. The paper aims to firstly identify these critical elements and to illustrate their potential implications to ventilation and smoke control. Study of feasible technical resolutions to cope with these adverse effects are then elaborated in detail with examples of computer simulation analyses and project reference of airflow testing data. Furthermore, the system design and implementation with real-time automatic system control and monitoring on relevant tunnel environmental elements are then discussed. Some innovative ideas of using more comprehensive tunnel and traffic data with Internet-of-Thing (IoT) are further illustrated as potential advancements for system control for future reference.

2. CRITICAL ELEMENTS AFFECTING PERFORMANCE

2.1. Tunnel geometry

Number of lanes and traffic gauge determine major dimensions of the tunnel. Besides, spatial provisions for other facilities (such as maintenance/safety walkway, zones on side wall for Electrical and Mechanical (E&M) equipment installation, ceiling crown and ventilation ducts, etc.) further refine the tunnel geometry. Arrangement of ventilation points along the tunnel shall be designed to suit the tunnel geometry in order to achieve a proper distribution of airflow pattern and pollutant control during normal operation. Moreover, a well-planned arrangement of ventilation points can facilitate efficient smoke extraction and maintain a tenable environment for evacuation during fire emergencies [5].

2.2. Gradient Effect

Pollutant emission rate from vehicles depends on the gradients of road alignment. For example, when the vehicle is running uphill, more fuel is being consumed, and thus more air pollutants are emitted. Under normal operation, the pollutant concentration level is building up along the traffic direction. This becomes a challenge of a semi-transverse tunnel ventilation system to limit the pollutant concentration level for a longer tunnel. Under a fire emergency, the gradient effect acting on smoke spread leads to a challenge in two folds: (1) to confine smoke within certain length for minimizing smoke spread to other sections, and (2) to create a tenable environment for evacuation and firefighting. The buoyancy effect of hot smoke creates a tendency to flow towards uphill direction with a faster smoke accumulation at higher side [6]. If the smoke could not be removed effectively, the escape path could be endangered by dropping of the smoke layer.

2.3. Traffic Flow

The movement of the vehicles inside the tunnel induces certain degree of tunnel airflow (i.e. “piston effect”). The higher the vehicle travelling speed, the larger “piston effect” can be generated. In general, ventilation of tunnel could be achieved with the “piston effect” by dragging fresh air into the tunnel from entry portal under a smooth traffic flow. The pollutant concentrations inside tunnel will be diluted by the fresh air and maintained within an acceptable level. However, under a congested scenario, the “piston effect” is significantly reduced while the pollutants emissions from the vehicle will be accumulated inside the tunnel. With reference to a recent tunnel project in Hong Kong, fresh air requirement for pollutant control and “piston effect” at various traffic speed are illustrated in figures.

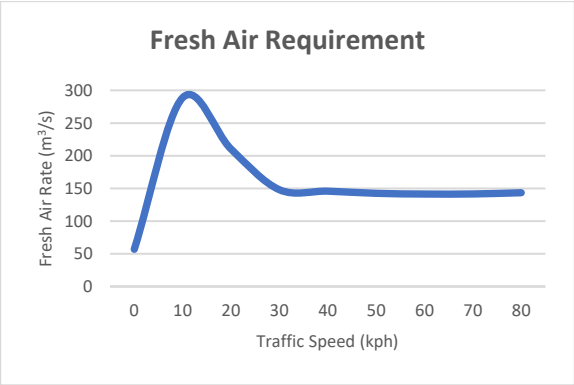


Figure 1: Fresh Air Requirement at various Traffic Speed

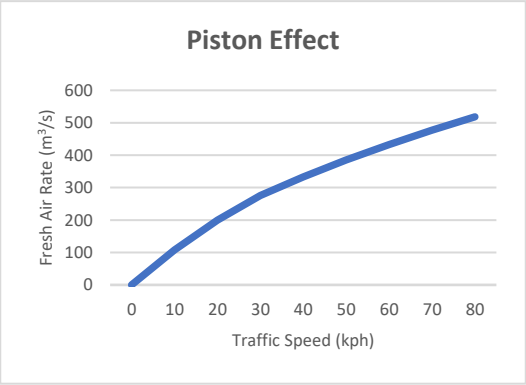


Figure 2: Piston Effect at various Traffic Speed

To achieve effective tunnel air quality control under various traffic flow, enhancement of the semi-transverse ventilation system operation with the "piston effect" is necessary.

2.4. Unbalance Air Flow Effect for Smoke Extraction

During a fire scenario, the tunnel ventilation system performs smoke extraction at the incident smoke zone through the Overhead Ventilation Duct (OHVD). Make-up air (i.e. fresh air introduced into the smoke zone to replace air removed by smoke extraction system) is naturally drawn from two tunnel portals at both sides. In certain cases when the fire locates closer to either end of the tunnel, more make-up airflow will be drawn from the closer end with high air velocity than that from another end. This would result in an unbalance amount of make-up airflow towards the fire site. Smoke layer may be disturbed by higher make-up air velocity and drops below the design smoke clear height faster, and thus tenable environment cannot be maintained on escape path. Figures below illustrate the adverse effect of unbalanced makeup airflow during smoke control.

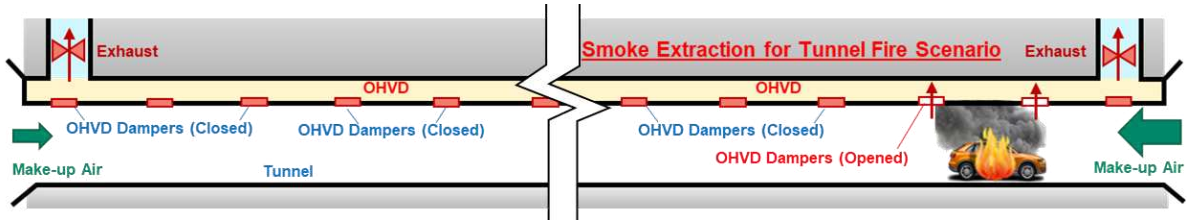


Figure 3: Unbalance Make-up Air for Tunnel Fire Scenario close to one Tunnel Portal during Smoke Extraction

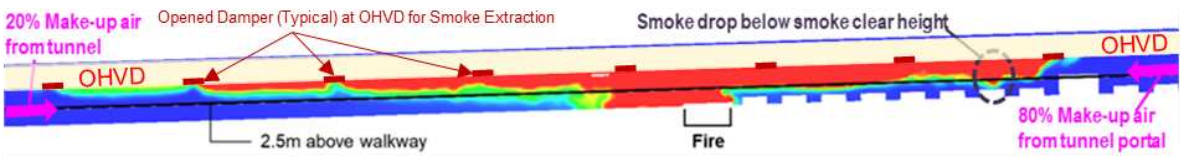


Figure 4: Computational Fluid Dynamic (CFD) Simulation reveals Smoke Drop below Smoke Clear Height due to Unbalance Make-up Air

3. STUDY OF FEASIBLE RESOLUTIONS FOR ENHANCEMENTS

3.1. Enhancement to suit Tunnel Geometry

For a 2-lane tunnel tube, ventilation points can be arranged in single (i.e. one ventilation point per tunnel cross-section) or double opening(s) (i.e. two ventilation points per tunnel cross-section) along the OHVD. For a 3-lane tunnel tube, the ventilation points would be better arranged with minimum double openings (i.e. two ventilation points per tunnel cross-section) along the OHVD for more evenly distributed smoke extraction performance. It is important to locate these ventilation points at high level so as to capture the smoke more effectively. As the smoke extraction rate is estimated based on design fire size against the design smoke clear height for escape path, the dimensions and distribution of the ventilation openings on the OHVD shall take account the effectiveness of smoke extraction. Therefore, "plug-hole" effect ("Plug-hole" effect occurs when the air velocity entering an extraction point is high enough to entrain clear air from below the smoke layer into the extraction point. The problem with "plug-hole" effect is that clear air will be extracted instead of smoke which resulting in reduction on effectiveness of smoke extraction system.) shall be carefully assessed and avoided with appropriate smoke extraction velocity passing through the ventilation point against depth of smoke layer below the point. To meet the design smoke extraction performance, more ventilation openings with smaller dimensions are required in some cases.

In some tunnel geometry, evacuation path or walkway is elevated (i.e. above road level). The design smoke clear height shall include this elevation to ensure a smoke clear path above the walkway for evacuation and firefighting uses. The smoke extraction rate and associated ventilation points of the semi-transverse tunnel ventilation system will be increased to meet performance requirement in this tunnel geometry.

3.2. Enhancement to tackle Gradient Effect

To evaluate vehicle emission of several common pollutants, PIARC has provided a comprehensive methodology regarding emissions of pollutants generated from the vehicles under various speed. This method also provides average emission factors for each pollutants accounting for associated gradient of the road where the vehicles are travelling on. These pollutants accumulate faster along the tunnel with longer uphill section towards downstream of the traffic. To maintain the pollutant concentration level within the maximum allowable limits throughout the tunnel, fresh air shall be supplied to the tunnel by two commonly used ventilation schemes:

(1) Constant rate along the tunnel to keep the pollutant concentration level under the design maximum allowable limits (refer to Figure 5), or;

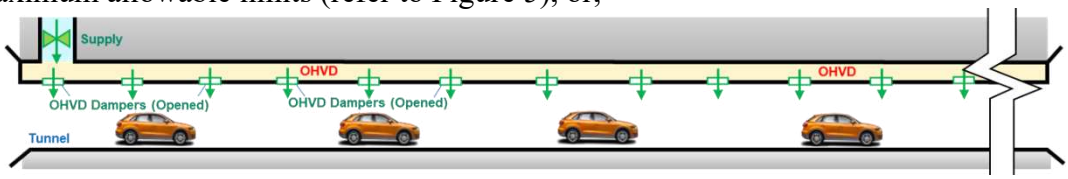


Figure 5: Evenly Distribution of Fresh Air Supply via OHVD Openings along tunnels

(2) Variable rate at dedicated location in tunnel that can bring down the pollutant concentration to certain level such that the subsequent "peaks" of the pollutant level remain under the design maximum allowable limits (refer to Figure 6).

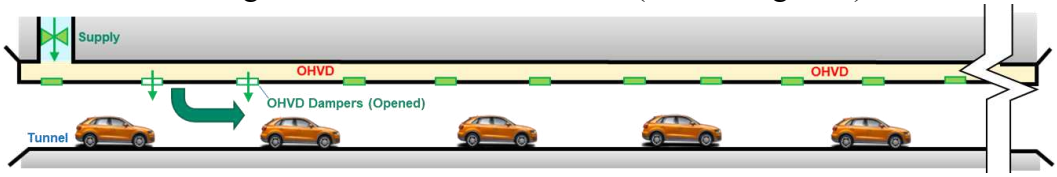


Figure 6: Variable Rate with Point Supply of Fresh Air Supply via OHVD Openings in tunnels

Table 1: Comparison of the two ventilation schemes

Factors of Comparison	Constant rate along tunnel	Variable rate at dedicated location
Balance of airflow at ventilation points	Airflow rate via majority of dampers on OHVD need to be balanced along tunnel	Airflow rate via dedicated zone(s) of dampers on OHVD need to be balanced
Number of dampers in operation	Majority of dampers on OHVD shall be open	Dedicated zones of dampers on OHVD shall be open
Flexibility for variation of gradient effect	Refinement of ventilation rate at each damper is required	Refinement of ventilation rate at dampers is not required
Flexibility for variation of traffic condition	Lower due to fixed setting of damper openings	Higher by adjustment of ventilation rates only

Furthermore, the design of semi-transverse ventilation system for smoke control involves more robust considerations to deal with the gradient effect. As the accumulation of smoke at higher side of the incident tunnel section is faster due to its buoyancy and therefore, this indicates a higher smoke extraction rate or smoke extraction density is required to maintain a design smoke clear height along the escape path. In another words, the same smoke extraction capacity shall be applied to a shorter tunnel smoke zone with higher gradient, while it is applied to a longer tunnel smoke zone with lower gradient. For various tunnel geometry and tunnel configurations, the required smoke extraction rate for different gradient section shall be verified or optimized by computer simulation analyses, for example, Subway Environment Simulation Programs (SES) and Computational Fluids Dynamic (CFD) simulation.

3.3. Enhancement to suit various Traffic Flow

Under the semi-transverse ventilation scheme, a Variable Supply Zone Method is recommended to tackle variation of the piston effect given from the change of traffic flow. This method is to provide fresh air supply via OHVD at specific supply zone in the tunnel at different traffic conditions. Change on piston effect due to different traffic conditions is monitored by airflow sensors installed in the tunnel. The specific supply zone will be activated corresponding to the airflow monitored by airflow sensors.

Considering a “weak” piston effect under congestion, fresh air is strategically supplied near the middle of the tunnel, such that the supplied fresh air dilutes pollutants and direct the airflow towards portals on both ends. When the piston effect increases with the traffic speed, majority of the supplied fresh air will be pushed by vehicle movement towards exit portal and the airflow rate travel towards entry portal will becomes less. In this case, the supply zone will be shifted towards to the entry portal such that the fresh air supply can ride on the piston effect to ventilate the tunnel. Each specific supply zone and its location corresponding to specific piston effect will be assessed by simulation analysis. The shifting of the supply zone on OHVD under different traffic flow conditions is illustrated in the Figures 7 to 9.

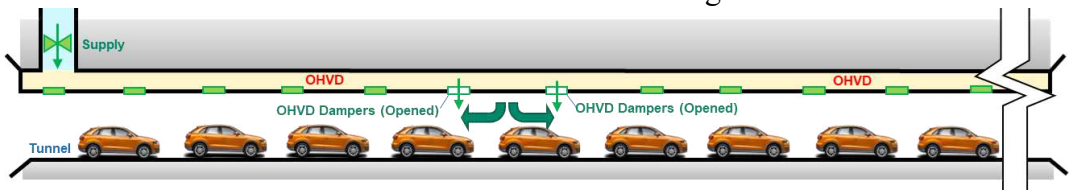


Figure 7: Zone Supply of Fresh Air Supply via OHVD Openings under Congested Traffic

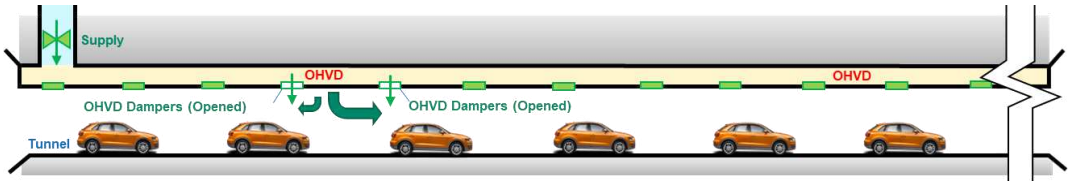


Figure 8: Zone Supply of Fresh Air Supply via OHVD Openings under Smooth Traffic

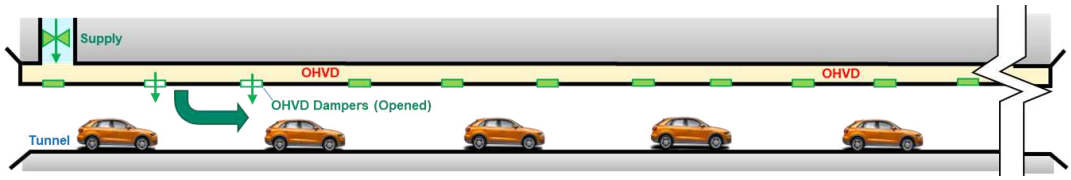


Figure 9: Zone Supply of Fresh Air Supply via OHVD Openings under High Traffic

The Variable Supply Zone Method can be adopted for changes of traffic condition as an effective ventilation strategy of the semi-transverse ventilation scheme. For a longer tunnel with larger aerodynamic resistance, the Method could be further enhanced with jet fans along the tunnel, and the jet fans can improve control of tunnel airflow by pushing towards to the exit portal regardless of traffic conditions (refer to Figure 10). Simulation analysis can be used to optimized distribution of supply airflow under various traffic speed.

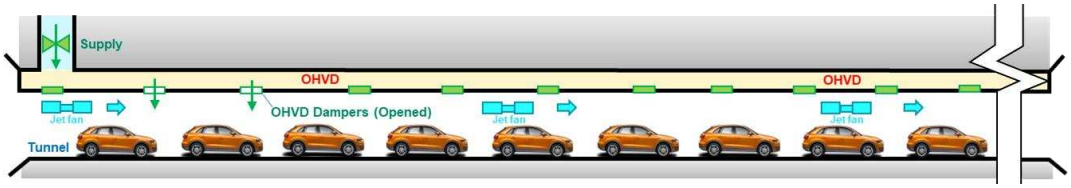


Figure 10: Zone Supply Method with Jet Fans for Fresh Air Supply via OHVD Openings

3.4. Enhancement to achieve a Balanced Makeup Airflow for Effective Smoke Control

As described in Section 2.4, the challenge of unbalanced natural markup airflow could cause ineffective smoke control with semi-transverse tunnel ventilation system. Taking a recent Hong Kong road tunnel project of approximate 3.2km long as an example, simulation analysis by using SES was performed to examine the natural make-up airflow rate on both sides of each smoke zone. SES results showed that a reasonable balance airflow effect could be obtained when the fire locates near the middle sections of the tunnel. The difference on make-up airflow quantity between two sides of the smoke zone increases when the fire location shifting towards tunnel portal on either side. The largest difference on make-up airflow between two sides of smoke zone (approx. 70% and 30% of natural make-up airflow from two sides respectively) happened when the fire site is located right next to a tunnel portal (refer to Figure 11).

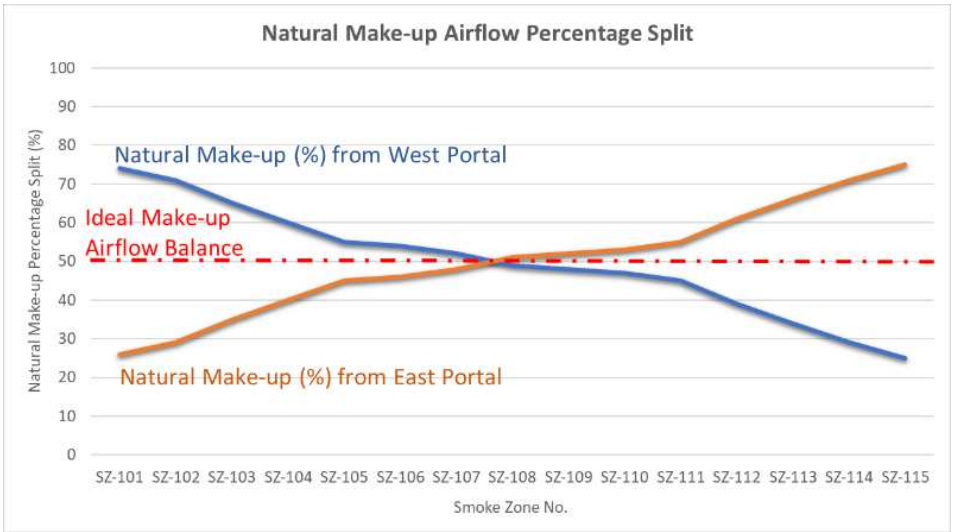


Figure 11: Natural Make-up Airflow Percentage Split

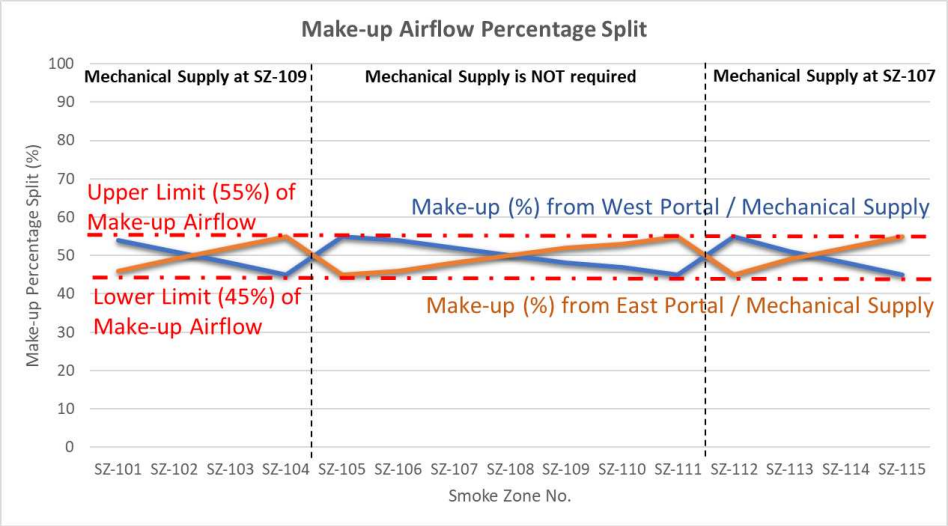


Figure 12: Make-up Airflow Percentage Split by Fixed Supply Zone Method

To enhance system operation for a balanced makeup airflow, a Fixed Supply Zone Method is implemented by air supply at dedicated vent zones with an acceptable range of make-up airflow in terms of percentage (for example, 45% - 55% split of make-up airflow from two ends). Simulation analysis shall be used to verify whether the range of makeup airflow split could result in design smoke clear height under the operation of smoke extraction system. The operation principle and ventilation zone arrangement are illustrated in the following Figure 13 for example. When the fire locates in zone A, B and C with smoke extraction system in operation, the mechanical make up air will be supplied on another end of tunnel at the fixed location (i.e. the fixed supply zone) with fixed supply make up airflow rate, so that 45% - 55% split of make-up airflow from two ends can be achieved. The graph in Figure 12 illustrates effective range of makeup airflow control for different locations of fire site where smoke extraction is performed.

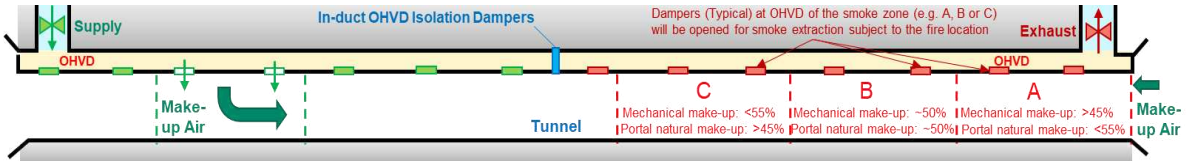


Figure 13: "Fixed Supply Zone Method" for smoke extraction and dedicated mechanical make-up air supply zone

This Method is successfully applied in the semi-transverse system design and operation for the recent road tunnel projects in Hong Kong. Result of CFD analysis in Figure 14 shows that tenable environment can be maintained by the smoke extraction system under the make-up airflow percentage split.

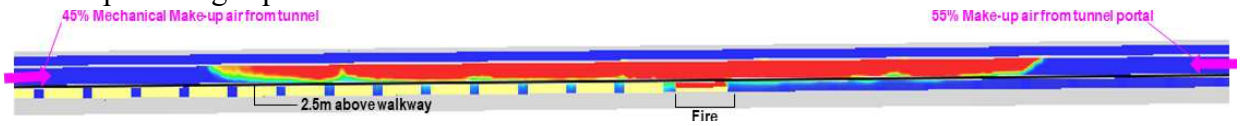


Figure 14: Computational Fluid Dynamic (CFD) Simulation reveals tenable environment can be achieved under a percentage split of 45% and 55% make-up airflow (CFD result from project reference)

4. TESTING OF TUNNEL AIRFLOW BALANCE CONTROL

4.1. Road Tunnel Test

This section presents the testing approach and results for a recent Hong Kong dual 2-lane road tunnel (approx. 4.8 km), focusing on fire-mode validation of the enhanced semi-transverse ventilation strategy adopting the "Fixed Zone Method" for mechanical make-up air. The installation comprises 24 tunnel ventilation fans (TVFs) rated at 85 m3/s across three Ventilation Buildings (VBs), connected to a reinforced concrete Over Head Ventilation Duct (OHVD) divided into two sections by a central dividing wall. Airflow distribution is controlled by 1,302 Motorized Fire and Smoke dampers (MFSDs).

Two representative smoke extraction scenarios were selected for field validation against SES/CFD design predictions, and the target make-up split of approximately 45–55%: Z-009 at the middle of the tunnel with natural make up air and Z-016 close to the tunnel exist portal are selected to validate the assumption of make-up air flow percentage split (45%-55%) from each side of the smoke zone. Lanes closed, no traffic; ambient wind monitored; steady-state achieved before logging.

4.2. On-site Air flow Measurement

OHVD MFSDs total flows (extraction and supply): By using calibrated hot-wire anemometers across the MFSD free area. Where practical, a suitable flow hood and differential manometer were used for corroboration. To enhance the flow measurement efficiency in this scale of projects, 4 groups of technicians utilized synchronized wireless data capture technology to measure a single smoke extraction mode in approximately 20 to 30 minutes. The precise time required varied based on the specific count of dampers within the active zone being tested.

Tunnel make-up airflow approaching the active smoke zone will be simultaneous multi-point velocity measurements, performed at 2 sections located about 10m upstream and 10m downstream from the active extraction zone, using hot-wire anemometers with synchronized logging at steady state. This gives the result of section-average velocity, volumetric flow rate (using surveyed cross-sectional area, and the percentage split of total make-up air from each side of the smoke zone.

Summary of Tunnel Airflow Measurement Results of Two Smoke Zones – Z009 and Z016 is illustrated in the table below. The summary aims to show the comparison between make up split predicted during design and actual measured data.

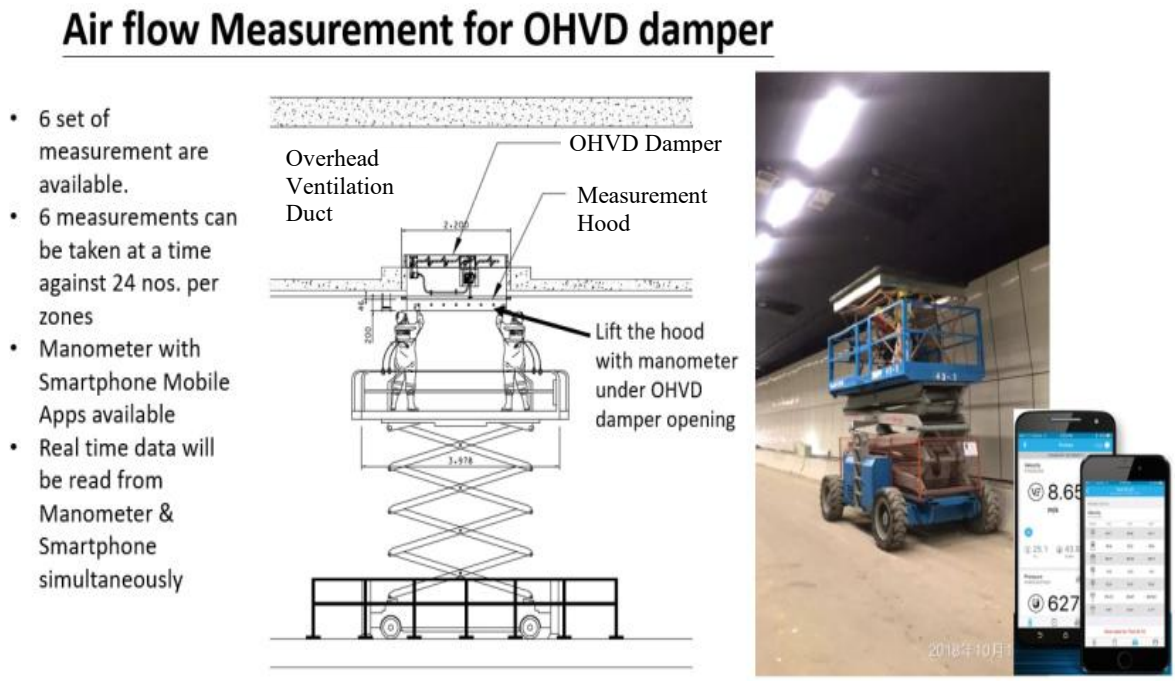


Figure 15: Air flow measurement for OHVD damper

Table 2: Actual Site Measurement

Smoke Zone No.	Total Extraction capacity	Make up air flow			
		Upstream		Downstream	
		Design	Actual	Design	Actual
Z009	323.49 m^3/s	Natural make up Split %: 41.9%	Natural make up Split %: **46.0%**	Natural make up Split %: 58.1%	Natural make up Split %: **54.0%**
Z016	348.91 m^3/s	Mechanical Make Up Split %: 41.7%	Mechanical Make Up Split %: **40.2%**	Natural make up Split %: 58.3%	Natural make up Split %: **59.8%**

4.3. Airflow Control Effectiveness

Results of tunnel airflow tests closely matched SES/CFD predictions and validated the Fixed Zone Method for smoke-mode operation in semi-transverse ventilation. For the mid-tunnel case (Z009) demonstrated balanced natural make-up without mechanical supply. On the other hand, the near-portal case (Z016) confirmed that a dedicated fixed mechanical make-up zone on the far side reliably delivers a balanced make-up split within the 45–55% acceptance range, supporting smoke layer stability and clear height targets for evacuation.

The adopted field methodology—Building Services Research and Information Association (BSRIA)-based MFSD face flow traverses plus simultaneous upstream/downstream section measurements—provided repeatable, efficient verification of extraction capacity and make-up split, enabling direct comparison with SES/CFD outputs and confirming the robustness and operational simplicity of the enhanced control strategy.

5. REAL-TIME AUTOMATIC SYSTEM CONTROL AND MONITORING

5.1. Centralized Monitoring & Control System

To achieve a real-time automation of the tunnel ventilation system, control and monitoring functions could be formed as a dedicated standalone system (i.e. Tunnel Ventilation Control System – TVCS) or integrated with a Centralized Monitoring & Control System (CMCS),

which performs multi-system interface and operational control functions. The system involves several major sub-systems as below:

(1) Tunnel Ventilation Control System (TVCS) – for determining operation modes to be activated based on signal/data received from other sub-systems and control the operation of all elements of the system such as fans (e.g. on/off/speed-control of fan-group or individual operation) and dampers (zonal/individual operation), etc.

(2) Air Quality Monitoring System (AQMS) – for monitoring of the tunnel air quality such as pollutant levels, airflow velocity and visibility, etc.

(3) Fire Detection and Alarm System – for detection of fire/heat/smoke in tunnel and generating alarm signal to associated systems (including tunnel ventilation system)

(4) Traffic Control & Surveillance System (TCSS) – for generating of traffic control signals during normal and emergency operation scenarios

5.2. Automatic Control under Normal Operation

During normal operation, pollutants' level and visibility along the tunnel are two major factors determine the tunnel ventilation requirement. Real-time measurement is carried out by the AQMS regarding concentration of CO, NO_x and visibility/PM level at critical locations along the tunnel, which are fed into the TVCS to check against the threshold limits of these factors. When any one of these factors is reaching an associated preset value, level-up operation of the tunnel ventilation system will be triggered by increasing speed or number of fans in operation to supply more fresh air into the tunnel and bring down the value(s) to an acceptable level. The control logic is the same but in reverse fan control for level-down operation, the speed or number of fans will be reduced when the factors are lower than preset values. This is a closed-loop automatic control method for the real-time control and monitoring functions which aim at energy-saving and cost-effective operation of the tunnel ventilation system.

In the enhanced semi-transverse tunnel ventilation system, locations of the AQMS sensors are essential to take account various traffic operations and conditions. For example, in a smooth un-directional traffic condition, higher "piston effect" will generate higher airflow velocity and the peak of the pollutant level along the tunnel is commonly close to the exit portal. However, during a congested traffic, the peak is likely shifted to the middle of the tunnel due to lower "piston effect" (i.e. lower tunnel airflow velocity). As such, tunnel sensors can be installed in closer interval so as to pick up the tunnel environmental conditions along the tunnel closely in order to for the TVCS to select the most appropriate operation mode as described in section 3.3 of this paper.

5.3. Automatic Control under Fire Emergency Operation

In case a fire accident occurring in a tunnel, location of the fire site shall be firstly identified by the tunnel fire detection and alarm system (e.g. linear heat detection system or heat/smoke detection system) with a corresponding smoke/vent zone(s). The associated signal of the fire location will then be sent to the TVCS and TCSS for verification, if necessary. Based on location of the incident smoke zone, a predefined emergency mode of the tunnel ventilation system shall be selected automatically by TVCS to actuate a TVS operation. As an enhanced smoke control strategy, suitable amount of mechanical makeup air will be supplied to the incident tunnel via a well-defined location/zone so as to facilitate an effective smoke control operation as explained in Section 3.4 of this paper.

At the same time, the tunnel fire alarm will also be triggered to actuate planned tunnel fire services (e.g. fire hydrant system and alarm/exit sign at cross-passages) as well as directly report the fire incident to the associated fire service departments. Moreover, the fire information could be sent to TCSS for further traffic control along the incident tunnel. For

example, TCSS could set up traffic control signs to direct those vehicles at downstream of the fire site out of the tunnel and to stop those vehicles at upstream of the fire site from moving toward the incident location.

5.4. Potential Application of Internet-of-Things (IoT) and Digital Twin Technologies

Following advancement of technology, more comprehensive tunnel, traffic and even atmospheric data could be monitored and integrated into the control system via IoT and digital twin technologies. Some potential innovative considerations are listed for further exploration:

(1) **Real-time traffic throughput and mix data** – Traffic flowrate and types of vehicles at entrance of a tunnel could be used to estimate changes of "piston effect" and pollutant emissions along the tunnel. If these data could be collected via TCSS and evaluated by TVCS in advance, more closely tracked tunnel ventilation capacity and mode operation could be actuated in advance to minimize gap of lead-lag condition between monitoring and control of the tunnel ventilation system.

(2) **Corelation among background air quality, tunnel air quality and portal emission** – Pollutants' concentration level in atmosphere is one of factors determine the fresh air requirement for the tunnels. The pollutants' concentration level will be built up along the tunnel and the air mixtures will be discharged back to the outside ambient in return. Real-time monitoring of the pollutants' concentration levels in these three entities could effectively evaluate not only the tunnel ventilation capacity but also the portal exhaust capacity, if portal emission control is necessary, based on the actual pollutants level for a cost-effective system operation.

(3) **Enhancement of monitoring and control of mechanical makeup for effective smoke control** – Referring to the enhanced smoke control strategy in Section 3.4, bi-directional airflow velocity measuring sensors can be installed in tunnel section near both portals. These sensors can carry out real-time monitoring of the markup airflow rates from both sides of the fire site, and the data could be fed into the TVCS to control the make-up fan capacity in order to achieve a relative balanced makeup airflow pattern to improve the smoke control performance.

With advancement of IoT to integrate connections among multiple data, which could be used in a digital twin model of the tunnel systems, it is anticipated that the tunnel operation could be more efficient and cost-effective in dealing with various conditions.

6. SUMMARY

For the commonly used semi-transverse tunnel ventilation scheme, the paper has identified major critical elements that may affect the operational effectiveness and efficiency of the associated tunnel ventilation system including tunnel geometry and alignment, traffic operation and unbalanced natural make-up in smoke control. Potential resolutions for these critical elements have been elaborated in detail with project reference of computer simulation analysis and on-site tunnel airflow test for illustration. Last but not the least, innovative ideas about real-time automatic system control and monitoring based on more comprehensive tunnel and traffic data collection are introduced riding on the advancement of IoT technology. These ideas could be further investigated and developed for implementation in future tunnel projects.

7. REFERENCES

[1] Lixia Yan, “Research on Intelligent Highway Tunnel Ventilation System Based on Vehicle Identification Technology”, Institute of Electrical and Electronics Engineers (IEEE), 2024 6th International Conference on Electronics and Communication, Network and Computer Technology, Oct. 9, 2024

[2] Jojo S.M.Li and W.K. Chow, “Vehicular Tunnel Ventilation Design and Application of CFD published by Department of Building Services Engineering”, The Hong Kong Polytechnic University, International Conference on Air Distribution in Rooms [ROOMVENT], Jan. 1, 2000

[3] Song Yang, Zubin Ai, Chao Zhang, Shun Dong, Xun Ouyang, Rong Liu and Ping Zhang, “Study on Optimization of Tunnel Ventilation Flow Field in Long Tunnel Based on CFD Computer Simulation Technology”, Multidisciplinary Digital Publishing Institute (MDPI), Sep. 2022, 14(18):11486

[4] Nikola Mirkovic, Predrag Mitkovic, Ljubo Divac, Slobodan Radovanovic & Dragoslav Sumarac, “Ventilation of Long Road Tunnels in Regular and Accidental conditions of Functioning”, the 5th International Conference – Contemporary achievements in civil engineering 21 Apr 2017, Subotica, SERBIA

[5] N. Faggioni, F. Bizzi and M. Bringiotti, “Transverse ventilation system applied to unidirectional road tunnel: Practical case of S2 Tunnel in Warsaw”, Tunnels and Underground Cities: Engineering and Innovation meet Archaeology, Architecture and Art, World Tunnel Congress 2019

[6] Yonghai Qiu & Bo Lou, “Research on the Semi-transverse Ventilation and Smoke Exhaust Strategy in Sloping Tunnels”, International Conference on Logistics Engineering, Management and Computer Science 2015, Atlantis Press

[7] Road Tunnels: Vehicle Emissions and Air Demand for Ventilation (2019) published by The World Road Association (PIARC).

[8] Road Tunnels: Operational Strategies For Emergency Ventilation (2011) published by The World Road Association (PIARC).

[9] NFPA 502: Standard for Road Tunnels, Bridges, and Other Limited Access Highways (2026 Edition) published by the National Fire Protection Association (NFPA).

[10] CIBSE Guide E: Fire Safety Engineering (2019 Edition) published by Chartered Institution of Building Services Engineers (CIBSE).

INNOVATION IN TUNNEL VENTILATION

Global Quality



FAN ENGINEERING

Rail-Mounted Sliding Tunnel Jet Fan

Patented Innovation by AIRONN

A Member Company of CFH HOLDING

Local Solution

%www.aironn.com.tr | ✉ info@aironn.com.tr| ☎ +90 216 524 56 96

PROVEN GLOBAL TRACK RECORD

11,500 UNITS WORLDWIDE

- Poland
- Georgia
- UAE
- KSA
- Algeria
- ...

- Bulgaria
- Albania
- Azerbaijan
- Oman
- Iraq
- ...



A Member Company of

CFH HOLDING

AIRONN

FAN ENGINEERING

%www.aironn.com.tr
✉ info@aironn.com.tr
☎ +90 216 524 56 96

VENTILATION CONTROL OPTIMISATION FOR SHORT LONGITUDINALLY VENTILATED ROAD TUNNELS IN CASE OF TEMPORARY BIDIRECTIONAL TRAFFIC OPERATION

Oliver Heger, Gregor Schmölzer

ILF Consulting Austria GmbH, AT

DOI 10.3217/978-3-99161-087-8-013 (CC BY-SA 4.0)
https://creativecommons.org/licenses/by/4.0/deed.de
This CC license does not apply to third party material (attributed to other sources) and content noted otherwise.

ABSTRACT

Maintenance closures in modern tunnel infrastructure often require temporary bidirectional operation of short, longitudinally ventilated road tunnels, creating significant challenges for ventilation control and fire safety. These tunnels, originally designed for unidirectional traffic, face increased risk during such phases, particularly when regulatory requirements cannot be fully met due to spatial and operational constraints. This paper examines optimization strategies for ventilation control under these conditions using a representative two-lane motorway tunnel as a case study. The Austrian TuRisMo risk assessment methodology was applied, combining quantitative scenario analysis with coupled 1D–3D smoke propagation modeling. A key focus was the impact of jet fan activation near fire locations, which can destroy smoke stratification and impair evacuation. To address this, an adapted modeling approach approximating jet fan-induced destratification was introduced. Results show that natural ventilation—deactivating jet fans in smoke-filled areas—can significantly reduce expected fatalities in certain scenarios compared to configurations involving temporary overblowing. However, controlled longitudinal ventilation remains advantageous in other cases. The findings highlight the need for flexible, risk-based approaches and performance-based design principles to balance safety, regulatory compliance, and operational feasibility during temporary bidirectional operation.

Keywords: tunnel ventilation, risk-based design, ventilation control optimisation

1. INTRODUCTION AND REGULATORY REQUIREMENTS

Short unidirectional tunnels are generally regarded as relatively safe components of underground transport infrastructure. This is primarily due to their enhanced accessibility for emergency services and shorter egress paths to open areas compared to longer tunnels. Their comparatively lower risk potential is also reflected in tunnel safety regulations, which—depending on tunnel length and traffic volume—typically permit longitudinal ventilation (either natural or mechanical) for short tunnels with free-flowing unidirectional traffic.

However, due to spatial constraints, designing ventilation systems for short tunnels can be challenging. Ventilation zones must be compact, and jet fans as well as anemometers are often installed at short intervals. Under normal conditions—such as moderate gradients and typical meteorological influences—these challenges are generally manageable. In recent years, however, many road tunnels, constructed or significantly upgraded following the implementation of EU Directive 2004/54/EC [1], have entered their next major maintenance cycle. As a result, numerous tunnels, including short unidirectional ones with mechanical longitudinal ventilation, require extended maintenance, often necessitating the closure of one

tube for prolonged periods. In such cases, it is practical to operate the remaining tube with bidirectional traffic to minimize the impact on overall traffic capacity. However, this temporary shift to bidirectional operation in a tunnel, designed for unidirectional flow, typically results in increased risk. Experience shows that this risk increase can often be mitigated by optimizing the longitudinal ventilation system for bidirectional traffic. This usually involves loop-controlled low-speed ventilation, maintaining the original airflow direction, and ensuring that jet fans are not activated in smoke-filled areas. Additional risk mitigation measures—such as significant speed reductions, traffic metering systems, or optimized maintenance scheduling (e.g., during night hours)—are also commonly implemented.

For short tunnels, however, the options for optimizing longitudinal ventilation control are significantly limited. Due to the short spacing between jet fans, it is often not possible to meet all regulatory requirements simultaneously. In some cases, jet fans located in potentially smoke-filled areas must be activated to maintain airflow control. Achieving full regulatory compliance would formally require the installation of a semi-transverse ventilation system. However, this is typically neither cost-effective nor feasible, as implementing such an upgrade would necessitate closing one tube—thus requiring bidirectional operation in the remaining tube in the first place. Therefore, the only viable approach is to optimize the existing longitudinal ventilation system and control strategies as much as possible, while reducing risk through supplementary safety measures, accepting a residual risk increase for a limited time. Current tunnel safety frameworks acknowledge this challenge and often permit cost-effectiveness analyses and ALARP (As Low As Reasonably Practicable) justifications in such scenarios.

For instance, the Austrian regulatory framework for tunnel ventilation design, the STSG [2] and the RVS guideline [3] formally require mechanical ventilation and, under normal bidirectional conditions, would not permit longitudinal ventilation without a risk analysis and/or compensatory measures for tunnels of a certain length and traffic volume (AADT). But RVS 09.11.03 explicitly allows for flexibility in temporary operational phases, enabling the use of longitudinal ventilation if equivalent safety can be demonstrated through a structured risk assessment or if additional measures would not be cost-effective with respect to the ALARP principle. Similar, also under the German guideline RE-ING [4], the use of longitudinal ventilation in bidirectional tunnels is conditionally permissible. For tunnels longer than 600 m and up to 1200 m, a risk analysis is required unless specific geometric and operational criteria are met. For tunnels exceeding 1200 m, smoke extraction systems are generally mandated. Actually, RE-lNG does not explicitly differentiate between permanent and temporary bidirectional operation. However, it is also common practice in Germany that longitudinal ventilation systems have been accepted for temporary bidirectional operation phases (e.g., during maintenance closures of one tube). For both regulatory frameworks, the use of longitudinal ventilation in permanent bidirectionally operated tunnels is restricted but there is regulatory and practical precedent for accepting longitudinal ventilation during temporary operational phases, provided that a comprehensive risk analysis is conducted, specific safety measures are implemented to mitigate the increased risk, and the equivalency of the residual risk, or alternatively the ALARP compliance of the temporary risk exceedance, is demonstrated.

Irrespective of the underlying directive, the regulatory requirements for longitudinal ventilation lead often to implementation issues in case of short tunnels (approx. 1.000 m). The spectrum of problems in such projects typically include undersized existing ventilation systems following expired guidelines or for downhill ventilation in case of tubes operated in uphill direction under normal (unidirectional) operation, short distances between fans and thus

compact fire zones, spatial restrictions for installation, in particular small cross-sections and restricted options for adding more jet fans, as well as longer back layering due to low-speed ventilation during bidirectional operation. Due to these issues, it is often not possible to meet all regulatory ventilation control requirements simultaneously – i.e. achieving desired airflow velocities under design conditions for both ventilation directions, avoiding activation of jet fans in areas where smoke is potentially present (i.e. downstream the fire site or within the back-layering length in upstream direction), and avoiding flow reversal. Therefore, optimization of the ventilation control to minimize potential casualties is necessary as a part of the risk assessment and ALARP compliance demonstration procedure.

This paper is intended to illustrates a promising approach for this optimization procedure based on a scenario analysis, using a generic two-lane unidirectional tunnel with a typical longitudinal ventilation layout. The presented technique has been developed with broader risk assessment framework implementation in mind. Therefore, a simplified method to account for smoke destratification caused by jet fan activation in smoke-filled areas within quantitative tunnel risk analysis, relying on coupled 1D-3D smoke propagation modelling approaches, where jet fans are not specifically modelled in the 3D domain, has been adopted. In section 2 a generic two-lane unidirectional tunnel with a typical longitudinal ventilation layout, temporarily operated with bidirectional traffic, is presented as an demonstrative example and the possible options for optimizing longitudinal ventilation control are discussed. Section 3 presents the methodology used for the scenario analysis as well as the approximative approach to account for smoke destratification due to jet fan activation in smoke filled areas. The detailed results for one exemplary fire scenario as well as the overall result for the different fire detection zones for the considered model tunnel are finally presented in section 4.

2. EXAMPLARY MODEL CASE

As an example, a 675 m long, two-lane motorway tunnel with horseshoe profile, which is temporarily operated with bidirectional traffic during refurbishment, is selected. The given ventilation system is designed and optimized for one-way traffic and essentially complies with the requirements of the current Austrian guideline RVS 09.02.31. The tunnel has two accessible cross passages. A summary of the relevant parameters can be found in Table 1. Due to the steep gradient (-3.6%) against the normal operation direction, the tunnel has a total of 12 jet fans, spread across 6 locations. The resulting fire detection zone lengths are generally around 100 m, the only exceptions are the portal zones with 60 /185 m (see also Figure 1).

Table 1: Key parameters of the example tunnel

Parameter	unit	value
Tunnel length	[m]	675
Gradient	[%]	-3,6
Cross section	[m²]	50,0
Cross passages	[#]	2
Design fire	[MW]	30
Target velocity (bidirectional traffic)	[m/s]	±1,5
Portal pressure difference	[Pa]	10
Hourly traffic	[veh/h]	2.200
HG traffic share	[%]	
Number of jet fans	[#]	12
Static thrust per jet fan	[N]	915

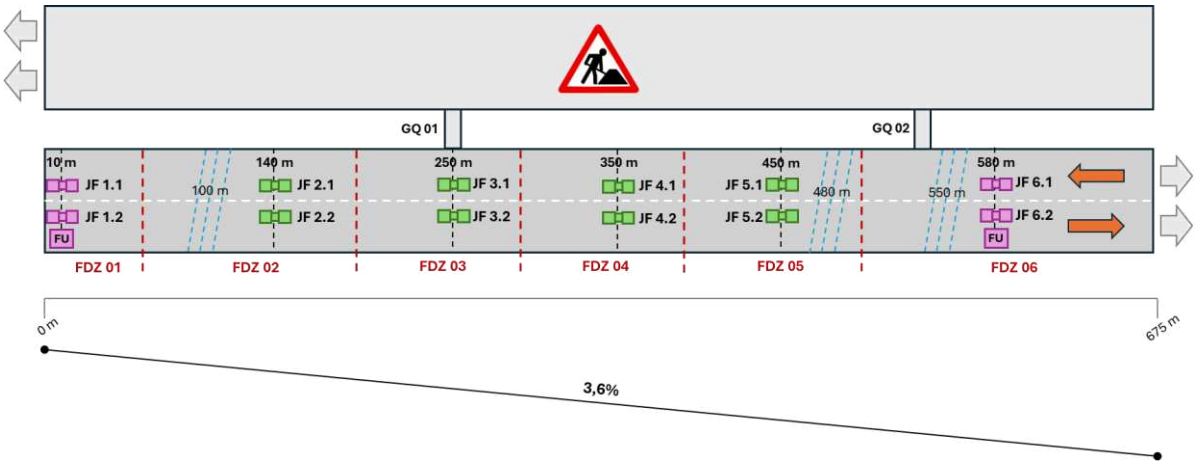


Figure 1: Ventilation scheme diagram for the example tunnel

In accordance with Austrian guideline RVS 09.02.31, during the temporary two-way traffic phase, the flow direction, prevailing in the tunnel at the time of fire detection, must be maintained, and an air speed upstream the fire of +/- 1.5 m/s must be achieved under design conditions. At the same time, jet fans in the smoke layer should not be activated to avoid unnecessarily and prematurely destroying any smoke stratification that may be present, which would significantly impair visibility and escape conditions. However, if this requirement is to be met, it means that all jet fans located between the fire and the respective exhaust portal must not be activated. Assuming that smoke is always extracted via the nearest portal in the portal zones, only 2 to 10 jet fans upstream of the fire are available for smoke extraction, depending on the location of the fire. Considering the system parameters for the selected tunnel (especially the steep gradient and short distances between jet fans), it can be assumed that it will not be possible to simultaneously meet all the requirements set out in the guideline, and consequently the following options, diverging from the regulatory requirements in one way or the other, remain:

- Full compliance with the required flow direction and velocity (according to RVS 09.02.31), but use of all jet fans that are not located in the immediate fire zone
- No use of jet fans downstream / too close upstream, but negative deviations in the achievable velocity (up to the extreme case of "natural ventilation") are accepted
- Fixed smoke extraction direction (intentional flow reversal, if required) to take advantage of the gradient (thermal buoyancy) or to have more jet fans available upstream at a sufficient distance from the fire location

In a first step, calculations were performed for each fire detection zone (FDZ) to determine whether ventilation in both directions, at a minimum speed of 1.5 m/s, is possible under design conditions using only jet fans located upstream of the fire. In cases where this is not possible, fixed smoke extraction in the direction for which positive calculated proof could be provided is selected for the time being.

The technically feasible smoke extraction strategies derived from these calculations are summarized in Figure 2 (left-hand side), considering the basic flow at the start of the fire. Due to the steep incline, in zones FDZ 01 to FDZ 04 ventilation is only possible uphill / northwards. In zone FDZ 05, smoke extraction in both directions is mathematically possible in accordance with the guidelines. In zone FDZ 06, active ventilation is only possible in the direction of the nearby south portal since there are no more jet fans available upstream of the fire for ventilation northward. With a fire load of 30 MW and the desired air speed of 1.5 m/s, a

significant backflow of smoke (back layering) is to be expected. Figure 2 (left-hand side) also shows the minimum distance between a fire and the nearest jet fan location required for ventilation. Depending on fire location and ventilation direction, this distance is 90 to 520 m. In some cases, under the given circumstances (slope, fire load, initial basic flow, forced flow reversal), it can be assumed that smoke backflow will temporarily or permanently, reach these locations. Scenarios where this could not be explicitly ruled out in advance are highlighted in yellow. For these cases, a possible alternative strategy has been defined as a potential optimization option to be assessed by means of a quantitative, simulation-based scenario analysis. The ventilation control alternatives for the affected fire zones are shown at the right-hand side of Figure 2. For the tunnel investigated, the only alternative still available in all affected zones is to dispense active, mechanical ventilation and to switch to natural ventilation instead.

ventilation concept according to design & feasibility

*initial flow ► south / **downhill***

JF	1.1/1.2	2.1/2.2	3.1/3.2	4.1/4.2	5.1/5.2	6.1/6.2	target value	min. distance to next active JF
FDZ 01	fire ◄	x	x	x	x	1	-1,5 m/s	520 m
FDZ 02	x	fire ◄	x	x	x	1	-1,5 m/s	390 m
FDZ 03	x	x	fire ◄	x	x	1	-1,5 m/s	290 m
FDZ 04	x	x	x	fire ◄	x	1	-1,5 m/s	190 m
FDZ 05	1	2	3	x	fire ►	x	+1,5 m/s	140 m
FDZ 06	1	2	3	x	x	fire ►	+1,5 m/s	240 m

possible alternative concept

*initial flow ► south / **downhill***

JF	1.1/1.2	2.1/2.2	3.1/3.2	4.1/4.2	5.1/5.2	6.1/6.2	target value	min. distance to next active JF
FDZ 02	x	fire ◄►	x	x	x	x	nat. vent.	-
FDZ 03	x	x	fire ◄►	x	x	x	nat. vent.	-
FDZ 04	x	x	x	fire ◄►	x	x	nat. vent.	-
FDZ 05	x	x	x	x	fire ◄►	x	nat. vent.	-

*initial flow ◄ north / **uphill***

JF	1.1/1.2	2.1/2.2	3.1/3.2	4.1/4.2	5.1/5.2	6.1/6.2	target value	min. distance to next active JF
FDZ 01	fire ◄	x	x	x	x	1	-1,5 m/s	520 m
FDZ 02	x	fire ◄	x	x	x	1	-1,5 m/s	390 m
FDZ 03	x	x	fire ◄	x	x	1	-1,5 m/s	290 m
FDZ 04	x	x	x	fire ◄	x	1	-1,5 m/s	190 m
FDZ 05	x	x	x	x	fire ◄	1	-1,5 m/s	90 m
FDZ 06	x	x	x	x	x	fire ◄►	nat. vent.	-

*initial flow ◄ north / **uphill***

JF	1.1/1.2	2.1/2.2	3.1/3.2	4.1/4.2	5.1/5.2	6.1/6.2	target value	min. distance to next active JF
FDZ 04	x	x	x	fire ◄►	x	x	nat. vent.	-
FDZ 05	x	x	x	x	fire ◄►	x	nat. vent.	-

Figure 2: Possible smoke extraction strategies Variant I (left) and Variant II (right) for the example tunnel

3. ASSESSMENT METHODOLOGY

3.1. The Austrian Tunnel Risk Assessment Methodology

In many regulatory contexts risk assessment is the tool of choice to allow for a deviation from the ventilation requirements prescribed in the respective guidelines in terms of a performance-based design approach. In this model case example, the Austrian tunnel risk assessment methodology (TuRisMo) is applied for this purpose. The Austrian methodology uses a fully integrated quantitative approach that allows for the detailed analysis of many kinds of safety measures and for interactions between them. The method combines a quantitative frequency analysis based on statistical evaluations and a quantitative consequence analysis that includes a mechanical collision-only part and a distinct fire consequence model [5]. The primary output of TuRisMo is the expected number of fatalities per year for the tunnel under consideration which is assessed by comparison with a reference risk value. In this relative approach the reference risk profile is obtained by applying the same quantitative model (TuRisMo) to a suitable reference tunnel, which is defined as a tunnel as similar as possible to the tunnel under investigation while fully in line with all applicable design regulations and guidelines.

The methodological core of TuRisMo, which is also essential to the comparison of ventilation control strategies in this study, is the quantitative fire consequence model. The fire consequence model used further on in the investigation of emergency ventilation strategies can be summarized as follows: For each considered fire scenario, a transient one-dimensional airflow simulation is performed, considering all important influencing factors, such as traffic volume, fire location, ventilation design and meteorological boundary conditions. In this study the commercial software IDA RTV is used for this purpose. The predicted development of the longitudinal airflow velocities is then used as boundary condition in a three-dimensional CFD simulation (FDS) in which local effects such as back-layering and smoke stratification are examined. Visibility-, heat- and toxic-gas concentrations generated in the three-dimensional CFD simulation are then combined with person-exposure distributions dependent upon the traffic configuration after the incident. Based on this superposition and using an accumulation and intoxication model describing the effects of fire hazards on evacuation speed and survivability of persons [6], the expected total number of fatalities is computed [7].

3.2. Approximative Consideration of Jet-Fan Overflow

One of the central questions in the ventilation design of short bidirectionally operated tunnels is whether it is better to accept the fact that small distances between activated jet fans and fire location might lead to a destratification of smoke, or whether keeping stratification up as long as possible thus accepting deviations from the desired airflow target directions and velocities is preferable. To analyze the potential impact of jet fans on layer formation, the local impact of jet fans on the flow field or at least on the smoke layer, needs to be considered in the CFD simulations. According to the fire-consequence modelling technique, adopted in TuRisMo as explained above, active longitudinal ventilation components are not explicitly modeled in the 3D-CFD simulations, and only directly considered in the 1D part of the smoke propagation model. In the 3D-CFD simulations, the impact of jet fans is only considered implicitly by applying the longitudinal velocity development, that is a result of the consideration of jet fans in the 1D simulation, as velocity boundary conditions at the 3D domain inlet. This simplification of jet fan consideration in the 1D-3D coupled approach is legitim, if the distance between activated jet fans and region of interest is large enough for the high vertical velocity gradients, caused by the high discharge velocity of jet fans, to have decreased significantly so that the assumption of a relatively homogeneous velocity field acting on the smoke/fresh air layer formation is justified. For standard use case of tunnel risk assessment models (longer tunnels with sufficiently broad ventilation zones, where the distance between fire location and activated jet fan is often several hundreds of meters long), this assumption is typically applicable. In the present case, however, ventilation zones are very compact and no can be generally considered as smoke free due to the low target airflow velocities. Therefore the existing fire consequence analysis methodology, and in particular the (one-way) coupled 1D-3D smoke propagation model must be adapted and the direct impact of active jet fans on the smoke-layer formation potentially causing destratification considered.

The most intuitive and straight forward approach would be to consider jet fans in the 3D model directly. In principle, this is technically possible and several 3D studies, focusing on jet fan performance in tunnels, have indeed been carried out recently (cf. [8], [9]) . However, the large vertical gradients in the near-field of activated jet fans call for very high mesh resolutions in the 3D CFD analysis, at least in the respective region, which would lead to significant increase in computation time compared to the standard smoke-propagation simulation approach. In addition, the 3D CFD modelling of jet fans is typically restricted to steady-state problems, while the problem at hand is highly transient, as the time-dependent propagation of smoke is of relevance. In addition, it has been demonstrated that FDS might be rather inaccurate in predicting the impact of jet fans on upstream smoke propagation, which would

necessitate the use of more adaptable CFD solvers like Ansys Fluent [8]. Due to these reasons and to be in line with the consequence analysis approach prescribed within the TuRisMo methodology, an alternative method to estimate the occurrence and impact of destratification due to effect of close active jet fans, at least in an approximative manner, has been adopted:

- In principle, the one-way coupling between the 1D and 3D CFD models is maintained, and the influence of jet fans on flow behavior is considered only in the transient 1D simulations. The results of the coupled flow simulation therefore do not include any consideration of 3D (or 2D) effects of the jet fans.

- To determine whether the smoke layer might potentially be destroyed by upstream jet fans, the result of the 3D simulation is examined regarding the extent of "back-layering." For this purpose, the cross-section-averaged temperature profiles at the boundaries of the influence zone of the nearest jet fan are analyzed, assuming an influence length of 60 m for a jet fan.

- If the cross-section-averaged temperature 60 m downstream of the jet fan closest to the fire site is elevated compared to the ambient temperature, it is assumed that the smoke stratification is destroyed for the duration of the temperature increase, and thus for the duration of the jet fan smoke-overflow

- To approximate the impact of a disrupted smoke stratification, the evacuation and survival simulations employ cross-section-averaged values for temperature and smoke gas concentration, rather than head-level values, for the duration of the jet fan smoke-overflow ($\bar{t}_1$) and the subsequent period required to purge the smoke-filled air column between the jet fan and the extraction portal at the prevailing flow velocity ($\bar{t}_2$)).

- The time it takes for the smoke-filled air column between the jet fan and the smoke extraction portal to be removed from the tunnel is derived from the temporal progression of the flow velocity and the distance between the jet fan and the smoke extraction portal, cf.

$$\bar{t}_2 : \int_{\bar{t}_1}^{\bar{t}_2} u(t, x_{SV}) dt := x_{Portal} - x_{SV+60m}$$

Equation 1: Estimated time duration for removal of destratified smoke

4. RESULTS

The options for ventilation control for the described model tunnel application discussed in section 0 have been assessed based on a direct comparison of the two possible ventilation alternatives with respect to the expected number of fatalities resulting from the application of the adapted TuRisMo fire consequence model. The detailed results for fire zone FDZ 04, characterized by an initial airflow direction toward the south, are presented in Figure **3** and Figure **4** as a representative example to illustrate the applied methodology. In Variant I, the targeted longitudinal airflow velocity was successfully achieved, as shown in the left part of Figure **3**. To reach this velocity, both authorized jet fans were activated. In Variant II, natural ventilation was applied. The distance between the fire location and the activated jet fan in Variant I was 190 m. Results from the 3D CFD simulation using FDS (Fire Dynamics Simulator) indicate an increase in cross-section-averaged temperatures 60 m downstream of the relevant jet fan between 110 s and 320 s after ignition, compare Figure **3** (right part). After

approximately 320 s, the back-layering was suppressed by the developing longitudinal airflow velocity of –1.5 m/s, leading to a re-establishment of smoke stratification.

This effect was incorporated into the evacuation and survival simulations by applying cross-section-averaged smoke gas and temperature values for the section between the smoke extraction portal (north portal) and the jet fan (580 m) during the period of expected smoke layer destruction (indicated as **CSA** Figure **4**- left**)**. For times before and after this period, Face-Level values were used (indicated as **FL** Figure **4** - left**)**. Since an instantaneous restoration of stratification after back-layering suppression cannot be assumed, the time required to purge the air column between the jet fan and the extraction portal (the zone of destroyed stratification) was also calculated. In a conservative approach, cross-section-averaged values were applied for this additional period as well. The integration of head-level and cross-section-averaged smoke gas and temperature values into a unified dataset for Fire Zone 04 is illustrated schematically in Figure **4**. Based on this dataset, evacuation and survival simulations were performed for three representative population groups, with different walking-speeds and pre-movement times considered.

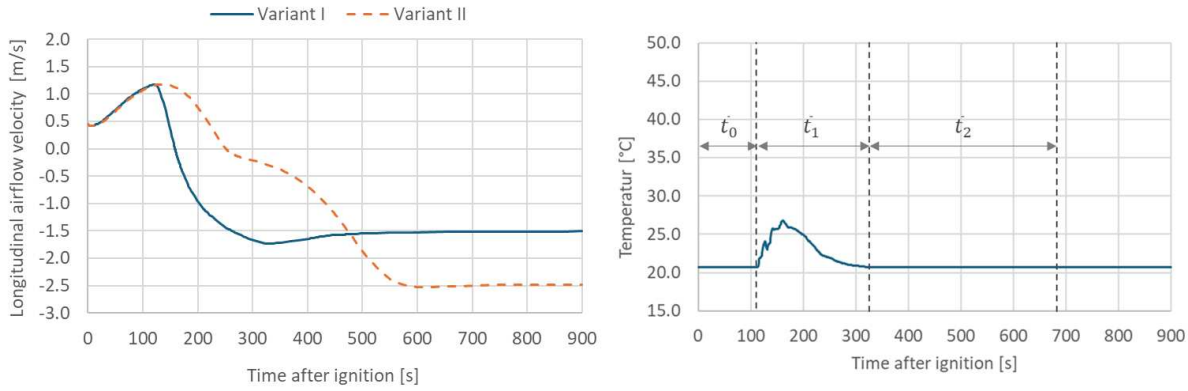


Figure 3: Time development of longitudinal Airflow (left): solid line Variant I vs. orange line Variant II, and temperature development 60 m downstream of activated jet fan for Variant I (right)

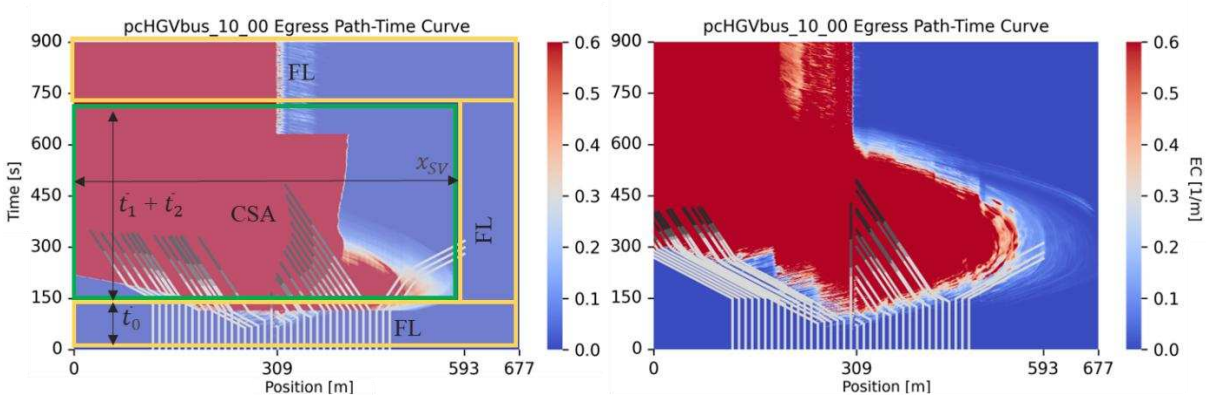


Figure 4: Temporal and spatial smoke density, along with path-time trajectories for one considered group of evacuating agents—Variant I (left) versus Variant II (right)

The spatial and temporal smoke density (expressed as extinction coefficient), together with the resulting path-time trajectories for one group of evacuating agents are also depicted in Figure **4**. Each trajectory represents an individual starting evacuation from a specific position within the vehicle queue. The trajectory color indicates intoxication level, ranging from light

(no impairment) to dark (severe impairment). Agents whose trajectories terminate at an emergency exit—portal or cross passage—or who survive until the end of the simulation period (900 s) are classified as successfully evacuated. Conversely, agents whose trajectories end prematurely before reaching an emergency exit are classified as fatalities. Both the numerical data and qualitative visualizations clearly demonstrate the superior performance of natural ventilation (Variant II) compared to the configuration involving temporary overblowing of activated jet fans (Variant I) for the considered scenario.

Table 2 presents the quantitative results of the scenario analysis, expressed as the number of fatalities per scenario and ventilation variant. For Fire Zones FDZ04 – south and FDZ05 – south, the outcomes are unambiguous: natural ventilation (Variant II) offers significant advantages during the self-rescue phase. This benefit is primarily due to the anticipated destruction of the smoke layer caused by activated jet fans in Variant I. For Fire Zone FDZ02 – south, Variant II also results in a slightly lower number of fatalities. However, considering the inherent uncertainties in modelling and parameter assumptions, as well as the fundamental advantages of controlled longitudinal ventilation—particularly the ability to maintain a defined airflow state—Variant I is selected despite the marginally higher fatality count. Due to the similarity of fire zones FDZ 02 – south and FDZ 03 – south as well as FDZ 04 – north and FDZ 05 – north , quantitative results for scenarios FDZ 02 – south and FDZ 05 – north have been used as decision basis for fire zones FDZ 03 – south and FDZ 04 – north, respectively.

Table 2: Quantitative Results for selected fire zones and scenarios

Fire Scenario	Fatalities Variant I	Fatalities Variant II	Suggested Variant
FDZ 02 – south	8.7	7.7	I
FDZ 03 – south	Not simulated	Not simulated	I
FDZ 04 – south	56.9	27.8	II
FDZ 05 – south	16.5	3.4	II
FDZ 04 – north	Not simulated	Not simulated	II
FDZ 05 – north	6.0	2.2	II

5. SUMMARY AND CONCLUSION

This study addressed the challenges of optimizing ventilation control in short, longitudinally ventilated road tunnels during temporary bidirectional traffic operation, a scenario increasingly relevant due to maintenance cycles in modern tunnel infrastructure. Using a representative model tunnel and the fire consequence analysis part of the Austrian TuRisMo methodology, ventilation strategies, focusing on the trade-off between regulatory compliance, operational feasibility, and safety outcomes were systematically analysed. Based on a discussion of the Austrian and German regulatory framework and the application of related requirements on a representative model tunnel it was demonstrated that, in short tunnels with compact ventilation zones, it is often not possible to fully satisfy all regulatory requirements for ventilation control during temporary bidirectional operation. In particular, the activation of jet fans in close proximity to a fire can lead to smoke destratification, significantly impairing visibility and evacuation conditions.

To optimize the ventilation control with respect to the available options and to potentially inform a following ALARP discussion and full risk assessment treatment, an adapted fire consequence modelling approach, which approximates the impact of jet fan-induced destratification, was adopted, enabling a more realistic assessment of the contrary ventilation

control approaches within the risk analysis framework. The results indicate that, for certain fire zones, natural ventilation (i.e., deactivating jet fans in smoke-filled areas) can substantially reduce the expected number of fatalities compared to configurations involving temporary overblowing by jet fans. However, in other scenarios, the advantages of controlled longitudinal ventilation—such as maintaining defined airflow and preventing smoke spread—may outweigh the risks associated with partial regulatory deviations.

Overall, the findings underscore the necessity of a flexible, risk-based approach to ventilation control during temporary bidirectional operation in short tunnels. By integrating quantitative scenario analysis and performance-based design principles, it is possible to identify ventilation strategies that achieve a maximum balance between safety, regulatory compliance, and operational constraints in the light of unavoidable safety requirement deviations and residual risk exceedance. The applied approximative approach to estimate the occurrence and impact of destratification because of activating close jet fans was particularly developed to be suitable for broader implementation in the full system-based risk analysis framework TuRisMo, which includes the quantitative treatment and simulation of hundreds of fire scenarios, and was thus kept this simple and approximative on purpose. This approach proved to be very efficient and produced overall plausible results. However, the utilization of 3D-CFD smoke propagation results, missing direct implementation of jet fans, in situations where jet-fan 3D-effects have the potential to severely impact the smoke-layer formation and thus the overall dynamics, is of course a strong oversimplification. This approach therefore bears the risk of leading to comparatively large uncertainties and modelling errors. It is therefore of utmost importance to attempt validation against experimental results or at least comparison to reliable 3D CFD simulations as part of the further development of the approach before integration of this approach in the overall risk analysis methodology.

REFERENCES

[1] European Parliament and Council, „Directive 2004/54/EC of the European Parliament and of the Council of 29 April 2004 on minimum safety requirements for tunnels in the Trans-European Road Network,“ *Official Journal of the European Union,* pp. L 167, 39–91, 2004.

[2] Bundesgesetzblatt, *Gesamte Rechtsvorschrift für Straßentunnel-Sicherheitsgesetz, Fassung vom 30.05.2025. BGBl. I Nr. 54/2006 idF BGBl. I Nr. 123/2022,* 2006.

[3] Austrian Research Association for Road-Rail Transport, *RVS 09.02.31 Tunnel Equipment - Ventilation Systems: Basic Principles,* Vienna: Austrian Federal Ministry for Traffic, Innovation and Technology, 2014.

[4] Bundesministerium für Digitales und Verkehr, *Richtlinien für den Entwurf, die konstruktive Ausbildung und Ausstattung von Ingenieurbauten: RE-ING Teil 3 Tunnel – Abschnitt 1: Planungsgrundsätze; Abschnitt 2: Konstruktive Anforderungen und bauliche Durchbildung; Abschnitt 3: Technische Ausstattung,* Bonn, 2023.

[5] Austrian Research Association for Road-Rail Transport, *RVS 09.03.11 - Methodology of Tunnel Risk Analysis,* Vienna: Austrian Federal Ministry for Traffic, Innovation and Technology, 2019.

[6] Purser, D. A., McAllister, J. L., „Assessment of Hazards to Occupants from Smoke, Toxic Gases, and Heat," in *SFPE Handbook of Fire Protection Engineerin (5th ed)*, Springer, 2016, pp. 2308-2428.

[7] Kohl, B., Senekowitsch, O., Nakahori, I., Sakaguchi, T., Vardy, A.E., „Risk assessment of fire emergency ventilation strategies during traffic congestion in unidirectional tunnels with longitudinal ventilation," in *Proceedings of the 17th International Symposium on Aerodynamics, Ventilation and Fire in Tunnels*, Lyon, 2017.

[8] Beyer M., Stacey C., „CFD Validation for Tunnel Smoke Control Design," in *Proceedings of the 11th International Conference on Tunnel Safety and Ventilation*, Graz, 2022.

[9] Khodadadi, R., Abbas ,T., Scriven P., Waldron, T., „Analysing the significance of turbulence models in predicting the installation efficiency of jet fans in tunnels: A comprehensive investigation," in *Proceedings of the 20th International Symposium on Aerodynamics, Ventilation and Fire in Tunnels*, Copenhagen, 2024.

EXTERNAL SMOKE MOVEMENT AND ITS IMPACT ON STATION DESIGN – GUIDANCE FOR VENTILATION LAYOUT

Jolyon Thompson, Mark Gilbey

WSP UK Ltd., UK

DOI 10.3217/978-3-99161-087-8-014 (CC BY-NC 4.0)
https://creativecommons.org/licenses/by/4.0/deed.de
This CC license does not apply to third party material (attributed to other sources) and content noted otherwise.

ABSTRACT

Space or planning considerations can lead to the need to use pavement level grilles for forced smoke exhaust from metros. The emitted smoke might be ingested into station entrances or stair pressurisation system intakes which could impact the ability to evacuate the station. This challenge is not unique to underground stations - guidance on vent separation distance is available with building codes, but the quantities of smoke in metro application vents can be much higher than commercial buildings. There is very limited similar guidance on vent separation available to the design engineer for metros/stations.

This paper explores the impact of smoke release at low level on key intakes for an assumed vent and entrance location for a simple station and urban configuration. It reviews a range of parameters which could impact upon the design and provides guidance on those which may be of importance. The paper also explores the benefits that an elevated release of smoke can offer so that the visual impact of an additional structure can be considered against the engineering consequences. The paper finally concludes with design advice that can be used during initial station layout. Whilst each station will have a wind microclimate that will affect smoke movement, some simple guidance as a starting point for laying out vents was considered as useful.

Keywords: Atmospheric dispersal, design guidance.

1. INTRODUCTION

Fire and smoke present hazards in underground stations and tunnels. To provide a safe environment to allow the passengers to evacuate in the event of a fire it is common to include a ventilation system. This may be natural or mechanical, but both will result in smoke being released to atmosphere local to the station.

Smoke rejected from the station can present an additional hazard to the station evacuation if the smoke interacts with entry/exits to the station or is drawn into the station via supply intakes. It is tempting in the initial stages of laying out a station to rely on building codes to define separation distances. Building industry standards such as BS 9999 in the UK for stair pressurization systems specifies a minimum separation of 5m [1]. This was presumably based on magnitudes of fire, ventilation, and smoke from buildings. Figure 1 shows the smoke emanating from pavement level grilles from the 2003 Daegu Metro fire in South Korea. The volume of smoke released from the vents and the impacts of wind were considerable, all of which suggests that building fires may not be a suitable proxy for underground station fires.



Figure 1: Daegu metro fire exterior conditions [2]

Smoke plumes and their dispersion in atmosphere have been studied extensively for many years, commonly using the Gaussian dispersion plume model. This approach is used to predict the dispersion of pollutants from a point source (like a chimney) in the atmosphere. It assumes the pollutant spreads in the crosswind (y) and vertical (z) directions according to a Gaussian (normal) distribution, with the mean wind advecting the plume downwind (x direction) [3][4]. The spread of the pollutants is assumed to be Gaussian driven and governed by the standard deviations in y and z which are typically developed from empirical data. This allows the user to select coefficients which will represent typical terrains and atmospheric stability. Over time these types of models have been extended to include for a variety of different factors including amongst others the impact that building wakes may have. The simplest models are variations on the Brigg's Gaussian model. These equations and formulas are often developed for very tall chimneys with minimal infrastructure downwind of the plume. In urban areas, the presence of buildings introduces complex, three-dimensional flow patterns that fundamentally alter plume behaviour compared to open terrain [5].

Buildings can block, deflect, or trap the plume, causing it to recirculate within street canyons or be ejected upwards or sideways at intersections [6]. Turbulence generated by flow separation and wakes around buildings increases the spread of the plume, often bringing it down to ground level more quickly than predicted by open-country models. The plume's path and concentration at any point can fluctuate rapidly due to coherent structures (e.g., vortex shedding, recirculation breakdown) and random turbulence [6]. Urban dispersion models (e.g., ADMS, OSPM) attempt to include building effects by parameterising street canyon recirculation, vertical exchange, and pollutant trapping, but still face challenges in highly mixed or varying environments [5][6][7]. Wind tunnel studies have also shown that buildings significantly affect dispersion patterns, introducing complexities such as recirculation zones, wake effects, and plume splitting. These effects go significantly beyond the empirical corrections that are currently available with the building impact often being reduced to a single coefficient. They also typically underestimate peak concentrations near buildings [5] which is the area of greatest concern for the ventilation engineer.

The Brigg's Gaussian models are most effective for distances of greater than 100m and durations of more than one hour [5]. These models were originally developed using assumptions of continuous release of pollutant which is not the type of release associated with station fires. Attempts to improve this limitation were developed for short duration releases of pollutants, or puffs. These puffs can be combined with multiple puffs making up a single simulation. This approach offers some improvement when considering mean pollutant concentration but due to advances in CFD, the simple models are no longer considered to be the best approach [7].

Where local and short-term effects are of importance, such as smoke release around metro stations, then it has been recommended that wind tunnel and Computational Fluid Dynamics (CFD) are conducted [5]. Large Eddy Simulation (LES) techniques are useful in this application as they can reasonably portray the dynamic nature of wind flows as well as offering reasonable accuracy and computational costs. Flemming and Rhodes used FDS to study smoke movement from metro fires and concluded that this approach was able to be used when used to assess above ground smoke movement [8]. Noteworthy in their paper is the need to validate the modelling approach and they provide reference to experimental data that can be used to do this. Models can resolve the complex, unsteady flow and pollutant dispersion in urban environments, capturing the effects of individual buildings, street canyons, and intersections.

2. SIMPLIFIED DISPERSION MODELLING

When it is not possible to obtain project specific CFD data, the following considerations are recommended when applying Gaussian models alone.

1. Model the system both with and without building wake interactions to get a spread of potential outcomes.
2. In recognition of the limitations and likely underestimation of Gaussian model predictions apply engineering judgement as to the applicability of the results. The safety factor to apply will depend upon the project circumstances and should be acknowledged as a source of uncertainty.
3. Where available use wind tunnel and CFD data for similar regions to calibrate and validate the empirical correlations used to determine the standard deviations. This is of increasing importance for complex urban and industrial locations.

Following the above steps is extremely challenging for the ventilation engineer as a large proportion of the approach is subjective, with limited guidance on how to select appropriate coefficients. CFD models can be time consuming and thus costly to develop and run and may be disproportionate in the initial stages of a station project design. However, if not considered early any later station design changes that arise can be expensive. It would therefore be useful to develop some simplified design guidance for early stages of projects.

The focus of the remainder of this paper is to try and provide specific data that can be used to inform initial design layout of a station smoke control system. This paper adopts the FDS modelling methodology described by Flemming and Rhodes [8] to develop a data set for a simplified station realm.

3. FDS MODELLING

3.1. General

A highly simplified test domain was developed to keep the results from this paper generic. The domain and analysis assumed that the only features of interest were the smoke release and a station entrance/air intake. Air was assumed to be entering the station entrance mimicking the effect of make-up air from a station smoke exhaust system.

The exhaust vent and intake relationships were tested using a parametric study varying the separation distance between the release point and intake, the external wind speed, the volumetric flow rate of the smoke exhaust, the volumetric flow rate of the intake and the differential height between the smoke exhaust and the intake. In all cases the wind was assumed to be blowing directly across the smoke exhaust vent towards the station intake. The model assumed upstream turbulence indicative of a metro located in an urban environment.

The wind was modelled using the Jarrin approach that was validated by Flemming and Rhodes [8].

The simulations were conducted to achieve quasi-steady conditions. The soot was exhausted at a constant mass fraction and temperature of 90°C. The mass fraction and temperature were selected based on the values measured across a wide range of station smoke control systems that the authors have worked on. They were not indicative of any specific scenario but could be appropriate for a train fire of between 7 and 14 MW. Therefore, the results should be interpreted based on relative comparisons rather than specific values. Warmer smoke would have been more buoyant but the analysis suggests that inertial forces were tangibly larger than buoyancy forces and hence the sensitivity to hotter smoke was not expected to be very high.

The results are presented as visibility at head height which was determined for a light reflecting sign and using a mass extinction coefficient of 8,700 m²/kg. This enables the results to be considered in a manner that the tunnel ventilation engineer is familiar with. For information, two trend lines were added to the results at 10m and 20m. The 10m visibility is the limit for tenable evacuation across a wide range of standards [9][10]. The 20m visibility is added to provide a limit that allows for some interaction of ingested smoke with smoke that is not extracted by the ventilation system.

3.2. Initial Findings

An initial data analysis was undertaken which varied separation distance, wind speed, smoke exhaust and intake flow rates which involved 270 parametric FDS simulations. The models predicted the expected fluctuations in wind that can be observed in nature. Therefore, if results are considered at snapshots in time this can mask overall trends. Therefore, all results in this paper are provided as 30s averages taken over the final 30s of the FDS model (when quasi-steady conditions had been achieved). These 30s average results for all 270 cases are presented in Figure 2 with all cases plotted as individual points. To make the chart easier to read and identify potential trends, coloured ‘patches’ are drawn around the most extreme points for each wind speed. The colours of the patches match the marker shown in the legend (i.e. the 4 m/s bubble is green etc). The two black lines show the 10m and 20m thresholds which were used for indicative assessment purposes.

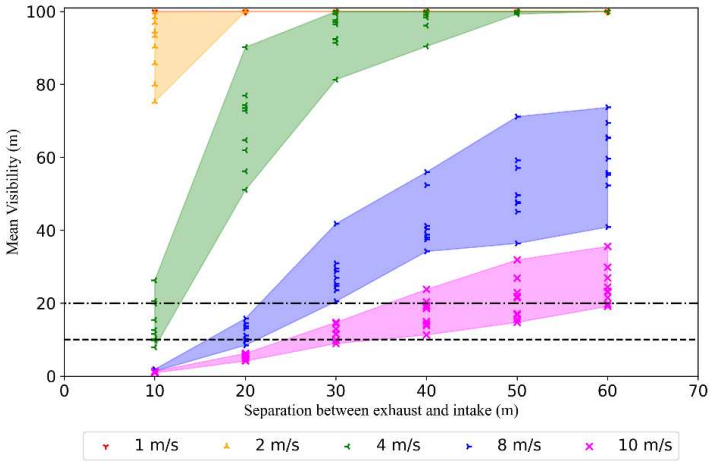


Figure 2: Variation of visibility averaged over 30s with wind speed

The initial data review considered trends against all variables tested. This indicated that variations in the flow rate of the smoke exhaust and intake did not have a significant impact on smoke dispersion, so no further comment is made on either of these variables. The analysis

covered a range of 70 to110 m³/s of smoke exhaust and an intake over a range of 10 to 30 m³/s. All remaining runs presented used a smoke exhaust of 90 m³/s and a station intake of 20 m³/s. The results are presented against wind speed as this was the only variable to exhibit a strong correlation between variables.

The visibility at ground level and head height was only reduced below the thresholds of 10 and 20m for wind speeds more than 4 m/s. The impact downstream was significantly increased with wind speed. This result was expected. The key takeaway in this chart though is shown in the coloured patches which show the spread of results that can occur in simulations.

3.3. Height differences

For smoke rejected at ground level the wind interactions were constrained by the ground plane. Elevating the smoke exhaust and intake (for example using small chimneys on the exhaust) so that they were less impacted by the ground plane was considered. Figure 3 shows plots for both exhaust and intake at the top of a single-story building (4m) and a two-story building (8m). For brevity both heights are plotted together but the 8m high results can be distinguished using the larger marker size. The new data are shown by symbols, and the shaded area shows the prior data from Figure 2.

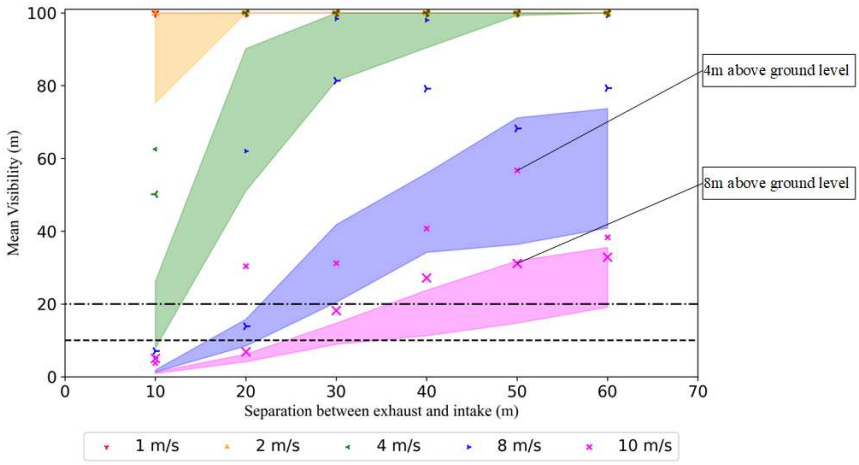


Figure 3: Impact of release height

Figure 3 shows that, all other actions being equal, releasing smoke at height is beneficial even without a height difference between the exhaust and intake. The loss of visibility was reduced at all points downstream. This is true for all wind speeds and shows that the lower elevation of the release of smoke, the greater the required separation that is required. In most cases 4m is shown to be more beneficial than 8m although not in all. This is thought to be due to the nature of the flow disturbance caused by the chimney used to elevate the exhaust and intake locations. However, this was not fully investigated during this paper and remains as a further area of study.

Height differences between the smoke exhaust and the intake were also tested. Depending on the layout these were favourable (intake below exhaust) or adverse (intake above exhaust). This finding was unremarkable and would be in line with an experienced practitioner's expectations. Therefore, this was not shown graphically for reasons of brevity.

3.4. Obstacles between exhaust and intake

Obstructions could consist of vegetation (trees or shrubs), buildings, walls, any other station infrastructure. It is not practicable to discuss many forms of blockages and obstruction within this paper. A generic structure was considered and the layout of the obstructions considered are shown schematically in Figure 4. The first was a thin wall located 2.5m downstream of the smoke exhaust marked 'A' in Figure 4. The thin wall was modelled as 1m wide ('W') and could be considered as a smoke screen intended to force smoke up. The second was a building which runs the full distance between the exhaust and intake with a 2.5m margin on either end (i.e. as separation distance increases the width of the obstruction increases). The purpose of the building is not relevant to this discussion.

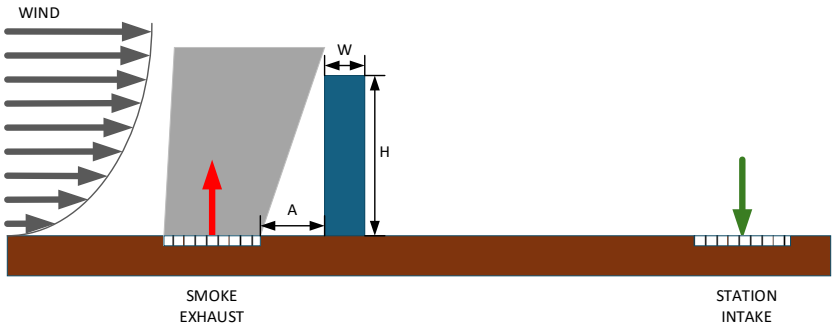


Figure 4: Obstructions used in FDS model

In both cases the obstructions were 10m long in the plane coming in and out of the page (and thus not shown in Figure 4). This 10m dimension was five times longer than the length of the smoke outlet. Time did not permit sensitivity tests to the 10m obstruction length used in the model. The obstruction was located such that the smoke exhaust and intake were on the centre line of the obstruction. This allowed air flow to flow around the obstruction and cause interactions between the building wake and the intake. The obstructions were initially implemented as being 6m high, H in Figure 4, which is representative of a two-story building or a reasonable spacious concourse.

The results are shown in Figure 5 again retain the same format of Figure 3 with the new results superposed over the shaded areas from Figure 2. This figure shows the results of building of different narrow widths (i.e. just a wall) with small markers and one with the width 5m less than the separation distance, (i.e. if the separation distance was 30m the obstruction width was 25m with the building centred between the exhaust and intake) with large markers.

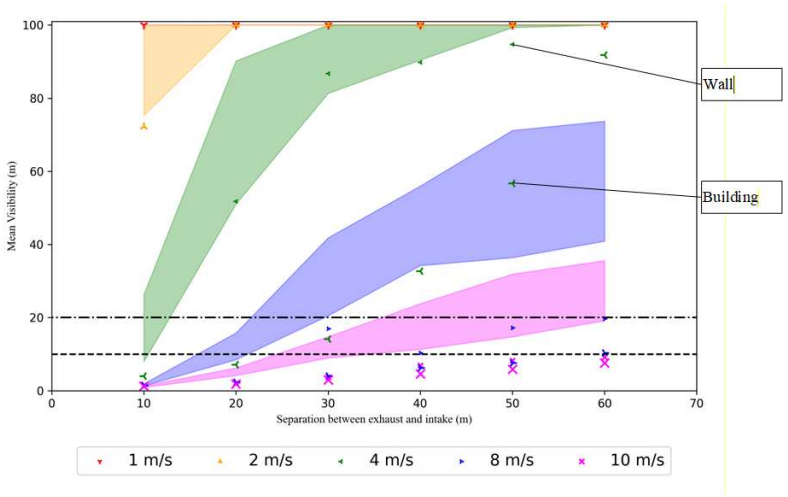


Figure 5: The impact of obstructions between the exhaust and intake for two different building widths

The buildings had a negative impact causing smoke to drop more quickly for all wind speeds. The extra turbulence caused by the obstruction seemed to cause more issues than it resolved. It was observed that the wider buildings caused the greater negative impact upon the visibility results.

The cases shown in Figure 5 were repeated for a building height of 15m rather than 6m. This was the only difference between the obstructed simulation sets. The results from this are presented in Figure 6.

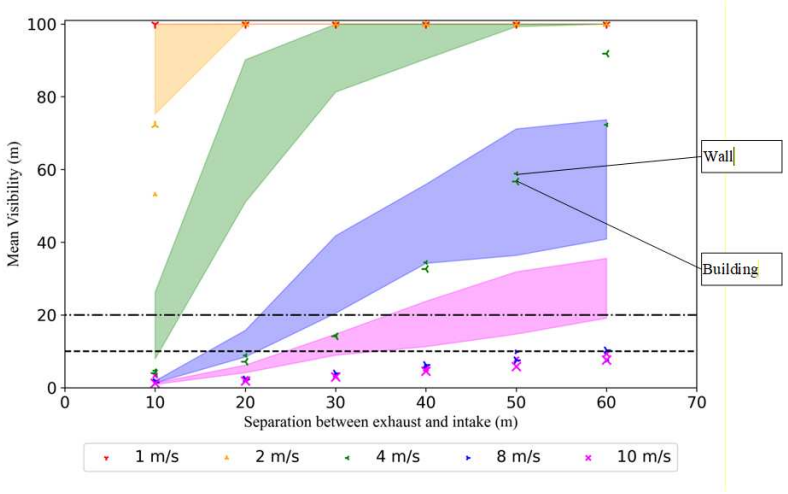


Figure 6: The impact of tall obstructions between the exhaust and intake for two different building widths

The results from the higher building were similar to the lower building at high wind speeds. The impact of the building height though was more pronounced at lower wind speeds with 4 m/s particularly changed as an impact of building height. The visibility became worse as the building height increased. Potentially the impact could have been less if the obstruction was longer/wider than 10m. The effect of building height is therefore wind speed dependent and is of importance to the ventilation engineer.

4. DESIGN IMPLICATIONS AND RECOMMENDATIONS

The results show that for some situations more than 50m may be needed between intake and exhaust which is significantly more than some building code requirements and suggest. A key early question to be resolved by the ventilation engineer is how much reduced visibility can be accepted at the entrance? One might argue that as long as the visibility is greater than 10m the situation is acceptable; however, lower visibility incoming air may mix with smoke in the station and result in an overall worsening of the outcome.

Greater separation was required for higher wind speeds and it is recommended that local microclimate information is obtained as early as practicable within the project and reviewed in the context of the design wind speed and extent of risk the project may accept. Releasing smoke at low elevation resulted in more smoke spread closer to ground level so where practicable release at height is recommended. Little sensitivity was shown to smoke exhaust and intake flow rates.

The impact of buildings is significant and was shown to be impacted by the height and overall shape of the building. The analysis highlighted the complexity of the problem with a two story building being shown to make the test case more vulnerable to cross contamination. Whilst the same was true for a five story building the impact was much more significant at the middle range of wind speed. This implies that changes in the building landscape, for example from over-site and adjacent site developments, should be subject to rigorous analysis to ensure that they don't generate a significant adverse impact on the system prior to their acceptance. Where over-site development is permitted or expected it is recommended that the buildings have microclimate studies undertaken very early in their development. This will enable suitable design modifications to be established early in the process. It is also recommended that a smoke stack through the building should be included where possible to minimize the risk of cross contamination to both the station and the development.

5. CONCLUSIONS

This paper presented a CFD study on the potential for cross contamination of smoke in underground station environments. The findings highlight several key considerations for the design and layout of ventilation systems in such settings.

Firstly, the results indicate that separation distances more than those noted in building codes are probably required. Secondly, wind speed and smoke release height play an important role in smoke dispersion. Finally, the impact of buildings and other obstructions was shown to be significant, with the height and shape of these structures affecting the potential for cross-contamination. The impact of the buildings tested was shown to be non-linear. However, it is acknowledged that further research is needed to provide quantified recommendations. Where buildings need to be considered it is recommended that a safety margin is included within initial station layout.

The findings in this paper are intended to guide the early stages of project development, with the understanding that detailed CFD analysis will be necessary at later stages.

6. REFERENCES

[1] British Standards Institute, 2017, Fire safety in the design, management and use of buildings – Code of Practice, BS 9999

[2] Associated Press, http://news.bbc.co.uk/1/hi/world/asia-pacific/2774561.stm, Retrieved on 10th October 2025

[3] Gary A. Briggs (1965) A Plume Rise Model Compared with Observations, Journal of the Air Pollution Control Association, 15:9, 433-438

[4] Turner DB, 1970, Workbook of atmospheric dispersion estimates, US Department of Health Education and Welfare

[5] Woodward H, Gallacher D, Robins A, Seaton M, ApSimon H, 2021. A review of the applicability of Gaussian modelling techniques to near-field dispersion, ADMLC project ADMLC-R11.

[6] ADMS User guide, 2023, Cambridge Environment Research Consultant Ltd.

[7] Bentham JHT, 2003. Microscale Modelling of Air Flow and Pollutant Dispersion in the Urban Environment. Ph.D. Thesis. Imperial College London.

[8] Flemming C. and Rhodes N., 2018, A validation of the fire dynamics simulator for smoke dispersion from metro stations, 9th Int Conf Tunnel safety and ventilation, Graz

[9] British Standards Institute, 2020, Fire safety in the design, management and use of rail infrastructure – Code of practice, BS 9992

[10] NFPA, 2026, Standard for fixed guideway transit and passenger rail systems, NFPA 130

SAFETY CHALLENGES OF HIGHWAY LIDS IN THE US

[1]Petr Pospisil, [2]Colin Santangelo, [1]Bernd Hagenah

[1]Tunnel Safety & Ventilation Consultant, US
[2]HNTB Corp., US

DOI 10.3217/978-3-99161-087-8-015 (CC BY-SA 4.0)
https://creativecommons.org/licenses/by/4.0/deed.de
This CC license does not apply to third party material (attributed to other sources) and content noted otherwise.

ABSTRACT

Covering highways with lids creates space for recreation and urban development, reduces noise and pollution, and improves traffic safety, among other benefits. Urban highways are characterized by large traffic numbers on multiple lanes with regular congestion. While actual road tunnel safety knowledge is mostly derived from European tunnels with two or three lanes per tunnel cell, there are a few examples of modern urban highway tunnels with many lanes in each direction. Local driving habits and codes need to be considered alongside the laws and provisions in the US.

Basis of design is a safety concept, describing safety systems and equipment in order of their effectiveness, prioritizing preventive measures. An Engineering Analysis for approval by the Authority Having Jurisdiction (AHJ) is required by the governing fire safety code NFPA 502. For that, we propose a Quantitative Risk Analysis (QRA), focusing on accident risks based on statistical data, and on fire risk based on simulations of smoke spread and egress for different scenarios under varying initial and boundary conditions. Statistical data about accidents and vehicles fires are available from the vast US road network. Tunnel specific European data and adapted to conditions in US high-way lids which differ from European tunnels. The appropriate simulation of different traffic scenarios is essential to understand the application of measures such as detection and traffic control, emergency exits, mechanical ventilation and Fixed Fire Fighting Systems. This paper describes a holistic approach to tunnel safety by providing a methodology for developing safety concepts and QRA with focus on tunnel ventilation aspects.

Keywords: Highway Lids, Tunnel Safety & Ventilation, Risk Analysis

1. INTRODUCTION

In many countries, highways have been built through cities, disconnecting urban centers and neighborhoods. Covering such highways with lids creates space for recreation and urban development, reduces noise and pollution, and improves traffic safety, among other benefits. Urban highways in the US are characterized by unidirectional traffic on multiple lanes with regular congestions, and large cross sections. Actual road tunnel safety knowledge is mostly derived from European tunnels with two or three lanes per tunnel cell, but there are few urban highway tunnels with many lanes in each direction.

Key differences between Europe and the US to be considered are:

- Legal framework
- Driving habits
- Operational experience

2. US SPECIFIC CONDITIONS

2.1. Legal Framework

Most European countries with extensive tunnel experience have a framework of road tunnel standards, providing coordinated and detailed requirements for the concept, design, operation and quality assurance of road tunnel structures and systems (e.g., [9]).

Details of the legal framework in the US are not subject of this paper, but it should be mentioned that in the US, road safety requirements are based on federal, state and AASHTO guidelines [3], and tunnel safety systems are determined by various guidelines e.g., the ANSI/IES guideline RP-8 [4] for tunnel lighting, the NFPA 502 standard [1] for fire safety measures including fire ventilation, the ANSI/ASHRAE Standard 217 [5] for operational (non-fire) ventilation, and the FHWA TOMIE manual [6] for operation and maintenance.

A tunnel project in the US must be approved by the local Authority Having Jurisdiction (AHJ), which is often the Fire Marshall. This AHJ usually refer to codes such as NFPA 502 (see [1]), which formulate performance-based requirements referring to an 'engineering analysis.' The specific methodology for this analysis is not detailed prescriptively, which can lead to different interpretations in practice.

Often, AHJ follow building codes for fire life safety, arguing that a road tunnel is a building. Consequently, tunnel systems in the US are sometimes planned by designers who apply a 'Fire Life Safety' approach derived from building codes. This approach may not always fully address the specific conditions unique to tunnel environments, in particular the vehicular traffic and resulting longitudinal airflow.

In cases of uncertainty, there may be a preference for a technical solution perceived as the most conservative, potentially placing less emphasis on cost-benefit considerations or long-term operational issues. That is explained in particular for the example of tunnel ventilation (section 5).

2.2. Driving Habits

In contrast to the conservative approach often seen in tunnel system design, road traffic fatality rates in the US are statistically higher than in many comparable European countries. E.g., in 2022, the road fatality rate per billion km driven was 8.2 in the US, and 4.6 in Germany (a country without speed limit on highways). The road traffic fatality rate per inhabitant is even approx. 4x higher than in Europe considering that Americans on average drive more.

Different driving behaviors may be a contributing factor. For example, the observance and enforcement of speed limits in the US may be less strict. On multi lane highways, weaving and sudden braking are major causes of collisions. This needs to be considered for road tunnel risk assessment and operational measures, in particular traffic management.

2.3. Operational Experience

The first US automobile tunnels were the Liberty tunnel in Pittsburgh opened in 1924 and the Holland tunnel under the Hudson river between New York and New Jersey in 1927.

Transversal tunnel ventilation for dilution of vehicle emissions was developed by the Pittsburgh Bureau of Mines. However, in the following decades, only few, mostly short road tunnels were built. Today, there are approx. 185 road tunnels with a length exceeding 300 m (1000 ft) in the US, according to the FHWA National Tunnel Inventory database (NTI).

In contrast, in Europe, there are over 4000 road tunnels with lengths exceeding 300 m, and much longer tunnels. After large fire incidents in the 1990s, European road tunnel safety has been substantially improved, and there is extensive operational experience with modern road tunnels and their safety systems.

Urban highway lids in the US were built since the 1970s, but most of the existing or actually planned or constructed lids are very short, with lengths rarely exceeding 500 m. On the other side, US highway lid cross sections are mostly larger than in European tunnels.

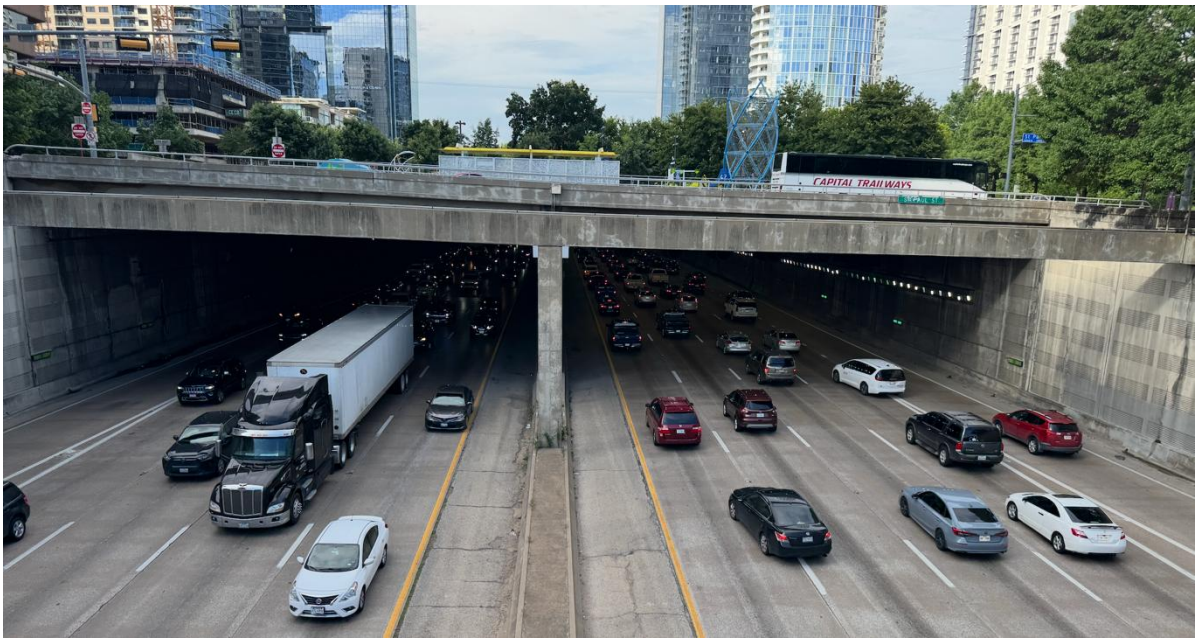


Figure 1: Klyde Warren Park, Dallas TX, 366 m long, opened 2012 (photo by author)

3. SAFETY CONCEPT

3.1. Overview

A holistic safety concept serves as the design basis for road and structural measures, systems and equipment, and has been described in other publications (e.g., [23]). Hazards are evaluated and assessed, safety goals are defined, and safety measures are ranked by effectiveness to prioritize prevention while complying with US codes and guidelines that focus on fire and life safety. The following discussion focuses on the most significant hazards in road tunnels and highway lids: collisions and fires. Other hazards, such as natural disasters or structural collapse, must also be considered within the safety concept but are beyond the scope of this paper.

3.2. Hazards: Collisions

Collisions impose the most significant risk to drivers on roads. The risk is largely related to driver behavior and vehicle properties.

Generally, there is an increased likelihood of collisions in tunnel portal zones, same as under wide bridges, due to changing light conditions. In contrast, the interior of tunnels provides

safe, uniform conditions. Drivers are shielded from changing light, unfavorable environmental conditions such as rain, snow and ice, and tunnels prevent collisions by inhibiting access to pedestrians and animals. Therefore, the collision risk in long road tunnels is lower compared to open roads.

3.3. Hazards: Fires

Fires on roads happen far less often than collisions. According to US NHTSA and NFPA data ([17], [18], [19]), and the PIARC report [15]:

- Approx. 70 - 80% of vehicle fires result from technical defects (mechanical, electrical), 10 - 20% from collisions.
- In 80 – 90% of fires "there is neither personal injury nor damage to property", that means most vehicle fires are insignificant.
- Approx. 0.3% of collisions result in fires.
- While collisions are not the primary cause of fires overall, they are the leading cause of particularly large fires that can result in fatalities and significant structural damage.
- Therefore, any safety measures that reduce the collision risk also reduce the fire risk.

4. SAFETY MEASURES

4.1. Prevention

Hazard prevention, primarily concerning collisions and fires, is the highest priority. The following prevention measures apply both to open roads [7] and tunnels:

- Driver education.
- Well maintained vehicles in good condition with on-board safety systems (e.g., driver assistance systems).
- Traffic concept and road alignment providing a smooth, constant travel through the tunnel as far as possible (e.g., by adequate lane & shoulder width, avoiding impact surfaces, avoiding lane merges in tunnels, avoid weaving, etc.).
- Measures to improve driver awareness and avoid distraction.
- Speed limit, adequate to sight distance and traffic conditions, that may be enforced.
- Traffic management, avoiding congestions.
- Traffic restrictions (permanent or temporary, e.g., on hazardous goods).

Tunnel specific prevention measures [16] are:

- Bright tunnel walls, shielding drivers from distraction, separating roadway directions, and serving as fire compartmentalization.
- Wide shoulders.
- Tunnel lighting, which is directly related to the permitted speed and sight distance. Appropriately designed and controlled lighting is especially important to reduce the collision risk in the portal zones.
- Floor guidance lights reduce the probability of accidents and serve as wayfinding lighting for egressing motorists in case of a fire.
- Mechanical ventilation to ensure acceptable air quality and visibility (see section 5)
- Regular inspection and maintenance of structure, systems, and equipment.

Since any traffic obstructions increase the collision and fire risk, lane closures for maintenance and construction works should be limited as far as possible.

4.2. Mitigation

Mitigation measures reduce the immediate impact of an incident when prevention failed.

- Fast incident detection, in particular:
  - Acoustic Detection System (ADS)
  - CCTV camera system with Automatic Incident Detection
  - Smoke detection / visibility measurement
  - Fire detection (Linear Heat Detection system)

  Reliability of detection is essential, because false alarms may have negative effects.
- Signals and barriers for lane or tunnel closures in case of an incident with adequate length for lane changes and deviations.
- Signals inside long tunnels, to prevent vehicles from approaching the incident site further.
- Traffic management in the adjacent road network, to allow for traffic leaving the tunnel in case of an incident.
- Fixed, automatic Fire Suppression System (FFFS).
- Drainage.

4.3. Evacuation

Evacuation measures facilitate the safe egress of tunnel occupants from the hazard zone to a designated place of safety.

- Wide shoulders to provide safe evacuation path beside active traffic lanes.
- Emergency exits in short distances, equipped with appropriate doors and signage.
- Emergency lighting and floor guidance lights.
- Public Addressing / Voice Alarm System (PA/VA).
- Mechanical ventilation / smoke control (see section 5).

4.4. Rescue

Rescue measures facilitate emergency service operations in rescuing motorists and suppressing fires.

- Emergency Response Plan.
- Emergency responder access routes.
- Staging areas at portals.
- Means of communication.
- Standpipes with FD connections.
- Staging areas at portals.
- Rescue equipment.
- Regular emergency responder training & exercises.

Those measures protect in first order life and health. Asset protection measures, such as structural fire protection, are treated separately.

5. TUNNEL VENTILATION

5.1. Basic Considerations

Tunnel ventilation is a key feature that can either mitigate or aggravate smoke spread in a tunnel, which affects tenable conditions for evacuation of motorists and access of first responders. For highway tunnels with unidirectional traffic, longitudinal ventilation with

impulse fans (jet fans or nozzles) is the mechanical ventilation system of choice. Additional concentrated smoke exhaust is required in some European countries for urban highway tunnels with high probability of congestions and blocked vehicles, but substantially increases costs and can bring additional risks (see Compendium [23]). Transversal ventilation systems, as applied until a few decades ago for the dilution of high vehicles emissions, are considered obsolete nowadays.

The key questions are, when does a mechanical ventilation make sense, and how should it be operated? As explained in the Compendium [23], in short tunnels, the number of motorists potentially exposed to smoke is low, escape routes to the portals are short, and short tunnels would be smoked-up across a large part before the ventilation could even react.

5.2. Comparison Europe – US

Referring to highway lids with unidirectional traffic, key differences between actual tunnel ventilation requirements in Europe and the US are as follows:

- According to the EU directive [8], which determines minimum requirements, mechanical tunnel ventilation is not required for tunnels under 500 m length. That may vary in country specific guidelines. E.g., in Switzerland, the minimal length for ventilation requirement in unidirectional traffic tunnels is 600 – 800 m [9]. Switzerland has only approx. 0.4% of the area of the US, but almost twice as many road tunnels exceeding 300 m length, and much longer tunnels.
- Currently in the US there are some very short highway lids with lengths under 500 m that are equipped or planned with a mechanical ventilation. The design basis may focus on a specific hypothetical scenario where ventilation is beneficial (see Figure 4). This might not fully account for dynamic effects, such as traffic-induced airflow, or scenarios where mechanical ventilation could be detrimental (see Figure 6). In practice, operational records show that some ventilation systems are not activated at all, even during fire incidents, while still requiring regular testing and maintenance.



Figure 2: Central 70 cover, Denver, CO, 307 m long, opened 2022 (photo by author)

- In Europe, ventilation requirements for urban highway tunnels with high probabilities of congestions are similar as for bidirectional tunnels, considering the possibility of motorists being exposed to smoke on both sides of a fire as described in the PIARC report [12] and many national tunnel ventilation guidelines. In contrast, in the NFPA 502 standard [1], there is no distinction between rural and urban tunnels with unidirectional traffic.
- Ventilation requirements could be compensated with other safety measures, e.g. shorter emergency distances. That can be evaluated by means of a risk analysis. That is also described in NFPA 502, but this approach has not yet seen widespread application in practice.

5.3. Flow Control

For fire ventilation, active control of longitudinal airflow is essential, in particular for urban highway tunnels, as described in the PIARC report [12] and the Compendium [23]. In principle, that would also be required to comply with actual NFPA 502 (2023 edition) requirements to 'control backlayering distance', or to 'keep longitudinal air velocity at low magnitudes where motorists can be on both sides of the fire side'. Until the 2020 edition, NFPA 502 required to achieve at least critical velocity in unidirectional traffic tunnels, ignoring the possibility of motorists downstream of the fire exposed to smoke. Active flow control has been applied in European tunnels for more than 20 years but not yet in the US [24].

However, in short tunnels, active flow control is not feasible, since there is no space for the necessary jet fans and anemometers at adequate distances, considering that jet fans close to a fire must not be operated, and instruments may provide distorted values, which need to be eliminated by a diligent plausibility check.

According to the PIARC report [12], without active flow control, a mechanical ventilation should not be operated at all when there is a possibility of congestions with motorists downstream of the fire exposed to smoke. That has been described e.g., by Bettelini for a 4-/5-lane highway lid [22]. Critical is particularly the case of a fire resulting from a rear-end crash at the end of a column of standing vehicles (see Figure 6).

Operating a tunnel ventilation without flow control may even increase the fire risk, as shall be explained for an example similar to the one in Figure 2. In short tunnels, the determining force is the wind pressure on the portals, which is in principle unknown and may strongly vary depending on the local meteorological conditions. Assuming a tunnel ventilation design case when the tunnel is filled with still standing vehicles in a congested situation over the whole length, the operating fans should achieve a flow velocity of approx. 3 m/s (critical velocity) against an assumed counter pressure of 10 Pa. But with a wind pressure of 10 Pa in the opposite direction and the tunnel filled only with 25% vehicles, the resulting flow velocity with the same number of operating fans would be 4.9 m/s. Such high flow velocities can fan a fire and accelerate downstream smoke spread, immediately disrupting smoke stratification. While small fires may allow for tenable conditions downstream due to smoke dilution within the large tunnel cross-section, large fires intensified by excessive airflow would endanger motorists exposed to the smoke.

A dynamic analysis shows that in case of congested traffic and strong wind against the traffic (see Figure 4), the smoke may have spread against traffic direction to the entry portal before that fire would be detected and any safety systems, particularly the mechanical ventilation, could react. When starting the jet fans in the smoke, a local backflow would occur, initially even driving the smoke against the traffic direction.

Moreover, the requirement to provide pressurization of the non-incident tube to prevent smoke spread through open cross passage doors (as specified e.g., in NFPA 502) cannot be met by providing only a row of fans at the entry portal.

5.4. Natural Smoke Exhaust

In some US highway lid project, designers proposed openings for natural smoke exhaust. In contrast, as part of refurbishment programs of some European tunnels, previous existing ceiling and wall openings had been closed based on operational experience. Arguments to be considered are:

- Natural smoke exhaust may work under favorable conditions of buoyancy driven flow, but in reality, the smoke is often driven by traffic or wind induced longitudinal flow past the opening along the tunnel.
- Ambient wind conditions outside the openings have a strong influence on smoke exhaust.
- Openings provide accident hotspots due to changing light conditions and entering rain and snow, increasing the risk.
- Openings are a source of noise, compromising one of the main benefits of the highway lid.

6. RISK ANALYSIS

6.1. General Description

Quantitative Risk Analysis (QRA) has been developed for a wide range of applications in the US, e.g., nuclear facilities, chemical industry and aerospace. There is a NPFA guide for evaluation of fire risks [2], and QRA is understood as an emerging practice for US road tunnels. In Europe, QRA is standardly applied to road tunnel projects, as described in PIARC [13] and many national guidelines and publications. For US road tunnel projects, we proposed to apply the German BASt methodology [20], [21] adapted to the conditions in the US.

The QRA focuses on accident risks based on statistical data, and on fire risk based on an event tree analysis for different scenarios. The scenarios are developed into an event tree, assigning probabilities to each scenario. The methodology has been described in the QRA report [20] and many publications (e.g. [26], [27]).

Analyzing only one or a few predetermined 'worst case' scenarios would lead to biased results. A serious analysis must evaluate 'worst cases' based on variations of traffic conditions (moving and standing vehicles), the type of fire, meteorological conditions, particularly wind on tunnel portals, fire buoyancy, and operating systems such as mechanical ventilation.

6.2. Traffic Scenarios

Beside wind pressure on the portals, moving traffic is the determining force influencing airflow and smoke spread in the initial phase of a fire in a tunnel, before the incident is detected and any systems can react. Therefore, defining different realistic traffic scenarios is essential for a serious analysis. Key scenarios are:

6.2.1. Free Flowing Unidirectional Traffic

During flowing unidirectional traffic, smoke spread is initially induced by moving traffic. Vehicles and motorists upstream are safe, vehicles downstream of fire should be able to drive out of the tunnel.

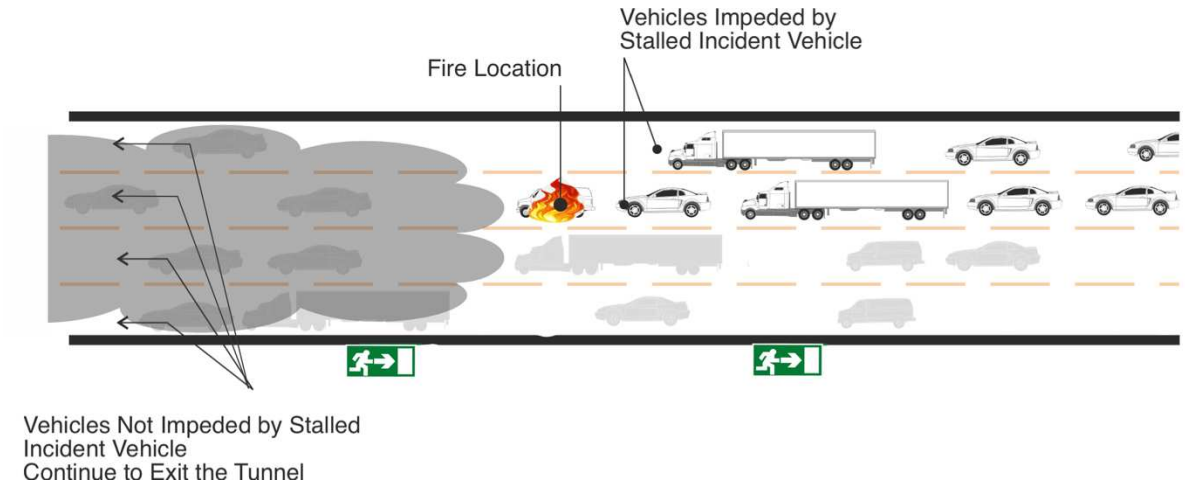


Figure 3: Free flowing unidirectional traffic

On the lanes behind the fire, vehicles are assumed to stop, as is modeled in common 1-D simulation tools (see Figure 7). However, in highway lids with 3 and more lanes, vehicles on the adjacent lanes are supposed to drive past the fire, further driving smoke spread in traffic direction. That must be considered for a realistic modeling.

As long as the traffic is moving, smoke is driven by the piston effect in the direction of the traffic. Motorists upstream (between the incident location and the entry portal) are situated in cold air and do not need to cross the active traffic lines to reach the cross passages.

Wind pressure and / or fire buoyancy may eventually lead to a flow reversal, which could be prevented by a mechanical ventilation.

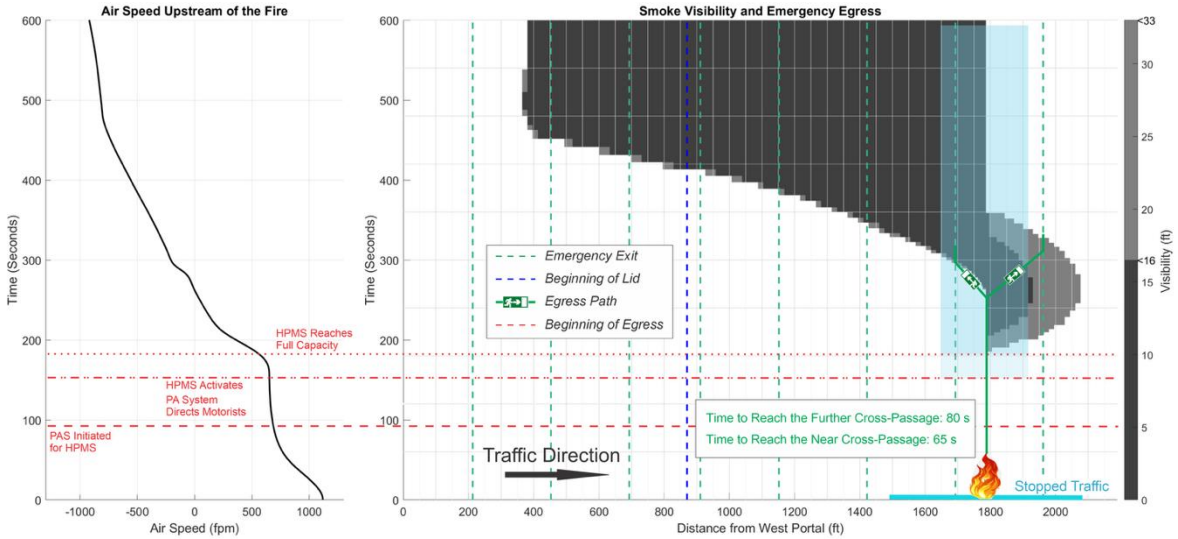


Figure 4: Simulation of flow and smoke spread with flow reversal

6.2.2. Congested Unidirectional Traffic

Congested traffic can be assumed as stop-and-go with low speed (e.g. 5 – 10 km/h). Still standing vehicles on all lanes for a long period are highly unlikely.

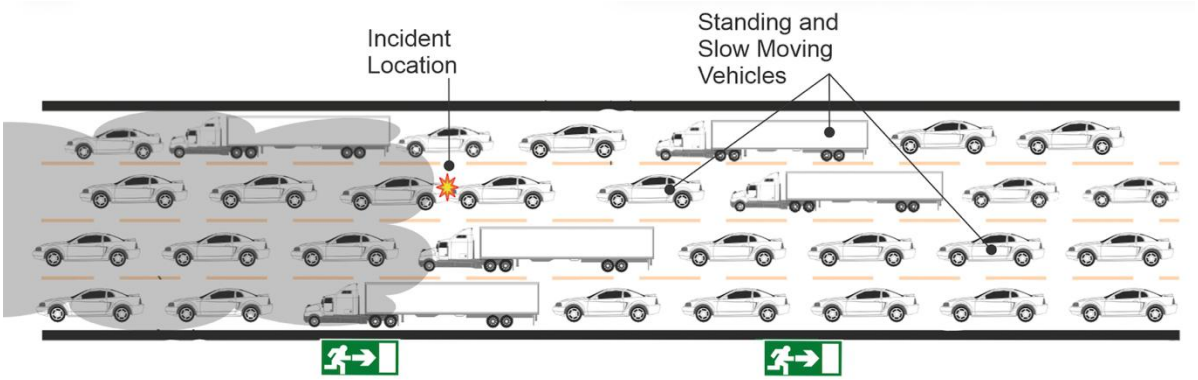


Figure 5: Congested unidirectional traffic

The likelihood of collisions with significant impact, and thus resulting fast developing large fires, is negligible. Nevertheless, fires from technical defects can occur and occasionally develop into large fires.

Strong wind pressure may lead to flow and smoke spread against traffic direction even in the initial phase. Cross passages serve for egress of motorists that are trapped in the smoke.

6.2.3. Unidirectional Traffic with Vehicles Blocked Downstream

The most dangerous scenario is when vehicles are blocked downstream of a fire, and motorists immediately exposed to smoke from a large fast developing fire. Such can occur e.g., resulting from a rear-end crash at a column of standing vehicles, which has led to some of the worst tunnel fire disasters (e.g., Tauern tunnel 1999, Yanhou tunnel 2014)

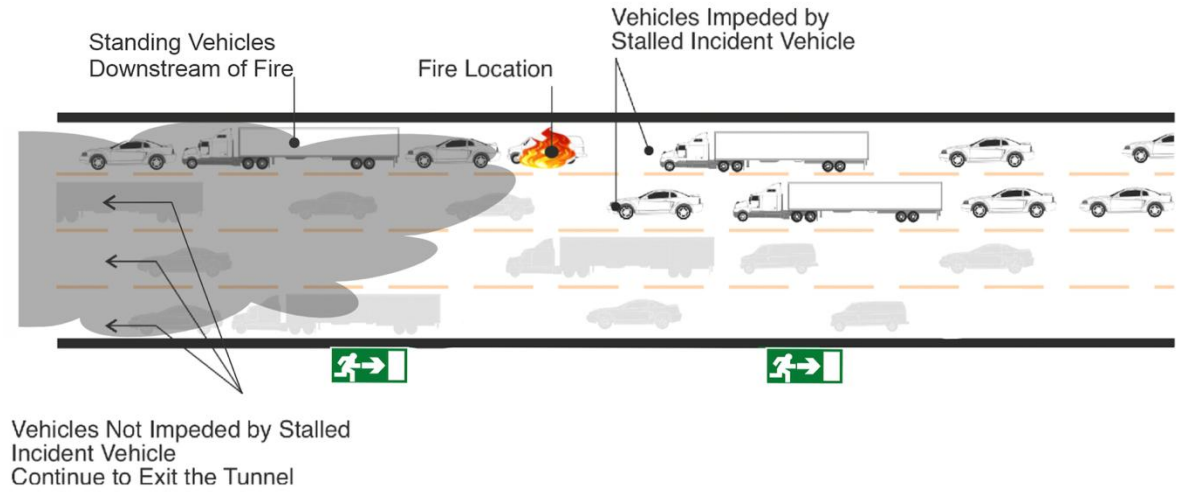


Figure 6: Unidirectional traffic with vehicles blocked downstream of the fire

Cross passages providing egress of motorists that are trapped downstream of the fire incident are essential. A mechanical longitudinal ventilation, blowing in traffic direction, would even deteriorate the conditions. A smoke exhaust system could limit the smoked up tunnel section, but the detection and reaction time needs to be considered when evaluating its benefit during the self rescue phase. Further, as explained in the Compendium [23], an additional risk arises due to the possibility of exhaust at the wrong place.

6.2.4. Bidirectional Traffic

Bidirectional traffic would also lead to motorists exposed to smoke on both sides of a fire, but is usually not considered in US urban highway lids. In case of a tunnel cell closure for maintenance or after an incident, the traffic is usually deviated to the surface road network.

6.3. 1-D vs 3-D modeling

Modeling is based on simplifications about aerodynamics and thermodynamics, using assumptions on physical parameters and boundary conditions.

Dynamic traffic and smoke spread modeling in road tunnels is usually conducted with 1-D models, as presented e.g. by Riess in 1999 [26], and developed into commercial simulation programs such as IDA.

However, actual models do not consider different traffic behavior on different lanes, as is the case in multiple lane highway tunnels. Therefore, we applied a combined approach with simulation of traffic on different lanes with different models which then needed to be combined.

1-D models do not display local effects, in particular smoke stratification and backlayering, asymmetric flow profiles, and turbulences, and therefore cannot be applied for complex geometrical structures. Smoke stratification during the evacuation phase provides tenable conditions up- and downstream of the fire, therefore a 1-D simulation considering only mean smoke densities is more conservative to assess how many motorists are affected by smoke in a given fire scenario, than a 3-D simulation with smoke stratification.

Most importantly, 1-D models can dynamically simulate moving and standing traffic and the resulting flow and smoke spread and are regularly validated by in-tunnel flow measurements and smoke detectors [25].

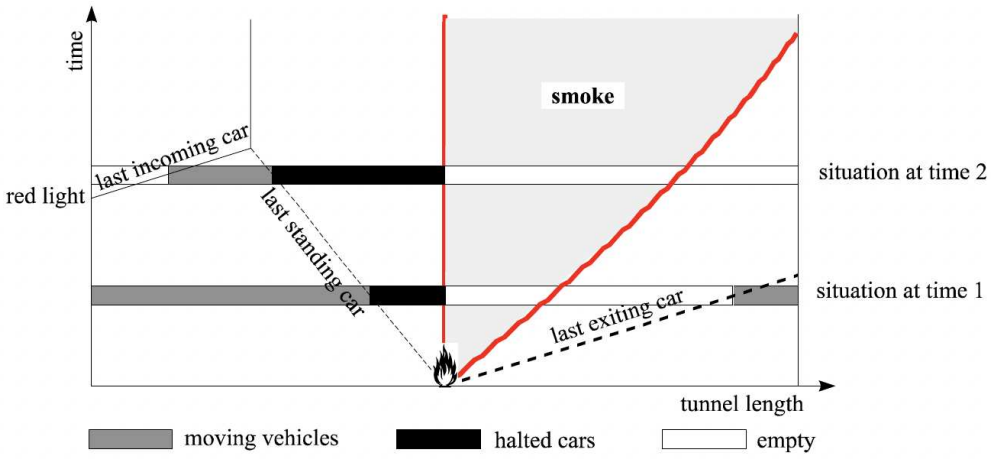


Figure 7: Traffic model and smoke spread for tunnel fire on 1-/2-lanes (from [26])

As a rule of thumb, a 1-D model is applicable for structures where the length is more than approx. 10x the width. For a 5 lane tunnel with a width of 25 m, that would mean that for lengths under approx. 250 m, 1-D modeling may be questionable.

On the other side, with 3-D models, moving vehicles cannot be adequately simulated with justifiable effort. 3-D models for road tunnels are useful for evaluating local aerodynamic effects, and fire modeling of buoyancy driven plumes, smoke stratification and backlayering. 3-D models can be particularly used to evaluate smoke stratification in critical scenarios that have been previously identified by 1-D simulations. Traffic induced flow can be modeled with

a 1-D model and then applied to the 3-D model as boundary condition, however that is not possible in short tunnels where the 3-D model comprises of the whole tunnel length.

3-D models cannot appropriately model turbulences, therefore simplified turbulence models are applied. In real tunnels, particularly under traffic or with operating jet fans, the flow field is so highly turbulent that details of 3-D results may be questioned in principle.

3-D tunnel fire models have been validated by a series of full-scale tests (e.g., 1995 Memorial tunnel in the US), but a validation for project specific tunnel geometry and aerodynamic flow conditions, particularly under traffic, is not possible. 3-D simulations strongly depend on arbitrary boundary conditions and assumptions, therefore, do not provide additional precision in the results in comparison to 1-D analysis, when only the mean flow and smoke density is considered.

7. SUMMARY AND CONCLUSION

With a systematic safety concept approach, improved tunnel safety and cost savings are possible by focusing on measures with best effectiveness, in particular prevention, and reduction of safety measures with little or even negative benefit. An important aspect of a safety assessment is to consider unwanted side effects and evaluate ‘what can go wrong’, considering practical experience.

An example is tunnel ventilation. Mechanical ventilation in unidirectional traffic tunnels is typically used to prevent smoke from spreading against traffic flow, but inappropriate operation without flow control could also lead to increased smoke spread and destratification, making conditions worse for motorists downstream of the fire. For facilitating egress, emergency exits in short distances are more effective.

With a Quantitative Risk Analysis, the risks can be brought in the right perspective. The accident risk in road tunnels is a magnitude higher than the fire risk, and can be derived from excessive statistical data and tunnel specific adjustments. Simulations of smoke spread and egress are a useful tool to assess the fire risk. Smoke spread depends on many different factors, especially the moving traffic in the initial fire phase, meteorological boundary conditions, and fire buoyancy in tunnels with considerable slope. Therefore, a series of simulations have to be conducted for different fire scenarios under different boundary and initial conditions.

3-D simulations, such as those used for buoyancy-driven smoke spread in buildings, may have limited applicability to road tunnels, as they often cannot adequately simulate the critical factor of moving vehicles. On the other side, 1-D models are not applicable for very short and wide highway lids. There is a principal limit of useful modeling with justifiable effort for such projects.

Therefore, it is proposed applying an analytical approach that incorporates extensive experience from international tunnel safety practices and adapts it to the specific conditions of US highway lid projects.

In particular:

- Safety measures should be evaluated based on a diligent Safety Concept, focusing in first order on prevention.
- The utility and possible risks of mechanical ventilation should be carefully evaluated for short urban highway tunnels, particularly where active flow control is not feasible.

- Compensatory measures may comprise of preventive measures like traffic management and floor guidance lights, fast and reliable incident detection, emergency exits in short distances, and possibly active fire suppression (FFFS).

8. REFERENCES

[1] NFPA 502, Standard for Road Tunnels, Bridges, and Other Limited Access Highways, 2023

[2] NFPA 551, Guide for the Evaluation of Fire Risk Assessments, 2022

[3] American Association of State Highway and Transportation Officials (AASHTO), A Policy on Geometric Design of Highways and Streets, 7th ed. 2018

[4] ANSI/IES RP-8-22, Lighting Roadway and Parking Facilities, 2022

[5] ANSI/ASHRAE Standard 217-2020, Non Emergency Ventilation in Enclosed Road, Rail, and Mass Transit Facilities, 2020

[6] FHWA HIF-15-005, Tunnel Operations, Maintenance, Inspection, and Evaluation (TOMIE) Manual, 2015

[7] FHWA, Road Safety Fundamentals, Concepts, Strategies and Practices that Reduce Fatalities and Injuries on the Roads, 2017

[8] Directive 2004/54/EC of the European Parliament and of the Council of 29 April 2004 on minimum safety requirements for tunnels in the Trans-European Road Network

[9] ASTRA 13001, Guideline Road Tunnel Ventilation, V3.01, 2021

[10] PIARC, Dangerous Goods Quantitative Risk Assessment Model (DG-QRAM), 2001

[11] PIARC 2008R15, Urban Road Tunnels, Recommendations to Managers and Operating Bodies for Design, Management, Operation and Maintenance

[12] PIARC 2011R02, Road Tunnels: Operational Strategies for Emergency Ventilation

[13] PIARC 2012R23, Current Practice for Risk Evaluation for Road Tunnels

[14] PIARC 2016R03, Fixed Fire Fighting Systems in Road Tunnels: Current Practices and Recommendations

[15] PIARC 2017R01, Design Fire Characteristics for Road Tunnels

[16] PIARC 2019R03, Prevention and Mitigation of Tunnel-related Collisions

[17] NHTSA, Motor Vehicle Fires in Traffic Crashes and the Effects of the Fuel System Integrity Standard, DOT HS 807 675, 1990

[18] Ahrens M., US vehicle fire trends and patterns, NFPA, 2005

[19] McGree T., Vehicle Fires, NFPA, 2024

[20] BASt B66, Assessing the Safety of Road Tunnels - Final Report & Appendices, 2007

[21] BASt B183, Assessing the Safety of Road Tunnels - Review of Assumptions and Parameters for Performing Risk Analyses, 2022

[22] Bettelini M., Rigert S., Ventilation and Escape Facilities for Short Cut-and-Cover Urban Tunnels, 7th International Conference 'Tunnel Safety and Ventilation' Graz, 2014

[23] Pospisil P., Road Tunnel Ventilation, Compendium and Practical Guidelines, 2nd ed. 2020

[24] Pospisil P., Woodward D., Haydn S., Flow Control in Tunnels, North American Tunneling Conference, Philadelphia, 2022

[25] Pospisil P., Hagenah B., Johnson D., Flow measurement for tunnel ventilation, BHR 20th ISAVT, Copenhagen, 2024

[26] Riess I., Bettelini M., The prediction of smoke propagation due to tunnel fires, ITC Conference Tunnel Fires and Escape from Tunnels, Lyon, 1999

[27] Riess I., On smoke stratification in a 1-D tunnel ventilation model, 11th International Conference 'Tunnel Safety and Ventilation' Graz, 2022

CULTURAL DIFFERENCES IN ROAD TUNNEL FIRE SAFETY

Conrad Stacey, Michael Beyer

Stacey Agnew Pty Ltd, AU

DOI 10.3217/978-3-99161-087-8-016 (CC BY-NC 4.0)
https://creativecommons.org/licenses/by/4.0/deed.de
This CC license does not apply to third party material (attributed to other sources) and content noted otherwise.

ABSTRACT

In these days of easy international travel, the world seems to be becoming more homogenous. You can get good sushi in Graz and Brisbane, good steak in Osaka and Graz, and schnitzel everywhere including Osaka and Brisbane. Why then are our approaches to tunnel fire safety so different? For real cultural experiences when you travel, forget the food – go and look at the tunnels. This paper notes differences in approaches to ventilation, fire suppression and tunnel operation and, within the limits of our knowledge, tries to rationalise them. Simply thinking about the differences may assist advancements in any of the jurisdictions, perhaps in a direction not identical to any of them.

Keywords: tunnel ventilation, fire suppression, tunnel operation.

1. INTRODUCTION

We are interested in why different jurisdictions have (sometimes quite different approaches to satisfying the same goal of building and operating tunnels with appropriate fire safety and fire resilience. These are our notes on differences in approach, including impressions on how the differences in approach came about. We emphasise that they are impressions. Reconstructing the background in an academically thorough way would be more involved than genealogical research.

We are not on a mission to prove a right way and a wrong way, as there are many solutions to such multifaceted problems, driven also by competing objectives with different weightings and informed by different knowledge bases. In some areas, there are ways we consider preferable, but we are aware that it is from our lens, with our understanding of the objective functions to be optimised. The important thing is to note the differences, and to think about whether the objective function that is applicable today might lead to a different answer from the one arrived at when the approach was first adopted.

Mathematicians like to optimise functions. Our view is that optimisation is generally easy if you can truly identify the objective, but that in the real world, objective functions are really really hard.

With that viewpoint as a basis, we look at the differences, focusing primarily on fixed fire suppression, ventilation, and operational management. We look at Japan, Australia and Europe as revealing interesting differences that may be usefully considered by others.

2. FIXED SUPPRESSION SYSTEMS

2.1. Europe

European tunnels eschewed fixed suppression systems until relatively recently, with PIARC taking a largely critical view in 1999 (for some plausible and some doubtful reasons), adopting a non-committal position in 2007, and offering cautiously favourable commentary in 2016. The European industry, driven by asset protection, has moved ahead in patches. Europe has a lot of older tunnels, and the lowest common denominator (least onerous on the budget) approach necessary in such an agglomeration of countries has likely contributed to the patchiness. On top of that, as the suppression in road tunnels is primarily an asset protection measure (once sufficient egress is provided), it is an economic decision rather than a public safety one.

There is also the issue of regulatory inertia. Whether or not suppression is beneficial to asset protection, business continuity or safety, where design requirements are set by regulation, those requirements will be followed. It is generally difficult to justify to financial oversight bodies any additional expenditure beyond the mandated standard. For example; German regulations, as at 2025, do not require suppression in road tunnels, and consequently such systems are typically not incorporated into German tunnel designs.

With mist being more effective than deluge (more on that later) and being far easier to retrofit to existing tunnels, their adoption has increased steadily. There are now 19 or more mist systems in European tunnels, both refits and new builds, after the first installation only in 2004. We understand that the road tubes of the Fehmarn Belt Tunnel will have a mist system.

2.2. Australia

Significant Australian road tunnels since Sydney Harbour Tunnel in 1992 almost all have 10 mm/minute deluge systems. Some bus tunnels have a lower application rate. One twin-tube road tunnel that missed out in 2000, the Heysen Tunnels in South Australia, was fitted with low pressure misting in 2024.

2.3. Japan

Japan also has a long history of road tunnel building and Japanese road tunnels have had deluge systems for so long that very few practitioners remember why they are sized the way they are (more on the design later). The answer is that the currently applied arrangement of deluge nozzles and piping is born from an extensive testing campaign in the 1960s. Although the reasons are not entirely clear to us, it seems that in the 1960s, and probably earlier, funding was available to support significant work on improving fire protection methods This led to extensive research on water spray systems, and helped establish the design principles that later shaped road tunnel fire suppression practice. The water application rate (around 7 mm/min), and the fundamental implementation techniques are generally understood to have changed little up to now (2026).

2.4. Business continuity considerations

On the benefits of suppression for business continuity, there may also be cultural differences in the acceptability of traffic disruption. As an example, on the 9th January 2026, a truck crashed and burnt entering the Brentenbergtunnel on the A10 in Austria. It was reopened with all lanes on the 17th January (8 days later) with some follow-on night works to be done. Regardless of whether the economic arguments about that period of closure and the structural damage caused due to the high heat exposure justify a suppression system, there are cultural matters around the inconvenience. It could be seen as acceptable to close a tunnel for a week

or two due to fire perhaps every 5 or 10 years. Where, in some European jurisdictions, that closure outcome may be accepted as just what happens, being the consequence of an extraordinary event, Australians might say that the closure should definitely have been kept to an hour or two by the (simple) measure of a suppression system. Japanese people, also used to suppression systems, might also think so, but probably wouldn't comment out loud like the sometimes blunt Aussies. The Australian view also comes out of a culture in which fewer question the level of expenditure than perhaps is the case in Europe. That is the case for anything presented as a safety feature, even if primarily for asset protection, with spending money seen as a reasonably practicable thing to do. So, the level of adoption of tunnel suppression systems may have quite a bit to do with a cultural view of knowing what could happen and dealing with it if it does, versus preventing it happening with some up-front and on-going expenditure.

2.5. Acceptability inertia

There is also an effect of 'acceptability inertia'. It is clear that society, with increasing standards of living (mostly), of wealth, and of infrastructure over the last lifetime has also changed its appetite for risk in many areas. Europe has had significant tunnels for longer than living memory. The acceptability of risk (to life and business continuity) was arguably quite different when the European cultures (there are several) around tunnel safety were established. In the absence of realised risk, there is not sufficient incentive to revisit approaches, despite that society generally has been creeping toward a more conservative risk view over decades. In the case of Europe, the impetus to revisit matters and overcome the inertia was a series of major incidents (Mont Blanc 1999, Tauern, also 1999, Gotthard 2001). They led to European Directive 2004/54/EC on minimum safety requirements for tunnels in the Trans-European Road Network. It also led to changes in perceptions generally.

The same circumstances could occur in Japan, but perhaps because there were already suppression systems in many tunnels, they haven't, and so there has been no need to revisit acceptability in that context. Australia is comfortably smug that they do water-based suppression better than anyone. That (cultural) comfort and smugness, together with the typical tunnel procurement processes, gave the status quo enormous inertia in Australia, and kept misting systems from being seriously looked at for at least a decade.

2.6. Implementation

Japanese deluge systems have a single distribution pipe along only one wall of the tunnel, with 2- or 3-part nozzle assemblies to throw the water across two or three lanes. There is the possibility of a tall truck shielding a large zone of the tunnel, with the hope in that case being that the fine droplets do what fine droplets do, and blow from upstream in sufficient density to suppress the shielded fire. There are of course reasons for accepting what seems an odd compromise. Installation is much simpler and cheaper with a single wall-mounted line of nozzles, but it is in the testing that the arrangement has the most benefit. Tokyo roads are quite heavily trafficked at all hours, and alternative routes are not always just a minor inconvenience, so the preference to keep one lane open is very strong. That is similar in other urban areas in Japan. The standard approach for nozzle testing is to capture the nozzle flow in a hose and measure the flowrate. A number of trucks equipped with arms to do that are used, such that flow from each of the nozzles (spaced at 5 m) can be captured separately. With the nozzles from one zone only on one wall of the tunnel, and the testing trucks in place, the zone may be tested end-to-end without the risk of wetting the traffic that is continuing to drive in the far lane. So, the typical Japanese installation is driven directly not only by history, but also by lane closure policy and the need to test performance of the whole chain right to water delivery.

Australian tunnels generally have surface routes that are reasonable in quieter traffic times, and so tube closures are possible. Deluge systems are zoned arrays up to 30 m long, with the nozzles in a grid pattern directly above the traffic space. The nozzle pattern is not so different from a high hazard building, which is where the scheme came from. With sufficient closures to exercise all zones once per year, there is no need to avoid having water on the roadway. In fact it is useful, to rinse off the road surface after the wall-washing truck has been through and left suds around.

2.7. Corollaries of suppression policy

If you have a system for applying Niagara Falls to any incident in your tunnel within 30 seconds or less, you can be confident of the rarity of seeing high temperatures in the tunnel more than just immediately above the truck that is on fire. That means that you don't try particularly hard to move services out of the way. In Australia, that is assisted by having no tunnels in areas with weather below 0ºC. Consequently, most Australian tunnels have local cabling exposed on tray above the traffic, and some have water main pipework exposed (obviously the suppression delivery pipework is exposed).

Provision of a fixed suppression system also means giving operators in-tunnel camera vision, controls, and training on when to operate the system.

2.8. Mist vs deluge

As Australia adopted of deluge for road tunnels in 1992, 5 years before the first ever road tunnel mist installation which was on the opposite side of the globe, deluge has become the default, and so 'acceptability inertia' meant that misting was not looked at too seriously. Contracting approaches, time pressures and frankly laziness contributed to that, and mist was often disparaged as a technique, probably that dealt with considerations without further ado.

Europeans had no such attachment to deluge, and so when mist came along, it had half a chance of being considered. That, plus the greater ease of installing the smaller valves and pipework in existing tunnels, has seen many tunnels adopt misting. Of course, the inertia in most of Europe makes having no suppression still quite likely, but where suppression is called for, it is more likely to be a mist system.

Japan has had deluge for so long, with good outcomes, that there has been little incentive to consider mist. There is some thought in Japan recently that maybe it is time to have another good look.

Besides the space saving, installation speed, and reduced water requirements, the comparable test data we have been able to find says that mist is better at both suppression and cooling than the larger droplet version of the same concept (deluge), so, as we see it, deluge systems will only be installed from now due to acceptability inertia.

3. VENTILATION CONTROL

In discussing ventilation control, we are not talking about model-based predictive control or inverter systems, we are talking about control policy. That is; what is the desired oncoming tunnel airspeed, possibly varying over time.

Australia has had a fairly simplistic approach mainly following the US (NFPA 502) policy of ensuring critical velocity to prevent backlayering. In US custom and practice, thinking about risk is essentially forbidden – you will do what 502 says. Following a critical velocity approach is made easier by the lack of significant bidirectional tunnels, and the generalization

that even heavily congested traffic is above the smoke speed (~10 km/h). Ventilation responses can be invoked automatically as there is no harm in keeping the air moving in the traffic direction, but potentially significant harm if it is allowed to reverse. It is noted that over-ventilating a minor fire will assist de-stratification of a smoke layer, and will of course make matters worse if there are any people downwind. In tunnels with flatish grades, an early stage response with low airspeed can be considered until the downwind area is known to be clear of people.

Of course, there are also great benefits to a simple approach. Trying too hard to tailor the response to specific scenario details can produce very bad results if the scenario is slightly different to what is sensed or expected. We have seen, in Japan, automatic sensing of traffic congestion used to decide between ventilating with traffic or stopping all air movement. That is great in theory, but when the cars stopping behind the fire are interpreted by the sensors as congested traffic and the algorithm stops all tunnel airflow, the stopped traffic can become immersed in smoke.

Policies in Europe mostly have air speed targets that are lower than critical velocity as a default, with an option to increase if clear downwind. The numbers are generally hard-coded into standards rather than being calculated based on fire sizes etc.. The result is expected to be a good outcome for all possible incidents, rather than a perfect outcome for any exactly specified incident. In that way, the European approach embodies the robustness of simplicity, but with a different view on the simplified optimum to that prevailing in the US, and also largely Australia.

When there are no people downwind, most Japanese tunnels target a view of critical velocity, which it seems has never been harmonised with any of the versions in the west. In the period 2017 to 2025, that was probably very wise, with NFPA 502 being grossly misled over that period. Recent thoughts in Japan are toward target airspeeds below critical velocity, considering also the time taken for a fire and backlayer to grow to be threatening, and the speed with which evacuation is likely.

4. OPERATIONAL MANAGEMENT

Some European tunnels have only an alarm to the local fire service. Here we are interested in heavily trafficked tunnels, which are usually monitored 24/7 by staffed control rooms. There are many such control rooms in Europe, Australia and Japan. Control rooms operators have some level of induction, and on-the-job training with early supervision. Australia may be unique in having a training and accreditation, organised externally from the tunnel operation, which gives formal training and accreditation as a Road Tunnel Operator. There are seven required units of competency in the Road Tunnel Operator Skill Set. In addition to that, there is training specific to the control room and tunnels where they are employed.

So, throughout Australia, tunnel operators are trained in the procedures and the risks, and are expected to make judgements and implement an appropriate response (which may be a pre-programmed one). The situation in Japan is not uniform. Some tunnel owners also expect operators to respond appropriately to emergencies, while at least one owner believes that it is appropriate to allow pre-programmed responses to be implemented automatically in an emergency. We do not fully understand why operators are expected to take an active role in in managing traffic and dispatching road patrollers, etc., but are then required to adopt a hands-off approach when operational demands become more critical. The answer apparently lies in legal liability. They cannot make a mistake that they are liable for if they are not involved in

the response. It would be interesting to understand if the system designer and the PLC programmer have the same appreciation of the approach reducing the operator's legal liability.

Providing operators with the knowledge to make judgement calls, and the training to implement resulting actions, is consistent with the view that a trained human will deal with complex decisions and actions better than an automated system. Certainly, in the sensed congestion in the Japanese tunnel noted earlier, a human operator would have realised that the only stopped vehicles (and tunnel occupants) were upwind of the fire (the video had been available from the start) and so the human judgement would not have permitted zero-flow control to be invoked.

Another example of automatic VS human response is in the Australian policy of having an 'unresponsive operator' timer on deluge activation. The idea is that if an operator makes no response to fire within 90 to 180 seconds, it should be discharged where the heat detector detected the fire's location. We have never seen an instance in which that was a useful fallback, with the operator always responding to multiple notifications (traffic, stopped vehicle, perhaps smoke and pedestrians) and taking command of the systems before the heat detection timer expires, and generally before the linear heat detector even alarms. However, automatic activation, even with a delay, can be problematic. There have been false activations of deluge in several tunnels also on live traffic. It can be because there was maintenance being done on the system by technicians, so the operator ignored the warning, or because there was a secondary back-door signal transmission in the system that couldn't be seen by the operator. Whatever the underlying reason was, there is always a chance of accidental operation in complex systems, and the system complexity conspired to dump deluge on live traffic. Without automatic activation being programmed in, that would not have happened. You cannot see out of your windscreen under 10 mm/min deluge. And to be surprised like that when driving in a tunnel at 80 km/h is not safe. Fortunately, no harm came from those incidents, but they were arguably more dangerous than a car burning unsuppressed in previously free-flowing traffic. Consequently, we do not include automatic deluge, or mist, release in designs.

5. SUMMARY AND CONCLUSION

You may never understand the culture of a country unless you were born there. Even then, there will be pockets you don't know about. You would think it would be easier to understand a country's tunnel fire safety culture, but the decisions hidden by the mists of time, and the sometimes random walk of systems development in a particular jurisdiction make logical explanations of why things are done as they are very difficult. Japan, Europe, and Australia have distinct differences in approach to a very similar fundamental problem, which is keeping people and the asset safe from fire.

This is in no way the end of a journey to explore and understand the differences. We hope to learn more over the next years. It is hoped that our thoughts so far might prompt new thoughts from practitioners in any jurisdiction. If so, we would love to hear them.

THE BEST THING FEDRO HAS PROVIDED US WITHIN RECENT YEARS! EXPERIENCES FROM OVER 50 OPERATIONAL CONCEPTS FOR SWISS ROAD TUNNELS

[1]Ralf Wetzel, [2]Christian Jäger

[1]ILF Beratende Ingenieure AG, CH
[2]WSP Ingenieure AG, CH

DOI 10.3217/978-3-99161-087-8-017 (CC BY-SA 4.0)
https://creativecommons.org/licenses/by/4.0/deed.de
This CC license does not apply to third party material (attributed to other sources) and content noted otherwise.

ABSTRACT

After a fire, various defects are discovered in the operating and safety equipment (OSE) of a tunnel! A truck enters a tunnel with an extended crane and damages the OSE in the entrance area! The system control of the tunnel ventilation fails! What to do?

In Switzerland, Regional Units (RU) are responsible for operating the national road tunnels. They are regularly confronted with these or similar issues. The options for further action are many: tunnel closure, tube closure, lane reduction, operation under minimum requirements or normal operation with/without measures. Other questions also arise: Act immediately or later? Who should be informed? Who decides?

The operating concepts (OC) for road tunnels enable the RU to correctly assess the situation in the event of system failures or external events (accident, fire, …), make quick decisions and involve the right people. This ensures the safety of road users and maximizes the availability of high-performance roads.

RU and planners can use the OC to optimize spare parts inventory. Components with long permissible downtimes do not need to be procured as spare parts. Components with short permissible downtimes or components whose failure would lead to operation under minimum conditions or to a tunnel closure must be available quickly and kept in stock as spare parts.

OC developed during the planning phase enables the planner to align his concepts at an early stage to clarify the availability and safety requirements of the project and agree them with the client. These include redundancy concepts, failure strategies and refurbishment concepts.

This article will share the experience of IG BeSt (ILF Beratende Ingenieure AG / WSP Ingenieure AG) from over 50 implemented OC and answer the question of why a RU employee describes them as the best that Federal Roads Office (FEDRO) has provided to RU in recent years.

Keywords: operational concept, operation under minimal requirements

1. INTRODUCTION

Modern road tunnels are highly complex infrastructure facilities. Their safe and efficient operation requires numerous technical, organisational and personnel resources. In cases of technical malfunctions, accidents or fire incidents, operators - the regional units (RU) - must quickly decide on measures to ensure the safety of road users and maintain the availability of national roads. Operational concepts (OC) for road tunnels, developed by the Federal Roads Office Winterthur in close collaboration with IG BeSt (ILF Beratende Ingenieure AG and WSP Ingenieure AG) and operators (RU VI and RU VII), provide a structured and practical foundation for this purpose. They enable the systematic evaluation of technical failures and external events, the derivation of suitable measures, and the targeted involvement of the relevant stakeholders. This significantly eases the burden on the RU and ensures clarity in critical situations, allowing for swift decision-making. This increases safety for all road users and ensures high route availability with minimal tunnel closure times and reductions in traffic capacity. This article highlights the practical advantages of operational concepts and illustrates their importance in tunnel project planning and operation. These insights are based on over 50 operational concepts implemented for Swiss road tunnels, as well as feedback from operators. The aim is to familiarise clients, planners and operators with the significance and benefits of these concepts.

2. OPERATIONAL STATES OF ROAD TUNNELS

Operational concepts for road tunnels distinguish three key states of operation, each of which has different requirements for measures, responsibilities and decision-making processes. These states are crucial for the structured evaluation of technical faults and events during tunnel operation.

2.1. Normal Operation / Permissible Deviation From Normal Operation

In this state, either no technical fault is present, or a technical fault or system failure exists that deviates from the target state, but which does not endanger road users' safety. Tunnel availability is maintained.

Generally, no special measures are necessary. However, faults must be resolved within a defined outage period (I0–I3, i.e. 24 hours to six months, see table 1).

Responsibility lies with the regional unit’s incident commander (ELG). In some cases, immediate action is required (e.g. manual switching) to ensure the safety of road users until repairs are completed.

Examples include individual failures of tunnel lighting or the failure of an HVAC-System.

Table 1: Permissible Outage Times
(* According to the OC, the permissible outage time does not begin with the first occurrence of a fault, but only once the damage has been clearly identified.)

Class	Intervention	Permissible Outage Time*	Significance for Operation
I0	immediate	6 to 24 hours	Critical faults must be resolved quickly. Immediate actions are usually required.
I1	short-term	< 72 hours	Fault of moderate urgency. Measures must be taken within three days.
I2	medium-term	< 3 weeks	Fault with lower risk. May require unscheduled lane/tube closures.
I3	long-term	< 6 months	Tolerable fault with minor impact. Resolutions can occur as part of regular maintenance.

2.2. Operation Under Minimal Requirements

This state involves a technical fault or system failure, in which case road user safety can only be ensured by immediate additional support measures, such as traffic metering, mobile ventilation or the closure of one driving direction. These measures restrict tunnel availability and increase the risk of traffic disruption. During this operational state, responsibility shifts from the regional unit's incident commander to the FEDRO incident commander (ELA).

Supporting measures and restoration of affected systems must be initiated immediately. No specific deadlines are set for resolving faults. The tunnel will remain in this operational state until the repairs are complete and any remaining faults can be assessed as permissible deviations from normal operation.

Examples include the failure of smoke extraction or fire detection systems in one tunnel tube of unidirectional tunnels

2.3. Tunnel Closure

In this state, road user safety cannot be guaranteed due to major faults or damage to the operational and safety equipment (OSE), even with supporting measures in place. The tunnel must therefore be closed to eliminate risks. This will lead to traffic disruption with potentially regional impacts. In this case, responsibility immediately shifts from the ELG to the ELA.

The tunnel will only reopen once safe conditions have been re-established. Examples include the failure of smoke extraction or fire detection systems in bidirectional tunnels with bypass options.

In exceptional cases where there is no suitable bypass, tunnel closure may be avoided if the risks on the bypass route would be higher than in the tunnel. In such cases, operation under minimal requirements is initiated and the associated residual risks is accepted by FEDRO.

3. STRUCTURE OF THE OPERATIONAL CONCEPTS

The OC for road tunnels are modular and follow a proven, uniform structure. These consist of five main modules, each of which contains specific information and action guidelines.

3.1. Module 1: Imprint & Abbreviation Directory

This module includes administrative details such as the client, operator and owner, as well asa change log and distribution list. Of particular importance is the object-specific abbreviation directory, which clarifies all abbreviations used in the concept.

Winterthur branch / Regional Unit VII
Tunnel

Tunnel Uetliberg

Closure! | Operation under minimum requirements required! | I0 = 6-24 h | I1 = < 72 h | I2 = < 3 Weeks | I3 = < 6 Months

Version 2.0 | Module 3 | M3_TUET_001

Overview of mandatory measures in the event of technical malfunctions

Nr.	Event	Classif.	Consequences	Immediate measure	Accompanying measures (functional replacement & risk reduction)				EVP-Nr.
①	②	③	④	Traffic/Operational and safety equipm./Infra./Information ⑤	Traffic ⑥	Operational and safety equipment ⑥	Infrastructure ⑥	Information ⑥	⑦
1.102.5	Failure of both transformers for the exhaust fans of one tube.		Total failure of the exhaust fans in this tube and thus total failure of the smoke extraction system.	**Information:** BLUR / VLZ: - PoI - ELG - NSU ELG: - StreMa - ELA **Traffic:** --- **Operational and safety equipment:** BLUR / GE VII BSA:Closure of one lane with TVR und VLS. **Infrastructur:** ---	**Function replacement:** NSU / PoI: Closure of a lane with scissor barriers and lane closure signage. **Risk reduction:** NSU: Signage indicating speed reduction to 60 km/h on open lane. GE VII / BLUR: Traffic metering with TVR.	**Function replacement:** BLUR / GE VII BSA: Manual ventilation control (see Module 4) FW: Provision of mobile SV including personnel if jet fans have failed at the same time. **Risk reduction:** ---	**Function replacement:** --- **Risk reduction::** ---	**Function replacement:** --- **Risk reduction:** Information to fire brigade ---	EVP 102 (MA)

① Table structure and numbering according to AKS CH
② Description of the technical malfunctions / system failure
③ Permissible downtime within which the fault must be rectified
Start time: Damage is known.
Failure to comply with permissible downtine: Information to ELA
④ Brief description of the consequences of the technical malfunction / system failure
⑤ Brief description of the immediate measures
Structured in traffic, operational and safety equipment , infrastructure & information
⑥ Brief description of the accompanying measures
Definition of responsibilities for each measure
⑦ Specification of the contingency planning number (EVP number)
Detailed information on the technical malfunction / system failure is described in the EVP (Module 4)

Figure 1: Explanations of the structure of Module 3 using an example (highlighted in light blue: failure with operation under minimum requirements) from the Uetliberg Tunnel (equipped with a semi-transverse ventilation system) [3] with a clear definition of responsibilities for each measure (underlined: e.g. BLUR – Urdorf Operations Control Centre)

3.2. Module 2: Tunnel Reflex Matrix

The tunnel reflex matrix is a key part of operational concepts, describing the automated responses of tunnel operations to specific events or conditions. It determines the actions triggered by the higher-level control system in the event of technical faults or safety-critical incidents.

3.3. Module 3: Overview of Measures

This central module provides a table listing all analysed technical faults and system failures. Entries are colour-coded as follows:

- **White:** Permissible deviation from normal operation
- **Light blue:** Operation under minimal requirements
- **Red:** Tunnel closure required

For each fault, the permissible outage time from I0 to I3 and the necessary immediate and supporting measures and responsibilities for each measure are clearly defined. In more complex cases involving immediate and supporting measures, Module 3 refers to contingency planning (CP), which is detailed in Module 4.

3.4. Contingency Planning (EVP)

Module 4 provides detailed descriptions of the complex faults defined in Module 3. Each CP includes at least:

- Description of the failure
- Consequences for operation and safety
- Detailed description of immediate and supporting measures
- Notes on tunnel availability and bypass options

The measures are categorised by traffic, OSE, infrastructure and information, and include concrete action instructions for responsible individuals.

3.5. Supplementary Documents

This module provides documentation on the standard operational and safety systems (OSE) of the tunnel, including the implemented redundancy concepts and failure strategies. It also contains notes and recommendations from the author of the OC, as well as information on the process of changes and mutations.

4. APPLICATION IN PRACTICE

Operational concepts for road tunnels are not just theoretical documents; they are essential tools for RU in their day-to-day work. They are applied in various operational situations. The possible use cases, along with their respective objectives, are compiled below.

Table 2: Typical use cases for operational concepts

Use Case	Example	Objective / Benefit
Technical fault / system failure OSE in normal operation	Failure of OSE such as: • Transformer • Escape route lighting • Ventilation control	• Assessment of impact • Initiation of appropriate measures
Support in event management	Events affecting OSE: • Fires • Accidents • Collisions with tunnel infrastructure	• Acceleration of event management • Evaluation and prioritisation of measures for route clearance
Tunnel renovations / modifications under traffic	Renovation of critical OSE with functional interruptions under traffic conditions: • MV switchgear • Ventilation control	• Preparation of work/measure planning • Fallback planning • Identification of optimisation potential
Spare parts inventory	• Definition of critical components based on delivery times & permissible outage times	• Optimisation of inventory • Maximisation of route availability • Synergy use of spare parts (different tunnels)

Training and education	• Introduction of new operator employees, • Training / refresher training	• Building operational competence • Safe and fast application of concepts

4.1. Technical Faults and System Failures

In the event of a fault, RU employees refer to the operational concept for the affected tunnel. Module 3 provides a tabular overview of all relevant failures, including their classification (permissible deviation, operation under minimal requirements or tunnel closure), the permissible outage time, the required measures and the responsibilities. For more complex cases, reference is made to the associated contingency planning in Module 4.

4.2. Support in Event Management

Even for external events, such as traffic accidents or fires, the operational concepts serve as a basis for decision-making. Depending on the severity of the event, various phases of event management are implemented (see Fig. 2). The operational concepts help to assess whether route clearance is possible and whether supporting measures are required.

4.3. Tunnel Renovations / Modifications Under Traffic

During planned tunnel renovations or modifications while the tunnel is in use, operational concepts provide initial guidance on the minimum required measures. Since interventions in the OSE are generally scheduled, additional measures are usually required. Table 3 shows an example of the conversion of an MV switchgear in a tunnel where there are no suitable bypass options.

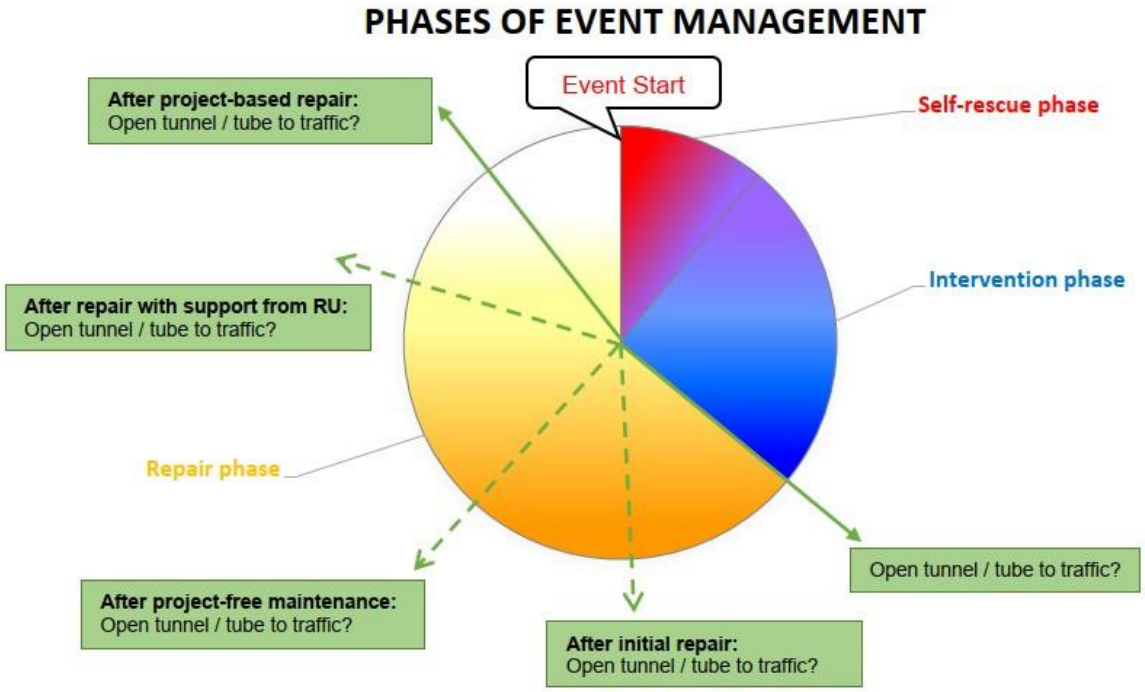


Figure 2: Operational concepts are applied in every phase when assessing route clearance. (derived from: Event Management Handbook, C+E Planing [1])

4.4. Spare Parts Inventory

Spare parts inventory is associated with high costs. Spare parts require storage space and must be procured and stored under specific climate conditions. Sometimes they also require maintenance to avoid storage damage. Therefore, it is crucial to keep on hand the components that are essential for ensuring the safe operation of tunnels and high route availability. These components can be identified in the OC. Those components that must be kept in stock are those whose failure would result in operation under minimal requirements or tunnel closure. Additionally, components must be stocked if their delivery times exceed the permissible outage time and if there are no alternatives for the failed component. Synergies between different tunnels can also be exploited to minimise overall inventory and associated costs.

4.5. Training and Education

In order to ensure that operational concepts can be applied safely and efficiently in an emergency, it is essential that RU personnel receive targeted training. OC form an integral part of initial and continuing education and are practised regularly in training sessions and learning checks.

New employees receive comprehensive training on operational concepts during their induction. This training covers not only the contents of Modules 1 to 5, but also the underlying systematics, the distribution of roles between RU, ELG and ELA staff, and the processes for technical faults and events.

The training is based on a standardised presentation format developed by RU VII and IG BeSt and includes basics and objectives of operational concepts, distinction from other concepts (e.g. emergency management), definitions and abbreviations, operational modes and accepted residual risks, interfaces to action plans and event management as well as practice-oriented exercises. Using real-life scenarios such as transformer, lighting or ventilation system failure, trainees practise applying the concepts.

They learn how to identify the fault in Module 3, to check measures and responsibilities and to initiate defined actions. These exercises foster understanding of and the routine in handling the concepts, thereby preparing staff for emergency situations.

Table 3: Application of operational concepts to planned renovations/modifications to BSA

Example: Uetliberg Tunnel	Operational Concept Measures	Measures for Conversion
The MS system is converted during operation and there is no bypass option. **Colour code** **Green**: Not required for a planned conversion measure as everyone has already been informed. **Black:** Measures that apply in both cases. **Blue:** Additional measures for planned	MS system failure: • Information from the police, head of operations GE VII, national road maintenance, fire brigade • Information from ASTRA operations manager • Closure of one lane using a traffic management system/tunnel traffic control (TVR) • Closure of the lane with scissor barriers and lane closure signage	Planned conversion of the MS system: • Testing of ventilation functions (longitudinal ventilation) • Informing the public to avoid the tunnel • Traffic is restricted to a single lane. • Use of emergency power generators for lighting, escape route signage, fire and flow measurement sensors,

interventions in the BSA	• Speed reduction to 60 km/h on open lane • Traffic control, e.g. with mobile traffic lights (to prevent congestion in the tunnel). • Connection of emergency power generators → Establishment of minimum functions (e.g. lighting) → Traffic metering with TVR → Manual ventilation control (longitudinal ventilation). → Use of mobile jet fans in the event of power failures	ventilation control and jet fans. • Yellow flashing lights and a reduced maximum speed limit • Permanent traffic monitoring and congestion avoidance in the tunnel by trained personnel • Preset permanent operation of longitudinal ventilation in the direction of travel, with manual control of steel fans by the area unit in the event of a fire. • Fire brigade on standby with emergency vehicles on site

5. WHAT MUST THE PLANNER OF OPERATIONAL CONCEPTS CONSIDER?

Operational concepts are primarily intended as a working and support tool for RU staff. As RU in Switzerland are not organised uniformly, their responsibilities and communication paths differ. Each RU also has its own processes for tunnel monitoring and fault message handling, as well as different RU requirements for implementing technical BSA solutions.

Therefore, operational concepts must address RU-specific processes and characteristics and cannot simply be transferred from one RU to another. They can only be created through close collaboration between the RU, the FEDRO and the planning office. All measures must be coordinated with the RU's capabilities. This includes personnel resources, material resources and distance between the operations centre/control centre and the tunnel.

A crucial aspect is the phased/stepwise development of OC, as these directly influence planning, tendering and the inventory of spare parts. During the planning phases, redundancy concepts, failure strategies, monitoring strategies and bypass options must be closely coordinated with the consequences and necessary measures for operating under minimum requirements or tunnel closure. The failure of a single component must not result in operation under minimal requirements or tunnel closure if the tunnel has high availability requirements.

OC must be developed during detail design (SIA Phase 32). All failures requiring measures must be monitored, and appropriate fault notifications must be sent to the operations control centre. Depending on the importance of the system and the measure, fault notifications can be prioritised. Considering the OC, the costs of spare parts, which must be tendered in the next project phase (SIA Phase 41), can be determined in this phase. Therefore, must be finalised by SIA Phase 41 at the latest.

6. SUMMARY AND CONCLUSION

Returning to the questions raised at the beginning of the abstract: Such events cannot be planned for and confront RU staff unexpectedly during daily business. What should be done? Six years ago, staff of the RU VI and VII had to answer these questions independently, hoping that all of their decisions to handle the event are correct.

Today the answer is simple: Use the OC!

Operational concepts for road tunnels enable RU staff to assess situations during system failures or external events (e.g. accidents or fires) quickly and accurately, make immediate decisions and involve the right people. Measures to maintain safe tunnel operation and high route availability are defined and coordinated with FEDRO. The remaining residual risks are known to and accepted by FEDRO. And most importantly: Operational concepts have repeatedly alleviated pressure on RU staff in situations like those described above.

- Situation assessment during events has become much easier!
- Reporting lines and responsibilities are now clearly defined!
- Everyone can now fully focus on their role and tasks in event management!

That is why a RU VII employee concluded: **'Operational concepts are the best thing FEDRO has provided us with in recent years!'**

7. REFERENCES

[1] FEDRO / C+E Planing: Ereignisbewältigung auf Nationalstrassen, Handbuch Teil 1: Konzept und Schulungsunterlagen, V 1.0, 2016

[2] FEDRO / IG BeSt: Betriebskonzepte Strassentunnel, Handbuch, V 2.0, 2022

[3] FEDRO / IG BeSt: Betriebskonzept Tunnel Uetliberg, V 2.0, 2020

THRUST COMPARISON OF CONVENTIONAL JET FANS AND FANS WITH SHAPED SILENCERS IN AN ITALIAN ROAD TUNNEL BASED ON IN-SITU MEASUREMENTS

[2]Fathi Tarada; [1]Luca Stantero; [1]Pier Bertacche;[3]Natalino Daniele Boffa;
[3]Francesco Bezzi; [4]Natalino Lucatelli

[1]Risk Design Engineering, IT
[2]Mosen Ltd, UK
[3]ANAS SpA, IT
[4]De Cardenas Fans & Service SRL, IT

DOI 10.3217/978-3-99161-087-8-018 (CC BY-SA 4.0)
https://creativecommons.org/licenses/by/4.0/deed.de
This CC license does not apply to third party material (attributed to other sources) and content noted otherwise.

ABSTRACT

This paper presents the results of an extensive in-situ measurement campaign aimed at quantifying the performance of conventional jet fans and using fans with shaped silencers. The tests were conducted at the Verta Tunnel, an existing 3.5 km long road tunnel with an arched cross-section operated by the Italian road authority (ANAS).

A detailed velocity grid measurement was undertaken within the tunnel, capturing the airflow profile across the entire cross-section. This measurement allowed for an evaluation of the flow distribution resulting from fan operation, as well as a calculation of the effective thrust generated by the two different jet fan types. Additional parameters, such as pressure differentials, were recorded at strategic locations to support the overall analysis.

The results demonstrate differences in thrust and flow development between conventional jet fans and those with shaped silencers. The findings not only provide insight into the in-tunnel thrust of each jet fan type, but also highlight the impact of tunnel geometry and installation layout on the actual ventilation performance.

Keywords: Jet fans, thrust, installation factor, aerodynamics

1. INTRODUCTION

Due to its versatility and modest construction cost implications, longitudinal ventilation using jet fans is an increasingly popular option for ventilating tunnels worldwide. Indeed, the use of jet fans has been the de-facto standard for the ventilation of Italian road tunnels for several decades. Despite their widespread use, jet fans are generally inefficient at producing airflow in tunnels because of aerodynamic friction with tunnel surfaces. It has been estimated that typical jet fan installations waste over half the supplied electrical power [Ref. 1]. On that basis, there has been significant interest in improving the efficiency of jet fan installations, in order to present a more sustainable and cost-effective solution to the issue of longitudinal tunnel ventilation [Ref. 2]. One of these methods is the use of shaped silencers attached to the fans, designed to deflect the jets away from the tunnel soffit and thereby enhancing the in-tunnel thrust [Refs. 3, 4]. This is the method that was considered in our measurement campaign, in which we compared back-to-back measurements using conventional jet fans and fans with shaped silencers.

2. TEST ARRANGEMENTS

2.1. Verta Tunnel

The Verta Tunnel, managed by ANAS, is a two-lane, 3.5 km long tunnel in the municipality of Omegna, within the Italian region of Piedmont. A cross-sectional view of the tunnel, showing one bank of jet fans, is provided in **Figure 1**.

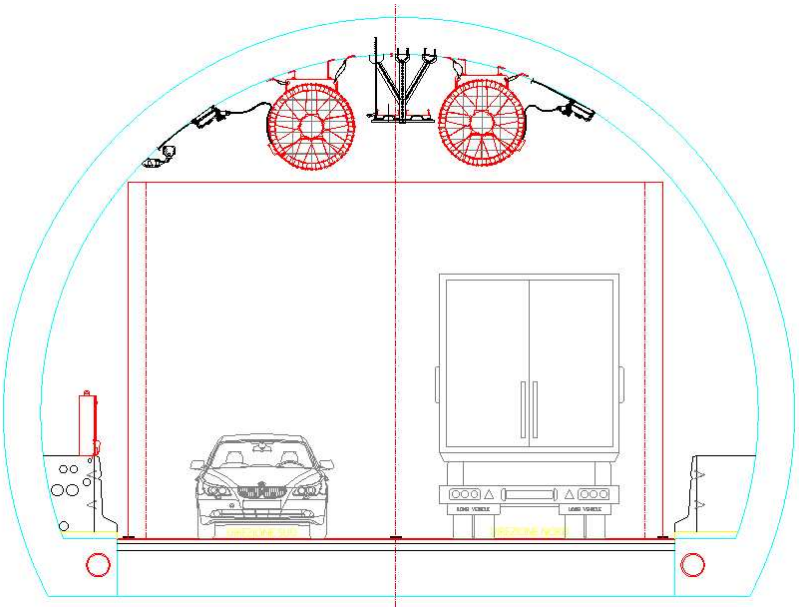


Figure 1: Cross-section of Verta Tunnel, showing jet fan installations

The Verta tunnel is equipped with 10 pairs of jet fans, each pair installed as a bank of fans. 5 pairs of jet fans are installed close to the north portal and a further 5 pairs of jet fans are located near the south portal. The first bank of jet fans is located 100m from each portal, and subsequent banks of fans are separated by 100m.

Our tests involved operating fans from the first four banks of fans closest to the north portal – the first two banks of fans installed with shaped silencers, and subsequent two banks of fans installed with conventional silencers.

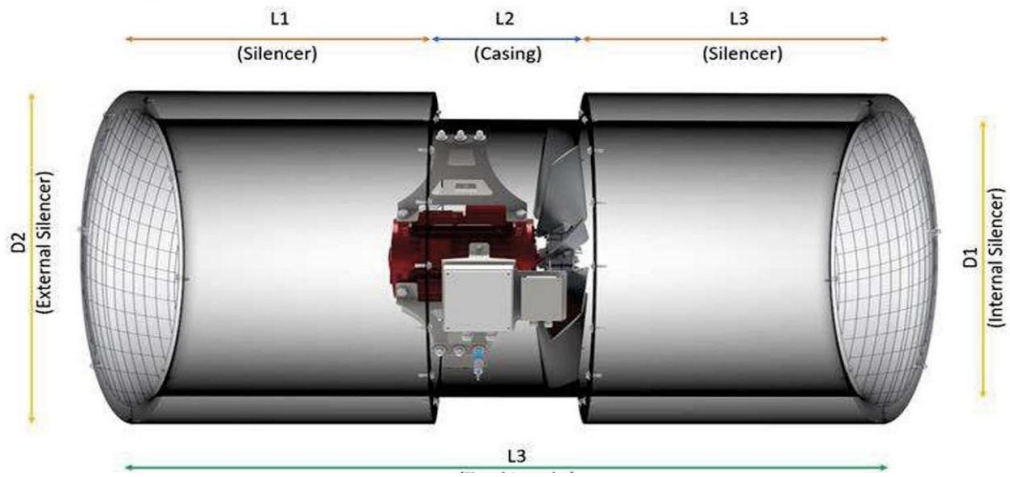
During the test, an operator located inside the electrical substation alternately operated either the two banks (four jet fans) with shaped silencers, or the two banks (four jet fans) with conventional silencers. The data was saved on a tablet that communicated with the anemometers via Bluetooth.

2.2. Jet Fans

All jet fans used in this test had the following specifications:

- Reversible fan operation
- Volumetric flowrate: 24.3 m^3/s
- Discharge velocity: 30.9 m/s
- Bench thrust: 900 N
- Rotational speed: 1480 rpm
- Absorbed power: 26 kW
- Sound pressure: 71±3 dB(A) (measured 10 m away, at a 45° angle from the fan axis)

There were no differences between the bench thrust, absorbed power or sound pressure values for the fans equipped with conventional or shaped silencers (within the measurement tolerances defined in ISO 13350:2015). The deflection of the discharged jet was therefore achieved by the shaped silencers without a reduction in thrust or an increase in power or noise, in contrast with deflection vanes which can cause a reduction in thrust and an increase in power and noise [Ref. 5]. The dimensions of the conventional jet fans are indicated in **Figure 2**. The lengths of the shaped silencers were the same as those of the conventional silencers. **Figure 3** shows a photograph of a bank of two jet fans, with shaped silencers.



L1 [mm]	L2 [mm]	L3 [mm]	D1 [mm]	D2 [mm]
1000	500	2500	1010	1210

Figure 2: Dimensions of Conventional Jet Fan



Figure 3: Bank of Jet Fans with Shaped Silencers

2.3. Measurement Locations

The longitudinal location chosen for the air velocity measurements was approximately 600 m from the north portal, and approximately 100 m after the second vehicular lay-by which is encountered on the left-hand side when traveling south through the tunnel. This section was located after the five pairs of fans in the vicinity of the north portal, and was sufficiently remote from the upstream fans and the lay-by to ensure a reasonably homogeneous flow profile.

The spatial distribution of measurement points across the tunnel cross-section was selected on the basis of EN ISO 5802_2008 +A1:2015. This standard requires that 36 measurement points be undertaken, with locations set in accordance with log-Tchebycheff rules. The area-averaged velocities were estimated on the basis of weighted coefficients defined in EN ISO 5802.

Figure 4 shows the locations of measurement points used in the tests.

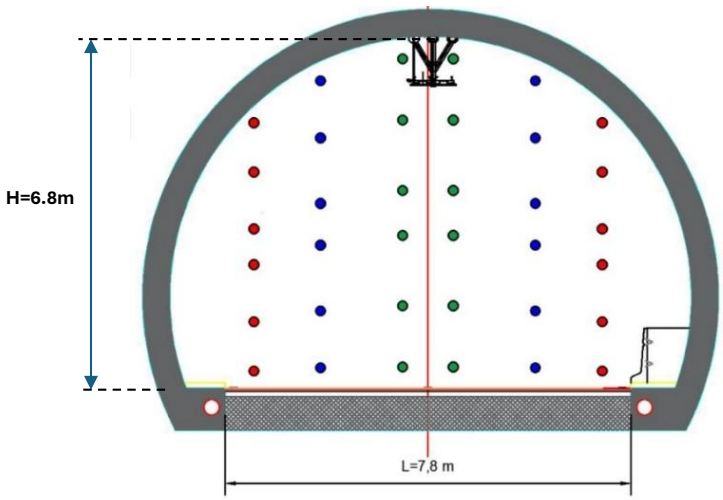


Figure 4: Velocity Measurement Locations

2.4. Measurement Equipment

The instruments used to measure air velocity were six Testo model 405i hot-wire anemometers and six Trotec model BA30WP hot-wire anemometers. The anemometers were securely fastened with hose clamps to two telescopic tripod supports at predetermined heights, which were set up during to the test preparation phase.

The six spanwise locations of the instruments were marked by chalk on the road surface, by measuring the required locations from the left-hand wall (when facing south). The vertical locations of the instruments were marked on the tripod supports.

Data acquisition was carried out with a tablet that recorded the measurements with a sampling interval of 5 seconds. Each set of measurements was undertaken for 120 seconds, after which the support was moved and the anemometers positioned at new locations.

To measure the differential pressure generated by a bank of jet fans, a Testo 400 universal instrument was used. The test consisted of placing a rubber tube across the fans, 50 m upstream and 50 m downstream of the bank (i.e. 100 m total chainage). The ends of the tube were inserted into the instrument, which detected the pressure difference at the two ends.

Figure 5 shows the tripod arrangements for the velocity and pressure measurements.



Figure 5: Tripod set-ups for velocity measurements (left) and pressure measurements (right)

3. MEASUREMENTS AND RESULTS

3.1. Test Campaign

The test campaign was carried out on 26/02/2025 and 11/06/2025. The campaign had the following objectives:

- Measure the tunnel friction factor using the rundown technique
- Measure air speed with 36 measurement points across the tunnel cross-section (as per **Figure 4**)
- Measure the installation factor of the fans using the pressure difference technique

3.2. External Wind Conditions

Wind speeds of up to 4 m/s and gust speeds of up to 5.6 m/s were measured at the north portal, as indicated in **Figure 6**. Estimates of the jet fan installation factor (as estimated by the technique described in section 3.5) are reasonably independent of meteorological conditions. The primary wind direction was towards the north, i.e. against the mechanical ventilation.

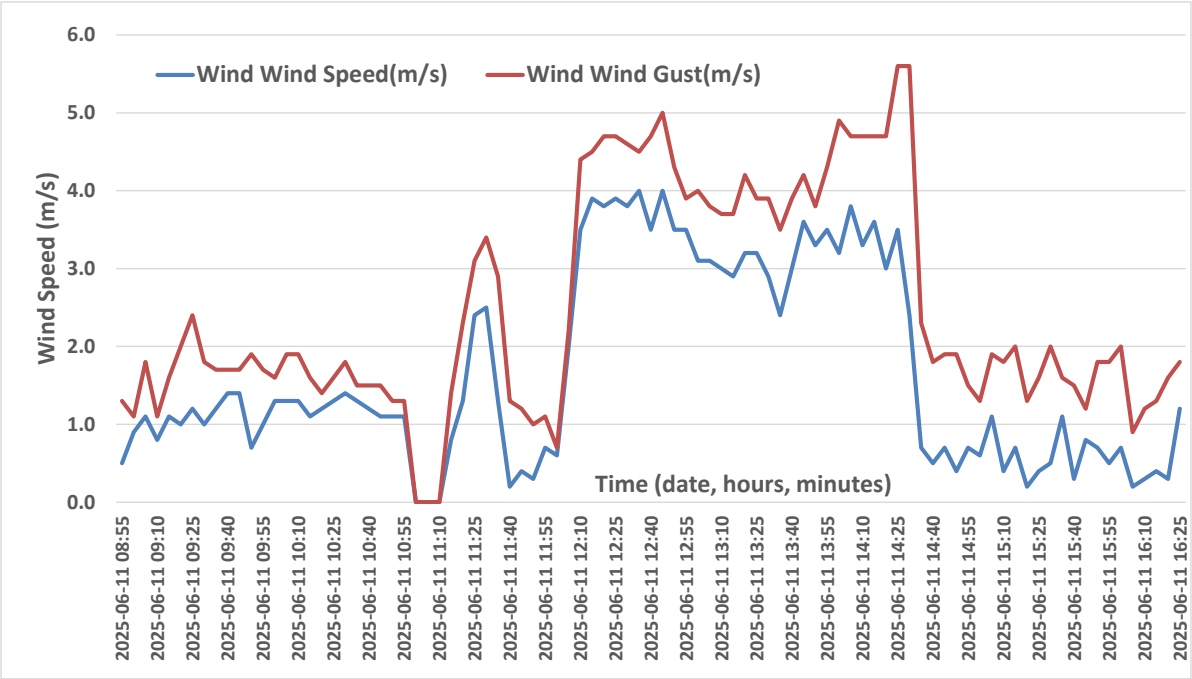


Figure 6: Wind (blue) and Gust (red) Speeds as a Function of Time

3.3. Run-Down Test

A run-down test was undertaken on 26/02/2025 to estimate the tunnel friction factor, based on the procedure proposed in [Ref. 6], initially using all jet fans on the northern side, and then using all jet fans in the tunnel. The result was a friction factor of 0.025, with a measurement uncertainty of +10%.

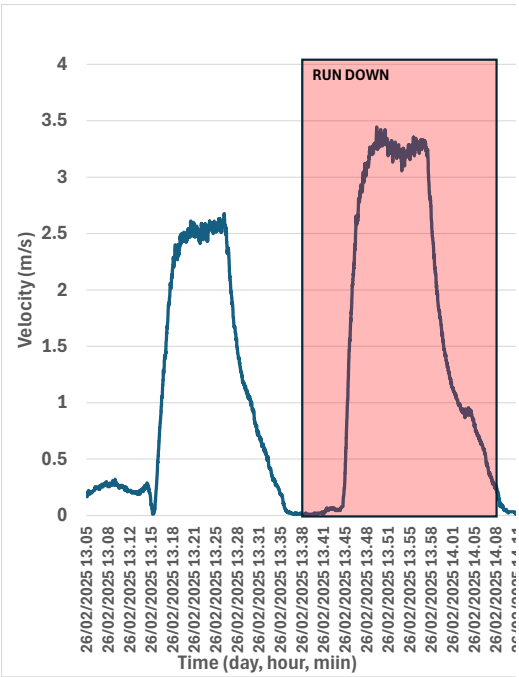


Figure 7: Run-down Test

3.4. Air Velocity Tests

Three separate sets of measurements were undertaken for the air velocities in the tunnel: one with conventional jet fans, and two with shaped silencers. The measurement periods, each of which lasted for 7 minutes, are indicated in **Figure 8**.

Table 1 reports the time-average velocity measurements for the three time periods. The thrust increase with shaped silencers can be estimated on the basis of the square of the measured velocities.

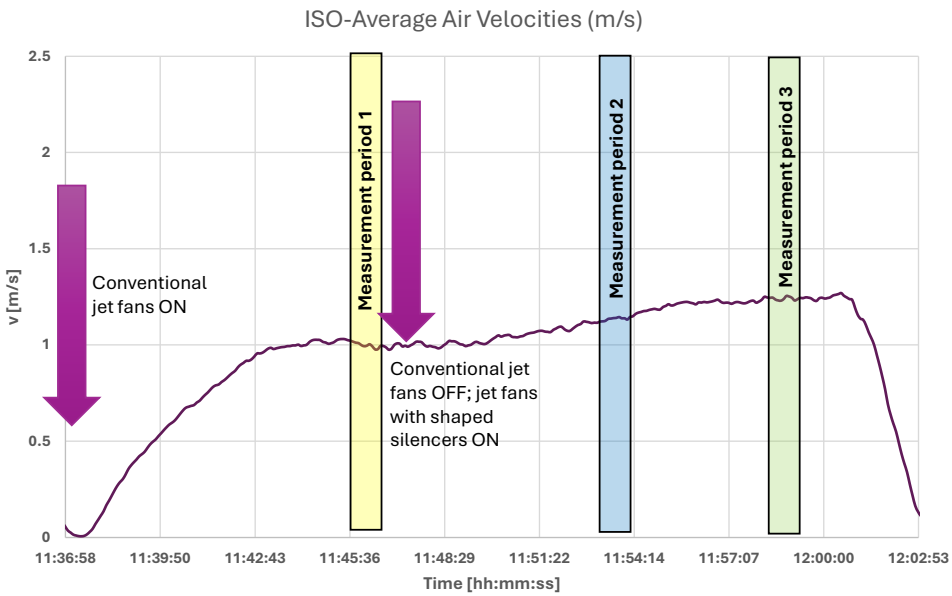


Figure 8: Variation of ISO-average tunnel velocities during the test

Table 1: Air Velocity Measurements

Measurement period no.	Jet fan type	ISO Area-Average Air Velocity (m/s)	Test average air velocity (m/s)
1	Conventional	1.016	1.016
2	Shaped silencers	1.118	1.182
3	Shaped silencers	1.246	

3.5. Pressure Difference Results

The jet fan installation factor, η, for both fan types was estimated using the measured pressure rise across the fans (Δp_{12}), as follows [Ref. 7]:

$$\eta = 100 \cdot \frac{\Delta p_{12} + \left(\frac{\lambda \cdot L_{12}}{D} + \zeta_{12}\right)\frac{\rho}{2}u_t^2}{n \cdot \rho u_s^2 \frac{A_s}{A_t} \cdot \left(1 - \frac{u_t}{u_s}\right)}$$

The measured pressure rise across a bank of fans and the estimated jet fan installation factors are listed in **Table 2**, based on the test-average results.

Table 2: Jet Fan Installation Factors from Pressure Differences

	Δp_{12} (Pa)	Installation Factor
Conventional	20.60	0.703
Shaped silencer	29.64	0.948

3.6. In-Line Jet Fan Tests

In-line arrangements of four conventional jet fans with four jet fans with shaped silencers, all installed near the north portal, were tested on 26th February 2025. These tests were conducted with the jet fans located near the south portal switched on (and blowing towards the south), in order to provide a background tunnel velocity and to counteract the effect of external wind. The installation factor results were similar to those reported here with jet fans arranged in banks of two – which increases the confidence that can be attached to the results, and suggests that there was no significant influence of external wind.

3.7. Measurement Errors

The measurements were subject to systematic uncertainties (e.g. due to anemometer calibrations, direction of probes, finite number of measuring points) and to random measurement errors. Most systematic uncertainties "cancelled out" due to comparative nature of exercise, since the same layout and measurement equipment was used for both the conventional and shaped silencer tests.

We estimate that the random errors for the velocity and pressure measurements were within 5%, to 95% confidence as described in EN ISO 5802:2008+A1:2015. One of the sources of random errors in this test was the external wind, which was moderate, but which had a temporal variability. Adding all random errors, including wind, implies an overall ±10% uncertainty to 95% confidence in the installation factor results.

4. DISCUSSION AND CONCLUSION

Measurements undertaken in the 3.5 km Verta Tunnel in Omegna, Italy sought to determine the performance difference between jet fans using conventional (cylindrical) silencers and those with shaped silencers. The latter are designed to deflect the airflow away from the tunnel soffit, and hence enhance the in-tunnel thrust.

The two types of measurements (velocity and pressure) suggest slightly different enhancements of shaped silencers compared to conventional silencers, albeit within the ranges of uncertainty.

The enhancement of jet fan in-tunnel thrust using shaped silencers has been well established from previous full-scale measurements [Ref. 3] and CFD [Ref. 8]. In particular, Ref. 3 reported a thrust enhancement of 29% in a similar arched tunnel profile, using shaped silencers. The measured jet fan installation factors align well with the results of Ref. 3 and with correlations proposed on the basis of extensive CFD calculations [Ref. 4].

In order to further reduce the measurement uncertainties, we recommend further tests with a larger number of jet fans, in order to provide additional confirmation of our test results.

5. REFERENCES

[1] Tarada, F., "Design, Testing and Application of an Energy-Efficient Longitudinal Ventilation System", 14th International Symposium on Aerodynamics and Ventilation of Tunnels, Dundee, Scotland, UK, 11 - 13 May 2011.

[2] "Sustainability of Tunnel Operation: New Approaches. A PIARC Briefing Note and Collection of Case Studies". Technical Committee 4.4 Tunnels, 2025R03EN, 2025.

[3] "Measurements and CFD Calculations with a MoJet and a Conventional Jet Fan", Fathi Tarada, Lars Lehmann and Pier Bertacche, 11th International Conference 'Tunnel Safety and Ventilation' 2022, Graz.

[4] "Jet Fan Installation Factor Correlations for Conventional Jet Fans and MoJets", Fathi Tarada, Pier Bertacche and Luca Stantero, 12th International Conference 'Tunnel Safety and Ventilation' 2024, Graz.

[5] "Deflectors for Tunnel Jet Fans", Fathi Tarada, 19th International Symposium on Aerodynamics, Ventilation & Fire in Tunnels, Brighton, 2022.

[6] "Theoretische und experimentelle Untersuchungen über die Lüftungsanlagen von Strassentunneln", Promotionsarbeit, ETH Zürich, Alex Haerter, 1961.

[7] "Evaluation of Jet Fan Performance in Tunnels", Beyer M., Sturm P.J., Saurwein M., Bacher M., 8th International Conference 'Tunnel Safety and Ventilation' 2016, Graz.

[8] "Jet Fan Installation Factors", Fathi Tarada and Pier Bertacche, 19th International Symposium on Aerodynamics, Ventilation & Fire in Tunnels, Brighton, 2022.

OPTIMIZATION OF THE MAIN FANS AND ASSOCIATED DRIVES FOR THE E4 STOCKHOLM BYPASS

[1,2]Rune Brandt, [3]Peter Stevelink,

[1]HBI Haerter, CH
[2]Trafikverket, SE
[3]Zitron, NL

DOI 10.3217/978-3-99161-087-8-019 (CC BY-SA 4.0)
https://creativecommons.org/licenses/by/4.0/deed.de
This CC license does not apply to third party material (attributed to other sources) and content noted otherwise.

ABSTRACT

The Stockholm Bypass project is part of the European motorway E4 and will connect the southern and northern regions of the Stockholm County. The Bypass is 21 km long, of which 18 km are in tunnels.

The ventilation system of the unidirectional tunnel consists of 241 jet fans (124 x 1000 N and 117 x 1500 N) and 47 main axial fans rated at 200 m³/s, installed in 17 ventilation stations. Minimising environmental impact is a key objective of the Swedish Transport Administration (Trafikverket). The total installed fan power amounts to 27 MW (17 MW for the main axial fans and 10 MW for the jet fans). Optimising fan and drive efficiency as well as minimising flow losses are therefore essential.

Eighteen of the 47 main axial fans must provide 120 m³/s in reverse-flow mode (60% reversibility), while the remaining 29 are operated only in forward direction. Pressure losses and ventilation regimes vary among the 17 ventilation stations. For system-redundancy reasons, all 47 motor-impeller units are required to be identical.

The paper discusses:

- design requirements for the axial fans and the resulting main design parameters
- duty points for the ventilation stations and for the axial fans
- evaluation of three variable-speed configurations:
  - A: variable speed drive (VSD),
  - B: two-speed 50% / 100 % (6/12-pole)
  - C: two-speed 75% / 100 % (6/8-pole).
- analysis of the performance of ventilation stations operating at 20 % to 100 % capacity
- evaluation for five typical operating scenarios to determine the most energy-efficient configuration

The study concludes that the intended configuration i.e. axial fans with variable pitch in motion combined with variable speed drives offers the highest overall energy efficiency. Only in one scenario is variant C marginally more efficient.

Keywords: Variable pitch in motion, axial fans, variable speed drives, two-speed motors

1. INTRODUCTION

The Stockholm Bypass project (Förbifahrt Stockholm) is part of the European motorway E4 and will connect the southern and northern regions of the Stockholm County. The bypass is 21 km long of which 18 km are in tunnels.

The unidirectional tunnel applies longitudinal ventilation with air-exchange stations. The ventilation system comprises 241 jet fans (124 x 1000 N with shaft power of 37 kW and 117 x 1500 N with shaft power of 45 kW) as well as 47 main axial fans with a nominal volume flow of 200 m³/s (46 fans at 355 kW and one at 75 kW[1]) installed in 17 ventilation stations. The total installed shaft power is 26,258 kW.

The specifications of the axial fans include:

- variable pitch in motion enabling reverse-flow operation
- design volume flow: Q =200 m³/s per fan (in forward direction)
- reverse volume flow: Q=120m³/s (60% of forward design flow)
- variable-speed drive operation
- suitable for parallel operation including start-up
- identical motor-impeller units for all stations
- installed motor shaft power: 355 kW
- certification for operation at 200°C for 120 minutes

An overview of the ventilation stations is provided in Table 1.

Table 1: Ventilation stations

Fan station	Type	Number installed fans	Number fans in operation
271	Exhaust	1	1
272	Exhaust	3	3
279	Exhaust	3 + 1 (redundant)	3
371	Exhaust	3	3
372	Exhaust/Supply	3	3
373	Exhaust/Supply	3	3
374	Exhaust	3	3
375	Exhaust	3	3
376	Exhaust/Supply	3	3
377	Exhaust/Supply	3	3
378	Exhaust	3	3
471	Exhaust	3	3
472	Exhaust/Supply	3	3
473	Exhaust/Supply	3	3
474	Exhaust	3	3
475*	Low-pressure shaft fan	1	1
571	Exhaust	3	3

*Special fan, which is not involved in this study

[1] The single 75 kW exhaust fan is a low-pressure shaft fan and is not considered in this analysis

2. OBJECTIVE OF THE STUDY

A key design criterion for the Stockholm Bypass ventilation system was to minimise power consumption. This raised the following question:

Are alternative fan–motor configurations feasible that eliminate the need for variable speed drives and thereby avoid converter-related losses?

To answer this question, the electrical power requirement had to be calculated for each configuration, taking into account the expected operating durations under various scenarios.

3. PRECONDITIONS

The fan selection was based on the following criteria:

a. The blade profile must be fully or partly reversible.
b. The fan diameter must be suitable for all required duty points (see Figure 1, Figure 2).
c. The hub diameter must be optimised for the required pressure rise and large enough to house the electric motor.
d. The number of blades must be optimised for pressure rise and maximum efficiency.
e. Identical motor-impeller units must be used in all ventilation stations.
f. Pressure losses across the complete fan unit must be minimised.
g. The maximum motor speed is determined by the pole number of a 50 Hz electric motor.

Figure 1 shows the required duty points for the fan stations:

– up to 200 m³/s with one fan in operation
– up to 600 m³/s with three fans in operation
– reverse extraction of at least –360 m³/s with three fans in operation

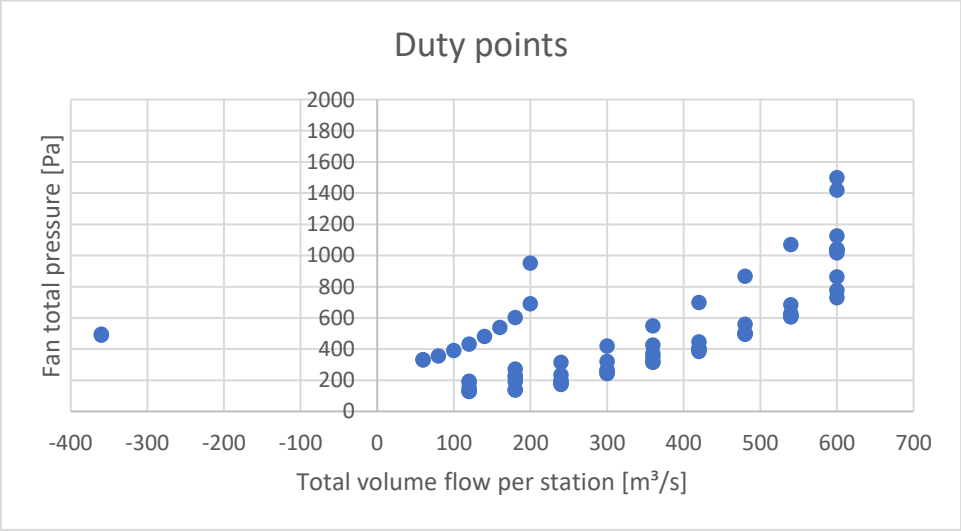


Figure 1: Duty points for the ventilation stations. For one fan up to 200 m³/s and with three fans up to 600 m³/s. Reversing three fans, the extraction capacity shall be at least -360 m³/s.

These station-level requirements translate into the fan duty points shown in Figure 2.

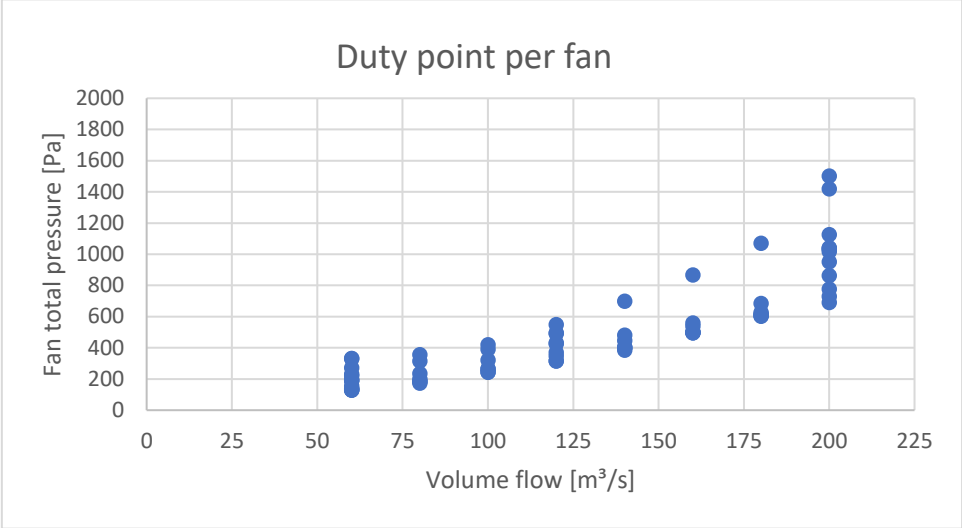


Figure 2: Fan duty points

4. INVESTIGATED VARIANTS

The optimal fan design (impeller diameter, hub diameter, blade count, and variable pitch in motion) was assumed fixed. Only the motor-speed configurations were varied:

- Variant A: fan with a variable speed drive (frequency converter)
- Variant B: fan with a Dahlander 6/12-pole motor (995/497 min^{-1})
- Variant C: fan with a 6/8-pole motor (995/746 min^{-1})
- Variant D: fan with a 6/10-poles motor (995/597 min^{-1})

Five operating scenarios were used to evaluate the total energy consumption (see section 4.6).

4.1. Required input

To calculate the electrical power demand, the following data were required for each duty point:

a. Blade angle
b. Aerodynamic fan efficiency
c. Fan rotational speed
d. Motor efficiency at the corresponding speed
e. For Variant A: variable speed drive efficiency

4.2. Variant A: Input Data

Variant A assumes a 355 kW, 6-pole motor (ABB M3BPW 355LKB 6) with a nominal speed of 995 rpm. The fan performance and motor efficiency characteristics are shown in Figure 3.

The variable speed drive efficiency as a function of torque is given in Table 2.

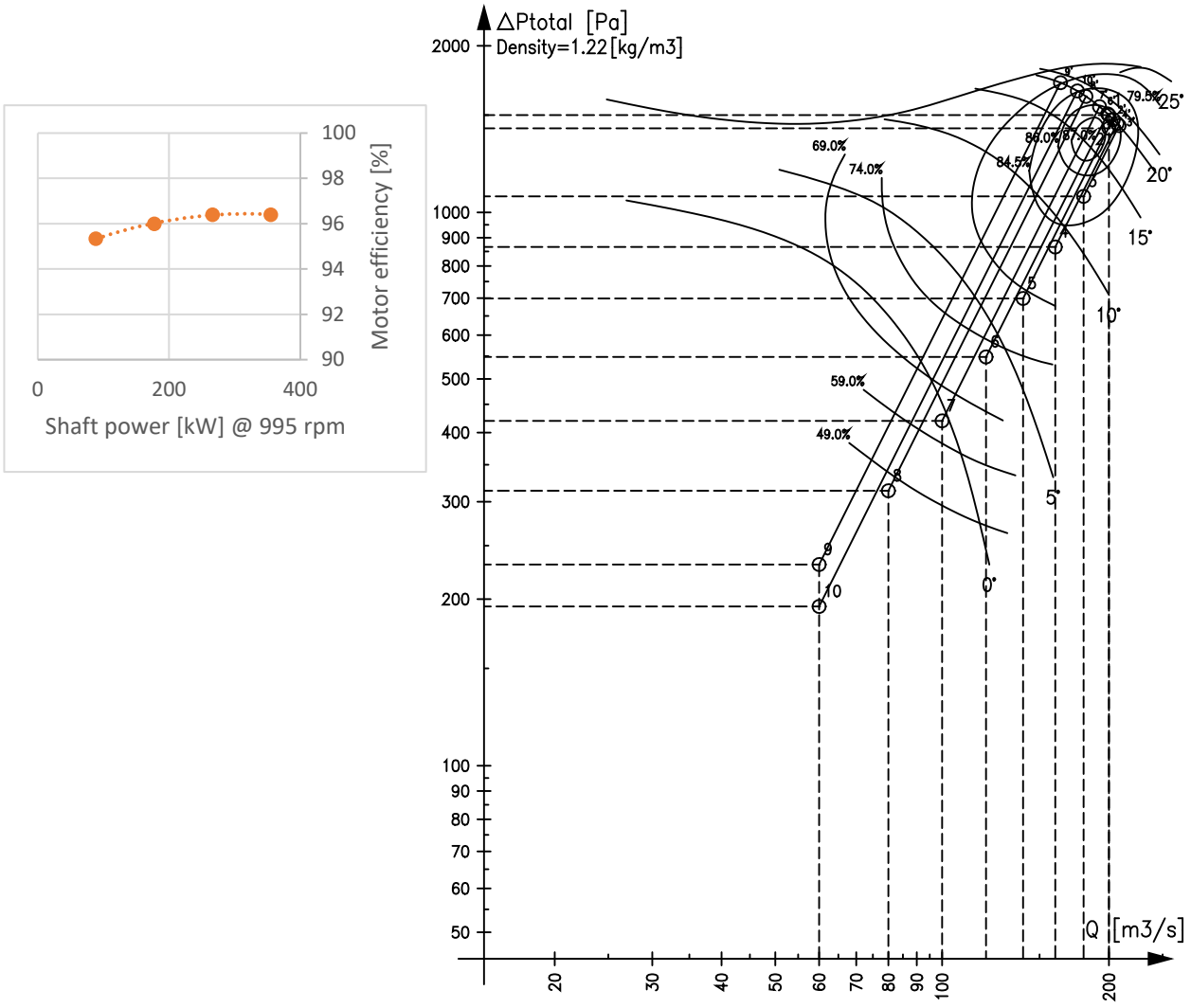


Figure 3: Variant A. Right: Fan curve. Left: Motor efficiency at full speed.

Table 2: Variant A: Efficiency of variable speed drive (frequency converter) including filters etc.

	Frequency converter together with harmonic filter, DU/DT filter, DC trottle										
Efficiency [%]	**Speed [%]**										
Torque [%]	**0%**	**10%**	**20%**	**30%**	**40%**	**50%**	**60%**	**70%**	**80%**	**90%**	**100%**
100%				97,67	97,68	97,68	97,70	97,69	97,69	97,67	97,67
90%				97,67	97,67	97,67	97,67	97,67	97,67	97,67	97,67
80%				97,67	97,67	97,67	97,67	97,67	97,67	97,67	97,67
70%				97,66	97,66	97,66	97,66	97,66	97,66	97,66	97,66
60%				97,63	97,63	97,63	97,63	97,63	97,63	97,63	97,63
50%				97,55	97,55	97,55	97,55	97,55	97,55	97,55	97,55
40%				97,39	97,39	97,39	97,39	97,39	97,39	97,39	97,39
30%				97,10	97,10	97,10	97,10	97,10	97,10	97,10	97,10
20%				96,51	96,51	96,51	96,51	96,51	96,51	96,51	96,51
10%				95,07	95,07	95,07	95,07	95,07	95,07	95,07	95,07
0%				88,75	88,75	88,75	88,75	88,75	88,75	88,75	88,75

4.3. Variant B: Input data

Variant B uses a 355 kW Dahlander 6/12-pole motor (ABB M3BPW 400LD 6G), capable of operating at full and half speed.

Fan performance and motor efficiency curves are shown in Figure 4.

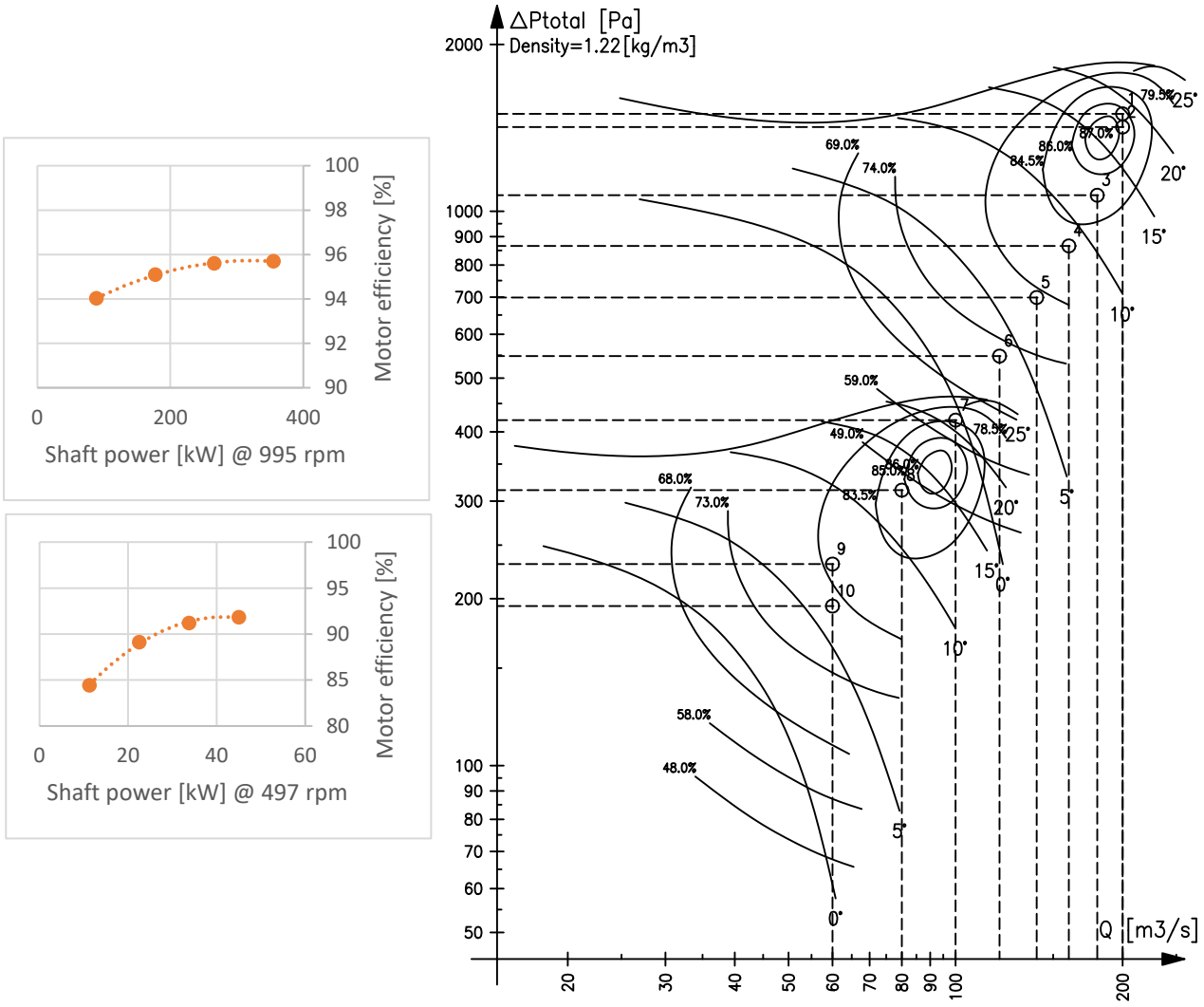


Figure 4: Variant B. Right: Fan curve.
Left: Motor efficiency at full speed (top) and at half speed (bottom)

4.4. Variant C: Input data

Variant C uses a 355 kW, 6/8-pole motor (ABB M3BP 400LB 6/8), providing 100% and 75% operating speeds.

Fan performance and motor efficiency curves are shown in Figure 5.

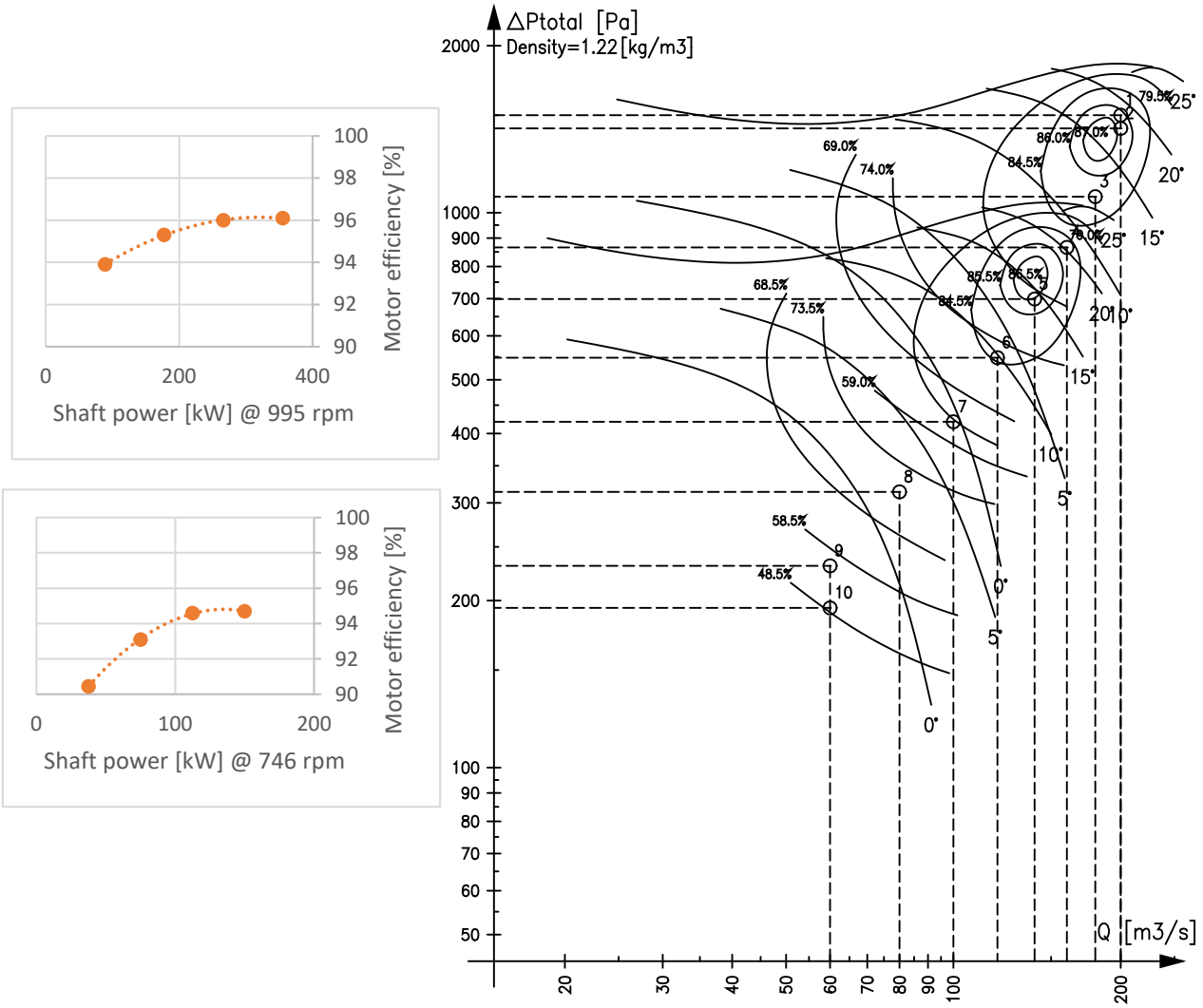


Figure 5: Variant C. Right: Fan curve.
Left: Motor efficiency at full speed (top) and at 75% speed (bottom)

4.5. Variant D: exclusion

During the study, it became clear that a dual-winding motor capable of 995 and 597 rpm would require a larger frame size than could be accommodated in the fan hub. Variant D was therefore excluded from further analysis.

4.6. Operating scenarios

Extensive simulations were used to define five representative operating scenarios for the calculations of operating costs.

Table **3** provides an overview. One station (279) is dedicated to smoke extraction and was therefore assigned only 0.01 daily operating hours.

Table 3: Five investigated operation scenarios. One fan station (279) is dedicated to smoke extraction, which therefore has been estimated to merely have 0.01 daily running hour.

Ventilation station capacity	Fan flow rate [m3/s]	Fans operating	Daily running hours				
			Scenario I	Scenario II	Scenario III	Scenario IV	Scenario V
100%, Smoke extraction	200	3	0.01	0.01	0.01	0.01	0.01
100%	200	3	0.01	1.00	0.00	0.00	1.00
90%	180	3	0.50	1.00	0.00	0.00	2.00
80%	160	3	1.00	1.00	0.50	0.50	2.00
70%	140	3	1.00	1.00	1.00	1.00	1.00
60%	120	3	1.50	1.00	1.50	4.00	0.50
50%	100	3	2.00	1.00	2.00	1.00	0.00
40%	80	3	2.50	1.00	2.50	0.50	0.00
30%	60	3	2.50	1.00	3.00	0.00	0.00
20%	60	2	1.00	1.00	3.50	0.00	0.00

5. RESULTS

Intermediate results for station 378 are presented below, as this station is representative of the stations 371, 374, 375, 471, and 474. Subsequently, aggregated results for all stations are summarised.

5.1. Intermediate results of fan station 378

The results for the three variants and their respective power consumption are shown below, see Table 4, Table 5 and Table 6.

Table 4: Variant A

VARIANT A (n=995min^{-1} with VSD)												
Operation percentage			100%	100%	90%	80%	70%	60%	50%	40%	30%	20%
Volume flow per fan	Q_{Fan}	[m³/s]	200	200	180	160	140	120	100	80	60	60
Total pressure loss	Δp_{total}	[Pa]	1126	863	684	558	446	426	321	235	271	190
Motor speed	n	[Min^{-1}]	995	923	826	740	656	606	517	431	417	365
Fan Efficiency	η_{Fan}	[%]	85.4%	81.9%	81.1%	81.5%	81.7%	84.2%	85.0%	85.8%	78.1%	84.4%
Shaft power	P_{shaft}	[kW]	263.7	210.7	151.8	109.5	76.4	60.7	37.8	21.9	20.8	13.5
Electrical power	$P_{elektric}$	[kW]	273.8	219.1	158.2	114.6	80.4	64.1	40.4	24.0	22.9	15.4
Motor efficiency	η_{motor}	[%]	96.3%	96.2%	95.9%	95.6%	95.1%	94.7%	93.4%	91.1%	90.9%	87.9%
Frequency Converter Efficiency	η_{VSD}	[%]	97.4%	97.4%	97.3%	97.2%	96.9%	96.8%	96.3%	95.4%	95.3%	94.3%
Electrical power	P_{grid}	[kW]	281.1	225.1	162.7	117.9	82.9	66.2	42.0	25.2	24.0	16.3
Total efficiency	η_{total}	[%]	80.1%	76.7%	75.7%	75.7%	75.3%	77.2%	76.5%	74.6%	67.6%	70.0%

Table 5: Variant B

VARIANT B (n=995/497min^{-1})												
Operation percentage			100%	100%	90%	80%	70%	60%	50%	40%	30%	20%
Volume flow per fan	Q_{Fan}	[m³/s]	200	200	180	160	140	120	100	80	60	60
Total pressure loss	Δp_{total}	[Pa]	1126	863	684	558	446	426	321	235	271	190
Motor speed	n	[Min^{-1}]	995	995	995	995	995	995	497	497	497	497
Fan Efficiency	η_{Fan}	[%]	85.4%	81.5%	80.0%	75.5%	71.0%	69.0%	85.4%	78.0%	80.0%	77.0%
Shaft power	P_{shaft}	[kW]	263.7	211.8	153.9	118.3	87.9	74.1	37.6	24.1	20.3	14.8
Electrical power	$P_{elektric}$	[kW]	276.1	222.1	162.0	125.0	93.6	79.2	41.1	26.9	22.9	17.1
Motor efficiency	η_{motor}	[%]	95.5%	95.3%	95.0%	94.6%	94.0%	93.6%	91.4%	89.6%	88.7%	86.7%
Total efficiency	η_{total}	[%]	81.6%	77.7%	76.0%	71.4%	66.7%	64.6%	78.0%	69.9%	71.0%	66.7%

Table 6: Variant C

VARIANT C (n=995/746min^{-1})												
Operation percentage			100%	100%	90%	80%	70%	60%	50%	40%	30%	20%
Volume flow per fan	Q_{Fan}	[m³/s]	200	200	180	160	140	120	100	80	60	60
Total pressure loss	Δp_{total}	[Pa]	1126	863	684	558	446	426	321	235	271	190
Motor speed	n	[Min^{-1}]	995	995	995	746	746	746	746	746	746	746
Fan Efficiency	η_{Fan}	[%]	85.4%	81.5%	80.0%	79.5%	80.5%	81.5%	80.5%	74.5%	64.0%	63.0%
Shaft power	P_{shaft}	[kW]	263.7	211.8	153.9	112.3	77.6	62.7	39.9	25.2	25.4	18.1
Electrical power	$P_{elektric}$	[kW]	276.1	222.1	162.0	120.1	83.4	67.7	43.5	28.0	28.2	20.4
Motor efficiency	η_{motor}	[%]	95.5%	95.3%	95.0%	93.5%	93.0%	92.7%	91.7%	90.2%	90.3%	88.7%
Total efficiency	η_{total}	[%]	81.6%	77.7%	76.0%	74.3%	74.9%	75.6%	73.8%	67.2%	57.8%	55.8%

5.2. Average efficiency

The average efficiency at each duty point - expressed as a percentage of volume flow - was calculated for all three variants and is shown in Figure 6.

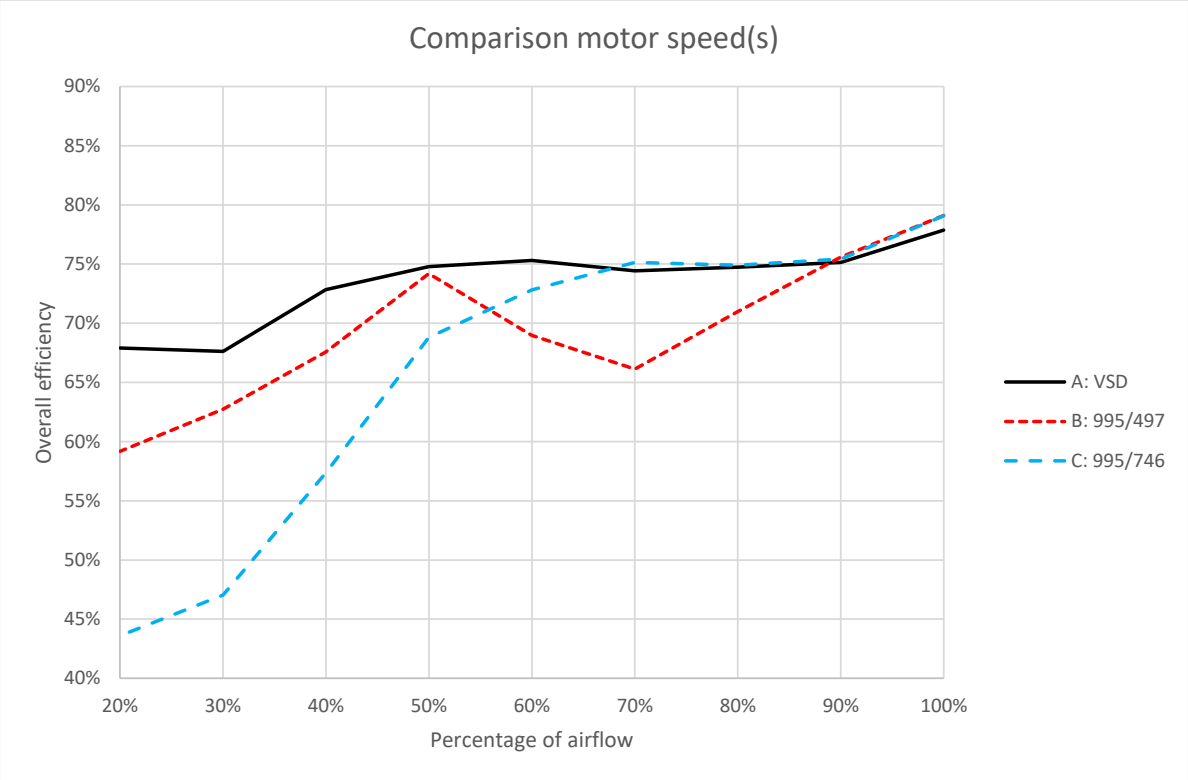


Figure 6: Comparison of efficiencies.

5.3. Annual power consumption

Annual energy demand was determined for each of the five operating scenarios (see Table 7), based on 310 operating days per year.

For comparison, Table 8 shows normalised values with 100% representing the most efficient variant for that particular scenario.

Table 7: Annual power consumption

Annual power consumption [kWh]			
	A: VSD	B: 995/497	C: 995/746
Scenario I	7 355 336	7 707 587	8 036 087
Scenario II	9 781 387	10 027 169	10 053 042
Scenario III	5 983 929	6 323 438	6 909 141
Scenario IV	5 651 667	6 127 297	5 853 981
Scenario V	11 776 474	12 043 032	11 705 719

Except for scenario V, Variant A with a VSD is the most energy-efficient solution.

The Dahlander configuration (Variant B) consistently exhibits the highest energy consumption.

Only in one scenario is Variant C marginally more efficient than Variant A.

Table 8: Normalised annual power consumption per scenario

Annual power consumption percentage [%]			
	A: VSD	B: 995/497	C: 995/746
Scenario I	100.00%	104.79%	109.26%
Scenario II	100.00%	102.51%	102.78%
Scenario III	100.00%	105.67%	115.46%
Scenario IV	100.00%	108.42%	103.58%
Scenario V	100.60%	102.88%	100.00%
Average	100.12%	104.85%	106.22%

6. CONCLUSIONS

For the Stockholm Bypass project, the following conclusions can be drawn:

- Fans operated via a variable speed drive (VSD) are slightly less efficient at maximum speed than fans with two-speed motors.
- However, when reduced speed is required, VSD-driven fans generally achieve significantly higher overall efficiency.
- Under typical operating conditions and expected yearly operating hours, the VSD solution is the most energy-efficient configuration.
- Only if the fans are expected to operate for many hours at maximum operation point may a two-speed configuration become more efficient.
- The originally planned configuration - axial fans with variable pitch in motion combined with variable speed drives - was confirmed to be the optimal solution.

EXPERIMENTAL INVESTIGATION OF THERMAL RUNAWAY IN LITHIUM-ION BATTERIES: IMPLICATIONS FOR TUNNEL SAFETY AND STRUCTURAL INTEGRITY

[1,2]Davide Papurello. [1,2]Luca Musso, [3]Carlo Barbetta, [1,2]Romano Borchiellini, [3]Maciej Sobótka, [4]Daniel Fruhwirt

[1]Department of Energy, Politecnico di Torino, IT
[2]Energy Center, Politecnico di Torino, IT
[3]Systemair GmbH, DE / Systemair Srl, IT
[4]Graz University of Technology, Institute of Thermodynamics and Sustainable Propulsion Systems, AT

DOI 10.3217/978-3-99161-087-8-020 (CC BY-NC 4.0)
https://creativecommons.org/licenses/by/4.0/deed.de
This CC license does not apply to third party material (attributed to other sources) and content noted otherwise.

ABSTRACT

The increasing use of lithium-ion batteries (LIBs) in electric vehicles and energy storage systems raises new safety concerns, particularly in confined environments such as road tunnels. This study presents an experimental investigation into thermal runaway (TR) events in LIBs triggered by mechanical, thermal, and electrical abuse conditions. The work focuses on characterising temperature and pressure evolution, gas emissions, and the effects of battery fires on surrounding structural materials, specifically concrete, representative of tunnel linings. Abuse tests, including nail penetration, overheating, and external short circuits, were conducted using an Accelerating Rate Calorimeter (ARC). The maximum temperature, pressure and released gases were monitored. Pre- and post-mortem computed tomography analyses provided insight into internal cell degradation and structural changes. Importantly, TR events in proximity to cement mortar samples revealed their thermal damage, leading to microstructure degradation (mostly microcrack network development) after repeated exposure. The results show that thermal runaway of cells can rapidly propagate in confined spaces, developing flammable gases, toxic substances and thermal loads capable of compromising tunnel structures. Cells triggered at higher ambient temperatures are more reactive, reaching higher peak temperatures and pressures during TR. The state of health (SOH) of cells influences the severity of TR, with degraded cells producing less intense but still dangerous reactions. Overheating tests demonstrated a critical delay window (~350 s) enabled by safety valve activation, crucial for mitigation in real tunnel scenarios. For external short circuit, no thermal runaway occurred for different SOC states. These findings contribute to a better understanding of LIB behaviour under critical conditions and support the development of safety strategies, emergency response plans, and structural containment systems for tunnels. The data will serve as a basis for future risk assessments and engineering models aimed at improving resilience to battery-induced fires in underground infrastructure.

Keywords: Thermal runaway; lithium-ion battery; nail penetration; overheating; tunnel safety; structural degradation.

1. INTRODUCTION

The global energy transition and decarbonization goals have accelerated the deployment of lithium-ion batteries (LIBs) for both electric vehicles (EVs) and stationary energy storage systems. These technologies are crucial for managing the intermittency of renewable energy sources and reducing greenhouse gas emissions from the electricity (32.3%) and transport (15.5%) sectors [1]. In 2024, global battery demand reached 1 TWh, with electric vehicles accounting for over 85% of this total; the most rapid growth was observed in electric trucks (+75%) [2]. However, the widespread use of LIBs introduces critical safety challenges, primarily related to thermal runaway (TR)—a rapid, self-sustained temperature rise caused by exothermic reactions within the cell. TR can lead to fires, explosions, and the release of toxic and flammable gases, posing risks in confined environments such as tunnels or enclosed transport systems. This aspect is increasingly felt at the level of risk management, due to the increase of electric vehicles, especially considering large vehicles (electric buses or trucks), for these vehicles the impacts can be extensive and experimental studies are scarce. Mechanistically, TR initiates when internal heat generation exceeds dissipation, leading to SEI and separator degradation at temperatures between 70–130 °C, followed by cathode decomposition and gas release above 150 °C, and full electrolyte breakdown near 200–300 °C [3], [4], [5]. These reactions may be triggered by mechanical, thermal, or electrical abuse—each capable of producing internal short circuits (IC) that start runaway reactions [6]. Existing safety standards, such as SAE J2464 (2009), require testing across four system levels—cell, module, pack, and vehicle—but this study focuses specifically on cell-level abuse behaviour [7]. Typical abuse mechanisms include:

- Mechanical: impact, crush, or penetration tests (e.g., nail tests).
- Thermal: overheating or exposure to extreme temperatures.
- Electrical: short circuits and overcharge conditions

This research aims to provide a comprehensive experimental investigation of LIB thermal runaway under realistic conditions, including interactions with structural materials such as concrete, which are critical for assessing safety in tunnel infrastructures. The work explores TR triggered by mechanical, thermal, and electrical abuse, analyzing thermal, pressure, and gas-emission profiles to develop improved safety models and mitigation strategies.

2. DATA AND METHODS

2.1. Experimental Setup

Tests were conducted using a Thermal Hazard Technology EV+ Accelerating Rate Calorimeter (ARC), equipped with thermocouples, pressure transducers, and a vent gas analysis system, see Figure 1.

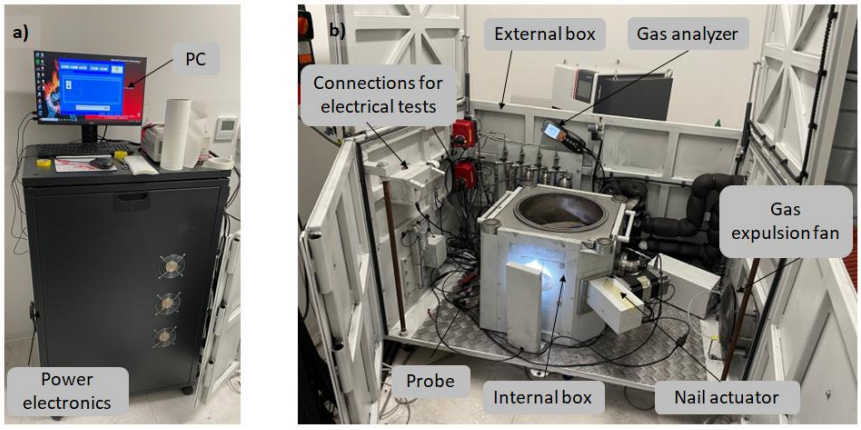


Figure 1: Thermal Hazard Technology EV+ Accelerating Rate Calorimeter (ARC): a) power electronics, b) testing tool.

Mechanical (nail penetration), thermal (overheating), and electrical (external short circuit) abuse conditions were applied to commercial cylindrical LIB cells (LG INR18650 M29 and Samsung INR21700-50E), see Table 1.

Table 1: cells tested datasheet.

Parameters	LG 18650	Samsung 21700
Technology	Li-NiMnCoO$_2$	Li-NiMnCoO$_2$
Nominal Capacity	2850 mAh	4900 mAh
Nominal Voltage	3.67 V	3.6 V
Charging Voltage	4.2 V	4.2 V
Charging Current	0.5C (1375 mA)	0.5C (2450 mA)
Max Charge Current	1C (2750 mA)	1C (4900 mA)
Max Discharge Current	10 A	14.7 A
Weight	45 g	69 g

Environmental temperature and state of charge (SOC) were systematically varied. Gas emissions (CO_2, CO, NO_x, O_2) were monitored using a Testo 330 gas analyser. Concrete samples representative of tunnel linings were placed in proximity to cells to observe flame and pressure effects, see Figure 2. Scanning electron microscopy (SEM/EDS) were used to assess internal cell damage and concrete microstructure degradation.

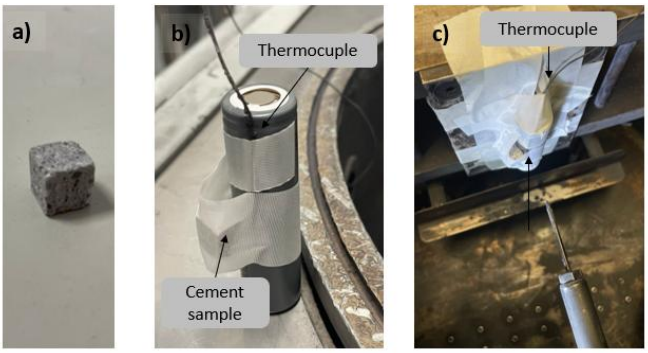


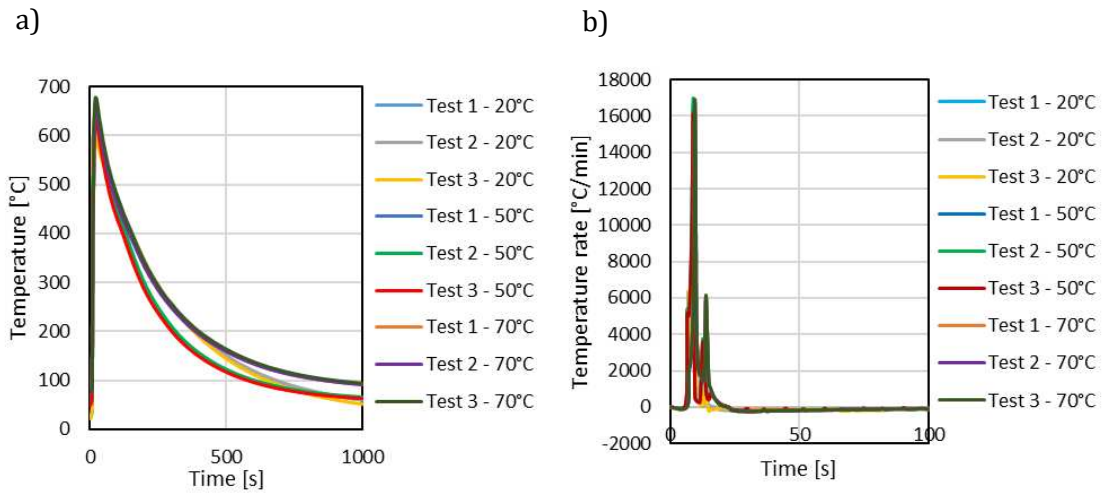
Figure 2: a) cement mortar sample, b) positioning of the concrete sample in contact with the surface and with the thermocouple, c) experimental setup in the THT instrument.

3. RESULTS AND DISCUSSION

Thermal runaway occurred during nail penetration and overheating tests, but not under external short-circuit conditions.

Mechanical abuse – nail penetration

Cells triggered at 70 °C ambient temperature exhibited more severe TR, with peak temperatures exceeding 660 °C and pressures above 2.3 bar, see Figure 3. Higher ambient temperatures increased reaction rates and gas production, primarily CO_2 and CO, see Table 2.



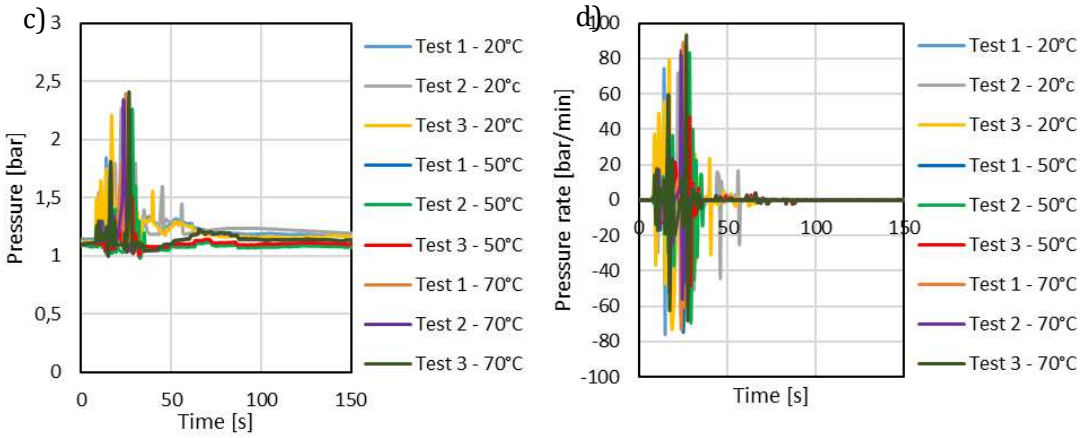


Figure 2: a) Temperature profile during TR for nail penetration tests, b) Temperature growth rate during TR for nail penetration tests, c) pressure profile during TR for nail penetration tests, d) pressure rate of temperature tests for nail penetration tests.

Table 2: Average key values of gas analysis.

Room temperature [°C]	CO_2 max [%]	O_2 min [%]	ppm(v) CO max	ppm(v) NO max
20	3.6	16.1	12359.7	23.3
50	4.0	15.1	14374.9	35.1
70	4.4	14.8	16553.7	50.8

In tests involving concrete samples, it was observed that the thermal runaway triggered by the nail penetration caused progressive degradation of the concrete matrix. After repeated TR events, microcracks developed in the concrete, particularly in the cement matrix, leading to structural damage. The extent of degradation was directly proportional to the number of TR events, with samples exposed to multiple battery explosions showing widening cracks and increased porosity, up to 8 µm wide and the incorporation of metallic inclusions from cell materials, see Figure 4-7.



Figure 3: Effects of explosions on concrete samples.

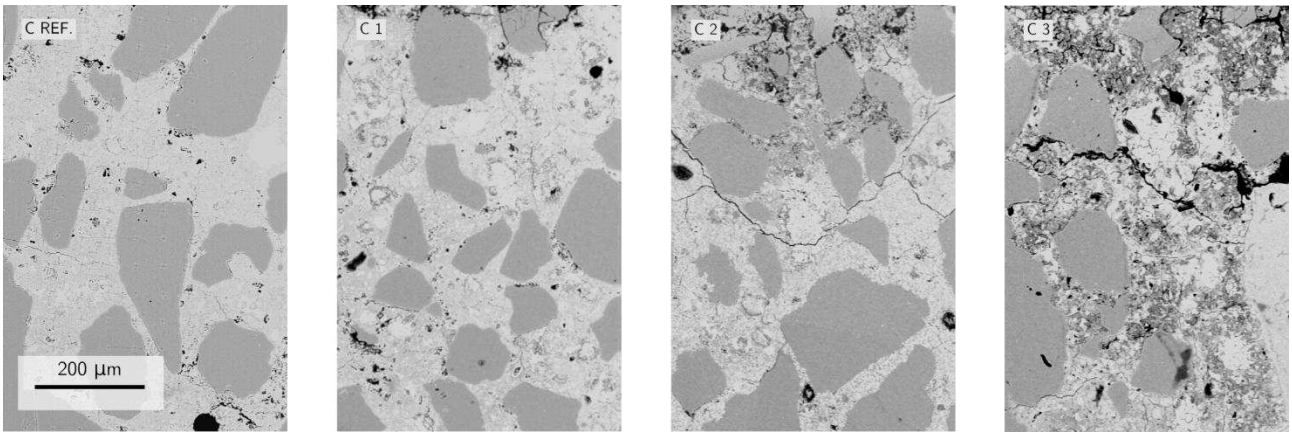


Figure 4: SEM micrographs of the samples after exposure to TR.

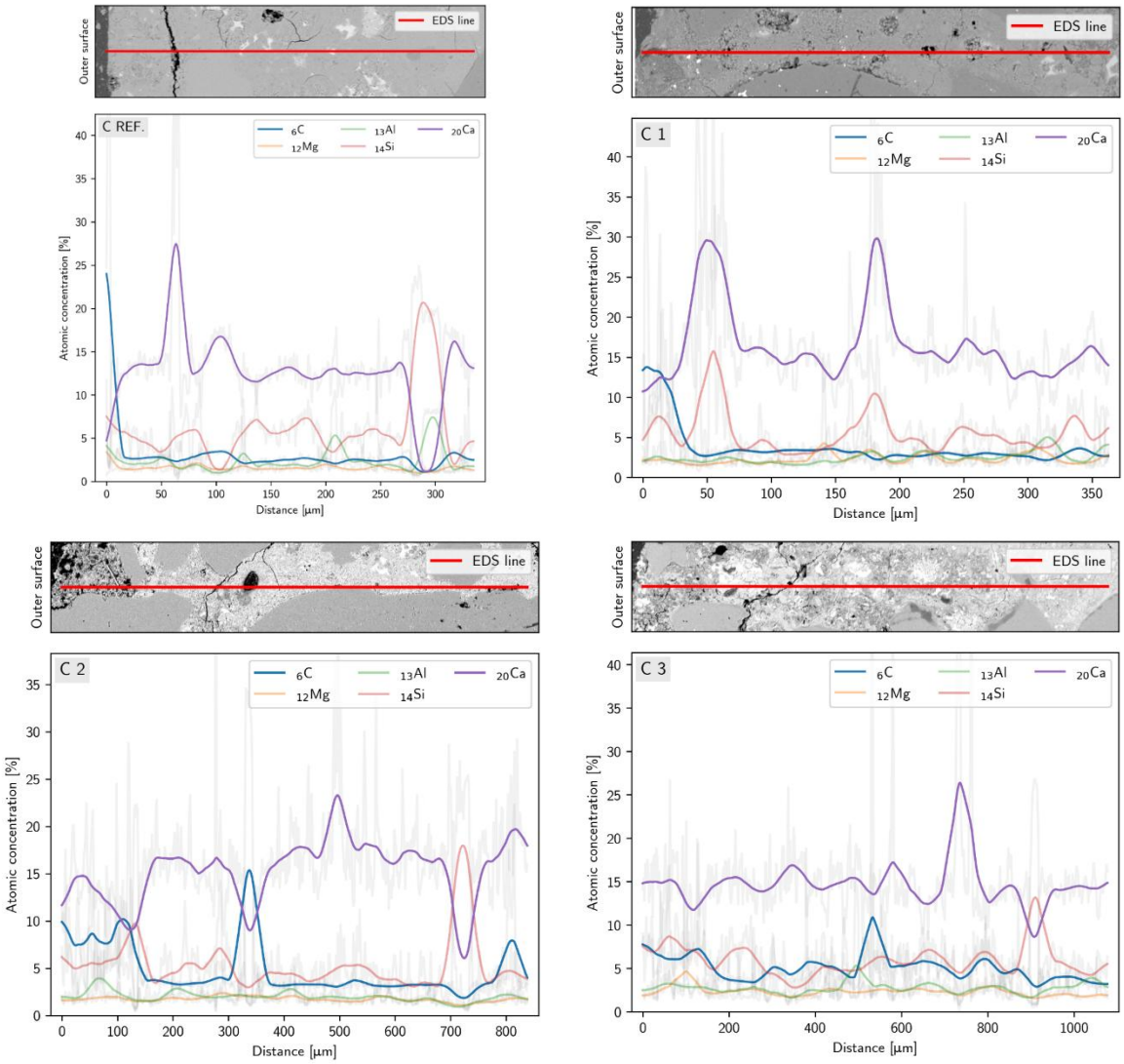


Figure 5: Changes in elemental composition of concrete samples in the vicinity of the surface subjected to cell explosions: a) reference sample, b) sample C 1 – after one cycle, c) sample C 2 – after two cycles and d) sample C 3 – after 3 cycles.

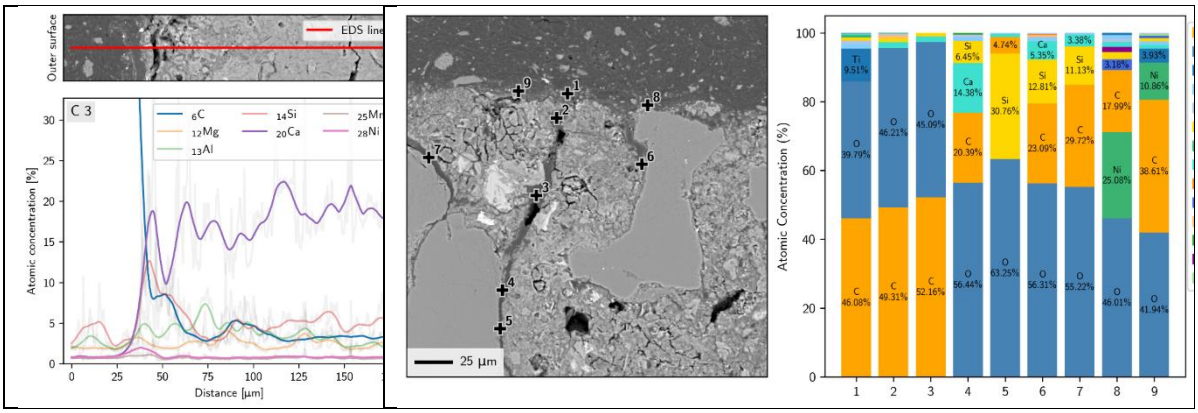


Figure 6: Combustion product penetration into concrete samples: elemental composition in concrete degradation zone, locations of spot measurements and measured atomic concentrations at selected points of concrete sample C 3.

The presence of nickel, cobalt, and manganese within the concrete samples was not uniform but concentrated in specific regions, particularly at the interfaces between the cracks and degraded matrix areas, confirming that these metallic elements originated from the battery cell and migrated into the concrete due to the thermal runaway reactions. This finding is critical for understanding the long-term impact of battery fires on the structural integrity of tunnel linings and other concrete infrastructure exposed to battery-induced fires.

Thermal abuse - Overheating

The overheating thermal abuse tests provided crucial insights into the behavior of lithium-ion cells under extreme thermal stress. A key finding was the rate of temperature increase, which was alarmingly fast, with some cells heating from 130 °C to over 1300 °C in just 1.8 seconds, see Figure 8. This rapid escalation results to the high reactivity of the cells when exposed to prolonged heat, compounded by reduced heat dissipation in an already-heated environment. As shown in previous studies, the combination of reduced cooling capacity and accelerated reaction kinetics at high temperatures makes thermal runaway more severe [8]. The pressure profiles observed in these tests also highlighted the importance of safety mechanisms, as gases released during TR caused significant pressure buildup inside the cell, peaking at 1.47 bar under the most extreme conditions, see Figure 9. The safety valve's role in relieving pressure helped mitigate some of the immediate risks associated with explosion or fire propagation, but it was evident that the reaction would continue to escalate once the valve had been triggered.

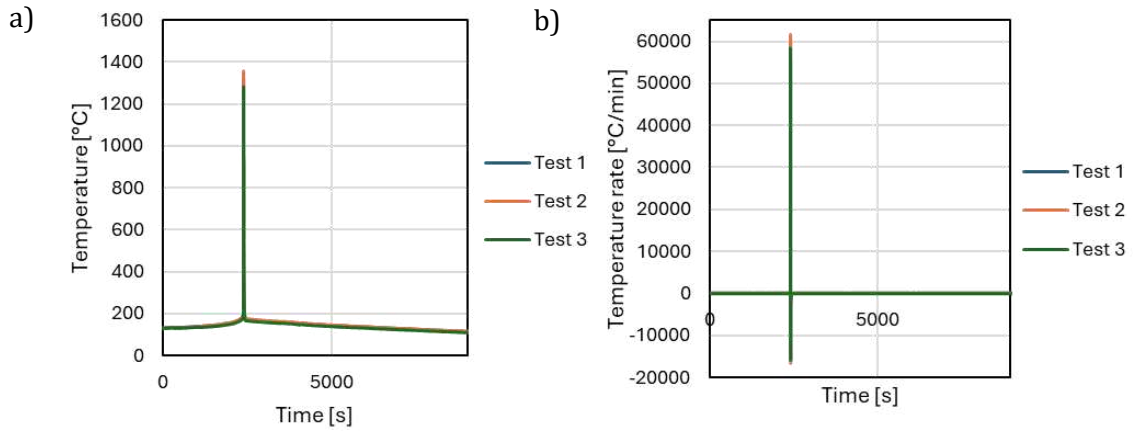


Figure 7: a) temperature profile of the cell during the overheating test,
b) temperature gradient profile of the cell during the overheating test.

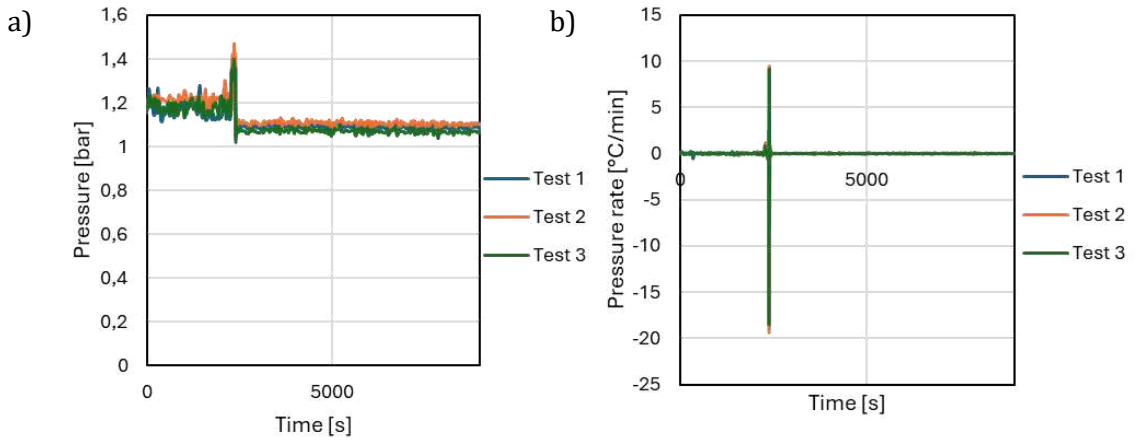
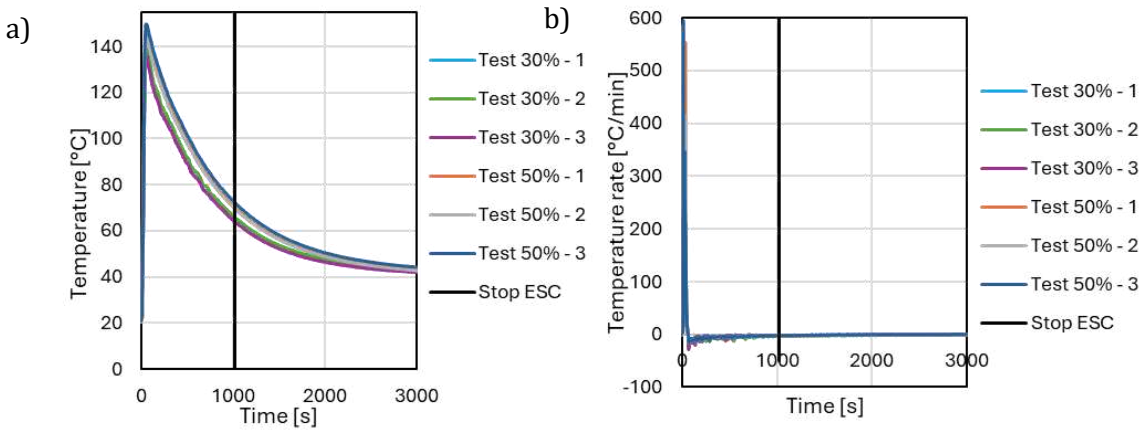


Figure 8: a) pressure profile during the overheating test,
b) pressure gradient profile during the overheating test.

Electrical abuse - External Short Circuit

During the ESC tests, the cells exhibited an increase in temperature; however, the rise was not sufficient to trigger TR. The maximum temperatures reached were relatively moderate, and temperature gradients remained within manageable levels. At both 30% and 50% states of charge (SOC), the temperature increase was slower compared to tests involving nail penetration or overheating, where the cells experienced rapid and extreme thermal escalation, see Figure 10. This indicates that external short circuits under these conditions do not generate the intense thermal reactions that lead to TR, likely due to the thermal protection mechanisms built into the cells, such as PTC (Positive Temperature Coefficient) thermistors and Current Interrupt Devices (CID).



c)

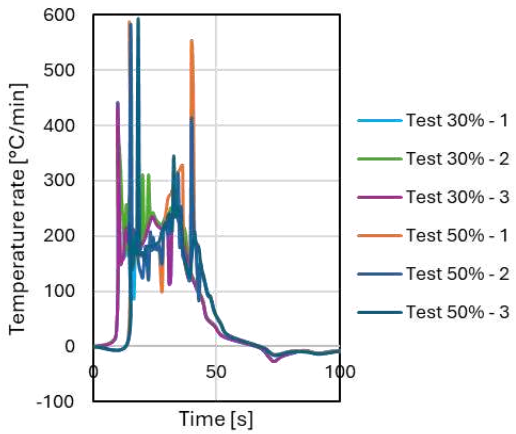


Figure 9: a) ESC test temperature profiles on 21700 cells at different SOCs,
b) ESC temperature gradient profiles on 21700 cells at different SOCs,
c) Temperature gradient profiles in the early stages of ESC on 21700 cells at different SOCs.

4. CONCLUSIONS

The experimental study revealed the critical parameters influencing lithium-ion battery thermal runaway under realistic conditions. TR events generate intense heat, pressure, and toxic gases that can compromise tunnel structures. Mechanical and thermal abuses were identified as dominant triggers, while electrical short-circuiting was mitigated by cell safety mechanisms. Concrete materials experienced cumulative degradation after repeated exposures, underlining the need for fire-resistant designs. The observed 300–350 s safety valve delay offers a crucial opportunity for emergency response in confined environments. These results provide a foundational dataset for developing safety models, risk mitigation measures, and structural protection strategies in underground applications.

5. REFERENCES

[1] L. Musso et al., 'Thermal runaway in lithium-ion batteries: experimental insights from mechanical, thermal, and electrical stress tests,' Applied Thermal Engineering, vol. 281, 2025.

[2] X. Feng et al., 'Thermal runaway mechanism of lithium-ion battery for electric vehicles: a review,' Energy Storage Materials, vol. 10, 2018.

[3] D.P. Finegan et al., 'In-operando high-speed tomography of lithium-ion batteries during thermal runaway,' Nature Communications, 2015.

[4] S. Doose et al., 'Development of a new procedure for nail penetration of lithium-ion cells,' Journal of The Electrochemical Society, 2020.

[5] Y. Li et al., 'Pressure effect on thermal runaway behaviours of lithium-ion battery in confined space,' Fire Technology, 2023.

[1] H. Ritchie, P. Rosado, and M. Roser, "Breakdown of carbon dioxide, methane, and nitrous oxide emissions by sector," Our World in Data, Jun. 2020, Accessed: Nov. 04, 2025. [Online]. Available: https://ourworldindata.org/emissions-by-sector

[2] "Electric vehicle batteries – Global EV Outlook 2025 – Analysis - IEA." Accessed: Nov. 04, 2025. [Online]. Available: https://www.iea.org/reports/global-ev-outlook-2025/electric-vehicle-batteries

[3] Q. Wang, P. Ping, X. Zhao, G. Chu, J. Sun, and C. Chen, “Thermal runaway caused fire and explosion of lithium ion battery,” J Power Sources, vol. 208, pp. 210–224, Jun. 2012, doi: 10.1016/J.JPOWSOUR.2012.02.038.

[4] C. Essl et al., “Comprehensive Hazard Analysis of Failing Automotive Lithium-Ion Batteries in Overtemperature Experiments,” Batteries 2020, Vol. 6, Page 30, vol. 6, no. 2, p. 30, May 2020, doi: 10.3390/BATTERIES6020030.

[5] F. Gao et al., “A Review on Materials for Flame Retarding and Improving the Thermal Stability of Lithium Ion Batteries,” Int J Electrochem Sci, vol. 15, no. 2, pp. 1391–1411, Feb. 2020, doi: 10.20964/2020.02.24.

[6] S. Mallick and D. Gayen, “Thermal behaviour and thermal runaway propagation in lithium-ion battery systems – A critical review,” J Energy Storage, vol. 62, p. 106894, Jun. 2023, doi: 10.1016/J.EST.2023.106894.

[7] “J2464_200911: Electric and Hybrid Electric Vehicle Rechargeable Energy Storage System (RESS) Safety and Abuse Testing - Recommended Practice.” Accessed: Nov. 04, 2025. [Online]. Available: https://saemobilus.sae.org/standards/j2464_200911-electric-hybrid-electric-vehicle-rechargeable-energy-storage-system-ress-safety-abuse-testing

[8] A. García, J. Monsalve-Serrano, R. Lago Sari, and S. Martinez-Boggio, “An optical investigation of thermal runaway phenomenon under thermal abuse conditions,” Energy Convers Manag, vol. 246, p. 114663, Oct. 2021, doi: 10.1016/J.ENCONMAN.2021.114663.

SMART TUNNEL IN INDUSTRY 5.0: IMPROVING ROAD TUNNEL RESILIENCE BY DYNAMIC RISK ANALYSIS

[1]Alessandro Focaracci, [2]Francesca Zacchei, [2]Luigi Martirano

[1]*Prometeoengineering.it S.r.l., IT*
[2]*La Sapienza - University of Rome, IT*

DOI 10.3217/978-3-99161-087-8-021 (CC BY-SA 4.0)
https://creativecommons.org/licenses/by/4.0/deed.de
This CC license does not apply to third party material (attributed to other sources) and content noted otherwise.

ABSTRACT

Safety in tunnels is being contemplated through a holistic approach due to accidents that occurred through years. Technological innovations have led to the tunnel concept evolution from civil to technological infrastructure, where technology overcomes the limits of the geometric design, increasing its operating capacity. This paper aims to illustrate SCADRA principles (Supervisory Control Acquisition and Dynamic Risk Analysis), developed thanks to EURAM (EUropean Risk Analysis Method) methodology, which assessed the risk of over 600 road tunnel tubes, focusing on the following values: users and managers' needs (Human-centricity), usage of green technologies and application of energy saving strategy (Sustainability), and improvement of tunnels resilience (Resilience). SCADRA is used in monitoring continuously the tunnel state by gathering the safety influence variables and performing a dynamic risk analysis, quantitative and probabilistic, in real-time. The system was installed in three Italian road tunnels, executing over 130,000 instantaneous risk analyses. The applications' results and the future developments will be presented according to tunnels' safety improvement, maintenance, and management.

Keywords: Dynamic Risk Analysis, Smart Tunnel, Real-time Monitoring, Infrastructure Resilience

1. INTRODUCTION

Italy's diverse geomorphological landscape, extending from mountains to plains, has made road tunnels essential for ensuring continuous and efficient national connectivity. Following the major accidents in the Mont Blanc, Tauern, and St. Gotthard tunnels (1999–2001), tunnel safety evolved toward a systemic and integrated approach, leading to the adoption of Directive 2004/54/EC and its national transposition through Legislative Decree No. 264/2006, which established minimum safety requirements for all TEN-T (Trans-European Transport Network) tunnels. This shift introduced the concept of the "tunnel system," where safety results from the interaction between infrastructure design, user behaviour, and operational control systems such as ventilation, lighting, communication, and fire protection. Advances in digital and automation technologies have transformed tunnels from civil works into intelligent infrastructures capable of real-time monitoring and adaptive management. Within this framework, the SCADRA system (Supervisory Control Acquisition and Dynamic Risk Analysis), developed according to the EURAM methodology, has been applied to over 600 Italian tunnels, providing real-time, risk-based safety assessment and marking a significant step toward data-driven, resilient, and sustainable tunnel management. The present paper

illustrates the fundamental principles of the SCADRA system (Supervisory Control Acquisition and Dynamic Risk Analysis), developed and implemented using the EURAM methodology and software [1], which has been applied to assess the safety level of over 600 Italian road tunnel tubes in accordance with Legislative Decree 264/06. The paper discusses the most significant results obtained, evaluates the system's contribution to safety improvement and infrastructure resilience, and outlines future developments for the enhancement of tunnel management, maintenance, and operational sustainability.

2. SMART TUNNEL

Smart Tunnel idea [2] comes from the achievement of Industry 4.0, in which there is a strong industrial automation that integrates the most innovative technologies, in order to improve the operating and safety conditions and increase the equipment productivity and quality. Smart Tunnels allow optimal tunnel management during operation and in emergency situations thanks to the installation of traditional and technological sensors and the real-time assessment of tunnels' safety level, as a function of climatic conditions, traffic data and equipment state, in accordance with the Legislative Decree No. 264/2006. Smart Tunnel together with SCADRA system (Figure 1) allow controlling the systems in the tunnel and improving the effectiveness of the operational and integrative measures increasing the safety of the users and producing also other advantages like energy savings and the improved scheduling of maintenance.

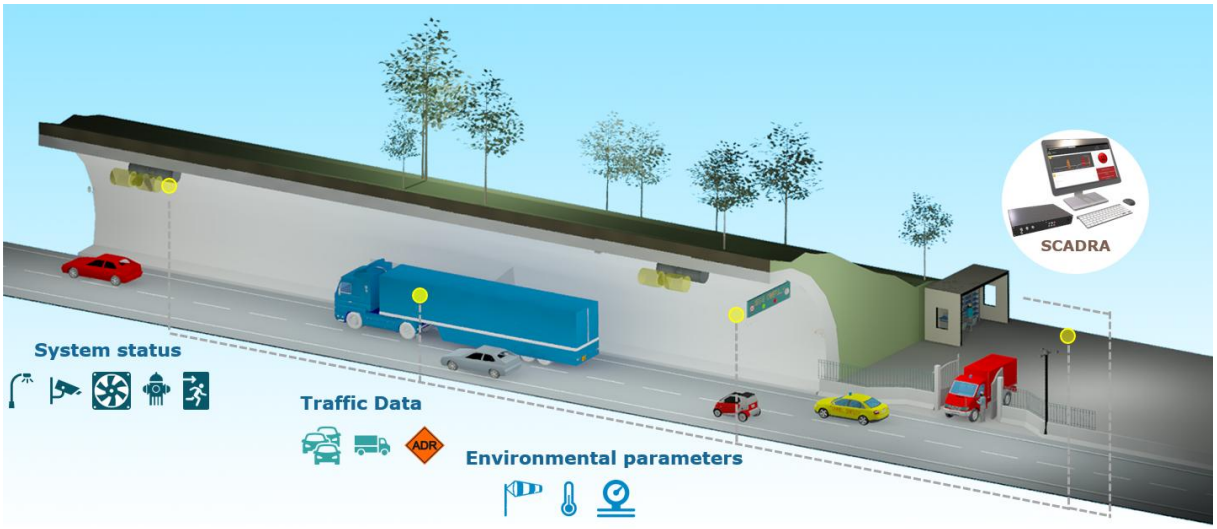


Figure 1: Smart Tunnel with SCADRA

SCADRA system was installed in three Italian road tunnels, executing over 130,000 instantaneous risk analyses in real situations and this report illustrates the main results and the considerations that can be drawn for a correct tunnel management during normal operation and emergency situations (Table 1).

Table 1: SCADRA analyses report

Tunnel	N. of instantaneous risk analyses executed	Analysis duration [h]
TUNNEL 1	8.640	2.160
TUNNEL 2	92.160	23.040
TUNNEL 3*	28.608	7.152

*Data analysed from 15/10/21 to 10/11/22.

3. SMART SYSTEM

SCADRA is a system that continuously monitors the tunnel state by collecting the variables that can influence the tunnel safety conditions (equipment and structures state, traffic data and environmental parameters) and performing a dynamic risk analysis, quantitative and probabilistic, at regular intervals or due to sudden change in the gathered data [2]. If the risk level grows towards the unacceptability threshold or in case of anomalous situations (traffic flows increase, equipment deterioration, etc.), SCADRA activates or signals the necessary safety measures in order to restore the required safety level. Instead, if the risk level is low for a certain amount of time, SCADRA suggests energy saving strategies to perform energy management for the lighting system [3].

SCADRA configuration sets alongside the traditional “Supervisory Control And Data Acquisition” systems (SCADA), a system of acquisition of all the parameters, that can influence the tunnel management (collecting data related not only to systems fault and malfunctions, but also on traffic type and intensity, dangerous goods and vehicles presence, air quality, visibility, wind speed, etc.) in order to get information on safety systems operating status, on environmental conditions and on traffic status within the tunnel, necessary for the subsequent dynamic risk analysis. Through the elaboration and analysis of all parameters, obtained from sensors and system, a continuous safety level monitoring of the tunnel is carried out, performing the Dynamic Risk Analysis at regular pre-established intervals, under normal operating conditions and in emergency case. The equipment installed elaborates an analysis on a series of external input data. These external input data have been divided into 2 macro categories: fixed inputs, related to the tunnel structure, and variable inputs, that may vary over time (weather, vehicular flow and tunnel systems efficiency, etc.). SCADRA subsystem acquires, as dynamic inputs, the input data and the parameters necessary for its processing, directly from the SCADA tunnel. The information provided by the sensors and the historical data recorded are processed by SCADRA through a specific software in order to execute a risk assessment in real-time and to determine if the risk is tolerable or if it is necessary to implement further safety measures. According to the expected level of risk, SCADRA provides a safety management (Figure 2) that can be used for: planning preventive measures, like reducing speed limits, minimum distance among vehicles and prohibition of overtaking for HGV, and executing protective measures, such as sending communications to users, fire brigade alert, interruption of the systems energy saving mode.

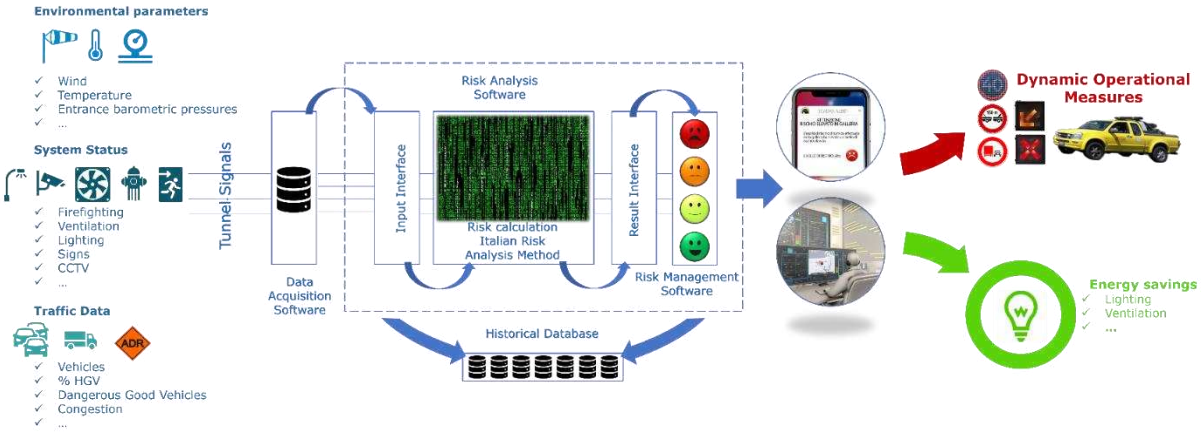


Figure 2: SCADRA system architecture

4. DYNAMIC RISK ANALYSIS (DRA)

SCADRA is based on the Dynamic Risk Analysis (DRA): the data are acquired by technical systems and specific sensors. Afterwards, a processor installed in the server performs the DRA and manages the residual risk (Figure 3).

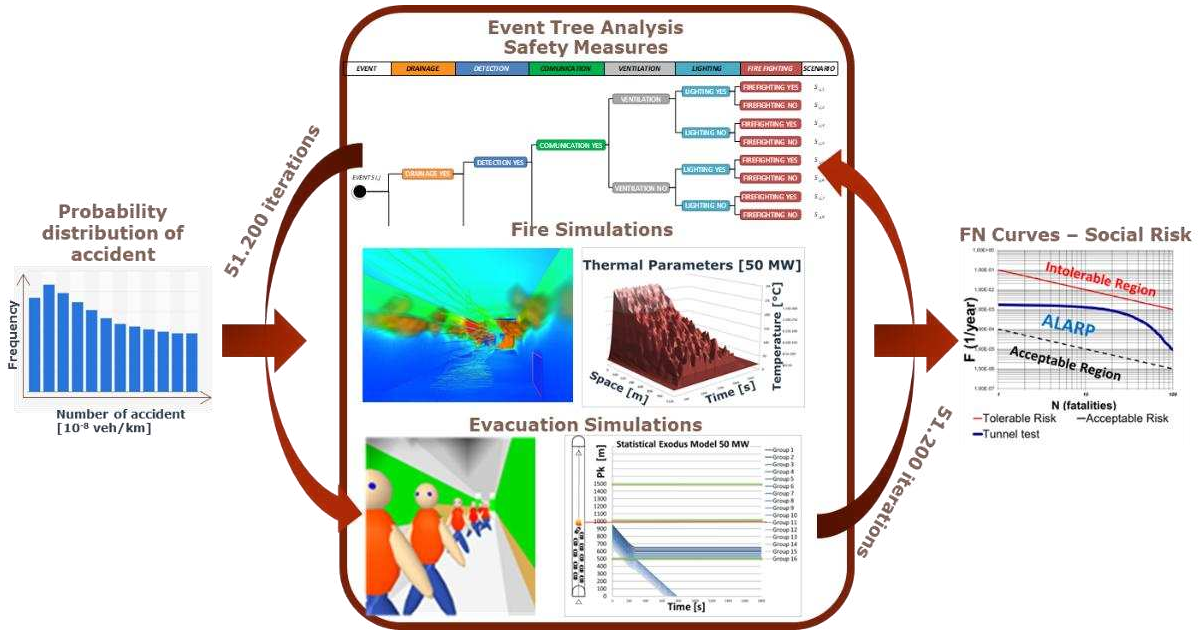


Figure 3: DRA methodology

The DRA results are processed in order to classify the value of the risk according to pre-established levels that allow to undertake the appropriate actions associated with them and envisaged in the risk management plan, and it is normally implemented every 10-15 minutes, during the operation period, and in case of sudden changes of traffic or environmental conditions and operating level of safety systems. The risk value is obtained by executing the quantitative probabilistic analysis, according to the method defined by the Italian Law (Italian Risk Analysis Method - IRAM), and the results are represented by the Live Expected Value of Damage (LEVD) and the F-N Curve, which defines the social risk. The tolerability and

acceptability criteria are settled by evaluating the risk level in real time (LEVD) and by comparing it with the reference value, assessed during the tunnel design and approved by the Administrative Authority. If the real-time risk becomes relevant, SCADRA starts to manage the technical systems and to introduce effective safety operational measures that can reduce it. The risk level has been classified according to 4 categories of instantaneous risk:

- Level 1 – Low Risk: LEVD well below reference values; energy-saving mode enabled;
- Level 2 – Normal Risk: standard operational safety;
- Level 3 – Pre-alert: increased LEVD; preventive measures suggested;
- Level 4 – Alarm: LEVD exceeds acceptable threshold and emergency measures are activated.

The risk levels are represented by a graphical interface, which shows different coloured emoticons according to the real-time risk level. The graphical interface shows the LEVD trend related to the surveys taken in the last 24 hours and it highlights the significant deviations of the input parameters. A browser-based graphical user interface was developed in order to be user-friendly to facilitate the control centre operator in the real-time risk level monitoring and to easily understand the causes behind the risk level increase and to quickly decide on the necessary safety interventions.

5. SCADRA AND ROAD TUNNEL RESILIENCE

Tunnel resilience has been defined, by PIARC Technical Committee 4.4 "Tunnel" [4], as “The ability to prepare and plan, resist / absorb, recover or adapt more successfully (promptly and efficiently) to the actual or potential negative effects of events or developments affecting the use of a tunnel. In this context, an acceptable level of safety is an essential constraint for the availability of the tunnel”. SCADRA system installation perfectly fits within improving road tunnel resilience, since it is always possible to know in real-time (instantaneously or by defining regular intervals to calculate the risk level) what happens inside the tunnel, the environmental conditions, the traffic data and the system status. Therefore, SCADRA allows to monitor continuously the tunnel risk level (Figure 4) and, if needed, to apply operational measures with the purpose of ensuring the required safety.

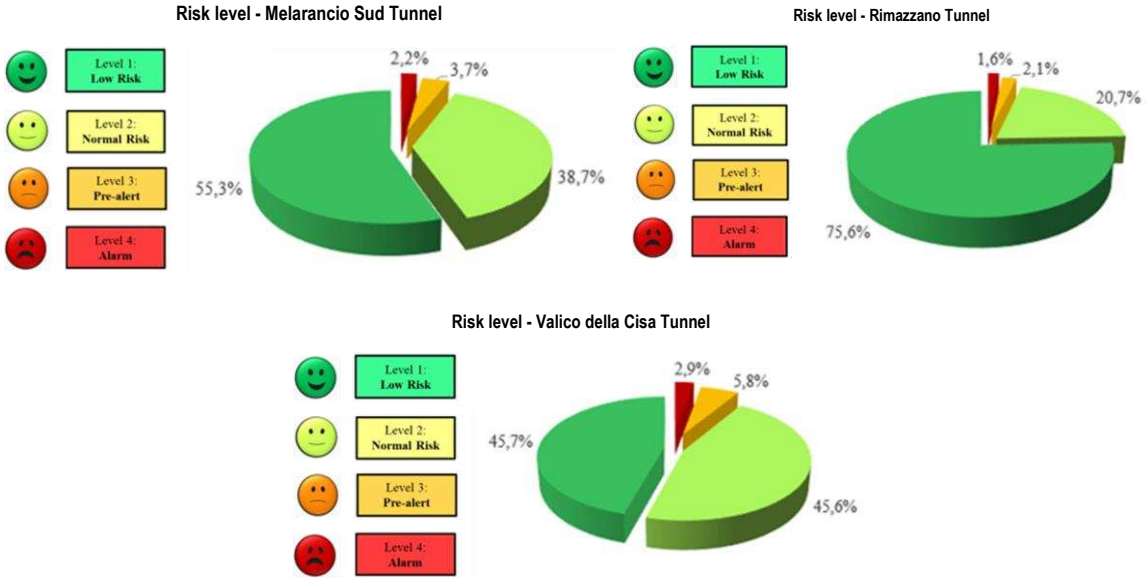


Figure 4: Risk Levels calculated by SCADRA system

Consequently, the system supports the increasing of the road tunnel resilience by preventing and planning safety measure according to every critical situation that might occur. SCADRA system can also represent an effective optimization for the firefighters' management, in order to reduce the instantaneous residual risk in critical conditions, such as congested traffic in a tunnel with longitudinal ventilation. Furthermore, through the continuous acquisition and processing of data, it is also possible to have preventive maintenance focused on user safety, with the aim of reducing interventions, operating costs, intervention times, MTTR (Mean Time To Repair), and system(s) unavailability. Therefore, SCADRA system allows to operate and manage technical systems improving the effectiveness of operational and integrative measures, by enhancing the maintenance design and planning and considering the users' safety.

5.1. Risk Influencing Factors

Risk Level 1 corresponds to optimal safety conditions, where the calculated Expected Value of Damage (EVD) remains significantly below the admissible limit established during the design phase. Under these circumstances, the system may authorise energy-saving strategies without compromising tunnel safety.

Key influencing factors typically associated with Risk Level 1 include:

- Low or moderate traffic flow, particularly during off-peak and night-time hours;
- High availability of safety-critical systems, including ventilation, fire-fighting installations, emergency signalling and communication systems;
- Favourable environmental conditions, such as normal visibility and stable meteorological conditions;
- Absence of critical alarms or operational anomalies in electromechanical and monitoring equipment.

Under Risk Level 1, the system may therefore recommend energy-saving actions by regulating technical systems to function at reduced operational performance compared with normal operation, without any compromise to safety requirements. Activation of this operating mode is permitted exclusively under optimal safety conditions, corresponding to a High Safety Level, thereby guaranteeing that the adoption of energy-saving measures does not produce any increase in risk beyond acceptable thresholds [3].

Risk Level 2 is representative of ordinary operating conditions, with values of risk slightly higher than in Level 1 but still well within the acceptable safety margin.

- Typical contributors to Level 2 behaviour include:
- Increased but still regular traffic volumes, including modest fluctuations in HGV share;
- Minor degradation or temporary unavailability of subsystems, without significant impact on global safety performance;
- Non-severe variations in environmental conditions (e.g., moderate temperature variations, low-intensity precipitation);
- Transient operational adjustments, such as maintenance switching or subsystem testing.

Risk Level 3 corresponds to a pre-alert condition, requiring heightened attention and, where necessary, preventive operational measures to maintain safety.

Observed triggers associated with Level 3 include:

- High traffic flows approaching design capacity, particularly during weekends and holiday peaks;
- Elevated proportion of HGV, generating increased fire load and impacting evacuation/ventilation dynamics;
- Combined minor inefficiencies in multiple systems, which, although individually insignificant, collectively influence the risk level;
- Transient anomalies in ventilation, fire-detection or communication systems;
- Adverse micro-climatic conditions or portal-effect phenomena with higher temperature gradients or smoke-stratification risk.

Risk Level 4 indicates a high-risk condition, requiring immediate operational action to ensure safe tunnel operation. Although rare during the monitoring period, Level 4 scenarios are critical for evaluating the system's responsiveness.

Typical situational drivers observed or simulated for Level 4 include:

- Simultaneous degradation/unavailability of safety systems, such as ventilation combined with emergency communication or fire-fighting system faults;
- Severe operational or environmental anomalies, including forced simulation conditions applied during system validation tests;
- Traffic conditions beyond anticipated thresholds, particularly when combined with system malfunctions or abnormal heavy-vehicle shares;
- Rapid parameter variations, requiring SCADRA to recompute the risk and recommend immediate mitigation measures.

Overall, the results of SCADRA applications clearly demonstrates the capability of SCADRA system to discriminate between different operational safety conditions and to reliably identify the key drivers influencing real-time risk evolution. Across all monitored scenarios - from optimal operating states to high-risk conditions - SCADRA consistently responded to variations in traffic intensity, subsystem availability, and environmental parameters, providing timely and accurate risk-level classification.

The progressive escalation of influencing factors across the four risk levels confirms the importance of adopting an integrated monitoring framework, in which traffic conditions alone are insufficient to characterise tunnel safety. Instead, the results highlight the necessity of evaluating the combined contribution of structural, technological, operational and environmental elements, validating the holistic approach underpinning SCADRA.

These findings reinforce the robustness and operational maturity of the system, demonstrating its effectiveness as a real-time decision-support tool for tunnel risk management. By enabling proactive responses and supporting energy-optimisation strategies under safe conditions, SCADRA represents a substantial advancement in the evolution from static, design-based safety assessment towards dynamic and intelligent tunnel-safety management.

5.2. Risk Consideration: Analysis of LEVD Variations

The monitoring data recorded demonstrate that the calculated risk level increases in conjunction with traffic peaks, particularly during typical weekend travel periods. As shown in Figure 5, this behaviour is highlighted by the red circles marking Easter Monday (18/04/2022) and during the Liberation Day holiday (25/04/2022). On both dates (red circles), the traffic volume reached approximately 60.000 vehicles/day, a value comparable to the tunnel's design traffic assumptions. Under such conditions, the inefficiency of even a single

safety-critical subsystem could temporarily result in a risk level comparable to or exceeding the static design LEVD value.

Nevertheless, even for Average Daily Traffic (ADT) values close to design conditions, the measured risk remained below the design LEVD, as the static risk assessment performed during the design stage already accounts for an admissible margin of subsystem unavailability.

This trend is expected, as a clear correlation exists between traffic flow (approximately 30.000 vehicles/day during the analysed weekends) and the increase in the calculated tunnel risk level. However, the risk level does not depend solely on traffic volume nor follow a strictly linear relationship. LEVD fluctuates as a function of multiple interacting parameters, including:

- Traffic conditions;
- Environmental conditions;
- Availability and performance of safety systems.

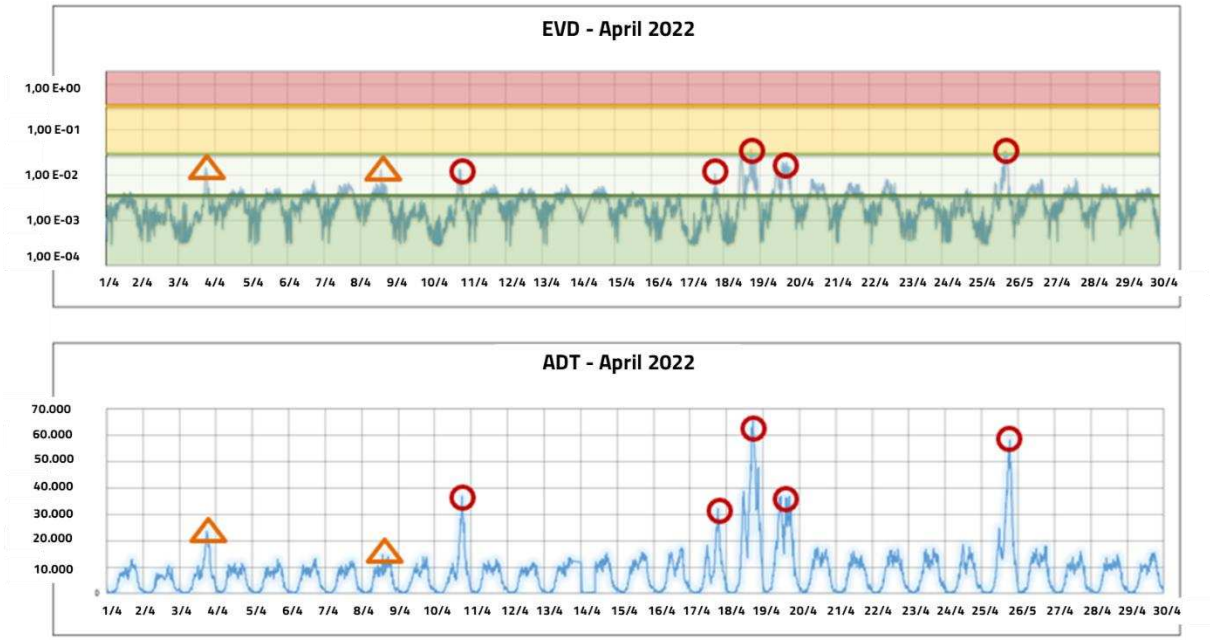


Figure 5: SCADRA system results (April 2022)

Overall, despite traffic variations and forced-input simulations, the calculated risk values consistently remained well below the design LEVD, indicated by the horizontal green reference line in the graph.

The correlation between LEVD and ADT, indicates that while traffic volume influences risk, other factors - such as system availability, environmental stability, and heavy-vehicle percentage - play decisive roles in determining the instantaneous safety level. SCADRA's multi-parametric model allows for a holistic representation of tunnel risk evolution, providing decision-makers with a reliable and actionable framework for dynamic tunnel management.

6. SUMMARY AND CONCLUSION

The analysis of SCADRA installations demonstrates that the system provides a robust, scalable, and adaptive solution for modern tunnel safety management. By integrating continuous data acquisition, probabilistic risk computation, and decision-support functionalities, SCADRA enables a transition from prescriptive design safety to proactive, data-driven governance. Its ability to manage residual risk, detect anomalies, and implement energy-saving measures under safe conditions positions it as a cornerstone technology within the Industry 5.0 framework.

Future developments will focus on extending SCADRA's application to metro and railway tunnels, integrating artificial intelligence for predictive risk modelling, and connecting the system with digital twin platforms for real-time simulation and training. These advancements will further enhance human-centricity, sustainability, and resilience—the three defining pillars of Industry 5.0.

7. REFERENCES

[1] A. Focaracci, "Italian Risk Analysis Method (IRAM)". 11th International Conference Underground Construction, Transport and City Tunnels, Prague 2010, pp. 837-845, 2011

[2] A. Focaracci, "Improving Road Tunnel Resilience by Dynamic Risk Analysis", PIARC 2nd International Conference on Road Tunnel Operations and Safety & VIII Spanish Tunnels Symposium, Granada, Spain, 25-28 October 2022

[3] A. Focaracci, L. Martirano, G. Greco, "Dynamic Risk Analysis and Energy Saving in Tunnels", 2019 IEEE International Conference on Environment and Electrical Engineering and 2019 IEEE Industrial and Commercial Power Systems Europe (EEEIC / I&CPS Europe), Genova, Italy, 11-14 June 2019

[4] PIARC Committee on Tunnels (TC4.4), "Improving Road Tunnel Resilience, Considering Safety and Availability", PIARC Literature Review, 2023

ACCEPTANCE CRITERIA FOR DESIGN OF LONGITUDINAL VENTILATION SYSTEMS IN ROAD TUNNELS: THEORETICAL FRAMEWORK

Matteo Pachera, Ranjit Chaudhary, Jef Van Nerom, Stefaan Vernieuwe

Sweco, BE

DOI 10.3217/978-3-99161-087-8-022 (CC BY-SA 4.0)
https://creativecommons.org/licenses/by/4.0/deed.de
This CC license does not apply to third party material (attributed to other sources) and content noted otherwise.

ABSTRACT

This paper investigates the relationship between fire risk and tunnel ventilation and its integration into the ventilation design process. Longitudinal ventilation is commonly applied in road tunnels with unidirectional traffic, as it confines smoke downstream of the fire and protects road users upstream of the incident. The risk of fatalities among road users in case of fire is primarily associated with the potential smoke propagation and exposure of road users. In addition, elevated temperatures during tunnel fires may cause damage to structural and electro-mechanical components, resulting in economic losses.

Both life safety and economic risks are related to the installed ventilation capacity and to air velocity in the tunnel for different fire sizes, fire locations and wind conditions. Two formulations are derived to quantify the equivalent risk indicators for road users and for the structural damage. These indicators are expressed as functions of tunnel geometry, traffic intensity, and traffic composition, enabling specific risk evaluation for each tunnel.

The proposed indicators are then applied to a case study in which the same tunnel is analysed under different traffic conditions. The results show that the tunnel ventilation design should not be based solely on critical velocity evaluation; but it should also consider other factors such as traffic conditions and tunnel connectivity. A comprehensive design should address both the risk associated with road user safety and with the business continuity in the event of a fire.

Keywords: Tunnel ventilation, risk, life safety, business continuity.

1. INTRODUCTION

Tunnel ventilation has been widely investigated as a safety measure to protect road users. Historically, ventilation was required to maintain acceptable air quality levels within tunnels [1]. However, as vehicle emissions progressively decreased, this problem became less severe. Conversely, catastrophic fires that occurred in tunnels have revealed new risks to road users and the infrastructure [2]. Mechanical longitudinal ventilation is typically required above a certain length and/or traffic intensity in road tunnels. However, its design is independent of the traffic conditions and the tunnel's functional role within the road network [3]. A longitudinal ventilation system is a widely adopted solution for unidirectional tunnels because it allows smoke to be confined downstream of the fire and protects road users [4]. In recent years, research has primarily focused on the calculation of the required velocity to confine or limit smoke spreading upstream of the fire [5][6][7]. This paper proposes a risk-based

framework for the design of the ventilation system that integrates the road-user safety and structural integrity risks in the design process.

2. ACCEPTABILITY CRITERION BASED ON LIFE SAFETY

The risk of fatalities due to fires in tunnels is commonly investigated with quantitative risk analyses [8]. However, these are often uncoupled from the design of the life safety systems. A longitudinal ventilation system is often installed in unidirectional tunnels because of its effectiveness and lower cost when compared to other solutions [12]. A longitudinal ventilation system confines smoke downstream of the fire, keeping a tenable environment upstream where road users may be trapped assuming no traffic congestion, **Figure 1**. The longitudinal velocity which confines the smoke downstream of the fire is referred to as critical velocity.

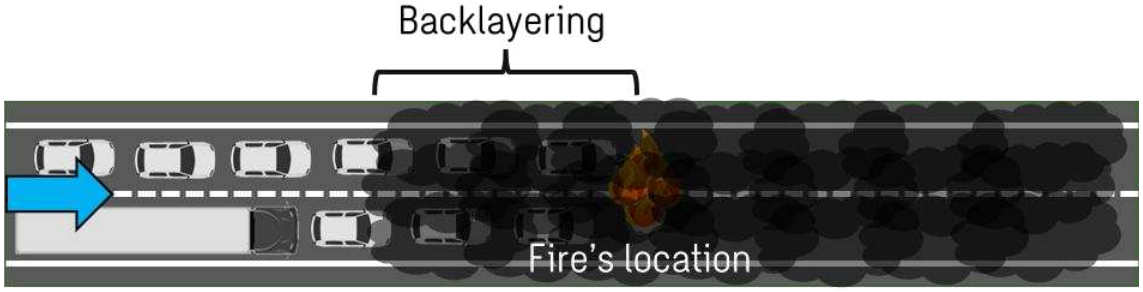


Figure 1: Schematic view of the ventilation conditions.

In several countries, the ventilation system is designed to guarantee that the longitudinal velocity in the tunnel exceeds the critical velocity in 95% of scenarios [10][11][12]. This residual risk accounts for unfavourable wind conditions or fire locations when the velocity does not meet the required criterion.

Nevertheless, applying a fixed acceptance criterion for the longitudinal ventilation design in tunnels with different traffic conditions results in different safety levels in case of fires. Tunnels with high traffic volumes and large fractions of heavy good vehicles (HGV) have higher frequencies of larger fires than tunnels with low traffic intensities and a higher fraction of passenger cars. Therefore, a fixed acceptance criterion might under-protect tunnels with higher fire risks while it overprotects tunnels with lower fire risks.

To address this limitation, the ventilation system should be designed to guarantee a consistent risk level for road users in case of fire among different tunnels. The risk per unit of length for road users R_f [n_f/year/km]. can be used as a design criterion. This is calculated as the sum of different risks that combine the consequences and the frequencies of different fire scenarios (S) as in the equation below:

$$R_f = \sum_S F_f \, N_f < R_{lim,f} \tag{1}$$

where F_f is the frequency of fire scenarios per unit of length [1/year/km] and N_f is the number of fatalities associated with them [n_f]. The scenarios (S) represent the different events that can occur in the tunnel as combinations of fire size, fire location, wind conditions. The risk R_f should be limited to an acceptable level $R_{lim,f}$ [n_f/year/km]. The limit risk can be represented as societal risk which is a function of number of fatalities and frequency or as individual risk which can be treated as a constant [13]. For the sake of simplicity in this first study, individual

risk is used, but conclusions are still valid with societal risk. The frequency of fires per unit of length F_f [1/year/km] is calculated in the equation below:

$$F_f = \sum_S f_S \, I_S = f \; C \; S \; N_{lanes} \sum_S X_S \tag{2}$$

The frequency of fire for a specific type of vehicle associated to the scenario S is the product of the number of vehicles driving through the tunnel I_S [veh/year] times the frequency of fires per driven kilometre f_S [1/veh/km]. The fire frequency is assumed to be constant for different types of vehicles in first instance (f) [1] so the equation can be rewritten as function of the traffic composition X_S [-], the number of lanes in the tunnel N_{lanes} [-], the lane's capacity C [veh/year] and the traffic saturation factor S [-].

The number of fatalities for a specific fire scenario is proportional to the number of road users exposed to untenable conditions in the specific scenario. Assuming the longitudinal ventilation system blows smoke downstream of the fire and road users are only blocked upstream of the fire, fatalities can occur when extensive backlayering takes place. The number of fatalities is calculated in the equation below:

$$N = D_{\mathrm{Occ}} N_{\mathrm{lanes}} \min(BL_s, x_{\mathrm{fire}}) \tag{3}$$

For a specific scenario, the number of fatalities can be estimated as first approximation as the product of the number of lanes N_{lanes} (that represents the number of rows of vehicles impacted) times the backlayering length BL [m], times the occupants' density D_{Occ} [pers/m]. In this study, BL is computed as a function of longitudinal velocity and tunnel geometry following reference [5]. Near the entry portal the backlayering can exceed the distance between the fire and the portal itself. In this case the affected zone is the minimum between the position of the fire measured from the entry portal and the backlayering length. The total risk obtained combining the equations above is written below:

$$R = f \; C \; S \; D_{\mathrm{Occ}} \; N_{lanes}^2 \sum_S \min\left(BL_s, x_{fire}\right) X_S \tag{4}$$

In the equation above, the fire frequency per kilometre, the lane's capacity and the occupant density are assumed to be constant values. The saturation factor, the number of lanes and the fractions of vehicle types are specific to the tunnel. The backlayering length is a function of the fire scenario, the ventilation system, the tunnel geometry, and the wind conditions. A simplified risk index R_{eq} [m] is derived from the equation above:

$$R_{eq,f} = \frac{R_{lim,f}}{f \; C \; D_{\mathrm{Occ}}} = \; S \; N_{lanes}^2 \sum_S \min\left(BL_s, x_{fire}\right) X_S \tag{5}$$

From the formulation above the following conclusions can drawn:

- The risk can be computed for the whole tunnel as an average risk over the length or locally for each fire location.
- The ventilation system has a direct impact on the backlayering length, the stronger the ventilation regime the lower the backlayering length and the equivalent risk.
- The traffic composition has a direct impact on the risk because a larger share of HGV (high Heat Release Rate (HRR)) increases the risk of larger fires while a larger share of light vehicles (low HRR) reduces this risk.

- The risk is proportional to the traffic intensity, the risk is linear in the saturation factor which ranges between 0 and 1 and quadratically proportional to the number of lanes. A larger number of lanes means that more road users are exposed to smoke and that the tunnel has more traffic.
- The risk is not a function of the tunnel's length because the risk is calculated per running km. Nevertheless, in short tunnels the risk is limited by the proximity of the fire to the entry portal.
- Fire locations close to the entry portal are less critical for the risk profile of the tunnel because the fire exposes less road users. Fire scenarios near the entry portal can be critical for the ventilation design of sunken tunnel which have large slopes near the portals.

On the other hand, this approach also requires simplifications to be applicable in a design process:

- The presence of emergency doors along the tunnel or means to stop the traffic outside the tunnel are not considered in the proposed formulation.
- At very low traffic intensities the model can overestimate the risk because it computes the backlayering length, however, the tunnel might be still empty because there are no vehicles in the tunnel or entering the tunnel.
- The calculation of the risk is a function of the traffic intensity and composition which can vary over time while the design should be valid for few decades. This requires foreseeing variations in traffic intensity and composition over a large span of time.
- The backlayering length provides a simple formula to correlate the longitudinal speed in the tunnel with the estimated number of fatalities. However, this can be overly conservative, because if the smoke layer does not remain high above road users it does not pose a direct threat to them. A more accurate estimate would require extensive CFD analyses that are specific for a specific tunnel geometry, and this is impractical for the purpose of the tunnel ventilation design. In this paper the formulation proposed by Ingason [5] is used to calculate the backlayering length as function of the tunnel's geometry and the longitudinal velocity.
- The reliability and availability of the ventilation system is not accounted in the current formulation. All the jet fans are assumed to work correctly if the temperature remains within the operating range.
- The acceptable risk is not discussed and investigated in this paper because other stakeholders should be involved in the discussion as well. It is also not decided whether the maximum risk along the tunnel or the average risk should be used as design criterion.
-

3. ACCEPTABILITY CRITERION BASED ON BUSINESS CONTINUITY

When designing ventilation systems for tunnels, it is also crucial to consider the consequences of the tunnel closure after a fire. The tunnel closure causes direct costs due to the required refurbishment and indirect costs due to increased travel time and possible lost income [17]. The economic risk associated with tunnel closure can be used as design criterion to effectively protect the tunnel as an infrastructure in the road network. The acceptable economic risk R_b [€/year] should be limited to an acceptable value ($R_{lim,b}$) [€/year].

$$R_b = \sum_S F_b \, N_b < R_{lim,b} \tag{6}$$

where F_b is the frequency of fire in the whole tunnel [1/ year] and N_b are the consequences [€]. In Eq (2), the frequency of fire F_f is normalized per unit length, while Eq. (7) calculates the total frequency of fire for a specific tunnel considering its length.

$$F_b = L \sum_S f_S \, I_S = Lf \; C \; S \; N_{lanes} \sum_S X_S \tag{7}$$

Where L is the length of the tunnel [m]. The consequences (N_b) in this case are not fatalities, but economic losses and are calculated as the product of the length of the damaged zone requiring repair (D_s) [m] and the economic loss associated with damage of the tunnel per unit length [€/m]. In Eq (8), the direct and indirect cost are both proportional to the length of fire damage in the tunnel. Direct costs are the cost of repair of both the structure and the equipment of the tunnel. The direct costs are generally much lower in magnitude than the indirect costs [18][19] and therefore have been ignored in the current study for simplification. Considering that the tunnel needs to be closed during the repair process, the indirect costs can be linked to the amount of traffic (I) that must be redirected, the time loss per road user (Δt_l) [h] associated with the tunnel's closure during repair.

$$N_b = \sum_S D_S \, I\Delta t = \Delta t \; C \; S \; N_{lanes} \sum_S D_S \tag{8}$$

When combining Eq (7) and Eq (8), the risk for loss of business continuity can be evaluated as follows:

$$R_b = Lf \; C^2 \; S^2 \; N_{lanes}^2 \Delta t \sum_S X_S D_S \tag{9}$$

In the equation above, the fire frequency per unit length (f) and the lane's capacity can be assumed constant. The length of the tunnel, the saturation factor, the number of lanes and the traffic composition are specific to the tunnel, while the length of the damage zone is function of the smoke temperature. A stronger longitudinal flow can enhance the cooling effect on the smoke and limit the damages associated with elevated temperature in the tunnel. Considering these aspects, a simplified risk index $R_{eq,b}$ [m²/h] is obtained as:

$$R_{eq,b} = \frac{R_{\mathrm{lim,b}}}{C^2 f} = L \; S^2 \; N_{lanes}^2 \Delta t \sum_S X_S D_S \tag{10}$$

Similar conclusions from the formulation for life safety can be drawn also for structural safety but with some differences:

- The impact of tunnel length appears explicitly in the risk formulation because a fire at any point of the tunnel can force closure of the entire infrastructure.
- Risk is quadratically proportional to the traffic intensity, since traffic affects both fire frequency and the number of road users who must be rerouted when the tunnel is closed.
- Network robustness is accounted for via the difference in travel times with and without the tunnel. Isolated tunnels with few alternatives have higher rerouting times — and thus higher risk — than urban tunnels with multiple alternative routes.
- Ventilation affects the extent of damage: higher longitudinal flow can cool smoke, reducing the zone exposed to damaging temperatures.

The proposed approach also requires assumptions and simplifications:

- The damaged length is estimated from average tunnel temperature. This may be inaccurate near the fire source, where a one-dimensional model underestimates peak temperatures; the choice of critical temperature for damage requires further study.
- The impact of fire fighters' operations trying to suppress the fire or the impact of active fire protection are not considered.
- Other dagames (e.g. explosions) are not accounted for in the current study but should be considered in tunnel design decisions if relevant.

4. APPLICATION OF THE PROPOSED CONCEPT TO A SAMPLE TUNNEL

The proposed approach to tunnel ventilation design is applied to a sample tunnel. The tunnel is 600 m long, 11 m wide and 6 m high with two traffic lanes. The tunnel is flat and has no longitudinal grade. The tunnel is equipped with jet fans at the entry portal and each fan has a nominal thrust of 1000 N. Different ventilation configurations are investigated for this exercise by varying the number of jet fans: 2, 4, 6 and 8.

Three different fire scenarios are evaluated: a car fire with an HRR of 10 MW, a bus or small truck fire with a HRR of 30 MW, and a HGV fire with a HRR of 200 MW [12][7][20].

The tunnel is simulated with a one-dimensional tunnel ventilation model considering the different fire sizes, fire locations, wind speeds and directions. A total of 3,180 simulations were performed to cover the combinations of variables for each jet-fan configuration. The model provides distributions for the different scenarios of the temperature, velocity and backlayering length inside the tunnel.

The critical velocity and the backlayering lengths are calculated for the different fire sizes with the formulation proposed in [7]. The critical velocity is close in all scenarios when referred to the gross tunnel area because of the different obstruction factors created by the vehicles. The critical velocity referred to the net area is presented for the sake of completeness, but it is not used.

Table 1: Critical velocity for the different fire scenarios.

Fire scenario	Obstruction area	Critical velocity (gross area)	Critical velocity (net area)
10 MW	3 m²	2.77 m/s	2.90 m/s
30 MW	10 m²	2.80 m/s	3.30 m/s
200 MW	10 m²	2.80 m/s	3.30 m/s

4.1. Car fire scenario 10 MW

The median longitudinal speed, Figure 2, and the median backlayering length, Figure 3, are calculated for different wind conditions and are presented as a function of the fire location for the fire scenario of a burning car 10 MW

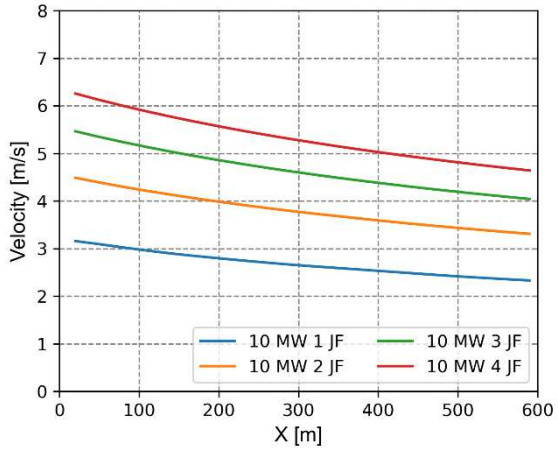


Figure 2: Longitudinal velocity as function of the fire location (scenario Car fire 10 MW)

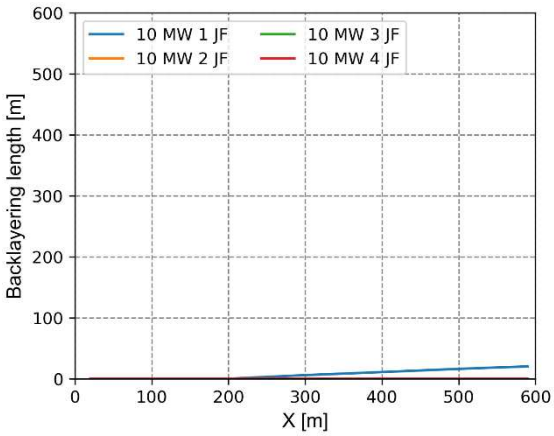


Figure 3: Backlayering length as function of the fire location (scenario Car fire 10 MW)

The cumulative distributions of the longitudinal velocity considering for ventilation configurations are presented in Figure 4. The length of the tunnel where the average temperature exceeds 400 °C is considered damaged and is shown for different ventilation configurations in Figure 5. The damaged length is negligible in this case due to the limited temperature rise induced by the fire.

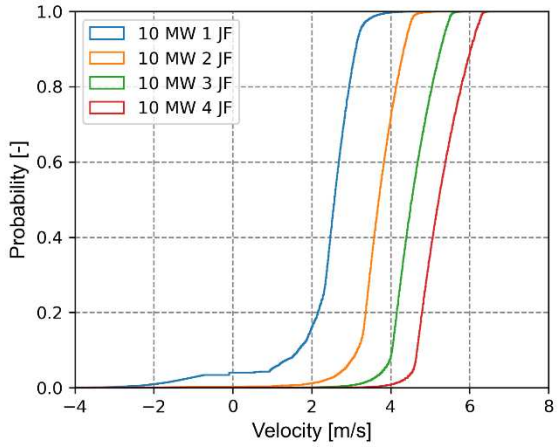


Figure 4: Distribution of the longitudinal velocity for a car fire.

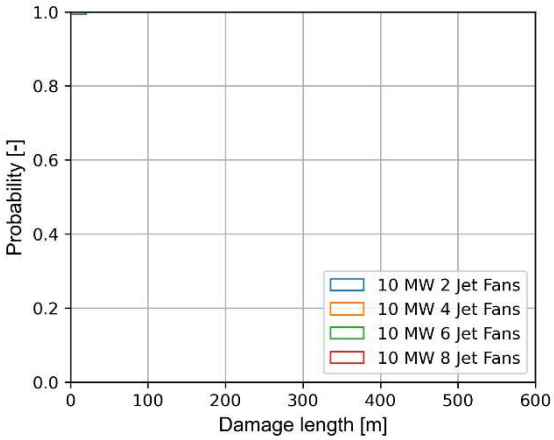


Figure 5: Distribution of the damaged length for a car fire.

4.2. Bus fire scenario 30 MW

The median longitudinal speed, Figure 6, and the median backlayering length, Figure 7, are presented for the fire scenario of a burning bus or small truck 30 MW.

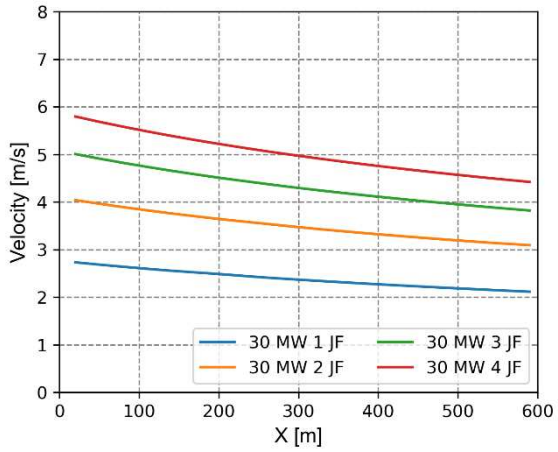


Figure 6: Longitudinal velocity as function of the fire location (scenario Bus fire 30 MW)

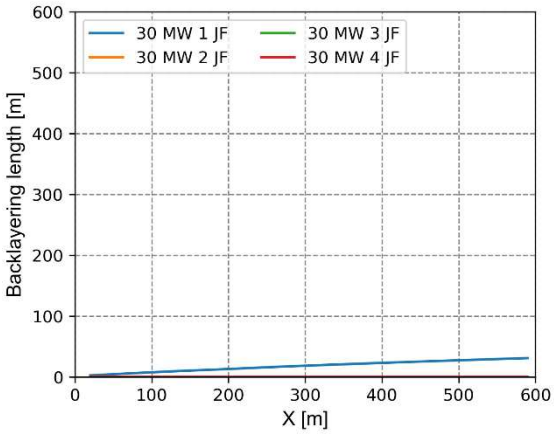


Figure 7: Backlayering length as function of the fire location (scenario Bus fire 30 MW)

The cumulative distributions of the longitudinal velocity as a function of the different ventilation configurations are presented in Figure 8. Again, the length of the damaged zone of the tunnel where the average temperature exceeds 400 °C is negligible for different ventilation configurations, see Figure 9.

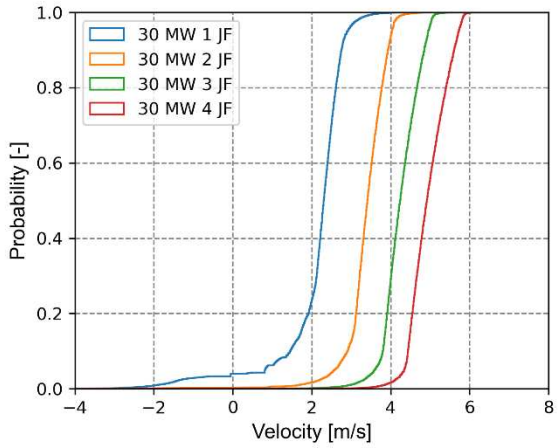


Figure 8: Distribution of the longitudinal velocity for a bus or small truck fire.

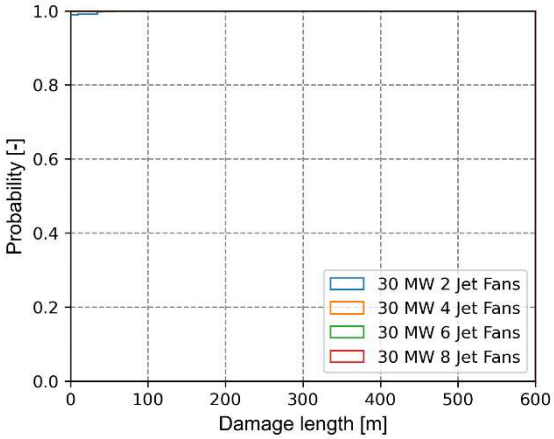


Figure 9: Distribution of the damaged length for a bus or small truck fire.

4.3. HGV fire scenario 200 MW

The median longitudinal speed, Figure 10, and the median backlayering length, Figure 11, are presented for the fire scenario of a burning HGV 200 MW.

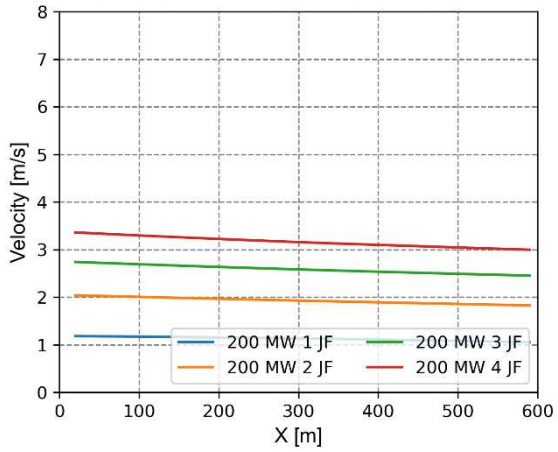


Figure 10: Longitudinal velocity as function of the fire location (scenario HGV fire 200 MW)

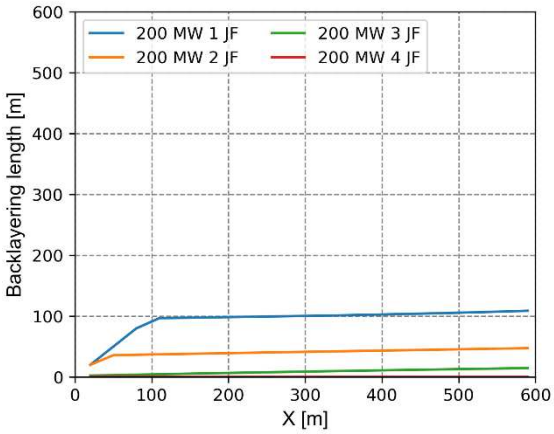


Figure 11: Backlayering length as function of the fire location (scenario HGV fire 200 MW)

The cumulative distributions of the longitudinal velocity as a function of the different ventilation configurations are presented in Figure 12. In Figure 13, as expected, the damaged length of the tunnel with average temperature higher than 400 °C is considerably higher than the previous two fire scenarios with lower fire load.

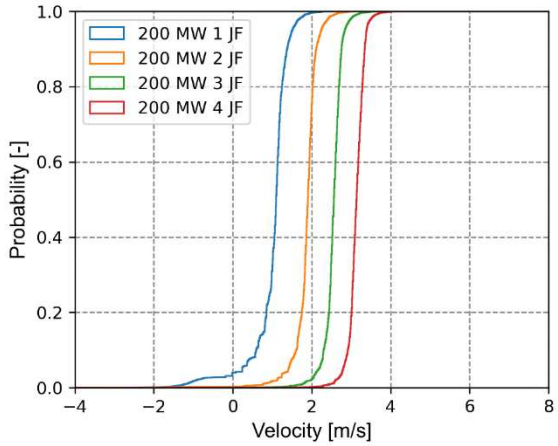


Figure 12: Longitudinal velocity distribution for an HGV fire

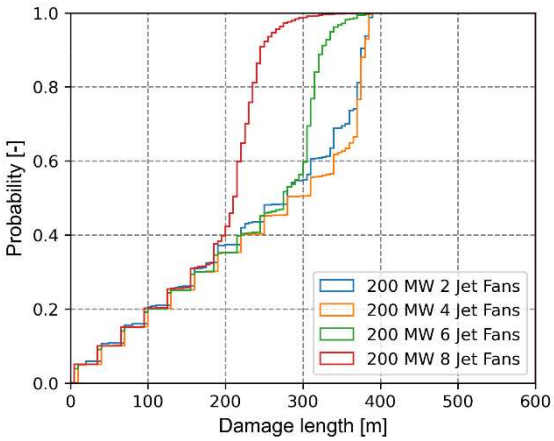


Figure 13: Distribution of the damaged length of the tunnel of an HGV fire.

4.4. Risk evaluation

The results discussed above present the longitudinal velocity, the backlayering length, and the damaged length for the different fire sizes and ventilation configurations. As fire size increases, longitudinal velocity decreases because the fire induces greater resistance, and backlayering increases accordingly. The damage to the tunnel due to elevated temperatures is negligible for the car- and bus-fire scenarios but becomes clearly visible for the HGV fire scenario. Typically, increasing the number of ventilators reduces the damaged length because ventilation cools the smoke in the tunnel.

Given the results of the analyses discussed above, the risk for road users and for the structure can be calculated considering different traffic conditions in the tunnel. Four hypothetical cases are considered for the study, and they are summarized in Table 2. In the first three cases the traffic intensity and the traffic composition are varied while the number of lanes is fixed to two. In the last case, the number of lanes is reduced to one to show the impact of the number of lanes on the risk.

Table 2: Input parameters of the four different test cases

	Case 1	Case 2	Case 3	Case 4
Saturation	0.3	0.5	0.8	0.5
Cars %	0.90	0.50	0.50	0.50
Bus %	0.05	0.20	0.20	0.20
HGV %	0.05	0.30	0.30	0.30
N_{lanes}	2	2	2	1

The equivalent risk for road users is summarized in Table 3 as a function of the number of jet fans installed in the tunnel. Both the maximum risk and the average risk indicators for life safety are presented for all the considered cases.

Table 3: Summary of the maximum and average risk indicator [m] for road users along the tunnel.

	Case 1		Case 2		Case 3		Case 4	
	Max	Mean	Max	Mean	Max	Mean	Max	Mean
2 jet fans	65.6	38.0	150.1	106.8	240.2	170.8	37.5	26.7
4 jet fans	7.0	4.9	36.0	29.9	57.6	47.8	9.0	7.5
6 jet fans	1.4	0.9	10.4	7.0	16.7	11.2	2.6	1.8
8 jet fans	0.14	0.08	0.55	0.36	0.87	0.57	0.14	0.09

The results for the considered cases are presented in Figure 14, Figure 15, Figure 16 and Figure 17. The risk profile is strongly affected by the percentage of vehicles in the tunnel because this affects the chance of an accident and the number of exposed users. There is a clear impact from the traffic composition, larger volumes of HGV can be associated to higher risks because of the higher frequency of large accidents. The number of lanes has a strong impact on the results because it affects both the fire frequency and the exposed number of road users. Therefore, ventilation-system design should not rely solely on critical-velocity criteria; design must also account for traffic sturation, HGV share, and lane count.

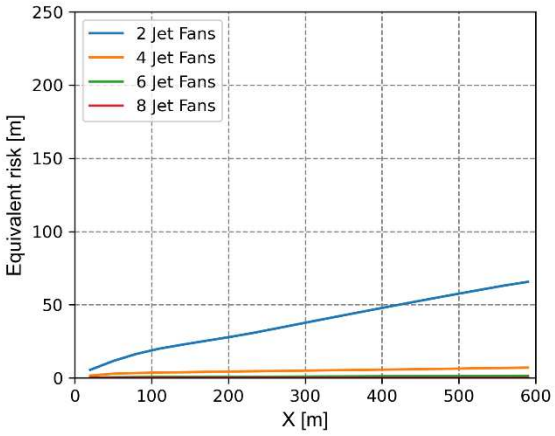


Figure 14: Risk profile for road users, Case 1.

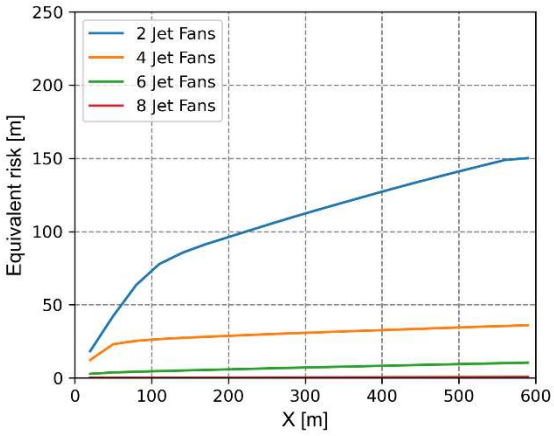


Figure 15: Risk profile for road users, Case 2.

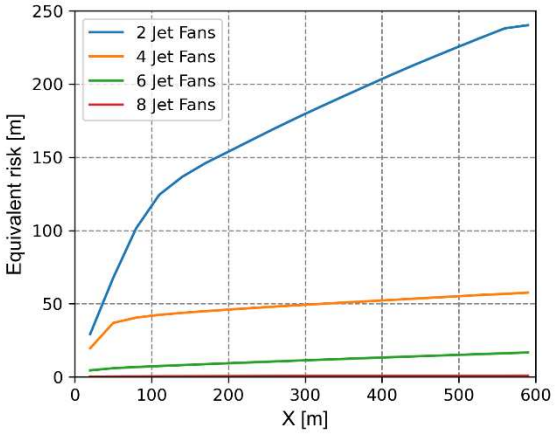


Figure 16: Risk profile for road users, Case 3.

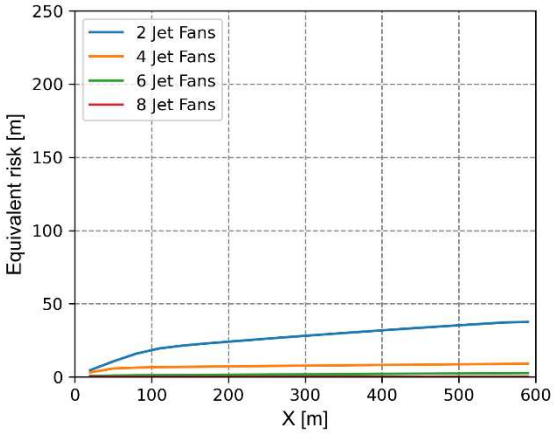


Figure 17: Risk profile for road users, Case 4.

The equivalent risk for the structure is calculated assuming that the rerouting due to the tunnel closure is 30 min (0.5 h). The equivalent risk for the structure is summarized in Table **4** as function of the number of jet fans installed in the tunnel. Both the maximum risk and the average risk for structural damage indicators are presented for the different cases.

Table 4: Summary of the maximum and average risk indicator [m²/h] for the structure along the tunnel.

	Case 1		Case 2		Case 3		Case 4	
	Max	Mean	Max	Mean	Max	Mean	Max	Mean
2 jet fans	1916	1345	31645	22206	81010	56848	7911	5552
4 jet fans	2027	1375	33780	22916	86477	58666	8445	5729
6 jet fans	1737	1238	28955	20646	74124	52855	7239	5162
8 jet fans	1319	989	21988	16484	56289	42200	5497	4121

The results are presented in **Figure 18**, **Figure 19**, **Figure 20** and **Figure 21**. Given the limited damage associated to the smaller fires (10 MW and 30 MW) the risk is directly proportional to the share of HGV in the tunnel. The risk is also quadratically proportional to the total traffic intensity (saturation factor times number of lanes), and this is visible comparing cases 1, 2 and 3. The figures highlight how the ventilation has a positive effect on cooling the smoke and limiting the damage caused by the fire. In the zone of the tunnel near the exit portal the damage is mostly limited by the length of the tunnel itself. The area affected by elevated temperature

cannot be longer than the distance between the fire and the exit portal. The equivalent risk level with 2 jet fans is lower than that with 4 jet fans because the configuration with 2 jet fans often has negative longitudinal flows induced by wind. This naturally limits the temperature inside the tunnel and the extent of the damage. Overall, these results demonstrate that traffic intensity, tunnel length, and lane count materially influence business-continuity risk and must be included in ventilation design decisions.

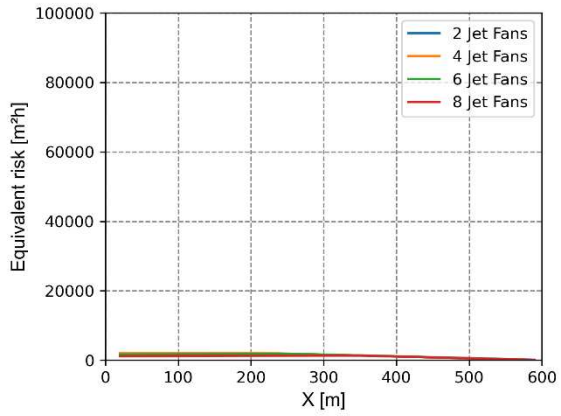


Figure 18: Risk profile for the structure, Case 1.

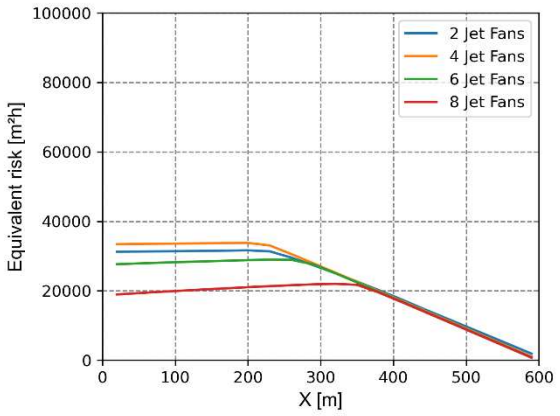


Figure 19: Risk profile for the structure, Case 2.

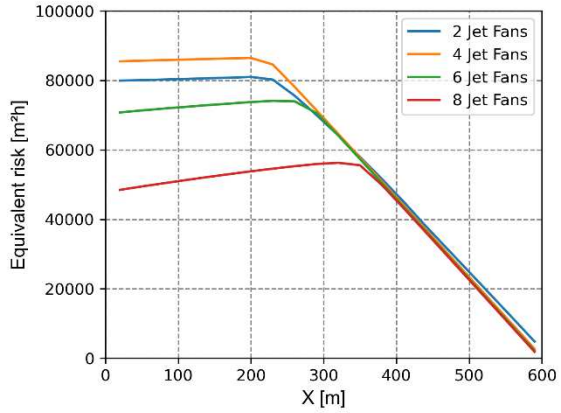


Figure 20: Risk profile for the structure, Case 3.

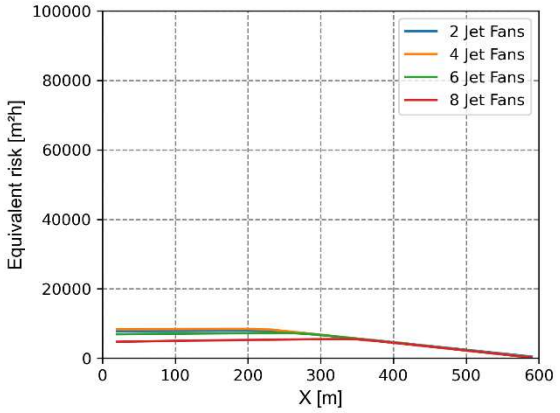


Figure 21: Risk profile for the structure, Case 4.

5. CONCLUSIONS

This paper proposes a risk-based framework for the design of longitudinal ventilation systems in road tunnels. Equivalent risk indicators are developed to address the risk to road users and the risk associated with the economic consequences resulting from tunnel fires. These indicators enable ventilation design to be driven by a target risk level, providing a uniform safety level across tunnels. The risk indicators are linked to tunnel geometry, traffic intensity, and traffic composition.

Tunnel ventilation can reduce backlayering and thus the number of road users exposed to smoke during a fire. The life-safety risk for road users can be related to backlayering length, and it also depends on traffic composition, traffic intensity and number of lanes, because these parameters affect fire frequency and the number of exposed users. Higher traffic intensities and larger shares of HGV increase the frequency of severe fires and therefore raise the overall risk.

For large fires, ventilation can also reduce smoke temperature and mitigate thermal damage inside the tunnel. The economic-loss risk is related to the damaged length, and is also influenced by tunnel geometry, traffic intensity and composition, and the rerouting time following tunnel closure, since these parameters affect both the frequency and the economic impact of fires. High traffic intensity and larger heavy-vehicle shares increase the likelihood of severe fires and the number of vehicles that must be rerouted, increasing economic risk.

Setting fixed acceptance criteria for backlayering length or longitudinal velocity simplifies ventilation design but can be inappropriate because it ignores differences in frequency and consequences of fires in different tunnels. Starting from a common acceptable risk level across tunnels, it is possible to derive tunnel-specific design criteria that reflect each tunnel's traffic, geometry, and exposure.

In practice, this means tunnels with high traffic intensity and large shares of HGV would receive greater protection through a better performing ventilation system, while tunnels with lower risk would receive proportionally less. This enables more efficient allocation of resources across the network. This paper aims to provide a conceptual basis for further development and practical implementation. The following topics should be investigated in future work:

- Stakeholder-based definition of acceptance criteria: analysis of acceptable thresholds for fatalities and economic damage, involving civil society, road authorities, emergency services and other stakeholders to define socially and politically acceptable risk levels.
- Expanded fire-scenario analysis: study of a broader set of fire sizes, locations, and vehicle types; compare the effect of different national/design fire recommendations on ventilation design.
- Validation and refinement of damage and backlayering correlations: further investigation of temperature thresholds that cause damage to electro-mechanical equipment and structural elements, and improved quantification of repair time and downtime.
- Tenability and occupant behaviour under blocked conditions: improved backlayering calculations that include tenability criteria (toxic and thermal exposure) and consider how blocked traffic and human behaviour influence exposure and evacuation outcomes.
- Uncertainty and sensitivity analysis: quantify uncertainty in input parameters (traffic projections, fire frequency, rerouting time, damage cost) and perform sensitivity studies to investigate the most important drivers of risk.

6. REFERENCES

[1] Piarc Technical Committee 5 "Road Tunnels: Emissions, Environment, Ventilation", World Road Association (PIARC), 1996.

[2] Beard, A., Carvel, R., "Handbook of Tunnel Fire Safety, 2nd Edition, Part I: Real Tunnel Fires", ICE Publishing, 2012.

[3] Frey, S., Riklin, N., Brandt R., Heger, O., Kohl B., "Modelling of tunnel ventilation's influence on fire risk – a detailed comparison of model assumptions and their potential influence" ISAVFT, 2019.

[4] Piarc Technical Committee 5: "Fire and Smoke Control in Road Tunnels" PIARC 1996

[5] Li Y., Z., Ingason H., “Study of critical velocity and backlayering length in longitudinally ventilated tunnel fires.” Fire Saf Journal 45:361–370, 2010.

[6] Stacey, C., Beyer, M. “On Li, Lei & Ingason’s Critical Velocity Data Treatment and Their Clarification.” *Fire Technology* (2025)

[7] NFPA 502, “Standard for Road Tunnels, Bridges, and Other Limited Access Highways,” The National Fire Protection Association, US, 2026

[8] RWS Steunpunt Tunnelveiligheid, “Achtergronddocument QRA-tunnels 2.0”, Rijkswaterstaat, 2012.

[9] FSV (Austrian Association for Research on Road, Rail and Transport) Guideline RVS 09.03.11 – Methodology of Tunnel Risk Analysis Vienna 2015

[10] Cuypers, H., Peerlink, J., “Vlaamse Tunnelrichtlijn: C301 Tunnelventilatie” Agentschap Wegen en Verkeer, Brussel (2023)

[11] CETU, “Dossier pilote des tunnels équipements Ventilation”, Ministère de l’Équipement, des Transports, du Logement, du Tourisme et de la Mer direction des routes, 200

[12] Huijben, J. W., P. Fournier, and B. P. Rigter. “Aanbevelingen ventilatie van verkeerstunnels.” Rijkswaterstaat, Utrecht 2006.

[13] Piarc Technical Committee 4 “Risk evaluation, current practice for risk evaluation for road tunnels”, World Road Association (PIARC), 2013.

[14] Rattei, G., Lentz, A., Kohl, B., “How frequent are fires in tunnels - analysis from Austrian tunnel incident statistics” 7thInternational Conference ‘Tunnel Safety and Ventilation’ 2014, Graz

[15] CETU: “Breakdowns, accidents and fires in road tunnels” Ministère de l’Équipement, des Transports, du Logement, du Tourisme et de la Mer direction des routes, 2022

[16] Agentschap Wegen en Verkeer, “Vademecum weginfrastructuur (VWI) deel Europese hoofdwegen” AWV, 2023

[17] Pachera, M., “Economic risk as an additional metric for tunnel’s design” Seminar Young Engineers @Work, Zaventum (2024).

[18] Leucker, R., Stieglitz, C. V., and Gielnik, B., “Economic feasibility study for the use of fire protection boards in road tunnels.” World Tunnel Congress (2022).

[19] Schepers, M., Deckers, X., Jovanović. B., Chaudhary, R.K., Van Coile, R., “FIERCE: a cost benefit analysis for tunnel fire safety.” In11th Tunnel Safety and Ventilation 2022.

[20] Piarc Technical Committee 3.3: “Design fire characteristics for road tunnels,” World Road Association (PIARC), 2016.

STATE OF THE ART AND LINES OF DEVELOPMENT FOR THE ARTU RISK ANALYSIS SOFTWARE

Rugiada Scozzari, Michele Fronterrè,
Cantene s.r.l, IT

DOI 10.3217/978-3-99161-087-8-023 (CC BY-NC 4.0)
https://creativecommons.org/licenses/by/4.0/deed.de
This CC license does not apply to third party material (attributed to other sources) and content noted otherwise.

ABSTRACT

ARTU, acronym for "Risk Analysis in Tunnels", determines the societal risk related to fire in road tunnels and calculates the FN-curve accordingly to the European Directive 2004/54/EC. ARTU performs a quantitative assessment of risk, coupling probabilistic Monte-Carlo and deterministic approach.

In the last years, some updates were made in order to make ARTU suitable to address a wider range of tunnel typologies. As an example, a multi-scale approach to fluid-dynamics has been included, based on a zone model developed by Lund University, called MZ.

At the same time, many efforts were put in assuring that ARTU results are reliable. Fire tests have been performed at the Lund University scale tunnel facility to validate the software and study the applicability limits.

Based on these results, a methodology has been drawn up to identify the cases in which ARTU gives satisfactory results and cases in which further analysis are needed. Regarding the smoke dynamic, the use of the 1D model introduces some errors in particular for what concerns the presence of stratification and back-layering. These errors are partially corrected by the multi-scale approach but could have a relevant effect in the risk estimation for tunnels with specific characteristics as the absence of mechanical ventilation or bidirectional traffic. In these case, further analysis, as CFD simulations, could be needed to obtain robust and appropriately conservative results. The methodology aims at a systematically classification of tunnels and procedure to be followed to properly assess the risk.

The present paper discusses the above mentioned methodology in the framework of existing risk analysis methods. The paper also includes an overview of main road tunnel risk analysis developed by ARTU. This allows to clarify the ARTU applicability limits, strong points and possible future developments.

Keywords: ARTU, risk assessment, fluid-dynamics model, methodology.

1. INTRODUCTION

According to PIARC, tunnel risk assessment methodology can be divided in scenario-based and system-based approach. In the scenario-based approach, a set of relevant scenarios is defined and risk assessment is done separately for each single scenario along with the estimation of the probability of occurrence. When applying a system-based approach, instead, risk value for an overall system is estimated, taking into account all events/scenarios which can affect persons in the system [1]. A limitation of scenario-based approach is its sensitivity

to the choice of the set of analysed scenarios. Not accounting for all possible different combinations of fire and evacuation scenarios, it does not consider uncertainties in an efficient way.

ARTU software implements a system-based approach. ARTU performs the risk assessment of a tunnel simulating a large number of scenarios, varying fire position and HRR (Heat Release Rate) curve and traffic conditions. Each scenario returns a certain number of fatalities, the results are cumulated and plotted on a FN diagram. Based on the case, the FN curve can be compared with a reference tunnel, which is a tunnel having the same characteristics of the one under examination, but fully compliant with the European Directive requirements. In this way, it is possible to assess if the lack of some measures, as an example the emergency exits, is likely to increase the risk or it is mitigated by the presence of additional measures.

ARTU includes different sub-models: queue formation, egress, interaction between smoke and people (based on FED – Fractional Effective Dose – parameter), one-dimensional (1D) and zone models fluid dynamics.

One-dimensional (1D) models resolve fluid mechanics equation by assuming that the physical parameters (temperature, velocity, pressure) are all uniform in the cross section [3]. The main advantage of 1D models is that they have low computational requirements, and are particularly attractive for parametric studies where a large number of simulations have to be conducted [4]. This is the case of the methodology implemented in the ARTU software, which aims at the simulation of a large number of scenarios varying the heat release rate (HRR) and position of fire. 1D models permit to model in a complete and compact way complex network systems, constituted by a tunnel and its ventilation ducts [3]. In the case of long tunnels using a transverse ventilation system, the 1D model is the only one capable of modelling the system in its entirety [4]. 1D models are well suited to the study of longitudinal ventilation, since they provide reliable and realistic results when the air velocity is above the critical value [4]. With other ventilation systems, as transverse or semi-transverse systems, using 1D models requires more expertise. Caution is required in interpreting results, due to the possible presence of stratification and back layering phenomena.

3D CFD models provides a solution of the Navier–Stokes equations. The need of appropriate boundary conditions along with detailed input data greatly influence the results [4]. Fluid flow processes are complex and, in order to judge the quality and accuracy of a simulation, an understanding of fluid mechanics and experience of the particular class of flows simulated is necessary [3]. CETU [4] suggests to perform and interpretate a preliminary 1D analysis where a 3D CFD model is used for the specific hazard investigation. In tunnel fire studies, the 3D CFD software FDS (Fire Dynamic Simulator) has become one of the primary tools [9]. Its characteristics allow for significantly larger cell volumes of the numerical mesh, making FDS particularly suitable in risk analysis even if the accuracy of course decreases with increasing volume of numerical grid cells [9], [10]. Nevertheless, some issues arise when applying FDS to tunnels [11][12].

In many cases, it is practical to use 3D CFD models to represent a small tunnel portion, and to account for the effects of the remaining portion of the tunnel by means of 1D models. This class of hybrid models, known as ‘multi-scale models’, are usually based on the coupling between multi-dimensional (e.g. CFD) and 1D (e.g. network model) solvers [3].

ARTU implements a multi-scale approach coupling 1D model with a multizone (MZ) model [5] developed specifically for the tunnel environment. The MZ model represents the entire enclosure through several smaller computational volumes (zones), for which the conservation of mass and energy are applied. Fire is specified as a heat release rate and empirical models

are used to represent the plume and the ceiling jet [5]. The model was originally developed by Lund University [13] for generic enclosures and has been improved [6] in order to make it suitable to the application in tunnels. The use of the MZ model makes it possible to represent two phenomena that cannot be modelled through 1D fluid-dynamic software, namely the smoke stratification and the presence of back-layering. The MZ model development includes continuous validation by means of scale tunnel fire tests, that lead to the definition of its applicability field. Currently, the MZ tool has been founded reliable in the analysis of fire up to 20MW, and in short domain (<200m from the fire) [6]. As a consequence, the necessity arises to define in which cases the 1D-MZ modelling procedure is suitable to produce reliable and satisfactory results. Further analysis, including more complex CFD solvers as the Fire Dynamic Simulator (FDS), are required case-by-case to validate the ARTU estimation of risk. This approach is in accordance with the recommendations of some regulatory authorities, as the Italian ANSFISA that requires [7] an evaluation of the applicability of the tool used to asses the risk to the specific tunnel under analysis.

Chapter 2 discusses the methodology followed by authors to identify the tunnels that requires specific evaluation in order to determine the best approach to assess the risk. The unreliability index automatically calculated by the ARTU software is presented. Chapter 3 presents a set of 41 case studies analysed following the presented methodology, in order to better clarify the role of the unreliability index and to present a qualitative assessment about the suitability of the ARTU tool in the risk assessment of road tunnels.

2. A METHODOLOGY TO IDENTIFY THE TUNNELS WHICH REQUIRES FURTHER ANALYSIS

In order to identify the tunnels that require in-depth analysis, a methodology has been developed, based on an analysis of the 1D fluid-dynamic and MZ models limitations. The fact that stratification and back-layering are not taken into account when estimating the interaction between tunnel users and smoke could lead to both an over-estimation or under-estimation of risk, depending on the case. The lacking representation of stratification phenomena leads generally to an over-estimation of risk, since the 1D models assumes the smoke as homogeneously distributed, while it can be well stratified at a considerable height, as depicted in **Figure 1**.

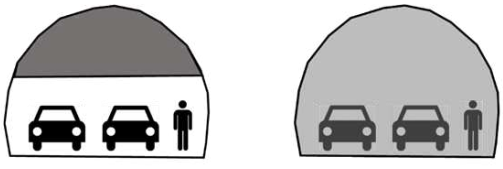


Figure 1: Lack of smoke stratification representation in 1D models

The lacking representation of back-layering has an effect that depends on the position of tunnel users respect to the fire. In some cases it leads to an under-estimation, while in other case the results is an over-estimation (**Figure 2**).

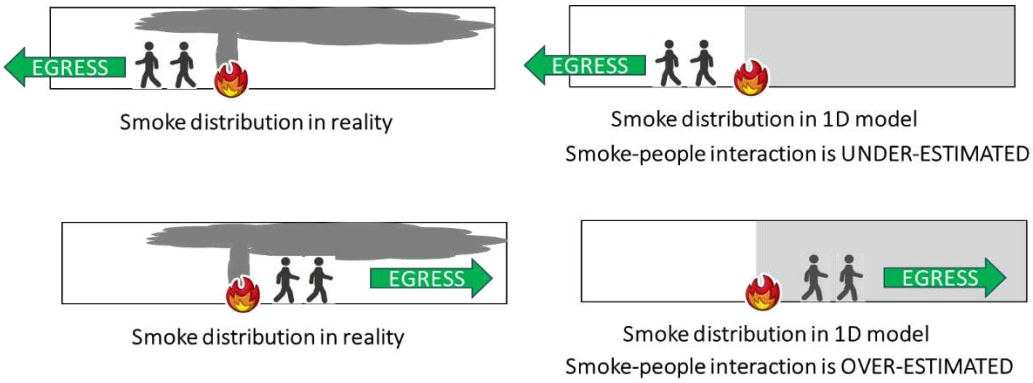


Figure 2: Effect of back-layering missing representation on the estimation of interaction between people and smoke

As previously mentioned, tunnel with longitudinal ventilation are generally well described by 1D models. MZ model is useful to model the first phase of fire, before the activation of emergency ventilation. Usually, this happens by 3-5 minutes from the ignition, and the 1D-MZ representation of smoke behaviour is appropriate. In some case, instead, the emergency ventilation is activated with a larger delay, for example in the case of bidirectional tunnels or monodirectional tunnels in which traffic congestion is frequent. In this case, the ventilation strategy is based on the control of the air velocity that should remain lower than 1 or 1.5m/s, depending on the specific case, in order to promote stratification of smoke and create a fresh air layer in the lower part of tunnel, to allow people egress. Hence, stratification and back-layering lasts for a long time (10-30 minutes) and involves a portion of tunnel for which the MZ application is not fully validated. As a consequence, a case-by-case evaluation is needed for bidirectional or monodirectional congested tunnels.

Regarding transverse and semi-transverse ventilation systems with more than one extraction damper, these always imply the stratification of smoke for the whole duration of emergency. In this case, the 1D representation of smoke could lead to an over-prediction of the interaction between people and smoke. Furthermore, back-layering could appear outside the extraction zone, due as an example to unbalanced pressure related to meteorological conditions at portals. Due to the wide range of possible architecture of the transverse and semi-transverse ventilation system, a case-by-case evaluation is needed.

Naturally ventilated tunnels can be considered as longitudinal ventilated tunnels if their slope is high enough to create a chimney effect able to produce an air flow with velocity similar to the critical value. Nevertheless, chimney effect depends on the position and magnitude of fire, and critical velocity is affected by the tunnel cross-section, so it is difficult to a-priori identify the tunnels that can be treated as longitudinal ventilated.

Finally, each tunnel that shows peculiar characteristics needs to undergo a specific analysis. As an example, a non-exhaustive list of peculiar characteristics includes strong winds at portals, intermediate access/exit ramps, fluid-dynamic connection with other tunnels. All tunnels included in these categories needs a specific evaluation in order to determine whether the risk assessment can be conducted with the ARTU tool or it is necessary to combine it with a scenario-based approach in order to deepen the effect of peculiar characteristics on the overall risk. Based in this discussion, the following flow-chart has been defined.

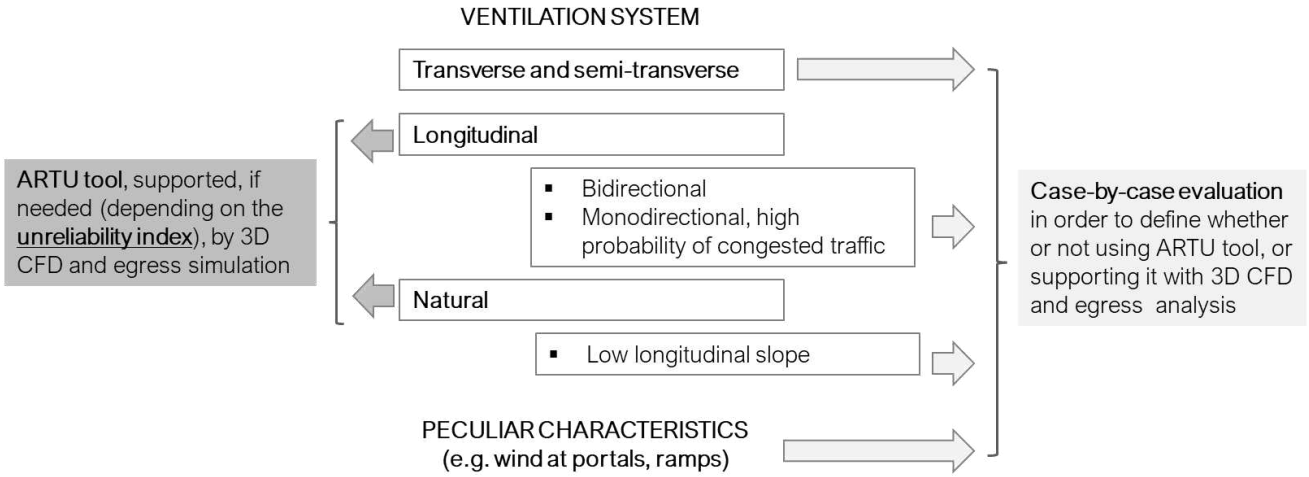


Figure 3: Methodology flow-chart

In any case, regardless a case-by-case evaluation is needed or not, ARTU tool computes an unreliability index in order to quantify the impact, on the FN curve estimation, related to the lacking representation of back-layering.

2.1. The unreliability index

An unreliability index is calculated during the execution of ARTU code, in order to monitor the error in the estimation, due to the use of 1D model, of the smoke-users interaction. The index is defined in order to monitor the cases in which a back-layering has not been taken into account by the 1D model, outside the applicability field of MZ model. The index returns the percentage of cases in which an under-estimation of the interaction between people and smoke could have been happened. The higher the index, the higher the potential under-estimation of risk.

An unreliability index equal to a certain value, as an example 10%, means that in the 10% of the scenarios that composes the FN curve, there is a significant (in terms of duration) lacking back-layering representation. The presence of back-layering does not automatically imply that people will interact with that back-layering. The unreliability index does not state that there is an interaction between people and smoke that was not represented by the software. It states that further analysis, by means of more sophisticated tools as 3D CFD simulations, are required to assess it.

Figure 4 shows the acceptance scale currently associated do the reliability index. Index lower than 25% (green zone) is considered sufficient to guarantee reliable results. Index higher than 75% (red zone) requires further analysis. Values in the range 25%÷75% (yellow zone) suggest to put particular attention in the analysis of ARTU results and, based on the user judgement, could require further analysis.



Figure 4: Acceptance scale used to compare the reliability index and dataset results

The acceptance scale (**Figure 4**) is set based on the experience and takes into account the fact that the FN curve obtained by ARTU is computed taking into account some thousands of cases, and only some of them (corresponding to the value of the unreliability index) are potentially affected by underestimation of fatalities. Since ARTU implicitly include conservative assumptions, due to the uncomplete representation of stratification, it is possible that fatalities are generally over-estimated, despite the potential error in back-layering representation.

When required due to the index falling in yellow or red area, further analysis involves additional 3D CFD and egress simulations. The results of 3D CFD and egress simulations, in terms of fatalities calculated by means of FED (Fractional Effective Dose) parameter, are compared with the ARTU results. Worst case scenarios, in terms of back-layering development, are selected.

Depending on the result of the comparison, the FN curve could be adjusted including the results obtained by 3D CFD and egress simulation. In the case the FN curve has to be adjusted, some qualitative considerations are done to extend results related to the specific scenarios analysed with 3D CFD + egress simulations to other scenarios. Such considerations take into account as an example longitudinal profile, cross-section variations, emergency exits position. The process to extend results of some specific scenario to the rest of tunnel involves what recommended in [8], which states that in a scenario-based approach, analysis of the results must be carried out with regard to the scenario considered and the choice of its parameters. For example, significant consequences must be put into perspective if the chosen parameters are unfavourable.

The number of scenarios to be analyses by means of 3D CFD and egress simulations depends on the characteristics of tunnel, namely geometry (slope, cross sectional area, length), ventilation system typology and architecture, and traffic conditions (congestion probability, percentage of heavy goods vehicle and bus). Indicatively, up to 1-4 3D CFD simulations can be needed, depending on the case. For each 3D CFD simulation, one or more egress simulations can be done, varying the number of people in the tunnel or egress-related parameters as the pre-movement time, accordingly to what ARTU does, in order to make results fully comparable.

3. ANALYSIS OF A SET OF CASE STUDIES DEVELOPED BY MEANS OF THE PRESENTED METHODOLOGY

For the present analysis, 41 road tunnels are considered. The larger part are motorway tunnel (37), remaining are rural (2) and urban (2). Tunnel length ranges from 471m to 4250m, with an average value equal to 1270m. 17 tunnels have a length larger than 1km. 37 tunnel have monodirectional traffic, and 4 bidirectional. Amongst the monodirectional tunnel, 22 have longitudinal ventilation system, 15 are naturally ventilated. Number of lanes is 2 for 35 tunnel, and 3 for 6. Cross sectional area varies from 47.6 m^2 to 123 m^2, with an average value of 68m^2.

Longitudinal profile shows a wide range of shapes and slope values. 8 tunnel have a humpbacked profile, 2 have a U-shaped profile. Globally, slope values ranges from 0 to 4.45%. Also the AADT (Annual Average Daily Traffic) ranges on a wide interval, from 4000 to 59100 with average value equal to 19300.

Figure 5 resumes the main characteristics of the tunnels dataset.

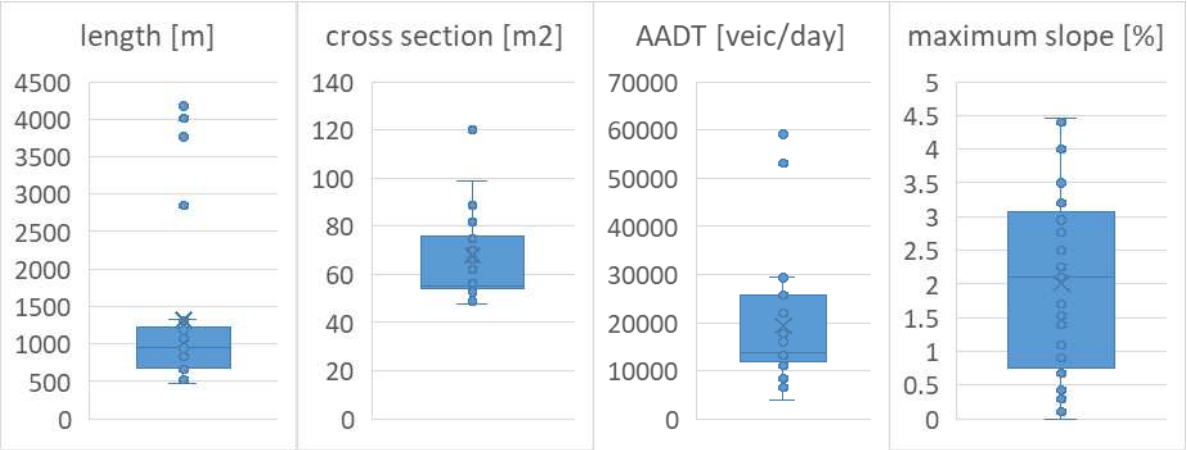


Figure 5: Main characteristics of the case studies dataset

Half of the analysed tunnels are monodirectional, with a length included in the range 500 ÷1200m and are provided with longitudinal ventilation system. Between them, nevertheless, 2 tunnels are characterized by a high probability of congested traffic occurrence (more than 3 hours per day).

7 tunnels required a case-by-case evaluation due to their peculiar characteristics, as resumed in **Table 1**. This was done preliminarily, before the analysis of the unreliability index. In particular, case 3 was out of ARTU applicability limit due to the slope = 0%.

Table 1: Outlier case studies

Case study	Tunnel characteristics	Approach to the risk estimation
1	Length = 4013m, bidirectional traffic, mixed (transverse and longitudinal, depending on fire position) ventilation system, few (2) emergency exit	ARTU analysis + semiqualitative analysis about the low number of exits
2	Length = 736m, monodirectional traffic, natural ventilation, frequent windy conditions (~4.5m/s) at portals	ARTU analysis + 4 3D CFD simulations, 3 of which took into account wind at portals, that lead to an adjustment of FN curve
3	Length = 714m, monodirectional traffic, natural ventilation, slope = 0%	ARTU cannot be used due to the 0% slope. 9 3D CFD simulations and 31 egress simulations have been done to draw the FN curve.
4	Length ~ 700m, monodirectional, longitudinal ventilation, high probability of congested traffic (3 hours per day)	ARTU analysis + 1 3D CFD analysis in order to assess the interaction between people and smoke in low longitudinal velocity (1m/s)
5		
6	Length ~ 500m, monodirectional, natural ventilation, high probability of congested traffic (3 hours per day)	
7		

Unreliability index varies from 0% to 100% in the analysed dataset. **Figure 6** shows the cumulate frequency of occurrence of different index values. 3 small squares over the graph indicates the percentage of cases in the dataset that fall in each zone (green, yellow and red).

It can be seen that 75% of dataset cases has an index ≤ 25%. 49% of analysed tunnels have an unreliability index equal to 0%.

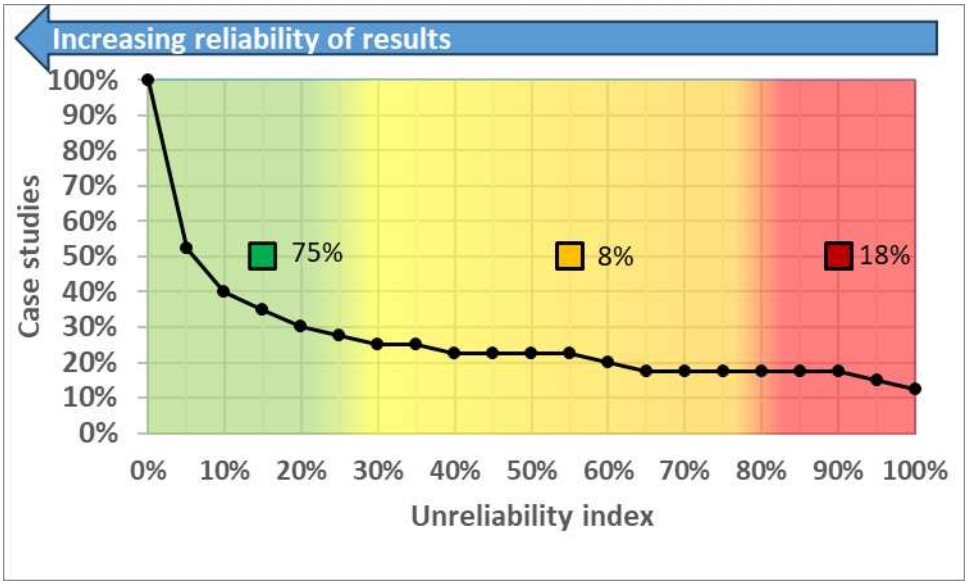


Figure 6: Cumulate frequency of occurrence of different index values

11 tunnels, having index higher than 25%, required a further 3D CFD and egress analysis. Amongst them, in 7 cases, this further analysis confirmed the ARTU estimation of risk. In the remaining cases it was necessary to adjust the FN curve. Hence, the correction was needed in 4 tunnels over 40 analysed with ARTU, in a dataset in which just 1 case (case 3 in **Table 1**) was out of applicability limits, due to the 0% longitudinal slope. Depending on the tunnel, the number of required 3D-CFD and egress simulations varied from 1 to 4. This number is far lower than the number of simulations that would have been required in a scenario-based approach. As an example, the outlier case 3 (see **Table 1**), which was not suitable to be analysed with ARTU required 9 3D CFD simulations and 31 egress simulation to produce the FN curve.

4. SUMMARY AND CONCLUSION

The need to check the suitability of the ARTU tool used in the tunnel risk assessment, combined with the necessity to keep the computational time reasonably low, lead to the development of a methodology that permits to evaluate, in a systematic and repeatable way, the suitability of the tool in the risk assessment of each specific tunnel. Beside the development of this methodology, an unreliability index was included in the code in order to estimate the accuracy of the ARTU risk estimation in a systematic way, taking into account the main limitations of its fluid-dynamic sub-routines, based on 1D model and the MZ (multi-zone) model.

An analysis carried out on 41 real tunnels showed that 7 of them were outlier, namely had peculiar characteristics that required specific analysis before launching ARTU analysis. Apart from that, based on the unreliability index, for 11 tunnels it was necessary to carry out further analysis based on 3D CFD analysis. Nevertheless, the number of 3D CFD simulations was far lower than the number of simulations that would have been required for the same tunnel if studied with a scenario-based approach. For 7 cases in 11, the additional 3D CFD analysis confirmed the results obtained by ARTU, while in 4 case it was necessary to adjust the FN curve.

Overall, the analysis showed that the software ARTU can manage a wide range of real cases, with a good accuracy, allowing a strong reduction in the number of necessary 3D CFD simulations. This is particularly significant considering that 3D CFD simulations require a

certain level of expertise, are generally time consuming and cannot cover the whole range of possible tunnel fire scenarios.

5. REFERENCES

[1] PIARC. Risk analysis for road tunnels. 2008

[2] Sandin, K., Grenberg, K., Husted, B. P., Scozzari, R., Fronterrè, M., & Ronchi, E. (2019). Verification and Validation of the ARTU (Tunnel Fire Risk analysis) tool. Lund, Sweden: Lund University, Department of Fire Safety Engineering. CETU. Guide to Road Tunnel Safety Documentation, booklet 4. 2003

[3] A. Beard, R. Carvel. Handbook of Tunnel Fire Safety, 2nd edition.

[4] CETU. Guide to Road Tunnel Safety Documentation, booklet 4. 2003

[5] Johansson N., Ronchi E., Scozzari R., Fronterrè M., (2023) The use of multi-zone modelling for tunnel fires, Tunnelling and Underground Space Technology, Volume 134, https://doi.org/10.1016/j.tust.2023.104996.

[6] Fronterrè M., Scozzari R. The Application Of Zone Modelling In The Risk Analysis Of Tunnels With ARTU Software. 11th International Conference 'Tunnel Safety and Ventilation' 2022, Graz

[7] Commissione Permanente per le Gallerie. Contenuti e modalità di presentazione della documentazione di sicurezza con particolare riguardo alle tematiche inerenti alla redazione dell'analisi di rischio. 20/02/2025

[8] CETU. Étude Spécifique Des Dangers Esd. Compléments au fascicule 4 du guide des dossiers de sécurité. 2023

[9] Heger O., Strum P. On The Accuracy Of Fds Smoke Propagation Models In The Context Of Tunnel Risk Analysis. 11th International Conference 'Tunnel Safety and Ventilation' 2022, Graz

[10] Backlayering and changes with grid resolution, discussion started in 2023 on FDS issue tracker (https://github.com/firemodels/fds/issues/11495)

[11] Ang C., Rein G. und Peiro J. (2020), Unexpected Oscillations in Fire Modelling Inside a Long Tunnel," Fire Technology, Nr. 56, pp. 1937-1941, 2020.

[12] McGrattan K. und McDermott R (2022) Response to "Unexpected Oscillations in Fire Modelling Inside a Long Tunnel" by Ang et al," National Institute of Standards and Technology, Gaithersburg, Maryland, USA, 2022

[13] Johansson, N. (2021). Evaluation of a zone model for fire safety engineering in large spaces. Fire Safety Journal 120.

HEAT TRANSMISSION BETWEEN GROUND AND TUNNEL AIR FOR DIFFERENT CONFIGURATIONS AND USES

Juan Manuel SANZ SACRISTÁN
Sener Mobility SA, ES

DOI 10.3217/978-3-99161-087-8-024 (CC BY-SA 4.0)
https://creativecommons.org/licenses/by/4.0/deed.de
This CC license does not apply to third party material (attributed to other sources) and content noted otherwise.

ABSTRACT:

From exhaustive measurements of the temperature variation in different positions of different tunnels, the phenomena of heat transmission between ground and air are explained for different configurations, depths and uses of the infrastructure.

The tunnels for which temperature data are available over time at different points and for which the processes of heat exchange between ground and air are analysed based on their comparison with the outside temperatures and air velocities inside are: urban tunnel of great extension and complexity (M30), metro line (L1 Metro de Barcelona) and 24 km long mountain railway tunnel (in its stage prior to operation). This data is complemented by calibrated 1D CFD simulation models of these infrastructures that allow for a deeper analysis of these phenomena and additional situations that have not occurred.

From these analyses we can conclude that the transmission of heat between the ground and the tunnel is a phenomenon of great importance to obtain in the design stage the evolution of the temperature over time and its variation between winter and summer. These conditions can imply natural currents due to the chimney effect at certain times of the year or cyclical currents throughout the day and that in the tunnels in operation can be masked by the piston effect. As an example, on the M30 every night there are important natural currents in a fixed direction at each point even though traffic is very low and that even in many areas it is contrary to the direction of traffic. This phenomenon occurs in the same direction and similar values throughout the year and it has been proven that its reason is that at night the temperature in the tunnel is close to the average day and it is higher than the lower temperatures of the night, which causes chimney effects between portals of different heights due to air density variations.

Heat transmission is also quantified according to the depth of the tunnel and connection points with the outside. This allows to calculate the transition distances between the outside and the ground temperature.

Keywords: Tunnel ventilation, heat transmission, chimney effect.

1. INTRODUCTION

The temperature of a tunnel wall varies over time. This variation is affected by several parameters, including:

- Ground characteristics
- Tunnel depth
- Ambient conditions in the area
- Air currents
- Heat dissipated within the tunnel by passing vehicles or installed systems

In turn, the wall temperature primarily influences the air temperature in the tunnel. The difference between the air inside the tunnel and the outside creates aerodynamic forces (derived from the chimney effect due to the difference in air density). These forces can modify the sizing and operation of the ventilation system. This aspect can also be of great importance in cases where it is considered necessary to maintain the temperature within certain temperature ranges (such as in meters or air conditioning of technical rooms) or where these differences are to be used for HVAC of nearby buildings.

The process of wall temperature variation has a daily component (usually cooler temperatures at night than during the day) and a seasonal component (with higher temperatures in summer and colder temperatures in winter). Depending on the airflow moving through the tunnel throughout the day, the thermal inertia of the system will be greater or lesser between winter and summer. If air currents are low, the tunnel will behave similarly to a cellar, with a constant average temperature, which means it is colder than the outside in summer and warmer than the outside in winter. If the air current is very high, the tunnel could behave similarly to a home, where the interior temperature is close to the outside temperature and the wall temperature could be considered close to the daily average.

This paper analyses the importance of the various parameters and phenomena that influence wall temperature and how it varies throughout the day and year. It also examines the influence of this value on air currents and temperature in the tunnel, as well as its impact on ventilation.

2. MAIN EFFECTS

The temperature of the tunnel wall depends on the depth below the surface. It is generally considered that the surface temperature of a ground layer (up to about 10 m deep) is influenced by the outside temperature. At the surface, the temperature varies between the average temperature of the coldest month and the average temperature of the warmest month. Due to its thermal inertia, the temperature variation from one day to the next is very small. Beyond a certain depth (about 10 m), the temperature remains practically constant and practically equal to the average annual temperature of the area.

This ground condition is used by geothermal installations, which attempt to take advantage of the lower ground temperature in summer and higher temperatures in winter. These installations use the ground as a thermal accumulator. In summer, they inject heat (we could say they extract cold) which they recover in winter. If the system's temperature is not balanced between cold and heat, the ground tends to increase or decrease in temperature relative to its natural temperature, so the system would stop working (or decrease its efficiency) when the ground temperature is close to that of the outside.

The temperature distribution of the ground would be like the following figure:

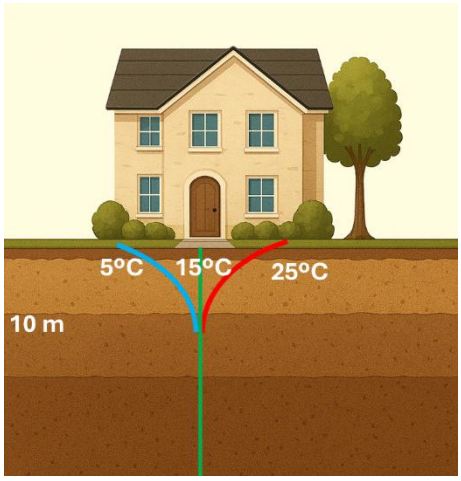


Figure 1: Ground temperature variation along the year with depth (Source Copilot)

At greater depths, the temperature of the ground increases because of geological pressure at values of around 25-30ºC per kilometre.

The first time the tunnel is excavated, the temperature of the walls will be the same as that of the unexcavated ground. As time passes and the air movement processes inside the tunnel will cause variations in ground temperature. Depending on the amount of air exchanged with the outside world and the heat dissipated within the tunnel, these variations will vary daily or seasonally, with varying degrees of variation and shorter or longer periods of equilibrium. In this regard, it is worth noting that some deep tunnels include cooling systems to compensate, if necessary, for the high temperatures expected in the rock at the time of excavation. In principle, we can assume that a ventilation system that moves a large flow of air along the tunnel would be sufficient to modify the long-term rock balance to values close to the average temperatures in the area.



Figure 2: Thermal equilibrium will depend on the external, geothermal and ventilation conditions of the tunnel.

The ambient temperature in a given area typically varies daily and seasonally. Although the climate varies from year to year, we can assume that the minimum temperatures are around the average values of previous years.

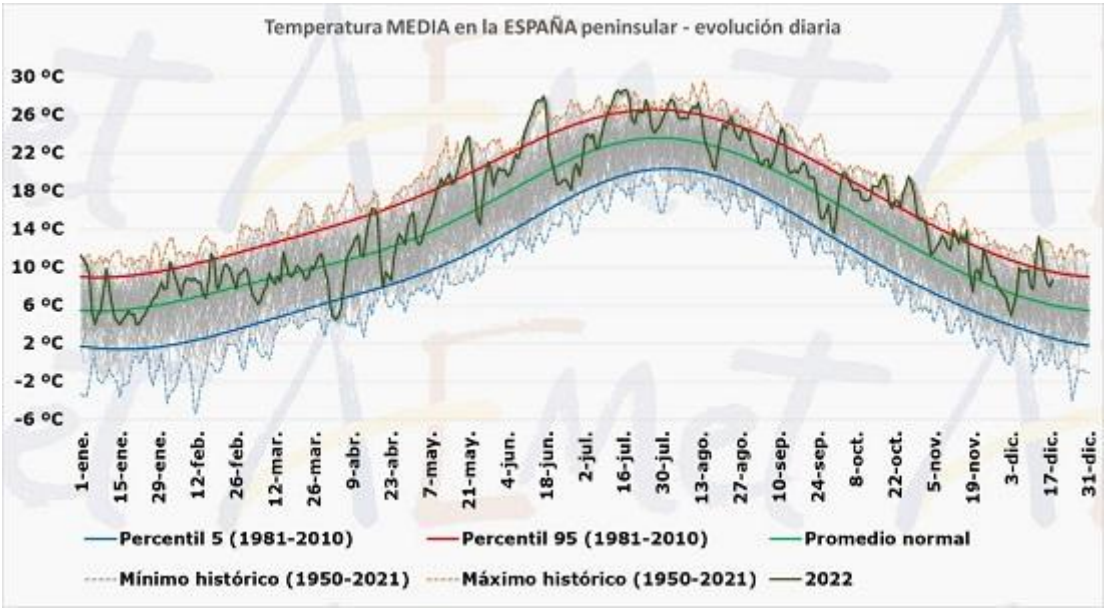


Figure 3: Annual temperature in Madrid (Source Aemet)

It is observed that a tunnel lags the outside temperature due to the thermal inertia of the ground. We will show various examples of this later in tunnels with different configurations.

In a cellar or tunnel with little air movement, the temperature will remain practically constant and close to the average annual temperature. This is because still air is considered good thermal insulation. In the case of rapid air movement, heat transmission with the walls is already higher. Furthermore, the continuous renewal of outside air implies (due to the temperature difference between the incoming and outgoing air) an exchange of heat with the outside, which modifies the temperature of the wall and the ground around the tunnel. Therefore, we will need to briefly explain the heating/cooling processes of solids and gases, as well as the heat transfer between solids and solids and between solids and gases, depending on the temperature difference and the type of transfer. Between solids and gases, it is very important to consider whether the air movement is shallow, laminar, or turbulent. These types of air movement are associated with heat exchange by conduction, or convection. Heat transmission by radiation will also occur, although generally to a lesser extent due to the small temperature differences between the walls and the air.

The equations for conduction are the following:

Fourier's Law of Heat Conduction: $q = -k \times \frac{dT}{dx}$

Where:

q: heat flux (W/m²)

k: thermal conductivity of the material (W/m·K)

dT / dx: temperature gradient

In gas-solid interactions, conduction is significant only in the thin layer of gas adjacent to the solid surface.

Table 1: Some examples of Thermal Conductivity

Material	*Typical k Value [W/m·K]*	*Notes*
Concrete	1.0 – 1.7	Common in tunnel walls and floors
Air	0.024 – 0.030	Thermal conductivity of air
Steel (carbon)	45 – 60	Used in reinforcements and structures
Aluminium	200 – 235	Used in ducts or panels
Rock (granite)	2.5 – 3.5	Found in natural tunnel environments
Insulation (mineral wool)	0.035 – 0.045	Used for thermal protection

The equations for convection are the following:

Newton's Law of Cooling: $q = h \cdot A \cdot (T_s - T_\infty)$

Where:

q: heat transfer rate (W)

h: convective heat transfer coefficient ($W/m^2 \cdot K$)

A: surface area (m^2)

Ts: temperature of the solid surface

T∞: temperature of the gas far from the surface

The value of h depends on whether the convection is natural (due to buoyancy) or forced (due to fans, pumps, etc.).

Table 2: Some examples of the Convective Heat Transfer Coefficient (Solid-Gas Interfaces)

Situation	*Typical h Value [W/m²·K]*	*Notes*
Air flowing over a flat wall (forced)	10 – 100	Depends on air speed and surface roughness
Natural convection (still air)	2 – 25	Occurs in stagnant zones
Air inside ventilation ducts	20 – 250	Higher with fans or forced flow
Turbulent flow over heated surface	100 – 1000+	Found in high-speed ventilation systems
Air moving at 2 m/s	H ≈ 30-50	

The amount of heat Q needed to increase the temperature of a substance (solid, liquid, or gas) is given by the formula: $Q = m \cdot c \cdot \Delta T$

Where:

Q: heat energy (in joules, J)

m: mass of the substance (in kilograms, kg)

c: specific heat capacity (in J/kg·K)

ΔT: change in temperature (in kelvin or °C)

Table 3: Specific Heat Capacity of Common Tunnel Materials

Material	*Typical c Value [J/kg·K]*	*Density (kg/m³)*	*Notes*
Concrete	840 – 1000	2300	Depends on composition and moisture content
Air (at 25°C)	1005	1,184	Common value for dry air at constant pressure
Steel (carbon)	450 – 500	7850	Lower than most building materials
Aluminium	900	2700	High for a metal, helps in heat dissipation
Granite (rock)	790 – 900	2600	Varies with mineral content
Mineral wool (insulation)	~840	30	Similar to concrete, but with low density

From all the above, and from the values measured in tunnels shown in the following chapters, we can deduce that at low speeds, air behaves as an insulator. With air speed higher than 1 m/s, common in tunnels, heat transfer between the wall and the air is high.

3. ANALYSIS OF TUNNELS IN OPERATION

Below we collect temperature variations recorded in various types of tunnels.

3.1. Urban tunnel

Air velocity and temperature records have been analysed in various areas of the Madrid urban road tunnel network (M30). The following figure shows the temperatures and velocities in the cut & cover area of Avenida de Portugal in the summer of 2021.

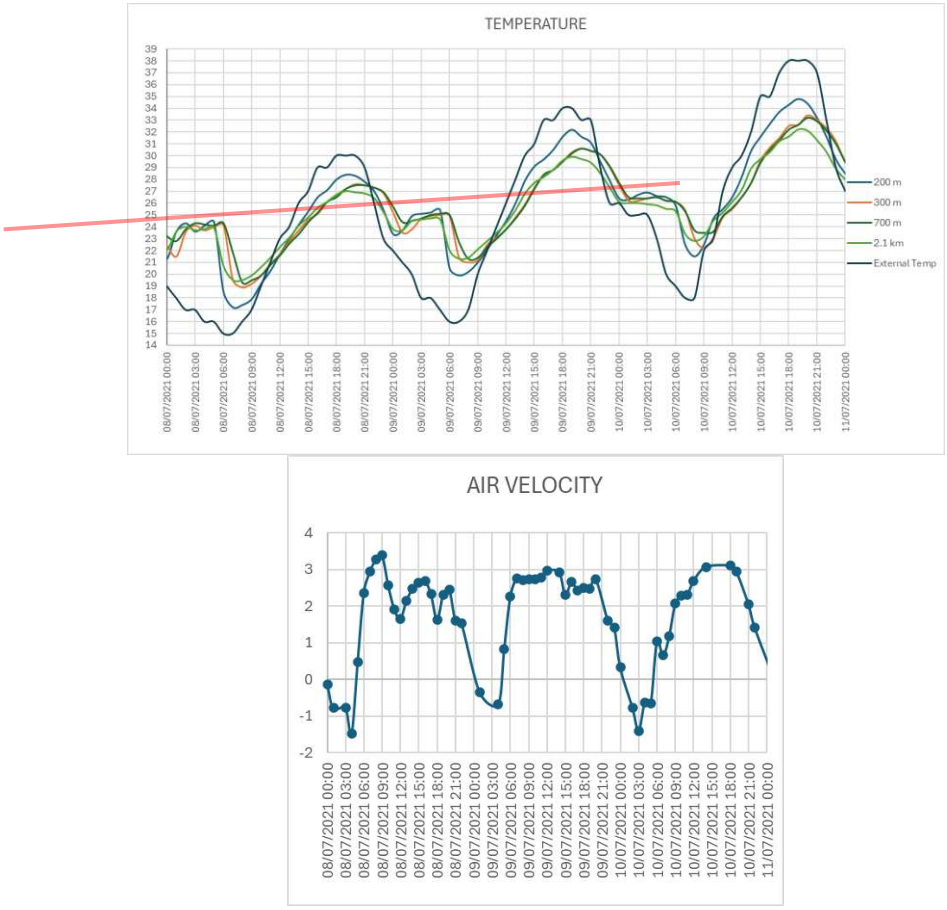


Figure 4: Temperature variation along the tunnel (with average evolution estimation) and air velocity

We can observe the following main aspects for this tube:

- There is a significant heat exchange between the walls and the air in the area near the portal.
- This exchange involves both heating and cooling the air depending on the temperature difference between inside and outside.
- During hours, when the outside temperature is lower than the inside and there is no significant piston effect, the air has natural draft in the opposite direction to traffic. Under these conditions, the temperature remains practically constant throughout the tunnel, at a value that could be considered the average for the infrastructure. This chimney effect can cause natural currents of the order of 2 m/s.
- The average temperature of the tunnel varies by up to 1°C from one day to the next, due to the summer period, when the infrastructure warms up because the average outside temperature is higher than that of the infrastructure.
- Thermal fluctuations reach 3°C in 200 m sections, with air velocities of around 2 m/s.
- Heat exchange with the walls is concentrated in the first 500 m of the infrastructure.

Considering the configuration and cross-section of this tunnel, whose area is about 100 m²:

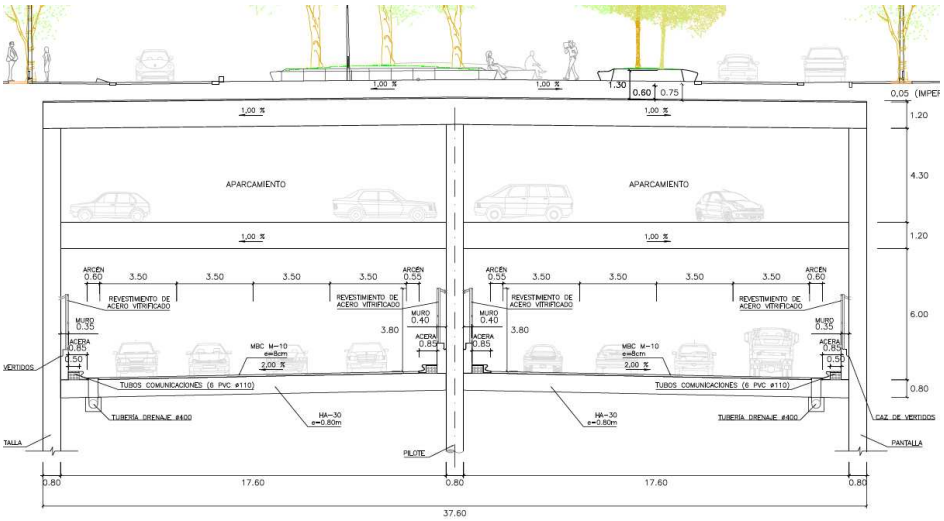


Figure 5: Typical cross section of the tunnel analysed

This implies a heat transfer in the portal area of approximately (during the hottest hours of midday and in 200 m length): 100 m² x 2 m/s x 1.184 kg/m³ x 1005 J/kg·K x 2 K = 476 kW. If we consider this heat over the tunnel perimeter, in a 10 cm thick concrete layer, we obtain a temperature change of approximately: 476000 J/s / (47.2 m x 0.1 m x 200 m x 2300 kg/m³ x 840 J/kg·K) = 26 x 10^{-5} K/s = 0.94°C/h. This confirms the observation of the temperature variations shown in the previous figures.

If we analyse the air temperature variation along the tunnel, we will obtain a figure like the following:

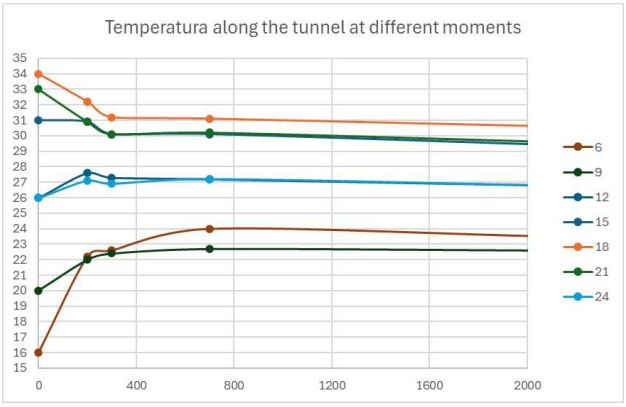


Figure 6: Temperature variation along the tunnel at the hours when the velocity is positive

We can observe a certain similarity between this distribution and the one mentioned above for the variation of the ground with depth, although in this case it does not converge on a constant value.

For more detailed analyses, it would be necessary to create a three-dimensional model of the tunnel and the surrounding ground, considering in this case that above the tunnel there is a parking lot that acts as insulation from the outside and the thermal conditions of the opposite tunnel. This model must consider the temperature variation of the tunnel structure, the heat transfer to the ground, and its storage capacity. 1D models analyse the transmission between the air and the tunnel and the temperature variation of the ground, although it is not easy to select the assumptions to be made (due to the lack of detailed knowledge of the ground conditions) nor to calibrate this for existing tunnels.

3.2. Metro tunnel

On Line 1 of the Barcelona Metro, an analysis has been carried out on the temperature evolution of the stations over time and its relationship with the outside temperature. The annual temperature evolution of a typical station is shown in the following figure in relation to the outside temperature:

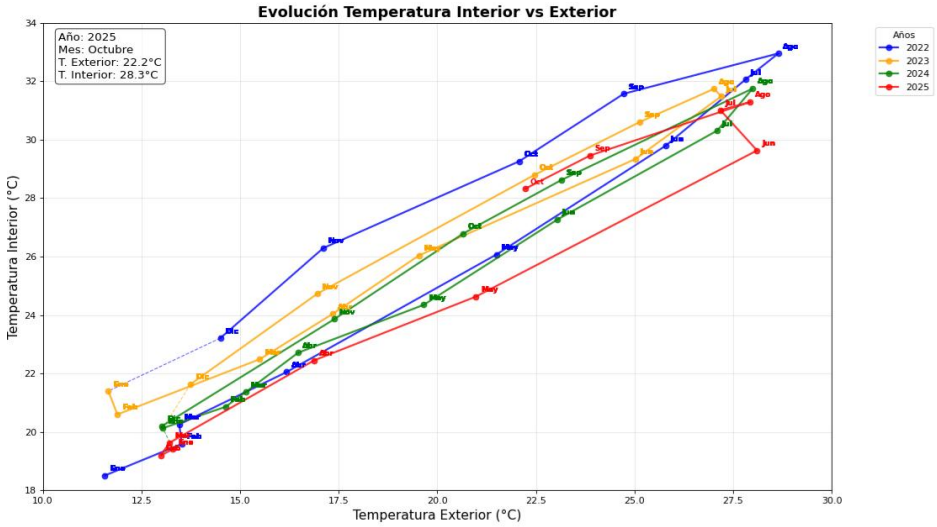


Figure 7: Temperature evolution of L1 of Metro Barcelona along different years.

The main temperature variation over the years in this case is due to the improvement of the ventilation algorithm, which applies Artificial Intelligence. With lower energy consumption each year, it optimizes the moments when outside air is introduced with the greatest temperature difference between outside and inside, to maximize the thermal storage capacity of the ground.

The daily temperature evolution of this line can be observed in the following figure:

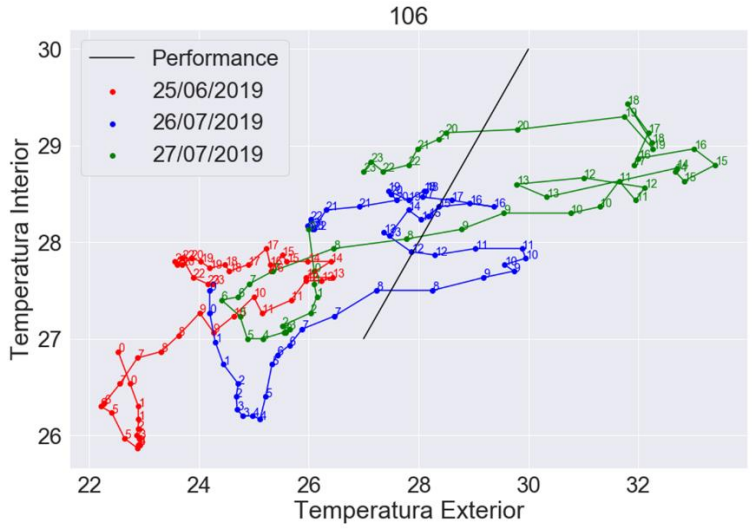


Figure 8: Temperature evolution of L1 Metro Barcelona along some days.

It can be observed that we have a similar evolution to that of the urban tunnel. The daily temperature of the tunnel varies similarly to the outside temperature, although with less variation due to the thermal inertia of the ground. In this case, the internal heat emitted by

vehicles and installations is much higher than in the road tunnel, so the interior temperatures are higher relative to the average outside temperatures.

3.3. Mountain tunnel

In the Pajares railway tunnel, during the equipment installation phase (tunnel excavated, not in operation and without ventilation) of 24 km in length, a campaign of air current and temperature measurements was carried out, from which the 1D ventilation model of the system was developed. In this case, the campaign was not continuous over time, so long-term evolution information is not available. However, some conclusions were drawn from the measurements taken and from the simulation model developed based on them.

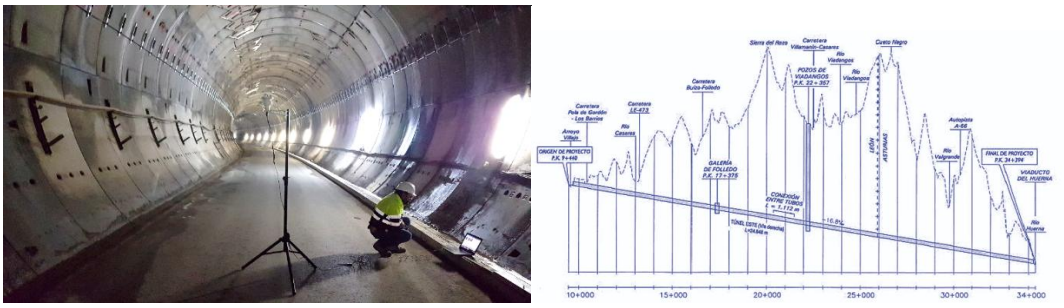


Figure 9: Measurement campaign and longitudinal profile.

The following graph shows the temperature variation in the tunnel in relation to the outside temperature and the air velocities and direction:

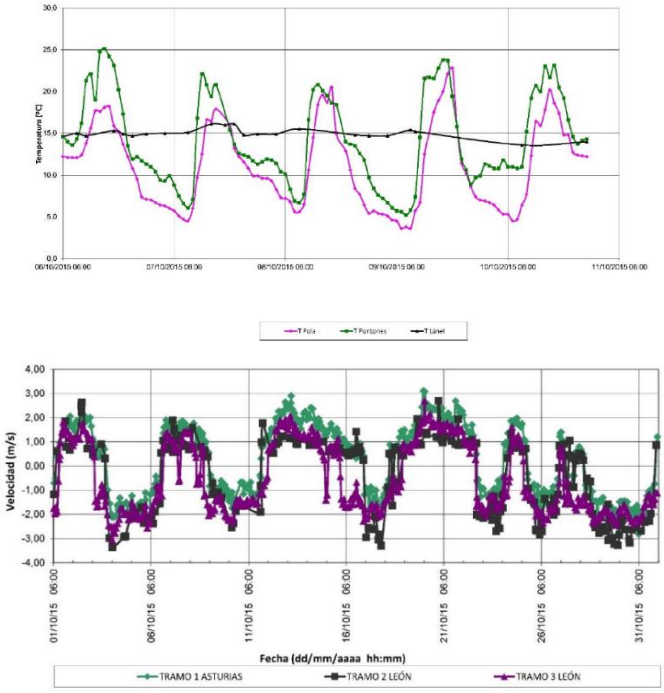


Figure 10: Tunnel and external temperature (left) and air velocity.

The main observed aspects are the following:

The temperature along the tunnel was practically constant and close to the average temperature of the area.

No temperature differences were observed due to the depth at which the tunnel was located.

External temperature variations only impact the first few meters from the portal, with a length of approximately 2000 m. The rest of the tunnel remains at a practically constant temperature.

In this case, variations in air speed and direction are influenced by temperature, but mainly by atmospheric pressure differences between the valleys connected by the tunnel.

4. SUMMARY AND CONCLUSIONS

Heat transfer between the air and the tunnel walls is significant when air currents exceed 1 m/s. This effect is mainly concentrated at the portals due to external temperature variations and their difference with the tunnel interior. The external influence zone is limited to a few hundred meters. In many cases, longitudinal air currents will occur without the need to activate ventilation, due to the piston effect of vehicles, temperature differences between the interior and exterior if the portals are at different heights, or climatic differences between both ends.

In the variation of the tunnel's interior temperature, daily and seasonal cycles are observed. By appropriately activating ventilation during periods of greater temperature difference between the interior and exterior, the infrastructure's temperature can be modified.

This phenomenon also involves the heat dissipated inside the tunnel (either by vehicles or installed systems), although this value is usually relatively constant during tunnel operation.

The variation in interior and exterior temperature can cause air currents (due to the chimney effect from density differences), which must be considered in the design of the ventilation system, as well as in its control algorithms.

The thermal inertia of the tunnel and the heat transfer to the ground have a damping effect in relation to external temperature variations.

ENHANCEMENT OF THE DISPERSION OF POLLUTANTS NEAR A TUNNEL ENDING IN A STREET CANYON, A CFD CASE STUDY

[1]Gabriel Remion, [1]Bruno Vidal, [1]Thierry Kubwimana, [1]Marouane Yaghzar, [1]Antoine Mos, [2]Romain Boissat, [2]Edwige Revelat, [2]Alexis Stepanian

[1]CETU, FR
[2]AtmoSud, FR

DOI 10.3217/978-3-99161-087-8-025 (CC BY-NC 4.0)
https://creativecommons.org/licenses/by/4.0/deed.de
This CC license does not apply to third party material (attributed to other sources) and content noted otherwise.

ABSTRACT

Covered expressways have several advantages in terms of quality of living inside cities. However, they concentrate pollutants at their portals, which are often located in street canyons. The configuration of these street canyons, which are often below the street level, hinders the wind inflow. This can result in the stagnation of pollutants and the exposure of people living or working in their vicinity. A mitigation solution has been assessed in order to enhance the dispersion of pollution, and thus, reduce the exposure risk. Urban tunnels are usually equipped with a ventilation system that dilutes pollutants to comply with regulatory thresholds. The idea of the mitigation solution is to additionally control the ventilation system using NO_2 sensors located outside of the tunnel. This article first aims at characterizing the exposure risk around the street canyon, and then at testing the influence of the proposed mitigation solution.

A Reynolds-Averaged Navier-Stokes model of a real field case with two tunnels ending in an cut street canyon in Marseille, France, was implemented. The topography, the thermal stability of the atmosphere, and buildings were modelled. An experimental campaign was also conducted to validate the model. Both the experimental campaign and the CFD model demonstrated the sensitivity of the site in terms of air quality. The risk of exceeding the hourly NO_2 regulatory threshold at the ground level, and on building facades, was ascertained. The proposed mitigation solution was found to be highly effective in reducing the exposure risk for people living or working near the street canyon.

Keywords: Pollutant dispersion, CFD model, street canyon, tunnel ventilation

1. INTRODUCTION

In order to reduce traffic nuisances inside cities, to save some land, and to avoid discontinuities at the city surface, urban planners often push for underground covered expressways. They have the advantage of improving the quality of life in the vicinity of these roads by tackling the three issues mentioned above. However, the challenge lies in the vicinity of tunnel portals, with traffic-induced pollutants levels that may concern people living or working there. Yet, urban tunnels often need to be divided into several tunnels separated by hundreds of meters for safety, economic or sobriety reasons, thus increasing the number of portals.

The aeraulic transparency separating two consecutive urban tunnels will be called here the “Cut Street Canyon (*CSC*)”, distinct from the “street canyon” often found in the literature,

which represents urban boulevard surrounded by arrays of buildings [1], [2], [3]. Street canyons may hamper the wind inflow, favouring the stagnation of pollutants. *CSCs* are even more critical because, unlike street canyons, their extremities do not allow wind inflow.

This article is part of a wider project [4] that aims to improve the air quality near a real *CSC* field-case, located in Marseille, France. A measurement campaign [5] demonstrated that the site was indeed sensitive to traffic pollution. The wider project also aims at testing a mitigation solution that will be called the "over-ventilation". The mitigation solution aims at triggering the tunnel ventilation system via NO_2 sensors installed around the *CSC*, in addition to those located inside the tunnel.

The present study focuses on a Computational Fluid Dynamics (*CFD*) model of the NO_2 dispersion around the *CSC* of interest. The *CFD* model was validated against results of the experimental campaign (see section 2.3). It was then used to better characterize the exposure risk of people living there (see section 3.1). Finally, the *CFD* model was used to test the mitigation solution. As a first step of the wider project, results will show the potential of the mitigation solution (see section 3.2).

2. METHODS

2.1. Site location, computational domain and grid

Figure 1 shows the site location, in Marseille, **France** along the L2 urban express ways represented by the white dashed line. The domain is quasi-cubic with a square base 8 km long and 2.5 km high. It is centered around the *CSC*, 194 m long, 40 m wide, and 14 m deep, which leads to a low penetration of the outside air. Furthermore, this particular configuration is worsened by the discharge of two tunnel portals, each with a 60,000 veh/day traffic.

The variation in altitude at the boundaries is about 150 m maximum. The height of the domain was determined in order to be significantly higher than the variation of the boundary altitude in order to avoid an artificial acceleration of the flow. The red circle in Figure 1 embraces any building that may have an influence on the flow field around the *CSC*. Indeed, it is often considered that a building can have an influence on the flow field until 5 times its height. Inside the red circle, buildings were carefully modelled. Outside of the circle, an aerodynamic rugosity (z_0) of 1 m was implemented to simulate the effect of buildings.

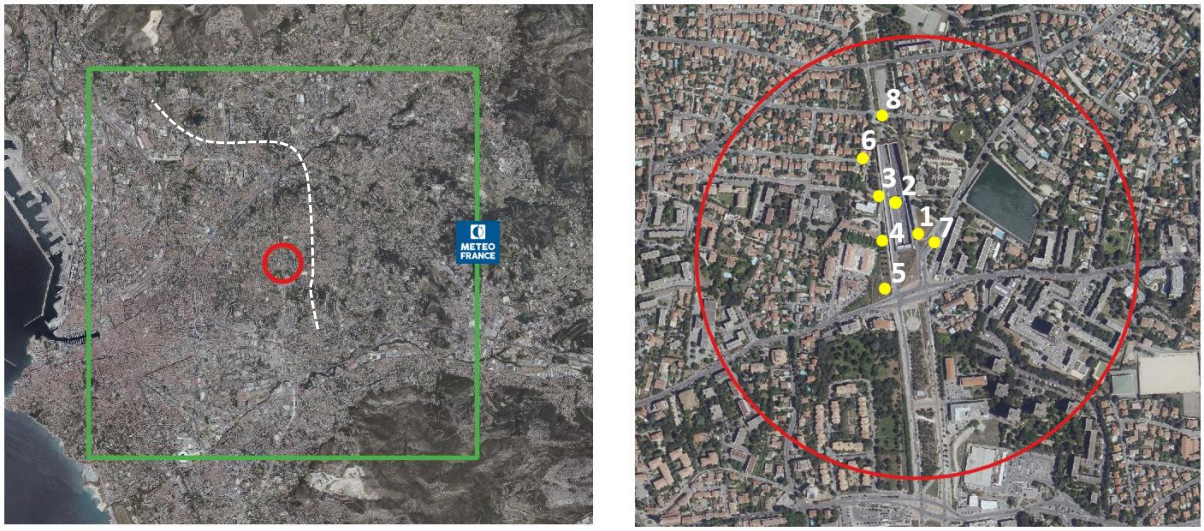


Figure 1: Site location and computational domain

Figure 2 shows the geometrical model focused on the zone of interest (the red circle in Figure 1) with the topography, influent buildings, and the *CSC*.

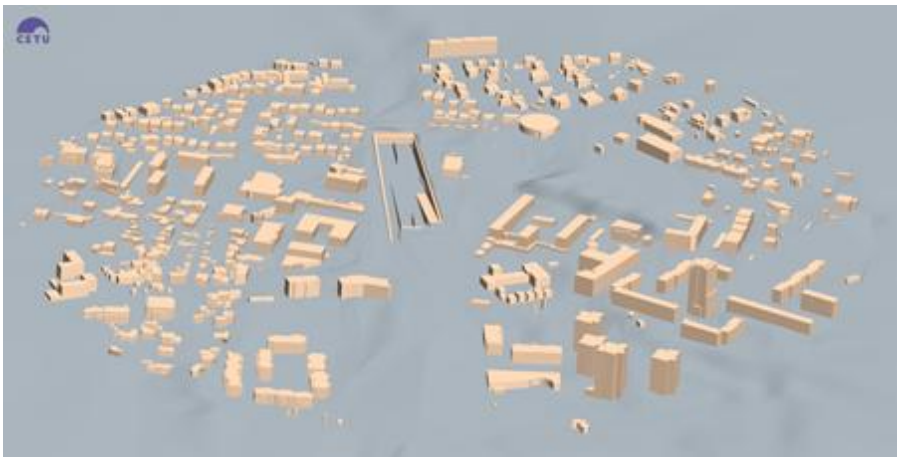


Figure 2: Geometric model of the site of interest

The mesh was implemented using polyhedral cells. Authors made sure that the following criteria were respected thanks to surface and volumetric controls: a number of cells below 10 million, at least 5 cells on each building height, at least 20 cells on the height of the *CSC*, at least 10 cells between the ground and the pedestrian level (2 m high) in the zone of interest, at least 10 cells between each building, and a geometric growth of 1.3 maximum. Inside the red circle of Figure 1, the target cell size is of 50 cm with a minimum of 20 cm allowed to respect the criteria. Far from the zone of interest, the cell size can reach 125 m. In total, the mesh grid represents about 9,5 million cells. Figure 3 shows some examples of the mesh on a building and on the street canyon.

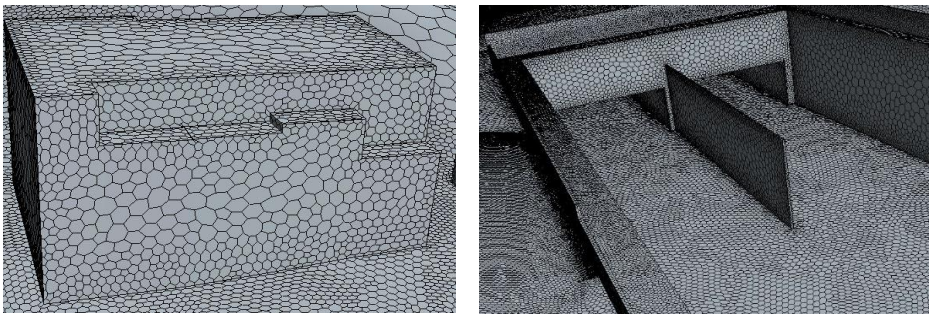


Figure 3: Screenshots of the mesh on a building and on the cut street canyon

2.2. The CFD model

We implemented a steady Reynolds Averaged Navier Stokes model, with a k-epsilon closure model. Because of its influence on the pollutant dispersion, the atmospheric stability was taken into account thanks to the Monin Obukhov Similarity Theory (*MOST*) [1], [3], [6], [7]. This theory provides the analytical formulas of the inlet profiles in physical equilibrium with the thermal transfer between the atmospheric boundary layer and the ground. Also, the k-epsilon model was modified through the integration of the $C_{3\varepsilon}$ parameter in the transport equations of turbulence parameters that intends to describe the production or destruction of turbulence by buoyancy. Several articles tackled the definition of the $C_{3\varepsilon}$ parameter [8], [9], but we used the one computed by StarCCM+. We performed a sensitivity analysis on this parameter, and it appeared to have a small influence in our zone of interest: close to the ground.

Figure 4 shows a schematic of the numerical model. Boundary conditions are specified. Blue arrows represent inlets of the domain, while red arrows represent outlets. The inlets of the domain are either boundaries from which the wind enters the model, or the exits of the tunnels, the latter being the only sources of pollutants. The pollutant considered here is the main tracer of road traffic: the nitrogen dioxide NO_2. In both cases, the inlets are set as velocity inlets where the temperature, velocity, and turbulence parameters are imposed, as well as the pollutant concentration.

Using directly NO_2 is an approximation as this gas is reactive: it is destructed under solar radiation or produced from NO in the presence of ozone [10]. We assumed that pollution episodes of NO_2 mainly occur during winter, when the ozone concentration is very low. The production of NO_2 from NO is, thus, very low as described in ref. [11] and we can consider than using NO_2 is conservative because its destruction is not considered.

Inlet profiles on boundaries from which the wind enters the model are all derived from the *MOST* theory [9]. Meteorological data measured at the closest weather station, such as the cloudiness, the temperature and velocities at 10 meters above the ground, and the solar radiation, fed analytical formulas of the inlet profiles of the temperature, the velocity, the turbulent kinetic energy, and the turbulent dissipation rate.

Regarding tunnel exits, boundaries are set a hundred meters upstream the tunnel exit in order for the boundary layer to be fully developed when it enters the *CSC*. The velocity and the temperature imposed at the boundaries are extracted from the measurement. Turbulence is introduced at the tunnel exits by means of the turbulent intensity I_t (*equation 1*) and the turbulent length scale l_t (*equation 2*) representative of a duct, where ρ is the reference density, U the longitudinal velocity, D_h the hydraulic diameter, and μ the dynamic viscosity.

$$I_t = 0.16 \left(\frac{\rho\, U\, D_h}{\mu}\right)^{-1/8} \quad (1)$$

$$l_t = 0.07\ D_h \tag{2}$$

The mass flow rate of each outlet is imposed in the light of what is usually done when modelling stratified atmospheric boundary layers [8], [12]. The top boundary is set as a symmetry condition, assuming the absence of vertical gradients near the top of the domain. In order for the system to be in equilibrium, an energy source (*Se)* is added in the upper layer. It intends to balance the heat transfer H_0 injected in the model from the ground.

The ground is set as a rough surface outside the circle, with an aerodynamic roughness height representative of a city (z_0 = 1 m). The ground is set as a smooth surface inside the circle where buildings are modelled. The heat transfer of the ground is imposed as a volumetric heat source H_0, which comes from a ground energy balance.

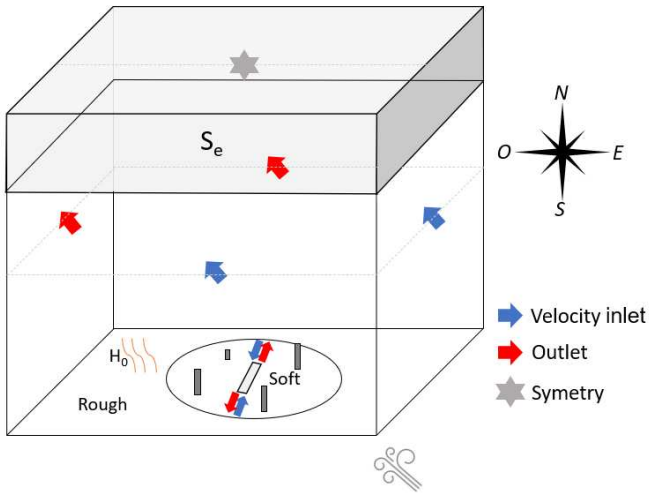


Figure 4: Schematics of the numerical model

2.3. Model validation

In addition to a confrontation with experimental data, the scientific community agrees on the need to check the horizontal homogeneity and the mesh independence to test the validity of *CFD* models [1], [6], [9]. It allows to ensure that governing equations of the model are consistent, and that the geometry is well discretized. The homogeneity test was assessed over 6 km on an empty domain and appeared validated with low deviations of the inlet profiles (see **Figure 5**).

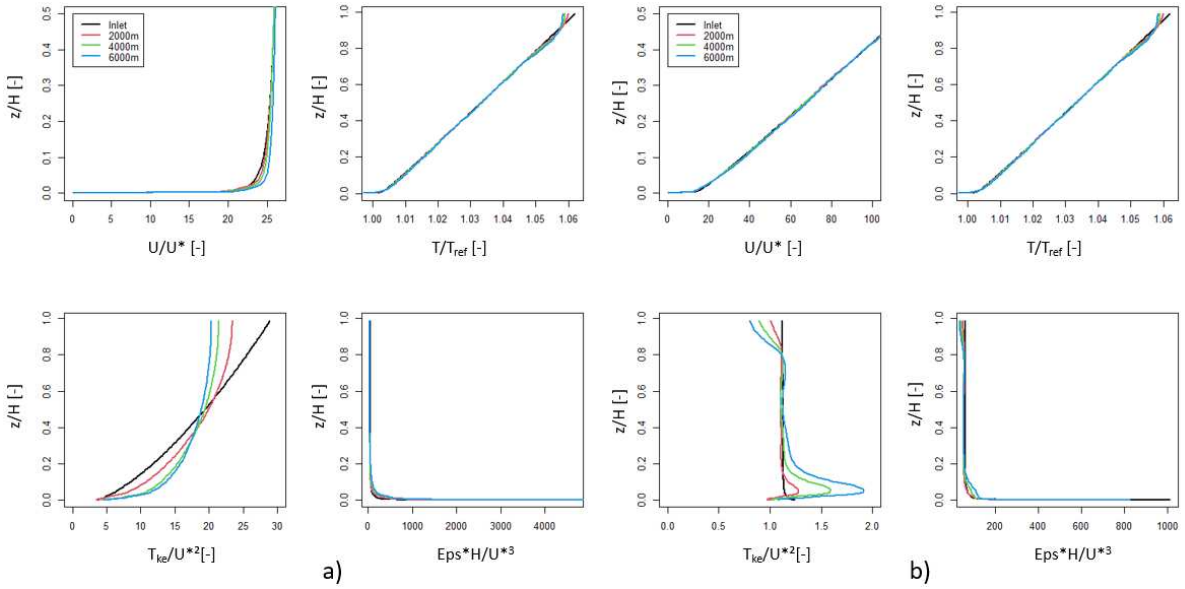


Figure 5 : Horizontal homogeneity test : (a) for an unstable atmosphere (LMO = -142 m), (b) for a stable atmosphere (LMO = 92 m)

The mesh sensitivity was questioned through two indicators: the maximum of NO_2 at 2 m above the ground, and the area of the pollution slick at 2 m above the ground. A refinement of 10% of the mesh on the zone of interest, which increased the number of cells from 9.5 to 16 million, led to deviations below 1%, which validated the mesh independence test.

Then, 30 configurations were selected from an experimental campaign, that provided NO_2 measurements at 8 locations around the *CSC* (see Figure 1), as well as inputs of the model such as the velocity and the concentration of both tunnel plumes. Other input data were extracted from the closest weather station, that is also considered as the most representative of the site of interest. NO_2 concentrations were then compared for the 30 configurations at each measurement points. Depending on the wind direction, only 3 to 4 sensors were located inside the plume for each condition. Only those points were selected for the comparison, in order for the confrontation to be more representative of the ability of the model to reconstruct the plume.

Chang and Hanna [13] have proposed some metrics, which are extensively used to validate pollutant dispersion models [14], [15]. They proposed to compare simulated and measured concentrations by means of 3 different metrics: the fractional bias *FB (equation 3)*, the Normalized Mean Square Error *NMSE (equation 4)*, and the factor 2 *FAC2 (equation 5)*.

$$FB = \frac{\overline{C_{exp}} - \overline{C_{sim}}}{0.5\,(\overline{C_{exp}} + \overline{C_{sim}})} \tag{3}$$

$$NMSE = \frac{\overline{(C_{exp} - C_{sim})^2}}{\overline{C_{exp} C_{sim}}} \tag{4}$$

$$FAC2 = \frac{1}{N}\sum_i n_i, n_i = 1 \; if \; 0.5 < \frac{C_{sim}}{C_{exp}} < 2 \; else \; n_i = 0, \tag{5}$$

Table 1 gives those metrics computed for each measurement points over the 30 configurations selected for the confrontation. Metrics were only calculated on points that were inside the plume. Sensor 8 was never in the plume on any of the tested configurations, so it has not been part of the confrontation. Chang et Hanna [13] proposed some threshold values to verify the reliability of the model : $-0.3 < FB < 0.3$; $NMSE < 1.5$; and $FAC2 > 0.5$, knowing that a

perfect model would lead to *NMSE* and *FB* equals to 0 and *FAC2* equal to 1. Only the fractional bias shows 2 points outside of the range (points 6 and 7), which is discussed next.

Table 1: metrics for the model validation

	Point 1	Point 2	Point 3	Point 4	Point 5	Point 6	Point 7	Point 8
FB	*1.9e-1*	*3.0e-1*	*1.1e-1*	*1.3e-1*	*2.1e-1*	*3.7e-1*	*5.2e-1*	*NaN*
NMSE	*6.0e-2*	*2.1e-1*	*1.5e-1*	*1.9e-2*	*1.1e-1*	*2.1e-1*	*3.4e-1*	*NaN*
FAC2	*1*	*7.7e-1*	*8.9e-1*	*1*	*1*	*8.7e-1*	*7.7e-1*	*NaN*
RD [%]	*15*	*22*	*1*	*3*	*15*	*29*	*40*	*NaN*

Table 1 also gives the Relative Deviation *(RD)* computed as:

$$RD = \frac{C_{exp} - C_{sim}}{C_{exp}} * 100 \quad (6)$$

The relative deviations are systematically positive, meaning that the model underestimates the measurements for each point. The average of the relative deviations among each measurement points is 18%. This systematic underestimation is consistent, because the *CSC* traffic is not taken into account. Assuming that the traffic of the *CSC* is the same as the traffic inside tunnels, this is possible to estimate the additional pollution it would represent by calculating the length ratios of the *CSC* compared to both tunnels. This would represent an additional pollutant emission of 25%, which is not taken into account by the model.

The systematic underestimation caused by not taking the *CSC* traffic into account explains why the *FB* is outside of the validity range for two sensors. Indeed, a bad fractional bias with good other metrics suggests that biases are small, but systematic.

The model is, therefore, considered as reliable and an offset of 18% is applied on the results to approximately account for the *CSC* traffic and reduce the systematic bias.

3. RESULTS

3.1. Sensitivity of the site to the hourly NO_2 regulatory threshold

In order to assess the sensitivity of the site to pollutant exposure above the hourly regulatory threshold, we considered two traffic conditions, three wind directions and a low wind speed of 0.5 m/s at 10 m above the ground. The latter parameter is particularly unfavourable in terms of pollutant dispersion. This tends to 6 simulations. The traffic condition is the main parameter that influences the source of pollutant: it characterizes the pollutant concentration and the speed of the plume of the tunnel. A traffic representative of rush hours (*T1*), and a traffic voluntarily critical (*T4*) relative to a full congestion inside both tunnels, were implemented. *T1* represents a traffic of roughly 4,628 veh/h circulating at a speed of 40 km/h. *T4* relates to the maximum traffic that can occur at a speed of 10 km/h: 3,000 veh/h.

The wind directions were chosen for their ability to orientate the plumes towards the denser zones of buildings around the *CSC*. Directions *D1*, *D2* and *D3* are related to representatively 300°, 110°, and 190°.

Figure 6 shows the areas at 2 m above the ground, as well as building facades, in which the NO2 excess the hourly regulatory threshold, namely the polluted area and exposed building facades. Those indicators are given for the three wind directions. The figure on the left refers to the “rush hour” traffic condition *T1*, and the figure on the right refers to the “congested”

traffic condition *T4*. Traffic *T1* leads to a couple of exposed buildings for the wind directions *D1* and *D3*, and 4 exposed buildings for the eastern wind direction *D2*.

The congested traffic logically leads to extended polluted areas for all the wind directions. The eastern wind direction is again the most critical with 18 exposed buildings. It seems quite consistent as this direction orientates the plume towards the denser built-up area around the *CSC*. Other wind directions also lead to a higher number of exposed buildings than traffic *T1*, but to a lesser extend: wind direction *D1* exposes an additional apartment building, and wind direction D3 exposes 4 additional houses.

The sensitivity of the site with a low wind speed condition has, thus, been demonstrated with both traffic conditions and the three wind directions: two to 18 buildings exposed buildings were listed among simulations.

A sensitivity analysis, which is not the topic of this article, demonstrated that the risky conditions leading to the exposure of one building at least, may occur during 3% of the time, which remains quite low.

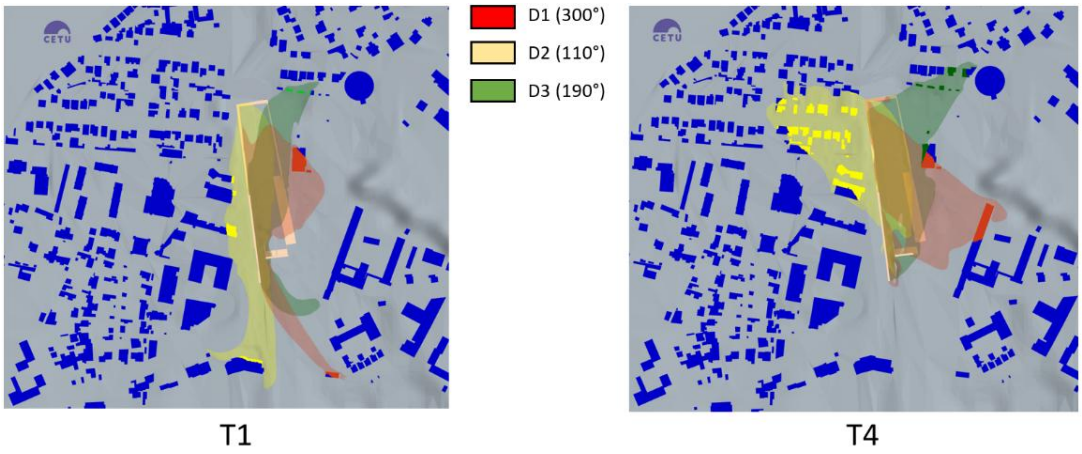


Figure 6: Pollution slicks with the three wind directions, for a rush hour traffic (a), congested traffic (b)

3.2. The mitigation solution

As described in the introduction, the mitigation solution proposed to improve the air quality around the *CSC* will be called over-ventilation. Triggering the over-ventilation led to air velocities between 4.6 and 7.8 m/s depending on scenarios, against velocities between 0.8 and 3.8 m/s without over-ventilation. To test its effectiveness, we assumed the same conditions as presented in section 3.1, and we calculated the new concentration and velocity of each plume consistent with the ventilation system of tunnels operating at its maximum speed. The over-ventilation strategy increases the velocity of plumes, while decreasing its pollutant concentration by the additional dilution it provides. Two over-ventilation scenarios were tested: an over-ventilation of the northern tunnel alone, and an over-ventilation of both tunnels simultaneously.

Figure 7 shows the influence of both over-ventilation scenarios in terms of reduction of both the polluted areas and the exposed building facades. Results are given for the congested traffic *T4* only, which has been demonstrated as the most critical in terms of air quality in the previous section. The three figures are relative to the three wind directions. Note that colours are identical to those in Figure 6, but they have here a different meaning: the red colour stands for the case with no over-ventilation, the green colour stands for the over-ventilation of the northern tunnel only, and the yellow colours refers to the over-ventilation of both tunnels.

The over-ventilation of the northern tunnel alone (green colour) seems to reduce slightly the area of the pollution slick, and deviates the plume towards the south for each wind direction. The deviation of the plume is consistent with the increased velocity of the plume of the northern tunnel compared to the one of the southern tunnel, that adds a dissymmetry of the flow inside the *CSC*. The velocity of the plume of the northern tunnel prevails over the one of the southern tunnel, thus orienting the global plume towards the south. The area of the pollution slick may still remain quite large (see *D1* and *D3*), but the zone in the south is a less densely built-up area. As a consequence, the number of exposed buildings is significantly reduced: one building (compared to 18 without over-ventilation) is exposed for the eastern wind direction (D2), and no more buildings are at risk for the two other wind directions.

The over-ventilation of both tunnels simultaneously allows to significantly reduce the area of the polluted areas, which remains located close to the *CSC*. Two buildings remain slightly exposed for the eastern direction (compared to 18 without over-ventilation).

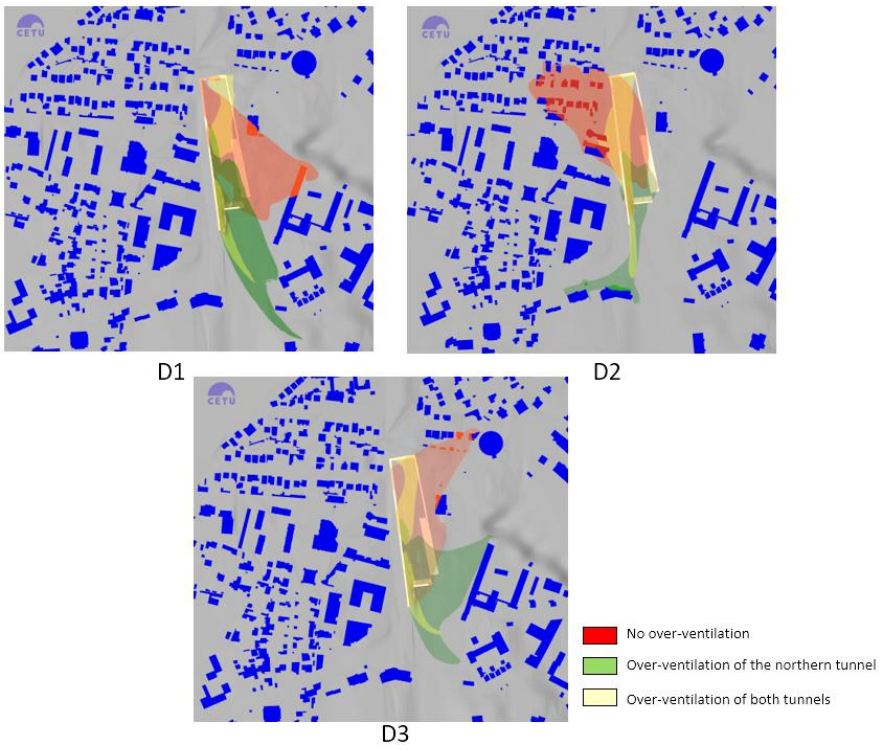


Figure 7: Influence of the over-ventilation for the congested traffic

Table 2 presents the averages and the standard deviations (Sd) of the areas of both the polluted areas and the exposed building facades on all simulations (including traffic condition *T1*). Results are given according to the over-ventilation scenario. Regarding the exposed building facades, the reduction allowed by both over-ventilation scenarios are significant: about 100 % and 95 % respectively for the over-ventilation of both and single tunnels. Reductions of the mean areas of the polluted areas are about 47 % and 24 % according to the over-ventilation scenario. In terms of polluted areas, the over-ventilation of both tunnels is, thus, significantly more effective. The significantly smaller standard deviations allowed by both over-ventilation scenarios suggest that pollution areas are less sensitive to other conditions (traffic and wind) than with no over-ventilation.

Table 2: Average areas of the polluted areas and the exposed building facades

	Building facades		Pollution slick	
	Mean [m²]	Sd [m²]	Mean [m²]	Sd [m²]
No over-ventilation	724,5	756,9	18503	2664
Over-ventilation both tunnels	1,3	3,1	9782	1334
Over-ventilation single tunnel	37,2	90,5	14050	1979

4. SUMMARY AND CONCLUSION

A CFD model of the pollutant dispersion around a real cut street canyon field-case has been carefully implemented and validated against experimental data. It was then used to identify the risk of exposure of buildings to NO_2 concentrations above the French hourly regulatory level. Simulations with a traffic representative of the rush hour with almost no wind showed that the site was indeed sensitive to traffic pollution, especially at the extreme proximity of the cut street canyon.

The potential of the mitigation solution called here “over-ventilation” was established by the significant reduction of both the polluted areas and the exposed facades of buildings. On average the over-ventilation of both tunnels allowed to reduce the exposed facades by 100% and the polluted areas by 47%. The next step would be to effectively control the ventilation system with NO_2 sensors located close to the most sensitive buildings. The technical challenges regarding the linking of sensors to the Tunnel Control System were not treated here and will be the subject of further development.

5. REFERENCES

[1] Y.-B. Wen, Z.-R. Huang, Y.-F. Tang, D.-R. Li, Y.-J. Zhang, et F.-Y. Zhao, « Air exchange rate and pollutant dispersion inside compact urban street canyons with combined wind and thermal driven natural ventilations: Effects of non-uniform building heights and unstable thermal stratifications », *Sci. Total Environ.*, vol. 851, p. 158053, déc. 2022, doi: 10.1016/j.scitotenv.2022.158053.

[2] X. Li, C. Liu, D. Leung, et K. Lam, « Recent progress in CFD modelling of wind field and pollutant transport in street canyons », *Atmos. Environ.*, vol. 40, n° 29, p. 5640-5658, sept. 2006, doi: 10.1016/j.atmosenv.2006.04.055.

[3] D. Guo, T. Han, F. Yang, Y. Li, J. Zhang, et X.-F. Wang, « Numerical simulation studies of the flow field and pollutant diffusion around street canyons under different thermal stratifications », *Atmospheric Pollut. Res.*, vol. 14, n° 8, p. 101829, août 2023, doi: 10.1016/j.apr.2023.101829.

[4] J.-F. Burkhart *et al.*, « Project Borée: controlling road-tunnel ventilation by means of a network of microsensors, in order to reduce the exposure of the local population to pollutants - Background, methodology and initial results », *18th Int. Symp. Aerodyn. Vent. Fire Tunn. ISAVFT Proc.*, p. 79-95, 2019.

[5] R. Boissat et E. Revelat, « Projet Borée - Novembre 2021 ». 2021.

[6] M. Lateb, R. N. Meroney, M. Yataghene, H. Fellouah, F. Saleh, et M. C. Boufadel, « On the use of numerical modelling for near-field pollutant dispersion in urban environments − A review », *Environ. Pollut.*, vol. 208, p. 271-283, janv. 2016, doi: 10.1016/j.envpol.2015.07.039.

[7] X. Zhou *et al.*, « Large eddy simulation of the effect of unstable thermal stratification on airflow and pollutant dispersion around a rectangular building », *J. Wind Eng. Ind. Aerodyn.*, vol. 211, p. 104526, avr. 2021, doi: 10.1016/j.jweia.2021.104526.

[8] C. Alinot, « Aerodynamic Simulations of Wind Turbines Operating in Atmospheric Boundary Layer With Various Thermal Stratifications », 2002.

[9] J. E. Pieterse et T. M. Harms, « CFD investigation of the atmospheric boundary layer under different thermal stability conditions », *J. Wind Eng. Ind. Aerodyn.*, vol. 121, p. 82-97, oct. 2013, doi: 10.1016/j.jweia.2013.07.014.

[10] L. Soulhac, P. Salizzoni, F.-X. Cierco, et R. Perkins, « The model SIRANE for atmospheric urban pollutant dispersion; part I, presentation of the model », *Atmos. Environ.*, vol. 45, n° 39, p. 7379-7395, déc. 2011, doi: 10.1016/j.atmosenv.2011.07.008.

[11] A. U. Weerasuriya, X. Zhang, K. T. Tse, C.-H. Liu, et K. C. S. Kwok, « RANS simulation of near-field dispersion of reactive air pollutants », *Build. Environ.*, vol. 207, p. 108553, janv. 2022, doi: 10.1016/j.buildenv.2021.108553.

[12] H. J. Breedt, K. J. Craig, et V. D. Jothiprakasam, « Monin-Obukhov similarity theory and its application to wind flow modelling over complex terrain », *J. Wind Eng. Ind. Aerodyn.*, vol. 182, p. 308-321, nov. 2018, doi: 10.1016/j.jweia.2018.09.026.

[13] J. C. Chang et S. R. Hanna, « Air quality model performance evaluation », *Meteorol. Atmospheric Phys.*, vol. 87, n° 1-3, sept. 2004, doi: 10.1007/s00703-003-0070-7.

[14] B. Alam, R. Nkenfack Soppi, A.-A. Feiz, P. Ngae, A. Chpoun, et P. Kumar, « CFD simulation of pollutant dispersion using anisotropic models: Application to an urban like environment under neutral and stable atmospheric conditions », *Atmos. Environ.*, vol. 318, p. 120263, févr. 2024, doi: 10.1016/j.atmosenv.2023.120263.

[15] S.-J. Mei, Y. Zhao, T. Talwar, J. Carmeliet, et C. Yuan, « Neighborhood scale traffic pollutant dispersion subject to different wind-buoyancy ratios: A LES case study in Singapore », *Build. Environ.*, vol. 228, p. 109831, janv. 2023, doi: 10.1016/j.buildenv.2022.109831.

SMOKE RECIRCULATION AT ROAD-TUNNEL PORTALS

Marco Bettelini, Marco Tobler, Raphaël Defert

Amberg Engineering Ltd, CH

DOI 10.3217/978-3-99161-087-8-026 (CC BY-NC 4.0)
https://creativecommons.org/licenses/by/4.0/deed.de
This CC license does not apply to third party material (attributed to other sources) and content noted otherwise.

ABSTRACT

In case of fire in twin-tube tunnel systems, the parallel tube is commonly used as a haven for self-rescue and plays an essential role for intervention. This requires a high level of protection against smoke penetration through cross connections and tunnel portals. Structural (e.g. shifting of portals or anti-recirculation walls) and technical measures (primarily appropriate ventilation control) are commonly adopted for preventing portal recirculation. Anti-recirculation walls are frequently unwanted, mainly because of their visual and operational impact as well as cost. Project-related detailed investigations showed that the benefits from anti-recirculation walls are at times lower than expected. This paper provides guidance for screening and detailed assessment of requirements and benefits. Appropriate numerical simulations can help to avoid large structural measures with low effectiveness.

Keywords: Road tunnel, portal smoke recirculation, anti-recirculation wall.

1. INTRODUCTION AND OBJECTIVES

In case of fire in twin-tube tunnel systems, the parallel tube plays an essential role as a haven for self-rescue and as access and working area for intervention. This requires a very high level of protection against smoke penetration through cross connections and tunnel portals. This paper focuses on portal smoke recirculation in twin-tube road tunnels.

Constructional and technical measures are commonly adopted for preventing portal recirculation, such as shifted portals or anti-recirculation walls. National regulations and international recommendations often provide specific prescriptions or functional guidance. Such measures can be invasive and are typically unwanted mainly because of their visual impact and cost. Technical reasons, such as load on bridges or viaducts directly connected with tunnel portals, might also play an important role in special cases. Portal recirculation is intimately related to geometric, operational and environmental conditions. Detailed analyses carried out for specific project-related configurations show widely variable benefits from anti-recirculation measures. While they play an essential role in most cases for ensuring a proper safety level, they only show marginal benefits in others.

The first part of this paper focuses on the phenomenological description of portal recirculation and discussion of relevant issues, requirements and design objectives, normative prescriptions and state-of-the-art. The second part provides specific guidance for the evaluation of practically relevant situations and describes methodological approaches for screening and analysis. Finally, representative real-life examples illustrate the approach for verifying the need and the effectiveness of anti-recirculation measures and how appropriate numerical simulations, involving coupled 1D and 3D simulations, can help to avoid costly constructional

measures with low effectiveness. The main focus here is set on methodological aspects rather than on technical details such as simulation technology and setup.

2. PHENOMENOLOGICAL DESCRIPTION AND SAFETY IMPLICATIONS

In twin-tube tunnels, self-rescue in case of a relevant accident is generally based on cross connections. Evacuees reach the parallel tunnel tube, where they can safely wait for rescue. The non-incident tube also plays an essential role in terms of intervention. Depending on the specific intervention strategy adopted by the first responders, it might host the bulk of the intervention effort or at least be used for the secondary intervention. Persons requiring emergency support and medical attention are generally carried into the parallel tube. The requirements on safety and air quality within the non-incident tunnel tube play therefore a central role in the overall safety concept. Smoke penetration through cross connections or through the portals must be prevented at any time. It is important to note that comparatively low levels of smoke penetration, resulting in smoke concentrations well below health-relevant thresholds, can have a significant impact. Persons escaping through a cross connection might perceive a partly smoke-filled parallel tunnel tube as unsafe and return to the fire tube. An additional requirement is the protection of the portal areas against noxious impacts, as evacuees may receive medical assistance or just wait in the immediate vicinity of the portals. The areas reserved for supporting and coordinating intervention are also located nearby.

In principle, portal recirculation can occur whenever smoke flows or is actively expelled from a tunnel portal. This phenomenon is particularly intense in case of air inflow into the parallel tunnel tube, unless the axial or lateral distance between the tunnel portals is sufficient. Portal configuration, wind and wind exposition also play an important role. The length of the influence area at the exhaust portal can generally be assumed to be in the order of 100 m. This can be significantly longer in case of smoke expulsion at high velocity (jet-type portal outflow with low thermal effects) and shorter e.g. in case of large fires coupled with comparatively low air velocity, where the hot smoke tends to rise rapidly at the portal. The area of influence at the inlet of the parallel tunnel tube is significantly shorter, in the order of 20 to 30 m. For this reason, portal shifting in axial direction is a very effective constructional measure against portal recirculation. This requires a prolongation / displacement of the exit portal by at least 30 m or of the entry portal by at least 100 m. An effective alternative is a roughly 30 m long separating wall between the two tunnel portals.

Tunnels equipped with longitudinal ventilation systems are particularly critical in terms of portal recirculation because of the steady smoke outflow from a portal during practically the whole duration of the emergency. The appropriate ventilation strategy in this case is flow reversal in the safe tunnel tube with an air velocity of at least 1 m/s. This measure is generally not sufficient for keeping the portal area free from smoke but effectively prevents smoke penetration into the safe tunnel tube. Flow reversal typically requires a few minutes, mainly because of the natural ventilation generated by the vehicles leaving the tunnel. Some level of smoke penetration during this initial stage cannot be entirely prevented by ventilation alone, particularly for long tunnels and in case of fires located close to the exit portal. Ventilation systems with smoke extraction are significantly less critical because smoke outflow from the tunnel portal only occurs during the first minutes after fire onset, before smoke confinement is effective, or in case of a fire located in the immediate vicinity of the exit portal, for which longitudinal smoke expulsion is typically the strategy of choice. Issues and prevention strategies are similar as in case of longitudinal ventilation.

Portal recirculation in short, naturally ventilated tunnels is significantly more complex. Different effects impact natural ventilation in the two tunnel tubes at different levels and at

different times. This particularly includes the initial traffic impact, the fire stack effect, which typically increases within the first minutes of a fire incident, and environmental effects, such as temperature difference, portal wind or barometric pressure difference. These environmental effects can vary rapidly during a fire incident and are likely to act in very different ways depending on season and meteorological conditions. These challenging conditions shall be addressed in more detail in Chapter 5.

For the purposes of this paper, it will be distinguished between transient (short-term) and sustained smoke recirculation. The former only occurs in the very first minutes of a fire scenario, e.g. before automatic fire ventilation can implement the proper fire ventilation strategy. Conversely, sustained portal recirculation is more or less a steady-state phenomenon, due e.g. to inappropriate ventilation strategy or to the combined action of natural ventilation and wind.

3. REGULATIONS AND STATE-OF-THE-ART

The risk of smoke recirculation at the portals of a twin-tube tunnel has found its way into the regulatory requirements in some countries, while other ones, e.g. France, just mention the issue and call for appropriate solutions without specification. National prescriptions are quite similar. The German RE-ING prescribes an offset between the portals of 30 m or a 30 m long anti-recirculation wall with the same height as the portal. The Swiss guideline for ventilation in road tunnels (ASTRA 13001) bases its requirements on the concept of an exhaust zone stretching 100 m from the exit portal and an intake zone for 30 m ahead of the entry portal. This results in largely similar requirements to the German guideline albeit accounting for the difference between air intake and expulsion jet behaviors. The Brazilian regulation requires a physical separation between the exhaust of the fire tube over a length of 100 m and the intake of the safe tunnel tube over a length of 30 m at each portal. Specific measures include a minimum lateral distance of 60 m between the portals, a longitudinal shift, the construction of anti-recirculation walls or combinations thereof.

Real-life experience and simulation proved that the normative prescriptions are generally effective. In several countries, e.g. Switzerland, anti-recirculation walls are a standard component for new or retrofitted tunnels. In other countries this issue has low or no priority.

4. RELEVANT PARAMETERS AND CLASSIFICATION

Various factors impact the risk and severity of portal recirculation in a twin-tube tunnel with a given portal arrangement, such as tunnel length, longitudinal slope, cross section, fire heat release rate, meteorological conditions, ventilation system, traffic volume, etc. This study mainly focuses on sustained portal recirculation that can have a relevant safety impact in terms of self-rescue or intervention. Tunnel length and tunnel ventilation system are two key parameters for smoke recirculation. Though countries differ in the details, the choice of ventilation system generally correlates directly with its length. Short tunnels allow for natural ventilation, intermediate ones are equipped with a longitudinal ventilation system using jet fans or Saccardo nozzles and long tunnels are equipped with smoke extraction systems. For twin-tube road tunnels with unidirectional traffic the classification of length is assumed herein to be roughly according to the following categories: short tunnels reach up to 1 km, intermediate ones up to 3-5 km and long tunnels beyond that. For the present purposes this simplified correlation is sufficient. Further key parameters include longitudinal slope, portal configuration and meteorological effects, such as wind, barometric pressure differences and natural thermal effects. Further parameters, such as traffic volumes and characteristics or

tunnel cross section, might play a role in some situations but are generally less relevant. Longitudinal slope, coupled with fire heat release rate, directly impacts longitudinal air velocity and smoke propagation. For these reasons, portal smoke recirculation shall be discussed primarily in terms of tunnel length / ventilation system and longitudinal slope in the fire tube. Fire intensity is subject to rapid variations in time and varies from case to case. It should be treated as range, with assumptions on the (traffic-dependent) likely maximum and development time.

A first rough categorization and ranking in terms of risk of portal smoke recirculation is summarized in Table 1. The classification "High" suggests that smoke recirculation is likely to be an issue deserving appropriate attention. "Low" suggests that it might be possible to evaluate deviations from normative requirements if they result in excessive functional, aesthetic or economic constraints.

Table 1: Categorization of tunnels in terms of risk of portal smoke recirculation

Tunnel categorization and expected risk of recirculation		Longitudinal slope		
		< -3%	**-1.5% to 1.5%**	**> 3%**
Tunnel length / Ventilation systems	**< 1 km Natural ventilation**	Low	Medium	High
	1 - 5 km Longitudinal ventilation	Medium	Medium	Medium
	> 5 km Smoke extraction	Low	Low	Low

5. SHORT TUNNELS WITH NATURAL VENTILATION

Short tunnels allow generally for short self-rescue times and natural ventilation is frequently the accepted solution. As a result, airflow is purely driven by a complex combination of traffic-related and natural effects. At times of high traffic, the airflow is mainly driven by traffic and at other times mostly driven by the wind. Barometric pressure differences and stack effect due to natural temperature differences are frequently negligible. In the event of a fire in a short tunnel, traffic influence quickly disappears, and transient portal smoke recirculation is virtually negligible. The driving parameters are in most cases external wind and stack effect.

In case of small tunnel slope (typically below 1%), the aerodynamics of smoke recirculation is largely governed by wind. Both tunnel tubes behave in a similar manner, the airflow in both tunnel tubes is generally in the same direction and the risk of relevant sustained smoke recirculation is low.

The situation in case of significant tunnel slope is more challenging. As fire develops, the incident-tube's airflow will be driven by the fire's stack effect and smoke will propagate towards the upper portal. In case of slopes over 2-3% and HGV fires with substantial heat-release rate, wind impacts on the incident tube will be relatively weak to negligible. Conversely, the non-incident tube will develop an airflow that depends on portal wind. This represents a significant risk, as this can easily lead to substantial airflows in the two tubes going in opposite directions for a tunnel that lacks mechanical ventilation to oppose these trends. The potential for strong, sustained smoke recirculation at the upper portal is therefore significant. Conversely, the lower portal will only experience short-term (transient) recirculation for up to 2-3 minutes with fire in the tube with descending traffic. Considering typical fire-development curves, this is mostly negligible. For fires in the tube for ascending

traffic, recirculation at lower portal is reduced/eliminated even further. There is hence potential for removing the anti-recirculation wall at the lower portal.

The risk of portal recirculation at the upper portal depends on the complex interaction between portal configuration and wind characteristics. Anti-recirculation walls should not be removed without a detailed analysis carried out considering the specific portal geometry and the local wind rose. Examples are presented in Chapter 8.

6. INTERMEDIATE TUNNELS WITH LONGITUDINAL VENTILATION

In principle, longitudinal ventilation systems provide ideal conditions for transient and sustained portal smoke recirculation. With the possible exception of extended traffic congestion, the preferred ventilation strategy is generally to support the natural airflow induced by the traffic in the tunnel using e.g. jet fans, resulting in opposite flow directions in the two tubes. The accepted ventilation strategy for mitigation of portal-recirculation into the safe tunnel tube is flow reversal. This can be assumed to work safely, independently of meteorological conditions and traffic, as long as ventilation is correctly designed. Smoke outflow can begin immediately in case of fire close to the tunnel exit or take up to roughly 15 minutes in case of a fire at the entrance of a 5 km tunnel. Flow reversal in the safe tunnel tube can typically be achieved in 5 to 10 minutes. An illustrative example (tunnel with length 4 km, slope 2.5%, 2 traffic lanes, longitudinal ventilation with jet fans, traffic per direction 1000 vehicles/h at 100 km/h, 50 MW fire developing within 10 minutes, no portal pressure differences) is presented in Figure 1. Fire is detected 2 minutes after onset and ventilation reaches full power 1 minute later. Under these specific conditions, significant smoke recirculation may occur between roughly 3 and 7 minutes after fire onset.

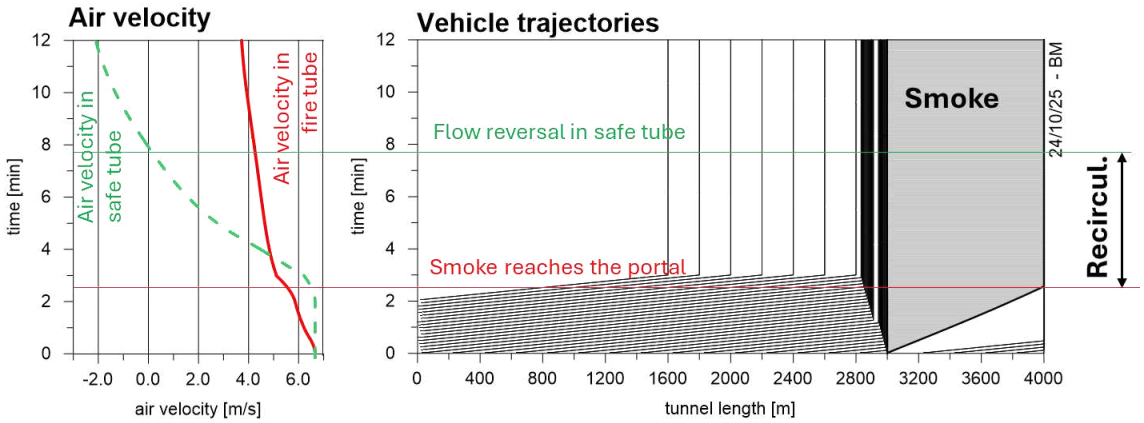


Figure 1: Vehicles trajectories and smoke propagation (right) and air velocity (left) [1].

Transient smoke recirculation into the safe tunnel tube might therefore last for at most 5-10 minutes. Depending on the specific conditions and considering typical fire heat-release rates in road-tunnel fires, this might be deemed acceptable, and one could consider eliminating the corresponding anti-recirculation walls. Under these conditions, smoke outflow from the fire tube might last for typically 30 to 60 minutes or longer. Appropriate considerations on specific portal configurations, and specifically the location of emergency meeting points and intervention points, are suggested, since smoke impact on these facilities would typically last for the whole duration of the fire. As a general conclusion, removal of accepted anti-recirculation facilities should only be considered, if they represent a real issue.

7. LONG TUNNELS WITH SMOKE EXTRATION

The preferred smoke-confinement strategy in case of transverse or semi-transverse ventilation with smoke extraction is concentrated smoke extraction in the immediate vicinity of the fire. Smoke extraction systems greatly alleviate the risk of sustained recirculation of smoke at the portals. Smoke extraction systems are designed to extract all smoke produced in the fire, thus preventing smoke propagation beyond the extraction. Smoke is therefore generally not expected to reach a portal in significant quantity/density. Hence, the risk of smoke recirculation in long tunnels only concerns smoke released at early stages, before smoke extraction reaches nominal operation, or for fires located close to the exit portal, where emergency ventilation cannot prevent smoke exhaustion at the portal. There is therefore generally no risk of sustained portal smoke recirculation once flow conditions in the tunnel system have reached steady state.

Fires located close to the exit portal (typically up to 200-300 m) represent a very important exception, since direct portal blowout typically represents the preferred strategy. The relevant phenomena in case of fire at the tunnel exit are analogous to the case of longitudinal ventilation, with the following particularities: under such conditions, smoke reaches the tunnel portal very rapidly and flow reversal in the opposite tunnel tube can take up to 15-20 minutes, the time required for traffic effects to decay to a level compatible with the capabilities of longitudinal airflow control. Self-rescue can therefore be inhibited by smoke penetration from the beginning and for a significant time period. This may also have a severe impact on intervention in the case of major tunnels with their own firefighting stations located by the tunnel portals (St. Gotthard, San Bernardino, Mont Blanc, Fréjus etc.).

The impact of transient smoke recirculation in case of a fire located farther away from the tunnel exit is generally very limited, despite the comparatively long time required for achieving smoke confinement. Self-rescue could be impacted by smoke recirculation, but only after several minutes, because of the time required for smoke to reach the portal and from there the cross connections used for self-rescue or intervention. Meteorological effects and tunnel longitudinal slope are also unlikely to have a significant impact, in spite of possibly very large barometric pressure differences of the order of several 100 Pa, since state-of-the-art ventilation systems are designed for mastering such effects.

8. ANALYSIS – METHODOLOGICAL APPROACH AND REAL-LIFE APPLICATIONS

8.1. Methodological approach

The preferred approach for assessing issues related to transient and sustained portal recirculation varies from project to project and is largely driven by the specific objectives of the investigation. Nevertheless, experience shows that the following general approach is appropriate in most cases:

1. Clear identification of the objectives of the investigation
2. Systematic gathering of all relevant tunnel, traffic and environmental conditions and identification of the specific scenarios which are relevant for portal recirculation
3. Preliminary screening based on 1D-simulation of relevant scenarios (airflow, smoke propagation and people movement) and engineering assessment
4. Detailed investigation of the potentially critical scenarios (if any) identified in the previous step

Based on the identified scenarios that pose a potential risk for portal recirculation, the airflow in the two tubes can be evaluated through 1D-simulation (step 3). A comprehensive model for this can already estimate the evolution of the smoke propagation in the incident tube. Together with the simulation of the non-incident tube, this provides a clear indication of when recirculation is possible (simultaneous smoke exhaustion at one portal and air intake in the parallel one). This leads to a prioritized list of scenarios and might lead to a conclusive evaluation for part of them.

The detailed investigation of the leading scenarios (step 4) needs to be based on 3D-simulation of smoke propagation in the tunnel and primarily in the area around the portals. This step enables full consideration of portal design in the evaluation, which is not feasible in the previous step. The conditions in the two tubes have been derived in the previous step and can be implemented into the boundary conditions of the 3D-simulation. Portal design as well as the surrounding landscape need to be appropriately represented in a 3D-model and included in the simulation with adequate accuracy (meshing and modeling of local wind conditions) and geometric extension, making these analyses quite expensive.

8.2. Application – Very short tunnel with large slope and natural ventilation

This example focuses on a short and very steep, short tunnel (length 280 m, slope 9%, 5 cross connections, daily traffic lower than 20’000 vehicles/day with low HGV percentage). Portal-recirculation patterns are clearly dominated by the interaction between portal wind and stack effect. Based on screening and 1D-simulation, the risk of sustained recirculation at the lower portal could be ruled out as virtually negligible and the corresponding anti-recirculation wall could be removed.

The analysis of the upper portal is much more complex because of the significant risk of sustained portal recirculation due to stack effect and unfavorable wind patterns. A screening procedure identified the most critical statistically relevant wind conditions. The corresponding scenarios with and without anti-recirculation wall were analyzed in detail using FDS [2]. The results without and with recirculation wall are shown in Figure 2 and Figure 3-The color contours represent visibility at 2 m height, ranging from 0 m (red contours) to 30 m or more (blue). The acceptable range, 10 to 20 m, is represented in green.

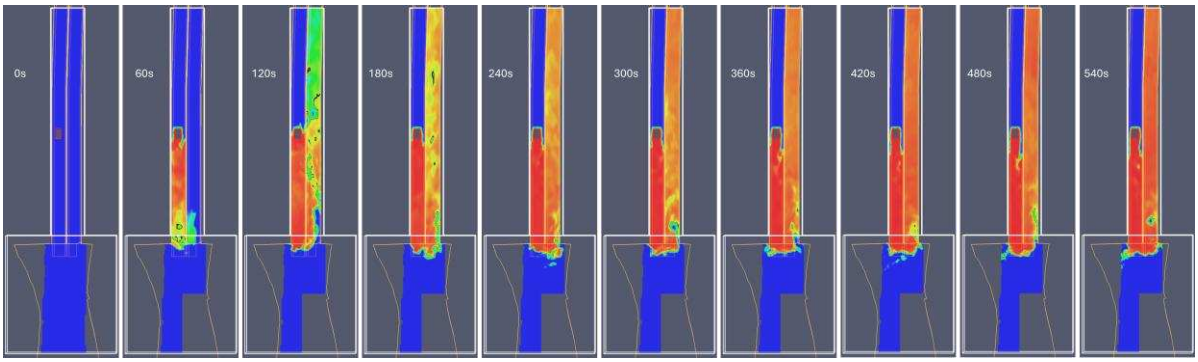


Figure 2: Smoke recirculation at upper portal without anti-recirculation wall.

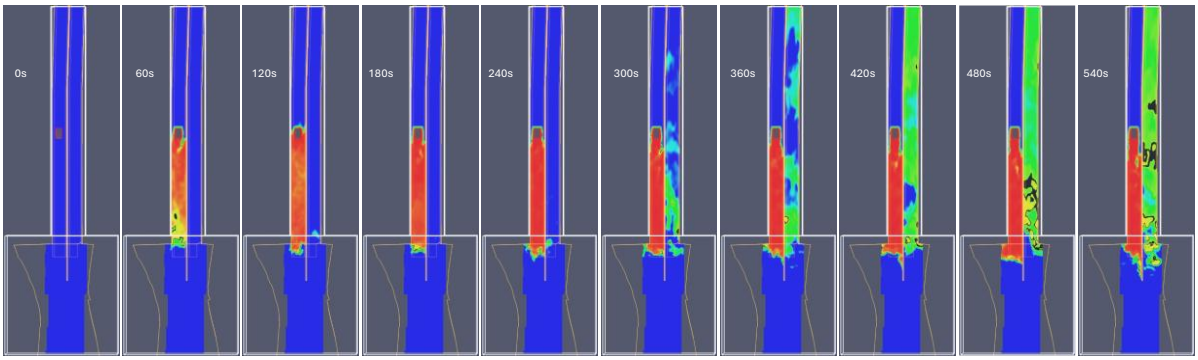


Figure 3: Smoke recirculation at upper portal with anti-recirculation wall.

The results clearly show that the anti-recirculation wall is required and very effective. Detailed analysis showed that its length can be safely reduced to 15-20 m.

8.3. Application – Tunnel with natural ventilation and low slope

A detailed investigation on smoke recirculation for the Swiss Riedberg tunnel (length 537 / 565 m, slope 1.2%, traffic volume 16'000 vehicles/day with 10% HGV) was carried out by Guetg et al. [3]. The realization of anti-recirculation walls in a very exposed area posed serious visual and static challenges, with tunnel exit on a bridge on one side. This is a typical example of a complex situation, where many different recirculation patterns result from complex portal configurations and wind conditions. A statistical approach was selected, based on a) Identification of specific potential damage patterns, b) Detailed analysis of all relevant scenarios, c) Identification of cases with strong / mild / minor recirculation and damage assessment and d) Consolidation in terms of expected number of fatalities and injuries per year. The final decision was based on a cost/benefit analysis.

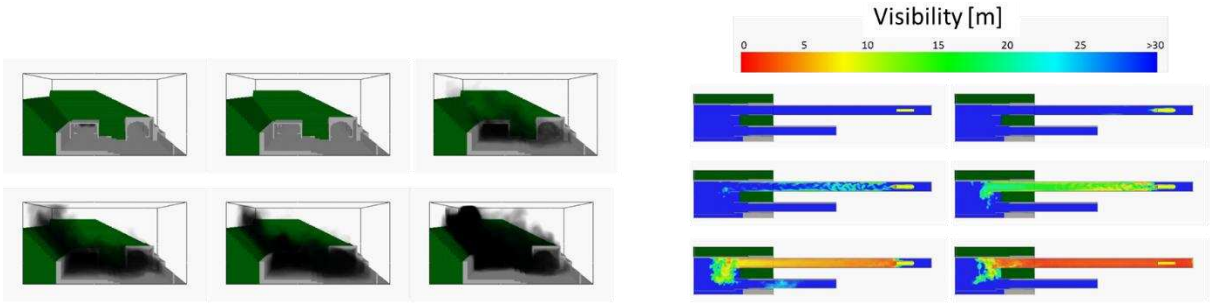


Figure 4: Leading smoke-recirculation scenarios for Riedberg tunnel [3].

9. SUMMARY AND CONCLUSION

Structural and technical measures against smoke recirculation through tunnel portals in case of fire are well established in several countries but are widely ignored elsewhere. Regulatory prescriptions, as they are formulated in several national regulations, are generally very effective but fail to catch the particularities and specific needs of each project. Short and intermediate-length tunnels with natural or longitudinal ventilation generally pose the highest requirements. Specific project-related investigations are strongly recommended.

The overall impact from structural measures can be very significant, particularly for urban tunnels. Simple screening procedures and detailed analysis as outlined herein help to establish project-specific requirements and to achieve tailored solutions for critical situations. As shown in the examples illustrated herein, the potential for preventing onerous measures with low effectiveness by means of appropriate screening and analysis is significant.

10. REFERENCES

[1] M. Bettelini, “Transient One-Dimensional Simulation for Optimum Road-Tunnel Ventilation”, ITA-AITES World Tunnel Congress, Sept. 19-25, 2008, Agra, India.

[2] Fire Dynamics Simulator (FDS), https://pages.nist.gov/fds-smv/

[3] F. Guetg, J. Amberg, M. Bettelini, “Prevention of portal recirculation for the Riedberg tunnel”, 19th International Symposium on Aerodynamics, Ventilation and Fire in Tunnels, Brighton, UK, 18th-30th September 2022.

APPLICATION OF LOW-TECH AND LEAN-TECH CONCEPTS TO ROAD TUNNELS FOR GREATER ENERGY EFFICIENCY

Tristan Regnier, Olivier Martinetto, Florent Guiral

Egis, FR

DOI 10.3217/978-3-99161-087-8-027 (CC BY-NC 4.0)
https://creativecommons.org/licenses/by/4.0/deed.de
This CC license does not apply to third party material (attributed to other sources) and content noted otherwise.

ABSTRACT

Our planet is facing a major climatic challenge, which is becoming increasingly acute and critical.

The need for underground communications infrastructure, to be maintained or created, remains strong in all countries to meet the needs of trade, travel and development.

These infrastructures can be money pits with a high carbon footprint. Simply optimising a system, is not enough to meet the challenges. The usual reliance on technology and the development of new systems in the hope of reducing the energy balance, while relevant in some cases, can be a headlong rush or an illusion with no guarantee of overall savings.

In this context, a different, holistic approach seems necessary in terms of design, operation and maintenance, and even use. The entire life cycle of the structure is concerned, particularly the design and operation phases:

- The design phase is totally structuring even if it is one of the shortest. It obviously involves a series of technical choices dictated by regulatory requirements, but which must also meet the specific constraints of operation and maintenance and the level of service expected of the structure, a level that is often poorly defined. It also deals with the criteria for choosing and procuring supplies, which are often neglected for lack of a suitable analysis tool.
- The operating phase, which is intended to be as long as possible, is crucial. Beyond the ‘established regime’, this phase includes major maintenance and renewal stages that must be taken into account right from the design stage.

This article looks at the practical implementation and convergence of different approaches:

- Low-Tech: using solutions technologically “sober” in terms of natural resources and energy consumption
- Lean-Tech: using technology as “leanly” as possible
- Design for Maintenance (DfM): maintenance/maintainability-oriented design
- Reliability Maintainability Availability Safety (RAMS) of “systems”

Keywords: low-tech, lean-tech, avoid, reduce, offset.

1. INTRODUCTION

The design of a road tunnel must take into account numerous parameters, including economic and social function, regulatory requirements, the environment surrounding the structure,

traffic characteristics, operating and maintenance resources, and investment and operating/maintenance budgets.

The equipment systems used are increasingly numerous and sophisticated in order to offer unrivalled levels of safety and service, at the risk of increasing energy consumption.

In this era of energy efficiency, beyond the usual levers for action on direct consumption specific to structures, it seems worthwhile to promote eco-design approaches such as low-tech or lean-tech and to highlight their similarities with more well-known approaches such as DfM and RAMS.

In terms of eco-design, road tunnels have multiple direct and indirect impacts and interactions with seven commonly identified environmental themes:



Figure 1: Environmental themes

Faced with the major climate challenge facing our planet, one of the basic principles is to avoid or reduce environmental impacts as much as possible (1), or where necessary to offset them, taking into account the entire life cycle of the structure. This 'ARO' (avoid, reduce offset) approach is illustrated below.

(1) *ensuring that improvements in one area do not significantly harm others.*

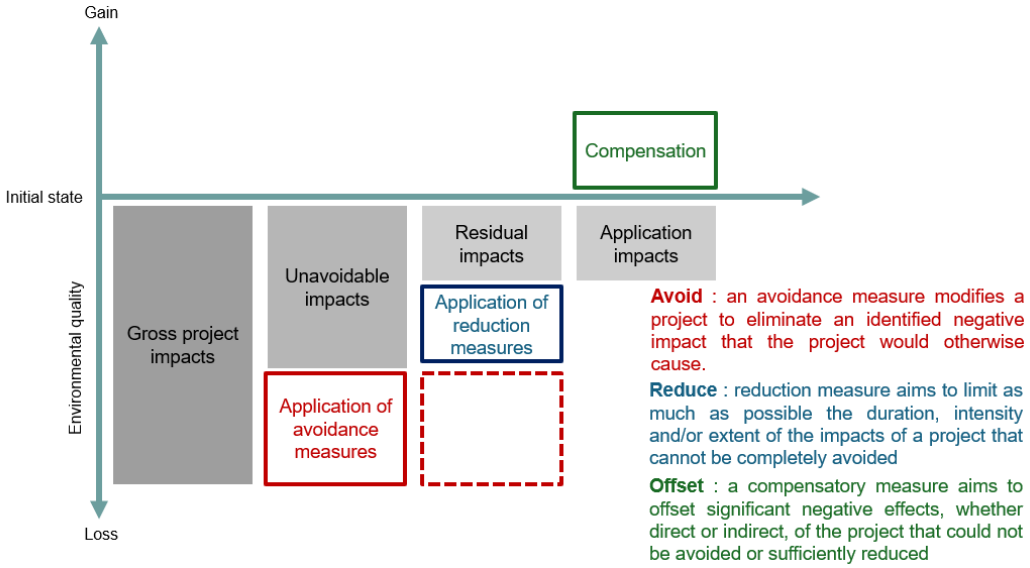


Figure 2: 'ARO' approach

The aim of this article is therefore to encourage design offices, project managers, contractors and operators of road tunnels to place eco-design at the heart of their concerns, with particular emphasis on energy and resource efficiency, the circular economy, carbon neutrality and

pollution control. To this end, the authors list a number of concrete solutions, propose avenues for reflection, open up new perspectives and share their questions. A methodology and recommendations are then suggested, before concluding.

The list of examples of solutions and avenues for consideration is structured around the first three phases of the project life cycle and some of the environmental themes. The contribution of each example to the ARO approach is indicated by a symbol. A R O

2. DESIGN PHASE

2.1. Energy efficiency

R
- Ensure economical design of the structure:
  - The layout (curves) impacts CCTV systems (and any associated automatic incident detection) and signalling systems.
  - the longitudinal profile (gradients, low points and high points) impacts drainage, lighting, fire protection, signalling, ventilation and video surveillance systems (and any associated automatic incident detection)
  - the cross-section (height, width, section) impacts lighting and ventilation systems

A
- Prioritise passive systems such as:
  - sunshades like those in the Jenner Tunnel (Le Havre, France), which replace supplementary lighting
  - gravity-fed firefighting and sanitation networks
  - buildings designed to limit heat gain and/or promote ventilation rather than air conditioning (Rtherm walls and doors).

A
- Eliminate redundancies that are not fully justified by the level of service or safety required and that prove to be energy-intensive, such as transformers and their no-load losses.

R
- Limit the need for electrical tracing (depth, insulation, circulation) related to sanitation and fire protection systems.

R
- Reduce the volume of effluent to be collected (intermediate collection, watertightness) from the sewerage network.

R
- Optimise lighting design criteria (exposure, environment, head treatment, road characteristics, provided that this does not involve transporting materials from too far away or negatively impacting the environment, permitted speed).

R
- Pay particular attention to the intrinsic efficiency of equipment and the optimisation of Joule losses, in particular:
  - efficiency of pumps and the delivery network (diameter and length of pipes, relay tanks)
  - efficiency of pumps and the fire protection network (diameter and length of pipes)
  - efficiency of inverters and variable speed drives of all kinds
  - efficiency of light sources and photometry of lighting fixtures
  - pooling of servers (virtualisation) required for supervision systems, networks, radio communications, emergency call networks, etc.

    This particular focus on efficiency, combined with the use of only the strictly necessary equipment, makes it possible to limit the resources required to equip the structure initially, then losses at source and therefore ventilation and/or air conditioning requirements, and finally the impact of GER works when they occur.

R
- Prioritise natural ventilation over forced ventilation and air conditioning.

2.2. Resource efficiency

A • Negotiate with the emergency services the possibility of providing fire suppression pressure using their fire engines rather than specific fixed installations (savings in installation, servicing, testing, maintenance, major maintenance renewal and associated easements).

? • Consider the choice of battery type for uninterrupted power supply and chargers (scarcity of metals/rare earths).

? • Which type of cable should you choose? Copper or aluminium? The following table looks at energy costs and CO_2 emissions, but does not mention the medium- or long-term availability of resources, their recycling rates, etc.

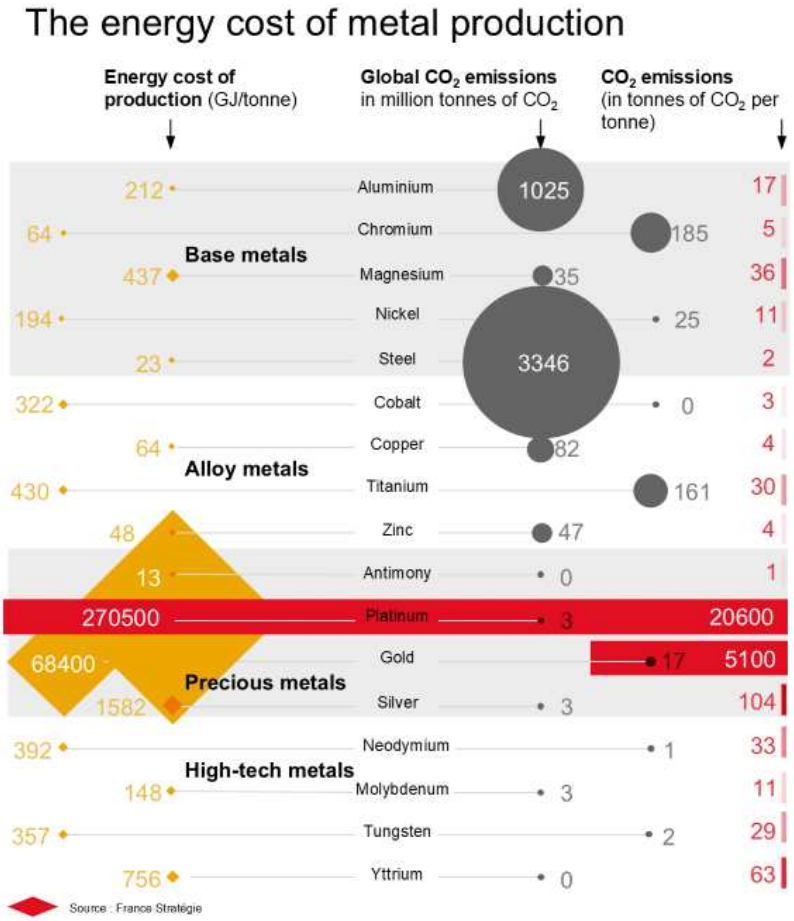


Figure 3: Energy cost of metal production

R • Avoid unnecessary equipment that is rarely or poorly used, as may be the case with the following systems:
  - o linear fire detection in tunnels
  - o extinguishing systems in technical rooms or tunnels

  In general, only install what is strictly necessary (in terms of equipment) and avoid compensating for weak civil engineering design with additional equipment: passive safety measures are always preferable to increased ventilation, a safe route is preferable to increased lighting and signage, etc.

R • Group equipment as much as possible on a limited number of technical sites – i.e. avoid isolated pockets of equipment.

R • Prioritise a robust design that is tailored to the specific context of the project.

R • Avoid corrosive materials and pay close attention to galvanic couples to ensure greater durability of sanitation, fire protection, ventilation, signalling and lighting systems, etc.

R • Require that repairs be possible and that components be replaceable rather than the entire piece of equipment or even the entire system (repairability index).

R • Respect the natural hydrological balance of the mountain ranges crossed, which may justify a roof-shaped longitudinal profile rather than a single slope.

O • Utilise surface water (separate network) for firefighting, filling siphon manholes or cooling premises.

2.3. Circular economy

R • Use recyclable or recycled materials that are abundant and easy or less difficult and energy-intensive to extract, produce or refine (steel rather than plastic, for example).

2.4. Carbon neutrality

A • Exclude SF6 from high-voltage equipment

A • Exclude (as far as possible) outdated technologies such as internal combustion engine generators.

R • Pay particular attention to the choice of heat transfer fluids for transformers and air conditioners, as well as the choice of acoustic insulation (for ventilation) and thermal insulation (for technical rooms).

R • Where possible, use renewable energy sources (solar, hydraulic, wind) for the needs of main technical rooms, for example.

R • Opt for a conventional heating system for technical and operating rooms rather than reversible air conditioning.

2.5. Pollution control

R • Limit gradients to reduce pollution from heavy vehicles.

A • Favour natural fluids in submerged transformers.

R • Choose paints carefully or limit their use.

2.6. Biodiversity

O • Provide wildlife crossings and other animal protection measures (toad tunnels, etc.).

3. IMPLEMENTATION PHASE

3.1. Energy efficiency

R • Ensure that the luminance meters and twilight sensors in the lighting system are correctly adjusted (including orientation) and, more generally, that all types of sensors are correctly calibrated.

3.2. Carbon neutrality / Circular economy

R • Consider the geographical origin of materials and equipment and promote reuse.

3.3. Biodiversity

R • Limit waste on the construction site and avoid polluting the natural environment.
R • Limit noise and light pollution, particularly at certain times of the year (breeding season, migration, nesting, etc.).
O • Respect or restore the various plantings.

4. OPERATION AND MAINTENANCE PHASE

4.1. Energy efficiency

R • Optimise functionalities, particularly self-tests (periodic testing of thermal engine backup groups, fire boosters, fans and accelerators).
R • Optimise operating times:
  - for signalling (lane assignment lights, variablemessage signs) used 'just in time' (which also has the advantage of better 'engaging' users)
  - for lighting
R • Limit the volume of data stored and data flows from supervision systems, video surveillance (and any automatic incident detection), emergency call networks, etc. to what is strictly necessary.
R • Enforce more virtuous use of the infrastructure by, for example, reducing the maximum speed allowed. This can have a significant impact on lighting and ventilation, two of the most energy-intensive systems.

4.2. Resource efficiency

R • Ensure regular maintenance and preventive maintenance in accordance with manufacturers' requirements to prolong the life of equipment while guaranteeing its performance.
? • Do not clean structures (less water, fewer pollutants, no paint) at the risk of irreparably clogging the piers and degrading the luminance?

4.3. Circular economy

R • Use recycled equipment or materials that some suppliers are beginning to offer.

5. METHODOLOGICAL ELEMENTS

The approach must be proactive, cross-functional/comprehensive and long-term. It is based on:

- Systematic questioning of each element of the 'tunnel system', in both civil engineering and equipment. This involves targeting all systems, obviously the large consumers, both occasional and permanent, but also the small permanent consumers.
- Analysis of equipment systems and their interactions (with each other and with the infrastructure).
- Consideration of the life cycle of the installations.

According to ADEME (The French Agency for Ecological Transition), 'The low-tech approach involves questioning needs with a view to retaining only what is essential, reducing technological complexity, and maintaining what already exists rather than replacing it.' The questioning can validly be based on the Avoid-Reduce-Offset criteria of the ARO approach, just as the RAMS approach requires questioning each of the criteria of Reliability, Maintainability, etc.

It may be useful to break down the ‘systems’ in order to better address their specific effects and be more comprehensive:

- sensors >>> quality (accuracy, reliability), adjustment
- operational part >>> functionalities (normal and degraded modes, self-tests, etc.)
- actuators >>> efficiency

It is also essential to consider ‘systems’ both as such and in the specific context of the project.

Taking into account the life cycle of installations (infrastructure and equipment) should make it possible to assess the environmental impact of specific equipment during the following phases:

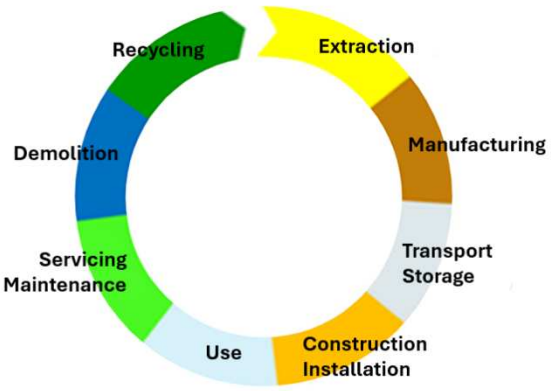


Figure 4: Life cycle

There are many ‘lean’ methods, often adapted to the context and modified over time. They generally aim to improve activities and products. Three of them seem likely to provide useful and effective support for reflection:

- the 5S method, which can be extrapolated to the design and maintenance process.
- the reduction of waste, including overproduction, overstocking, unnecessary transport, overprocessing, defects and scrap.
- ‘total productive maintenance’ with its concepts of planned maintenance and maintenance-oriented design.

In fact, there is a clear convergence between ‘low-tech’ and ‘lean-tech’ approaches, methods and concepts and the more common RAMS and DfM approaches. All aim to ensure the efficiency of activities (operation and maintenance) and the availability of facilities, and therefore of infrastructure, the primary motivation for which, it should be remembered, is to improve an economic or social function. The objectives of repairability, sustainability, standardisation, scalability, simplicity, etc. are therefore common to all.

6. RECOMMENDATIONS

Given the environmental challenges we face, the systematic questioning mentioned in the methodology section is no longer an option: it is a moral obligation before it becomes, perhaps in the near future, a regulatory or legal obligation in the same way as safety and RAMS objectives.

Firstly, it is necessary to clearly define the level of service [(1)] expected from the infrastructure of which the tunnel is a part. Although this step is fundamental, it is rarely explained in detail. This often results in oversizing due to the reproduction of unsuitable designs, which could be avoided by analysing needs (low-tech) and reducing waste (lean-tech).

(1) *There are many criteria, including safety, availability, reliability, predictability (journey time, traffic information, etc.), comfort, cost, etc.*

When it is not possible to completely eliminate energy consumption, the aim is to reduce requirements as much as possible and optimise existing systems. To this end, it is recommended to:

- accurately characterise consumption by implementing sufficiently sophisticated measurement and monitoring tools;
- ideally, focus on the most impactful parameters of each system;
- at a minimum, carry out the simplest and quickest optimisations;
- address the causes rather than their effects as a priority.

Efforts can also be made to optimise servicing and maintenance operations by avoiding systematic replacements that are too early and favouring scheduled operation. The latter option aims to limit unplanned interventions, which generate additional costs for operating services and also for users who are unable to organise themselves in advance.

Generally speaking, the principle of 'keep it simple' (2) seems as relevant in an ARO approach as it is in an RAMS or DfM approach. 'Technological escapism' should be avoided at all costs, and any increase in complexity must be firmly justified by necessity.

(2) *Albert Einstein proposed the following variation: 'Everything should be made as simple as possible, but not simpler.' In other words, the design of a system should be as simple as possible, to the point of reaching a minimal form.*

Finally, it should be emphasised here that none of these recommendations are in any way contrary to compliance with regulatory and fundamental safety requirements – quite the contrary. In other words, these requirements cannot justify a lack of concern for the environment, which, as we have seen, converges with the RAMS and DfM approaches.

7. SUMMARY AND CONCLUSION

The few examples listed show that most avoidance and reduction measures can be decided (1) during the design phase. However, there are also options during the construction and operational phases.

(1) *To be more precise, it should be said that they 'must be decided during the design phase' because postponing them may make them difficult or even impossible to implement later on. As such, calls for tenders and works contracts should/must include selection criteria during both the selection phase and the detailed design phase.*

Furthermore, it should be noted that most measures consist of reducing environmental impacts, rather than avoiding them entirely, which is more difficult to achieve. Compensation measures are also possible; these are obviously important but are not the primary objective. In any case, concrete and relatively simple measures are possible for many equipment systems!

You (readers) may have thought, 'I already do some or all of this.' Well, that's great! There is no doubt that there are many Mr Jourdains of eco-design and that, thanks to them, to you, environmental concerns will be better taken into account because, when it comes to environmental issues, every action counts, big or small! ARO measures must therefore be encouraged, developed and systematised wherever possible, in all areas and throughout the entire life cycle of facilities.

Faced with the major climate challenge facing our planet, the eco-design approach is no longer an option, especially since:

- It is fully compatible with regulatory safety requirements.
- It converges with RAMS, DfM and cybersecurity approaches.
- It does not preclude making the most of Intelligent Transport Systems (which could revolutionise mobility and contribute to safety) or Artificial Intelligence (enabling optimised management of certain processes).
- It is essential for meeting infrastructure resilience requirements.
- It can help control overall construction, operating and maintenance costs.

VID FIREKILL®
LOW PRESSURE WATERMIST

TUNPROTEC®



Advanced low-pressure water mist. High-efficiency protection for tunnel.

VID FIREKILL's **TUNPROTEC®** low-pressure water mist system is designed for the most demanding tunnel fire scenarios.
Tested under full-scale conditions up to 250 MW, it provides rapid fire suppression, reduces heat release and limits fire spread, even in complex environments with active ventilation and restricted access.

Engineered as a zoned deluge solution, it enables fast, targeted activation while optimizing water use and system efficiency. Using water as the suppression medium and operating at low pressure, the system also reduces water and energy demand compared to traditional solutions.

Fully aligned with NFPA502 and international tunnel safety guidelines, TUNPROTEC® delivers reliable, performance-driven protection for both new infrastructure and retrofit projects.

Discover our full range of solutions at **vidfirekill.com**

Norgesvej 2
5700 Svendborg, Denmark
+45 62621024

www.vidfirekill.com

NFPA®

VID FIREKILL®
LOW PRESSURE WATERMIST

TUNPROTEC®



Heysen Tunnel

When Tunnel Fire Protection Becomes Critical Infrastructure

Australia's first road tunnel equipped with water mist fire suppression

The Heysen Tunnel upgrade marks a step forward in how fire safety is engineered in operational road tunnels.

Upgrading fire protection in an operational tunnel requires more than compliance. It demands solutions that work within existing infrastructure, minimize disruption and respond effectively to high-risk fire scenarios.

VID FIREKILL's low-pressure water mist system was implemented as part of a broader safety upgrade, designed to deliver rapid response, controlled water use and reliable performance under real tunnel conditions.

- Protects critical infrastructure where evacuation time is limited
- Reduces thermal impact and structural damage
- Supports faster recovery and operational continuity
- Uses significantly less water compared to traditional systems

Designed for real risks. Proven in real tunnels.

Norgesvej 2
5700 Svendborg, Denmark
+45 62621024

www.vidfirekill.com

NFPA®

EFFECTS OF CONTRIBUTING TO DECARBONIZATION BY MODEL-BASED PREDICTIVE VENTILATION CONTROL (MPVC) ON EXPRESSWAYS

[1]Hiroki Ueda, [2]Atsushi Ichikawa, [3]Minoru Yuhara, [1]Masaki Hiro, [1]Yuichiro Fujita, [4]Wataru Takahashi and [5]Alan Vardy

[1]Nippon Expressway Research Institute Company Limited, JP
[2]East Nippon Expressway Company Limited, JP
[3]AMEC Consultants Company Limited, JP
[4]Central Nippon Highway Engineering Nagoya Company Limited, JP
[5]University of Dundee, UK

DOI 10.3217/978-3-99161-087-8-028 (CC BY-NC 4.0)
https://creativecommons.org/licenses/by/4.0/deed.de
This CC license does not apply to third party material (attributed to other sources) and content noted otherwise.

ABSTRACT

Although the scale of ventilation in highway tunnels has been decreasing due to stricter exhaust gas regulations, normal ventilation is still required under special conditions, such as long tunnels with two-way traffic and tunnels that require environmental measures at the portal. Historically, achieving stable, effective ventilation control in such complex tunnels without wasteful power consumption has been an issue. To address this, the NEXCO Research Institute and NEXCO companies have introduced the tunnel ventilation control software MPVC, which performs optimal control Based on a survey of the operational status of tunnels where MPVC has been introduced, this paper evaluates the optimization of control and the effect of reducing power consumption, and clarifies the contribution to decarbonization, future issues, and prospects.

Keywords: MPVC, Tunnel ventilation control, Decarbonization, Predictive control, Power consumption

1. INTRODUCTION

The amount of soot and other such pollutants exhausted by vehicles has decreased significantly thanks to stricter exhaust gas regulations. Currently, optimising emergency tunnel ventilation in the event of fire has become the mainstream. Nevertheless, tunnels under special conditions, such as long tunnels with two-way traffic and urban tunnels that need environmental measures at the portal, still require normal ventilation. Controlling ventilation in such tunnels is challenging, and unless controlled efficiently, power consumption will be high. For this reason, NEXCO Research Institute and the three NEXCO companies have introduced and are operating tunnel ventilation software MPVC (Model-based Predictive Ventilation Control) since 2007. [3],[4],[5] This software allows an accurate prediction of the ventilation status in the tunnel through multiple real-time simulations and provides an optimal control to reduce the amount of electricity for fans while maintaining various control values. This paper investigates the actual operational status of tunnel ventilation where MPVC is introduced, evaluates the optimization of ventilation control and the reduction of power

consumption, and also describes the effects of MPVC, including its contribution to decarbonization. In addition, issues extracted from the investigation are summarized and prospects of future tunnel ventilation are also mentioned.

2. CONVENTIONAL VENTILATION CONTROL

Tunnel ventilation must be controlled so that jet fans, exhaust fans and other such equipment, installed to prevent air pollution caused by automobile exhaust gas, are operated while maintaining various control values to avoid excessive power consumption. Conventional control methods adopted in Japan are mainly classified into the following three types.

2.1. FB (Feed Back) control

This method operates fans by comparing measured VI (Visibility Index) and CO levels against target values. Because operation only triggers after levels reach the target, rapid air quality deterioration can lead to recovery delays. Its simplicity, while reliable, can result in operational inefficiency.

2.2. FF (Feed Forward) control

This method determines fan output by predicting future tunnel conditions based on upstream traffic data. While potentially more efficient, any discrepancy between predictions and actual traffic can lead to unnecessary energy use or deviations from target environmental values.

2.3. AI Fuzzy control

This approach combines FB and FF methods to mitigate their respective weaknesses. Although Fuzzy theory aimed to improve prediction accuracy, adjusting fluctuating parameters (like soot volume) proved difficult. Unlike modern data-driven AI, this "expert system" relies on manual IF-THEN rules and specialized technical knowledge.

3. OVERVIEW & CHARACTERISTICS OF MPVC

3.1. Overview

The MPVC, a solution to cope with the issues facing conventional ventilation control, simulates and predicts conditions inside the tunnel using traffic data from traffic counters and data from other measurement instruments inside the tunnel to best control ventilation. In addition, it automatically corrects various parameters by comparing the predicted and actually measured values, and then applies the corrected parameters to the next calculation to repeatedly improve them. This ventilation control software has been installed and operated in tunnels in Japan since 2007. The followings describe the operation flow of MPVC (Figure 1).

1) Predict traffic flow inside the tunnel for a certain later time period from the traffic volume of each large and small vehicles measured by a traffic counters. (Traffic simulation)
2) Create combinations of all fans that can be transitioned, considering the situation of fans operating at the time of control.
3) Based on the predicted traffic flow, compute post-operation target control values (VI/CO, etc.) for all fan combinations. (Ventilation simulation)

4) Select the combination that satisfies the target control value and consumes least power from all of the results, and give instructions for ventilation control.
5) Lastly, compare traffic simulation values and ventilation simulation values to actually measured values, and correct parameters. (Traffic reconciliation, ventilation reconciliation)

3.2. Simulation in real time

As a result of real-time simulations, the graph shown in Figure 2 is created in the work processes 2 to 4. This graph is a comparison of power consumption of multiple, simulated fan combinations in post-control tunnel environment simulations created based on actual tunnel conditions. In the graph, those that have satisfied the control target are coloured. In other words, next time, the operation order will be to carry out the combination with the least power consumption among the coloured ones. In addition, the next control instruction also implements control to suppress sudden changes in ventilation machine operation. The idea of simulating, analysing, and predicting in virtual space is exactly the same as modern digital twin technology, and the fact that it was already implemented some 20 years ago means the technology was pioneering.

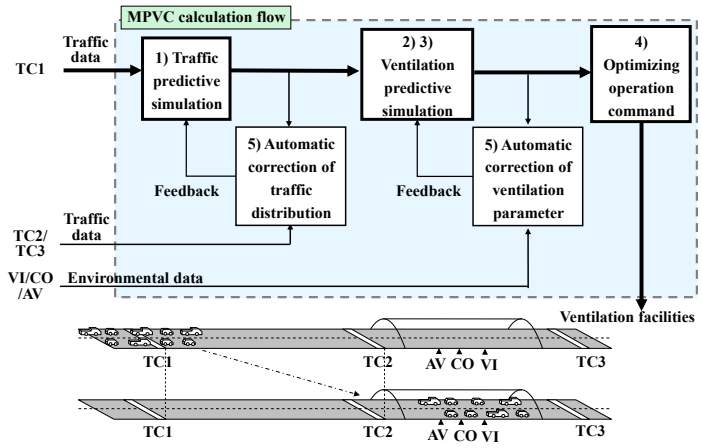


Figure 1: MPVC system flow diagram in the model tunnel

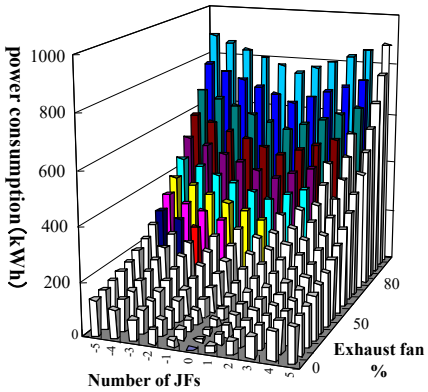


Figure 2: Ventilation combination and power consumption

3.3. Auto-correction of parameters

Parameters for forecasting ventilation fluctuate. These parameters, such as emission coefficients of automobile exhaust gas, which is decreasing year by year, and front projection area that differ per vehicle, are automatically corrected. Conventional AI fuzzy control and the like do not have this function, and parameters were changed manually after analysing the data and verifying them when necessary. This took time, but MPVC automatically corrects them in real-time.[6],[7]

4. POWER CONSUMPTION OF MPVC INTRODUCED TUNNELS

Currently there are about 2,000 tunnel tubes operated by East, Central and West NEXCO companies. Of them some 300 tubes are equipped with ventilation facilities, the majority of which are designed for smoke exhaust, as this has become the mainstream solution in the event of fire. MPVC is effective in long two-way tunnels, urban tunnels requiring environmental

measures at the portals and other tunnels where controlling ventilation to meet their special conditions is complicated. At the present, the three NEXCO companies have introduced and are operating 12 systems in 23 tubes (Table 1).

The annual power consumption on expressways operated by the three NEXCO companies is 1,143,095MWh (2023 results), of which some 22,406MWh, 2 % of the total, is consumed by ventilation equipment (Figure 3). In addition, the power consumption of tunnels with MPVC is 12,891MWh, which means more than half of the power consumed by ventilation is controlled by MPVC (Figure 4).

Compared with the power consumption in 2003, before the introduction of MPVC, the total power consumption has decreased, even though the extension of expressways in service has increased in the intervening 20 years. Looking at the breakdown, the share of consumption by lightings and ventilation equipment has decreased (The annual power consumption of tunnel ventilation decreased about 70% in 20 years.). Lightings switched to LED, more efficiently controlled tunnel ventilation systems by MPVC, and the review of design standards leading to lower automobile emissions are considered to be the factors for the reduction. NEXCO Research Institute has contributed to decarbonization by revising the design criteria.

Table 1: Tunnels with MPVC in Japanese Expressways

No.	Tunnel name	Traffic direction	Length [m]	Facilities	Control target
1	Oyubari	Two-way	4,213	JF×8	VI, CO & Humidity
	Kaede	Two-way	1,955	JF×3	VI & CO
	Osawa	Two-way	1,541	JF×3	VI & CO
	Hobetsu	Two-way	4,318	JF×9	VI & CO
	Shimukappu	Two-way	3,824	JF×7	VI & CO
2	Tenguyama	Two-way	2,978	JF×4	VI & CO
	Tenjin Second	Two-way	2,872	JF×4	VI & CO
3	Waga-sennin	Two-way	3,775	JF×4	VI & CO
4	Kan-etsu	One-way	11,055	Supply fan×6 / Exhaust fan×4	AV
5	Ome	One-way	2,062	JF×4 / Exhaust fan×2	VI, CO & AV
6	Tarutouge	Two-way	4,998	JF×11	VI, CO & Humidity
	Moriyama	Two-way	1,734	JF×4	VI & CO
	Tozurasawa	Two-way	2,295	JF×3	VI & CO
7	Hachioji-joseki	One-way	2,380	JF×4 / Exhaust fan×2	VI, CO & NOx
	Takaosan	One-way	1,329	JF×14 / Exhaust fan×2	VI, CO & NOx
8	Hida	Two-way	10,700	JF×15 / Exhaust fan×10	VI, CO & Humidity
9	Fujishiro [up]	One-way	1,805	JF×9 / Exhaust fan×2	VI, CO & SPM
	Fujishiro [down]	One-way	2,136	JF×2 / ESP×1	VI, CO & SPM
10	Shimotsu [up]	One-way	1,243	JF×7 / Exhaust fan×2	VI, CO & SPM
	Shimotsu [down]	One-way	1,287	ESP×1	VI, CO & SPM
11	Nagamine [up]	One-way	3,831	JF×3 / ESP×1	VI, CO & SPM
	Nagamine [down]	One-way	4,043	JF×3 / ESP×2	VI, CO & SPM
12	Kanmon	Two-way	3,461	Supply fan×8 / Exhaust fan×8	VI, CO & AV

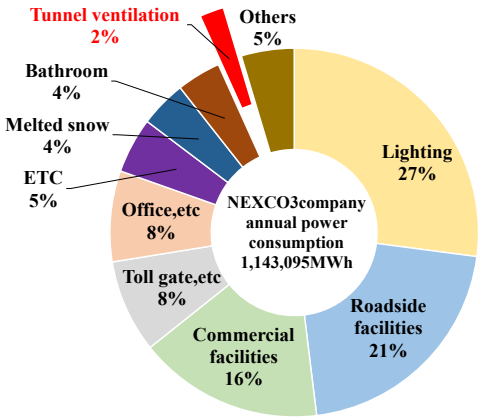


Figure 3: NEXCO 3 companies' annual power consumption usage breakdown in 2023

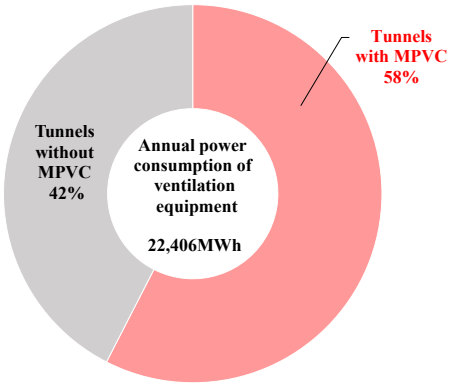


Figure 4: Breakdown of tunnel ventilation power consumption

5. EVALUATION OF MPVC

The 2023 log data on tunnels with MPVC were collected to the extent possible and various analyses have been carried out to evaluate the method.

5.1. Evaluation of ventilation control optimization

The purpose of controlling tunnel ventilation is to operate ventilation observing the tolerance and other values so that the tunnel interior and portal environment are optimized. To do that, the tolerance and actual values for each tunnel were evaluated. Figure 5 and Figure 6 show the actual VI and CO values of each tunnel in 2023. The results show that tolerance values are maintained throughout the year, i.e., MPVC controls ventilation so that the tunnel environment is maintained optimally. It was also confirmed that optimum tunnel outside portal environment was also maintained for SPM (Suspended Particulate Matter) targeted tunnel where the airflow velocity was the target value for controlling ventilation.

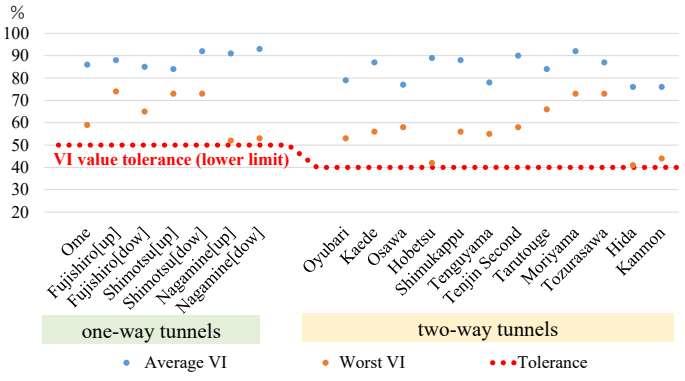


Figure 5: VI value

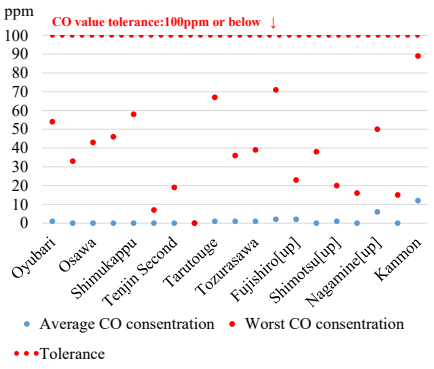


Figure 6: CO concentration

5.2. Evaluation of power consumption reduction

The purpose of MPVC is to optimize the tunnel environment with minimal power consumption. The optimization of ventilation control is guaranteed, as mentioned above, and the effect on the reduction of power consumption was evaluated on this premise. The evaluation was conducted in a tunnel where changes in power consumption can be seen before and after the introduction of MPVC (Table 2). As a result, 32% to 57% reduction was seen in each tunnel, and the total amount of reduction was about 30%. Based on this reduction amount, the cumulative CO2 reduction calculated from the time of MPVC introduction in each tunnel

is approximately 8,000t. Assuming all tunnels with MPVC reduced 30% of their CO2 emissions, the cumulative CO2 reduction from the time of introduction is about 36,000t-CO2, which is equivalent to the amount of annual CO2 emitted by about 10,000 ordinary households in Japan.

Table 2: Annual power consumption reduction effect by MPVC

Tunnel name	Ventilation power consumption		Reduced power consumption [MWh]	Reduction rate
	Before MPVC introduce [MWh]	After MPVC introduce [MWh]		
Osawa & Hobetsu	101	43	58	57%
Shimukappu	61	29	32	52%
Kan-etsu	3,171	2,150	1,021	32%
Kanmon	2,241	1,527	714	32%

5.3. Focus on the specific MPVC

We took a close-up look at the actual state of controlling ventilation in tunnels with MPVC to evaluate the effects of MPVC for different ventilation systems. While there are several other MPVC applications, such as the Hida Tunnel [8], two representative cases are presented below.

5.3.1. Transversal ventilation control system (Kanmon Tunnel)

Figure 7 shows the ventilation system at Kanmon Tunnel. The tunnel is a two-way tunnel with a transversal ventilation system with 4 shafts. Ventilation is controlled to optimize VI/CO in the tunnel and also to simultaneously control wind speed so that it is maintained within ± 2.5m/s to obtain a rapid response in exhausting smoke. Figure 8 and Figure 9 compare daily ventilation trends in the Kanmon Tunnel on a day before and after the implementation of MPVC when traffic conditions were similar. Before the implementation of MPVC (hereinafter “old control”) controlling ventilation meant operating supply fans and exhaust fans of each shaft simultaneously, and the operation tended to be relatively continuous. On the other hand, after the introduction of MPVC (hereinafter “new control”), supply fans and exhaust fans are operated independently, and thus more finely, to reduce power consumption. As a result, though VI decreased in the morning and evening in the old control, the new control maintained a stable and good environment throughout the day. Power consumption was 3,946kWh for the old control, but it decreased 30% and was 2,713kWh for the new control.

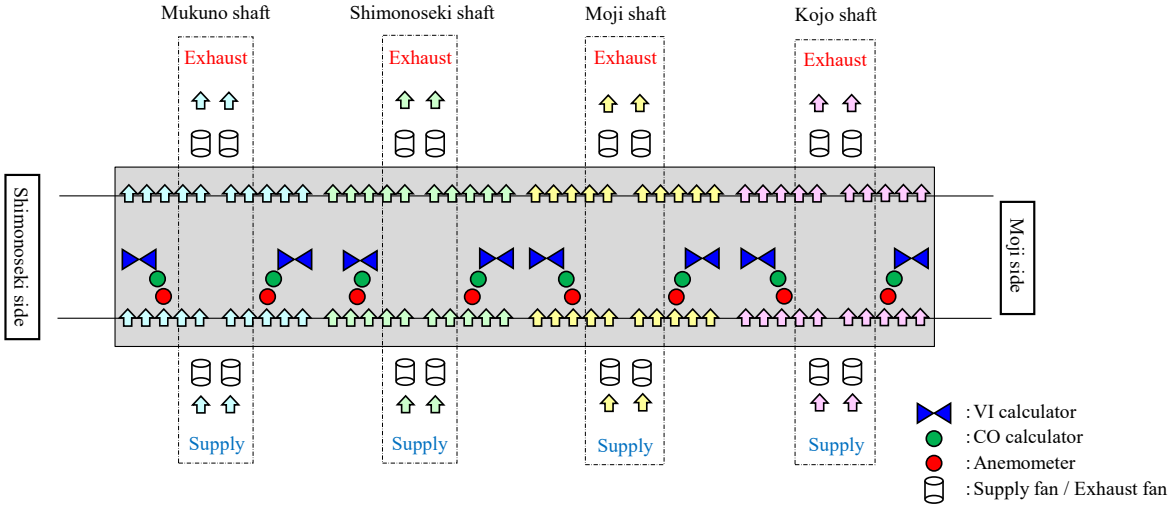


Figure 7: Kanmon Tunnel’s ventilation system diagram

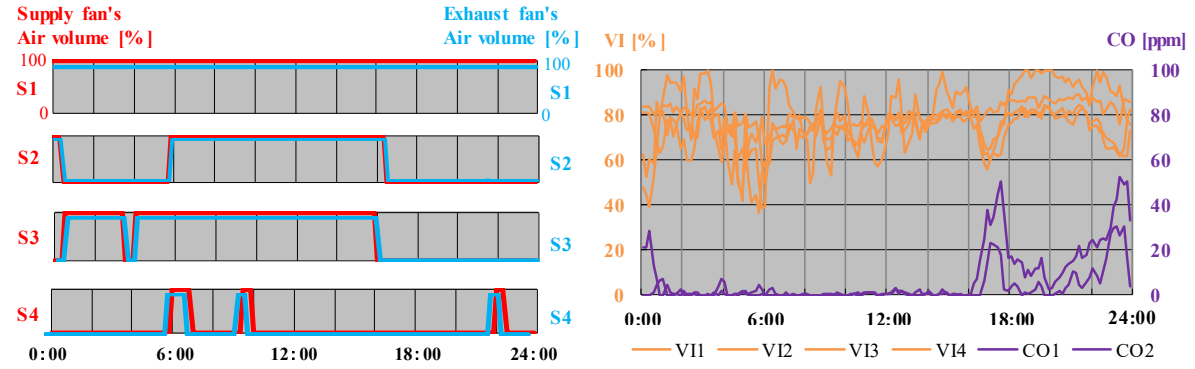


Figure 8: Ventilation trends without MPVC

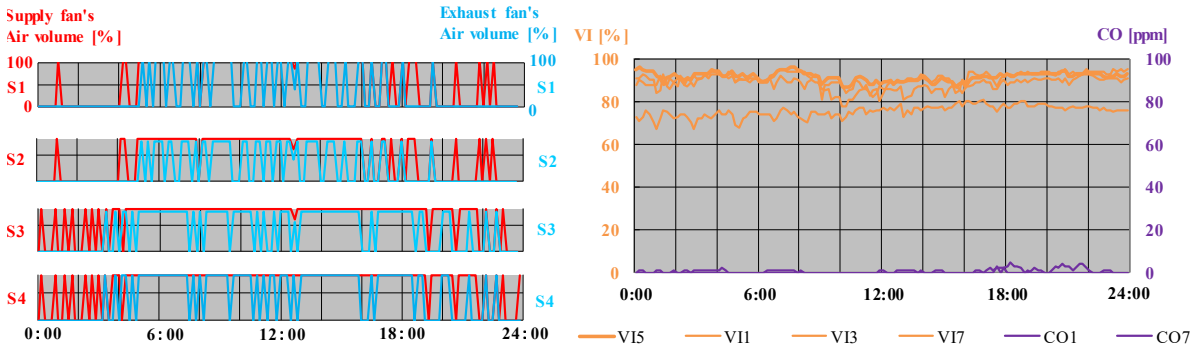


Figure 9: Ventilation trends with MPVC

5.3.2. Temperature & humidity ventilation control system (Oyubari Tunnel)

Figure 10 is the ventilation system at Oyubari Tunnel. The tunnel is a two-way tunnel with a longitudinal ventilation system operating 8 jet fans to control ventilation so that optimum VI/CO level is maintained. The tunnel is in one of the coldest regions in Japan and the relationship between the difference in the inside and outside temperature and saturated humidity may cause fog inside the tunnel in the winter, leading to poor visibility and vehicle windshields quickly fogging up. As a countermeasure, jet fans are operated to reduce the inside and outside temperature difference and prevent poor visibility.[9]

Figure 11 shows the trend of a day when jet fans were most heavily operated by this control method. By operating the jet fans when the outside and inside temperature difference is large and controlling ventilation so that outside air flows in, the temperature difference which was 20°C or more lowered to a daily average of about 2°C (Figure 11). As a result, the VI values were stabilized and poor visibility did not occur, as shown in Figure 12. In addition, MPVC maintains a small, controlled fluctuation in the temperature difference between the inside and outside of the tunnel, thereby preventing poor visibility caused by large temperature differences.

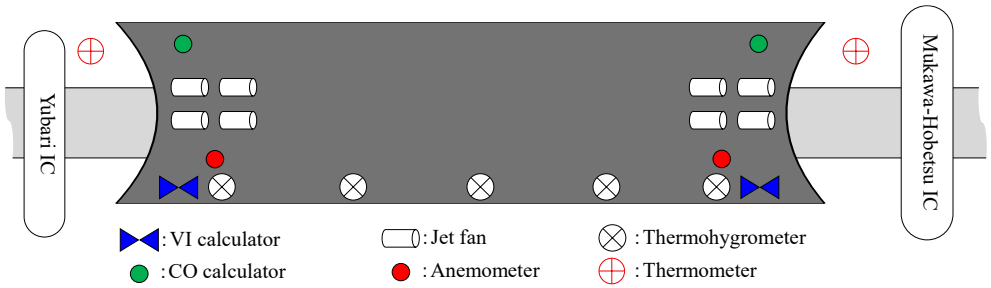


Figure 10: Oyubari Tunnel's ventilation system diagram

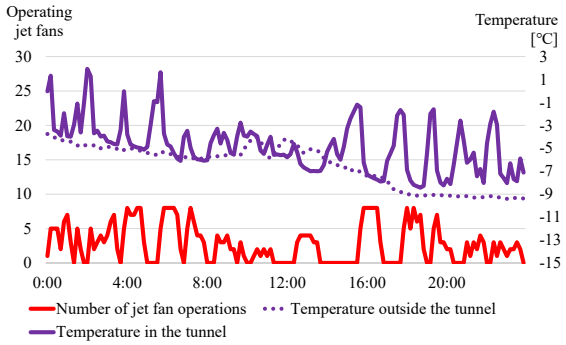


Figure 11: Temperatures inside and outside the tunnel and jet fan operation

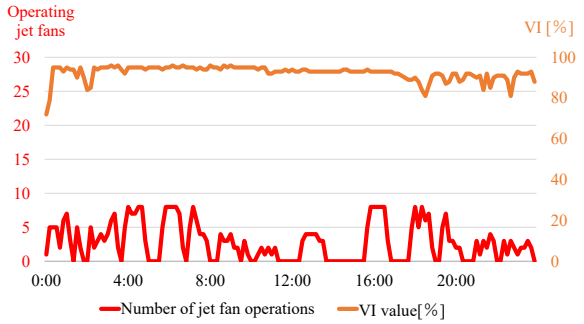


Figure 12: Jet fan operation trend and VI value

5.4. Consideration of auto-corrected parameters

Automatic parameter correction, a feature of MPVC, is aimed at improving prediction accuracy. Nevertheless, it was found that there are differences between the corrected values of each tunnel and the design ventilation values. Table 3 shows the difference between the average value of the log data correction and the current design guideline values. It can be seen that vehicle equivalent resistance area and soot, smoke and CO emissions values are less than those in the design criteria. We consider that MPVC cannot only control ventilation but also has the potential to sense and evaluate ventilation design values.

Table 3: The actual situation of auto-corrected parameters

Parameter	Automobile equivalent area [m^2]		Soot and smoke emissions [m^2/km・number]		CO emissions [m^2/km・number]	
	Large	Small	Large	Small	Large	Small
Design specification value	6.88	2.45	0.66	0.23	0.003	0.003
The above value corrected by the average compensation value	5.60	2.14	0.55	0.18	0.002	0.001
Auto-correction reference difference	-1.277	-0.313	-0.113	-0.049	-0.001	-0.002

6. CONCLUSION

Some 20 years have passed since MPVC was first introduced in Japanese tunnels. This was the first time that we have evaluated and verified the software by collecting annual logs comprehensively. Although power consumption by tunnel ventilation systems for the entire road network is decreasing, MPVC has been introduced for the purpose of efficient ventilation control in tunnels where complex ventilation control is required. From the results of our

verification, it has once again become clear that MPVC is an excellent ventilation control software that contributes to decarbonization by achieving both accurate ventilation and reduction in power consumption by 30% (estimated cumulative CO2 reduction: approx. 36,000t). Furthermore, by using MPVC's auto-parameter correction function, it is thought that the values of the design criteria may be evaluated and the data that are more in line with the actual situation be applied in the revisions of the guidelines.
A future issue is that because the log data required for evaluation and verification are stored at the site of each tunnel, it takes a lot of work to collect the data, and therefore, cannot be used in real-time. To counter this issue, it is necessary to systematize constant monitoring of logs to save labour and conduct regular evaluation and verification.
Controlling ventilation is expected to become even more complicated in tunnels where MPVC is scheduled to be introduced. But we would like to make use of what we have learned from the evaluation and verification this time so that we may contribute to decarbonization and optimization of road management.

7. REFERENCES

[1] Vardy A. E., Ichikawa A. Pollution-cost balance in road tunnel ventilation. Proc. Instn Mech. Engrs, Part A, Journal of Power and Energy, 2000, 214(A6), 677–690.

[2] Ichikawa A, Vardy AE & Brown JMB(2001) "Model-based predictive control using genetic algorithms" Proc I Mech E, J Power & Energy, 215, Part A, 623-638

[3] Vardy AE, Mori E, Yokota M & Nakahori I (2003) "Model-based predictive control of road tunnel portal emissions" ITA World Tunnelling Congress on Reclaiming the Underground Space, Amsterdam, The Netherlands, 12-17 April, International Tunnelling Association, Vol 1, 207-212

[4] Tokeida H, Mori E, Yamada S, Vardy AE, Mitani A & Yokota M (2006) "Full-scale test for verification to put MPVC into practical use for tunnels with the concentrated exhaust system at portal" Proc 12th int symp on the Aerodynamics and Ventilation of Vehicle Tunnels, Portoroz, Slovenia, 11-13 Jul, BHR Group, 723-733

[5] Tokieda H, "Development and Implement of MPVC," Japan Society of Mechanical Engineers, Mechanical Engineering Journal Vol. 1644 (2007)

[6] Azuma S, Nomura H, Ichikawa A, Kawashima S, Mitani A & Vardy AE (2011) "Application of MPVC to the two longest road tunnels in Japan" Proc 14th int symp on Aerodynamics and Ventilation of Tunnels Dundee, UK, 11-13 May 2011, BHR Group, 419-430

[7] Niimi T, "Development and Effect of MPVC Tunnel Ventilation Control Software," Japan Society of Mechanical Engineers, Mechanical Engineering Journal Vol. S0540201 (2016)

[8] Shirahige O, Kon I and Yuhara M "The improving effects of traffic prediction method for tunnel ventilation device" Bordeaux,5-9 October 2015, 22nd ITS World Congress

[9] Akaishi M, Ichikawa A, Azuma T, Azuma S, Sasagawa Y and Yuhara M "Application of Model-based Predictive Ventilation Control (MPVC) to Misty Haze Prevention in tunnels" Lyon,13 September 2017, ISAVFT 741

IMPROVING ENERGY EFFICIENCY IN ROAD TUNNELS

[1]Lorenz Kirchebner, [1]Alexander Wierer, [2]Christof Sistenich, [3]Michael Bacher, [3]Marlene Hinterhofer, [4]Thomas Marcher, [4]Georg Kaml

[1]crypta.sec conceptum GmbH, AT
[2]BASt, Federal Highway and Transport Research Institute, DE
[3]Graz University of Technology, Institute of Thermodynamics and Sustainable Propulsion Systems, AT
[4]Graz University of Technology, Institute of Rock Mechanics and Tunnelling, AT

DOI 10.3217/978-3-99161-087-8-029 (CC BY-NC 4.0)
https://creativecommons.org/licenses/by/4.0/deed.de
This CC license does not apply to third party material (attributed to other sources) and content noted otherwise.

ABSTRACT

The operation of road tunnels leads to considerable energy costs, which are expected to increase further due to the rising energy prices and stricter climate policies. This elaboration highlights technical, operation and planning-based approaches to reduce energy demand and life-cycle costs, based on the findings of the BASt research project “Ermittlung und Bewertung zur Steigerung der Energieeffizienz”.

Energy consumption data from more than 35 road tunnels have been analyzed, revealing that lighting accounts for the largest share – 50 % to 60 % – of the total energy demand, consistent with findings across the DACH region (Germany, Austria and Switzerland). Based on these insights, the project identifies three main pillars for energy optimization:

- Energy sources near or within the tunnel: integration of renewable energy systems, such as photovoltaic panels, hydropower from drainage systems and electricity generation from natural airflows
- Energy saving measures: implementation of energy-efficient components and design strategies, including optimized tunnel portals, high-reflectivity road surfaces and daylight-introducing elements like entrance light shafts
- Operation strategies: improves system control and regular maintenance, such as adaptive lighting control, demand-based ventilation control and implementation of energy monitoring with benchmark integration

Beyond technical measures a methodical framework for assessing tunnel energy performance as a basis for systematic energy management is developed. These results contribute to the development of a practical planning tool that supports sustainable tunnel operation and energy-efficient infrastructure design.

Keywords: Energy efficiency, sustainable tunnel operation, energy monitoring, energy management, energy-reducing measures

1. INTRODUCTION

Energy efficiency has become a central concern in the planning and operation of road tunnels. The continuous operation of lighting, ventilation and safety systems leads to a substantial energy demand and operating costs, which are expected to increase further due to increasing

energy prices and ambitious climate and carbon neutrality targets like the European directive [1] and energy efficiency reform act in Austria [2]. Nevertheless, energy consumption has historically been neglected in design and operation.

To address this need the „Bundesanstalt für Straßen- und Verkehrswesen (BASt)“ initiated the research project „Ermittlung und Bewertung von Maßnahmen zur Steigerung der Energieeffizienz von Straßentunneln bei Planung und Betrieb (FE 15.0705/2022/ERB)“. The project was funded by the „Bundesministerium für Digitales und Verkehr (BMDV)“ and conducted in cooperation with tunnel operators and planners. Its objectives were:

- To establish a comprehensive understanding of energy flows in road tunnels and their dependency on design and operation parameters
- To identify and evaluate energy-saving measures and renewable energy integration options
- To develop a practical energy management framework for both existing tunnels and new constructions
- To provide decision support and planning tools enabling operators and planners to balance safety, functionality and energy efficiency

The methodological approach in the project combined theoretical, empirical and computational elements. A literature review and regulatory analysis (e.g. RE-ING [3], RVS [4]) established the boundary conditions for tunnel equipment and operation. Real energy consumption data from over 35 German tunnels were collected and normalized to ensure comparability between tunnels with different length, geometry and equipment levels. Complementary simulation models were used to estimate energy demand and evaluate substitution potentials. The results formed the foundation for a structured catalogue of efficiency measures, grouped into technical, operation and strategic categories.

This paper provides an overview of the projects’ key content and results. The main focus is on the structure and applicability of energy management, its operational implementation in planning practice and the derivation of relevant measures to reduce energy consumption in tunnel operations.

2. ENERGY DEMAND AND CONSUMPTION CHARACTERISTICS

2.1. Installed Power vs. Operational Consumption

Energy demand in road tunnels is defined by the total installed electrical power of the installed subsystems. However, actual energy consumption is primarily governed by operation control, external conditions and system usage.

Ventilation systems typically represent the largest portion of installed power (up to 80 %, **Figure 1**) but their actual energy consumption often remains below 10 % of the total energy consumption (**Figure 2**) – full-load operation occurs only during maintenance or emergency scenarios. In contrast, lighting systems – especially entrance and transitions zones – show continuous operation making them the dominant consumer in daily tunnel operation (**Figure 2**).

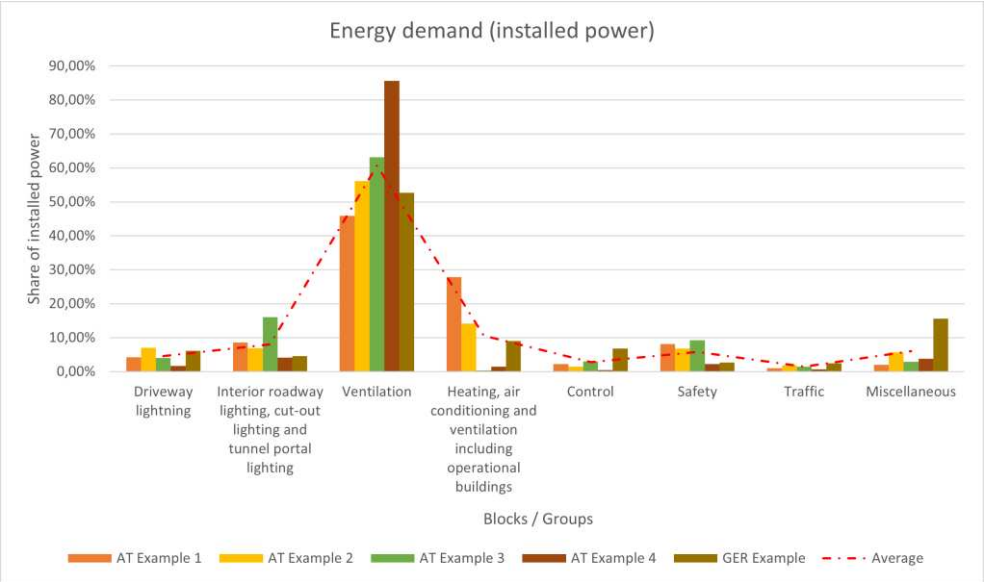


Figure 1: Example installed power of five tunnel systems.

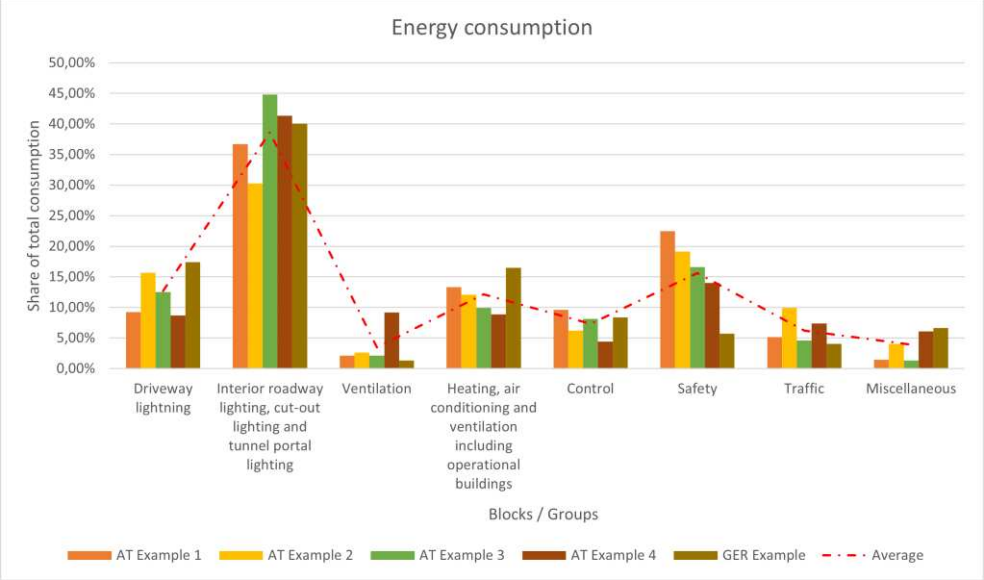


Figure 2: Example consumption of the same five tunnel systems.

The energy demand of tunnel systems fluctuates seasonally and diurnally. Lighting demand is directly linked to external luminance, which varies with weather, season and geographic orientation of the portals. On the other hand, ventilation demand depends on traffic load, air quality thresholds and control strategies.

This imbalance in **Figure 1** and **Figure 2** underlines the necessity for measurement-based energy assessment rather than relying solely on installed power. Furthermore, it becomes clear that significant savings can be achieved through operational optimization without the need to replace major hardware.

3. ENERGY CONSUMPTION IN THE DACH-REGION

The DACH comparison (Germany, Austria and Switzerland) provides insights into structural and operational factors influencing tunnel energy use. The analysis covered tunnels from Germany (38), Austria (51) and Switzerland (35) with a wide variety of different tunnel types (direction of traffic, ventilation system, length, number of bores, etc.).

3.1. Comparative Energy Distribution

For a direct comparison one single-way tunnel with longitudinal ventilation was compared for each country in the DACH region. Energy consumers were divided into similar groups. Normalized energy data (kWh per lane-meter) showed a consistent dominance of lighting energy in all three countries with shares ranging between 50 % and 60 % of total consumption, as seen in **Figure 3**.

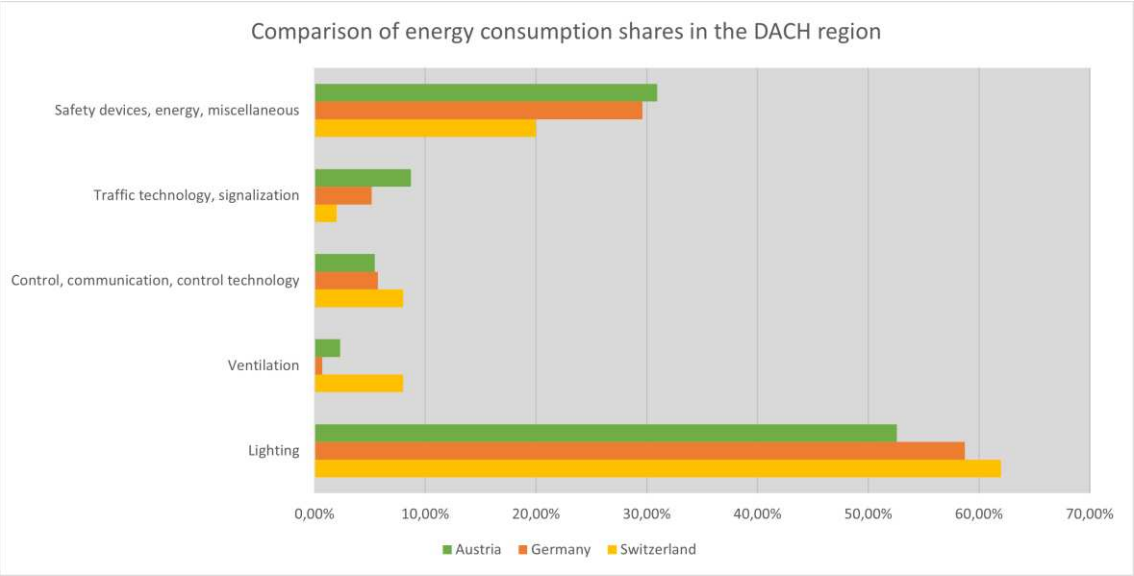


Figure 3: Comparison of energy consumption shares in the DACH region

Differences between countries are mainly attributed to design standards and lighting concepts. Austrian tunnels employ shorter entrance zones and lower luminance levels under dry conditions while Germany and Switzerland dimension for wet pavement reflections and apply symmetric lighting resulting in higher average energy demand.

4. ENERGY MANAGEMENT FRAMEWORK

The developed framework defines a systematic approach to record, evaluate and improve energy performance in tunnel operation. It consists of two interconnected levels:

- Strategic Energy Planning Aid
- Operational Planning Aid

4.1. Strategic Energy Planning Aid

The strategic guide provides the organizational and regulatory foundation for energy management. It defines responsibilities and procedures for energy-related decisions. Key elements include:

- Definition of an energy policy at operator level
- Identification of legal and economic boundary conditions
- Assessment of potential renewable energy sources near the tunnel site
- Integration of energy criteria into design and procurement processes
- Role of the electricity energy mix
- Importance of planning cycles, tendering models and make-or-buy decisions

4.2. Operational Planning Aid

At the operational level, energy management focuses on monitoring, analysis and optimization. The key steps are:

- Energy flow analysis: identification of main consumers and efficiency bottlenecks
- Energy performance indicators: development of comparable metrics
- Benchmarking: comparison against similar tunnels to identify outliers
- Evaluation: assessment of potential savings, costs and life-cycle developments
- Visualization: visual representation and its advantage of the energy flow within the tunnel
- Measures: selection of suitable measures to increase energy efficiency and reduce energy consumption

This framework supports operators in prioritizing investments and ensures that energy efficiency becomes a continuous and verifiable management process rather than a one-time action.

5. CATALOGUE OF ENERGY EFFICIENCY MEASURES

A detailed catalogue of measures was developed within the project to support practical implementation. It groups individual measures in three key pillars for increasing the efficiency of road tunnels (**Figure 4**).

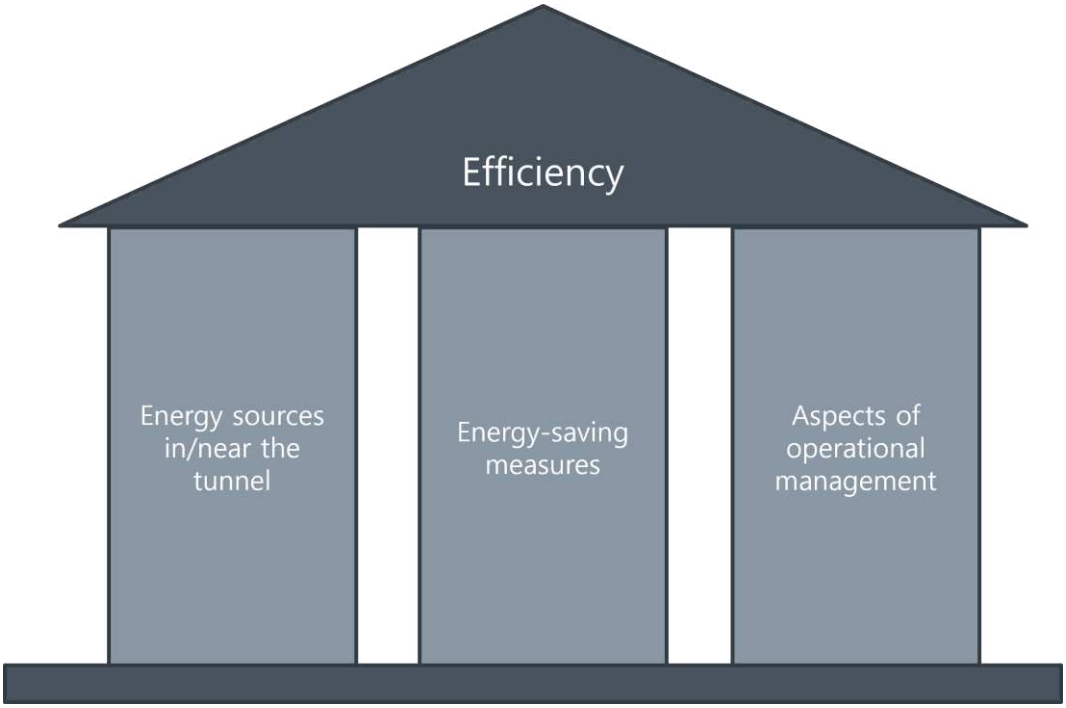


Figure 4: Key pillars for increasing the efficiency of road tunnels

The three main categories include the following measures (**Table 1**).

Table 1: Categories and analyzed measures

Category	Measures
EQ – Energy sources [5], [6], [7], [8], [9], [10], [11], [12], [13]	Generation of electrical energy from air currents in tunnels using meteorological portal pressure differences and buoyancy currents
	Geothermal energy – absorber tubes
	Geothermal energy – combination of open system with absorber tubes
	Geothermal mountain water utilization
	Photovoltaic system
	Wind turbine
EM – Energy-saving measures [14], [15], [16], [17], [18]	Use of test engineers during construction
	Coating of the tunnel ceiling with reflective materials
	Increasing the reflectance of the tunnel wall through wall panels
	Use of components with higher efficiency
	Retrofitting existing systems with LED-technology – the original luminaire positions are retained
	Re-equipping with LEDs vs. existing sodium vapor lamps – the luminaire positions are re-determined
	Counter-beam principle for entrance lighting
	Road surface with different luminance coefficients (q_0)
	Lightwell (saw-tooth roofs) in the viewing section (= section with the length of the stopping sight distance immediately behind the tunnel entrance)
	Wetness-dependent speed reduction
	Portal design
	Energy-saving potential through the use of frequency-controlled jet fans
AB – Aspects of operational management [19], [20], [21], [22]	Annual calibration of sensors
	Recording of energy data and benchmarks
	Demand-based control of the ventilation system during normal operation
	Regulation-compliant nighttime dimming of tunnel lighting
	Demand-based control of entrance lighting based on L_{20}

Each measure was evaluated for applicability, effectiveness and lifecycle cost impact. Measures at impact levels 1 to 3 typically reduce the expected annual energy consumption by a few percent. Measures at levels 4 and 5 achieve significantly higher savings – starting around 8-10 % and in individual cases even reaching up to 30 % of the total energy consumption. Some measures have a certain range of impact levels and a specific quantification depends on the respective project and must be determined individually.

A small selection of measures and their levels can be seen in **Figure 5** and illustrates the following measures:

- EQ1 – Generation of electrical energy from air currents
- EQ2 – Geothermal energy – absorber tubes
- EQ3 – Geothermal energy – combination of open system with absorber tubes
- EQ4 – Photovoltaic system
- EM1 – Use of test engineers during construction
- EM2 – Coating of the tunnel ceiling with reflective materials
- EM3 – Increasing the reflectance of the tunnel wall through wall panels
- EM4 – Use of components with higher efficiency
- EM5 – Retrofitting existing systems with LED-technology – the original luminaire positions are retained
- AB1 – Annual calibration of sensors
- AB2 – Recording of energy data and benchmarks
- AB3 – Demand-based control of the ventilation system during normal operation

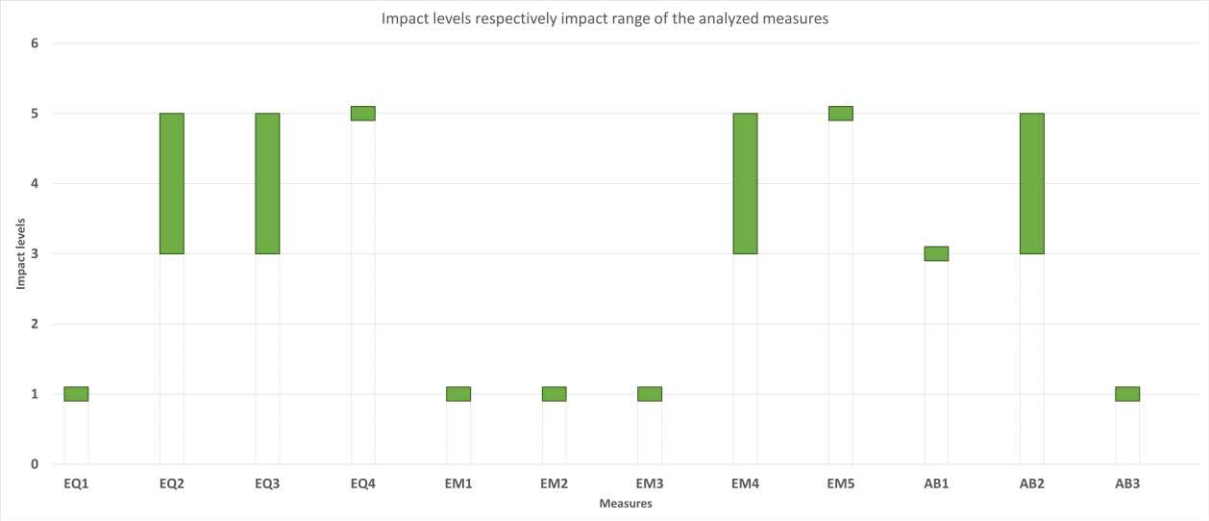


Figure 5: Excerpt from the range of impact levels of measures

In addition to quantitative effects, qualitative benefits such as improved visibility, safety and reliability are a by-product of some measures and were assessed. The catalogue is designed as a living tool, allowing future updates as new technologies and operational experiences emerge.

6. SUMMARY AND CONCLUSION

The presented results demonstrate that energy management and efficiency improvement in road tunnels is in many ways feasible. The analysis of the tunnels across the DACH region confirmed that lighting is the dominant energy consumer, emphasizing the relevance of optimized design, control and maintenance.

The developed energy management framework provides a practical methodology to:

- Identify and monitor energy flows and consumption patterns
- Integrate renewable energy sources directly into tunnel infrastructure
- Evaluate and prioritize efficiency measures based on technical and economic criteria
- Establish transparent performance indicators and benchmarks

Applying these principles can achieve measurable reductions in operational costs and CO_2 emissions while maintaining full safety and functionality. Furthermore, the proposed framework aligns with current European energy efficiency regulations and supports long-term sustainability goals in tunnel infrastructure management.

Future work should focus on expanding the availability and resolution of real energy demand data to further refine benchmarks. In combination with digital monitoring and predictive control systems, these developments will enable data-driven and adaptive tunnel operation, forming the foundation of future energy-efficient and resilient road infrastructure.

7. REFERENCES

[1] *Richtlinie (EU) 2023/1791 des Europäischen Parlaments und des Rates vom 13. September 2023 zur Energieeffizienz und zur Änderung der Verordnung (EU) 2023/955 (Neufassung) (Text von Bedeutung für den EWR), ABl. L 231 vom , pp. 1–111.*

[2] *Energieeffizienz-Reformgesetz 2023 – EEff-RefG 2023 (240/ME).*

[3] BMDV, *Bundesministerium für Digitales und Verkehr,* Berlin, 2024.

[4] Österreichische Forschungsgesellschaft Strasse, Schiene, Verkehr (FSV), *Richtlinien und Vorschriften (RVS) für den Straßenbau,* Wien.

[5] A. PEÑA-GARCÍA und D. GÓMEZ-LORENTE, Installation of solar panels in the surroundings of tunnel portals: A double-targeted strategy to decrease lighting requirements and consumption, Grenada: Tunnelling and Underground Space Technology, 2020.

[6] P. STURM, D. FRUHWIRT, R. SEEBACHER und K. KRISCHAN, „Tunnelkraftwerk - Möglichkeit von Stromerzeugung aus meteorologisch oder thermisch bedingten Luftströmungen in Straßentunneln," Graz University of Technology, Graz, 2023.

[7] OVE ARUP & PARTNERS LIMITED, „Geothermal use of tunnels," ohne Verlag, London, 2022.

[8] T. GEISLER, „Assessment of geothermal power in tunnels using open hydrothermal systems and engineering optimization option," Institute of Rock Mechanics and Tunnelling, Graz, 2024.

[9] T. GEISLER, G. KAML und T. MARCHER, „Sustainable energy from the depths: Optimization strategies for hydrothermal tunnel water systems," *Geomechanics and Tunnelling,* Bd. 17, Nr. 5, pp. 426-436, 1 Oktober 2024.

[10] C. MOORMANN, G. MARZAHN, I. KAUNDINYA und M. POZYBILL, „Nachhaltigkeit im Tief- und Tunnelbau durch innovative geothermische Konzepte," ohne Verlag, Stuttgart, 2022.

[11] R. BORRMANN, K. REHFELDT und D. KRUSE, „Volllaststunden von Windenergieanlagen an Land - Entwicklung, Einflüsse, Auswirkungen," Deutsche WindGuard GmbH, Varel, 2020.

[12] S. LÜERS und A.-K. WALLASCH, „Vorbereitung und Begleitung bei der Erstellung eines Erfahrungsberichtes gemäß § 97 Erneuerbare-Energien-Gesetz (EEG 2017) zum spartenspezifischen Vorhaben Windenergie an Land - Kostensituation der Windenergie an Land Stand 2023," Deutsche WindGuard, Varel, 2023.

[13] T. HOCHSTEIN, E. SCHRECK, C. MOORMANN und T. KUGLER, „Geothermal use of groundwater in tunnels combined with direct passive road surface temperature control," *Geomechanics and Tunnelling,* Bd. 17, Nr. 5, pp. 437-444, 1 Oktober 2024.

[14] crypta.sec conceptum GmbH, „B171 Tiroler Straße, Stadtbergtunnel Rattenberg, Beleuchtungsmessungen," Amt der Tiroler Landesregierung, 2022.

[15] S. KRISPEL, M. PEYERL und G. MAIER, „Erhöhung der Sicherheit und Energieeinsparung in Tunnelbauwerken durch Optimierung der Materialauswahl von Fahrbahndecken," pp. 499-508, 31 Mai 2019.

[16] C. YANG und S. FAN, „Energy-Saving Performance Studies of Road Tunnel Luminaries," *Applied Mechanics And Materials,* Bd. 291 bis 294, pp. 654-660, 2013.

[17] F. SALATA, I. GOLASI, A. POLIZIANIA, A. FUTIA, E. VOLLARO, M. COPPI und A. VOLLARO, „Management Optimization of the Luminous Flux Regulation of a Lighting System in Road Tunnels. A First Approach to the Exertion of Predictive Control Systems," *Sustainability,* Bd. 8, Nr. 11, p. 1092, 25 Oktober 2016.

[18] L. MORETTI, G. CANTISANI, L. CARRARINI, F. BEZZI, V. CHERUBINI und S. NICOTRA, „Italian Road Tunnels: Economic and Environmental Effects of an On-Going Project to Reduce Lighting Consumption," *Sustainability,* Bd. 11, Nr. 17, p. 4631, 26 August 2019.

[19] M. PEHNT, M. ARENS, M. DUSCHA und W. EICHHAMMER, „Energieeffizienz: Potenziale, volkswirtschaftliche Effekte und innovative Handlungs- und Förderfelder für die Nationale Klimaschutzinitiative. Endbericht," Institut für Energie- und Umweltforschung (ifeu), Heidelberg, 2011.

[20] A.-C. AGRICOLA, J. PERNER, S. JOEST, D. BOTHE, M. CZERNIE, R. HEUKE, D. KALINOWSKA und S. PETERS, „Steigerung der Energieeffizienz mit Hilfe von Energieeffizienz-Verpflichtungssystemen," Deuschte Energie-Agentur & Frontier Economics, Berlin, 2013.

[21] T. FLEITER, B. SCHLOMANN und W. EICHHAMMER, Energieverbrauch und CO2-Emissionen industrieller Prozesstechnologien - Einsparpotenziale, Hemmnisse und Instrumente (ISI-Schriftenreihe "Innovationspotenziale"), Stuttgart: Fraunhofer-Verlag, 2013.

[22] Autonome Provinz Bozen - Südtirol, „Autonome Provinz Bozen - Südtirol," 2013. [Online]. Available: https://news.provinz.bz.it/de/news-archive/432391. [Zugriff am 20 Oktober 2025].

ON SMOKE DETECTION SYSTEMS IN ROAD TUNNELS – A QUANTITATIVE COMPARISON

[1]Samuel Gehrig, [2]Simon Frey, [1]Benjamin Pollinger, [3]Reto Buchmann, [4]Bernard Crausaz

[1]AFRY Switzerland AG, CH
[2]HBI Haerter, CH
[3]buntech GmbH, CH
[4]Federal Roads Office FEDRO, CH

DOI 10.3217/978-3-99161-087-8-030 (CC BY-NC 4.0)
https://creativecommons.org/licenses/by/4.0/deed.de
This CC license does not apply to third party material (attributed to other sources) and content noted otherwise.

ABSTRACT

Reliable incident detection is crucial for safety and operation of road tunnels. On the one hand, rapid and accurate detection of incidents allows for timely activation of electromechanical equipment such as tunnel closure or ventilation systems. On the other hand, high reliability or low false alarm rates is a prerequisite for daily operations and user satisfaction.

In Swiss road tunnels, smoke sensors based on visibility measurement have been in use for nearly 20 years. Combined with an evaluation logic to distinguish between moving and stationary smoke sources, this has become an established solution. Nevertheless, continuous optimisation and development is being performed regarding sensor technology, sensor placement as well as evaluation logic. Video based Automatic Incident Detection (V-AID) is only sporadically used for fire detection, primarily due to the perceived lack of quality and reliability.

As part of a general study on smoke detection in road tunnels, the performance of conventional smoke detection and of modern V-AID systems is quantitatively compared, based on a large number of smoke tests. The tests include both moving and stationary smoke sources as well as different longitudinal airflows (intensity and direction). Each test was performed at least 3 times to account for variations. The performance of both systems is evaluated and compared using various parameters and, in particular, a dimensionless number accounting for the spatial and temporal sequence of smoke detection.

The work shows promising results using V-AID regarding the detection quality but also reveals a certain number of points to be addressed, prior to a wide use of modern V-AID systems for smoke detection.

Keywords: Smoke Detection, Video Automatic Incident Detection (V-AID), Comparison, Quality of Detection, Smoke Tests

1. INTRODUCTION

For nearly 20 years, fire detection in road tunnels in Switzerland has been relying on two detection methods: linear thermal detection for either elevated or rapidly rising temperatures, and smoke detection using optical sensors. As described in [1] and [2], smoke detection systems must be able to make a distinction between a moving smoke source and a stationary smoke source and must be able to cope with the transition from moving to stationary. The

related challenges are described for example in [3] or [4]. A major disadvantage of such systems is the pointwise measurement with sensors typically spaced by 100 m (compared to e.g. 5 - 10 m for thermal detection) and the fact that sufficient quantities of smoke must be transported to the detector and persist for a sufficient period of time. The main advantage of such systems is the fact that the measurement has a direct physically meaning including the integration of (multiple) thresholds and that the detection of fog can be eliminated when using integrated heating elements.

Even though widely spread, video automatic incident detection (V-AID) is primarily used for selected incident types such as a stopped vehicle, a vehicle moving in the wrong direction or pedestrians. As opposed to other countries, V-AID is in Switzerland not in use for smoke or fire detection, mainly due to the associated false alarm rates in conjunction with the fact that operators are not solely responsible for tunnel operation but primarily for general emergencies response. Modern V-AID systems, based on general image analysis (machine learning, with or without artificial intelligence), instead of pixel-based image processing are advertised as an important step forward regarding detection quality as well as robustness. Especially regarding smoke detection, V-AID systems offer one important advantage: volumetric detection instead of pointwise detection. Therefore, a single detector (a camera) can detect smoke independently of its effective position within the field of sight of the camera. On the contrary, as there is only a binary information: “absence of smoke” or “presence of smoke” thresholds cannot be used and no information on smoke concentration is available.

As part of a more general study on smoke detection in road tunnels, the performance of conventional smoke detection and modern V-AID is quantitatively compared in order to evaluate the future use of V-AID smoke detection in Swiss road tunnels. The purpose of this study is to evaluate and compare the effectiveness of traditional and video-based smoke detection systems under varied tunnel conditions so as to shape future tunnel safety strategies.

2. METHODOLGY

2.1. Experimental Setup

As smoke source, two different types of smoke generators (paraffine oil based as well as propylene glycol based) mounted on a trailer are used. The set up allows for smoke production rates of up to 1700 m^3/min. The produced smoke is at ambient temperature, dense, long lasting and resistant to slight temperature increase. **Figure 1** shows the trailer with the smoke generators. The smoke generators are mounted slightly tilted upwards or are equipped with deflector nozzles to achieve a more realistic smoke propagation.



Figure 1: Experimental setup with smoke generators on trailer

The tests consisted basically of the smoke source traveling at constant speed over up to 2’000 m. In order to reflect the situation in bidirectional tunnels, tests are conducted at

airspeeds in the tunnels of 1,5 – 2,0 m/s, 2,5 – 3,0 m/s as well as 4,0 – 4,5 m/s, whereas the direction of travel of the smoke source was in the direction of the airflow as well as opposed to it. **Figure 2** shows the different combinations of airflow direction and direction of travel. To verify the repeatability of the results, each test is repeated three times under the same conditions. This results in a set with a total of 36 tests. So far, the tests have been carried out in two different tunnels with different types of smoke detectors and the same type of V-AID system.

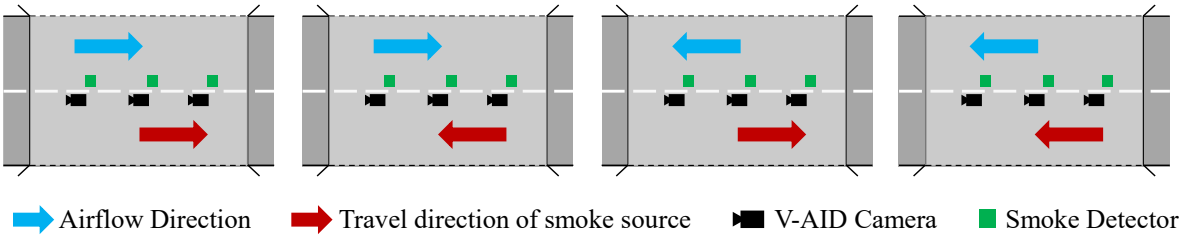


Figure 2: Combinations of airflow direction and direction of travel (schematic representation)

2.2. Tunnels under Investigation

The results from two Swiss tunnels are reported hereafter. The parameters relevant for this investigation are shown below. The cross section and the speed of travel are similar in both cases. Important differences are the smoke detector technology used and the applied thresholds. The V-AID algorithms are similar and distinguish smoke from fog.

Table 1: Tunnel parameters relevant to the investigation

Parameter	Tunnel 1	Tunnel 2
Tunnel cross section area	45,0 m^2	48,3 m^2
Type	Bifurcation in the centre	Single tube w/o bifurcation
Mean altitude	657 m.a.s.l	428 m.a.s.l
Smoke detector	Sigrist FireGuard 2	Sick VISIC50SF-1000
Extinction thresholds 1 and 2 in the smoke detectors	10 / 30 mE/m	20 / 70 mE/m
V-AID algorithm	Citilog CT-ADL 2024R1.E	Citilog CT-ADL 2024R2.3 (V9.1R2E5.P3)
Smoke source´s speed of travel	33 km/h	34 km/h

2.3. Quantitative (Statistical) Evaluation

2.3.1. Delay of Detection Δt_{VS} and Sequence of Detection τ

This study examines how much time elapses between passing by a sensor and the effective detection at this sensor (detection delay), and whether the sensors detect the actual order of passing by (detection sequence). The detection delay Δt_{VS} is given in seconds, and the detection sequence is the dimensionless number τ described below. For a better understanding of the following, please refer to **Figure 3**.

Given are the position $x_{S,i}$ of sensor i in the tunnel, the timestamp $t_{V,i}$ when passing by sensor i and the timestamp $t_{S,j}$ of the detection of the sensor to the threshold S at position $x_{S,j}$.

Therefore, there are two time series: $(t_{V,i}, x_{S,i})$ the time series of travel, and $(t_{S,j}, x_{S,j})$ the time series of detection, which are linked to each other by the sensor positions $x_{S,i}$ and $x_{S,j}$.

For each sensor j on the route of the vehicle which reacts to the threshold S during a test, there is a timestamp $t_{V,j}$ of passing by and a timestamp $t_{S,j}$ of detection. The difference

$$\Delta t_{VS,j} = t_{S,j} - t_{V,j}$$

is called detection delay. Due to the test setup, the detection delay only takes positive values.

Inconsistent, heavily varying detection delays may lead to an inconsistent detection sequence: e.g. sensor 3 detecting prior to sensor 2 within the sequence 1 → 2 → 3. Therefore, a number describing the quality of the detection sequence is sought after, which is independent of the vehicle's velocity and of the distance in between sensors, allowing to compare different tests and technologies against each other.

The time interval of the detection sequence is made of the two consecutive timestamps of detection $\Delta t_{S,j} = t_{S,j} - t_{S,j-1}$. The indices are chosen to look backwards ($j-1$ and j) because algorithms distinguishing moving from stationary smoke sources look backwards too. The sequence of the indices is not connected to the spatial detection sequence, but to the time of detection. Using the spatial connection of the two timeseries described above, the timestamps $t_{V,l}$ respectively $t_{V,k}$ of passing by under the sensors $x_{S,j}$ resp. $x_{S,j-1}$ are assigned to the timestamps of the detection. Thus, the interval of passing $\Delta t_{V,j} = t_{V,l} - t_{V,k}$ between these sensors is determined. $\Delta t_{V,j}$ can take any, especially negative, values.

- A positive value means that the vehicle passed by the sensor $x_{S,j-1}$ earlier than by the sensor $x_{S,j}$, which means that the sequence of detection corresponds to the sequence of passing by.
- A negative value however indicates an inversed sequence of detection, related to a much bigger detection delay $\Delta t_{VS,j}$ at sensor j than $\Delta t_{VS,j-1}$ at sensor $j-1$.

Scaling the interval of detection $\Delta t_{S,j}$ by the assigned interval of passing by $\Delta t_{V,j}$ leads to the dimensionless sequence of detection $\tau_{S,j}$, defined as the ratio of $\Delta t_{S,j}$ and $\Delta t_{V,j}$:

$$\tau_{S,j} = \frac{\Delta t_{S,j}}{\Delta t_{V,j}}$$

The sequence of detection $\tau_{S,j}$ allows for a more accurate interpretation than $\Delta t_{S,j}$ alone. The values of τ can be interpreted as follows:

- $\tau < 0$: the detection sequence is inverted (opposed to travel direction),
- $0 < \tau < 1$: this can be written as $0 < \Delta t_{S,j} < \Delta t_{V,j}$, which means that the sequence of detection is in the right order, but slower than the passing by,
- $\tau = 1$: travel and detection are perfectly marching in step,
- $\tau > 1$: this can be written $\Delta t_{V,j} < \Delta t_{S,j}$, which means that the sequence of detection is in the right order, but faster than the passing by.

In conclusion: The delay of detection Δt_{VS} answers the question how fast a technology detects smoke, whereas the sequence of detection τ evaluates how good the detection of moving smoke is. A technology is good, when there are no negative values of τ and all values are gathered around 1.

Figure 3 illustrates these relationships. Both cases discussed above are represented, case 1 for $\Delta t_{V,j} > 0$ and case 2 for $\Delta t_{V,j} < 0$. The green field represents values of τ greater than zero and the red one values smaller than zero. The vectors v_{smoke} represent the velocity of the smoke calculated from the detection points. The horizontal bold dashed line shows the target value $\tau = 1$.

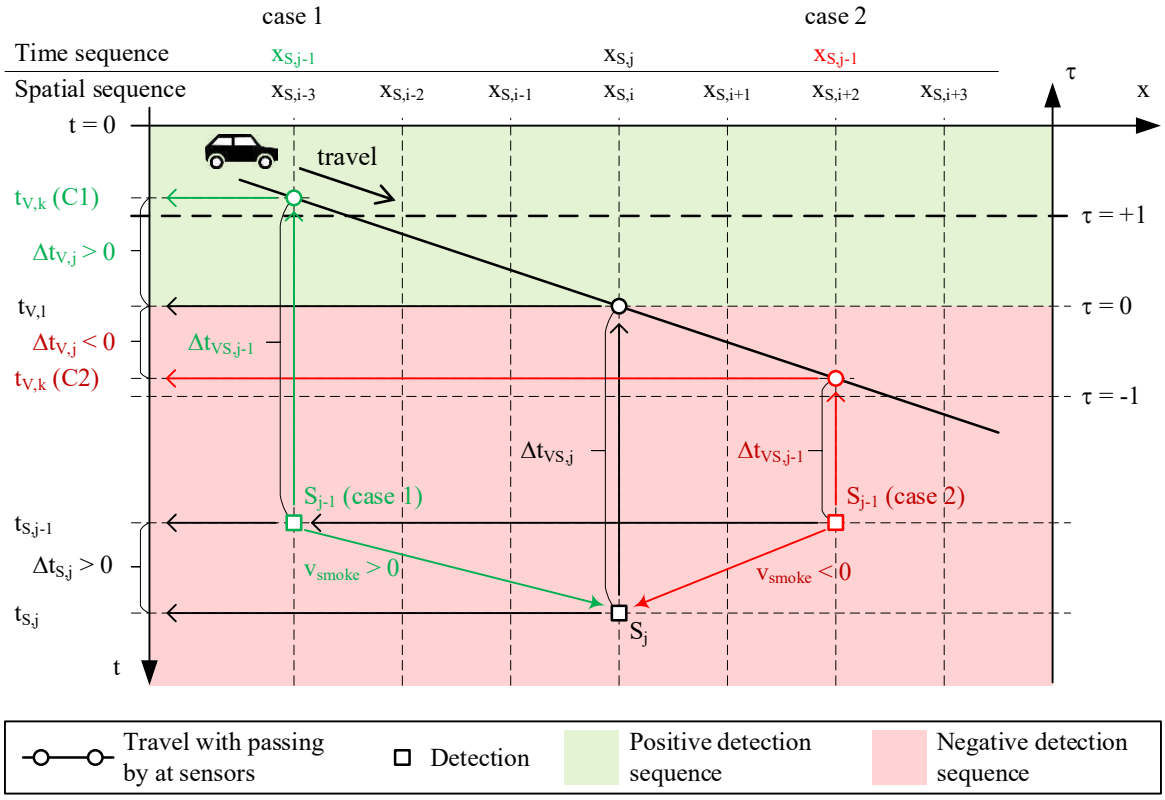


Figure 3: Schematical space-time chart for the time interpretation of τ

2.3.2. Space-Time-Velocity Charts and Boxplots

The results of the tests are evaluated and represented using two different types of plots:

- Space-time-velocity charts for representing the time and location of the detection points and the travel of the vehicle in the tunnel for each test. These charts allow to judge qualitatively the results and repeatability of a series of tests, as well as to detect patterns and anomalies in the tests.
- Boxplots for the statistical evaluation of the delay and sequence of Δt_{VS} and τ over several tests for different categories of parameters.

The so-called boxplot of a random variable uses boxes and lines to represent its distribution on one line, instead of on a plane like a histogram (cf. for an example **Figure 5**). Such plots show at a glance:

- The median of the distribution: the line in the box.
- The quartiles: 50% of the data lies inside the box; the lower edge is the lower quartile (25%) and the upper edge the upper quartile (75%).
- The extrema: the minimum and maximum of the distribution lie at the end of the line ("whiskers") below and above the box.
- The outliers: the points below and above the extrema.

The notch around the median "displays the variability of the median between samples" [5].

3. RESULTS

3.1. Space-Time-Velocity Charts

Two examples of space-time-velocity charts from both tunnels presented in section 2.2 are shown in **Figure 4** in the appendix. They have in common: the speed of travel (between 33 and 34 km/h), the intermediate air speed (between 2.5 and 3.0 m/s) and the direction of travel against the flow direction. The examples are chosen to illustrate how different the experimental results can be even for similar setups.

Whereas in **Figure 4a** all sensor types display a well behaved delay and sequence of detection, this is not the case in **Figure 4b**: The delay of detection is very long for all three sensors, the sequence of detection of the smoke detectors using threshold 1 (SD:TH1) is very chaotic, and most smoke detectors detect at threshold 2 (SD:TH2) only during the extraction of the smoke after the regular end of the test. The cameras (V-AID:SM) are behaving in a similar manner.

The reasons for this behaviour are yet not well understood and a matter of ongoing research.

3.2. Delay of Detection Δt_{VS}

Several boxplots of the delay of detection Δt_{VS} are presented in **Figure 5**. The data are divided into four categories: by sensor, by tunnel, by flow velocity and by driving direction with respect to the flow direction. The main parameters of the distributions: median, quartiles and sample size (number of samples), are presented in **Table 2** for the smoke detectors and in **Table 3** for the V-AID.

Figure 5a displays on the left the delay of detection of the smoke detectors relative to threshold 1 (SD:TH1) in tunnel 1. The median delay is shorter when driving in flow direction than when driving against the flow direction. In both directions, the median delay and the width of the distribution decrease with increasing flow velocity. On the right the same data are displayed for tunnel 2. Here also the median delay is always shorter when driving in flow direction than in the opposite direction. However, the median delay and the width of the distribution do not decrease with the flow velocity, as noted in tunnel 1, but rather increase. This is consistent with the behaviour observed in the space-time charts in **Figure 4b**. In tunnel 1 the median delay lies between 73 and 29 seconds, and in tunnel 2 between 115 and 21 seconds.

Table 2: Median, quartiles and sample size of delay plots in **Figure 5a** (SD:TH1)

Tunnel	Parameter	Unit	1,5-2,0 m/s		2,5-3,0 m/s		4,0-4,5 m/s	
			Against	With	Against	With	Against	With
1	Median and quartiles	[s]	$73{,}0^{92{,}2}_{56{,}5}$	$38{,}6^{51{,}7}_{32{,}3}$	$64{,}4^{71{,}0}_{56{,}0}$	$33{,}2^{37.8}_{30.4}$	$61{,}8^{66{,}8}_{54{,}5}$	$29{,}2^{30{,}0}_{27{,}7}$
	Sample size	[pc.]	69	72	116	118	69	72
2	Median and quartiles	[s]	$85{,}7^{125{,}9}_{67{,}1}$	$71{,}2^{97{,}1}_{47{,}8}$	$114{,}8^{141{,}0}_{98{,}5}$	$37.2^{43.6}_{32.3}$	$114{,}0^{153{,}2}_{87{,}4}$	$21{,}4^{23{,}2}_{20{,}0}$
	Sample size	[pc.]	84	66	93	84	49	77

Figure 5b displays the delay of smoke detection of the V-AID (V-AID:SM). In tunnel 1 the distributions are very narrow at all flow velocities and directions, with median delays between 35 and 40 seconds. The data displays a slight increase in the median with increasing flow velocity. The slight differences observed with respect to the driving direction are statistically insignificant, as the notches overlap at a given velocity. In tunnel 2, when driving in the direction of the flow, the distributions are also very narrow, the median delay lies between 17,4 and 17,9 seconds and no effect of the flow velocity is observed. However, when driving

against the flow direction, the distributions are very broad, the median delays very high and the sample sizes small. This is consistent with the behaviour observed in the space-time charts in **Figure 4b**.

Table 3: Median, quartiles and sample size of delay plots in **Figure 5b** (V-AID:SM)

Tunnel	Parameter	Unit	1,5-2,0 m/s		2,5-3,0 m/s		4,0-4,5 m/s	
			Against	With	Against	With	Against	With
1	Median and quartiles	[s]	$36{,}4^{38{,}0}_{34{,}2}$	$35{,}2^{36{,}7}_{33{,}5}$	$38{,}7^{41{,}1}_{37{,}1}$	$38{,}7^{39{,}9}_{37{,}4}$	$38{,}5^{40{,}8}_{37{,}2}$	$39{,}7^{41{,}2}_{38{,}7}$
	Sample size	[pc.]	57	72	97	111	54	65
2	Median and quartiles	[s]	$94{,}1^{127{,}7}_{56{,}3}$	$17{,}4^{19{,}1}_{15{,}5}$	$83{,}8^{115{,}2}_{40{,}7}$	$17{,}9^{19{,}6}_{16{,}2}$	$83{,}5^{105{,}3}_{54{,}8}$	$17{,}8^{19{,}4}_{16{,}4}$
	Sample size	[pc.]	41	86	57	129	35	115

The tunnels are equipped with different types of smoke detectors configured to react at different levels of smoke concentration. However, the data presented above displays certain similarities. The delay in detection using smoke detectors is very sensitive:

a) to the flow velocity in the tunnel: it decreases with increasing flow velocity,
b) to the driving direction relative to the flow direction: it is much shorter when driving with the flow than opposite to the flow direction.

The tunnels are equipped with similar V-AID cameras and algorithms. The delay in smoke detection using V-AID is:

a) independent from the flow velocity,
b) independent from the driving direction relative to the flow direction, if one only considers tunnel 1.

Regarding the delay of detection, V-AID delivers reproducible results, independent from flow velocity and direction. It appears that this is much less the case with traditional smoke detectors. The significant difference in delay of the V-AID between the two tunnels is potentially caused by the parametrization of the image processing algorithm.

3.3. Sequence of Detection τ

Several boxplots of the sequence of detection τ are presented in **Figure 6**. The data are divided into three categories: by tunnel, by flow velocity and by sensor. The main parameter of the distributions: median, quartiles, sample size and negative samples, are presented in **Table 4**.

Figure 6a displays on the left the sequence of the smoke detectors, threshold 1 (SD:TH1) and the V-AID (V-AID:SM) in tunnel 1. The median sequence of the V-AID:SM lies very close to one at all flow velocities; the distributions are very narrow, the whiskers lie above zero with few outliers below zero (less than 5,4%), which indicates a correct and repeatable sequence of detection independent of the flow velocity most of the time. In contrast, the median sequence of the smoke detectors is poor, much lower than 1, but increases with increasing flow velocity (between 0.56 and 0.84). Also, the percentage of negative sequences is much higher (15,7 to 21,5%). The algorithms distinguishing moving from stationary smoke sources must specifically be able to cope with such cases. The trends are similar in tunnel 2: median sequence close to 1 and independent of flow velocity for the V-AID, low median sequence increasing with flow velocity for the smoke detectors. However, the performance of both detection systems in tunnel 2 is inferior to tunnel 1: all median sequences are lower in tunnel 1, especially for the smoke detectors; the distributions of the V-AID sequence is much wider, and the percentage of negative sequences is much higher, about 20% for the V-AID and up to

42% for the smoke detectors. This is consistent with the behaviour observed in the space-time-charts in **Figure 4b**.

Table 4: Median, quartiles, sample size and negative samples of sequence plots in **Figure 6**

Tunnel	Parameter	Unit	1,5-2,0 m/s		2,5-3,0 m/s		4,0-4,5 m/s	
			SD: TH1	V-AID: SM	SD: TH1	V-AID: SM	SD: TH1	V-AID: SM
1	Median and quartiles	[-]	$0{,}56^{1{,}08}_{0{,}04}$	$0{,}98^{1{,}16}_{0{,}76}$	$0{,}73^{1{,}19}_{0{,}23}$	$1{,}00^{1{,}14}_{0{,}75}$	$0{,}84^{1{,}06}_{0{,}28}$	$0{,}95^{1{,}15}_{0{,}74}$
	Sample size	[pc.]	130	112	223	184	133	101
	Negative samples (τ<0)	[%]	21,5	3,6	15,7	5,4	17,3	5,0
2	Median and quartiles	[-]	$0{,}03^{0{,}29}_{-0{,}17}$	$0{,}87^{1{,}07}_{0{,}21}$	$0{,}34^{0{,}84}_{0{,}00}$	$0{,}88^{1{,}06}_{0{,}24}$	$0{,}77^{1{,}04}_{0{,}11}$	$0{,}89^{1{,}07}_{0{,}33}$
	Sample size	[pc.]	132	105	148	164	109	137
	Negative samples (τ<0)	[%]	41,7	21,9	24,3	20,1	16,5	19,0
All	Median and quartiles	[-]	$0{,}17^{0{,}66}_{-0{,}10}$	$0{,}93^{1{,}13}_{0{,}61}$	$0{,}60^{1{,}07}_{0{,}06}$	$0{,}91^{1{,}10}_{0{,}66}$	$0{,}81^{1{,}05}_{0{,}20}$	$0{,}90^{1{,}10}_{0{,}53}$
	Sample size	[pc.]	262	217	371	348	242	238
	Negative samples (τ<0)	[%]	31,7	12,4	19,1	12,4	16,9	13,0

Figure 6b shows the sequence of detection when the datasets of tunnels 1 and 2 are merged. This merger assumes that the results of two different smoke detector technologies can be compared directly. The same general trends as described above are observed here. The sequence of detection using the smoke detectors:

a) Is very sensitive to the flow velocity; its median is low (close to zero) at low velocity and increases with increasing velocity (close to one),
b) Displays a high percentage of negative sequences, above 17% and up to 32% in this case.

On the other hand, the sequence of smoke detection using V-AID:

a) Is independent of the flow velocity,
b) Is very close to one in the median,
c) Displays a low percentage of negative sequences, below 13% in this case.

As a summary, the smoke detection using V-AID delivers reproducible and correct sequences of detection that are independent from the flow velocity in the tunnel most of the time. This is not the case with smoke detectors.

4. CONCLUSION AND OUTLOOK

The quantitative evaluation of the smoke tests uses the delay of detection Δt_{VS} and the dimensionless sequence of detection τ. It shows that within the executed tests, the smoke detection by V-AID performs significantly better than the detection with smoke detectors based on extinction measurements, because:

a) V-AID detects faster with a smaller dispersion,
b) V-AID detects dependably with a smaller dispersion, which means that the sequence of detection is closer to 1 and scatters less than in case of smoke detectors,
c) V-AID is less prone to false detection of reverse sequences ($\tau < 0$).

As the sample size for τ of SD:TH1 and V-AID:SM of both tunnels is greater than 800 data points, these conclusions are very reliable.

The tests have shown that the quality of detection of the smoke detectors at threshold 1 depends on the direction of travel with respect to the flow direction and velocity. The quality of detection increases with increasing flow velocity and is better when driving with the flow direction than opposite to it. Yet it is assumed that this is heavily related to smoke density and local flow structures in the wake of the vehicle

It has to be noted that V-AID can lead to bad results under certain conditions. These conditions are not understood yet. As with smoke detectors, this could be related to the lower smoke density when driving against the flow. On the other hand, the lack of quality can also be related to parametrization and training of the image processing algorithm.

In order to gather a better understanding of V-AID systems but also of traditional smoke detectors, the study must be extended to more objects and, in particular, more V-AID algorithms. Furthermore, effects related to fog, camera placement, pollution of the cameras, changes in lighting condition etc. must be analysed prior to qualifying V-AID based smoke detection as potential replacement of traditional technologies. Also, regarding the reliability and in particular the distinction of moving / stationary smoke sources, the impact of the lack of thresholds has to be investigated and parametrization of V-AID systems must potentially be optimized.

5. LIST OF ABBREVIATIONS

Table 5: List of abbreviations

Shorthand	Meaning
Bif.	Bifurcation
SD:TH1	Smoke detector, detection of smoke at threshold 1
SD:TH2	Smoke detector, detection of smoke at threshold 2
V-AID	Video based automatic incident detection
V-AID:SM	Video based automatic incident detection, detection of smoke
v_{air}	Air velocity in tunnel

6. REFERENCES

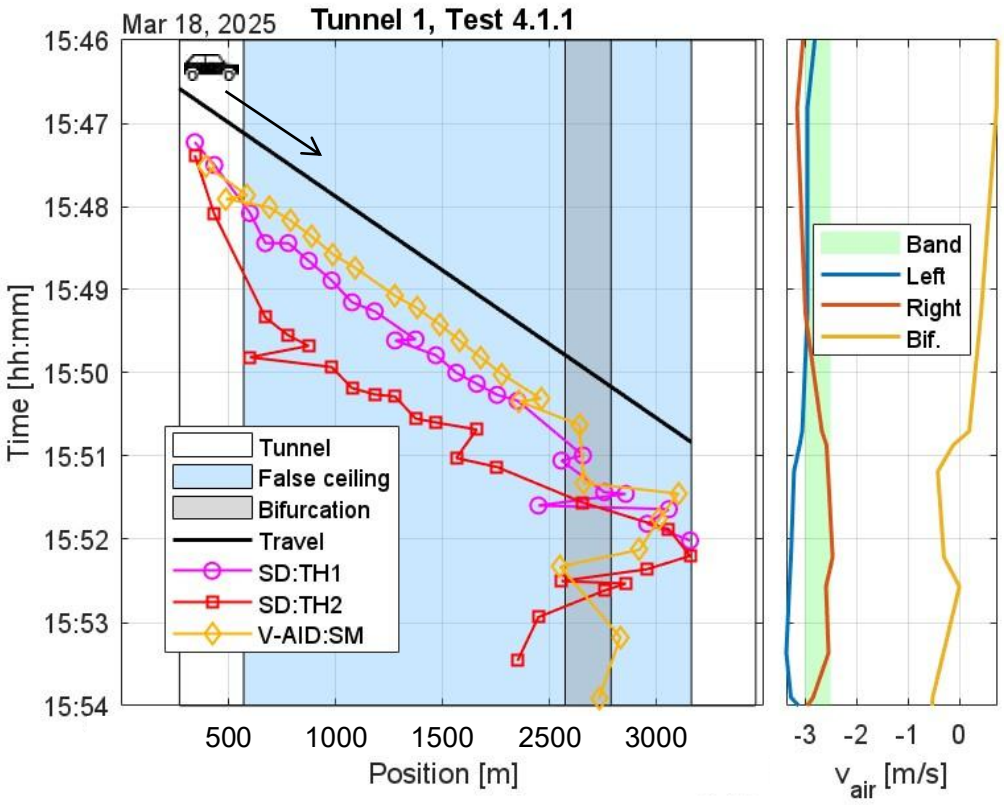
[1] Swiss Federal Roads Administration FEDRO, ASTRA 13004, “Branddetektion in Strassentunneln”, V2.10, 2007

[2] Swiss Federal Roads Administration FEDRO, ASTRA 23001, “Fachhandbuch Betriebs- und Sicherheitsausrüstungen (FHB BSA)”, 2025

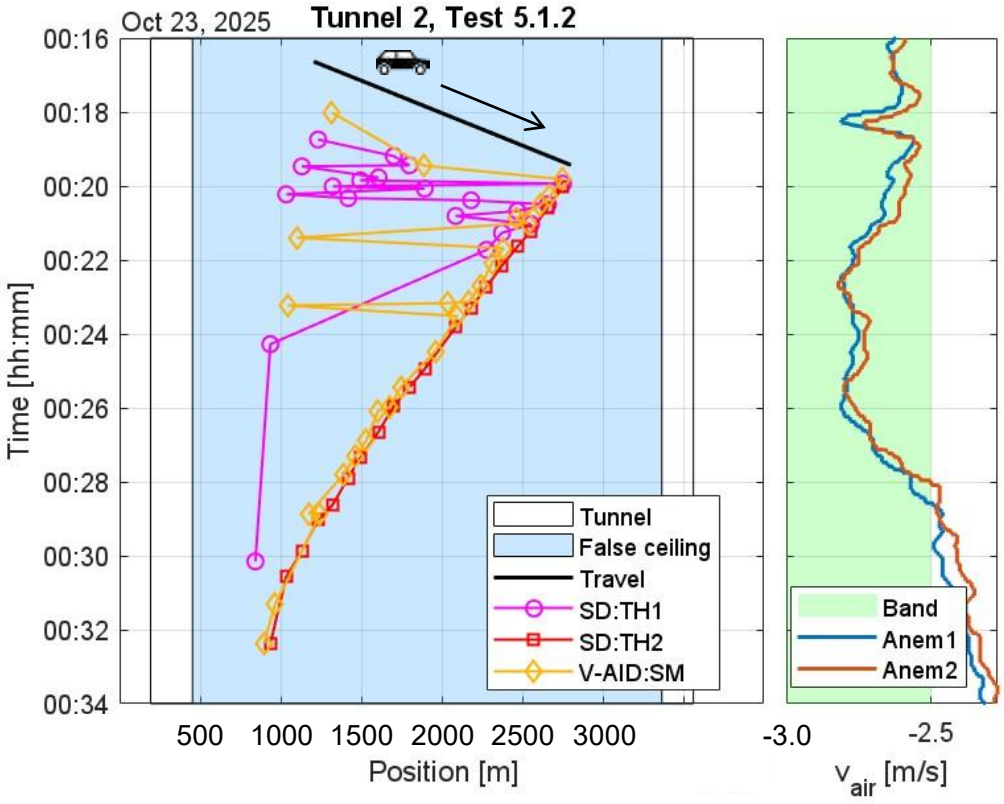
[3] M. Lempp, N. Riklin, V. Butty, F. Zumsteg, M. Eisenlohr, P. Wartmann, “Smoke detection in road tunnels leading to automatic incident response”, 9th International Conference ‘Tunnel Safety and Ventilation’, Graz, 2018

[4] M. Ehrensperger, V. Butty, S. Frey, “Smoke detection in branching tunnels”, International Symposium of Aerodynamics, Ventilation and Fire in Tunnels, Copenhagen, 2024

[5] MATLAB Help Center, Documentation, Compare Grouped Data Using Box Plots, 1994-2025 The MathWorks, Inc

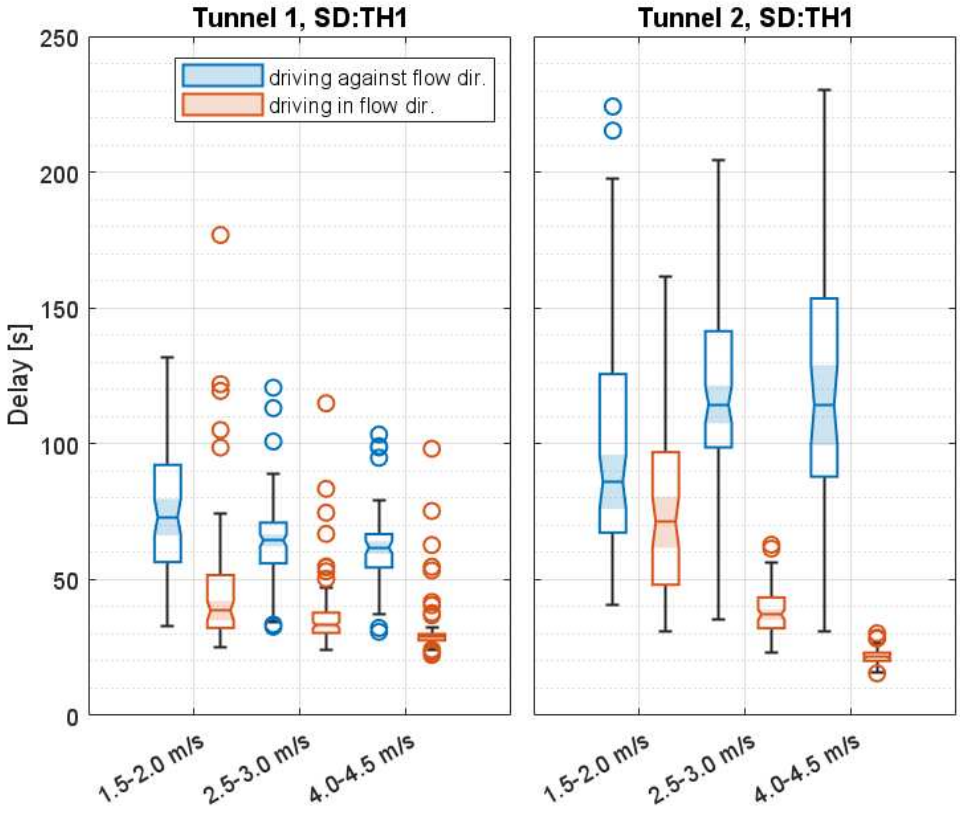


(a)

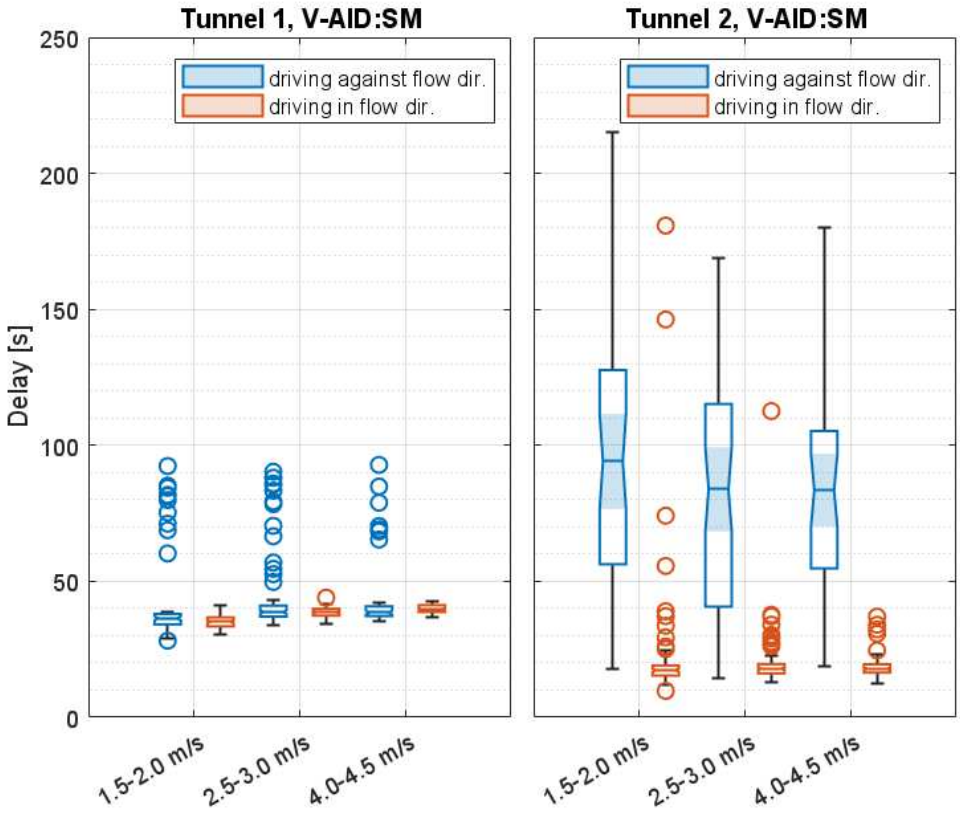


(b)

Figure 4: Space-time-velocity charts, two examples of two different tunnels at intermediate flow rate. travel direction against flow direction.

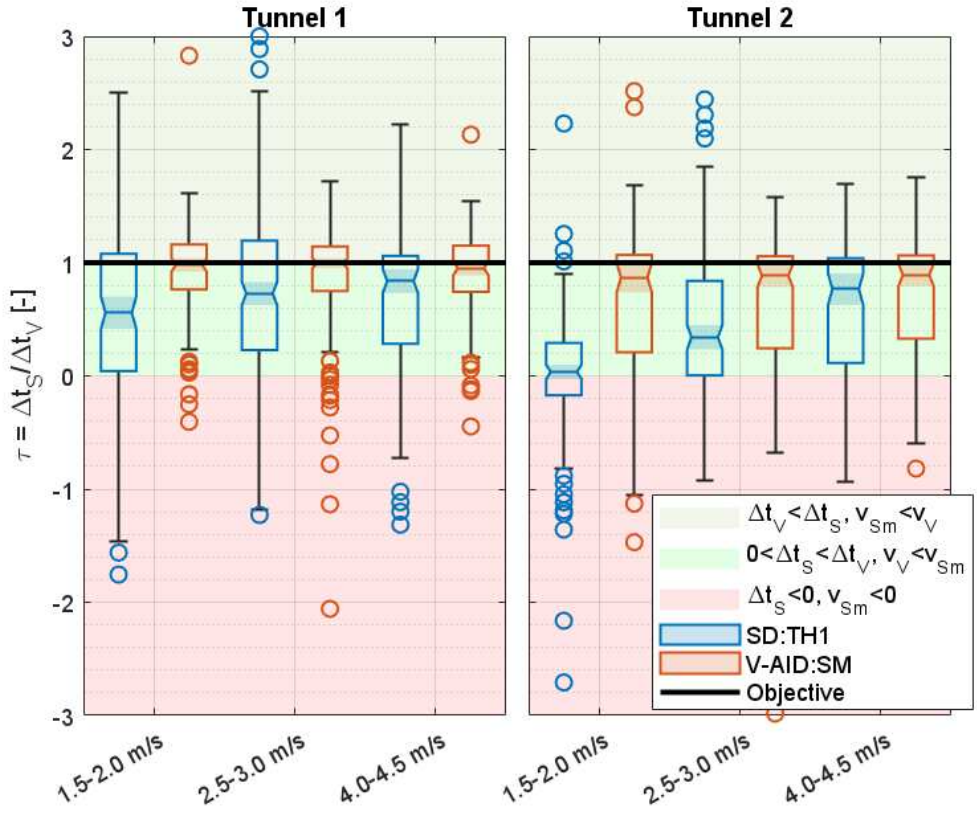


(a)

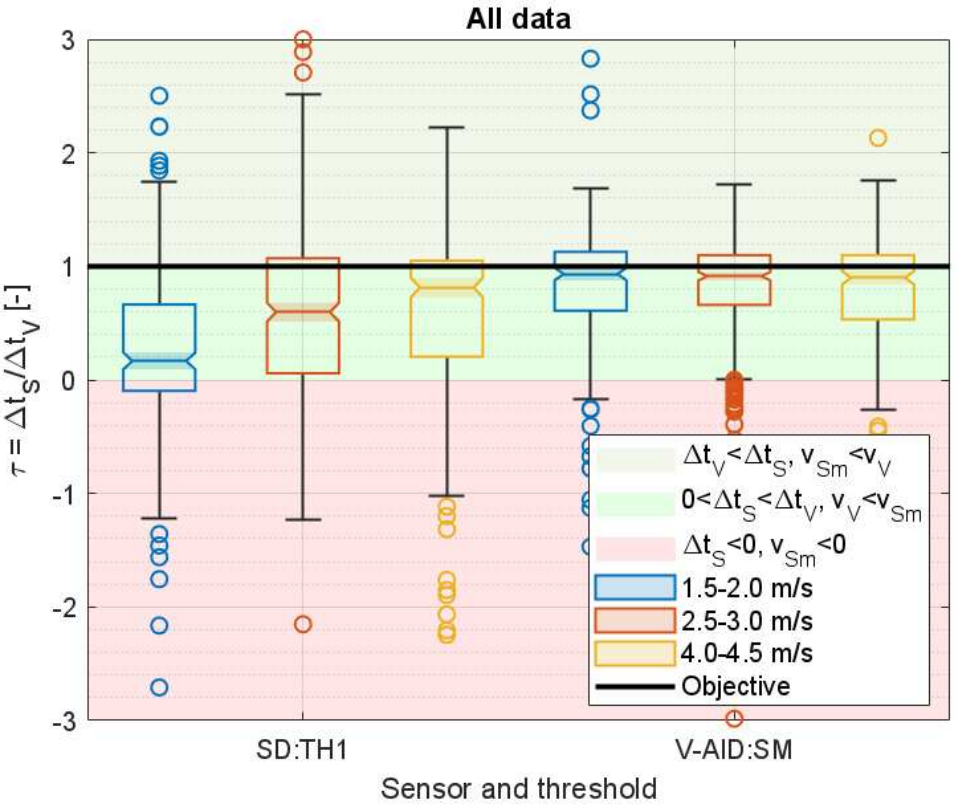


(b)

Figure 5: Boxplots of the delay of detection by flow velocity, by driving direction relative to the flow direction and by tunnel (a) for smoke detectors, threshold 1, and (b) for V-AID, smoke



(a)



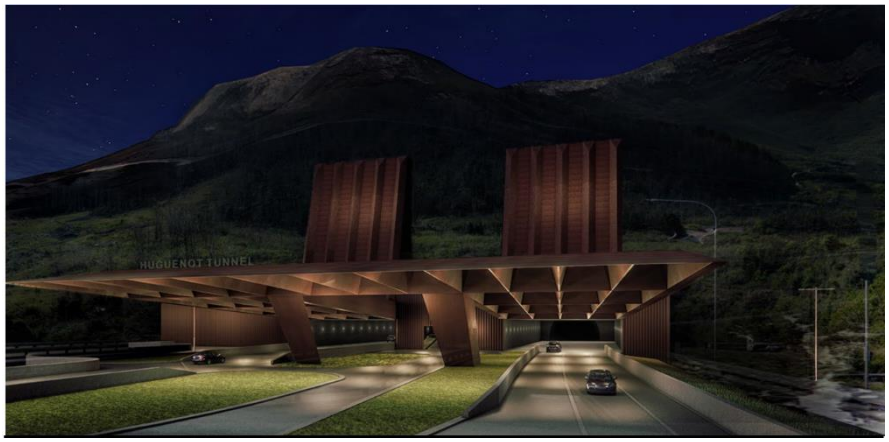
(b)

Figure 6: Boxplots of the sequence of detection for smoke detectors, threshold 1, and V-AID, smoke, by flow velocity and (a) by tunnel and (b) all data merged

VENTILATION SYSTEM UPGRADE FOR HUGUENOT TUNNEL IN SOUTH AFRICA

Tiago Massingue[1], Julia Kearns[2]

[1]*The South African National Roads Agency SOC Ltd, ZA*
[2]*SMEC South Africa (Pty) Ltd, ZA*



DOI 10.3217/978-3-99161-087-8-031 (CC BY-NC 4.0)
https://creativecommons.org/licenses/by/4.0/deed.de
This CC license does not apply to third party material (attributed to other sources) and content noted otherwise.

ABSTRACT

Worldwide, tunnel operators increasingly adopt modern ventilation technologies to enhance safety and operational standards. This is the case for ventilation systems in the Huguenot Tunnel, South Africa, where the current ventilation system that has been in operation since 1982, is now inadequate and subject to immediate replacement.

The major drive for this effort is that the existing system, built in the 80s, no longer meets the requirements of a modern tunnel. A single 375 KVA axial fan in each 4km bore for both air inlet and extraction partnered with one for extraction at the portal of each bore cannot respond to the 100 MW fire load requirement. The two axial fans are located exactly at the ceiling portal at less than 5 m from the entry. 'While ventilation alone cannot fully mitigate fire risks, modern localized solutions significantly improve tunnel safety.



Figure 1: The Huguenot Tunnel in South Africa build in 1982

A semi-transverse system is being introduced to mitigate the current shortfalls. The proposed new system aims to introduce a single point extraction through the provision of air and smoke extraction dampers at approximately 80 m intervals. These new dampers above each existing ceiling slot will also block fresh air. Replacement of the exhaust fan bypass door with a damper system will increase the extraction capability to 200-250 m^3/s in line, with internationally acceptable standards, whilst the introduction of new jet and axial fans will enhance the air control and ability to extract air at a fire incident.

1. INTRODUCTION

The South African National Roads SOC Agency (SANRAL) has identified the need to upgrade the Huguenot Tunnel from a two-lane single bore to twin bore tunnel configuration with separated traffic flows. The proposed intervention will address traffic capacity issues, provide upgrades to the fire and ventilation resilience systems to respond to a 100MW fire, improve vehicle and pedestrian cross connections as well as provide a new concrete pavement structure. Currently, SANRAL is undertaking repair works to the existing Huguenot Tunnel South Bore, comprising the following activities: installation of a new back-up generator; replacement of variable message signs (VMS), electronic signage, fire detection and suppression systems; and installation of new radio and re-broadcast systems to enhance tunnel public announcement systems. The Huguenot Tunnel is the main transportation link between the coastal plains of the Western Cape and the interior. It eliminates a steep climb of 500m over the 23 km long Du Toits Kloof Pass and contributes significantly to the national economy in terms of savings in logistics, road user costs and accident costs. It is expected that once all works are complete not only will there be an enhanced tunnel safety environment but also it will also comply with international tunnel safety standards (EU Directive 2004 for Tunnel Operations). The South Bore, in operation alone for 37 years has carried a total of 110 million vehicles of which 90 million were light and 20 million Heavy Goods Vehicles. It is therefore of strategic significance for the South African National Roads Network.

2. VENTILATION SYSTEM

The current Huguenot Tunnel ventilation system is old and obsolete. It is therefore essential, as part of the major tunnel upgrade, to modernize this ventilation system. The single 375 KVA axial fan in each 4km bore for both air inlet and extraction partnered with one for extraction at the portal of each bore cannot respond to the 100 MW fire load requirement likely in the case of a major fire. Upgrading the tunnel to eliminate ventilation constraints has been prioritized by SANRAL.

2.1. Existing ventilation capability

Two modes of operation are currently in use. These two independent components operating separately aim to address possible opposing scenarios within the tunnel ventilation environment. The fresh air duct aims to supply fresh air into the tunnel. Then the smoke extraction system aims to exhaust fumes in case of fire or any other undesirable fumes in the tunnel. The two systems are facilitated by means of bypass doors which are used as deemed necessary. The bypass door is as important as any other system because its failure would mean the tunnel would be reduced to fresh air or exhaust air systems only.

Figure 2 A) below shows the day-to-day operation at the natural barometric pressure where the fresh air inlet is continuously made available through the ceiling and underneath the vertical wall panels along the tunnel length. The bypass door/valve used critically for extraction also contributes for enhanced air inlet in normal operation.
Operation in the event of a fire is shown in Figure 2 B) and demonstrates that, for operation in the event of fire, only the extraction capability is maximized. The lack of dampers is a major constraint for effective operation standards in the tunnel.

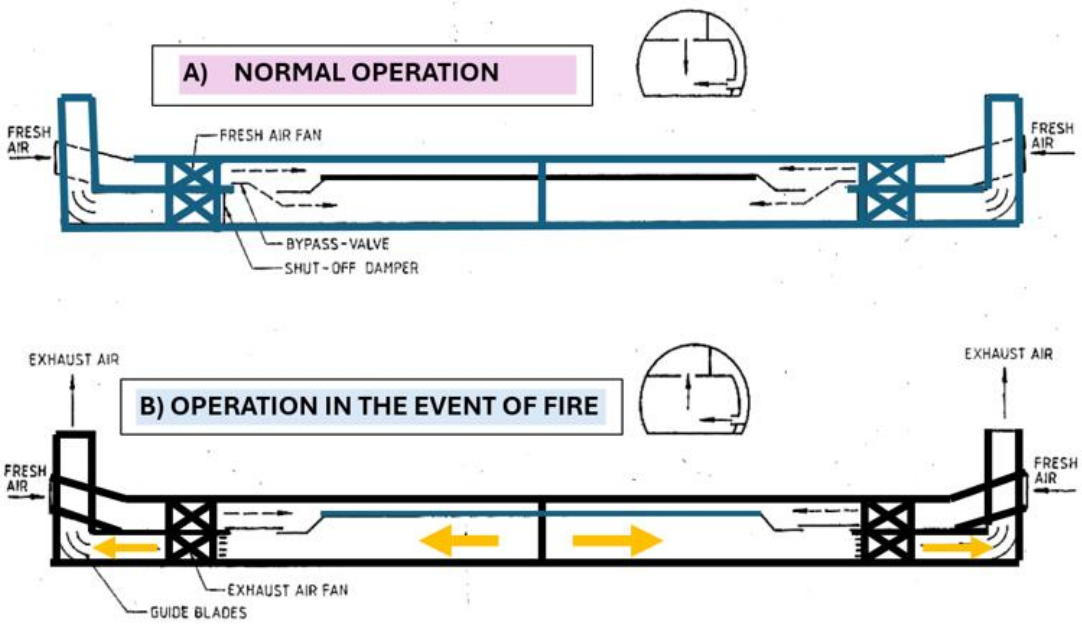


Figure 2: Normal Operation & Operation in the event of fire

3. VENTILATION IMPROVEMENT DESIGN CONCEPT

Several ventilation methods, namely longitudinal, transverse ventilation (including semi-transverse) and single point extraction were assessed for feasibility at the preliminary stage. Single point extraction was selected as most effective functionally for both bi-directional as well as unidirectional traffic flow scenarios. This option was found to offer the following benefits:

- Energy efficient – The system fully utilizes the fresh air and take full advantage natural air velocity for tunnel ventilation.
- Reduces portal air short circuiting.
- Fire Safety – The system can limit the fire affected zone to enable safe evacuation and firefighting. As a result, fire fighters can approach the fire from both sides.
- Operation Flexibility – The system can cater for bi-directional and unidirectional traffic without changing the system operational concept.
- Fast Response – As the exhaust fans are running for pollution ventilation, the exhaust location can be switched to the fire site within a shorter period. This can reduce movement and spread of smoke.
- Fast Recovery – Single point extraction system can limit the smoke affected zone to a reasonably short distance in the tunnel. This will limit the fire damage to a short distance, resulting in fast recovery and cost-effective repair/refurbishment after a fire incident.

3.1. Design Strategy

The Computational Fluid Dynamics (CFD) model developed for the project indicated that for a 100 MW fire load the axial fans would operate at 175 to 300m/second. New axial fans would be required to replace the old 375 KVA axial fan, but modernization of the existing fans would also be required. World Road Association (PIARC) guidelines on air quality parameters as well as the recommended CO levels were used for comparison. Based on the above, the pollution control ventilation rates were calculated for different project phases including bi-directional traffic and unidirectional traffic. For bi-directional traffic for year 2025, the peak airflow rates for East Bound and West Bound were 152.8m³/s (40kph) and 139.5m³/s (40kph) respectively. Similarly, for unidirectional traffic in year 2028, the peak airflow rates for East Bound and West Bound were 223.6m³/s (20kph) and 198.4m³/s (20kph) respectively. The limits of the airflow rates in Fig 2 below were therefore assumed at the range of 200m³/s to 300m³/s respectively.

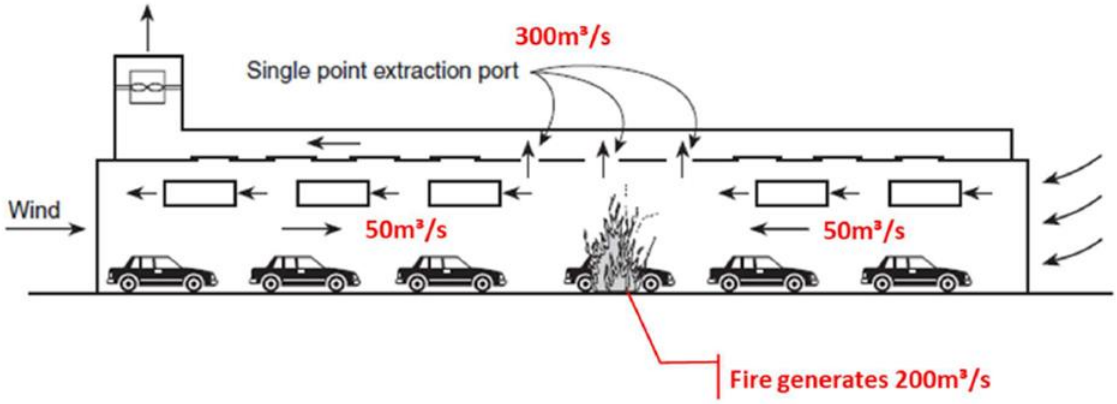


Figure 3: Limits of the airflow rates as per the CFD calculations

3.2. Key Equipment Components

The commissioning of the Huguenot Tunnel North Bore, and the upgrade of the Huguenot Tunnel South Bore has defined key equipment components to be used in line with CFD Models, previously discussed. These entail, the:

Provision of new axial fans,

- Provision of new jet fans,
- Introduction of new dampers, and,
- Retrofitting of the tunnel crown for the South Bore

a) New axial fans

Based on research of current suppliers, as well as supporting the (CFD) requirements, the following axial fans were selected for the North and South Bore Tunnels:

Table 1: Ventilation design requirements for new axial fans

Number of Tunnel Ventilation Buildings	2
Airflow rate per fan	100 m³/s
Total Tunnel Ventilation Fans in operation at peak load normal operation	3
Normal operation (Bi-directional traffic)	300 m³/s
Total Tunnel Ventilation Fans in operation for emergency	3
Emergency Operation	300 m³/s

b) New jet fans

The CFD model tested three different jet fans sizes of 900, 1200 and 1600 mm diameter to counter the natural air velocity during the emergency. Subsequently, the 1600 mm diameter fans were selected, and the summary of their output specifications was as follows:

Table 2: Ventilation design requirements for jet fans

Jet fan diameter	1600 mm
Thrust	2160 N
Number of fans per niche	3
Total duty fans	30
Standby fans	3
Total number of niches per tunnel	11

c) New dampers

The provision of dampers to effectively contribute to the extraction capability of smoke in normal and critical operations. The new improvement not only will provide working teams with proper fresh air in their normal activities, but it will be used also to exhaust fumes and gases that are detrimental to human lives and can be the major cause of fatalities in case of fires. This improvement is one of the most important technical contributions to a previously designed tunnel without ventilation dampers. The concluded design has established that the size of dampers will vary between 3 m³and 5 m³ for spacing intervals of 50 to 100 m. Due to high temperatures of the smoke in the extraction zone, the dampers will feature a heat resistance of at least 400 ℃ for 90 minutes. The time required for opening or closing the dampers should not exceed 25 seconds.

d) Reprofiling the tunnel crown

All design improvements being introduced at the Huguenot Tunnel North Bore must be replicated in the South Bore and for that purpose the tunnel crown of the south bore must be reprofiled to cater for the substantial 1600 mm diameter jet fans. This is an operation requirement which is made by specialist ventilation firms however it triggers a substantial level of new work in the currently operational bore.

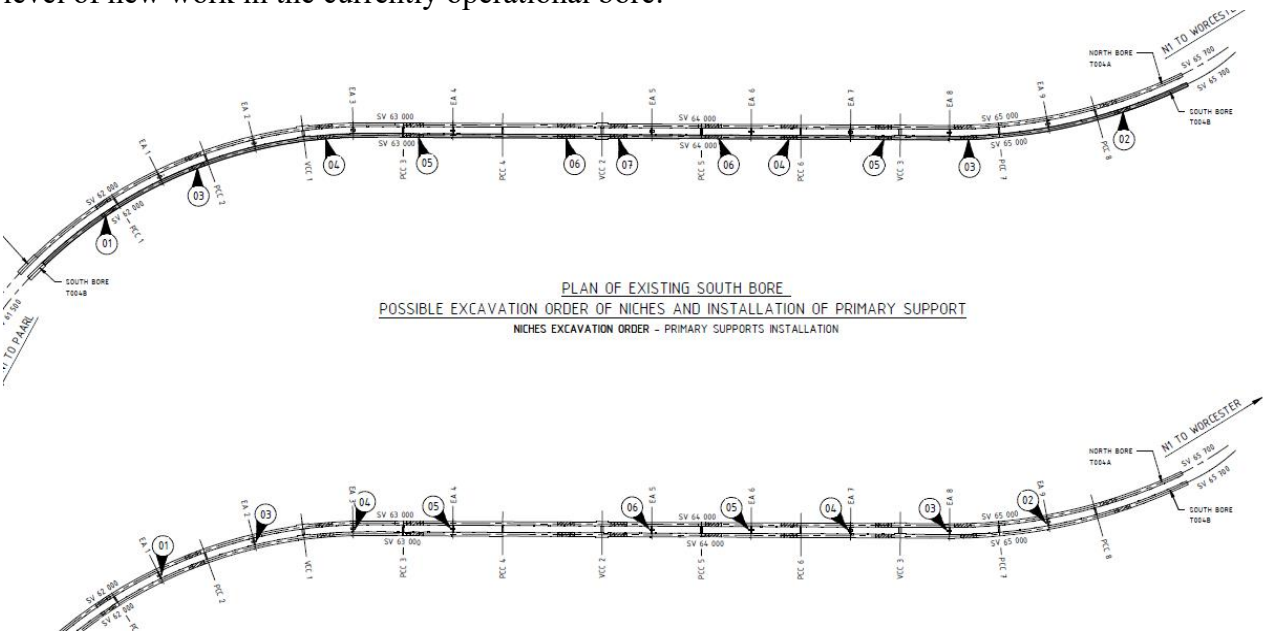


Figure 4: Niches layout

3.3. Retrofitting new design components

In terms of the ventilation design, 11 no. vertical niches are to be excavated into the roof of both tunnels to accommodate banks of jet fans. Niches are 56 m long and approximately 330 m apart. Vertical niches accommodate 11 banks of 3 no. reversible jet fans at each niche location, as shown in Fig 4 and Fig 5. Speed controls, including variable speed drives and power reticulation to jet fans is supplied from the 9-no. new cross connections and electrical adits. Fixed fire suppression system with misting nozzles will be installed to both North and South Bores. The misting system will be mounted to the underside of the tunnel ceiling. Monitoring will include cameras with 100% coverage (optical and thermal), heat detectors, sensors, all fully connected to Tunnel Supervisory Control System. Fig 4, 5 & 6 shows the design strategy applicable to North and South bores encompassing new niche locations, typical elevation and cross section as well as the expected final outcome.

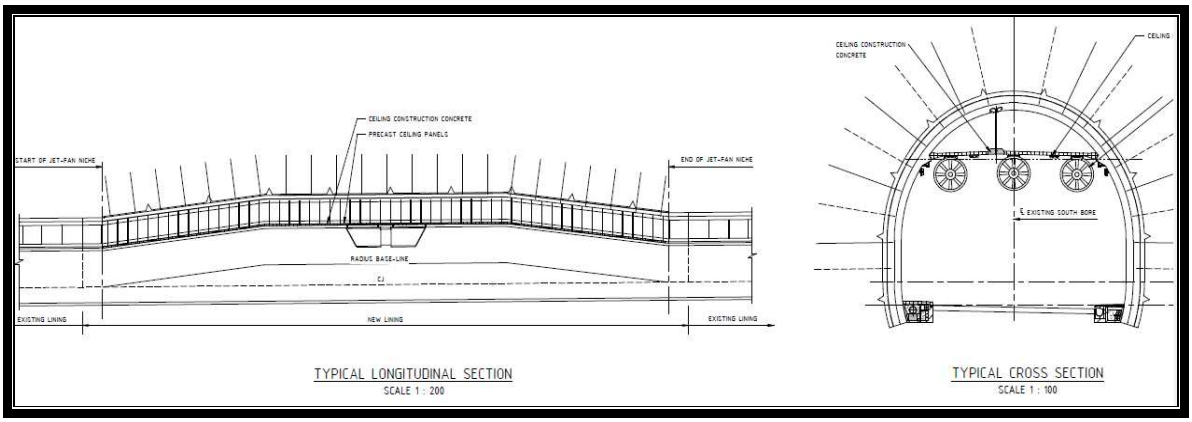


Figure 5: Niche longitudinal and cross sections

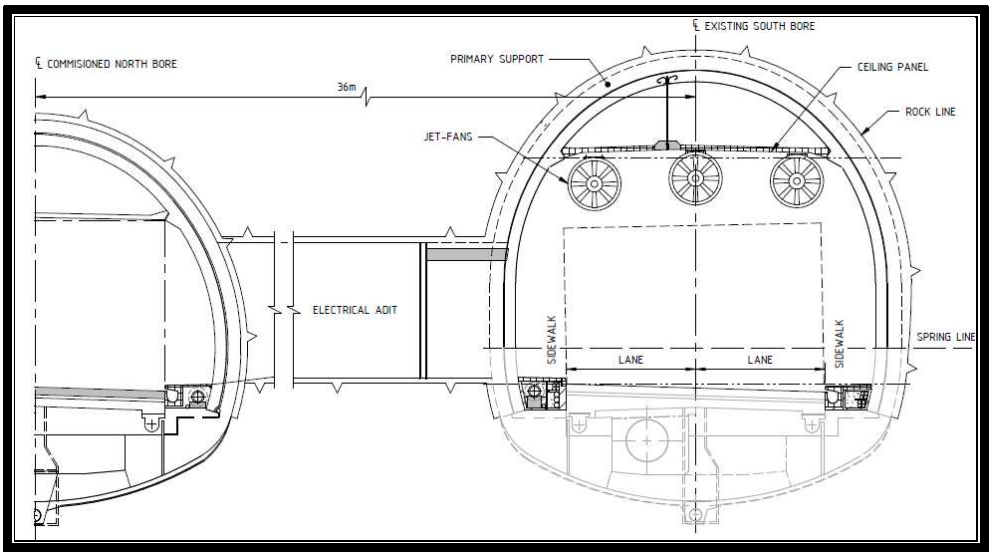


Figure 6: Design consideration for new niche after reprofiling tunnel crown

4. CONCLUSIONS

The South African National Road Agency is committed to develop the Huguenot tunnel as a twin bore mega infrastructure. All design steps for achieving this have been concluded and the appointment of contractors for civil work is at a final stage. The ventilation design and the retrofitting of its main components namely the new north bore, and the existing south bores are part of the scope of work that must be implemented for the safety of road users. As a project of unique complexity in the past 40 years one would expect some challenges related to experience of construction firms and possible implementation delays. The Huguenot Tunnel upgrade represents a significant advancement in South Africa's tunnel infrastructure, aligning with international safety standards and ensuring operational resilience. Fig 7 is the expected North and the South Bore tunnel portals as it is completed in 2029.

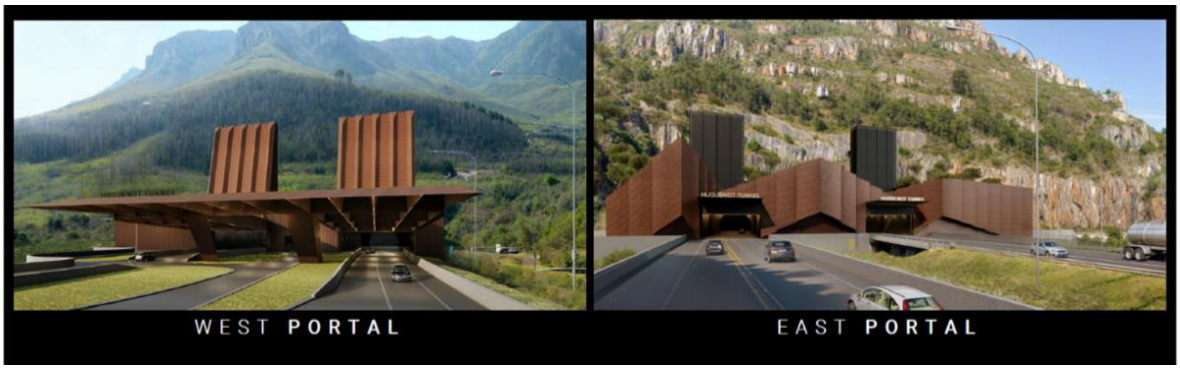


Figure 7: Architect's impression of tunnel portals after completion of the works

5. PLANNED UPGRADE WORKS

Based on the findings of the detailed design for the works, the upgrade of the Huguenot Tunnel has outlined the following activities beyond the topic discussed in this paper. These are:

- Upgrading of the N1/1 to a divided dual carriageway between km 56.430 and km 69.290 (12.86 km) with concrete-lined median drain on both approaches to the Huguenot Tunnel.
- Upgrading of the Southern Bore of the Huguenot Tunnel, including associated upgrades to the electrical, electronic, ventilation and fire suppression systems.
- Commissioning of the Northern Bore of the Huguenot Tunnel, designed for a 100 MW fire load; and including an international best practice point extraction ventilation system.
- Upgrading of the Southern Bore of the Huguenot Tunnel, to allow for a 100 MW fire load; and include an international best practice point extraction ventilation system.
- Installation of a low-pressure mist-type fixed fire-fighting system.
- Upgrading of the Main Control Centre Building, Portal Building East and Portal Building West to accommodate the upgrade of the Huguenot Tunnel.
- Upgrading of the power supply through construction of a new (132/11kV) Newland
- Substation and a back-up supply system for South Africa's state-owned electricity utility (Eskom).
- Upgrading of the tunnel electronic and control systems.
- Pavement rehabilitation of the existing N1/1 within the Planning Limits to cater for future attracted traffic.
- Providing 5 No. new bridge structures: Hugos River Viaduct Bridge A at km 60.180, Elands River Bridge at 65.690, Molenaars.
- Bridge 1A at 66.040, Molenaars Bridge 2B at 67.980 and a grade separation of the N1/R101 at 68.100.
- Incorporate findings of further geotechnical investigations in detailed design.

WEB-SCADA: A WEB-BASED SUPERVISORY CONTROL AND DATA ACQUISITION PLATFORM FOR ROAD TUNNEL SAFETY IN JAPAN

[1]Leon Dickel, [1]Mathis Ruffieux, [1]Jean Rouge, [1]Yen-Hung Lai,
[2]Masahide Nakamura, [3]Alan Vardy

[1]Sohatsu Systems Laboratory Inc., JP
[2]Kobe University, JP
[3]University of Dundee, Dundee, UK

DOI 10.3217/978-3-99161-087-8-032 (CC BY-NC 4.0)
https://creativecommons.org/licenses/by/4.0/deed.de
This CC license does not apply to third party material (attributed to other sources) and content noted otherwise.

ABSTRACT

The proposed paper introduces a web-based, remote-access platform for tunnel supervisory control and data acquisition ("SCADA"). The system enables operators and emergency services to monitor safety systems (e.g. fire detection and location) and ventilation systems, and to activate desired responses. The platform consists of an operational technology (OT) layer where real-time data is collected in a conventional database, and an information technology (IT) layer where web-based technology has replaced conventional display methods on monitoring screens.

We propose a Web-SCADA architecture built on the latest web technology. It is designed to support ubiquitous monitoring, with data displayed not only on conventional PC screens at the control centre, but also on tablets and smartphone screens in the office or even at home. By enabling direct access to the data in this way, the system facilitates fast responses by the police and fire services as well as by tunnel controllers. Also, by ensuring that everyone has access to the same up-to-date information, it enhances both the speed and reliability of information transfer, frees up humans for other tasks, and reduces the risk of potentially-flawed human communication. Simulation-based modelling is integrated into the web-SCADA to extend the real-time modelling with forecasts of the potential development of conditions (e.g. fire and smoke propagation). The modelling also assists in the detection of potential failures of sensors and other equipment.

Overall, the platform represents a significant enhancement of tunnel management whilst simultaneously reducing the need for human resources (a particular concern in Japan). It is expected to enhance both safety and operational efficiency.

Keywords: Web-based SCADA; Multimodal perception; Real-time simulation; Fire detection

1. INTRODUCTION

Road tunnel safety demands rapid incident detection, coordinated response, and precise ventilation control. This paper proposes Web-SCADA, a web-based supervision architecture that integrates multimodal sensing, edge inference and model-based simulation to support rapid incident detection and operational decision-making. The system introduces a modular OT/IT architecture enabling end-to-end data flow from sensors to simulation and visualization,

probabilistic model-based decision support for operators, and an operational sensor-health monitoring module based on the variance-ratio (σ_1/σ_0) method for detecting and isolating faulty telemetry. The paper presents three original contributions: (i) a modular web-based SCADA architecture for tunnel supervision, (ii) an integrated multimodal perception and data-fusion approach within SCADA, and (iii) the integration of simulation modules for predictive monitoring and sensor-health assessment.

Scope and limitations. The architecture presented here is a vendor-neutral design and a research prototype. While selected modules have been prototyped by the authors, this paper primarily outlines the proposed architecture, design rationale and example workflows; full experimental validation and large-scale deployment remain topics for future work.

2. TECHNOLOGICAL CHOICES

We select a modern, modular web architecture: PHP (Laravel) on the server side for the API, job orchestration and workflow management; Vue.js on the client side for a reactive, responsive UI that can be adapted to different roles (operators, firefighters, other stakeholders); MySQL as the primary transactional database for configuration, sensor data, events (alerts), tickets and simulation outputs; and Python for the model-base (simulations and scientific computations), which writes its results into the SQL database consumed by the web-SCADA. Multi-channel notifications (email, SMS, LINE for Japan, Slack for enterprise) are handled asynchronously via Laravel queues to ensure retries and traceability.

This choice builds on the "web-SCADA" paradigm documented in the literature [1] - early Web/Java implementations around 1995–2000 demonstrated the feasibility of browser-based supervisory control and lightweight client deployment, advantages that we exploit here using contemporary, industrially supported technologies.

For field data acquisition, the architecture uses a programmable logic controller (PLC) to perform direct sensor reading (AV, CO, VI, traffic counters, I/O) and to manage local real-time control logic. Complementarily, an edge inference module (YOLOv5) may be deployed on an edge device connected to cameras to reduce latency and bandwidth; both PLC and edge streams are then integrated into the web-SCADA supervision layer.

3. EQUIPMENT AND MULTIMODAL PERCEPTION

The detection and supervision system relies on multimodal perception combining the following sensors:

- Dual thermal + optical cameras - rapid thermal detection and visual classification, with the optical channel used for image-based inference (e.g., YOLOv5). [2]
- Acoustic microphones / arrays - audio signatures for collisions, tyre bursts, horns or voices; valuable in low-visibility conditions. [3]
- Linear temperature sensing cable - continuous temperature measurement along the ceiling with metre-scale localisation for fast pre-alarm confirmation. [4]
- Variable-speed (inverter) jet-fans - ventilation actuators supporting demand-driven / zero-flow strategies and accepting model-based setpoints. [5]
- Traffic counters (visible / thermal modes) - vehicle counts and class estimates feeding the model-base.
- VI / CO / AV probes - visibility index (VI), carbon monoxide (CO) and longitudinal air velocity (AV) sensors supplying quantitative inputs to the simulator.

Sensor streams (video, audio, probe measurements, linear-temperature traces and counts) are time-synchronized to enable multimodal fusion and corroborated alerts.

4. SYSTEM ARCHITECTURE AND CYBERSECURITY

The proposed system architecture follows a layered and modular design, connecting on-site sensors and control devices in the tunnel to a local monitoring and supervision platform hosted in the control room. All field data are acquired through industrial interfaces and transferred securely to the local SCADA server for visualization, analysis, and decision support (see Annex 1 for the architecture diagram).

4.1. Field layer - tunnel instrumentation

For the purpose of illustration, the scenarios in this paper assume a hypothetical tunnel instrumented with the sensors listed in Section 3, deployed and cabled to provide synchronized telemetry to the local PLC and SCADA server. Field signals include sampled probe measurements (VI, CO, AV), event streams (count, detection bounding boxes), continuous linear-temperature traces and archived video/audio.

4.2. Control and monitoring rooms

In a typical deployment, the electrical room would include an inverter panel which controls the variable-speed jet-fans (JF), and the control panel which collects signals from field sensors (AV, CO, VI, TC, linear temperature cable). A LAN cable connects the electrical room to the monitoring room, where the local web server and SQL database are installed. Sensor readings and events (video, acoustic, linear-temperature and probe measurements) are stored as structured SQL data, while video recordings are archived as MP4 files. The monitoring system can operate offline (without internet connection) for safety and independence. When connected to the internet, remote access to the web server is possible through a secure VPN, allowing authorized operators, maintenance teams and external stakeholders (e.g., emergency services) to monitor the system and receive notifications.

4.3. Cybersecurity considerations

Following industrial best practices [6], the system applies a multi-layer security posture: end-to-end encryption, multi-factor authentication for remote/VPN access, continuous IDS logging, and strict network segmentation/firewalls isolating PLC/control networks. Operational policies for patching, access control and audit logging complete the protection strategy.

5. HMI / HCI: OPERATOR INTERFACE AND USABILITY

As highlighted in the same reference [6], operator experience is critical to the effectiveness of SCADA systems. This section summarizes the design goals and usability considerations of the monitoring interface, focusing on role-adapted presentation, rapid situational awareness, and support for decision-making under stress.

5.1. Main monitoring view and role-based notifications

The monitoring screen is organised as a single operational view that presents critical information with minimal navigation (see Annex 2 for a screenshot). The central video panel shows the selected camera pair (thermal + visible) with adjacent pairs as thumbnails; a linear temperature ribbon overlays thermal readings and active detections and indicates the precise

location of a detected fire, while intervention devices (e.g. water spray) and their status are shown in context. Beneath the video, a compact sensor panel reports key environmental and ventilation values (VI, CO, AV) and jet-fan rotation rate, and a status table summarises active alerts and severity. Each operator has a personal notifications page listing alerts, comments and required actions; notifications may also be pushed to external channels (email, SMS, LINE, Slack) and filtered by type (e.g. fire only). A simplified, mobile-oriented view for emergency responders prioritises essential items only (fire location, presence of people, AV/direction, estimated time of arrival to ventilation target, thermal camera access and escape-route status).

5.2. User testing and planned evaluations

Preliminary user testing was performed iteratively to validate interaction concepts and prioritize design decisions. Early tests involved eight external participants across multiple regions and devices; their feedback guided incremental improvements to the layout, alert prioritization and responsiveness. Future evaluations will target the actual user populations (tunnel operators and emergency responders) and will include formal usability assessments with quantitative metrics such as detection and decision times, error rates, and subjective usability scores.

6. USE OF THE MODEL-BASE IN FIRE SCENARIOS

At the start of the processing chain, YOLOv5 is employed as the vehicle-classification module: its primary role is to detect and classify objects (cars, buses, trucks, etc.) in real time and to estimate their approximate dimensions from camera imagery. The vehicle class information is then mapped to an initial estimate of the fire scale (heat release rate, HRR, in MW) using type-conditioned prior distributions (national tables / PIARC) and an image→HRR calibration. In this way, visual classification does not merely describe traffic; it provides the key input—or a probabilistic prior—required to initialize the fire simulation and to predict subsequent smoke and ventilation dynamics.

6.1. Proposed architecture - detection and classification

YOLOv5 is deployed at the edge of existing camera streams (visible or thermal) to deliver low-latency vehicle type and size estimates. Importantly, YOLOv5 can be applied to any camera type, but satisfactory performance on a given sensor requires fine-tuning on images acquired from that sensor. The detector outputs both a class label and an uncertainty score; this uncertainty is propagated into the probabilistic HRR estimate used by the simulator. The presence of smoke, occlusions or adverse viewing angles degrades classification reliability and must therefore be reflected in the weighting of priors and in the confidence communicated to operators.

6.2. Fire-scale (HRR) selection - indicative table

To define design-fire scenarios, we rely on published ranges from PIARC [7], national guidance [9], and experimental findings from Nakahori et al. [13]. The indicative HRR ranges and the nominal values adopted in this work for simulation experiments are summarized in Annex 3.

6.3. Role and utility of the model-base in a fire

The model-base is a computationally light, fast simulation that ingests: (i) an initial fire-scale estimate (from YOLOv5 and/or operator input), (ii) traffic counts and flows from the traffic counter, and (iii) the pre-event state of tunnel sensors (visibility, CO, longitudinal air velocity AV, etc.). From these inputs the simulator produces near-real-time outputs: (a) smoke

propagation forecasts (arrival times and estimated VI per tunnel section), (b) traffic and congestion evolution (vehicle positions and evacuation probabilities), (c) the temporal trajectory of longitudinal air velocity (AV) and the estimated time-to-target (e.g. AV → 0 $m \cdot s^{-1}$), and (d) operational recommendations for jet-fan (JF) rotational speeds to balance evacuation facilitation and smoke control. The operational aim is to supply operators and emergency responders with actionable quantities (median and uncertainty intervals) that support safe, timely and documented evacuation decisions.

6.4. Software implementation and real-time pipeline

The simulation framework is implemented in Python. Structured prediction outputs are periodically written to a relational SQL database. A web-based SCADA frontend reads these records in real time (API / WebSocket) and visualizes: smoke arrival maps, AV time series, recommended JF setpoints and associated confidence metrics. The operational loop is therefore: sensor detection (camera / audio) → initial HRR estimate (AI ± operator) → fast simulation → write predictions to SQL → SCADA read/display → human decision/action. The model-base is subject to regular recalibration - parameter priors and image→HRR mappings are updated from operational feedback, simulation studies and available experimental data - to limit model drift and preserve prediction fidelity.

6.5. Methodological detail

The mathematical formulation of the model-base - covering vehicle dynamics, longitudinal airflow, jet-fan control and smoke advection - is summarised here; full equations and implementation notes are provided in Annex 6 (see also Annex 5 for nomenclature).

The traffic module computes vehicle positions, types and speeds at one-second intervals; traffic volume Mt (veh·h^{-1}) and mean speed Vt (km·h^{-1}) set the mean vehicle spacing $\Delta x=(Vt \cdot 1000)/Mt$. Vehicle motion uses an Optimal Velocity Model (OVM) to derive target speeds and accelerations as functions of headway, with simple stop-logic for vehicles affected by incidents.

Airflow dynamics are modelled by per-section momentum balances: portal pressure differences (natural ventilation), the piston effect of traffic, thrust from jet-fans, and frictional/resistive losses are combined to yield longitudinal velocity states used by the simulator. When a fire is detected, according to zero-flow strategy, jet-fan operation is represented by a feedback controller (PID-like) that computes target rotation/thrust setpoints from deviations between measured and desired air velocity; actuator limits and anti-windup are applied in practice.

Smoke is represented by an extinction coefficient (x,t) (m^{-1}) whose transport is computed with a 1-D advection–diffusion equation augmented by fire source terms parameterised from HRR(t). The simulator couples these modules in real time to produce forecasts (smoke arrival, visibility, AV trajectory) and recommended JF setpoints; probabilistic updates and Bayesian refinement of priors from operational feedback are also supported. See Annex 6 for the full model equations, discretisation, parameter values and numerical notes.

6.6. Operational benefit for evacuation

By combining an initial, classifier-driven fire-scale estimate with a fast, uncertainty-aware simulator, the system yields critical spatio-temporal horizons (e.g., time available before smoke reaches a given section; time until AV meets a specified threshold). Presenting these forecasts with quantified uncertainty in the web-SCADA console materially improves the ability of

operators and fire crews to coordinate evacuations, select safe ingress/egress routes, and sequence ventilation actions. Crucially, the human operator remains in the loop: when classifier confidence is low or uncertainty bands are wide, operator validation or override can be requested before automated recommendations are enacted.

7. SENSOR-FAILURE DETECTION FOR ROUTINE OPERATION

We adopt the variance-ratio σ_1/σ_0 method [10] (Annex 5 - Nomenclature) as a lightweight, operational data-quality monitor validated in case studies. The method compares the short-term residual standard deviation σ_1 (measured − predicted over a short operational window) with a reference σ_0 established during a long calibration period; $\sigma\text{-ratio}(t) = \sigma_1/\sigma_0$. Values near 1 indicate healthy sensors, while sustained values $\gg 1$ indicate suspect telemetry. Typical thresholds and an illustrative calculation and rolling-plot are provided in Annex 4. The module provides three practical outputs for operators: (i) early anomaly detection; (ii) temporal evidence (residual time series and plots) to support visual verification; and (iii) ranked, timestamped alerts to prioritise maintenance and enable audit.

7.1. Recommended operator procedures (practical examples)

We propose the following operational procedure, implemented in the web-based SCADA as alerts and action buttons. Computation and thresholds (indicative, to be calibrated): compute σ_1 continuously over a short window (W_short ≈ 5–30 min), with σ_0 derived from a long calibration period. Raise an alert if `$\sigma_1/\sigma_0 \geq 3$` and the condition persists for `T_confirm ≈ 5–15 min`.

- Level 1 - Warning (elevated σ-ratio, short persistence): display a yellow indicator in the sensor-health panel and notify the operator. Recommended action: monitor the sensor, visually inspect correlated camera frames, collect logs and schedule an inspection if the anomaly recurs.
- Level 2 - Critical (elevated σ-ratio with persistence > T_confirm): display a red indicator, tag the telemetry as “suspect”, and recommend actions: (i) switch affected automatic control loops to manual, (ii) create a high-priority maintenance ticket, (iii) temporarily exclude suspect data from automatic control loops if severity warrants.

Validation actions: the operator must compare the alert against available evidence (camera frames, short audio snippets, residual evolution) and choose an action (`acknowledge` / `defer`/ `escalate`). All operator decisions are timestamped and stored for audit.

7.2. UI / SCADA integration

In the web interface each sensor shall expose a compact “health indicator” showing status (OK / WARN / FAULT), the current σ-ratio value, a small residual plot (last 24 h) and action buttons (Acknowledge / Isolate / Create ticket). For critical alerts the system can auto-populate an incident report with residual plots, representative image(s) and the suspicious time window to assist field crews.

7.3. Practical limitations and uncaptured phenomena

The σ-ratio method is robust and operationally simple but has well-known limitations that should be communicated to operators:

- Slow drifts. Progressive offsets (slow bias) may not be detected by variance monitoring alone; σ-ratio is relatively insensitive to slow mean shifts.

- Cascade failures. A faulty traffic counter (TC) or other reference sensor may generate correlated residuals across many derived predictions, producing multiple alerts; σ-ratio alone will not identify the root cause. In such cases operators must cross-check other sources (cameras, logs, external data) before executing maintenance.
- Benign external events. Legitimate transient events (heavy rain, tunnel cleaning operations, large traffic surges) can temporarily increase σ_1/σ_0; persistence logic and visual validation are therefore essential to limit false positives.

7.4. Outlook - future methods

For reference and future development (but not as part of the initial operational deployment), the σ-ratio module can be complemented by more sensitive and diagnostic techniques: EWMA/CUSUM procedures for detecting slow drifts [11], regularized Mahalanobis-type multivariate monitoring for identifying cascade failures [12], or multivariate machine learning (ML) methods to classify fault types. These extensions require separate development and systematic validation (simulation and fault injection) and are therefore planned as subsequent enhancements to the baseline σ-ratio solution, rather than as a substitute for the validated, operationally ready method adopted here.

8. SUMMARY AND CONCLUSION

In practice, the proposed system enhances situational awareness and shortens the response time of first responders by combining multimodal evidence and predictive simulation within a single web-based interface. Overall, the web-SCADA framework provides a practical and scalable approach to tunnel incident detection, forecasting, and operational coordination by delivering synchronized, uncertainty-aware predictions and ventilation recommendations to operators and emergency services. Future work will include simulation and experimental validation campaigns to quantify performance gains, usability studies with operators and emergency responders, enhanced system resilience for large-scale deployment and continued efforts toward AI-based diagnostic methods.

9. REFERENCES

[1] B. Qiu and H. B. Gooi, “Web-based SCADA display systems (WSDS) for access via Internet,” IEEE Transactions on Power Systems, vol. 15, no. 2, pp. 681–686, May 2000, doi: 10.1109/59.867159.

[2] T. Matsumoto, T. Oshiro, K. Furuhashi, H. Uemura, and A. Vardy, “Rapid fire detection and notification using a dual thermal + optical camera,” in Proc. Tunnel Safety & Ventilation Conf., 2022.

[3] K. Hoyer, R. Schmidt, H. Kammerer, F. Graf, M. Dobrounig, and T. Kalina, “Influence of acoustic tunnel monitoring AKUT on tunnel safety,” in Tunnel Conference Proceedings, 2024.

[4] I. Nakahori, T. Oshiro, K. Fukuda, T. Matsumoto, and S. Abe, “Fast fire detection by linear temperature sensor cable and its application,” in Proc. Tunnel Safety & Ventilation Conf., Graz, Austria, 2018.

[5] I. Nakahori, T. Sakaguchi, B. Kohl, C. Forster, and A. Vardy, “Risk assessment of zero-flow ventilation strategy for fires in bidirectional tunnels with longitudinal ventilation,” in Proc. Tunnel Safety & Ventilation Conf., 2020.

[6] M. M. R. Enam, M. M. I. Joarder, M. T. Y. Taimun, and S. M. M. Islam Sharan, "Framework for Smart SCADA Systems: Integrating Cloud Computing, IIoT, and Cybersecurity for Enhanced Industrial Automation," Scholars Journal of Engineering and Technology, vol. 10, no. 4, pp. 37–44, Apr. 2025, doi: 10.36348/sjet.2025.v10i04.005.

[7] PIARC, Fire and Smoke Control in Road Tunnels: Design Fires, World Road Association (PIARC), Technical Committee C4.2, 2010.

[8] Directive 2004/54/EC of the European Parliament and of the Council of 29 April 2004 on minimum safety requirements for tunnels in the Trans-European Road Network, Official Journal of the European Union, L167, pp. 39–51, 2004.

[9] National Tunnel Safety Guidelines (e.g., UK Highways Agency, Guidelines for the Assessment of Tunnel Fires, 2007).

[10] I. Nakahori, T. Sakaguchi, A. Mitani, and A. E. Vardy, "Sensor Failure Detection in Road Tunnel Ventilation," in Proc. 6th International Conference on Tunnel Safety and Ventilation, Graz, Austria, 2012.

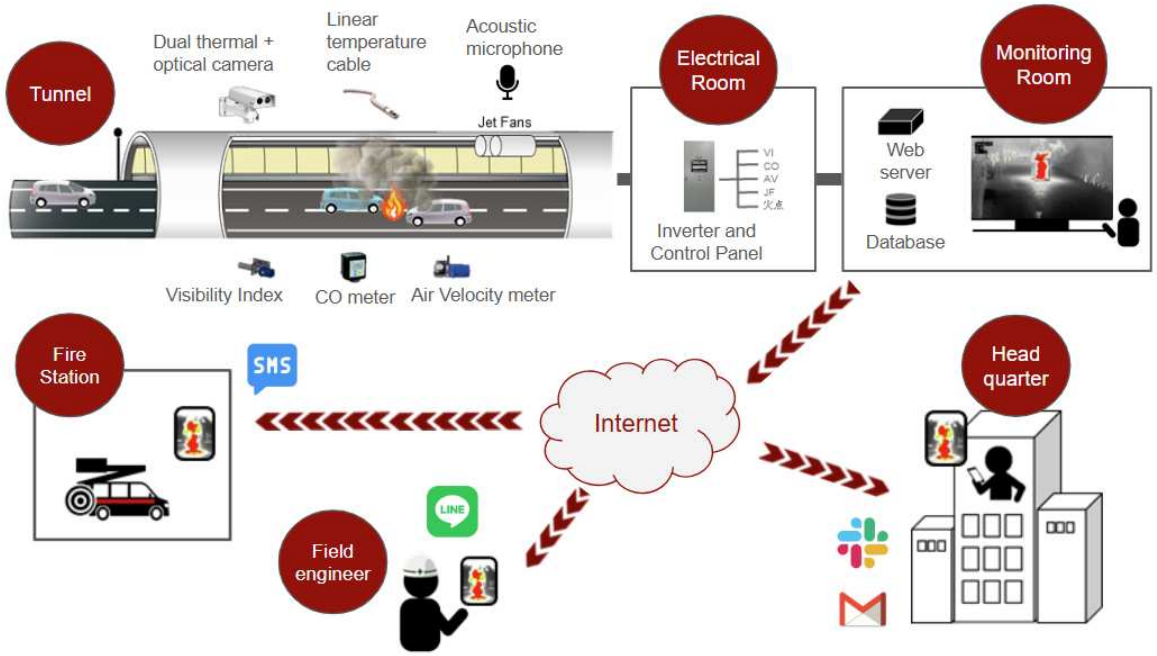
[11] D. C. Montgomery, Introduction to Statistical Quality Control, 7th ed., Wiley, 2013.

[12] J. F. MacGregor and T. Kourti, "Statistical Process Control of Multivariate Processes," Control Engineering Practice, vol. 3, no. 3, pp. 403–414, 1995.

[13] I. Nakahori, T. Sakaguchi, A. Nakano, A. Mitani, and A. E. Vardy, "Real-Time Estimation of Heat Release Rates in Tunnel Fires," in Proc. 7th International Conference on Tunnel Safety and Ventilation, Graz, Austria, 2014.

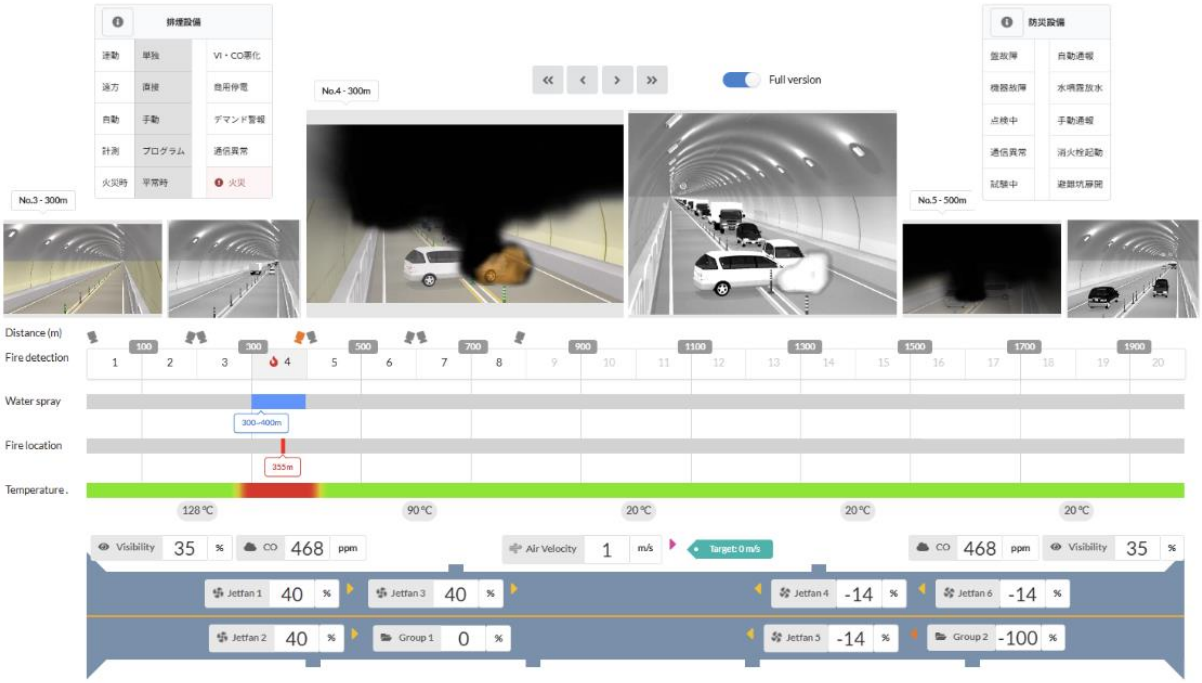
[14] M. Bando, K. Hasebe, A. Nakayama, A. Shibata, and Y. Sugiyama, "Dynamical model of traffic congestion and numerical simulation," Physical Review E, vol. 51, no. 2, pp. 1035–1042, 1995.

10. ANNEXES



Annex 1: Architecture diagram

Note: This diagram illustrates the layered and modular SCADA system connecting field devices to the control room platform, highlighting data flow and interfaces.



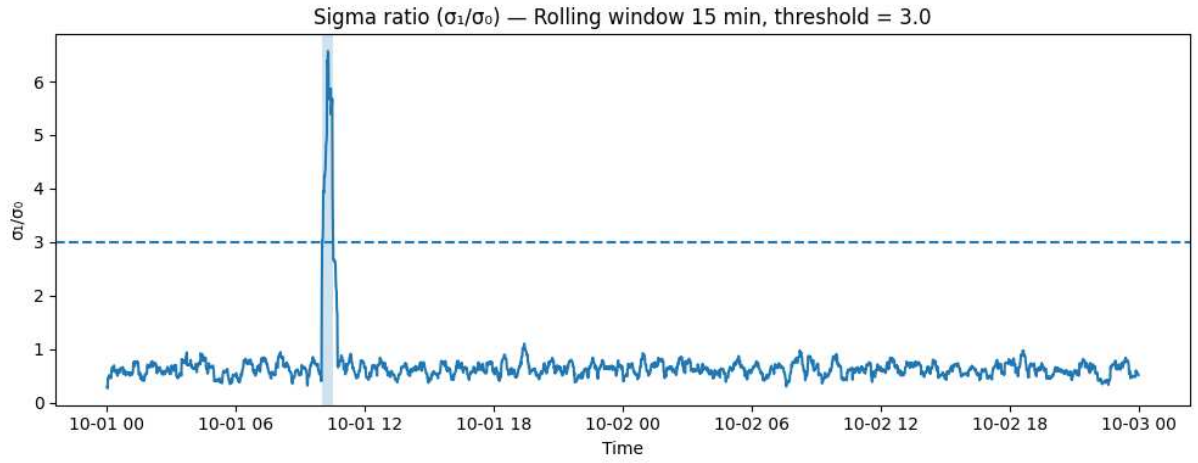
Annex 2: Screenshot of the monitoring screen

Note: This figure illustrates the main operational view of the SCADA system, including video feeds, sensor panels, ventilation status, and alert tables, providing a consolidated interface for tunnel operators.

Vehicle type / scenario	Indicative HRR range (MW)	Nominal value used (MW)
Passenger car	2 - 8	5
Bus / coach	10 - 30	20
Small loaded truck	20 - 50	30
Large loaded truck / HGV	50 - 150	100
Pool fire / tanker leak	100 - 300	200

Annex 3: Indicative HRR ranges

Note: These values are indicative design-fires. Battery fires and special cargoes can significantly deviate from these medians; consequently, the HRR estimate is treated probabilistically (type-conditioned prior + online update). The European Directive 2004/54/EC [8] frames tunnel-safety requirements but does not mandate fixed HRR values; selection of design-fires remains a national/engineering decision.



Annex 4: Sigma ratio (σ_1/σ_0) - rolling-window σ_1 divided by σ_0 with a dashed line for the threshold (3.0).

Note: Rolling-window σ_1 divided by σ_0, with a dashed line indicating the threshold (≈ 3.0). This visualization illustrates how persistent deviations trigger critical alerts for suspect sensors. Example: $\sigma_0 = 0.5$, $\sigma_1 = 1.6 \rightarrow$ σ-ratio = 3.2

Annex 5: Nomenclature

Symbols

σ_0 - Reference standard deviation (calibration period)
σ_1 - Short-term residual standard deviation (operational window)
σ-ratio(t) - σ_1/σ_0, variance ratio at time t (dimensionless)
HRR(t) - Heat release rate as a function of time (MW)
Mt - Traffic volume (vehicles per hour, veh·h^{-1}).
Vt - Average traffic speed used to compute spacing (km·h^{-1}).
Δx - Mean vehicle spacing (m).
(Δxi) - Optimal velocity for vehicle i as a function of headway (m·s^{-1}).
Vmax - Maximum vehicle velocity (m·s^{-1}).
hc - Critical headway (m).
Δh - Smoothness parameter for the OVM (m).
a - Sensitivity (reaction) coefficient in OVM (s^{-1}).
i - Vehicle index (integer).
k - Tunnel section index (integer).
ΔPk - Total air pressure difference in section k (Pa).
ΔPn, - Pressure difference from natural ventilation in section k (Pa).
ΔPt, - Pressure change from piston effect (traffic) in section k (Pa).
ΔPj, - Thrust contribution from jet-fans in section k (Pa).
ΔPr, - Pressure loss due to resistance in section k (Pa).
Mk - Mass of air in section k (kg).
Vk - Longitudinal air velocity in section k (m·s^{-1}).
Ar, - Cross-sectional area of section k (m²).
RJtg - Targeted rotation/thrust setpoint for jet-fans (unit depends on controller: rpm or normalized thrust).

Kp, Ki, Kd - Proportional, integral and derivative gains in PID-like controller (units consistent with controller design).
Δt - Controller sampling interval (s).
(x, t) - Smoke extinction coefficient at position x and time t ($1 \cdot m^{-1}$).
$q$out - Volumetric exhaust flow rate ($m^3 \cdot s^{-1}$).
D - Effective diffusion/advection coefficient ($m^2 \cdot s^{-1}$).
$\xi(x, t)$ - Smoke source term from the fire ($1 \cdot m^{-1} \cdot s^{-1}$, parameterised from HRR).
x - Longitudinal coordinate along tunnel (m).
t - Time (s).
W_short - Short rolling window duration (e.g., 5–30 min)
T_confirm - Confirmation persistence threshold (e.g., 5–15 min)

Acronyms
API - Application Programming Interface
AV - Air velocity (see symbol $Uk/\ Ur$)
CUSUM - Cumulative Sum (statistical method for monitoring shifts in process mean or variance)
ETA - Estimated Time of Arrival (time to reach a given target value, e.g., Air velocity target)
EWMA - Exponentially Weighted Moving Average (statistical process control method for detecting slow changes)
HCI - Human–Computer Interaction
HMI - Human–Machine Interface
HRR - Heat Release Rate (see symbol HRR(t))
IIoT - Industrial Internet of Things
JF - Jet-fan (ventilation actuator)
ML - Machine Learning (data-driven methods for pattern recognition, classification, or prediction)
OVM - Optimal Velocity Model
PLC - Programmable Logic Controller
SCADA - Supervisory Control and Data Acquisition
SQL - Structured Query Language
TC - Traffic Counter
VI - Visibility Index (distance in m)
YOLOv5 - You Only Look Once v5 (object detector)

Annex 6: Model Equations

(See Annex 5 for full nomenclature and units.)

A. Traffic dynamics (OVM and spacing)

$$\Delta x = \frac{V_t \cdot 1000}{M_t} \tag{A1}$$

$$V(\Delta x_i) = V_{max}\left(\tanh\left(\frac{\Delta x_i - h_c}{\Delta h}\right) + \tanh\left(\frac{h_c}{\Delta h}\right)\right) \tag{A2}$$

$$\ddot{x}_i = a(V(\Delta x_i) - \dot{x}_i) \tag{A3}$$

We employ an Optimal Velocity Model (OVM) for vehicle motion; this approach is standard in microscopic traffic modelling and numerical studies [14] (or see eqs. A1–A3).

where:

i - vehicle index; Mt - traffic volume (veh/h); Vt - average speed (km/h); Δx - mean spacing (m); Vmax - maximum vehicle speed (m/s or km/h consistent with Vt); hc - critical headway (m); Δh - smoothness parameter (m); a - sensitivity coefficient (s^{-1}).

B. Longitudinal airflow - pressure balance and section dynamics

Global pressure-balance over tunnel sections:

$$\sum_{k=1}^{i} \Delta P_k = \sum_{k=1}^{i} \left(\Delta P_{n,k} + \Delta P_{t,k} + \Delta P_{j,k} + \Delta P_{r,k}\right) = 0 \quad \text{(A4)}$$

Per-section momentum relation (Newtonian form):

$$M_k \frac{dV_k}{dt} = A_{r,k}\Delta P_k = A_{r,k}(\Delta P_{n,k} + \Delta P_{t,k} + \Delta P_{j,k} + \Delta P_{r,k}) \quad \text{(A5)}$$

where:

k - section index; ΔPk - total pressure difference (Pa) in section k; $\Delta Pn,k$ - natural ventilation pressure term (Pa); $\Delta Pt,k$ - piston-effect pressure from traffic (Pa); $\Delta Pj,k$ - thrust from jet-fans (Pa); $\Delta Pr,k$ - pressure loss due to resistance (Pa); Mk - mass of air in section k (kg); Vk - average AV in section k (m/s); Ak - cross-sectional area (m^2).

Notes on modelling choices:

- ΔPt, is computed from the summed momentum exchange of vehicles in the section, following OVM-derived traffic states [14].
- ΔPr, is typically modelled using Darcy–Weisbach or empirical friction relations [7,9].
- ΔPj, maps fan rotation to thrust via simplified quadratic laws or manufacturer curves [5].

C. Jet-fan control (PID-like setpoint computation)

Discrete-time controller (sampled at Δt):

$$RJ_{tg}(t) = K_p(V_r(\mathrm{t}) - V_d) + K_i \times \sum_{\tau=t_0}^{t} (V(\tau) - V_d)\,\Delta\mathrm{t} + K_d \frac{V(t) - V(t - \Delta\mathrm{t})}{\Delta t}$$

where:

RJtg - targeted rotation/thrust setpoint for fan(s); V - measured/reported longitudinal AV (m/s); Vd - desired AV (setpoint, m/s, e.g. 0 for zero-flow); Kp, Ki, Kd - controller gains; Δt - controller sampling interval.

Implementation note: in practice we may omit the derivative term (Kd = 0) for robustness and use anti-windup on the integral term when fans saturate. PID-like control for ventilation is widely used in tunnel airflow studies [5].

D. Advection–diffusion of smoke (1-D model)

PDE for smoke extinction coefficient (x, t) (m⁻¹):

$$\frac{\partial C}{\partial t} + \frac{\partial (C V_r)}{\partial x} + \frac{q_{out}}{A_r} C = D \frac{\partial^2 C}{\partial x^2} + \xi_f(x,t) \quad \text{(A7)}$$

where:

C - smoke extinction coefficient (m⁻¹); x - longitudinal coordinate (m); Vr - local longitudinal air velocity (m/s); $q$out - exhaust volumetric flow (m³/s); Ar - cross-sectional area (m²); D - effective diffusion/advection coefficient (m²/s); ξf - smoke source term (m⁻¹·s) parameterised from HRR and combustion properties [13].

Discretization & boundary conditions: the PDE is discretized using an upwind or flux-conservative finite-volume scheme consistent with the sectioning used for airflow; boundary conditions at portals reflect ambient exchange and exhaust extraction. The extinction coefficient C is mapped to visibility index (VI) using an empirical relation (e.g., Koschmieder law or tunnel-specific calibration) [7,9] - see Annex 5 for the chosen mapping.

TOWARDS ACCURATE TUNNEL FIRE SIMULATIONS: GRID SENSITIVITY AND LES MODEL COMPARISON IN FIRE DYNAMICS SIMULATOR

[1]Mahfuz Sarwar, [2] K.A.M. Moinuddin

[1]*Fire Rescue Victoria (FRV), Major Community Infrastructure Unit (MCIU), AU*
[2]*Centre for Environmental Safety and Risk Engineering (CESARE), Victoria University, AU*

DOI 10.3217/978-3-99161-087-8-033 (CC BY-NC 4.0)
https://creativecommons.org/licenses/by/4.0/deed.de
This CC license does not apply to third party material (attributed to other sources) and content noted otherwise.

ABSTRACT

This study examines the grid sensitivity of four Large Eddy Simulation (LES) sub-grid scale (SGS) turbulence models available in Fire Dynamics Simulator (FDS) namely the Standard Smagorinsky, Dynamic Smagorinsky, Deardorff, and Vreman models using a backward-facing step benchmark. Results show that grid resolution has a stronger influence on LES performance than the choice of SGS model, highlighting the inherent challenge of achieving grid-independent solutions in implicitly filtered LES. Among the models assessed, the Standard Smagorinsky model exhibits the most consistent convergence behaviour and produces the closest agreement with experimental data, even though full grid convergence remains elusive. Additional refinement confirms that FDS's second-order scheme can deliver acceptable accuracy when sufficiently fine meshes are used.

These outcomes are directly relevant to tunnel CFD fire simulations, where accurate prediction of smoke movement, temperature distribution, and fire-induced flow fields is critical for occupant safety, ventilation design, and regulatory compliance. By providing a detailed understanding of SGS model behaviour and grid sensitivity, this study highlights the importance of carefully designed mesh strategies and informed SGS selection particularly the Standard Smagorinsky model, which exhibits the strongest convergence tendencies for reducing modelling uncertainty. The insights gained from this work enable more reliable simulation of flow separation, recirculation, and smoke stratification, thereby enhancing the robustness and credibility of FDS-based tunnel fire assessments and supporting better-informed engineering decisions and performance-based design approvals.

Keywords: Fire Dynamics Simulator (FDS), Large Eddy Simulation (LES), Sub-grid scale (SGS) models, Grid sensitivity, Turbulence modelling.

1. INTRODUCTION

The development of FDS was motivated by the need to simulate building-fires. It is a CFD based fire model initially developed to simulate low speed thermal buoyancy driven flows, namely flows of smoke and hot gases generated by fires. Subsequently, pyrolysis and combustion submodels have been added making it a state of the art fire model. FDS is an open source code which employs a second-order numerical scheme and it incorporates an LES model that is invoked by default. FDS offers the user a choice of four SGS models, namely the Standard Smagorinsky, the dynamic Smagorinsky, the Deardorff and the Vreman models. As all of these are implicitly filtered schemes, it poses challenges to the adequacy and efficiency of these SGS models and their sensitivity to grids [1]. In this paper, the grid sensitivity of FDS' SGS models has been studied. In the process, the adequacy of the second-order numerical scheme (accurate in time and space) has also been assessed. A well-defined

problem is studied namely turbulent flow over a backward facing step to compare the predicted flow fields with published experimental results. Those presented by Jovic and Driver (1994) [2] for flow over a backward facing step are used for evaluating the various sub-grid scale models.

The backward-facing step was selected due to its simple geometry yet complex flow physics. It is a classical benchmark in fluid mechanics because it captures several key flow features within a canonical configuration, including geometrically induced separation at a sharp edge, the formation of a recirculation zone, downstream reattachment, and strong turbulence and shear-stress gradients. These characteristics make it particularly suitable for validating turbulence models and numerical methods. Despite its geometric simplicity, the configuration is relevant to many practical engineering applications. Moreover, a plethora of well-established numerical and experimental results are available in the literature [3] for the case studied.

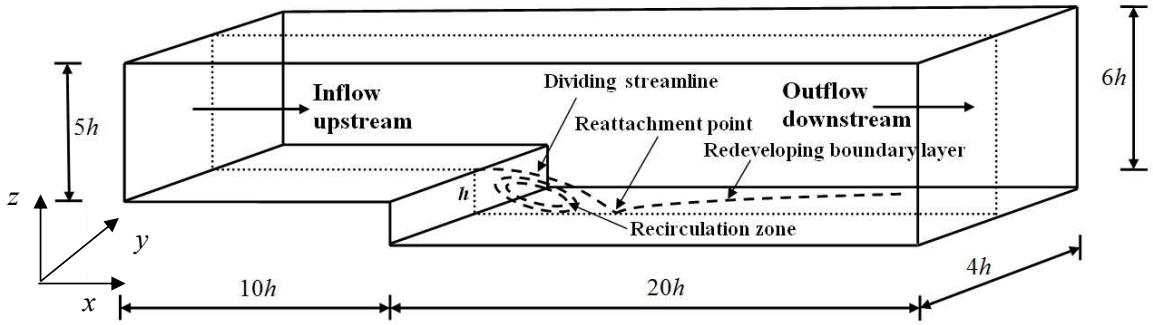


Figure 1: Schematic view of backward facing step flow configuration (not to scale)

Tunnel fires represent one of the most demanding environments for CFD fire modelling. Smoke transport, back-layering behavior, longitudinal ventilation effectiveness, and tenability predictions are all highly sensitive to the accuracy of turbulence representation. LES-based solvers like FDS are increasingly used for smoke stratification assessment under mechanical ventilation, critical velocity determination, analysis of fire-induced flow reversals, performance-based tunnel fire safety design [4].

However, uncertainties in LES turbulence modelling can propagate directly into tunnel fire predictions. For example, over-dissipation from an SGS model may suppress key flow structures, inaccurately predicting smoke spread or back-layering length. Under-dissipation may lead to numerical instabilities or unphysical oscillations, affecting tenability predictions. Grid-sensitive behavior may lead to inconsistent results between mesh configurations, undermining confidence in fire safety decisions and regulatory submissions.

By rigorously evaluating grid sensitivity and SGS model performance under controlled conditions, this research provides foundational insight into how FDS behaves in flows representative of tunnel environments. The conclusions can guide tunnel fire engineers in selecting more robust SGS models for longitudinal tunnel simulations, designing mesh strategies that improve predictive reliability, understanding when convergence is achievable or fundamentally limited, improving interpretation of FDS results used for regulatory compliance or performance-based design. In essence, although this study focuses on canonical flow, its implications extend directly to more reliable prediction of smoke movement and fire-induced flow fields in real tunnel scenarios.

1.1. Rationale for Selecting the Backward-Facing Step Configuration

A full tunnel fire scenario involves buoyancy, combustion, radiation, and ventilation effects that can mask the influence of grid resolution and sub-grid scale (SGS) model behavior. To

isolate and evaluate these fundamental turbulence-modelling issues, a simpler but still relevant flow configuration was required.

The backward-facing step (BFS) provides this balance. Despite its simple geometry, it exhibits key turbulent features of flow separation, shear-layer development, recirculation, and reattachment that are directly relevant to smoke movement and fire-induced ventilation flows in tunnels. These mechanisms influence smoke stratification, back-layering tendencies, and mixing processes that are critical in tunnel fire modelling.

Using an isothermal, non-reacting BFS flow removes confounding variables, allowing a clear assessment of how grid refinement and FDS's SGS models affect LES accuracy. Importantly, the BFS is supported by a robust experimental database (e.g., Jovic & Driver, 1994 [2]), enabling objective validation something not feasible for most real tunnel fire scenarios.

As a well-established LES benchmark, the BFS is highly sensitive to grid and SGS choices, making it an ideal test case for evaluating FDS performance. Insights gained from this controlled environment can therefore be confidently extended to improve the reliability and consistency of FDS-based predictions of smoke movement and fire-induced flow fields in tunnels.

2. NUMERICAL SIMULATION

The computational domain of the numerical simulation of the backward facing step is set up exactly according to the well-established numerical study of Le Moin and Kim (1997) [3]. According to their study, it is found that the configuration under consideration is sufficient for capturing all the prominent flow features of turbulent flow over a backward facing step as also in the experiment conducted by Jovic and Driver (1992) [2] and requires less computational resources.

Figure 1 shows a schematic of the configuration, indicating the dividing streamline and recirculation zone that forms as the fluid flows over the step. It also shows the reattachment zone and redevelopment of the boundary layer after the fluid passes the reattachment zone downstream of the step. These complex flow features render it a useful and demanding benchmark case for validation of LES schemes.

The fluid is air at a temperature of $20°\,\mathrm{C}$, and the kinematic viscosity (ν) and density (ρ) are taken to be $1.53 \times 10^{-5}\,\mathrm{m^2/s}$ and $1.2\,\mathrm{kg/m^3}$, respectively. The step height (h) is 9.6×10^{-3} m. The streamwise length of the upstream portion is $10h$ and the length of the downstream outflow section is $20h$. The flow width is $4h$. The height of the upstream and downstream sections are $5h$ and $6h$, respectively, corresponding to an expansion ratio (ER) of 1.2 and calculated as $ER = L_z/(L_z - h)$. The Reynolds number ($Re_h = hU_0/\nu$) is 5100 based on the step height h and the reference velocity U_0. In the experiment the reference flow speed (U_0) was maintained at $7.72 \pm 0.03\,\mathrm{m/s}$ at section $3h$ upstream of the step. The difficulty to obtain desired reference velocity in the numerical simulation is well known. In this study, the overall velocity is maintained 7.96 m/s for different viscosity models which is almost 2.5% higher than ideally desired at location 3h upstream of the step. The streamwise velocities are normalized using the upstream free stream reference velocity U_0. The reference velocity fluctuation for different viscosity models is maintained within ± 0.02 m/s. Mean velocities and turbulence statistics are analysed at two different stations ($x/h = 4$ and $x/h = 6$) along the streamwise direction. The dimensionless mean(u/U_o) velocity components and turbulence intensities or Reynolds stresses ($\overline{u'u'}$) normalized by the reference velocity U_0^2 are compared against the vertical axis (z/h) in order to obtain agreement between the simulated and experimental data. Generally, energy is transferred from the largest eddies to the smallest ones on a timescale of about one large eddy turnover. In this flow case, one recirculation time

(t_E) near the step height (h) is calculated as $5 \times 10^{-3} s$ which is considered as unit eddy turnover time. The flow achieved statistically steady state at approximately $800t_E$. After an initial run of $800t_E$, the flow velocity is averaged over the time for another $2000t_E$. The average velocity data was obtained at 0.01s interval (that means nearly two eddy turnover time) and statistical average of 1000 data points was taken which is considered adequate.

Three uniform computational resolutions namely coarse, medium and fine, are used along the streamwise(N_x), spanwise (N_y) and vertical (N_z) directions. The grid resolved quantities are physically interpreted as cell means. In implicit LES, the filter width is taken as the cube root of the cell volume, $\Delta = V_c^{\frac{1}{3}}$, the cell volume $V_c = \delta x\, \delta y\, \delta z$; where $\delta x,\ \delta y$ and δz are the grid spacings along the three directions of the Cartesian coordinate system. The filter width to grid spacing ($\Delta/\delta x$) is considered as one since the filter width (Δ) is equivalent to the grid spacing (δx). For the grid sensitivity study, instead of random grid selection, for the convenience grids are refined in terms of the step height to grid spacing ratios ($h/\delta z$) in this study. This grid selection process is adopted from the LES study of flow over a backward facing step by Panjwani (2010) [5] and Toms (2015) [6]. The step height to grid spacing ratios are considered as $h/\delta z = 3$, 5 and 10. Table 1 presents the selected grid resolutions, considered model coefficients of SGS models implemented in the numerical simulation along with the measured wall unit n^+_{min} values which represents the minimum grid spacing in the wall-normal direction at the outflow test section. It can be observed that despite the same grid resolution, resolution in terms of nominal minimum wall can be different.

Table 1: Considered model coefficients and estimated wall unit (n^+) values of SGS models

SGS models		**Smagorinsky**	**Dynamic Smagorinsky**	**Deardorff**	**Vreman**
Model coefficients(C_*)		0.20	--	0.10	0.07
Grid	$N_x \times N_y \times N_z$	n^+_{Wall}	n^+_{Wall}	n^+_{Wall}	n^+_{Wall}
Coarse (C)	$90 \times 40 \times 60$	≤ 3.80	≤ 3.98	≤ 4.34	≤ 4.45
Medium (M)	$150 \times 60 \times 100$	≤ 2.17	≤ 2.32	≤ 2.56	≤ 2.71
Fine (F)	$300 \times 120 \times 200$	≤ 0.83	≤ 1.02	≤ 1.17	≤ 1.28

It is to be noted that in the DNS study of Le, Moin & Kim (1997) [3] the wall unit ranged from $n^+_{min} \approx 0.3$ to $n^+_{max} \approx 31$. Furthermore, while Akselvoll and Moin (1993) [7] performed a LES of backward facing step with $Re_h = 5100$ (based on the step height, h) which is similar to this study, they refined the resolution to a nominal wall unit, $n^+ = 0.8$.

3. BOUNDARY CONDITIONS

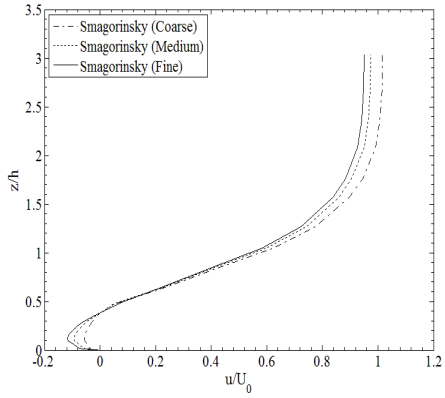
Boundary conditions play an important role in any numerical simulations and this is particularly true for LES to obtain appropriate solutions. Inlet boundary conditions are important as in most of the cases the downstream flow development is largely influenced by the inlet flow behavior. The boundary conditions for the backward facing step simulations are as follows. In Figure 1, at the inflow on the left end of the domain a constant and uniform atmospheric pressure is applied. At the outlet on the right end of the domain gradients of pressure and velocity are prescribed as zero. The lower boundary is a solid wall with the near wall behavior modelled by the Werner-Wengle approximation to the log-law [8]. Zero pressure gradient and a no-slip boundary condition is applied at the walls (side and bottom) while at the upper boundary the vertical velocity is $w = 0$ while streamwise and vertical velocity gradients are $\partial u/\partial z = \partial w/\partial z = 0$ which is consistent with Le, Moin and Kim (1997) [3]. The turbulence was initialized by some random perturbation.

4. RESULTS AND DISCUSSIONS - GRID SENSITIVITY

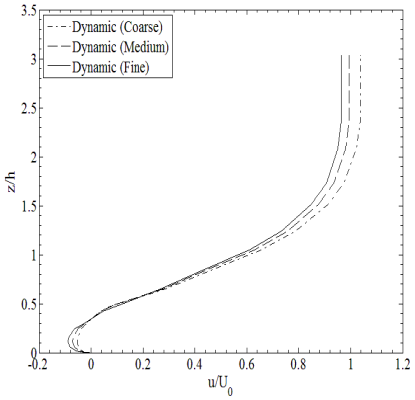
With the implicitly filtered SGS models (the standard Smagorinsky, the dynamic Smagorinsky, the Deardorff and the Vreman SGS models), simulations of flow over a backward facing step were performed for the three grid resolutions (coarse, medium and fine) as shown in Table 1. All the simulations were carried out to examine the influence of refinement of grids on their solutions. The simulated results are analysed based on the mean velocity and the turbulence intensity. Results are compared at two different test locations $x/h = 4$ and 6. The grid sensitivity is analysed both graphically and quantitatively. The main purpose of this analysis is to identify the most promising SGS model among the four for the conversion to an explicit LES model.

4.1. Graphical Comparison - Mean Velocity and Turbulence Intensity

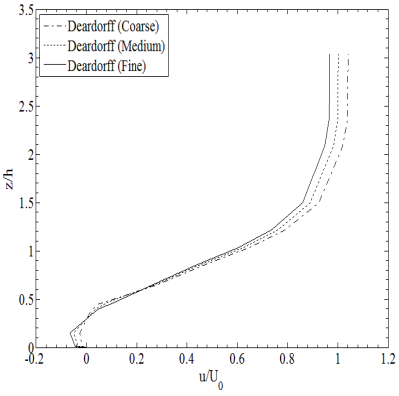
Figure 2 and Figure 3 present the comparison of the mean velocity profiles from simulations with four SGS models at stations $x/h = 4$ and $x/h = 6$. This parameter was averaged in time and non-dimensionalised with the free stream reference velocity U_0. As shown in Table 1, at fine grid resolutions, the wall units (n^+_{min}) along the vertical direction are reported in the range of 0.8 to 1.3 for all the four models. It also appears from the Figure 2 to Figure 5 that the tendency of numerical convergence of the standard Smagorinsky model is relatively better compared to other three SGS models at both locations. It is to be noted that when a coarser grid is used, a thicker boundary layer is predicted near the surfaces compared to the simulations where a finer grid is used.



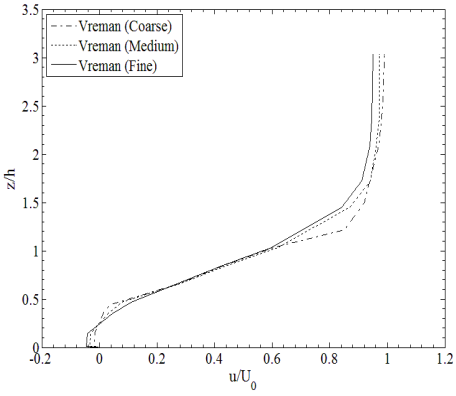
(a) Standard Smagorinsky



(b) Dynamic Smagorinsky

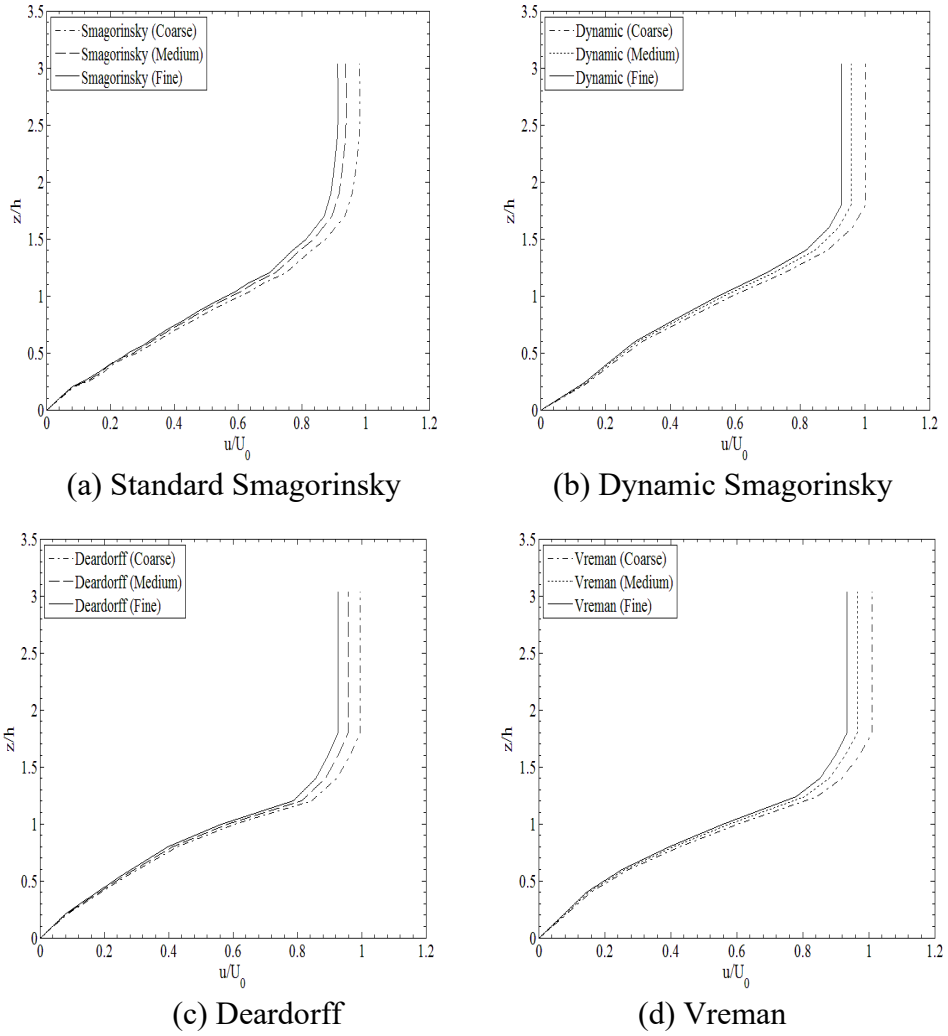


(c) Deardorff



(d) Vreman

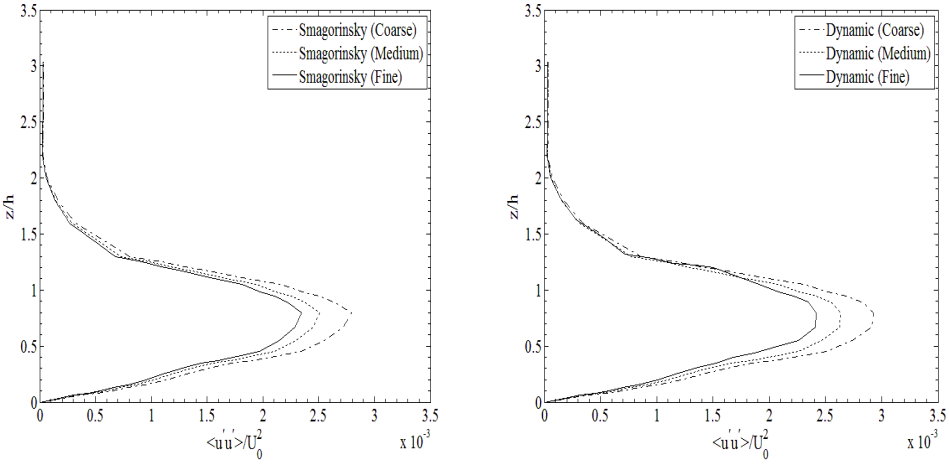
Figure 2: Mean velocity profiles at test section *x/h=4* for the SGS models



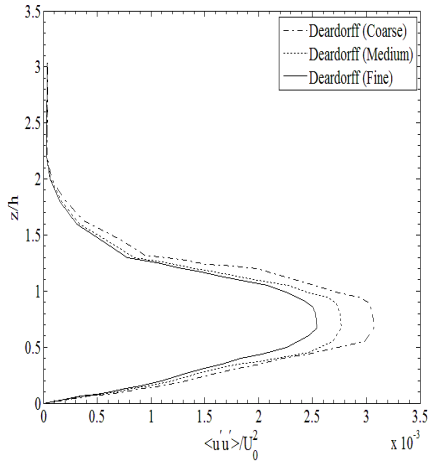
(a) Standard Smagorinsky (b) Dynamic Smagorinsky

(c) Deardorff (d) Vreman

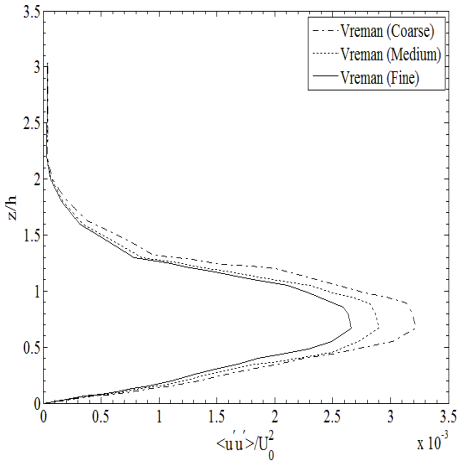
Figure 3: Mean velocity profiles at test section *x/h=6* for the SGS models



(a) Standard Smagorinsky (b) Dynamic Smagorinsky

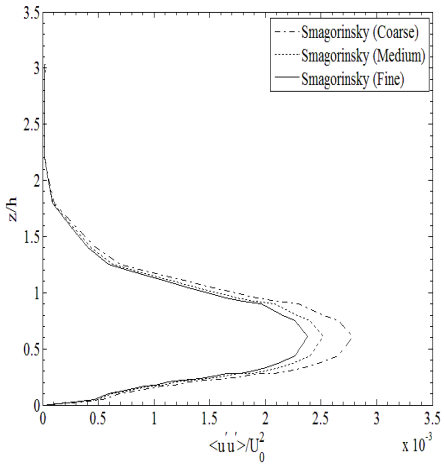


(c) Deardorff

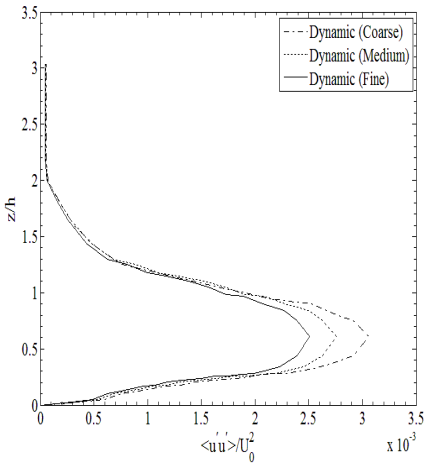


(d) Vreman

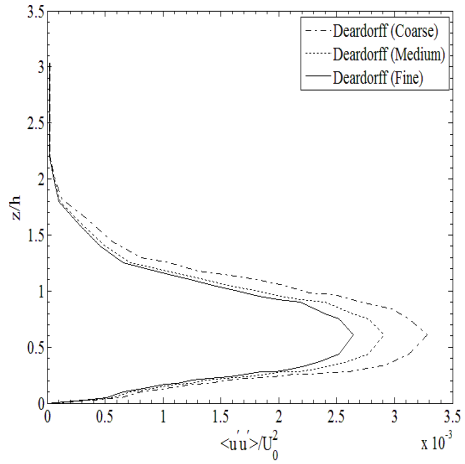
Figure 4: Turbulence intensities at test section *x/h=4* for the SGS models



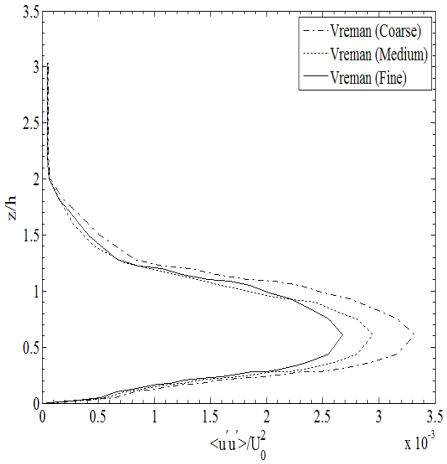
(a) Standard Smagorinsky



(b) Dynamic Smagorinsky



(c) Deardorff



(d) Vreman

Figure 5: Turbulence intensities at test section *x/h=6* for the SGS models

Turbulent flows are highly diffusive in nature due to continuous three-dimensional fluctuations of the fluid throughout the computational domain. Turbulence intensity arises due to the non-linear diffusive nature of fluid flow. It is an important flow parameter to quantify the nature of the turbulent flow.

The rms profiles of the turbulence intensities or Reynolds stresses ($\overline{u'u'}$) at different locations along the streamwise direction are normalized by the reference velocity U_0^2. Figure 4 and Figure 5 present the turbulence intensities at two test locations $x/h = 4$ and $x/h = 6$ for the SGS models. Similar to the mean velocity profile, it appears from the figure that SGS models turbulence intensity profiles at selected test locations are unable to achieve grid convergence. Out of four models, it also appears the tendency of grid convergence of the standard Smagorinsky model is relatively better compared to the other three models which is consistent with Figure 2 and Figure 3. From these figures, it is observed that although the grids are sufficiently refined (up to $n^+_{min} \approx 1$) but none of the SGS models is able to attain the numerical convergence.

4.2. Quantitative Comparison - Mean Velocity and Turbulence Intensity

From the above graphical presentation of the grid sensitivity study of the mean velocity and turbulence intensity, it appears that none of the flow variables is able to attain grid convergence despite sufficient refinement of the grid resolution. Hence, it is important to evaluate the grid convergence tendency of the four models to identify the most promising one. In this section, the focus was given on estimation of grid convergence error of the mean velocity and the turbulence intensity to quantify their tendency towards the grid convergence.

The grid convergence method was proposed by Roache (1992) [9] to estimate the grid convergence error which is based on the Richardson extrapolation [10]. Roache (1992) [9] and Richardson [10] point out that a grid convergence study requires a minimum of three grid solutions. The grid convergence index (GCI) provides a measure of convergence for grid refinement studies. GCI (%) can be expressed as follows

$$GCI\ (\%) = F_S \frac{\epsilon_{rms}}{r^p - 1} \times 100 \tag{1}$$

Where, p is the order of the numerical scheme and for second-order scheme $p = 2$, F_s is the factor of safety and the recommended value is $F_s = 3$ (Roache 1992) [9], r represents the grid refinement ratio, can be calculated as $r = (N_{fine}/N_{coarse})^{1/3}$, and ϵ_{rms} is the rms value of the relative error which provide an initial measure of grid convergence for individual points n as

$$\epsilon_{rms} = \left(\frac{\sum_{i=1}^{n} \epsilon_i^2}{n} \right)^{1/2} \tag{2}$$

where, the relative error (ϵ_i) at a certain point for a flow variable (say velocity u_i) can be calculated as the magnitude between the coarse and fine solutions

$$\epsilon_i = \left| \frac{u_{i,coarse} - u_{i,fine}}{u_{i,fine}} \right| \tag{3}$$

GCI has been calculated for three grid resolutions presented in Table 1. Results of this comparison in the form of grid convergence values (GCI) of the mean velocity and the turbulence intensity are reported in Table 2 and Table 3. From the comparison, it is found that there is a reduction in GCI values in the successive grid refinements ($GCI_{M/C} < GCI_{F/M}$) for each of the two variables for the SGS models. The GCI of the finer grid ($GCI_{F/M}$) is relatively

low compared to the coarser grid ($GCI_{M/C}$) which indicates that the dependency of the numerical solutions of the simulations on the grid size has been reduced.

Table 2: Grid convergence measures (GCI) of the mean velocity profiles at stations x/h=4 and x/h=6 for flow over a backward facing step

Grids	Test sections (x/h)	Grid convergence index (%)			
		Standard Smagorinsky	Dynamics Smagorinsky	Deardorff	Vreman
Medium- Coarse (M/C)	4	12.65	16.19	19.33	22.16
Fine- Medium (F/M)	4	6.32	10.03	15.17	14.52
Medium-Coarse (M/C)	6	13.12	15.94	16.87	19.57
Fine-Medium (F/M)	6	6.45	10.31	12.68	14.11

Table 3: Grid convergence measures (GCI) of the turbulence intensity at stations x/h= 4 and x/h=6 for flow over a backward facing step

Grids	Test sections (x/h)	Grid convergence index (%)			
		Standard Smagorinsky	Dynamics Smagorinsky	Deardorff	Vreman
Medium-Coarse (M/C)	4	15.18	22.67	27.06	31.02
Fine-Medium (F/M)	4	7.58	14.04	21.24	20.33
Medium-Coarse (M/C)	6	15.74	22.32	23.62	27.40
Fine-Medium (F/M)	6	7.38	14.43	14.75	19.75

From the comparison of GCI, it can be seen that the GCI value is almost halved for the standard Smagorinsky model between ($GCI_{M/C}$) and ($GCI_{F/M}$), whereas other three SGS models only reduced the error by roughly one-third. This quantitatively shows that among the four SGS models the grid convergence tendency of the standard Smagorinsky model is relatively high compared to the other three models. Roy (2003) [11] recommended that GCI is should be $\leq$ 4% for both higher and lower order numerical schemes to confirm the quality of simulations. However further grid refinement may provide reduction in GCI leading to grid converged solutions (especially for the standard Smagorinsky model) which may fall in the DNS resolution range ($n^+_{min} \approx 0.3$).

5. RESULTS AND DISCUSSIONS - PREDICTED OUTCOMES

The quality and efficiency of the SGS models can be justified by comparing the best converged LES solution (based on the grid convergence study shown above) with experimental results of Jovic and Driver (1994) [2]. This is done quantitatively and graphically in this section.

5.1. Statistical Analysis of Predicted Outcomes

The results using the fine mesh have been selected to determine the statistical relative error between the numerical solution and the experimental data of Jovic and Driver (1994) [2]. The method of Ierardi et al. (2003) [12] has been followed. According to this approach, the relative error (ξ) can be calculated as,

$$\xi = \frac{(\mathcal{R} - \psi)}{\psi} \tag{4}$$

where, $\mathcal{R}$ and ψ are the reference and predicted values respectively. The mean relative error (ξ_m) can be calculated by the absolute values of error in individual points n. Therefore, the over-predictions or under-predictions are of the same magnitude and the resultant error will not be zero,

$$\xi_m = \frac{\sum_{i=1}^{n}\left(\left|\frac{\mathcal{R}-\psi}{\psi}\right|\right)}{n} \tag{5}$$

The relative errors are presented in Table 4 and Table 5 for the mean velocity and turbulence intensity profiles. Relative errors for the SGS models considered are calculated by taking the average of the relative mean errors at each of the two stations. From the Table 4, as can be seen, the relative error of the standard Smagorinsky model at fine resolution is almost two fold less than those of the dynamic Smagorinsky and the Deardorff models and almost three folds less than the Vreman model. Therefore, on the basis of mean relative error analysis, it can be said that standard Smagorinsky is the most efficient model (in terms of obtaining closest to experimental results with the same grid resolution) among the four SGS models for the considered test case. Table 5 results show a sharp increase of relative error in the turbulence intensities than the mean velocity components which indicate that the turbulence intensities are more sensitive to the SGS models. However, once again the standard Smagorinsky model is found to be the most efficient model, this time in relation to the prediction of turbulence intensities.

Table 4: Relative error analysis of the mean velocity profile (fine resolution) at stations x/h=4 and x/h=6 for flow over a backward facing step

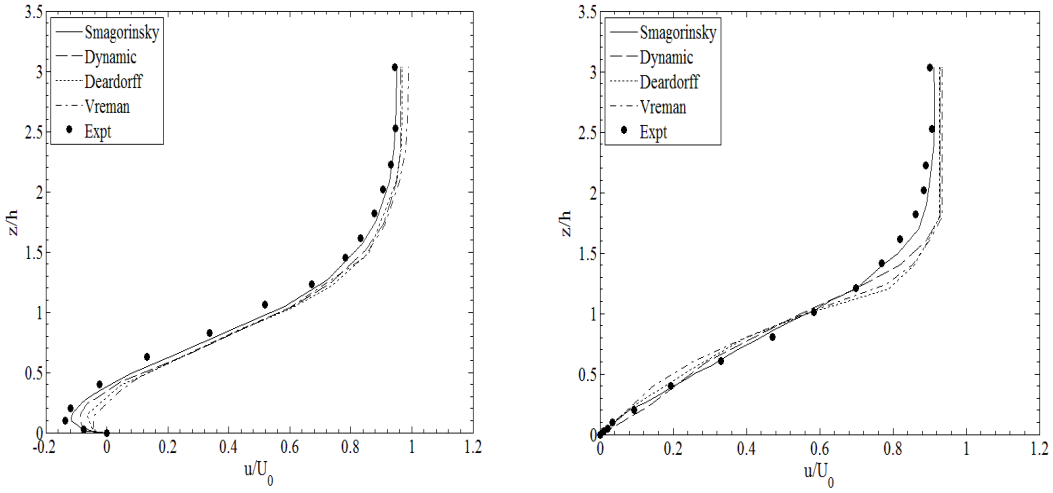
Test Locations (x/h)	Standard Smagorinsky (%)	Dynamics Smagorinsky (%)	Deardorff (%)	Vreman (%)
4	9.32	18.18	22.21	27.59
6	12.56	19.45	23.58	28.93
Average	10.94	18.81	22.90	28.26

Table 5: Relative error analysis of the turbulence intensity (fine resolution) at stations x/h= 4 and x/h=6 for flow over a backward facing step

Test Locations (x/h)	Standard Smagorinsky (%)	Dynamics Smagorinsky (%)	Deardorff (%)	Vreman (%)
4	15.04	25.45	31.09	39.62
6	17.62	28.33	33.01	36.50
Average	16.33	26.89	32.05	38.06

5.2. Mean velocity

Figure 6 represents the results for the dimensionless mean streamwise velocity at test sections x/h=4 and x/h=6 at a fine grid resolution. In Figure 6 (a), at section x/h=4, it appears that a reverse flow takes place between the step height level and wall region. It seems that the standard Smagorinsky model captures the secondary vortices near the step relatively better than other models and shows relatively better agreement with the experimental data. At the same location, among the other three eddy models, the Deardorff and the dynamic Smagorinsky model display almost the same phenomena except near the step height, but the Vreman model demonstrates poor agreement with experimental values compared to the other two models in the region near the step height and away from the wall. At section y/h=6 (Figure 6 (b)), it is appears that the flow is attached to the wall. In that section the standard Smagorinsky model shows relatively better agreement with experimental data but other models exhibit moderate agreement along the vertical axis. From the comparison, as can be clearly seen, the most accurate model (for the given absolute spatial resolution) overall is the standard Smagorinsky model, the dynamic Smagorinsky model is the intermediate and the Deardorff and the Vreman model are the least well performing SGS models.

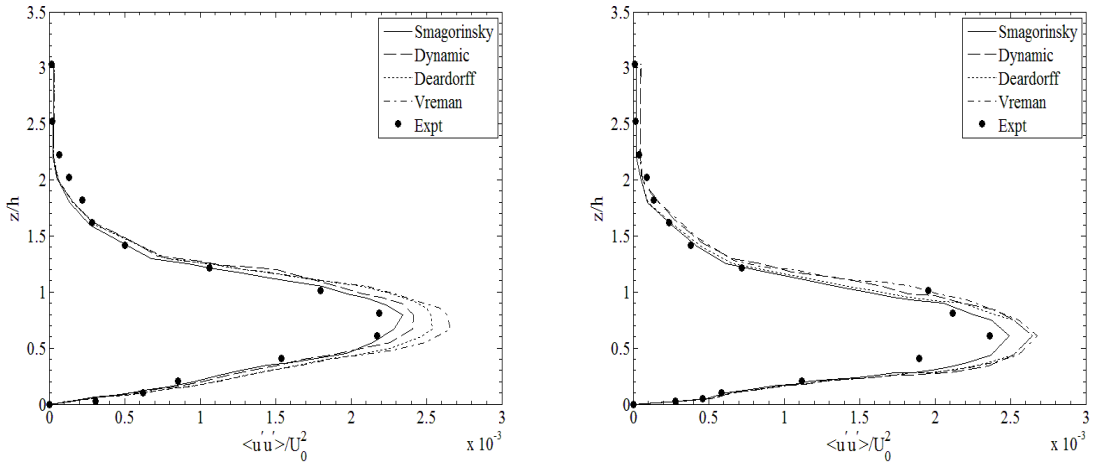


(a) at section *x/h=4* (b) at section *x/h=6*

Figure 6: Comparison of the mean velocity profile at test sections *x/h=4* and *x/h=6* for the SGS models

5.3. Turbulence intensity

Figure 7 represents the results comparison for turbulence intensities at selected test locations at fine grid resolutions. At test sections x/h=4 (Figure 7 (a)) and x/h=6 (Figure 7 (b)), it is found that similar to the mean velocity profiles the overall agreement of the turbulence intensity profiles of the standard Smagorinsky model with experimental data is relatively better compared to the other models. From the comparison, it can be concluded that the most accurate model (for the given absolute spatial resolution) overall is the standard Smagorinsky model, the dynamic Smagorinsky model is the intermediate and the Deardorff and the Vreman model are the least performing SGS models at both test locations for the turbulent intensities which is consistent with the mean velocity profiles in figure 6.



(a) at section *x/h=4* (b) at section *x/h=6*

Figure 7: Comparison of the turbulence intensity profile at test sections *x/h=4* and *x/h=6* for the SGS models

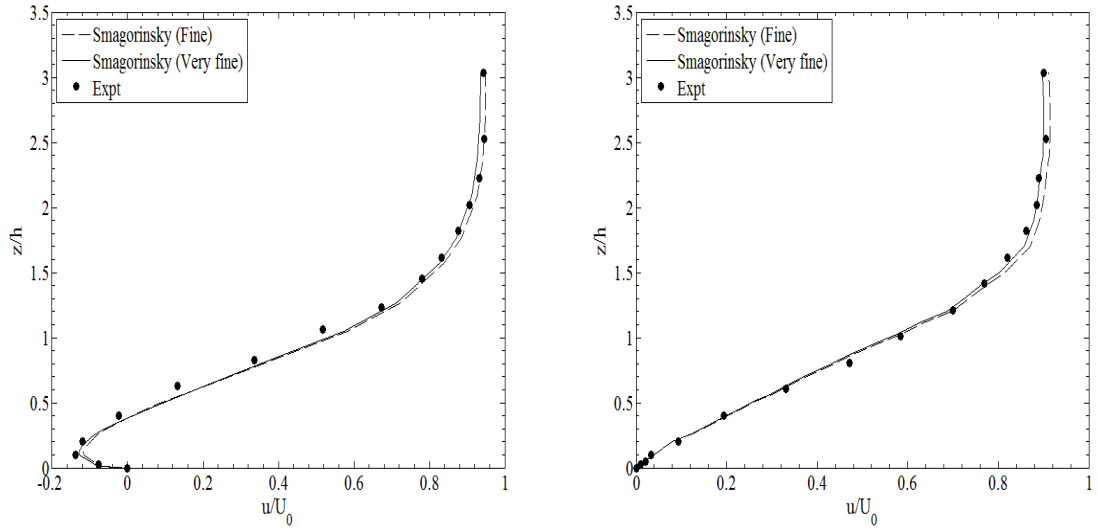
In summary, from the grid convergence study and the statistical relative error analysis along with graphical comparison of the mean velocity and the turbulence intensity profiles with experimental data, it appears that the standard Smagorinsky model is the most promising SGS model in FDS out of four despite it is unable to achieve grid convergence. Akselvoll and Moin

(1993) [7] application of LES to a backward facing step with $Re_h = 5100$ (based on the step height; h) shows that even with $n^+_{wall} = 0.8$ resolution, they were unable to achieve a grid converged solution with implicitly filtered LES. It seems the results of this present study are consistent with the findings of Akselvoll and Moin (1993) [7] and Toms (2015) [6] which also exhibit the elusive nature of grid convergence in implicitly filtered LES. However another simulation is conducted with the most promising standard Smagorinsky model when the grid resolution is further refined to $h/\delta z = 20$. This is to assess the adequacy of the second-order scheme.

6. FURTHER SIMULATION WITH STANDARD SMAGORINSKY MODEL

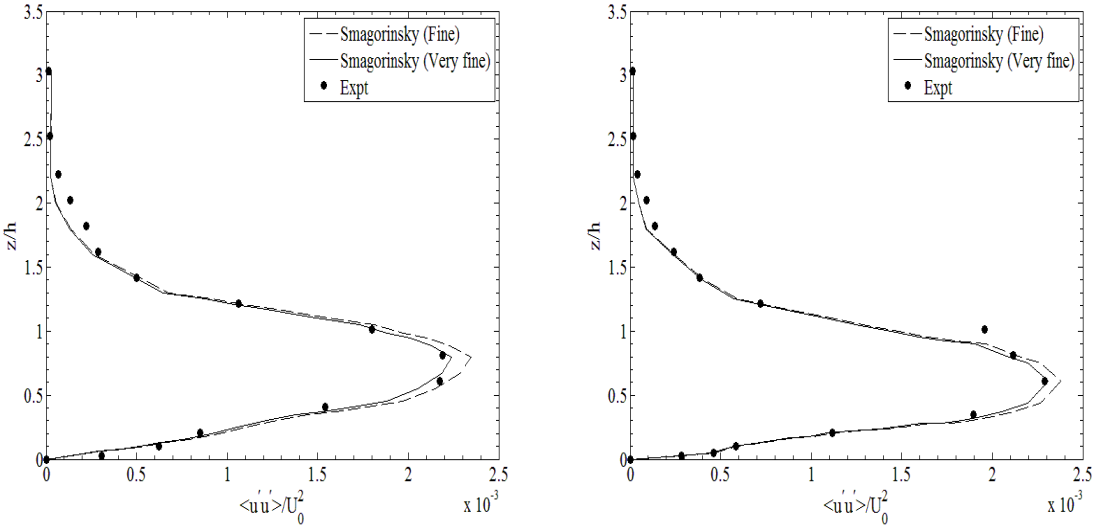
To assess the adequacy of second-order scheme, the grid is further refined as $h/\delta z = 20$ (very fine) where the grid resolution is $240 \times 600 \times 400$ and the nominal wall unit is measured as $n^+_{min} \approx 0.46$. Results of the mean velocity and the turbulence intensity of the very fine grid (VF) are presented in the Figure 8 and Figure 9 along with fine grid (F) to show VF's tendency of grid converge and also compared with the experimental data. From the figures, it can be said that for both mean velocity and turbulence intensity, the very fine grid shows relatively better agreement with experimental data compared to the fine grid. In the similar way, grid convergence index and relative errors of the mean velocity and the turbulence intensity have been calculated to assess the grid convergence tendency and the relative accuracy of the model with VF grid that are presented in the Tables 6 and 7 respectively.

As mentioned earlier Roy (2003) [11] recommended a GCI value of $\leq 4\%$ to confirm the quality of simulations. From the Table 6, it appears that GCI (%) of the flow variables are around this range, but still some grid sensitivity remains.



(a) at section *x/h=4* (b) at section *x/h=6*

Figure 8: Comparison of the mean velocity profile at test sections x/h=4 and x/h=6 for the standard Smagorinsky model for h/δz=20



(a) at section *x/h=4* (b) at section *x/h=6*

Figure 9: Comparison of the turbulence intensity profile at test sections x/h=4 and x/h=6 for the standard Smagorinsky model for h/δz=20

Table 6: GCI of the mean velocity and the turbulence intensity profiles of standard Smagorinsky model at stations *x/h=4* and *x/h=6* with very fine grid (*h/δz=20*)

Grid	Test section *(x/h)*	Grid convergence index (%)	
		Mean velocity	Turbulence intensity
Very fine-Fine (VF/F)	4	3.27	4.18
	6	3.43	4.07

Table 7: Relative errors of the mean velocity and the turbulence intensity profiles of standard Smagorinsky model at stations x/h=4 and x/h=6 with very fine grid (h/δz=20)

Test section (x/h)	Relative errors (%)	
	Mean velocity	Turbulence intensity
4	4.38	6.58
6	5.73	7.12
Average	5.05	6.85

Accuracy of the obtained solution of the mean velocity and the turbulence intensity is presented in the Table 7.

Table **7** shows that average relative errors of the mean velocity and the turbulence intensity at two stations are approximately 5% and 7%. According to Roache (1992) [9] and Roy (2003) [11], for the numerical validation of turbulent flow cases errors are expected to be within 5%. Therefore it can be observed that obtained results of mean flow from very fine grid (VF) simulation are almost within acceptable range. The turbulence intensity failed to satisfy this condition. However from the trend, it can be expected that further refinement of grid may provide more accurate results but it will be similar or higher than that of grid resolution considered in DNS (Le, Moin and Kim 1997 [3]) in terms of nominal n^+_{min}. This shows the elusiveness of grid convergence. This particular simulation using standard Smagorinsky model with very fine grid reduces the relative errors of both flow variables within the

acceptable range and shows very good agreement with the experimental data which demonstrates the adequacy of the second-order numerical scheme. In the process, this study also shows the elusiveness of the grid convergence of implicitly filtered LES.

7. CONCLUSIONS

This study evaluated the performance and grid sensitivity of four LES sub-grid scale (SGS) turbulence models namely Standard Smagorinsky, Dynamic Smagorinsky, Deardorff, and Vreman using FDS for a backward-facing step benchmark. The results demonstrate that grid resolution has a stronger influence on LES predictions than the choice of SGS model, highlighting the challenges of achieving grid-independent solutions in implicitly filtered LES. Among the models considered, the Standard Smagorinsky model exhibits the strongest convergence tendency, confirmed through additional simulations at very fine grid resolution (nominal $n^+ \approx 0.46$). Analysis of relative errors and grid convergence indices indicates that the second-order numerical scheme in FDS is adequate when sufficiently fine meshes are employed.

The findings of this paper highlight the persistent elusiveness of grid convergence in implicitly filtered LES, underscoring the critical importance of careful grid design, appropriate mesh refinement, and sub-grid scale (SGS) model selection in CFD based fire simulations using FDS.

8. FURTHER STUDIES

This work demonstrates that grid resolution exerts a dominant influence on LES performance in FDS and that the Standard Smagorinsky model delivers the most stable and consistent behavior among the SGS models evaluated. Although the backward-facing step configuration provided a well-controlled environment for isolating turbulence-modelling effects, further research is required to examine how these insights translate to the more complex flow physics of real tunnel fire scenarios, where buoyancy, heat release, radiation, and ventilation interact in coupled and highly unsteady ways. Future investigations should extend grid-sensitivity and SGS assessments to buoyant, fire-driven tunnel flows and develop mesh-design approaches suited to long, confined geometries. In addition, incorporating formal uncertainty quantification into FDS-based analyses will enhance confidence in numerical predictions and support more reliable performance-based fire engineering for tunnel applications.

9. REFERENCES

[1] Mahfuz Sarwar, Cleary, MJ, Moinuddin, KAM and Thorpe, GR 2017, ‘On linking the filter width to the boundary layer thickness in explicitly filtered large eddy simulations of wall bounded flows’, *International Journal of Heat and Fluid Flow,* Vol 65, pp 73–89.

[2] Jovic, S & Driver, DM 1994, ‘Backward-facing measurement at low Reynolds number Re_h = 5000’, *NASA Technical Memorandum 108807*, pp. 1–24.

[3] Le, H, & Moin, P & Kim 1997, ‘Direct numerical simulation of turbulent flow over a backward facing step’, *Journal of Fluid Mechanics*, vol. 330, pp. 349–374

[4] McGrattan, KB, Klien, B, Hostikka, S & Floyd, J 2014, *Fire Dynamics Simulator Version 6: Technical Reference Guide*, National Institute of Standards and Technology, Special Publication, pp. 1018–6

[5] Panjwani, B, I. S. Ertesvag, A. Gruber, K. E. Rian 2010. Large eddy simulation of backward facing step flow, 5th National Conference on Computational Mechanics, Trondheim, Norway.

[6] Toms BA, 2015. Large-eddy Simulation of Flow over a Backward Facing Step: Assessment of Inflow Boundary Conditions, Eddy Viscosity Models, and Wall Functions, Journal of Applied Mechanical Engineering, vol. 4: pp(169).

[7] Akselvoll, K, & Moin, P 1993. Large eddy simulation of turbulent confined co-annular jets and turbulent flow over a backward facing step, RTF-63. Thermo-sciences Division, Dept of Mech. Engng, Stanford University.

[8] H. Werner and H. Wengle. 1991 Large-eddy simulation of turbulent flow over and around a cube in a plate channel. In 8th Symposium on Turbulent Shear Flows, Munich, Germany, Technische University Munich, pages 155–168.

[9] Roache PJ, 1992. Quantification of uncertainty in computational fluid dynamics, Annual Review Fluid Mechanics, vol. 29:123–60

[10] Richardson, LF 1922, 'The supply of energy from and to atmospheric eddies', Proceedings of the Royal Society of London, vol. 97, p. 686

[11] Roy, CJ. 2003. Grid Convergence Error Analysis for Mixed-Order Numerical Schemes, AIAA Journal, vol. 41, pp no. 4

[12] Ierardi, M. J., & Blevins, R. D. (2003). Analysis of a three-dimensional vortex-induced vibration problem by a statistical relative error method. Journal of Fluids Engineering, 125(3), 526-531.

ON THE FLOW RESISTANCE OF TUNNEL FIRES – VALIDATION BY FULL-SCALE FIRE TESTS

[1]Ingo Riess, [2]Rajdeep. Deb, [2]Alex Weber

[1]Riess Ingenieur-GmbH, CH
[2]OST Ostschweizer Fachhochschule, CH

DOI 10.3217/978-3-99161-087-8-034 (CC BY-SA 4.0)
https://creativecommons.org/licenses/by/4.0/deed.de
This CC license does not apply to third party material (attributed to other sources) and content noted otherwise.

ABSTRACT

The aerodynamic resistance of a tunnel fire in longitudinal ventilation, also known as "throttling effect", is relevant for the design and operation of longitudinal tunnel ventilation systems. The throttling effect has been investigated in an extensive CFD study, as presented at the Tunnel Safety Conference in 2020 [1]. It was found that the temperature and airflow stratification downstream of the fire contributes to the pressure drop even far beyond the extent of the fire. A 1-D model of various factors contributing to the air-flow resistance of a tunnel fire has been presented.

In June 2024, we performed full scale fire tests in the test facility at the "San Pedro des Anes" Experimental Centre in Spain. The test facility allows controlled fires with a heat release rate up to 10 MW, jet-fan induced longitudinal flow and sufficient distance from the downstream portal to investigate temperature stratification. The experimental setup allowed direct pressure measurements between the tunnel and a parallel service gallery. Still, the observed pressure differentials were small and external meteorological pressures influenced the measurements in some of the tests.

It was not possible to validate the increased pressure drop downstream of the fire that was observed in the CFD simulations of the 2020 study. In this paper, an updated 1-D model for the throttling effect is presented that is supported by experimental data and by improved CFD modelling.

Furthermore, a frequency analysis of the static pressure has been performed with the goal of comparing the observed frequencies to the characteristic frequencies of the fire source and of the tunnel.

Keywords: throttling effect, tunnel, fire, flow resistance, pressure drop.

1. INTRODUCTION

The research project "Flow Resistance of Fires in Road Tunnels" ([1] to [3]) concluded that many longitudinal tunnel ventilation systems are under-dimensioned, as the flow resistance is generally underestimated. The project includes a theoretical investigation of flow resistance and its relevance for the tunnel ventilation design for smoke control.

The flow resistance of a fire consists of several contributions. Some can be determined from the one-dimensional conservation equations:

- Decrease in static pressure at the fire site due to heating, expansion and acceleration of the tunnel air,
- Increased wall friction downstream of the fire due to increased flow velocity with reduced air density,
- Increase in static pressure due to the deceleration of the air flow due to cooling on the tunnel wall.

An additional pressure loss was found due to spatial effects. It was determined from a series of 3-D CFD simulations.

- Increased flow resistance due to temperature stratification downstream of the fire.

Similar work on the flow resistance of tunnel fires has been done by other researchers ([4] to [8]). All studies were based entirely on analytical approaches, flow simulations and model experiments, since practically no large-scale experimental data was available at the time. Before the results can be applied in practice, simulations must be validated using large-scale fire tests.

Validation is the verification of a computational physical model with experimental measurements. In this case, validation pursues the following objectives:

- Measurement of the physical quantities required to validate the results of the study [2]: the pressure profile along the tunnel and the cross-sections of the flow velocity and temperature downstream of the fire.
- Comparison of the measurements with the results of the study.

This article concentrates on the fire tests and on the validation of the 1-D model. As part of the project, additional CFD simulations were done. These results are published in separate articles [9], [10] and in the project report [11].

2. METHODOLOGY

2.1. Test Tunnel

The fire tests were performed at the tunnel San Pedro de Anes near Gijon, Spain. The tunnel cross-section is shown in **Figure 1**. Key dimensions of the tunnel are:

- Length: 600 m
- Height under the false ceiling: 5.17 m
- Cross section (with false ceiling): 48 m^2
- Longitudinal gradient: -1% south to north

2.2. Fire Source

The fire was formed by fire pans that were placed close to the road surface. Fire pans represent a minimal geometric pressure loss. The heat release rate was estimated from the area of the fire pans. In the test, it was measured indirectly using gas analysis of the exhaust air. The average heat release rate was also determined by the amount of fuel and the duration of the fire.

- Test 1: 4.0 m^2 147 l
- Test 2: 4.0 m^2 150 l
- Test 3: 6.1 m^2 230 l

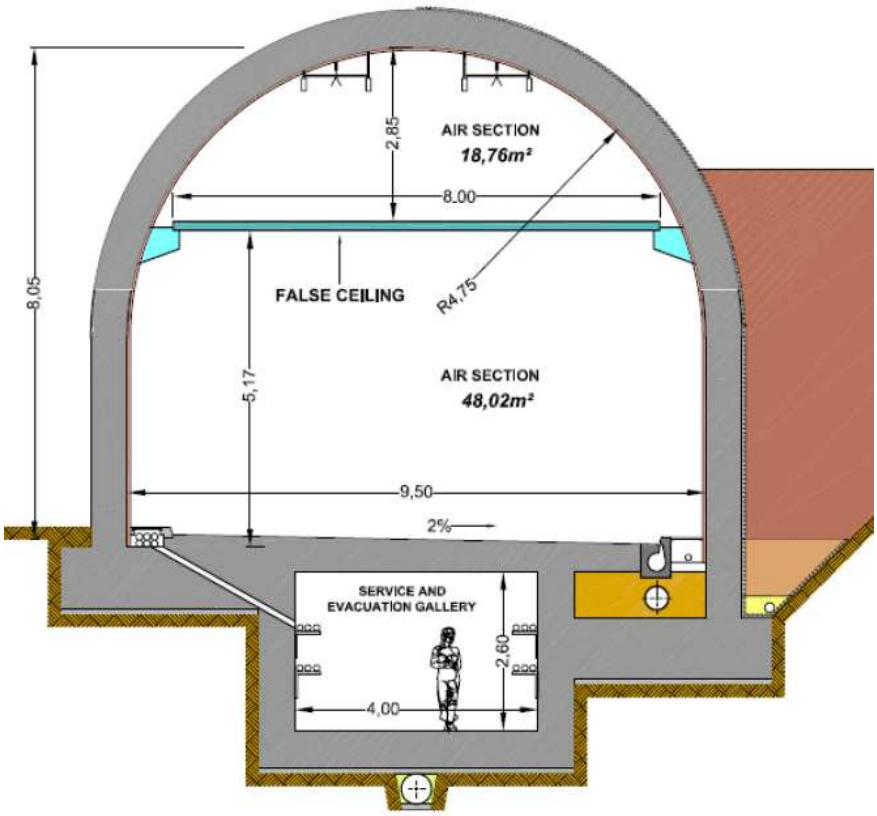


Figure 1: Normal profile of the test tunnel San Pedro des Anes

2.3. Ventilation

The target value of the longitudinal ventilation was an airflow of 3 m/s towards the fire, corresponding to the design value of the longitudinal flow according to the Swiss design code ASTRA 13001. The jet fans are supplied via soft starter on/off. The jet fans were set prior to the tests to achieve the intended airflow.

2.4. Instrumentation

The setup is shown in **Figure 2**. The airflow measurement downstream of the fire was supposed to consist of 25 independent velocity monitors to assess the average flow velocity in the tunnel as well as the flow profile in the cross-section. For the tests, however, only 6 differential pressure monitors were available. This only allowed to record a vertical flow profile with five pitot tubes recording the average dynamic pressure across the tunnel.

For temperature measurement, 25 gas thermocouples were installed at PK522 in the same grid points as the pitot tubes.

The static pressure profile along the tunnel was measured as a differential pressure between the tunnel and the service gallery underneath. The service gallery was open to ambient air at PK600 and no airflow was present. Therefore, the service gallery has been considered as being at reference pressure. In the tunnel, the pressure measurement was located at the tunnel wall, 2 m above ground. The opening of the pressure tube was arranged perpendicular to the longitudinal flow to avoid any influence of the flow velocity. In CFD simulations, it was verified that the measured differential pressure was representative of the average pressure in the tunnel cross-section.

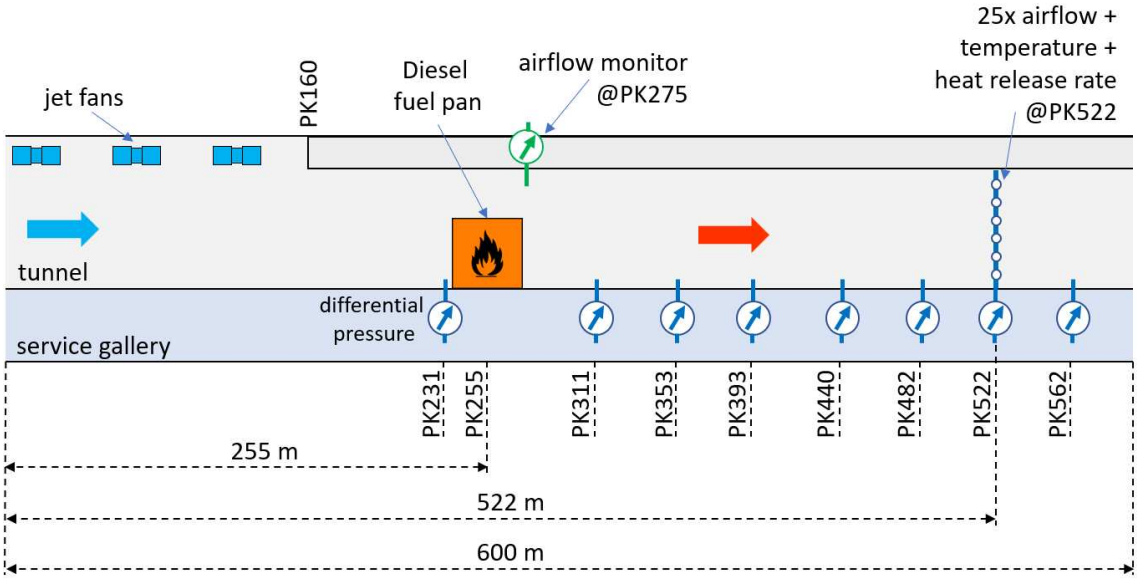


Figure 2: Test setup

An additional differential pressure measurement was located at PK231. The installation was like the installation of the differential pressure measurement described above. This pressure sensor was used to collect short time measurements at higher sampling frequencies of 100 and 2000 Hz.

The heat release rate was evaluated by measuring the total mass flow rate and various gas concentrations (CO, CO_2, O_2 and H_2O). The heat release rate was then derived from these mass flow rates.

3. MODEL

3.1. 1-D Model

A 1-D model for the throttling effect was proposed in the research report ([1] to [3]). With the assumption that fuel mass flow is neglected, the calculation model is presented in a compact formulation. Equations (1) to (5) were developed from classical fluid dynamics analysis, such as pipe flow pressure drop and momentum balance.

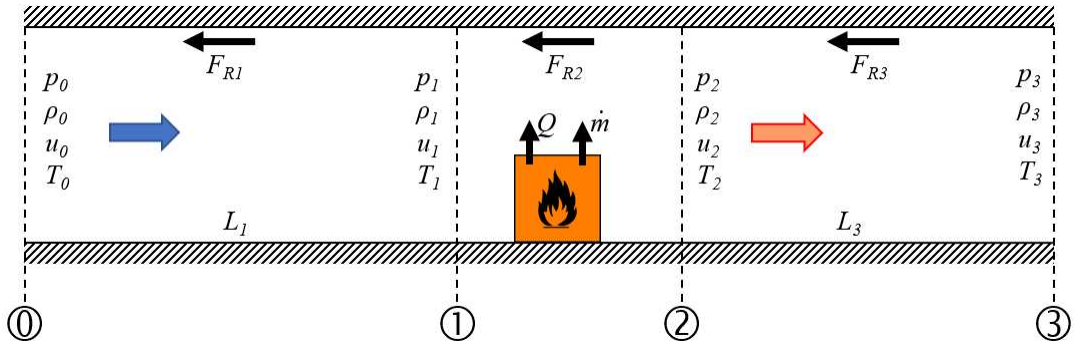


Figure 3: Definitions

The variation of static pressure due to wall friction in the inflow section results in

$$\Delta p_{0-1} = -\frac{\rho_0}{2} \cdot u_0^2 \cdot \frac{\lambda\, L_1}{D_h} \tag{1}$$

The change of static pressure at the fire location is simplified to

$$\Delta p_{1-2} = -\frac{Q_c\, u_0}{c_p A_T T_0} \tag{2}$$

The change in static pressure downstream from the fire includes two components. The wall friction corresponds to the inflow section. However, the flow velocity is increased and the density reduced. This results in an increased pressure drop.

$$\Delta p_{2-3A} = -\frac{\lambda}{2D_h}\int_0^{L_3} \rho(x)\cdot u(x)^2 \cdot dx \tag{3}$$

$$\Delta p_{2-3A} = -\frac{\rho_0}{2}\cdot u_0^2 \cdot \frac{\lambda}{D_h}\cdot\left[\frac{Q_c}{\alpha U_T T_0}\left(1 - exp\left(-\frac{\alpha U_T L_3}{\rho_0 u_0 A_T c_p}\right)\right) + L_3\right] \tag{4}$$

The recovery of static pressure by cooling and the resulting deceleration of the flow is

$$\Delta p_{2-3B} = \frac{Q_c\, u_0}{c_p A_T T_0}\left(1 - exp\left(-\frac{\alpha U_T L_3}{\rho_0 u_0 A_T c_p}\right)\right) \tag{5}$$

with

u	airflow velocity	L	length	Q_c	conv. heat release rate
ρ	air density	A_T	cross-section	c_p	heat capacity
p	static pressure	D_h	hydr. diameter	α	heat transfer coeff.
T	temperature	U_T	tunnel wet perimeter	λ	friction coefficient

The study ([1] to [3]) described an additional pressure loss due to temperature stratification. This was derived from OpenFoam CFD simulations. The evaluation of the test data made apparent that the strong flow stratification and the additional pressure loss were an artefact of the CFD simulations. It is now assumed that the pressure loss was caused by an insufficient resolution of the near-wall flow field (for the Large Eddy Simulation) and/or an inadequate application of wall functions.

For this analysis of the experimental data, the 1-D model following equations (1) to (5) were implemented in the 1-D numerical model Spitfire [12] for comparison with the experimental data and with additional CFD simulations.

3.2. CFD

In addition to the 1-D simulations, three different 3-D CFD codes were used for the preparation of the fire tests and for a comparison with the collected data

- RANS, Star-CCM+
- LES, Fire Dynamic Simulator
- DES, ANSYS Fluent

A detailed documentation of the CFD simulations, i.e. geometry, sub-models, boundary conditions etc. are described in the project report [11].

The Star-CCM+ version v2302 was used for the RANS simulations. The simulations were carried out in stationary mode with 2nd order coupled flow and energy. Due to the expected high temperature gradients, the air is assumed to be compressible. Viscosity, thermal conductivity and heat capacity of the air are calculated as a function of temperature using Sutherland's Law. The gravity term is included to take account of buoyancy forces. For inclined tunnel geometries, only the gravity vector is modified.

Fire Dynamic Simulator FDS v6.8.0 was used for the LES simulations. For analysis of the pressure curve of fires in long tunnels, the transient Very Large Eddy Simulation VLES in combination with the standard FFT-based solver has been used, as recommended in the FDS user manual.

Detached Eddy Simulation (DES) is a hybrid turbulence model that combines RANS and Large Eddy Simulation (LES). Near solid boundaries and close to the fire, where turbulence scales are small and resolving them is computationally expensive, DES applies RANS to model turbulence efficiently. Away from walls, in regions with large turbulent structures, DES switches to LES, which directly resolves unsteady eddies. DES provides a balance between accuracy and cost, capturing large-scale turbulent motions in separated flows while avoiding the excessive computational demand of a full LES.

3.3. Oscillations

The study ([2], [3]) describes pressure oscillations in the fire-affected tunnel, affecting the time averaged pressure profile in a tunnel. Physical oscillations may cause difficulties with the convergence of numerical models. They can be initiated by flame oscillation and amplified with the frequency of the air column in the tunnel. The flame frequency is correlated to the size of the fire pan [13]. In Test 1 it is estimated as 1.3 Hz from the 4 m^2 square pan. The natural frequency of the tunnel is given by the ratio of twice the tunnel length and the speed of sound. For the test tunnel, this gives a first natural frequency of 0.29 Hz and higher order frequencies as multiples $n \cdot 0.29\ Hz$.

4. RESULTS

4.1. Pressure Profile Test 1

Figure 4 shows a comparison of the four pressure profiles along the tunnel with the measured differential pressure. Three of the pressure monitors (PK231, PK482 and PK562) showed erratic behaviour in the dynamics of the test as well as in the time averages for the pressure profile. The installation has been re-checked after the test, but no explanation has been found. The data are shown in the graph but disregarded in the analysis. The measurement at PK231 is replaced by the high-frequency monitor.

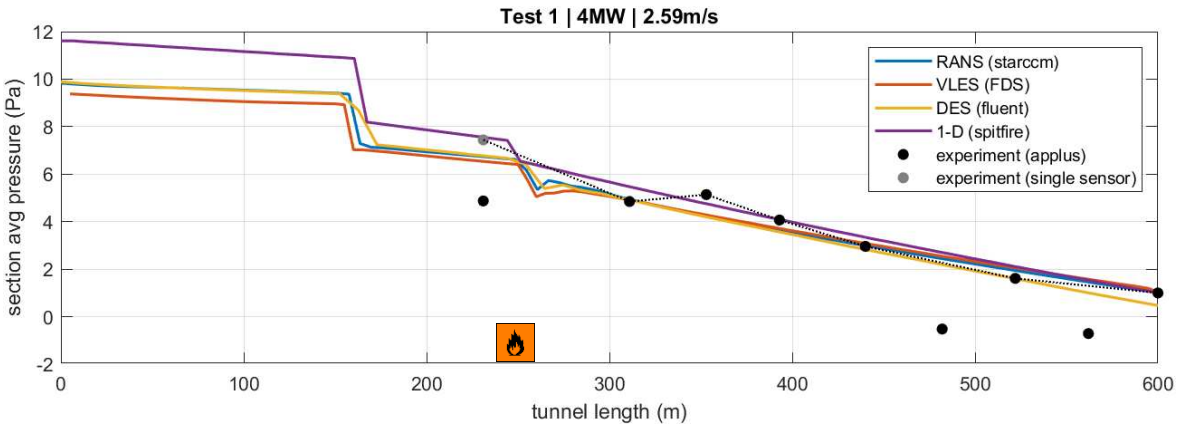


Figure 4: Pressure profile along the tunnel Test 1

The three CFD simulations show very good agreement with the measurements, while the 1-D simulation shows a slightly increased wall friction downstream, and an increased pressure drop at the cross-section change at PK160. The agreement with the measurement is surprising given the difficulty of the pressure measurement between the tunnel and the service gallery.

4.2. Pressure Fluctuations Test 1

The dynamic pressure data is best represented by a frequency analysis for a longer period with developed fire. For Test 1, this is shown in **Figure 5**. The oscillations include the dominant oscillations as well as the turbulence frequency spectrum. A dominant oscillation is visible at ~0.30 Hz, which represents the fundamental frequency of the tunnel tube with open portals. Higher order natural frequencies ($n \cdot 0.29\ Hz$) are not visible.

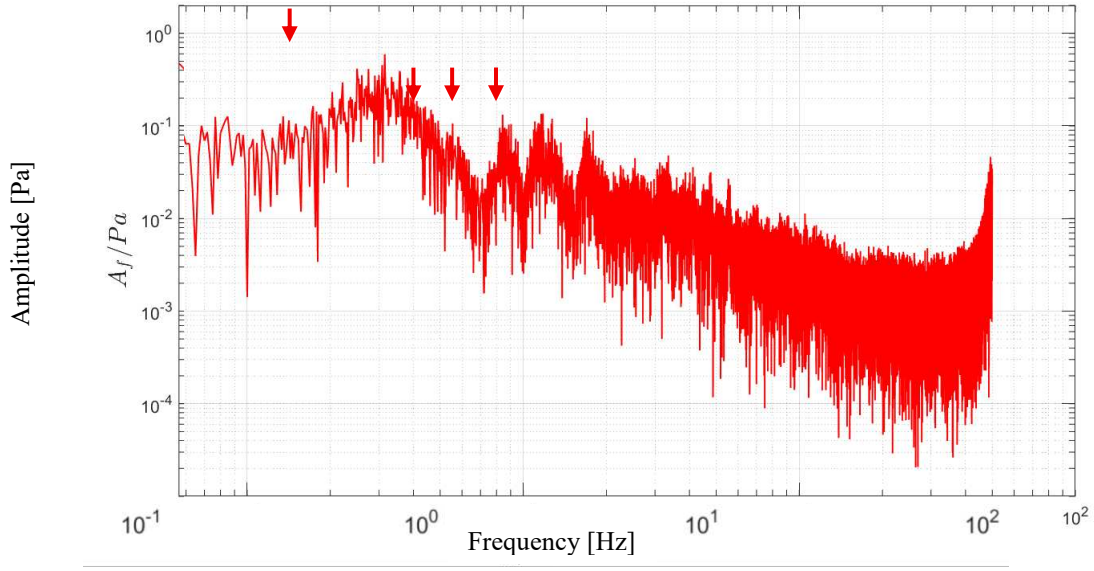


Figure 5: Frequency analysis Test 1, Sampling Rate 100 Hz

The graph also includes three distinct maximums at 0.85 Hz, 1.1 Hz and 1.5 Hz. Although these do not match the frequency of the flame oscillation according to [13], the oscillations are most likely driven by the fire. Further research is required to evaluate possible causes, such as eddy separation of the plume in crossflow.

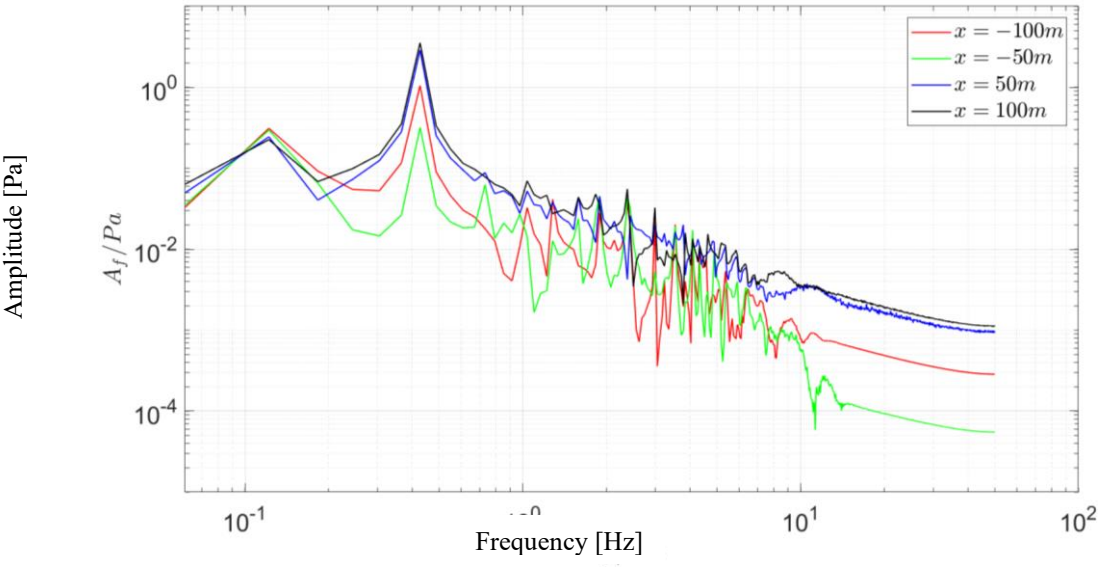


Figure 6: Frequency analysis Test 1, DES simulation

Figure 6 shows the frequency analysis for the DES simulation. We observe a peak frequency at 0.43 Hz, which matches the second harmonic frequency of a tube with one closed and one open end (0.425 Hz). The boundary conditions of the CFD model cause the tunnel oscillations to behave like a tube closed at one end (i.e. fixed flow rate).

4.3. Scaling to Higher Heat Release Rates

While the different models agreed well for the fire tests, the simulations must be scaled to typical tunnel design fires in the range of 30 to 50 MW. These simulations were done with the 1-D model, RANS and VLES.

For the scaled simulations, the tunnel geometry is changed to represent a tunnel with constant cross-section of 65 m^2. The shape of the cross-section varied from a wide rectangular tunnel to a high arched tunnel. A 900 m long tunnel with 1% gradient was modelled. The upstream airflow was set to 3 m/s and the heat release rate to 4 to 50 MW. **Figure 7** shows the static pressure profile along the tunnel for the RANS, VLES and 1-D simulations for a 30 MW fire.

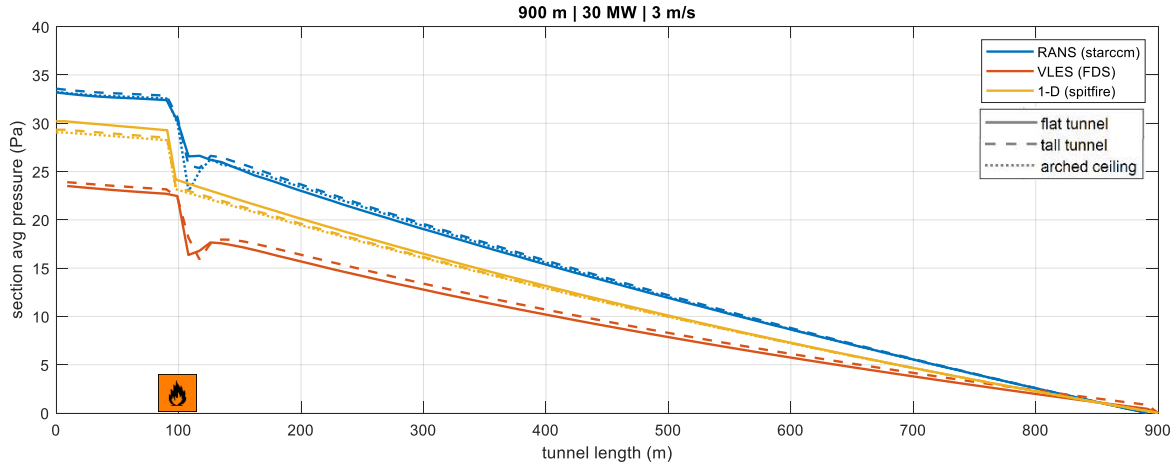


Figure 7: Pressure profile along the tunnel for a 30 MW fire

For all models, the shape of the tunnel cross-section appears to have a minor effect on the pressure drop. But, although the models agreed well for conditions of the fire tests, there is a significant difference for the larger fire with RANS giving the highest and VLES giving the lowest pressure drop.

It was the intention to conduct further simulations without gradient to separate the throttling effect from buoyancy on a downward gradient. At the time, new versions of FDS (v6.9.1 and v6.10.0) were published. The pressure profiles were significantly different from the previous version. These differences are visible in the respective user manuals chapter 21.3 [14]. It does not appear useful to validate a CFD model with such significant changes between versions. The differences in **Figure 7** can be attributed to temperature driven buoyancy on the gradient.

The simulations for larger fires indicate that model validation for experimental data from small fires has limitations regarding regular design scenarios. More data is required for larger fires.

5. SUMMARY AND CONCLUSION

Full size fire tests with heat release rates of 4 to 10 MW have been performed. The tests include measurements of downstream temperature and flow profile as well as pressure profiles along the tunnel. Although the measurement of small pressure differentials between the tunnel and the service gallery proves difficult, the data can be used for the validation of tunnel fire simulations.

The measurements are compared to 1-D simulations and to various 3-D CFD simulations. While the models agree well with the test data, upscaling the models to larger heat release rates shows significant differences, mostly to the temperature and buoyancy downstream of

the fire. FDS versions v6.8.0, v6.9.1 and v6.10.0 show significant differences in the pressure profile for tunnel fires.

Equations (1) to (5) give a good 1-D approximation for the throttling effect of tunnel fires in longitudinal ventilation. The equations can be implemented in dynamic 1-D models for the simulation of tunnel fires.

The fire tests are documented in "Flow Resistance of Fires in Road Tunnels – Validation" [11]. The documentation including the raw measurement data is available as download:

https://doi.org/10.5281/zenodo.17938708

6. REFERENCES

[1] I. Riess, D. Weber, M. Steck, "On the airflow resistance of fires in longitudinal ventilation – the throttling effect" in *10th International Conference Tunnel Safety and Ventilation*, Graz, 2020.

[2] I. Riess, D. Weber, M. Steck, "Strömungswiderstand von Bränden in Strassentunneln" in *Report 1679 Project AGT 2017/005*, 2020.

[3] I. Riess, "Aerodynamic Resistance of Fires in Tunnels", *Riess Ingenieur-GmbH Report 1904002*, Dezember 2020.

[4] E. Ang, I. Riess, J. Peiro & G. Rein, "Understanding and modelling the fire throttling effect in longitudinally ventilated tunnels", in *12th Asia-Oceania Symposium on Fire Science and Technology*, Brisbane, Dezember 2021.

[5] R. Hansen, "Modelling the throttle effect in a mine drift" in Journal of Sustainable Mining, Volume 20 issue 4, https://doi.org/10.46873/2300-3960.1329, 2021

[6] E. Ang, J. Peiro, I. Riess & G. Rein, "Analysis of fire throttling in longitudinally ventilated tunnels with a one-dimensional model" in *Fire Technology Volume 58, pp. 2925-2947*, 2022

[7] D. Gay, "CFD Simulation of the Throttling Effect in Tunnels", *MSc Thesis, Imperial College London*, September 2022

[8] E. Ang, "Engineering simulations in the design and analysis of tunnels for fire safety and smoke ventilation", *PhD Thesis, Imperial College London*, March 2024

[9] R. Deb, A. Weber, I. Riess, "Numerical investigation of flow resistance of fires in road tunnels" in *20th International Symposion on Aerodynamics, Ventilation and Fire in Tunnels*, Copenhagen, October 2024

[10] R. Deb, A. Weber, I. Riess, "Numerical modeling and experimental investigation of flow resistance of fire in longitudinal ventilation along a tunnel", submitted for publication in *Journal of Wind Engineering and Industrial Aerodynamics*, July 2025

[11] M. Friedl, A. Weber, R. Deb, I. Riess, "Flow Resistance of Fires in Road Tunnels – Validation", *Project BGT 20_00A_01*, report submitted for publication.

[12] I. Riess, "On smoke stratification in a 1-D tunnel ventilation model" in *11th International Conference Tunnel Safety and Ventilation*, Graz, 2022.

[13] H. Ingason, Y. Zhen Li, A. Lönnermark, "Tunnel Fire Dynamics", *Springer, DOI 10.1007/978-1-4939-2199-7*, 2015

[14] Fire Dynamics Simulator User's Guide, Versions v6.8.0, v6.9.1 and 6.10.0

EFFECT OF ROAD TUNNEL FITOUT ON SMOKE CONTROL

Michael Beyer, Conrad Stacey

Stacey Agnew Pty Ltd, AU

DOI 10.3217/978-3-99161-087-8-035 (CC BY-NC 4.0)
https://creativecommons.org/licenses/by/4.0/deed.de
This CC license does not apply to third party material (attributed to other sources) and content noted otherwise.

ABSTRACT

A CFD model, previously validated against the Memorial Tunnel fire tests with longitudinal ventilation, is used to investigate the influence of ceiling-mounted road tunnel equipment on upstream smoke propagation in case of a road tunnel fire. Typical road tunnel installations, including cable trays, hangers, lighting, signage, misting pipes, speakers, etc. were incorporated into a representative three-lane TBM tunnel geometry and compared with an otherwise identical tunnel without ceiling obstructions.

The study examines differences in smoke behaviour for both the critical velocity case, defined by the prevention of upstream backlayering, and the confinement velocity case, defined by limiting the upstream backlayering length to 30 m. The observed differences are interesting as the tunnel equipment does not materially alter critical velocity required to prevent backlayering. However, for the confinement velocity case, the presence of ceiling obstructions significantly affects upstream smoke propagation, resulting in increased backlayering lengths for the same applied ventilation flow rate.

The results are configuration-specific and reinforce the need for project-specific, validated CFD assessments when determining confinement velocity in tunnels with obstructed ceiling spaces.

Keywords: Smoke control, smoke propagation, confinement velocity, critical velocity, backlayering.

1. INTRODUCTION

In 2023, NFPA 502 [1] changed the design criteria for road tunnels from the absolute prevention of backlayering (critical velocity) to allowing some backlayering (confinement velocity). That made sense from a tunnel safety perspective regarding avoiding over-ventilation and consequent oversizing of the ventilation system. However, it is not clear how to determine a design confinement velocity. NFPA 502 does not provide a calculation method for determining confinement velocity as there is no such reliable method that can be used for real (full-scale) tunnels. It is recommended to use a CFD model validated against appropriate full-scale data to explore appropriate confinement velocity values.

It is noted that the absolute prevention of smoke backlayering is not universally adopted as a primary design objective in European tunnel fire safety practice. In several European guidelines and design approaches [2], [3], [4], [5] limited upstream smoke propagation may be considered acceptable as part of a balanced smoke control strategy, recognising that excessive longitudinal ventilation can disrupt smoke stratification and, under certain conditions, promote faster fire growth, higher peak heat release rates, and increased fire spread, as also discussed here [6], [7]. The low velocity philosophy, which seeks to balance smoke control effectiveness against adverse fire ventilation interactions, aligns with the

underlying rationale of the confinement velocity concept as a design criterion introduced in NFPA 502.

A previous study [8] explored some key influences on confinement velocity based on a validated CFD model [9], but the example tunnel used had no fittings, equipment or any other installations included. This may be appropriate for most tunnels in Europe where the tunnel ceiling is smooth and usually free of any equipment with considerable obstruction of the air path. In other regions, especially in Australia, it is common and more cost efficient to have cable trays, trusses, lights and other equipment hanging from the ceiling, potentially influencing the upstream smoke propagation.

To better understand the influence of obstructed ceiling space on smoke propagation, the same tunnel geometry and CFD methodology used for the previous study [8] was modified to incorporate tunnel equipment, with an example in Figure 1 (left). Using this updated geometry, the simulation parameters, methodology, and target flow conditions to achieve critical velocity (preventing the onset of backlayering) and confinement velocity (i.e., limiting upstream smoke propagation to a backlayering length of 30 m) were maintained as established previously [8]. The effect of the installed tunnel fitout on smoke propagation was then investigated.



Figure 1: Typical tunnel fitout in Australia (left, Heysen tunnel) and in Austria (right, Niklasdorftunnel [10])

2. CFD METHODOLOGY

The CFD model was created based on the methodology used for evaluating critical velocity by Beyer & Stacey [9]. The simulation software ANSYS Fluent [11], [12], [13] was used.

Following the previous study [8], the modelled example tunnel has a typical 3-lane TBM profile with a cross-section area of 93 m^2, a hydraulic diameter of 9.9 m, and a height from floor to ceiling of 8.92 m. The tunnel domain has a total length of 500 m. The fire source was placed 300 m downstream of the inlet portal on the floor in the middle of the tunnel. The "clean" tunnel geometry (no ceiling mounted equipment) was modified to include a typical tunnel fitout (i.e. lighting, cameras, cable trays, speakers, signage, misting pipes, and hangers or cross-tunnel bean mountings for all that equipment) as illustrated in Figure 2. The surface of the fitout was conservatively considered to be adiabatic, therefore not removing any heat from the smoke. The change to the unobstructed tunnel cross section at the fire front due to the added equipment is negligible (<0.1%). However, even with the overall tunnel area being about the same (resulting in about the same average air velocity for the same tunnel air flow rate), the lower flow around the obstructions can still have a considerable impact on the local and overall velocity distributions.

The overall mesh size in the modified domain and especially within the vicinity of the fire was kept the same as employed in the model without the tunnel fitout. A finer surface mesh (~10 mm) was applied to the tunnel fitout to resolve geometric details, resulting in increased mesh density and a three times higher total cell count relative to the original model [9]. To manage computational demands, tunnel equipment was only included around the fire and for 110 m upstream. Adopted design fire parameters as proposed in [14] for a 50 MW fire, and other input parameters, are listed in Table 1.

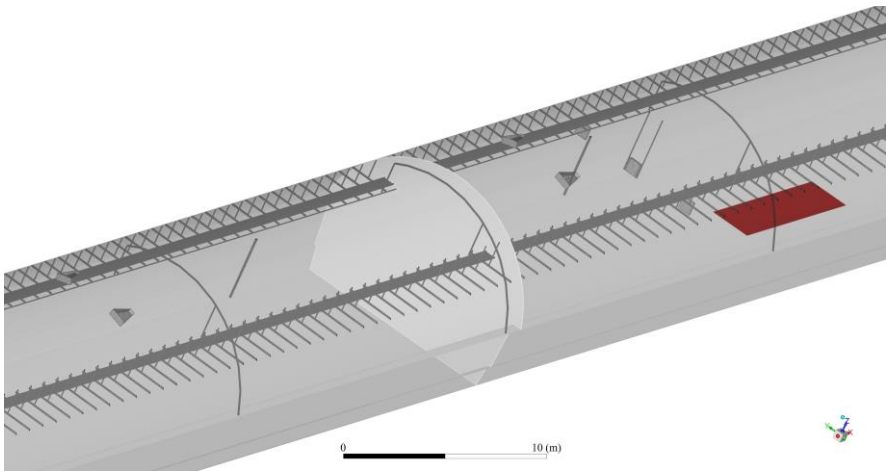


Figure 2: Adopted tunnel fitout for CFD study, including hangers for equipment.

Table 1: Input parameters used for the CFD model.

Parameter	Value
Tunnel air temperature	30°C
Tunnel wall temperature (constant)	30°C
Tunnel wall roughness height K_S	1.5e-03 m
Wall roughness height K_S of fitout	1.6e-04 m
Tunnel slope	Flat (0%)
Total Fire HRR	50 MW
Radiative fraction	0.2
Fire width	2.5 m
Fire intensity	2.25 MW/m^2
Fire length	8.889 m
Fuel	Fuel-oil ($C_{19}H_{30}$)
Combustion efficiency based on total HRR (relevant for additional CO_2 and H_2O source)	0.95

The required flow rate for just preventing smoke backlayering and confining the backlayering length to 30 m as previously concluded in the "Empty" tunnel was applied in the modified tunnel to explore the change in the smoke propagation with the obstructions in the ceiling space. The results are discussed and compared in Section 3 below.

3. RESULTS OF CFD STUDY

For the previously assessed tunnel without ceiling obstructions, the critical and confinement velocities were 3.54 m/s and 3.28 m/s respectively, for the assumed fire parameters in a flat tunnel. The confinement velocity corresponds to a controlled upstream backlayering length

of 30 m in the tunnel without the fitout. For the tunnel including ceiling-mounted equipment, the same upstream flow rates were applied for both cases, enabling a direct comparison of upstream smoke propagation with and without the additional equipment. In a further step, the smoke propagation of the confinement velocity case was also compared with and without the tunnel fitout in the 4% downgrade tunnel.

The characterisation of the flow regime, as well as a detailed discussion of the fire plume and smoke backlayer dynamics, is presented in previous work [8] and not repeated here.

3.1. Critical velocity (flat tunnel)

The critical velocity is 3.54 m/s in the example tunnel without the fitout [8]. The same flow rate applied with the ceiling-mounted equipment present resulted in the ceiling smoke jet right above the fire being more diluted (cooler) and pushed slightly further back (see

Figure **3** and Figure 4). Based on the example chosen, the results indicate that the ceiling obstructions do not significantly change the critical velocity required to prevent backlayering, and perhaps reduce it.

Figure **5** compares a contour plot of the velocity component along the tunnel axis in the tunnel cross section at the fire front, for the case with and without the ceiling-mounted equipment. The obstructions in the ceiling locally increase the velocity everywhere else in the cross section, including in the unobstructed ceiling area, compared to the case without the equipment in place. At the front of the fire, this is further enhanced by the plume front also creating some sort of obstruction for the oncoming flow, and pushing the air around, both sideways and up towards the ceiling. The left plot of Figure 6 shows the x-velocity vertical profiles at the centre of the fire front for both cases, which quantifies the higher ceiling velocity at the centre line. The right plot of Figure 6 compares the x-velocity profiles on a horizontal line at 6.4 m height at the fire front, going across the cable tray props which also support the lights, misting pipes etc.). The right plot also shows the higher upstream velocity in the unobstructed ceiling area. The slightly higher ceiling velocity in the unobstructed area and in the tunnel centre may be an explanation for the slight push back of the hot ceiling jet right above the fire source. The minor differences observed in smoke propagation for the critical velocity case are also related to the specific configuration of the tunnel fitout and the arrangement of certain installations (e.g. signage) relative to the fire location. In the example analysed, the fire is centred in the tunnel, and the obstructed ceiling areas are at the sides. Also, the larger signs could be local to the fire, or further away (12 m upstream in this example - Figure 4). The results here could be different if those things change. Therefore, the findings reported herein should not be interpreted as universally applicable, and project-specific assessments remain necessary.

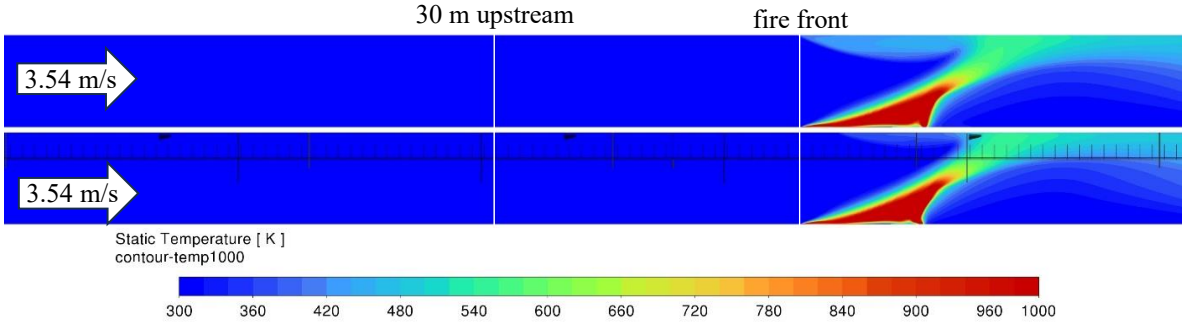


Figure 3: Contour plot of temperature distribution through the centre of the tunnel for the tunnel without fitout (top) [8] and with the fitout (bottom) for the critical velocity case. Temperature is clipped to 1000 K for better presentation.

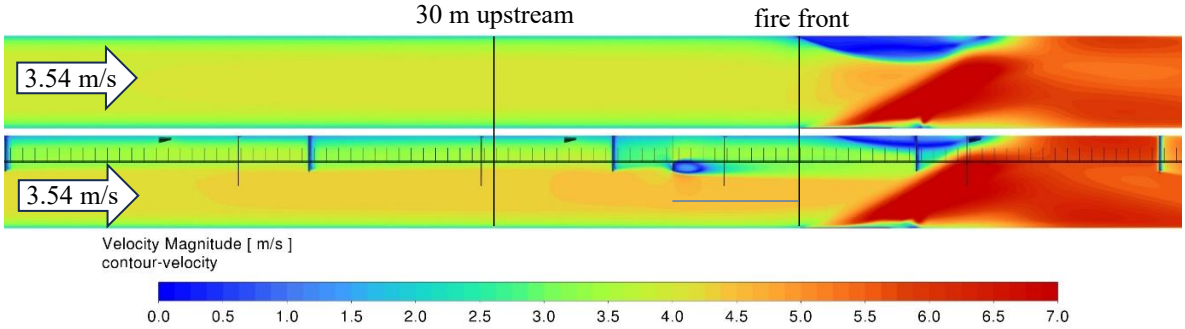


Figure 4: Contour plot of velocity distribution through the centre of the tunnel for the tunnel without fitout (top) [8] and with the fitout (bottom) for the critical velocity case. Velocity is clipped to 7 m/s for better presentation.

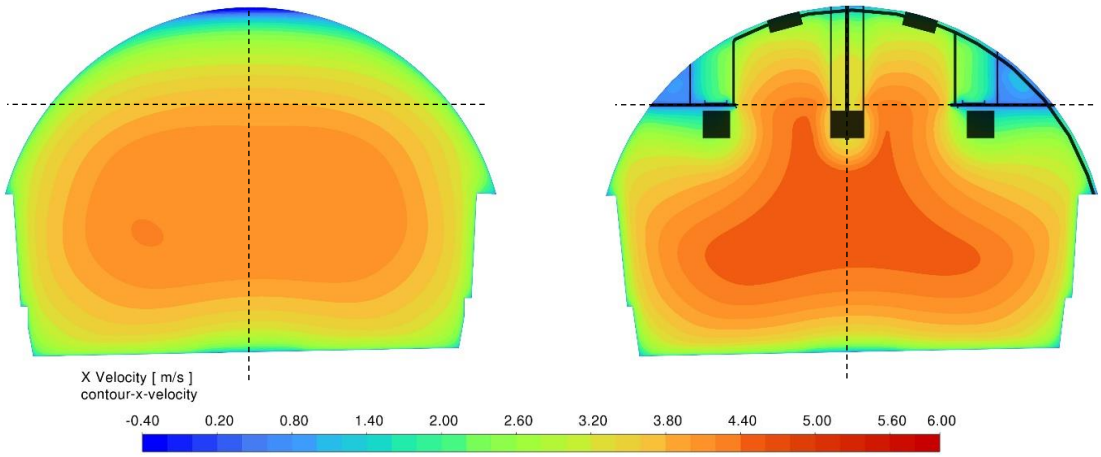


Figure 5: Contour plot of velocity along the tunnel (x-velocity) in the tunnel cross section at the fire front for the critical velocity case with fitout (right) and without the tunnel fitout (left) [8]. Detailed comparison of velocity profiles along the dashed lines is shown in Figure 6**.**

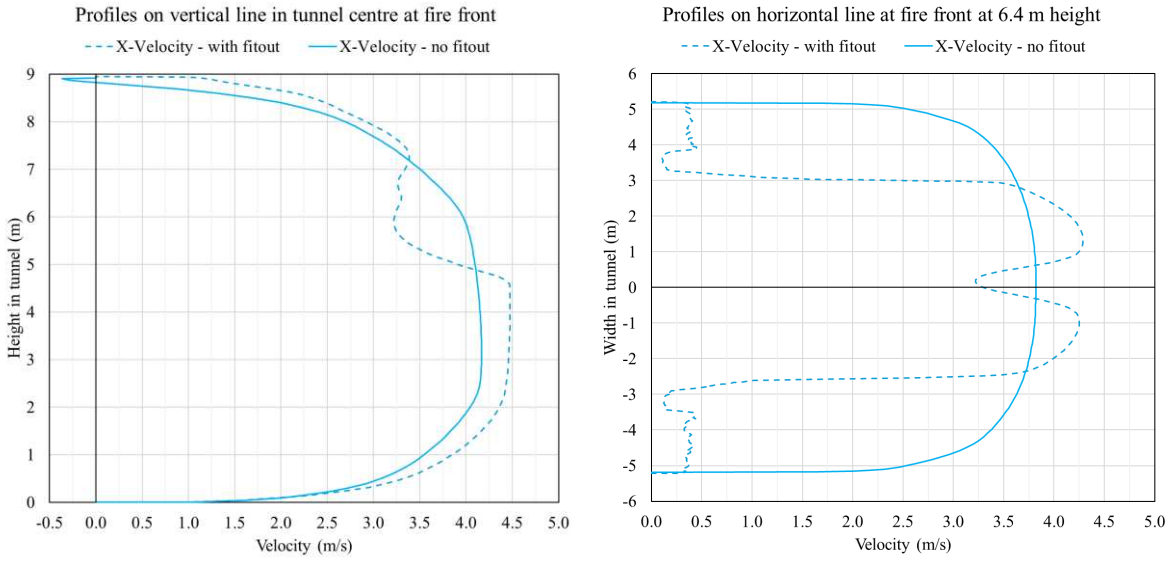


Figure 6: Velocity profile at the fire front for the critical velocity case with and without the tunnel fitout. Left: The profiles were taken on a vertical line from tunnel floor to ceiling on the centre line of the tunnel at the fire front. Right: The profiles were taken on a horizontal line from tunnel wall to tunnel wall at the fire front at 6.4 m height.

3.2. Confinement velocity (flat tunnel)

The influence of the tunnel fitout on the smoke propagation is quite different for the confinement velocity case where a hot smoke layer upstream of the fire is already present to a certain distance (here 30 m upstream of the fire front). With the same fire scenario and the same upstream flow in both tunnels (with and without the fitout) the backlayering length increases by about 50% (from 30 m to 43 m) in the tunnel with the fitout (see Figure 7 and Figure 8).

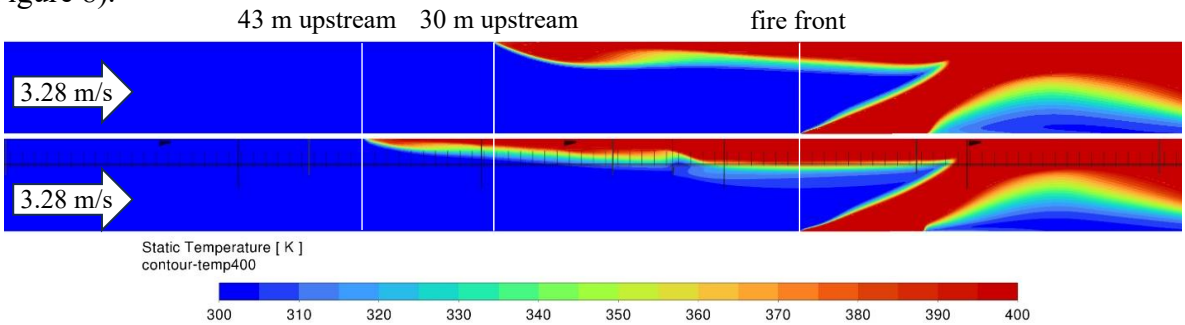


Figure 7: Contour plot of temperature distribution through the centre of the tunnel for the tunnel without (top) [8] and with the fitout (bottom) for the confinement velocity case. Temperature is clipped to 400 K for better presentation.

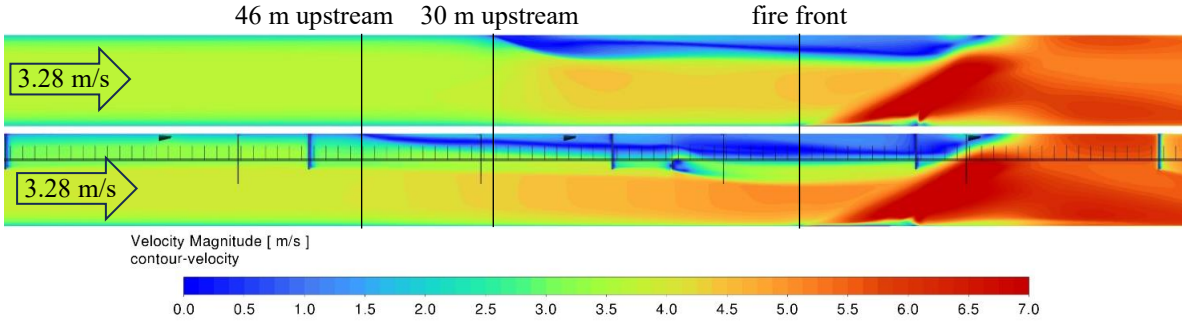


Figure 8: Contour plot of velocity distribution through the centre of the tunnel for the tunnel without fitout (top) and with the fitout (bottom) for the confinement velocity case. Velocity is clipped to 7 m/s for better presentation**.**

This is believed to be related to two factors. First, the comparison of the velocity profile in the middle of the tunnel for the two cases (Figure 9, left plot) shows that the oncoming velocity close to the ceiling is approximately 10% lower in the tunnel with the fitout. The lower velocity along the ceiling reduces the near-ceiling momentum of the approaching flow that opposes the advancing smoke layer. The velocity profiles shown in the left plot of Figure 9 were taken further upstream of the backlayering (58 m upstream of the fire front). At that location, there is no additional blockage due to either the fire plume (which displaces air sideways and up) or the hot smoke layer that also displaces the oncoming air. The higher ceiling velocity is only present at the fire front but not further upstream. The incoming velocity profile at the upstream extent of the smoke layer is then a different circumstance between the backlayer location at critical and confinement velocities. Secondly, the average velocity gradient in the shear layer between the approaching air and the hot smoke in the backlayer is approximately 35% lower in the tunnel with the fitout compared to the case with the unobstructed ceiling (see Figure 9, right plot). This reduces the shear stress and counteracting force on the backlayer, consistent with a greater upstream propagation of the hot smoke. The air speed around the obstructed areas in the ceiling is reduced, which provides more scope for the backlayer to develop upstream and to increase in thickness (see Figure 7 to Figure 8). The reduction of flow at high level increases the airspeed onto the plume underneath the smoke layer (see Figure 8), which obviously does not strongly influence the

plume behavior at the fire (see Figure 7). The thickness of the backlayer increases significantly, while the relative velocity between smoke backlayer and approaching air is not much changed. This is consistent with a reduced shear stress. This is depicted by the temperature and velocity profile at the fire front as shown in the right plot of Figure 9.

Based on the example chosen, the results indicate that the confinement velocity needs to be appropriately increased in the tunnel with the obstructed ceiling space, if it is desired to restrict the backlayer to the same length observed in the tunnel without the fitout.

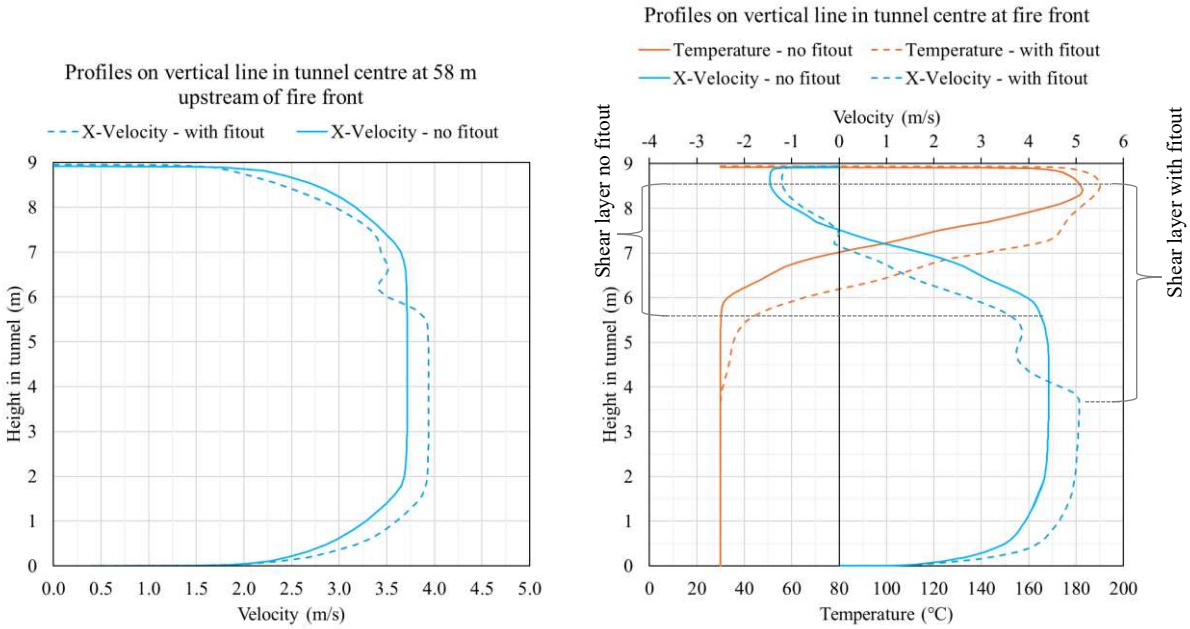


Figure 9: Velocity profiles 58 m upstream of the fire front (left) and at the fire front (right) for the confinement velocity case with and without the tunnel fitout in a flat tunnel. The profiles were taken on a vertical line from tunnel floor to ceiling on the centre line of the tunnel profile.

3.3. Confinement velocity (4% downgrade)

Figure 10 and Figure 11 plot contours of temperature and absolute velocity on a plane through the centre of the tunnel and compare the confinement velocity case results for 4% downgrade. The simulations are for the same fire scenario as before, and have the same upstream flowrate as for the flat tunnel confinement cases, but in a 4% downgrade tunnel.

The instability of the backlayering in the downgrade tunnel due to the additional buoyancy force in the smoke backlayer is already well explained in previous work [8] and will not be discussed again here.

Figure 12 compares the x-velocity vertical profiles in the centre of the tunnel at 58 m upstream of the fire front (left plot) and the x-velocity and temperature profile at the fire front (right plot). The left plot again shows that the approaching air velocity along the obstructed ceiling is about 10% lower than in the case without the fitout. In both cases, the velocity profiles at the fire front show that the initial velocity of the smoke propagating upstream is much higher in the downgrade tunnel compared to the flat tunnel (Figure 12 right plot vs. Figure 9 right plot).

The ceiling-mounted equipment reduces the momentum of the near-ceiling flow. This allows the smoke to propagate more freely upstream as discussed in Section 3.2, leading to much longer backlayering. The additional buoyancy force in the backlayer in the downgrade tunnel increases the backlayering length by approximately 10% compared to the flat tunnel case,

when comparing the two cases with the tunnel fitout (Figure 7 bottom vs. Figure 10 bottom). Also, the backlayering in the downgrade tunnel was seen to be more stable, without the oscillations that were observed in the tunnel without the ceiling mounted equipment.

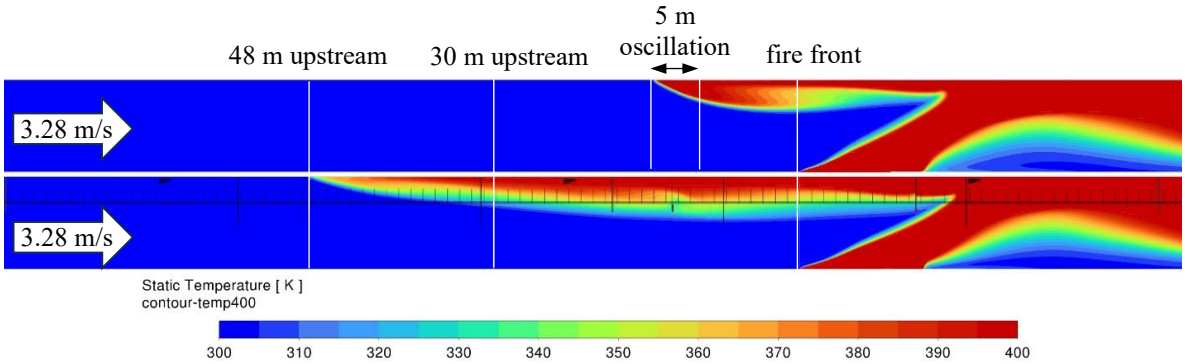


Figure 10: Contour plot of temperature distribution through the centre of the tunnel for the tunnel without fitout (top) and with the fitout (bottom) for the confinement velocity case with 4% downgrade. Temperature is clipped to 400 K for better presentation.

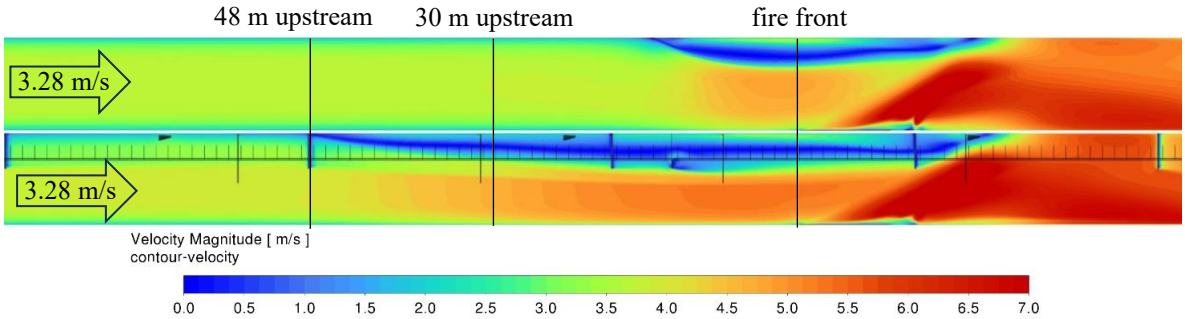


Figure 11: Contour plot of velocity distribution through the centre of the tunnel for the tunnel without fitout (top) and with the fitout (bottom) for the confinement velocity case with 4% downgrade. Velocity is clipped to 7 m/s for better presentation.

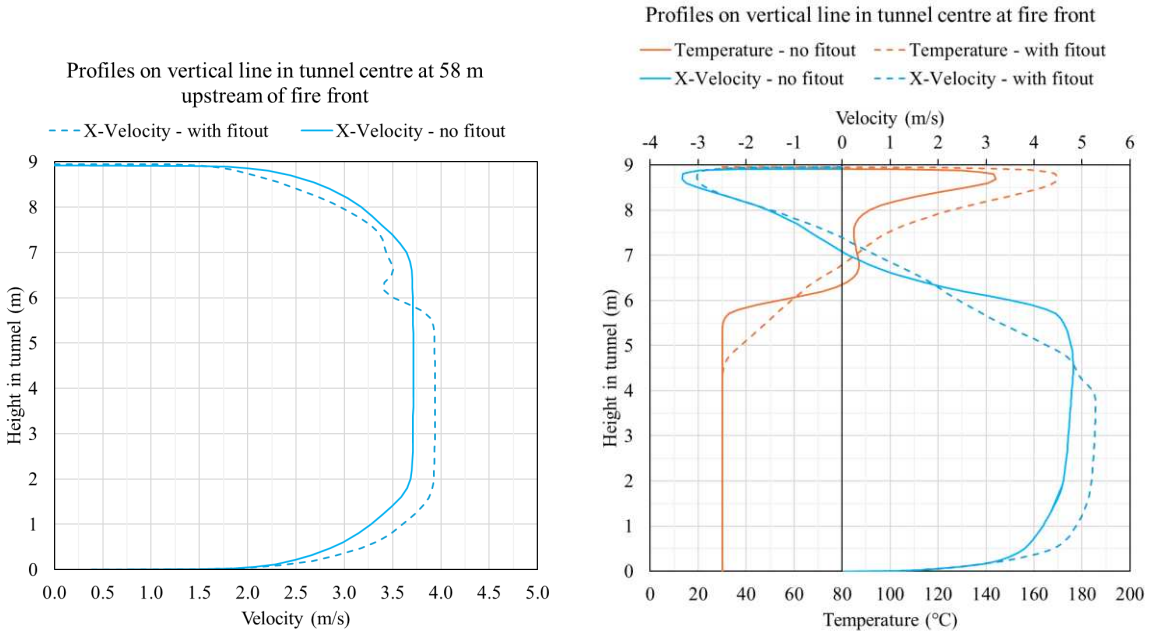


Figure 12: Velocity profile 58 m upstream of the fire front (left) and at the fire front (right) for the confinement velocity case with and without the tunnel fitout in a 4% downgrade tunnel. The profiles were taken on a vertical line from tunnel floor to ceiling on the tunnel centre line.

4. SUMMARY AND CONCLUSION

This study examined the influence of ceiling-mounted tunnel fitout on smoke propagation under longitudinal ventilation using a CFD model validated against the Memorial Tunnel fire tests. A representative three-lane TBM tunnel was analysed with and without typical ceiling-mounted equipment to assess the implications for fitout on critical and confinement velocity concepts adopted in NFPA 502.

For the critical velocity case, the inclusion of ceiling-mounted equipment did not result in a meaningful change in the velocity required to prevent upstream smoke propagation. Local redistribution of the approaching flow was observed near the ceiling, caused by both the presence of equipment and the fire plume acting as an obstacle to the oncoming air. This led to locally increased velocities in unobstructed ceiling regions at the fire front, resulting in slightly enhanced smoke dilution and a marginal displacement of the upstream ceiling jet right above the fire source. These effects were minor and strongly depend on the specific configuration of the tunnel fitout and their arrangement relative to the fire source. Therefore, no generalised influence of ceiling-mounted equipment on critical velocity should be inferred based on the results presented. However, it seems that critical velocity is not sensitive to ceiling fitout. Some sensitivity had been anticipated.

In contrast, the confinement velocity case showed a strong sensitivity to ceiling obstructions. For the same upstream flow rate that limited backlayering to 30 m in the clean tunnel, the inclusion of ceiling mounted equipment increased the backlayering length by approximately 50% in the flat tunnel. This behaviour is attributed to reduced approaching air velocity near the ceiling and a significantly lower velocity gradient across the shear layer between the incoming airflow and the hot smoke backlayer, resulting in reduction of the shear stress opposing upstream smoke propagation.

In the 4% downgrade tunnel, these effects were further amplified by the increased longitudinal component of buoyancy forces in the smoke layer, leading to longer and more stable backlayering relative to the tunnel configuration without the fitout. That is the opposite trend to that we found without the fitout, where the backlayer length in the downgrade tunnel reduced compared to the flat tunnel [8].

Overall, the results indicate that ceiling-mounted tunnel fitout has little influence on critical velocity but can significantly affect confinement velocity and backlayering behaviour, particularly where an established upstream smoke layer is present. The confinement velocity is highly sensitive to local ceiling-level flow conditions, which may be substantially affected by tunnel equipment even when the overall tunnel cross-sectional area is largely unchanged.

The findings presented in this study are based on a specific tunnel geometry, ventilation configuration, fire scenario, and a representative arrangement of ceiling-mounted tunnel fitout. While the CFD methodology has been validated against relevant experimental data obtained from full-scale tunnel fire tests, the results are sensitive to the detailed geometry, arrangement of the tunnel fitout, as well as tunnel slope, fire location, and design fire size.

For tunnels incorporating significant ceiling-mounted installations, the determination of critical and confinement velocity should therefore be undertaken on a project-specific basis, using CFD models validated against appropriate full-scale data and reflecting the actual tunnel geometry and fitout arrangement. Simplified or generic design values may not adequately capture the impact of ceiling obstructions on upstream smoke propagation.

5. REFERENCES

[1] NFPA 502, "Standard for Road Tunnels, Bridges, and Other Limited Access Highways," The National Fire Protection Association, US, 2023.

[2] RVS 09.02.31, "Tunnel / Tunnel Equipment / Ventilation Systems - Basic Principles," Richtlinie, Österreichische Forschungsgesellschaft Straße - Schiene - Verkehr, Wien, AT, 2014.

[3] RABT, "Richtlinie für die Ausstattung und den Betrieb von Straßentunnel (RABT)," Richtlinie, Forschungsgesellschaft für Straßen- und Verkehrswesen , Arbeitsgruppe Verkehrsführung und Verkehrssicherheit, Germany, 2016.

[4] ASTRA, "Lüftung der Strassentunnel - Systemwahl, Dimensionierung und Ausstattung (2008 V2.03)," Richtlinie, Bundesamt für Strassen ASTRA, Bern, CH, 2008.

[5] PIARC (C3.3), "Operational Strategies for Emergency Ventilation (P. C. (C3.3), Ed.)," World Road Association (PIARC), 2011.

[6] P. Sturm, M. Beyer and M. Rafiei, "On the problem of ventilation control in case of a tunnel fire event," *Case Studies in Fire safety, CSFS 22, Elsevier publishing, doi: 10.1016/j.csfs.2015.11.001,* 2015.

[7] M. Beyer, C. Stacey and A. Dix, "Critical velocity and tunnel smoke control Part 2, Filling the NFPA 502 void," *Australian Tunnelling Society,* p. 6, 2021, https://australiantunnellingsociety.com.au/2021/05/03/critical-velocity-and-tunnel-smoke-control-part-two/.

[8] M. Beyer and C. Stacey, "Confinement Velocity for Smoke in Tunnels – How to Poke a Stick at it," in *12th International Conference Tunnel Safety and Ventilation*, Graz, https://openlib.tugraz.at/download.php?id=661e41e159503&location=browse, 2024.

[9] M. Beyer and C. Stacey, "CFD Validation for Tunnel Smoke Control Design," in *11th International Conference Tunnel Safety and Ventilation*, Graz, 9th and 10th May 2022.

[10] M. Beyer, P. Sturm, M. Saurwein and M. Bacher, "Evaluation of Jet Fan Performance in Tunnels," in *8th International Conference 'Tunnel Safety and Ventilation'*, Graz, 2016.

[11] Ansys, Inc, "ANSYS Fluent Theory Guide, Release January 2023 R2," USA, 2023b.

[12] Ansys, Inc, "ANSYS Fluent User's Guide, Release January 2023 R2," USA, 2023a.

[13] Ansys, Inc, "ANSYS Fluid Dynamics Verification Manual, Release January 2023 R2," USA, 2023c.

[14] M. Beyer, C. Stacey and G. Brenn, "A Mixed Convection Model for Estimating the Critical Velocity to Prevent Smoke Backlayering in Tunnels," *Springer Fire Technology,* no. prepring, p. 50, 2024.

CONSEQUENCES FROM LARGE EV FIRES IN A TUNNEL – A DACH RESEARCH ACTIVITY

[1]Daniel Fruhwirt, [1]Alexander Kores, [2]Robert Galler, [2]Robert Wenighofer, [3]Bastiaan Lotmann, [4]Simon Frey, [5]Christian Thienert, [5]Frank Leismann, [6]Christoph Schneider [6]

[1]Graz University of Technology, AT
[2]Technical University of Leoben, AT
[3]ILF Consulting Engineers Austria GmbH, AT
[4]HBI Haerter AG, CH
[5]Studiengesellschaft für Tunnel und Verkehrsanlagen – STUVA – e. V., DE
[6]WSP Switzerland, CH

DOI 10.3217/978-3-99161-087-8-036 (CC BY-NC 4.0)
https://creativecommons.org/licenses/by/4.0/deed.de
This CC license does not apply to third party material (attributed to other sources) and content noted otherwise.

ABSTRACT

In recent years, battery-electric vehicles have reached a significant market share. Although this statement mainly refers to passenger car applications, meanwhile e-mobility has also reached heavy duty vehicles and buses. Many research activities have been conducted in order to evaluate the fire characteristics and the hazards posed by EVs. Available data from full-scale testing of small BEVs show no significant increase of risk compared to fires of conventional vehicles. However, there is only little information available about the fire risk of large EVs. For this reason, the DACH research area has initiated a dedicated research project in order to evaluate the fire characteristics of battery-electric trucks and its consequences for road tunnel safety. A key element of the DACH research activity is to perform a full-scale fire test of an EV truck in a road tunnel environment. Thereby, assessing both the consequences for tunnel users and the tunnel structure. This paper provides a comparative overview of today´s EV landscape and an introduction to the eTRUCK-DACH project.

1. INTRODUCTION – THE EVOLUTION OF VIDEO ANALYTICS

E-mobility is a key element of the transition of mobility towards more sustainability, by eliminating tailpipe emissions. In recent years the number of battery electric vehicles on European roads has steadily increased. In 2025 the share of newly registered EV passenger cars was 20%. The total number of registered EV passenger cars in the European Union has reached 7.7 million and another 5 million for plug-in hybrid vehicles.

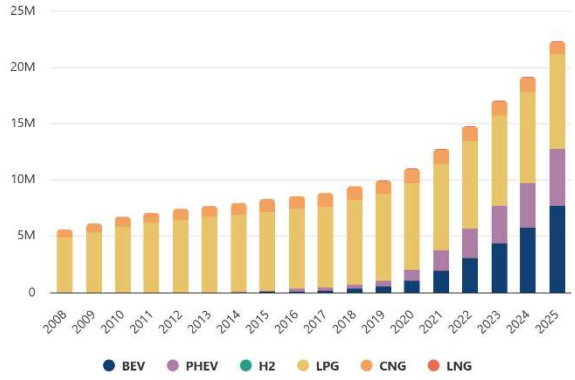


Figure 1: Number of registered alternative fuel vehicles in the European Union - passenger cars [1]

The number of large BEVs on European roads is significantly lower, although the number of newly registered vehicles strongly increases. According to the European Alternative Fuel Observatory [1], in 2025 12.300 BEV trucks have been registered, leading to a total number of 26.000 registered vehicles.

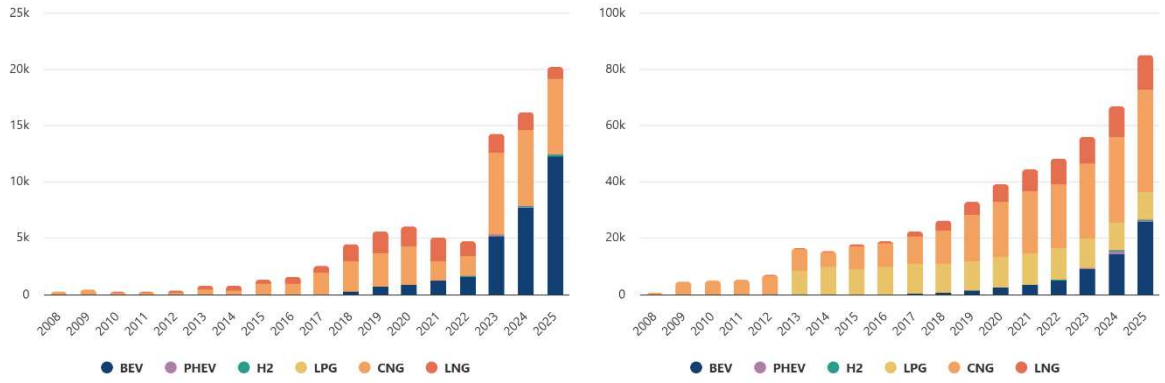


Figure 2: left – new registrations of alternative fuel trucks in the European Union,
right – total number of registered alternative fuel truck in the European Union [1]

These numbers showcast the trend in European mobility and highlight the need for an evaluation of safety concepts, which are mainly based on experiences with incidents involving conventional vehicles. Therefore, the D-A-CH region, who comprises the transport authorities of Germany, Austria and Switzerland has initiated a dedicated research project in order to scientificly investigate the fire characteristics of EV trucks in a road tunnel.

2. CHARACTERISTIC OF LARGE BATTERY-ELECTRIC VEHICLES

2.1. Battery technology

Modern electric vehicles predominantly use lithium-ion batteries because they offer higher volumetric energy density (capacity per cubic meter) and much lower self-discharge than legacy chemistries such as lead–acid, nickel–cadmium, or nickel–metal hydride. A lithium-ion cell comprises a negative and a positive electrode (whose roles as anode/cathode swap between charge and discharge), an electrolyte that enables lithium-ion transport, and a separator that electrically insulates the electrodes. The most common cathode chemistries include lithium iron phosphate (LFP), lithium cobalt oxide (LCO), lithium manganese oxide (LMO), lithium nickel cobalt aluminum oxide (NCA), and lithium nickel manganese cobalt oxide (NMC/NCM). NMC variants are defined by their Ni:Mn:Co ratios, for example NMC 111/333 with equal thirds and NMC 811 with an 80/10/10 split.

Compared with LFP, NMC cells typically provide higher nominal voltage and energy density. Nominal cell voltage is about 3.3 V for LFP and 3.7 V for NMC. Volumetric energy density is roughly 190–300 kWh/m³ for LFP versus about 325 kWh/m³ for NMC, while gravimetric energy density spans about 90–120 kWh/t for LFP and roughly 150-280 kWh/t across NMC variants (111/333, 622, 811). As a result, for the same size, NMC batteries offer approximately 10–70% more capacity at lower weight. Cost differences remain: in 2023, LFP averaged about $100 per kWh versus about $132 per kWh for NMC (roughly 30% higher), reflecting manufacturing complexity and the use of critical raw materials. Safety, however, favors LFP, which is more chemically stable and less prone to severe reactions under abuse.

Thermal runaway data from multiple studies (e.g., [2][3]) show lower onset temperatures for NMC cells, typically around 150–200°C, compared with about 270°C for LFP. At the module level [2], NMC modules initiated runaway near a surface temperature of approximately 370°C and propagated completely within about 390 s, whereas LFP modules initiated around 435°C and took roughly 1,850 s to fully propagate. These differences underline that battery chemistry strongly influences the fire hazard profile of BEVs. Market adoption also varies by region: in Europe, NMC dominates with roughly 95% of installed capacity, while globally NMC accounts for about 60%. OEMs deploy both chemistries (e.g., LFP by Mercedes and NMC by MAN).

2.2. System architecture

Battery technology has developed rapid in recent years and has reached all road applications. Nevertheless, the requirements on the battery technology differ significantly between passenger cars and trucks. This mainly refers to the required battery capacity to reach acceptable ranges. While the battery capacity of a common passenger car is 35 – 90 kWh, EV trucks require significantly larger batteries of 300 – 1000 kWh. In consequence, the system architecture of the applications varies. First of all, the battery of a EV passenger car commonly comprises one single battery pack, installed between the front and the rear axle. As an example the battery pack layout as well as the system layout of the AUDI etron is depicted in **Figure 3**

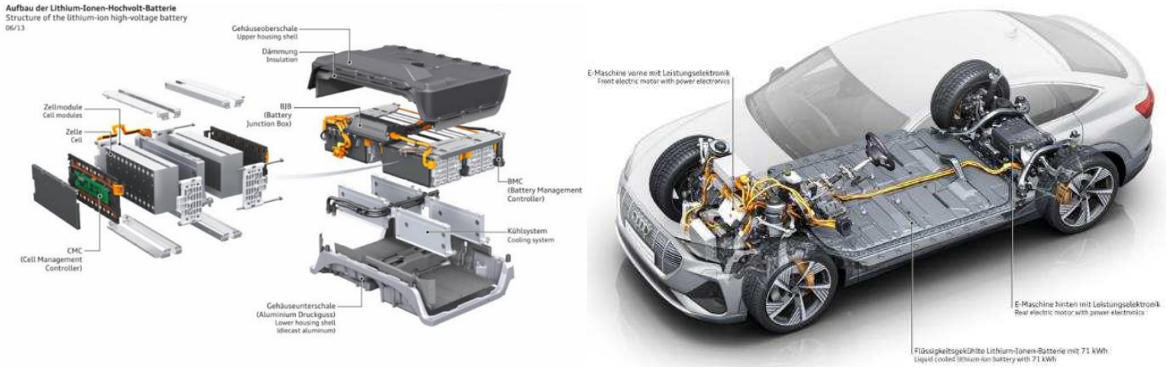


Figure 3: left – layout of a battery pack for passenger car applications,
right – system configuration of the AUDI eTron [4]

In contrast, the battery of an EV truck usually is divided in several battery packs installed at different positions. The exact layout is subject to manufacturers preferences. As an example, **Figure 4** illustrates the layout of a MAN battery pack and the arrangement of packs on an MAN eTGX truck. Battery packs of trucks are usually arranged in multiple layers. This is due to limitations in available space and to achieve highest possible battery capacity. The MAN truck depicted in **Figure 4** comprises six battery packs (either NMC 622 oder NMC 811), one situated beneath the cabin, one rear the cabin and four more packs at the location of the tanks of conventional trucks. The total battery capacity is 480 kWh.

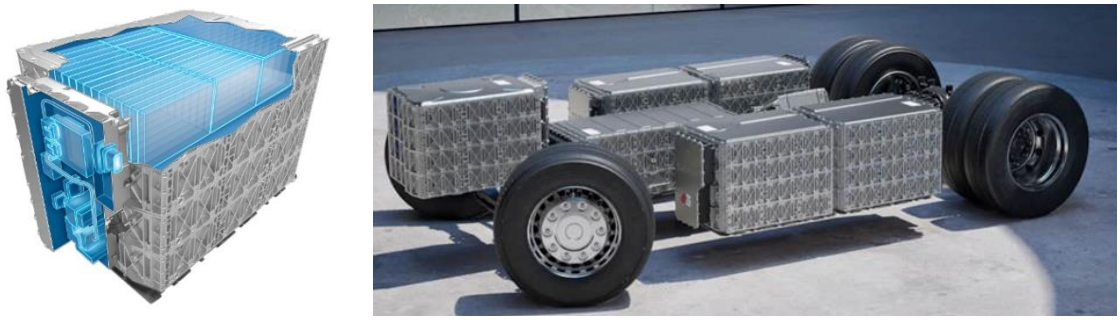


Figure 4: left – Battery pack layout, right- arrangement of battery packs on a MAN truck [5]

AS a comparison, **Figure 5** shows the EV trucks of Designwerk (member of Volvo Group) as well as the Mercedes eActros 600. Both trucks comprise three battery packs. However, the capacity of the Designwerk is 1017 kWh (NMC) and the capacity of the eActros is 621 kWh (LFP). Another difference of these vehicles is the arrangement of battery packs. While the Designwerk has its packs installed rear the cabin and laterally between the first and second axles, the eActros follows a contrary architecture by having the battery packs installed between the axles and 90° to the truck´s longitudinal axis.

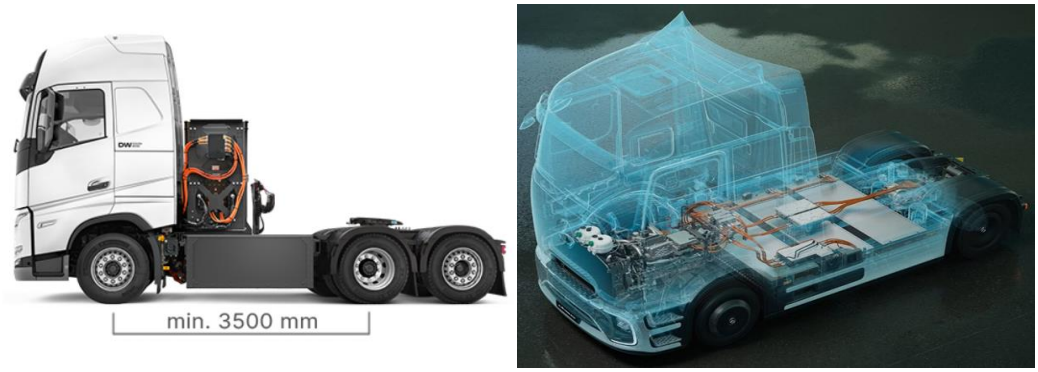


Figure 5: left – system architecture of a Designwerk truck [6],
right – system architecture Mercedes eActros 600 [7]

The presented trucks already demonstrate the variety of system configuration of EV trucks, which already suggest that different fire development can be expected for these trucks. Furthermore, large differences in system architecture make firefighting more difficult.

2.3. Hazards posed by large EVs

2.3.1. Fire dynamics

The heat release of a vehicle fire can be assessed theoretically and experimentally. Theoretical derivations (e.g., [8], [9]) are highly sensitive to assumptions about fire spread between battery modules and, for trucks in particular, about fire spread to the cargo—areas where data are scarce, making predictions uncertain. This approach is discussed in detail in Chapter 2.3. Experimental work to date has mostly focused on single battery modules or vehicles with battery capacities smaller than those of heavy-duty trucks. These tests indicate that heat release rates (HRR) of battery electric vehicles (BEVs) and conventionally powered vehicles are not fundamentally different; however, more recent programs [10][12]have reported up to 30% higher peak HRR for BEVs, a difference suspected to stem from the higher battery capacities [3].

When considering total heat release (THR), a clear correlation with battery capacity emerges. As a first-order estimate, 1 kWh is approximately 50,000 kJ of total released heat. Thus, an electric truck with a 600 kWh battery would yield roughly 30 GJ of THR, excluding any contribution from cargo. By comparison, conventional truck fire tests [11] measured total heat releases of 87 GJ, and 64 GJ in a follow-up test without the tractor. While the setups are not directly comparable, the implied contribution of the tractor unit in the conventional scenario is of a similar order of magnitude to that of an electric tractor unit (about 23 GJ versus approximately 30 GJ). These findings underscore both the dependence of HRR/THR on battery capacity and the importance of robust assumptions about fire spread when projecting outcomes for heavy-duty BEVs.

2.3.2. Toxic release

Multiple studies including [12] on combustion gases from large-scale EV fire tests, [13] on the effect of heating rate on degassing and combustion of cylindrical Li-ion cells, [14], and [15] show that BEV fires produce higher concentrations of hydrogen fluoride (HF; hydrofluoric acid in aqueous form) and elevated levels of battery-specific metals such as cobalt, nickel, and manganese when compared with internal combustion engine (ICE) vehicle fires. Special attention is required for extinguishing and cooling water, which can become a significant vector for dissolved HF and metal contamination. Despite these battery-related toxicants, carbon monoxide (CO) remains a critical hazard for tunnel users in BEV fire scenarios, similar to conventional vehicle fires.

2.3.3. Challenges in fire fighting

For practical firefighting, the vehicle's propulsion type (ICE versus BEV) is not the primary determinant of incident response strategy. Equally important are the typical timelines between incident onset and the start of effective suppression—often up to 30 minutes, depending on access and the duration of external rescue phases. By that time, thermal runaway in the battery is largely complete and the event has typically transitioned from a battery fire to a conventional vehicle fire. Nevertheless, directly introducing water into the battery can create additional hazards for responders. Correctly identifying the vehicle as an EV and knowing the battery's location and compartmentalization remain critical. Fully extinguishing a battery fire is generally not feasible, but cooling can significantly reduce reaction rates; flooding the battery with water is the most effective approach. Batteries positioned deep within the vehicle diminish the effectiveness of traditional hose streams as well as sprinkler or water-mist systems. Post-incident, the vehicle wreck and especially the battery require special handling. In Switzerland, the Federal Roads Office (ASTRA), together with Auto-Strassenhilfen-Schweiz, has issued guidelines for dealing with EV wrecks [16].

2.3.4. Resilience of tunnel infrastructure

Existing studies [14][15] do not indicate an inherently higher risk to tunnel infrastructure from battery electric vehicle (BEV) fires compared with conventional vehicle fires; however, this conclusion is based on tests with battery capacities far smaller than those of electric heavy trucks (about 80 kWh versus 600-1,000 kWh). Owing to the substances released during BEV fires, more extensive treatment of extinguishing water and more comprehensive post-incident cleaning are required, which directly affect the need for retention basins and increase the duration of tunnel downtime. Moreover, the potential impact of flames emerging in the underfloor area on cut-and-cover tunnel structures—particularly the structural stability of the central wall—and on utility ducts beneath the roadway remains an open question to be addressed by the eTruch-DACH research project.

3. DACH RESEARCH PROJECT

The DACH research track is a joint Germany–Austria–Switzerland initiative that prioritizes harmonized, practice-oriented research with direct utility for operators, regulators, and industry. Its core principles include cross-border collaboration and shared funding, standardised methods to ensure comparability and reproducibility, and scalability from laboratory to full-scale trials. It emphasizes evidence-based risk assessment, safety and resilience of critical infrastructure, and rapid knowledge transfer into guidelines and standards. The program fosters open dissemination, stakeholder involvement across academia and industry, alignment with European and international standards, and technology-neutral, sustainability-focused solutions that can be implemented consistently across the DACH region.

Originating from the DACH research call 2024, eTruckDACH represents a research project with focus on the consequences of an EV Truck fire in a road tunnel. The project´s aim is to provide detailed information about the fire characteristics and ist consequences for tunnel users and tunnel structure based on experimental data derived from full-scale testing, thereby answering a set of research questions.

3.1. Research Questions

The fire load of a truck strongly depends on the cargo, which in most cases is decisive for peak heat release rates (HRR) as well as total energy released (TER). The powertrain itself and in particular the energy carrier most likely contributes to the fire growth and fire dynamics, but is not the dominant element for HRR and TER. Obviously, the main research question in eTruckDACH is:

Are traction batteries oft rucks a gamechanger in terms of fire propagation towards the cargo?

Attached to this question, several other questions have been raised in the context of large EV fires in road tunnels:

- What can/must be considered “proper firefighting,” and how do fires involving large electric vehicles differ from fires involving electric passenger cars under various tunnel conditions?
- How can the protection of responders and the load-bearing tunnel structure be ensured during hard-to-extinguish large fires involving batteries? Which boundary conditions must be considered for potential rescue measures in fires involving large electric vehicles (ventilation fundamentals, tunnel geometry, risk of intermediate ceiling collapse, smoke spread, etc.)?
- How does battery fire propagation to potentially fire-prone cargo with high fire load occur, and which preventive measures can be taken in advance to avoid such spread (e.g., simultaneous battery cooling and prevention of spark transfer to the cargo during recovery, possible tractor/trailer separation devices)?
- How can recovery and removal of accident vehicles be ensured in confined environments (while simultaneously implementing stabilizing measures for the battery)?
- Battery fires generate toxic gases and thereby deposits (especially heavy metals) on tunnel structures. This gives rise to the following questions:
    - Which additional measures, beyond those already in place, can be provided to protect the environment from contamination?

  - By what means can fires involving large electric vehicles—or their impacts—in tunnels be fundamentally prevented/limited/combated (from adaptations to respiratory protection to the use of retention basins, etc.)?
  - What role do location (urban or rural) and/or tunnel design play in the choice of possible protection or firefighting measures?
  - Existing technical developments for passenger cars to contain battery fires include, for example, containers/cooling bags or piercing lances for water injection into the battery housing. What is the state of such measures for fires involving large electric vehicles in tunnels?
- Which factors must be considered for tunnel closures/permits for large electric vehicles? Do these differ from those for general transports and/or hazardous-materials transports with combustion-engine vehicles?

eTruckDACH aims at answering all aforementioned questions by conducting a full-scale fire test including advanced analysis methods, comprehensive risk analysis, analysis of structural impact, interviews with firefighters, etc.

4. CONCLUSIONS AND OUTLOOK

Past research activities have demonstrated that EVs do not cause a severe increase of risk in the context of road tunnel safety. However, this statement is limited to passenger cars, as for large EV applications no published solid data exist. In order to keep the safety of road tunnels on a high level, the DACH research track has initiated a dedicated research project that will provide evidence-based statements regarding the consequences for tunnel users and tunnel structure posed by a EV truck fire. The key element of this research activity is a full-scale fire test in a road tunnel environment, which aims at investigating the development of a fire starting in the batteries. The main question in that context is, if the batteries accelerate the fire propagation to the cargo, thereby causing a more rapid fire growth and reducing the available time to escape and to intervene respectively. Subsequent investigations also focus on the performance of passive fire protection solutions such as fire protection panels and mortar, the implementation of large EV fire scenarios in a road tunnel risk assessment framework, development of strategies for firefighters and transfer of results to similar infrastructures such as bridges and underpasses. By reducing the large uncertainties associated with large EV fires in tunnels, the eTruckDACH project represents a significant contribution to sustainably ensure safe road tunnels.

REFERENCES

[1] European Commission, European Alternative Fuels Observatory, 2026; https://alternative-fuels-observatory.ec.europa.eu/transport-mode/road/european-union-eu27/vehicles-and-fleet [accessed: 28.03.2026]

[2] Schöberl, J., Ank, M., Schreiber, M., Wassiliadis, N. & Lienkamp, M. (2024) Thermal runaway propagation in automotive lithium-ion batteries with NMC-811 and LFP cathodes: Safety requirements and impact on system integration. eTransportation, 19, p. 100305. doi: 10.1016/j.etran.2023.100305.

[3] Fößleitner, P. (2024) Challenges of alternative fuel vehicles and their impact on safety in road tunnels. PhD Thesis. Graz: University of Technology Graz. doi: 10.3217/mk26s-s1544.

[4] Audi AG (2018), *Audi e-tron drivetrain and battery system (technical illustration)*. Available at: https://www.audi-mediacenter.com (Accessed: 29 March 2026).

[5] MAN Truck and Bus SE; Der neue MAN eTGX: Der eTruck für die Langstrecke; Website, 2026; https://www.man.eu/at/de/lkw/alle-modelle/der-man-tgx/der-man-etgx/uebersicht.html [accessed: 29.03.2026]

[6] Designwerk Technologies AG; HIGH CAB - Der E-LKW für weite Strecken, Website, 2026; https://www.designwerk.com/elektro-lkw-high-cab/ [accessed: 29.03.2026]

[7] Daimler Truck AG, eActros600 - ProCabin , Website, 2026; https://www.mercedes-benz-trucks.com/at/de/trucks/eactros.html#layer-eactros-600-procabin [accessed: 29.03.2026]

[8] Voigt, S., Pahl, M., Lienenlüke, S., Berger, A. and Bräuer, A. S. (2023) 'An empirical model for lithium-ion battery fires for CFD applications', *Fire Safety Journal*, 135, p. 103725. doi: 10.1016/j.firesaf.2022.103725.

[9] Ingason, H., Li, Y.Z. and Lönnermark, A. (2015) Tunnel Fire Dynamics. Cham: Springer. doi:10.1007/978-1-4939-2199-7.

[10] Sturm, P. Fößleitner, P., Fruhwirt, D., Galler, R., Wenighofer, R., Heindl, S.F., Krausbar, S., Heger, O.; Fire tests with lithium-ion battery electric vehicles in road tunnels, Fire Saf. J., 134 (2022), Article 103695, 10.1016/j.firesaf.2022.103695

[11] Haack, A. (1998) Fire protection in traffic tunnels: General aspects and results of the EUREKA project. Tunnelling and Underground Space Technology, 13(4), pp. 377–381. doi: 10.1016/S0886-7798(98)00080-7

[12] Hynynen, J., Willstrand, O., Blomqvist, P. and Andersson, P. (2022), Analysis of combustion gases from large-scale electric vehicle fire tests, Fire Safety Journal, 131, 103597. https://doi.org/10.1016/j.firesaf.2022.103597

[13] Goupil, V., Gaya, C., Boisard, A. and Robert, E. (2022), Effect of the heating rate on the degassing and combustion of cylindrical Li-Ion cells, Journal of Power Sources, 523, 231030. https://doi.org/10.1016/j.jpowsour.2022.231030

[14] Sturm, P.-J., Fößleitner, P., Fruhwirt, D., Heindl, S.F., Kohl, B., Heger, O., Galler, R., Wenighofer, R. and Krausbar, S. (2021), BRAFA – Brandauswirkungen von Fahrzeugen mit alternativen Antriebssystemen: Ergebnisbericht. Graz: Technische Universität Graz, Institut für Verbrennungskraftmaschinen und Thermodynamik. https://doi.org/10.3217/8vj91-gc832

[15] Mellert, L.D., Welte, U., Tuchschmid, M., Held, M., Hermann, M., Kompatscher, M., Tesson, M. and Nachef, L. (2020), Risk minimisation of electric vehicle fires in underground traffic infrastructures. Final report AGT Project 2018/006. Zurich: Swiss Association of Road and Transport Experts (VSS)

[16] ASTRA & BTVE Working Group (2022) Guideline for the recovery, transportation, storage and disposal of vehicles with electric drive [PDF]. Bern: Bundesamt für Strassen (ASTRA). Available at: https://www.astra.admin.ch/dam/astra/de/dokumente/abteilung_strassenverkehrallgemein/btve-leitfaden-efahrzeuge-entsorgung.pdf.download.pdf/leitfaden-bergung-transport-verwahrung-entsorgung.pdf [Accessed: 29.03.2026].

MODELLING AIRBORNE BRAKE WEAR PARTICLE TRANSPORT IN SUBWAY SYSTEMS: A LINE-SCALE FRAMEWORK

Rodrigo Herrero, Carla Sánchez, Laura Rodríguez

Metro de Madrid (MdM), ES

DOI 10.3217/978-3-99161-087-8-037 (CC BY-NC 4.0)
https://creativecommons.org/licenses/by/4.0/deed.de
This CC license does not apply to third party material (attributed to other sources) and content noted otherwise.

ABSTRACT

Subway systems present specific challenges for indoor air quality and associated health risks. Stations, platforms and tunnels constitute enclosed or semi-enclosed environments characterized by complex airflow patterns. This paper proposes a one-dimensional advection–diffusion transport model to represent the evolution of pollutants generated by mechanical braking along an entire subway line (Line 1 in Metro de Madrid). The formulation incorporates source terms, deposition (sink) mechanisms, detailed station and track geometry, the real dynamics of moving trains, the configuration of ventilation shafts, and time-dependent forced-ventilation operating schedules. The model makes it possible to proportionally quantify the spatial and temporal distribution of pollutant emissions resulting from the different mass-transport mechanisms involved in this environment, and it also enables the prediction of accumulated total values under various operating conditions. This framework enables comparative evaluation of different mitigation strategies aimed at reducing the impact of particulate emissions on air quality, with particular emphasis on assessing on board retrofit filtration systems designed by Tallano technologies to reduce pollutant mechanical brake generation at the source, beyond the conventional strategies of ventilation control and cleaning programs.

Keywords:Railway Mechanical Braking, Subway Air Quality, On-board Brake Filtration

1. INTRODUCTION

Over the past two decades, the improvement of air quality has become firmly established as one of the priority pillars of public health and urban sustainability policies. The growing social awareness of the effects of atmospheric pollution, together with the accumulated scientific evidence on its respiratory, cardiovascular, and neurocognitive impacts, has driven the deployment of monitoring programs, emission reduction plans, and increasingly stringent regulatory frameworks [1]. Among regulated and emerging pollutants, particulate matter (PM) occupies a central place due to its ability to penetrate the respiratory system, its high specific surface area that promotes the adsorption of toxic compounds, its compositional heterogeneity, and its robust relationship with morbidity and premature mortality [2].

In urban environments, underground infrastructures—and particularly subway systems—present specific challenges for indoor air quality. Stations and tunnels constitute enclosed volumes where airflow patterns are governed by geometry, ventilation regimes, and the piston effect induced by train movement, as well as by interactions with the outdoor environment through entrances and air intakes. In addition to the inletting of outdoor pollutants, there is

significant internal generation associated with wheel–rail contact, mechanical braking processes, catenary–pantograph interactions, the off-service operation of auxiliary diesel vehicles, the resuspension of deposited dust driven by passenger movement and train passages [3]. As a result, PM concentrations in this environment often exceed those outdoors and exhibit pronounced space-time variations, being sensitive to station typology, tunnel geometry, ventilation modes, train frequency and speed, and cleaning protocols [4 - 6].

This context requires the development of quantitative tools capable of describing and predicting particle dispersion, to support the optimization of ventilation, cleaning, and emission control strategies, as well as the assessment of exposure levels for passengers and employees. In the case of Metro de Madrid, due to the scale of the system, the diversity of station typologies, the variability in tunnel depth and cross-section, and the operational regimes constitute an ideal testing framework. The possibility of extrapolating insights to other stations and lines reinforces the value of a scalable and replicable approach, with potential for technological transfer to other urban networks. Given the diversity of emission sources, each characterized by its own specific generation mechanism, it is of particular interest to analyse the emissions associated with rolling-stock circulation, and specifically those linked to the operation of mechanical braking systems that complement regenerative braking in railway environments.

During peak hours, the high train density and the continuous acceleration–braking cycles resulting from short inter-station distances enhance the effectiveness of regenerative braking. However, the geometric constraints associated with platform stopping points require the final approach to stations to be supplemented with mechanical braking. Conversely, during off-peak hours, the available windows for energy exchange between trains are reduced, leading to increased reliance on mechanical braking systems. Emissions generated by mechanical braking processes consist primarily of Fe as the major component, along with trace metals characteristic of railway wear, such as Mn, Cu, Zn, Sb, Mg and Si, as well as significant fractions of elemental carbon and organic carbon [7]. Source apportionment studies based on single-particle analysis using SEM-EDX and on mass balance approaches indicate that wear particles associated with the braking system can account for approximately 15 to 24% of the PM10 mass in metro stations. Within this group, the emissions generated by brake pads and brake discs exhibit a particle size dependent distribution, as summarized in Table 1.

Table 1: Relative source contributions of brake-related components (pads and discs only) by particle size fraction, expressed in particle number and particle mass compared with other sources [7].

Source		Particle numbers (%)			Particle mass (%)		
		1–10µm	1 – 2.5µm	2.5 – 10µm	1–10µm	1–2.5µm	2.5 – 10µm
Brake wear	Discs	3%	2%	5%	5%	3%	6%
	Pads	21%	21%	15%	11%	19%	9%
Track -wheel		33%	23%	61%	52%	29%	62%
Wire-pantograph		1%	1%	1%	0.4%	1%	0.5%
Other external sources		39%	49%	16%	30%	45%	21%

Due to the complexity of the underlying generation process—dependent on the condition and typology of the railway braking components, especially pads, disc and wheel in case of tread units, as well as on train speed and process temperature—it is highly beneficial to rely on results obtained from dedicated test-bench experiments to quantify their magnitude as a source term.

For the development of the present study, data from pollution tests carried out on the UIC test bench of TU Graz were used, corresponding to commercial service of rolling stock operating on lines 5 and 10 of Metro de Madrid. These activities have been performed in the context of the EU-funded VERA project, which aims at developing retrofit systems for tailpipe and brake emissions from road and rail vehicles. On top of that, VERA expands to exposure studies, particularly within confined environments, such as the underground stations, and assesses the impacts on air quality and human health.

2. METHODOLOGY

Mathematical model

The present study develops a one-dimensional space-time numerical model based on the advection-diffusion equation with time-dependent source terms. The model incorporates dynamic variability in the air velocity, associated with the train's piston effect and the forced ventilation system, as well as in the intensity of emissions linked to mechanical braking [8]. This formulation makes it possible to coherently represent the transients induced by railway operation and to capture the non-stationary evolution of the concentration along the tunnel-station domain.

Simplifying assumptions

To reduce the complexity of the physical model and facilitate the numerical resolution of pollutant transport in the underground system, a series of simplifying assumptions are adopted based on typical metro operating conditions and on the spatial and temporal scales of interest [9]. The working fluid is the air contained within tunnels and stations, treated as incompressible and of constant density during the periods analyzed, managing mean velocity along each section. The flow is assumed to remain in a subcritical regime, without compressibility effects or the presence of shock waves, in accordance with the criteria established for ventilation modeling in underground transport systems [10]. It is also assumed that the pollutant is sufficiently well mixed throughout the medium (well-stirred model), because of the high Reynolds numbers and the resulting turbulence.

The mean airflow is approximated as one-dimensional and aligned with the longitudinal axis of the tunnel, neglecting lateral and vertical variations in velocity, concentration, and pressure in comparison with variations along the main flow direction. Consequently, the suspended particle concentration represents an average value over the cross-section. The thermal and pressure properties of the air are considered uniform and slowly varying, so buoyancy effects induced by thermal or density gradients are negligible at the scales analysed [11]. Emission and deposition processes are represented through equivalent source and sink terms, without explicitly resolving aerosol microphysics. The combined action of forced ventilation and the piston effect induced by train movement is incorporated through a time-dependent mean air velocity. Instantaneous mixing within each tunnel or station cross-section is assumed, ensuring that the computed concentration corresponds to the spatial average consistent with mass conservation in a one-dimensional model [9].

Governing equations

The set of equations used to model the phenomenon includes a transport equation for a scalar magnitude $u(x,t)$, which represents the average pollutant concentration $[ug/m^3]$ along the subway infrastructure described by a one-dimensional advection–diffusion equation into a domain $\Omega = \{(x,t) \in \mathbb{R}^2 : 0 \leq x \leq L,\ 0 \leq t \leq T\}$ [12] as follows:

$$\frac{\partial u(x,t)}{\partial t} + c(x)\frac{\partial u(x,t)}{\partial x} + k(x)u(x,t) - \frac{\partial}{\partial x}\left[D(x)\frac{\partial u(x,t)}{\partial x}\right] = F(x,t) \qquad (1)$$

Where $c(x)$ represents the airflow velocity averaged over each section $S(x)$; $D(x)$ corresponds to the longitudinal turbulent diffusivity; $k(x)$ represents the term accounting the deposition/resuspension mechanism of material onto/from the surface of the tunnels and stations and $F(x,t)$ is the volumetric particle source in this study associated with the generation of PM due to brake system wear of each entire train moving along the line.

To model the air flow dynamics, the conservation equations of mass and momentum for incompressible flow at high Reynolds numbers are considered, including the arrangement of ventilation shafts along the line. So Ω is divided into adjacent characteristic subdomains, representative of station sections, tunnel segments, and compensation, supply, or extraction vents:

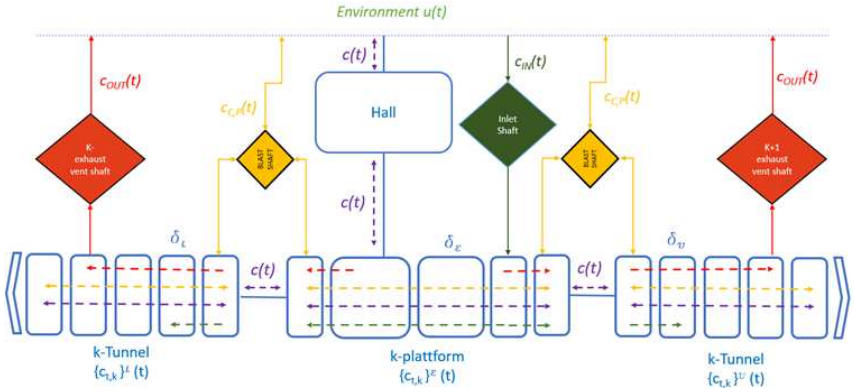


Figure 1: Schematic representation of a typical subway alignment section.

The operation of the forced-ventilation system consists of supplying fresh air through the fans installed in the shafts located at the stations and exhausting it to the outside through the fans installed in the shafts located inside the tunnels. In addition, there are compensation vents that regulate pressure imbalances and dampen the pressure waves associated with train movement.

To account for the flow induced by train motion, the velocity term $c(x)$ is transformed into a temporal coordinate, $c(t)$, train velocity $v_{train}(t)$ along the domain. By assembling these contributions for the set of s-th subdomains contained in the model, the following expression is obtained:

$$\rho\left\{\boldsymbol{\theta}\frac{\partial c(t)}{\partial t}\right\}_s = \left\{\boldsymbol{\omega}(\theta, f, g, c(t), v_{train}(t), x_{shaft})\right\}_s \quad (2)$$

Where $\boldsymbol{\theta}$ is a geometric factor that accounts for both train and infrastructure parameters—such as the train's frontal area S_t[m²], train length l[m], tunnel or station length L, and the cross-sectional area distribution $S(x)$. Its value depends on the presence (or absence) of trains within each s-th subdomain at time t. The term $\boldsymbol{\omega}$ represents the aggregated pressure-gradient contributions $\sum\Delta p_s$associated with train motion and airflow through tunnels, shafts, and stations. These contributions are determined by friction factors f, gravity g (track gradient), train velocity $v_{\text{train}}(t)$, shaft locations x_{shaft}, and the mean flow velocity $c(t)$ within each s-th subdomain.

At $t = 0$, an air-velocity field is imposed because of the operation of the forced-ventilation system, with no train motion, such that $c(x,0) = C_0(x)$, varying with the cross-section $S(x)$in each segment. Likewise, an initial pollutant distribution is assumed, $u(x,0) = h(x)$. As boundary conditions, atmospheric pressure is prescribed at the locations of each compensation vent. At the tunnel endpoints, $x = 0$ and $x = L$, the pressure gradients produced by the fans in the shafts are imposed, $\Delta p_{x\,shaft}$ and a temporal pollutant distribution is assigned at the

inlet and outlet stations, corresponding to the departure and arrival stations, respectively, such that $u(0,t) = Z_0(t)$ and $u(L,t) = Z_L(t)$. So, the strong formulation of the model is completed with this set of boundary conditions.

Numerical implementation

The implemented procedure consists of first solving the velocity $c(t)$ and pressure $p(t)$ fields from (2) using non-linear hydraulic impedance method [13] through different sub-domains by numerical approach. Once $c(t) \rightarrow c(x)$ is obtained, equation (1) is solved using an explicit finite-difference scheme on a regular spatial grid of N_x nodes and a uniform time step. Spatial derivatives are discretized using a first-order upwind scheme for the advective term and a second-order centered difference approximation for the diffusive term. The upwind formulation ensures correct physical propagation of the scalar field in the direction of the airflow and prevents non-physical oscillations, while the centered discretization of diffusion provides a balanced representation of longitudinal mixing. The time step is determined according to classical stability criteria for both advection and diffusion, satisfying the Courant–Friedrichs–Lewy (CFL) condition and the standard diffusion stability constraint to avoid numerical instability or dispersion errors due to insufficient discretization.

$$\Delta t \leq \ min\left(\frac{CFL\,\Delta x}{c_{max}}, \frac{\Delta x^2}{2\,D}, \frac{2\,D}{c^2}\right) \quad (3)$$

3. PARAMETER ESTIMATION

Deposition term $k(x)$

$k(x)$ represents the settling constant of airborne PM. This coefficient captures the combined effects of gravitational settling and residual removal processes under low-ventilation conditions. It was estimated using data from the blackout of April 28th, 2025, which temporarily halted both railway traffic and ventilation systems, while the battery-powered air-quality monitoring devices continued recording. This exceptional situation created a period with an almost complete absence of source emissions and particle resuspension, allowing PM concentrations to decay naturally over a much longer interval than the usual 4-hour service shutdown between 2 a.m. and 6 a.m. each day. The temporal evolution of PM levels was fitted using an exponential decay model, from which an effective first-order removal coefficient was derived. Measurements were obtained using calibrated monitoring devices compliant with the UNE 17660-1:2022 standard.

Diffusion term $D(x)$

$D(x)$ is the turbulent diffusivity [m^2/s] representing the longitudinal mixing induced by train movement and ventilation within the tunnel. In this study, it is treated as an effective parameter that aggregates the turbulent dispersion processed unresolved in the model. Its magnitude was selected based on values reported in experimental studies and Computational Fluid Dynamics (CFD) simulations of railway tunnels, where it typically ranges between 0.1 and 0.8 m^2/s under induced ventilation conditions [10].

Source term $F(x,t)$

To quantify the source term associated with mechanical braking processes, we used the results of the tests carried out on the UIC dynamometric test bench at the Technical University of Graz, using railway equipment supplied by Metro de Madrid, together with an innovative retrofit emission-reduction system developed by Tallano technologies, capable of suctioning and filtering a large fraction of brake-generated particles before they disperse into the railway

environment. The tests enabled the characterization of emissions as a function of parameters such as train speed and applied braking effort, for different railway braking system configurations—TBU (tread brake unit) and DBU (disc brake unit)—tested both with and without the retrofit system.



Figure 2: From Left to right, original DBU pad, modified DBU pad, modified DBU pad holder, modified TBU sole.

This experimental characterization allowed the parametrization of the source term $F(x,t)$ referred to in (1), taking into consideration the specific braking configuration of the trains operating on the modeled metro line, which consist of six-car trainsets with three motor cars and three trailer cars, equipped with DBU systems on the 12 axles of the motor cars and TBU systems on the 24 wheels of the trailer cars. For the purposes of this study, reference is made to the PM2.5 granulometry in order to compare it with measurements recorded by the monitoring equipment installed in the network.

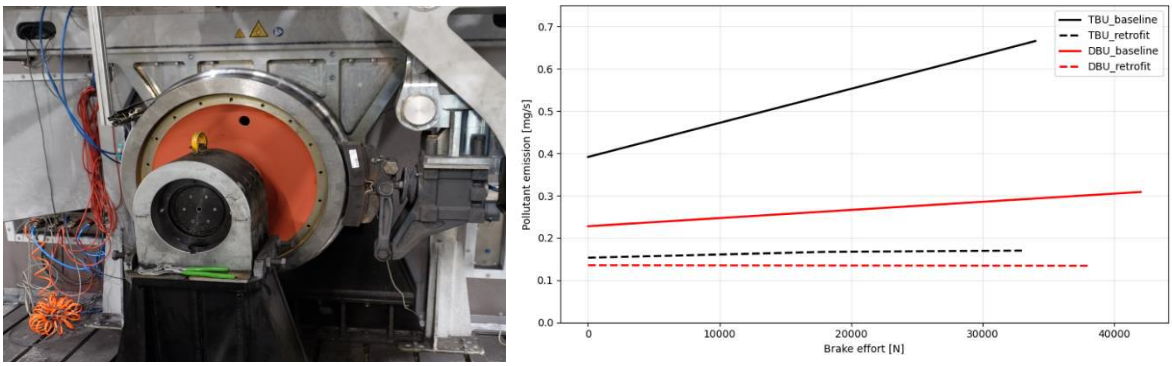


Figure 3: Arrangement of tread brake unit (TBU) on wheel rim in the test bench (left). Emission results according to the tested configurations (DBU, TBU, with/without retrofit system) (right).

4. RESULTS AND DISCUSSION

This section presents the results of the numerical simulations conducted to assess airborne, settled and exhausted to outdoor pollutant dynamics generated by brake emissions in different segments on Line 1 of Metro de Madrid.

Line 1 is the oldest line of the Madrid Metro, inaugurated in 1919, and runs between Pinar de Chamartín and Valdecarros, crossing the city diagonally from the North to the Southeast. It spans approximately 24 km/way of narrow-gauge tunnel and includes 33 stations/way. The total round-trip travel time (complete cycle on both tracks, way I and II) is 119 minutes. Line 1 crosses key central districts such as Sol, Gran Vía, and Atocha, forming a major north–

southeast axis of the city. It is one of the busiest lines in the network, carrying over 112,6 million passengers in 2025, up to 15% of the entire net. During peak hours, the line is operated with up to 38 six-car 2000 series trains (the oldest currently in operation), with headways of under 3 minutes.

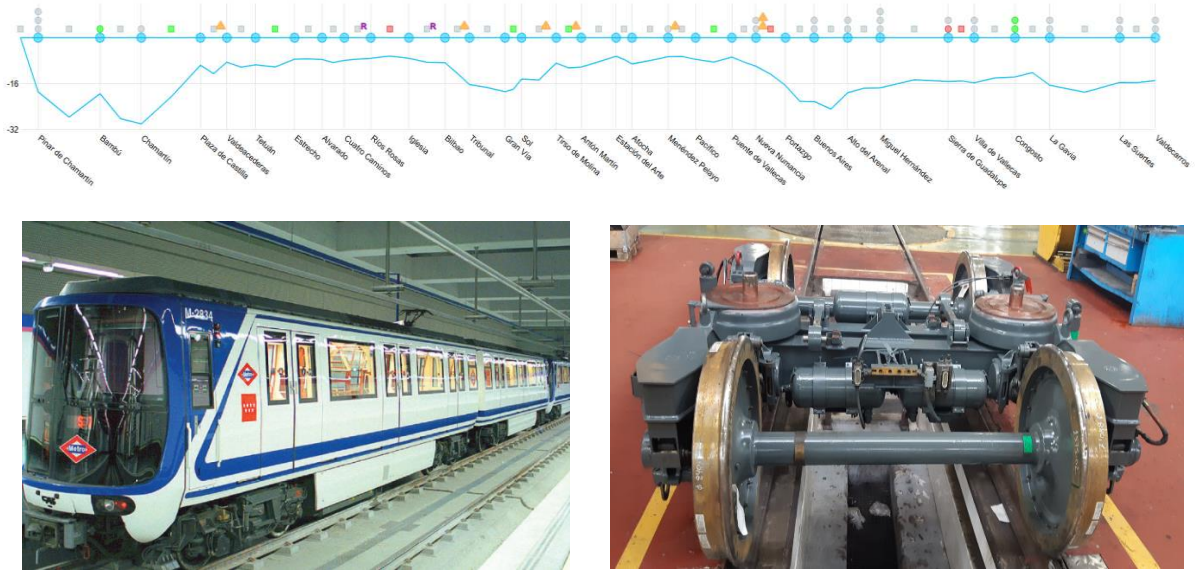


Figure 4: Track profile (upper); 2000-series operated on L1(left); bogie configuration (right).

This line is particularly relevant for the purposes of this study because the rolling stock operating on it is equipped with a mechanical braking system that combines both DBU and TBU technologies. Additionally, since half of the cars in each train consist of non-motorized trailers, the proportion of recoverable regenerative braking (75%) is lower than on other lines with more modern or more highly motorized trains (up to 85-90%). This results in a higher reliance on mechanical braking and therefore increases the significance of this line for the present analysis.

The Line 1 tunnel is equipped with pressure-compensation shafts located at both ends of each station, as well as extraction shafts equipped with axial fans in the mid-tunnel sections between stations. The layout of these shafts has been incorporated into the model to properly parametrize airflow patterns— and therefore the relevance of the convective transport terms — as well as to quantify the amount of pollutants exhausted through the ventilation shafts.

First, pollutant concentration is evaluated under four operational scenarios defined by the relative position of a second train. Figure 5 shows the resulting space–time concentration fields for the Estrecho–Alvarado segment, a short interstation characterized by high operating speeds. In the single-train reference case (Fig. 5a), the pollutant plume follows a predominantly advective pattern, with maximum concentrations occurring near the final braking zone and a progressive longitudinal spreading governed by piston-induced airflow and turbulent diffusion. When the crossing occurs at the initial platform (Fig. 5b), the departing train enhances outward transport, elongating the plume and reducing local accumulation in the upstream section. In contrast, the tunnel-crossing scenario (Fig. 5c) generates the highest concentration levels and the widest dispersion region, as the interaction between the airflow fronts induced by both trains limits immediate evacuation and promotes temporary pollutant retention within the confine domain. Finally, when the crossing takes place at final platform (Fig. 5d), the departing train from final platform partially extract the plume generated by the approaching train, resulting in lower peak accumulation.

The analysis was extended to the La Gavia–Las Suertes segment, which is characterized by a longer travel distance, Figure 6. After comparison with the shorter segment previously analyzed, it is observed that the increased distance allows advective transport to act over a larger domain, while turbulent diffusion has more time to smooth concentration gradients before reaching the final platform. As a result, the plume appears more elongated and spatially distributed, particularly in the tunnel-crossing scenario, where the interaction between the airflow fronts induced by both trains affects a wider region of the tunnel. Overall, a greater interstation length amplifies the spatial footprint of the emission event and reduces the sharp localization of peak concentrations.

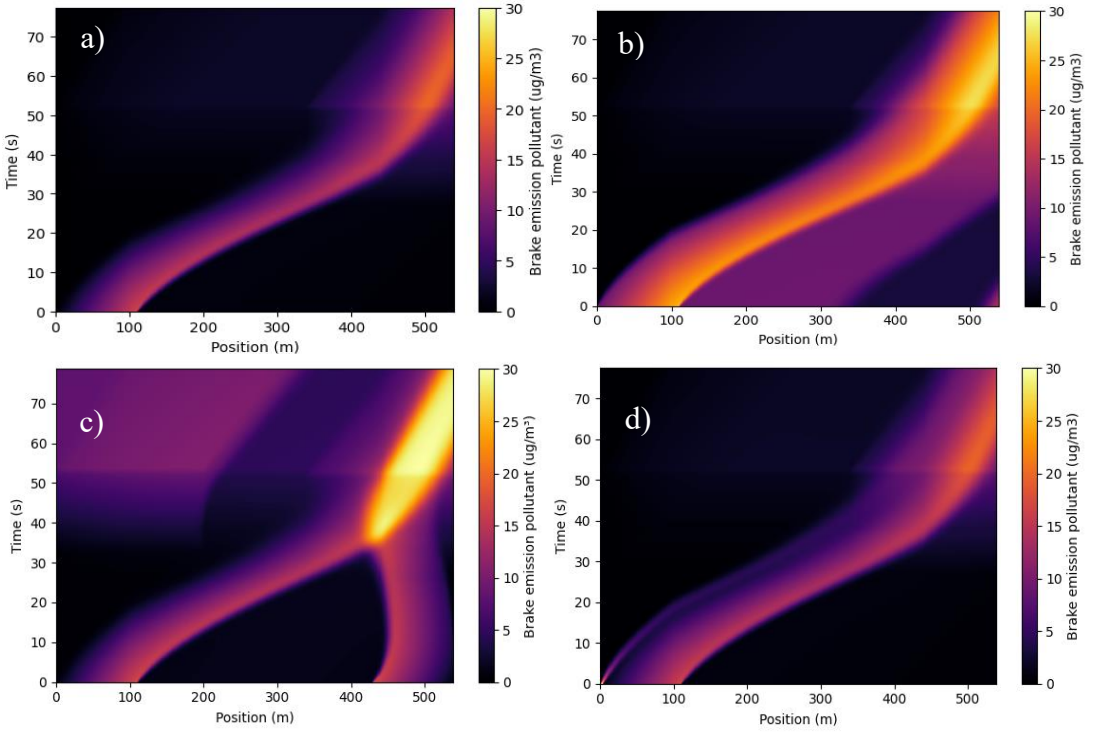


Figure 5: Spatial-temporal evolution of airborne pollutant concentration along the Estrecho–Alvarado segment (Way 1) under four operational scenarios: a) single train; b) crossing into initial platform; c) crossing inside tunnel; d) crossing final platform.

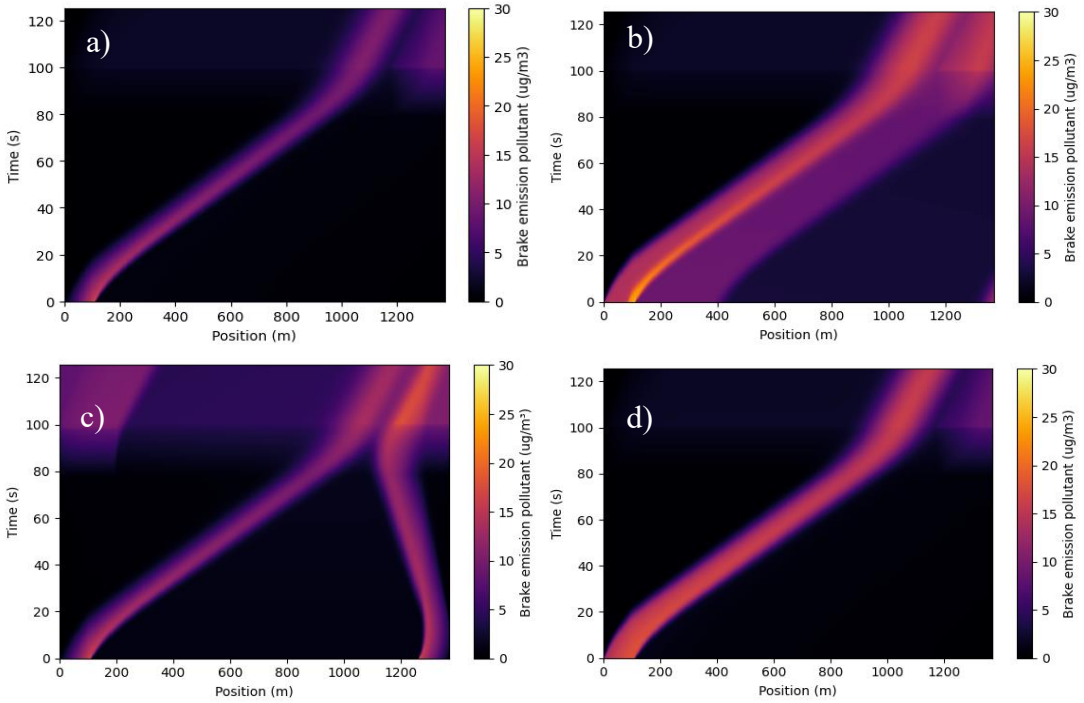


Figure 6: Spatial-temporal evolution of airborne pollutant concentration along the La Gavia -Las Suertes segment (Way 1) under four operational scenarios: a) single train; b) crossing into initial platform; c) crossing inside tunnel; d) crossing final platform.

In addition, the distribution of brake-emission pollutants accumulated over one hour of peak operation (38 trains/h) is analysed. The results quantify the fraction of emitted particles that remain airborne within the tunnel–platform domain, the fraction deposited on track and platform surfaces, and the fraction removed through ventilation.

Figures 7 show that the dominant fraction of pollutants generated by braking corresponds to particles deposited on track and platform surfaces, followed by the fraction remaining airborne, while the portion removed through ventilation is lower in both sections. The spatial distribution exhibits localized maxima that coincide with zones of higher braking demand, associated with descending gradients as well as geometric variations of the alignment. A correlation can be observed between the longitudinal gradient profile and the accumulation curves in Figure 8: segments with unfavourable slopes increase the need for pneumatic braking, thereby intensifying emissions and, consequently, the mass deposited and remaining airborne at those locations. The longitudinal redistribution of pollutants — both deposited and airborne — in the longer La Gavia–Las Suertes segment extends over a wider distance, indicating that the increased travel duration allows a more progressive dispersion of emissions.

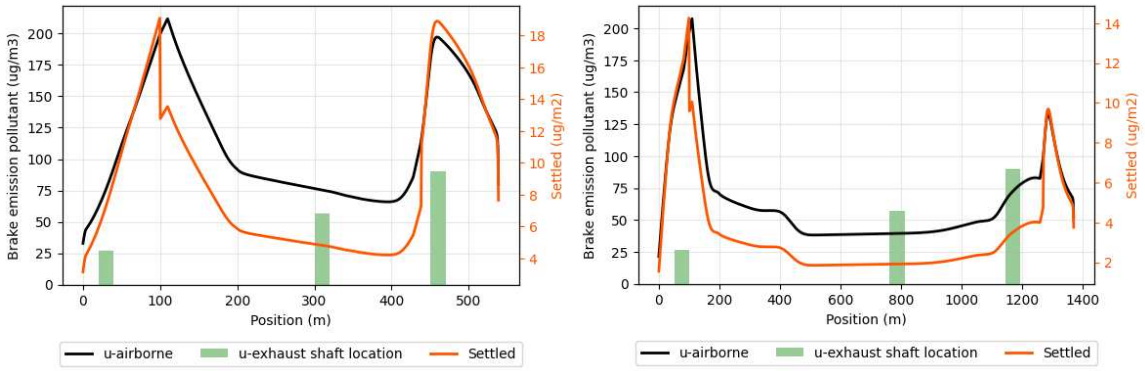


Figure 7: Airborne, settled on track–platform, outlet (exhaust) accumulated [1 h] pollutant during peak hour (38 trains interval 180 s): Estrecho–Alvarado section, Way I (left), and La Gavia -Las Suertes section, Way I (right).

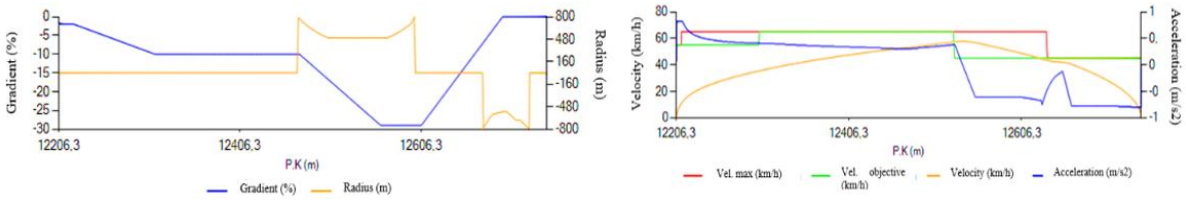


Figure 8: Example of longitudinal train dynamics profile Estrecho–Alvarado section, Way I.

To assess the impact of the retrofit system on emission dynamics, additional simulations were performed for the same segment under two configurations: conventional braking (baseline) and braking equipped with the Tallano retrofit device capable of suctioning and filtering a large fraction of brake-generated particles before they disperse into the railway environment.

The results clearly demonstrate a consistent reduction in emitted mass and peak concentrations when the Tallano retrofit system is implemented, underscoring the effectiveness of particle capture at the source and its direct impact on pollutant levels within the tunnel–platform environment (Figure 9). Overall, the net reduction approaches 70 % compared with the baseline scenario, highlighting the substantial mitigation potential of the system. These findings confirm that source-control technologies can play a decisive role in improving air quality in enclosed railway infrastructures.

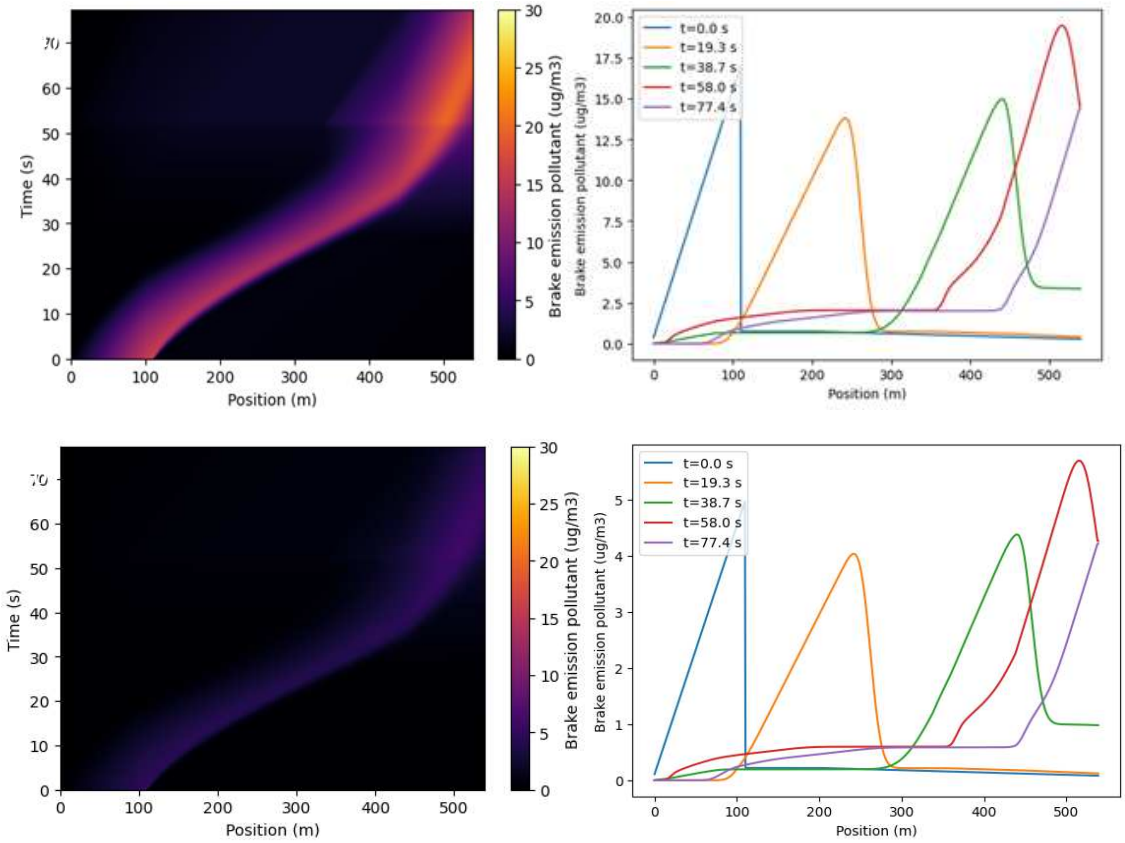


Figure 9: Spatial-temporal evolution of airborne pollutant concentration generated by brake emissions: a) Baseline and b) Retrofit system. Estrecho–Alvarado section, Way I.

Finally, Figure 10 shows the cumulative distribution of pollutants over one hour of operation for three cases: field measurements carried out using Class A air quality measurement devices at different Metro de Madrid locations (lines 8, 9 and 10), providing a realistic reference value; the model results under conventional configuration (without retrofit system); and the simulated case with the retrofit system activated. This comparison allows a direct contrast between numerical results and real data, as well as a quantitative assessment of the emission reduction associated with the implementation of the on-board filtration system. It should be noted that the measured in situ value encompasses the PM2.5 measured in the underground environment, including contributions from all potential sources (track–wheel interaction, wire–pantograph contact, external inputs, ancillary vehicles, infrastructure wear, among others). Since the developed model explicitly represents only the fraction associated with brake wear emissions (pads and discs), the experimental reference value has been proportionally adjusted according to the reported contribution of these components approximately 20% [7].



Figure 10: Comparative distribution airborne, settled on track–platform, outlet (exhaust) accumulated [1 h] pollutant during peak hour (38 trains interval 180 s).

In the case of Line 1, the trains have a higher proportion of motorized trains compared with trains running in Lines 8, 9 or 10, newer than L1 rolling stock), which implies a greater reliance on mechanical braking compared to the line where the in situ measurements were conducted. Consequently, the fraction of emissions attributable to brake wear is expected to be higher, which explains why the model results are greater than the experimentally measured values from other lines.

5. CONCLUSION

This study underscores the need for predictive tools capable of characterizing $PM_{2.5}$ dynamics generated by mechanical braking at the scale of an entire subway line under real operating conditions. The proposed one-dimensional transient framework integrates infrastructure geometry, ventilation shaft configuration, and can be parametrized for different forced-ventilation schedules, train intervals, and train dynamics within a simple yet physically consistent and computationally efficient formulation. This approach enables the representation of non-stationary pollutant transport and deposition processes in complex underground environments.

Comparison with measurement campaigns conducted at multiple locations along Metro de Madrid shows that the model reproduces the correct order of magnitude and captures the relevant spatiotemporal patterns, reinforcing its validity as a predictive tool despite the simplifying assumptions adopted. This experimental validation strengthens the robustness of the parametrization strategy and supports the physical coherence of the proposed formulation.

Beyond the evaluation of specific operational scenarios, the main contribution of this model lies in providing a scalable methodological platform for emissions assessment and for the evaluation of mitigation strategies—such as optimized velocity profiles that reduce pneumatic braking, enhanced cleaning protocols, improved ventilation schedules or the integration of onboard systems for emissions capture and filtration, such as the system tested and analyzed in this paper—at a network level. The model directly addresses a current need in the environmental management of metropolitan transit systems and establishes a foundation for further refinement, additional validation for other particle size fractions, and integration with exposure and health-impact assessment studies.

ACKNOWLEDGEMENT

This work has been funded by the VERA project, which has received funding from the European Union's Horizon Europe research and innovation program under grant agreement No. 101056893.

6. REFERENCES

[1] Smith, J. D., Barratt, B. M., Fuller, G. W., Kelly, F. J., Loxham, M., Nicolosi, E., Priestman, M., Tremper, A. H., Green, D. C. "PM2.5 on the London Underground." Environment International, 134, 105188 (2020).

[2] Moreno, T., Pérez, N., Reche, C., Martins, V., de Miguel, E., Capdevila, M., et al. "Subway platform air quality: assessing the influences of tunnel ventilation, train piston effect and station design." Science of the Total Environment, 511, 711–722 (2014).

[3] Wang, X. (Richard), Gao, H. O. "Exposure to fine particle mass and number concentrations in urban transportation environments of New York City." Atmospheric Environment, 45(5), 1202–1211 (2011).

[4] Moreno, T., Pérez, N., Reche, C., Martins, V., de Miguel, E., Capdevila, M., et al. “Subway platform air quality: assessing the influences of tunnel ventilation, train piston effect and station design.” Science of the Total Environment, 511, 711–722 (2014).

[5] Nieuwenhuijsen, M. J., Gómez-Perales, J. E., Colvile, R. N. “Levels of particulate air pollution, its elemental composition, determinants and health effects in metro systems.” Science of the Total Environment, 377(1), 394–406 (2007).

[6] Querol, X., Moreno, T., Karanasiou, A., Reche, C., Alastuey, A., Viana, M., et al. “Variability of levels and composition of PM10 and PM2.5 in the Barcelona metro system.” Atmospheric Chemistry and Physics, 12, 5055–5076 (2012).

[7] VERA Project – Metro de Madrid. Technical Report 2025. Metro de Madrid, Madrid (2025).

[8] Zhang, X., et al. "Indoor air particulate matter concentration forecast for subway station platforms using a deep learning framework." Building and Environment, 2024.

[9] Gómez Giraldo, A., Álvarez-Villa, O.D., Monsalve, G., Vélez, J.I., & Blessent, D. (2017). Simulación del transporte de contaminantes en un medio subterráneo heterogéneo mediante el rastreo aleatorio de partículas. Aqua-LAC, 9(2), 15–32.

[10] Xu, X., Zhou, Y., Sun, H., Duan, X., & Wu, Y. (2010). A Model for Dispersion of Contaminants in the Subway. Tunnelling and Underground Space Technology, 2010.

[11] Fernández Gómez, C. (2004). Modelos matemáticos aplicables a los impactos ambientales. Consejería de Medio Ambiente, Región de Murcia.

[12] Coke, L. R., Sanchez, J. G., & Policastro, A. J. (2000). A model for the dispersion of contaminants in the subway environment (ANL/DIS/CP-101582). Argonne National Laboratory. U.S. Department of Energy. https://www.osti.gov/servlets/purl/755859

[13] Sajben, M. (1971). Fluid Mechanics of Train-Tunnel Svstems in Unsteady Motion. AIAA Journal, 9(8), 1538-1545

[14] HAWE Hydraulics, “Impedance Z,” 2024. https://www.hawe.com/es-es/fluid-lexicon/impedance-z/

FROM MOTION TO UNDERSTANDING: HOW DEEP LEARNING ENHANCES AUTOMATIC INCIDENT DETECTION

Emmanuel MARCHAND, Maciej SEKULA, Christophe COLOMBEL

Citilog, FR

DOI 10.3217/978-3-99161-087-8-038 (CC BY-SA 4.0)
https://creativecommons.org/licenses/by/4.0/deed.de
This CC license does not apply to third party material (attributed to other sources) and content noted otherwise.

ABSTRACT

Automatic Incident Detection (AID) through video analytics is a cornerstone of modern traffic management. Historically, AID systems relied on pixel-based algorithms, detecting incidents by analysing changes in pixel intensity and movement over time. While foundational, these traditional methods often struggle with environmental noise and static scenes, leading to missed incidents and high false alarm frequencies.

This presentation by Citilog explores the paradigm shift brought by Deep Learning (DL) in AID. Unlike pixel-based methods that track abstract motion, DL models are trained for true object recognition and scene understanding. We will demonstrate how this transition fundamentally improves detection quality – simultaneously increasing true detection rates and drastically decreasing false alarms – through three key examples:

- **Stopped Vehicle Detection:** Traditional pixel-based systems frequently trigger false alarms from moving shadows or sudden lighting changes. Deep Learning accurately distinguishes between a cast shadow and an actual stationary vehicle, ensuring high reliability.

- **Pedestrian Detection:** Legacy analytics typically require tracking a small group of pixels over a long trajectory to confidently identify a pedestrian. In contrast, Deep Learning can recognize a human form instantly within a single frame, enabling much faster and more accurate detection.

- **Smoke Detection:** Pixel-based methods are largely limited to detecting a general loss of visibility by comparing the current scene against historical reference images. This requires time to establish a baseline and often cannot confirm if the visibility drop is actually smoke. Deep Learning, however, can instantly recognize the unique visual structure and patterns of smoke within a single frame, resulting in significantly faster and more precise alerts.

Deep Learning participates to define a new standard for AID accuracy, paving the way for safer, more efficient, and highly responsive road networks.

1. INTRODUCTION – THE EVOLUTION OF VIDEO ANALYTICS

For decades, Automatic Incident Detection (AID) has served as the critical "eyes" of Traffic Control Centres. However, those eyes have traditionally been limited by their reliance on **pixel-based background subtraction**. This method functions by establishing a "background" image and identifying moving objects as "foreground" based on changes in pixel intensity and contrast. While revolutionary at its inception, pixel-based analytics are fundamentally reactive: they detect *change*, but they do not *understand* the context of that change.

The inherent weakness of pixel-based systems lies in their extreme sensitivity to environmental noise. In complex infrastructures like tunnels or high-traffic corridors, variables such as shifting shadows, headlight reflections, and swaying equipment all trigger pixel changes that the system misinterprets as incidents. This leads to "false alarm fatigue," where the sheer volume of nuisance alerts can cause operators to miss real emergencies.

The Deep Learning Shift

Citilog's transition to Deep Learning (DL) represents a move from simple motion detection to **Advanced Computer Vision**. Instead of calculating pixel differentials, DL models (Convolutional Neural Networks) are trained on thousands of annotated images to recognize the "features" of objects—the specific geometry of a vehicle, the silhouette of a pedestrian, or the unique texture of smoke. This paper explores how this shift from tracking movement to identifying objects has delivered a significant improvement in detection quality, simultaneously increasing safety and operational efficiency across three critical use cases.

2. CASE STUDY 1 – STOPPED VEHICLE DETECTION

Stopped Vehicle Detection is the most frequent requirement for AID, yet it is where pixel-based systems are most prone to error due to the dynamic lighting environments of modern tunnels.

The Challenge: Luminance Adaptation and "Ghost" Incidents

Tunnels are quite stable environments; but the interior lighting is constantly adapted to match outdoor ambient light levels to ensure driver safety. As the sun moves, banks of lights are turned on, off, or dimmed in stages. To a pixel-based system, these **intensity variations** or **outdoor light entering the tunnel** are indistinguishable from physical movement. When a light bank dims, the algorithm interprets the sudden darkening as a large, stationary object. Furthermore, these lighting shifts create "new" shadows from infrastructure. Because the pixel-based logic only sees a change against a stored reference, these daily luminance adjustments may trigger "ghost" alarms, forcing operators to manually verify many non-events.

The Deep Learning Advantage

By utilizing Deep Learning, new algorithms perform **True Object Classification**. The system identifies a vehicle based on its structural features—wheels, windshields, and body contours—rather than just detecting a change in light and dark pixel clusters.

- **Feature-Based Recognition:** A shadow created by a lighting transition lacks a chassis or a roofline; the DL model ignores it as environmental noise.
- **Operational Efficiency:** This ensures that operators only receive alerts for actual physical hazards, neutralizing the impact of daily lighting cycles.



Figure 1: Stopped vehicle in a tunnel, Source: *Citilog CT-IM-AID_Functions_specifications-RevL.pdf*

Stopped vehicle	Detection rate	False alarm (FA) frequency
Pixel-based analytics	Indoor > 97 %; Outdoor > 95 %	Indoor: < 0,2 FA/camera/day Outdoor: < **1 FA/camera/day**
Deep Learning	Indoor > 99 %; Outdoor > 97 %	Indoor: < 0.02–0.1 FA/cam/day; Outdoor: < **0.1–0.25 FA/cam/day**

Sources: audits done for a tunnel for Service Public de Wallonie, Citilog CT-IM-AID_Functions_specifications-RevL.pdf

3. CASE STUDY 2 – PEDESTRIAN DETECTION

Detecting a pedestrian on a highway or in a tunnel is a high-stakes task where speed of detection is as critical as accuracy.

The Limitation of Trajectories

Pixel-based analytics struggle with pedestrians because a human being represents a very small number of pixels compared to a vehicle. To avoid false alarms from birds or debris, traditional systems usually require a **"validation trajectory."** The system must track the movement of those pixels over a significant distance and time (often several seconds) to confirm the "blob" moves like a human. In a fast-moving traffic environment, these lost seconds are a safety risk.

The Deep Learning Advantage

Deep Learning enables **Instantaneous Detection**. Because the model has been trained on the human form (the "skeleton" and posture), it can identify a pedestrian from a single frame.

- **Speed:** Detection occurs the moment a person enters the field of view, even if they are standing still or only partially visible behind a barrier.
- **Reliability:** By recognizing the object itself rather than its path, the system is far less likely to be fooled by non-human movement.



Figure 2: Pedestrian detected when entering the FoV, Source: www.citilog.com

Pedestrian detection	Detection rate	False alarm (FA) frequency
Pixel-based analytics	97% Only on **sidewalks**	< 0,1 FA/camera/day
Deep Learning	99% On **any traffic lane or sidewalk**	< 0,05 FA/camera/day

Sources: Citilog CT-IM-AID_Functions_specifications-RevL.pdf, indoor

4. CASE STUDY 3 – SMOKE DETECTION

Smoke detection is perhaps the most technically demanding AID task due to the semi-transparent, non-rigid, and shifting nature of the "object."

The Problem with View Obstruction

Traditional smoke detection relies on **Visibility Analysis**, comparing the live feed against a "historical reference image." This method assumes that any significant "loss of detail" or "graying" of the image is smoke. A major flaw occurs when a **large vehicle, such as a truck, stops directly in front of the camera**. The truck's flat side "hides" the background details of the tunnel. The pixel-based system sees that the reference (the tunnel wall or road) has disappeared and incorrectly triggers a "Loss of Visibility" or "Smoke" alarm, despite there being no fire.

The Deep Learning Advantage

Deep Learning treats smoke as a **distinct visual texture and pattern** rather than a mere lack of visibility. It looks for the characteristic turbulent flow and opacity gradients unique to smoke.

- **Contextual Intelligence:** When a large truck stops and covers the Field of View, the DL model identifies the object as a "Truck." It understands that the background is obstructed by a solid object, not obscured by an airborne particulate.
- **No Reference Required:** Because the model recognizes smoke "on sight," it does not need a historical baseline. It can detect smoke the second it appears, even if the camera has just been turned on.

- **Superior Accuracy:** By differentiating between a solid obstruction (a truck) and a fluid one (smoke), Citilog provides a much higher level of confidence for fire response teams



Figure 3: Smoke in a tunnel, Source: www.citilog.com

Smoke detection	Detection rate	False alarm (FA) frequency
Pixel-based analytics	95% Any type of loss of visibility, not specific	< 0,1 FA/camera/day
Deep Learning	95% Specific for **smoke**	< 0,05 FA/camera/day

Sources: Citilog CT-IM-AID_Functions_specifications-RevL.pdf, indoor

5. CONCLUSION – A NEW STANDARD FOR ROAD SAFETY

The transition from pixel-based analytics to Deep Learning is a fundamental re-engineering of how we monitor road safety. By moving from **Motion to Understanding**, using Deep Learning has addressed the two greatest pain points of traffic control centre operators: the "missed event" and the "nuisance alarm."

Summary of Improvements:

- **Reliable stopped vehicle detection:** The system is no longer fooled by necessary daily **luminance adaptations** or "ghost" shadows created by tunnel lighting cycles.
- **Instantaneous Pedestrian Alerts:** Detection is based on **visual form** rather than movement trajectories, allowing for immediate intervention.
- **Intelligent Smoke Detection:** The system distinguishes between **physical obstructions** (like a stopped truck) and actual smoke, ensuring fire alarms are only triggered by true threats.

As Deep Learning models continue to evolve and edge computing power increases, the gap between traditional analytics and DL-based systems will only widen. This technology represents a significant step forward, ensuring that traffic managers can move away from managing software filters and back to their primary mission: responding to incidents and saving lives in a complex, ever-changing environment.

INFLUENCE OF THE TUNNEL CROSS-SECTION ON TUNNEL AERODYNAMICS

Verena Langner, Andreas Huber, Johannes Rodler

Gruner GmbH Wien, AT

DOI 10.3217/978-3-99161-087-8-039 (CC BY-NC 4.0)
https://creativecommons.org/licenses/by/4.0/deed.de
This CC license does not apply to third party material (attributed to other sources) and content noted otherwise.

ABSTRACT

In addition to technical aspects, financial considerations also play a role in the planning of a railway tunnel. Since the tunnel shell accounts for a significant portion of the construction costs, efforts are made to keep the excavated volume as small as possible. This often results in very small tunnel cross-sections, which, in combination with high train speeds, lead to pressure changes with high amplitudes. The loads caused by the pressure changes generally represent the design reference for the load limit of trains and the components installed in railway tunnels. It has been shown that some of the cost savings in shell construction are offset by increased expenditure on tunnel equipment. In addition, small cross-sections can cause the problem of a so-called “sonic boom”, which can only be solved by additional construction work.

This article aims to highlight the connection between tunnel cross-sections and the associated aerodynamic aspects and to raise awareness of the importance of careful coordination of construction planning with regard to these aspects.

Keywords: rail tunnel, high-speed train, pressure wave, tunnel cross-section, aerodynamic burden, sonic boom

1. INTRODUCTION

When a train enters a tunnel at high speeds it induces static and dynamic pressures inside the tunnel. They affect tunnel equipment, as well as the train body. Furthermore, static pressure has effect on passenger comfort inside the train and can even cause medical injuries.

Train induced pressures are highly reliant on the tunnel cross-section. Besides geological and hydrological aspects the choice of the tunnel cross-section has significant influence on the construction costs. Hence tunnels are usually planned as small as possible with respect to the required clearance gauge and other requirements like dewatering. Aerodynamic considerations play a minor role in the planning phase of tunnel tubes. This can come back to haunt you later.

This paper aims to highlight the influence of the tunnel cross-section on various aerodynamic aspects and the associated problems. The following aerodynamic aspects are strongly depending on the tunnel cross-section:

- 10 kPa Health Criterion [1][2][4][5]
- Aerodynamic loads on tunnel structures and train body
- Pressure Comfort
- Aerodynamic Drag
- Sonic Boom

2. FUNDAMENTALS

When a train passes through a tunnel, pressure waves at nearly the speed of sound are propagated in the tunnel. Due to the superposition of waves, the pressure amplitude increases, leading to high loads on tunnel equipment and rolling stock. Besides this, the size and the direction of the impact forces change very quickly.

2.1. Static Pressure

Static pressure inside the tunnel is not directional and has impact on airtight structures like tunnel doors and the train which's coaches are sealed. Pressure transiently changes along the tunnel due to the train induced pressure wave. These fast pressure changes are overlayed by static pressure changes caused by train movement inside the tunnel. Free, non-airtight installations like traffic signs are not affected by the static pressure. Static pressure changes also can be recognised by the human ear which can be uncomfortable (pressure comfort) or even health affecting when the pressure variations are too high within a short time. **Figure 1** shows the characteristic train induced pressure wave measured near the entry portal.

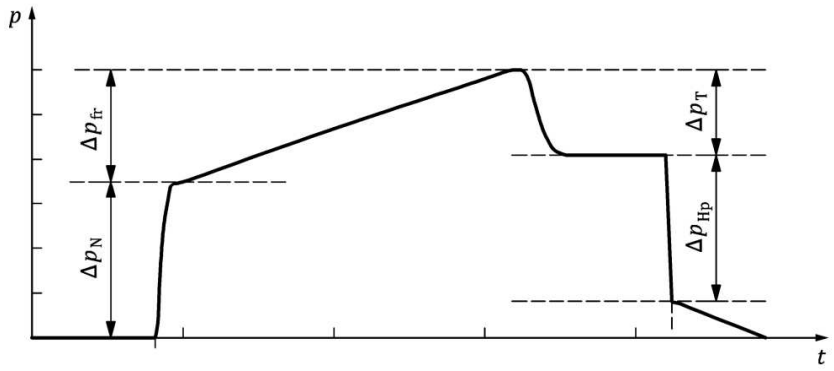


Figure 1: Pressure Wave induced by train entry (EN14067-5)

Δp_N pressure rise due to trains nose entry
Δp_{fr} pressure rise due to wall friction
Δp_T pressure drop due to entry of the trains tail
Δp_{HP} pressure drop due to train nose passing the fixed measurement position

This pressure wave travels through the tunnel at the speed of sound and is reflected by the portals. Hence pressure waves can superimpose especially in double track tunnels.

2.2. Dynamic Pressure

Dynamic pressure is directional and affects non-airtight tunnel installations (traffic signs, cables, signalling systems, etc.) that are exposed to the air currents caused by the train. The air flow in the direction of travel is caused by the piston effect, and the wake directly behind the train can exert high forces on the tunnel installations with multiple load changes.

2.3. Influencing Factors

Static as well as dynamic pressure inside rail tunnels depend on several influencing factors:

- Tunnel geometry (cross-section, length, area changes, niches, shafts etc.),
- Train geometry (cross-section, length),
- Tunnel and train wall friction,
- Train nose and tail shape.

However, the most important factor influencing the pressure level in tunnels is the blockage ratio:

$$\frac{A_{Train}}{A_{Tunnel}}$$

3. NORMATIVE TEXT AND GUIDELINES

This section lists normative texts and guidelines that deal with tunnel cross-sections and their aerodynamic aspects. Since aerodynamic aspects depend on both the railway infrastructure and the rolling stock, there are usually restrictions on the pressure inside a tunnel or inside a train rather than a minimum cross-sectional size.

3.1. TSI LOC&PAS / TSI Infrastructure:

The European Commission has passed technical specifications for the interoperability (TSI) in the trans-European high-speed and the conventional railway system and has published them in the respective gazettes of the European communities.

The TSI LOK&PAS and EN14067-5 provide reference scenarios given in Table 1. Those requirements must be met by trains to be TSI conform. The given tunnel cross-sections are not the minimum of acceptable cross-sections but gives a rough hint for the design of it.

The relevant aerodynamic properties of rolling stock are determined based on 1:1-tests and compared with the directives of TSI. The tests serve as basis for the approval and authorisation of trains and tunnels. Since 1:1-measuring of every train/tunnel combination is not possible, calculation results with validated calculation models are accepted too.

The two reference scenarios can be used to calibrate a train for 1D simulations to estimate the pressure loads inside a tunnel with a different cross-section. The reference trains lead to conservative pressure loads inside the tunnel. Modern highspeed trains usually have better aerodynamic characteristic.

Table 1: Reference cases according to TSI LOC&PAS and EN14067-5

	Reference Case		Requirements		
	V_{tr}	A_{tu}	Δp_N	$\Delta p_N+\Delta p_{Fr}$	$\Delta p_N+\Delta p_{FR}+\Delta p_T$
< 250 km/h	200 km/h	53.6 m²	≤ 1750 Pa	≤ 3000 Pa	≤ 3700 Pa
≥ 250 km/h	250 km/h	63.0 m²	≤ 1600 Pa	≤ 3000 Pa	≤ 4100 Pa

Figure 2 shows the calculated pressure wave induced by a TSI train which exactly fits the limitations shown in Table 1 (1D simulation by Gruner).

The verification is based on 1:1 -tests carried out at the reference speed or a higher speed in a tunnel with a cross-section that is as close as possible to the reference case. The transfer to the reference requirement must then be carried out using verified simulation software.

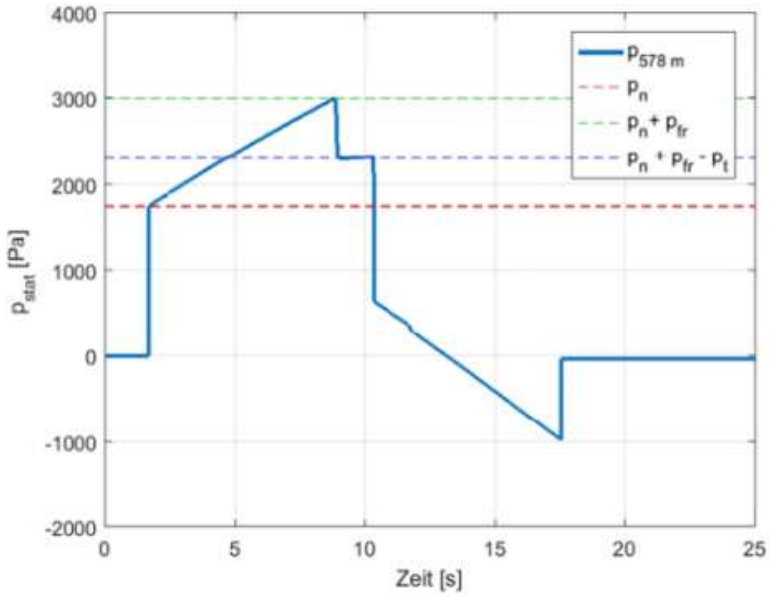


Figure 2: Reference Scenario (v_{train} < 250 km/h)

3.2. German Railway (DB)

The German Railway Service demands the following tunnel cross-sections for newly built tunnels shorter than 11 km (**Table 2**). Longer tunnels with more complex properties like air shafts, adjacent train stations or additional aerodynamically connected bores need further investigation.

Table 2: Tunnel cross-sections according to DB RIL 853 ([4])

	V_{tr}	No. Tracks	A_{tu}
High-Speed Trains	230 – 300 km/h	1	≥ 69.7 m²
	230 – 300 km/h	2	≥ 92.0 m²
Express Trains	160 – 230 km/h	1	≥ 53.7 m²
	160 – 230 km/h	2	≥ 79.2 m²

Figure 3 shows maximum pressure loads in German rail tunnels. In all cases the requirements regarding static pressure loads must be met.

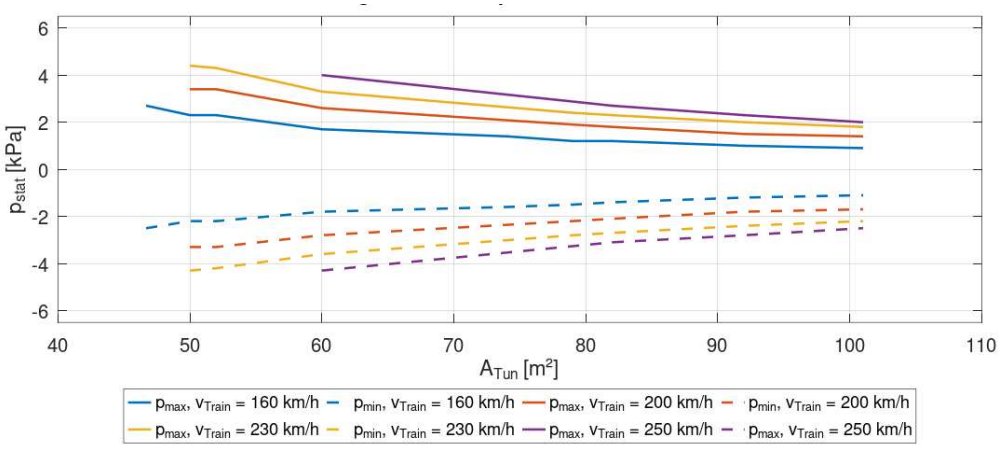


Figure 3: RIL853, Frequent pressure loads (single track)

3.3. Austrian Railway (ÖBB)

The ÖBB's actual standard cross-section for single track tunnels amounts to 54.2 m² [8]. This guideline is relatively new. Tunnels in Austria that are currently in the equipment phase, or have recently been put into operation, have smaller tunnel cross-sections. (e.g. Granitztaltunnel, Koralmtunnel, Semmering base tunnel).

4. ASSESSMENT

4.1. Static Pressure

The static pressure inside rail tunnels can be predicted by 1D simulations. For already existing tunnels pressure can be obtained by full-scale measurement.

In 2016, Gruner conducted parametric 1D simulation studies on static pressure caused by trains in tunnels. The TSI reference train (**Table 1**) was applied to simulation cases in which the parameters of train speed, tunnel cross-section, and tunnel length were varied. Pressure maxima and minima were calculated (see **Figure 4**). The figures can be used to estimate the expected static pressures as a function of the tunnel cross-section. In a further study [6], a general formula was derived with which a known characteristic pressure (e.g., maximum pressure) can be transferred to another cross-section.

Equation 1: $$\pm p_{char,tun} = p_{char,ref} * \left(\frac{A_{ref}}{A_{tun}}\right)^{\frac{3}{2}} [kN/m^2]$$

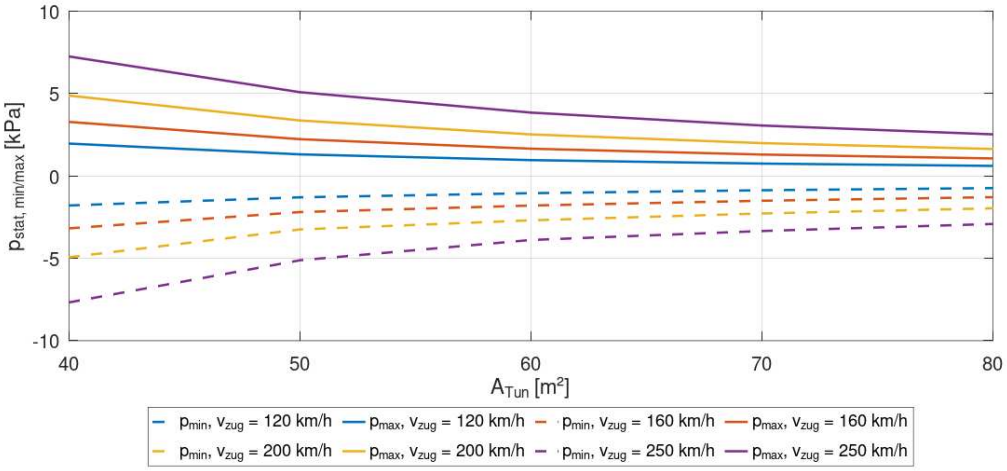


Figure 4: Static Pressure, Solo passages in long single-track tunnels

4.2. Dynamic Pressure

Dynamic pressure loads can be assessed according to RIL 853 [4]. First a dimensionless velocity is calculated using the formula below. For TSI conform tracks 0.05 must be added. Only tunnel cross-sections ranging from 32 to 101 m² are considered.

Equation 2: $$u^* = \frac{41}{A_{tun}} + 0.05 \text{ [-]}$$

Once u* is calculated the dynamic pressure loads can be calculated.

Equation 3: $$\pm q_{std} = \pm 0.04726 * u^{*2} * v_{train}^2 \text{ [Pa]}$$

The forces on tunnel equipment induced by dynamic pressure can be calculated as follows:

Equation 4: $$\pm F_{std} = \pm q_{std} * A_{comp} * c_{f,comp} \text{ [N]}$$

Figure 5 shows the dynamic pressure over different tunnel cross-sections.

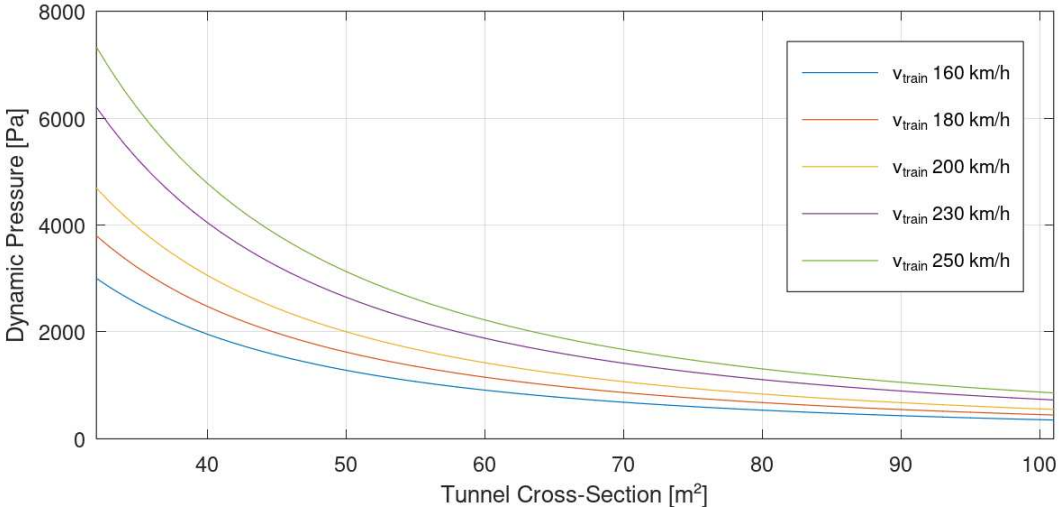


Figure 5: Characteristic dynamic pressure

5. SUBJECTS TO CONSIDER AND LIMITATIONS

5.1. The 10 kPa Criterion ("Infrastructure Reference Case")

The 10 kPa criterion refers to static pressure inside the tunnel as described in chapter 2.1. The pressure variations in tunnels during a passage of trains with a maximum speed equal or more than 200 km/h must not exceed 10 kPa. This limitation can be found in almost every normative text and guideline related to aerodynamical aspects of trains in tunnels ([1][2][3][4][5]). EN14067-5 defines the 10 kPa criterion as the maximum peak to peak pressure measured outside a train during a tunnel passage. It is a limitation for tunnel design. It can be assessed by 1D simulations using the reference train at maximum design speed described in chapter 3.1 inside the tunnel of interest. For single track tunnels a single train passage is sufficient. In doubletrack tunnels the superposition of pressure waves must be considered by variation of train entry times.

5.2. Pressure comfort

Pressure comfort refers to the pressure change per time unit inside a train passing a tunnel. It depends on the static pressure the train is exposed to and the quality of the train sealing which has a damping effect when outside pressure is transferred to the trains inside. The better the train sealing (commonly assessed using a Tau value in seconds), the more comfortable the pressure variations inside the train which the passengers are exposed to.

The Tau value is a measure for the relationship between external pressure p_e and the internal pressure p_i of a passenger coach or locomotive. The transient internal pressure can be calculated as follows:

Equation 5: $$\frac{dp_i}{dt} = \frac{1}{\tau_{dyn}}[p_e(t) - p_i(t)] \text{ [Pa/s]}$$

As train bodies are not perfectly stiff the formula can be extended by the variable k_T (usually between 0.05 and 0.1), a measure for the stiffness of the train structure. Neglecting this parameter would lead to an overestimation of the Tau value. The extended formula is

Equation 6:
$$\frac{dp_i}{dt} = \frac{k_r}{1+k_r} * \frac{dp_e(t)}{dt} + \frac{1}{\tau_{dyn}*(1+k_r)}[p_e(t) - p_i(t)]$$

Pressure comfort must be considered for all tunnels longer than 50 m [1]. It's up to the provider of the infrastructure to build tunnels in which pressure comfort can be achieved with a common pressure sealing (τ_{dyn} = 4 - 20 s). The train manufacturer must provide adequate sealing of their trains.

The ÖNORM EN 14067-5 recommends following pressure changes inside trains during tunnel passages:

Non-sealed trains (τ_{dyn} < 0.5 s)

- Double Track Tunnels: 4500 Pa within 4 seconds (critical train encounter)
- Single Track Tunnels: 3000 Pa within 4 seconds

Sealed Trains (τ_{dyn} > 0.5 s)

- 1000 Pa within 1 seconds
- 1600 Pa within 4 seconds
- 2000 Pa within 10 seconds

The values can be considered during tunnel design but aren't generally binding because the inside pressure is highly dependent on the trains using the infrastructure.

5.3. Sonic Boom

The pressure wave, which is generated when a train enters a tunnel, travels through the tunnel at the speed of sound. Most of the pressure wave is reflected into the tunnel at the exit portal. A small portion escapes at the exit portal as a micro pressure wave, which is radiated into the surrounding area. This micro pressure wave is perceived as a portal bang (sonic boom), which can have a negative impact on the immediate vicinity of the exit portal. The intensity of this phenomenon depends on the gradient of the pressure wave at the exit portal. The development of a sonic boom can be divided into 3 stages:

Entry wave

As described in chapter 2.1 the train induces a pressure wave to the tunnel. The highest temporal gradient is usually induced by nose entry (dp_N/dt, **Figure 6**).

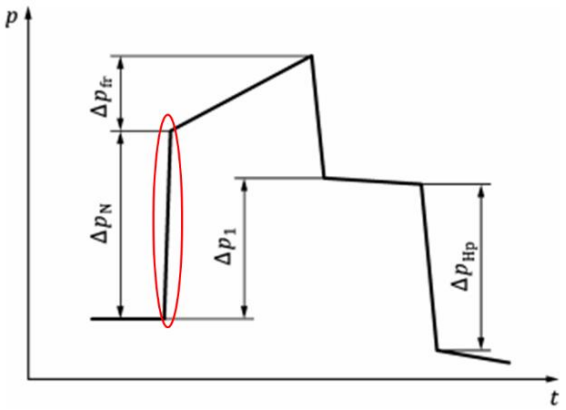


Figure 6: Entry Wave

While the gradient depends on the time the train nose needs to enter the tunnel, the magnitude Δp_N is influenced by following parameters:

- Blockage ratio (train cross-section / tunnel cross-section)
- Train speed (high speeds reduce the entry time)
- Nose length (long noses portals enhance the entry time)
- Portal shape (slanted portals enhance the entry time)

Friction has neglectable influence at this stage.

Wave steepening along the tunnel

When the pressure wave travels through the tunnel its gradient may steepen up. This is due to spatial pressure differences before and after the wave leading to differences of sonic speed. This means in some cases the pressure gradient rises along the tunnel.

Wall friction and other damping tunnel structures like shafts, niches or cross-passages reduce the amplitude of the pressure wave. **Figure 7** schematically shows the pressure wave's steepening as well as the reduction of its amplitude.

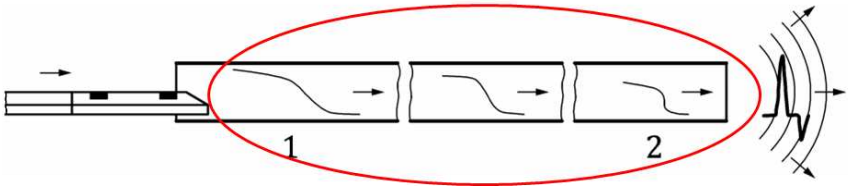


Figure 7: Pressure wave evolution along a tunnel [1] and MPW emission

Figure 8 shows the pressure gradient near the exit portal depending on the gradient near the entry portal for different tunnel lengths. The pressure gradient at the exit portal rises exponentially with gradient of the initial wave. The longer the tunnel, the more time the gradient has steepened up.

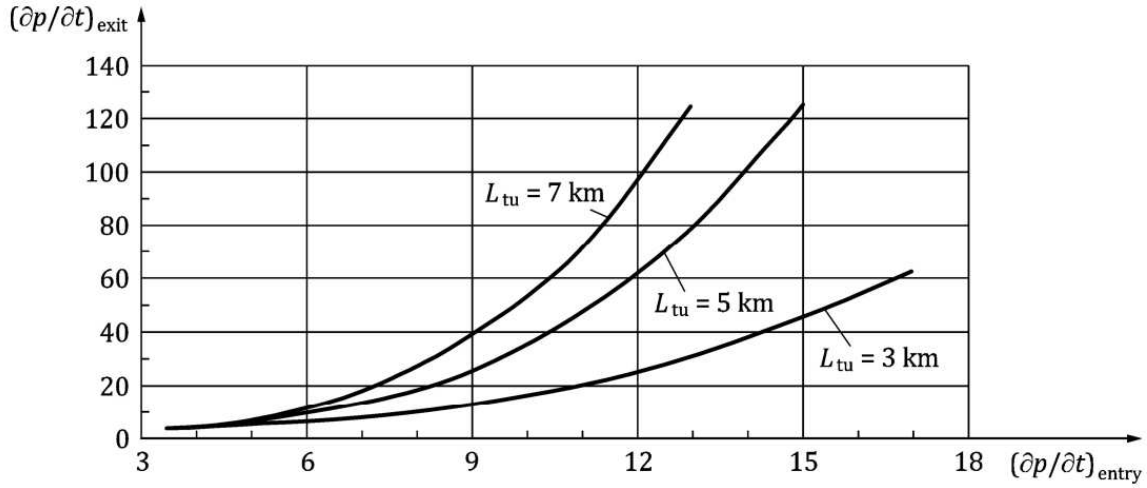


Figure 8: Wave steepening ([1])

The following factors are influencing steepening of the pressure wave:

- High blockage ratio increases the steepening effect.
- Slab tracks give advantage to a sonic boom, because they lack the damping effect of ballasted tracks (no sonic boom was reported in ballasted track tunnels).
- Wall friction and tunnel geometry (cross – passages, niches, shafts).

Micro Pressure Wave Emission

The emitted micro pressure wave (MPW) is directly proportional to the pressure gradient inside the tunnel near the exit portal. For simple portals, the MPW can be roughly estimated using Equation 7. Besides the term $(dp/dt)_{exit}$ the magnitude of the MPW depends on the tunnel cross-section (A_{tu}), the distance between the portal and the measurement position (r) and a factor **Ω** which is the spatial angle the MPW can be emitted (usually between 2 and 4). The variable c is the speed of sound.

Equation 7: $\Delta p(r,t) = \frac{2A_{tun}}{\Omega cr} * (\frac{dp}{dt})_{exit}$ [Pa]

Mitigation

As described above tunnel cross-section effects the sonic boom in two ways:

- The initial pressure gradient is higher due to higher pressure magnitudes and
- the wave's steepening effect is increased at small tunnel cross-sections.

An efficient way to mitigate sonic boom is to build a portal hood with a larger cross-section than the tunnel cross-section (Figure 10). This reduces the entry gradient. A popular example for a portal hood is the Katzenbergtunnel in Germany.

Influencing factors are:

- Hood cross-section / tunnel cross-section ratio (typically 1.5-2),
- Hood length
- Openings (area, amount, position), cf. **Figure 9**,
- Portal shape.

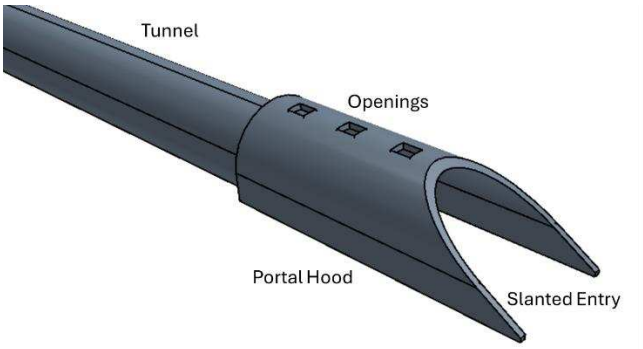


Figure 9: Portal Hood (illustriative)

Efficient portals lead to a reduction of the entry gradient of up to 50%. The performance can be assessed in advance by 3D-CFD simulation.

5.4. Aerodynamic Drag

A train is exposed to higher aerodynamic drag in a tunnel than on open track. Consequently, the train consumes more energy when passing a tunnel. The aerodynamic drag depends, besides other factors, on the tunnel cross-section as well as the tunnel length.

A common way to describe the aerodynamic drag in tunnels is the tunnel factor which is the ratio between the aerodynamic drag inside the tunnel and the open track. Typical values for the tunnel factor are between 1.0 (short tunnel, large cross-section) and 2.0 (long tunnel, small cross-section). The longer the train, the higher the tunnel factor.

6. SUMMARY AND CONCLUSION

Small tunnel cross-sections combined with high train speeds lead to pressure changes with high amplitudes. The stresses caused by these pressure changes are usually the design reference for the load limit of trains and the components installed in railway tunnels. In addition, small cross-sections can cause the problem of a so-called “sonic boom.” The mechanisms that lead to the formation of high-pressure amplitudes in tunnels were presented and the associated aerodynamic aspects were identified.

The sonic boom is a phenomenon that is often underestimated in this context. The description of the parameters influencing the supersonic boom shows that predicting it is anything but easy.

7. REFERENCES

[1] ÖNORM EN 14067-5, 2022-04-01, "Bahnanwendungen — Aerodynamik Teil 5: Anforderungen und Prüfverfahren für Aerodynamik im Tunne1

[2] TSI INFRA, VERORDNUNG (EU) Nr. 1299/2014 DER KOMMISSION vom 18. November 2014 über die technische Spezifikation für die Interoperabilität des Teilsystems „Infrastruktur“ des Eisenbahnsystems in der Europäischen Union

[3] TSI LOC&PAS, VERORDNUNG (EU) Nr. 1302/2014 DER KOMMISSION vom 18. November 2014 über eine technische Spezifikation für die Interoperabilität des Teilsystems „Fahrzeuge — Lokomotiven und Personenwagen“ des Eisenbahnsystems in der Europäischen Union

[4] Richtlinie 853, Deutsche Bahn, Eisenbahntunnel planen, bauen und instandhalten

[5] UIC 799-11, 2005 (deprecated)

[6] Dynamische Analyse des Anregungs- und Reaktionsverhaltens von Lärmschutzwänden und Tunneltüren bei Bahninfrastrukturprojekten, Dipl.-Ing. Dr.techn. Michael Reiterer, REVOTEC zt gmbh, Wien, 2016

[7] Michael Reiterer, Janez Schellander; AUFSATZ; Aerodynamische Belastungen auf bahntechnischen, Einbauten in schnell befahrenen Eisenbahntunneln, BATE 7/2022, AUFSATZ: 202100097

[8] ÖBB Regelwerk ÖBB 10.01.02.01 "Bautechnik"

[9] U.S. Department of Transportation, Federal Railroad Administration, "Aerodynamic Assessment and Mitigation – Design Considerations for High-Speed Rail"

Zitrón
NEDERLAND

SPECIALISTS IN VENTILATION SYSTEMS FOR TUNNELS AND METRO

Zitron Nederland B.V. is a leading European manufacturer of rail and road tunnel ventilation systems.
We can justifiably call ourselves tunnel ventilation system experts.



OUR EXPERTISE

- Verification of the ventilation system design
- Engineering
- Fabrication and assembly
- Full scale factory acceptance test
- Installation and commissioning
- Site acceptance tests
- Maintenance
- Fan overhaul







Zitron Nederland B.V.
Kanaalstraat 19, 7553 GP Hengelo
The Netherlands

Telephone: +31 (0)74 240 8260
www.zitron.nl
info@zitron.nl

VCA
ISO 9001:2015

Zitrón
NEDERLAND

SPEZIALISTEN FÜR LÜFTUNGSANLAGEN FÜR TUNNEL UND METRO

Zitron Nederland B.V. zählt zu den führenden Unternehmen Europas im Bereich der Lüftungssysteme für Bahn- und Straßentunnel. Das Unternehmen kann sich mit Recht als Spezialist für Tunnelbelüftung bezeichnen.



UNSERE KOMPETENZ

- Prüfung der Lüftungsauslegung
- Engineering
- Herstellung und Zusammenbau
- Werksabnahme in Großausführung
- Montage und Inbetriebnahme
- Abnahmen im Tunnel
- Wartung
- Lüftersanierung







Zitron Nederland B.V.
Kanaalstraat 19, 7553 GP Hengelo
Niederlande

Telefon: +31 (0)74 240 8260
www.zitron.nl
info@zitron.nl

VCA
ISO 9001:2015

AIR SPEEDS NEAR SERVICES ON TUNNEL WALLS

[1]Mark Gilbey, [1]Dami Ajewole, [2]David Soper, [2]Mike Jesson, [3]Ian Strudwick

[1]WSP Ltd, UK
[2]University of Birmingham, UK
[3]HS2 Ltd, UK

DOI 10.3217/978-3-99161-087-8-040 (CC BY-NC 4.0)
https://creativecommons.org/licenses/by/4.0/deed.de
This CC license does not apply to third party material (attributed to other sources) and content noted otherwise.

ABSTRACT

Tunnel services can be exposed to pressures and airflows that subject them and their supports to fatigue loads. The fatigue loads can be significant in high-speed tunnels. Pressure changes from train movements in tunnels are well covered by available modelling techniques, and for services completely immersed in the pressure these changes do not often form the design cases. Air speeds in train wakes are less well predicted by numerical modelling, specifically the range and scale of the 3-D velocity fluctuations generated by their highly turbulent nature.

This paper describes testing of moving trains in 1/25th scale tunnels. Model trains were fired at high-speed into the scale model tunnels and the tunnel air speeds near the walls measured at high frequency in three directions and at several locations. Different diameter tunnels and train designs and consists were tested. The data from the testing was interpreted using rainflow counting to estimate fatigue loads for discrete (small) items of equipment in the tunnels as well as longer elements where the wake velocity may affect the equipment in different ways.

Keywords: Air speeds, aerodynamics, scale model testing, fatigue, tunnel services.

1. INTRODUCTION

1.1. Project context

Services are required within tunnels to support operational, life safety and firefighting objectives. Services are often located on tunnel walls, which exposes them to the pressures and air speeds resulting from vehicle movement in the tunnels. The services tend to be immersed within the pressure environment meaning that a differential pressure, and thus pressure loading, does not manifest. The air speeds, however, can impact upon the services causing differential pressure loading because of the stagnation of the air on face of the element perpendicular to the flow direction. These loadings from air speeds can be frequent and fluctuating, creating a fatigue loading that must be accounted for in the design. The air speeds tend to be higher in high-speed tunnels.

In the UK a new high-speed railway (HS2) is under construction that differs from other recent high-speed railways. Firstly, the tunnels combine high line speeds with relatively small tunnel cross-section due to a decision to require more stringent train stiffness to manage interior pressure comfort rather than larger tunnels. Secondly, the train speeds will be higher than typical - there will be approximately 50 km of tunnels on the route with a typical train speed of 320 km/h (88 m/s) in the tunnels longer than 3 km and 360 km/h (100 m/s) in the shorter tunnels. Finally, high-level side walkways are used which for several reasons make the

embedment of many of the services into the walkway more difficult and hence tunnel services will be mounted onto the tunnel walls. Collectively, these factors made it important for HS2 to understand the air speeds and fatigue loads to which the tunnel services will be exposed and account for these in their design, fabrication and fixing.

1.2. The Nature of Train Induced Air speeds in Tunnels

The air movement around trains is usually referred to as the slipstream and is caused by air being dragged by the movement of a train due to friction between the train and the air [1]. Exemplar slipstream research [2][3] often presented results in a non-dimensional coefficient form, normalized by train speed for the U (along the train length), V (side to side perpendicular to the train) and W (up and down perpendicular to the train). The square root of the sum of the squares of the dimensionless U and V elements (which tend to be the dominant) is often reported as U_{res}.

Results from several studies conducted in the open air have identified specific flow regions created within the slipstream of passenger trains [4]. They include (a) an upstream and nose region characterized by an increase in flow velocity before the front of the vehicle; (b) a highly turbulent boundary layer region growing along the side of the vehicle; (c) a near wake region with a large velocity peak; and (d) a far wake region with turbulent flow with shedding vortices induced by the train (see Figure 1). Similar findings have been observed across a range of scales and techniques, from full-scale, operational trackside studies [5], to reduced scale physical modelling experiments [6] and computational fluid dynamics (CFD) simulations [7]. A detailed overview of characteristics associated with each region can be found in [1].

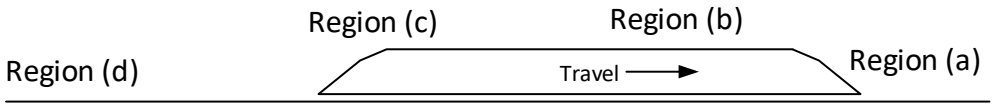


Figure 1: Wake regions

For tunnels, aerodynamic research has historically focused on the initiation and development of pressure waves and the emission of micro-pressure waves [1]. Whilst data related to slipstream flow development within tunnels is sparse, a small number of papers can be found [8][9][10]. These have observed similar flow regions to those discussed for the open air above, albeit with different aerodynamic characteristics due to confinement [10][11]. Within a tunnel key facets of the flow field include:

- Upstream – characterized by an increase in flow velocity due to a piston effect created by the solid train nose pushing air along the confined tunnel environment.
- Nose region - characterized by a sharp positive increase in flow velocity magnitude directly before the front of the vehicle, leading to a localized velocity peak. This is highly dependent on the train shape and is followed by a large reduction in flow magnitude to a negative velocity peak, caused by separation from the leading edge of the train nose and the influence of the small gap in the anulus between the train surface and tunnel wall.
- Boundary layer region – characterized by a reversal in the dominant flow direction due to an anulus flow effect created by the very confined space between the train surface and the tunnel wall. This region has highly turbulent flow with rapid changes in localized flow direction and a decreasing flow magnitude with train length.
- Tail and near wake region – characterized by further reversal in flow direction following the passage of the train tail. Here a positive peak in velocity is created by the air being dragged along behind the train within the tunnel.

- Far wake region - characterized by turbulent flow with shedding vortices induced by the train. Overall, flow magnitudes decrease in this region, and the flow again is influenced by localized pressure wave effects.

These general flow characteristics have been observed across a range of scales and techniques, from full-scale trackside studies [10], to reduced scale physical modelling experiments [11] [12] and computational fluid dynamics (CFD) simulations [8][9][13][14][15]. Further studies [10] have illustrated the influence of train type (high-speed, conventional and freight trains) on each characteristic flow region. However, to date, it has not been possible to identify any studies that appropriately consider further velocity components beyond U or U_{res}.

1.3. Motivation for Testing

HS2 originally set out their design criteria for tunnel air speeds based on published scale model tests [12]. Concept design studies and protype testing of cable management systems resulted in several fatigue failures, some of which indicated genuine areas where design improvements would be required and some of which were difficult to explain considering that similar designs had been used with success, albeit in slower tunnels, without reported issues. The data from the Gilbert tests [12] had some uncertainties regarding the downward direction W velocity components, which is important for horizontal cable ladder, and did not include a side walkway which was speculated may assist in disrupting the wake before it became impingent on the tunnel services. The data set also did not provide adequate data to evaluate the number of fatigue cycles. Additional data was therefore sought by HS2. Full-scale measurements within the somewhat similar HS1 tunnels were not possible in the required time scales and CFD modelling was considered unlikely to be able to confidently predict the wake region. Therefore, further scale modelling was undertaken.

2. SCALE MODEL SETUP

2.1. General

WSP Ltd, on behalf of HS2, and the University of Birmingham (UoB), collaborated to develop a series of requirements for tests which UoB conducted and both parties interpreted and reported on. The tests used the TRansient Aerodynamic INvestigation (TRAIN) rig which is a moving model testing facility specifically designed to examine the transient aerodynamics of vehicles [16]. Reduced scale vehicles are propelled at speeds up to 75 m/s, along three 150 m tracks. Aerodynamic flow properties around the train, acting on a train or trackside structures were measured. Moving model testing facilities are advantageous, in comparison to typical stationary wind tunnels, due to the capability of correctly simulating the relative motion between a vehicle and the ground/structures and tunnel micro-pressure waves relative to a moving train, which in turn is important for accurately modelling the characteristic development and magnitude of slipstream velocities within the tunnel environment. Moving model techniques have been thoroughly validated against full-scale experimental data in numerous studies [4][16][17] and are therefore a good route for providing a detailed understanding of the aerodynamic flow development around potential high-speed passenger trains within the confined tunnel configurations identified in this project.

A pre-tensioned elastic bungee cord system is used to accelerate reduced scale models in a 50 m firing section to a specified experiment speed. This method ensures no additional propulsion devices are needed; however, a slight reduction in model speed is observed as a result of friction and aerodynamic drag. In the open-air test section, an average deceleration of 2.5 m/s^2

has been estimated for this study. Models are brought to a stop in a 40 m braking section using a friction device.

2.2. Tunnels

Two tunnel configurations were considered for this study. At full-scale, the majority of HS2 tunnels have an internal diameter of 8.8 m, with the central axis at approximately 3.1 m above top of rail, whereas the HS1 tunnel has a 7.15 m internal diameter with the central axis approximately 2.5 m above the top of rail. Both tunnels have an escape walkway that extends approximately 0.76 m above the top of rail. The HS1 tunnel also includes a maintenance walkway that extends 0.5 m above the top or rail.

Each model tunnel was 24 m in length at model-scale, equivalent to a 600 m long tunnel at full-scale considering a 1:25 modelling scale. The remainder of the 150m test track was utilised for the acceleration section, the open route wake verification section and (after the 24m test tunnel) a braking/decceleration section. The tunnels were cast in 2.4 m long sections from glass reinforced plastic, with the escape walkways included in the tunnel section but modelled separately in medium-density fibreboard. Further modelling details, i.e. several small cable ladders as per engineering drawings of the full-scale case, were installed along the tunnel length. These cable ladders were modelled in aluminium, with the adopted design chosen to provide a representative structure with a similar blockage ratio to that of the full-scale case loaded with cables.

2.3. Trains

Representative train models and configurations were used based on models that were available from prior tests. These were (1) Alstom AGV – 5 car configuration; (2) Alstom AGV – 8 car configuration (5 car + 3 car); (3) Alstom Class 373 Eurostar – 5 car configuration; and (4) Alstom Class 373 Eurostar – 8 car configuration (5 car + 3 car). The basic dimensions at model scale are given in Table 1.

Table 1: Train Characteristics

Train Type	Number of Cars	Length (mm)	Width (mm)	Height (mm)
AGV	5	3870	118	166
AGV	8	6324	118	166
Class 373	5	4393	108	152.5
Class 373	8	7015	108	152.5

The configurations of a 5-car and 8-car train were chosen to enable modelling of the ‘V-shape’ section between joined train sets, which affects the overall flow dynamics. The train lengths were chosen as a balance based on maximum operating weights at the TRAIN rig facility, with a view to realizing high test speeds to maximize Reynolds numbers, and the need to appropriately capture aerodynamic transitions along the length of train within different flow regions, as discussed in the results.

The trains were created using a cast and mould system. Simplifications to the overall geometry through the removal of many small components were made to ensure that Reynolds number effects due to small scale train details were not created, but the overall geometry was maintained accurately. The model shells were mounted to a specially designed chassis and trailing wheel system and attached the propulsion/braking devices.

Figure 2 shows images of a typical test tunnel and two of the train models.



Typical test tunnel AGV Class 373

Figure 2: Model Features

2.4. Instrumentation

A series of Dantec triple fibre-film wire hot-wire probes were used to measure instantaneous three components of velocity in the tunnel (**Figure 3**). Similarly, a series of Turbulent Flow Instrumentation multi-hole pressure probes were used to measure instantaneous local static pressure and three components of velocity in the open-air test section.

The hot-wire probes were calibrated for each test configuration using a Dantec StreamLine Pro Automatic Calibrator, with automatic temperature compensation built into the multichannel constant temperature anemometry system. The probes were calibrated in steps across the typical range of expected velocities, for 0° and 25° flow angles to within ±0.1 m/s and ±1° for velocities. The sensors form an orthogonal system with an acceptance cone of 70.4°. To account for this acceptance cone when the train is passing the probes were mounted in two orientations: longitudinally along the tunnel facing the on-coming train (Case 1) and longitudinally along the tunnel facing away from the on-coming train (Case 2). The relative uncertainty of results based on the instrumentation accuracy, using a propagation of error approach, was found to be on average 2%. The positions of these probes are shown in Table 2.

Measurements were also made of slipstream outside of the tunnels to allow for comparison against open-air standards and measurements. For all slipstream measurements at least 20 runs were made for each measuring location and each train configuration examined, aligning with typical methodologies for slipstream measurements outlined in [20]. All instrumentation was set to record at a 5000 Hz sampling frequency.

Table 2: Probe locations

Probe Number Probe Number	HS1 test tunnel		HS2 test tunnel		Distance along tunnel (m)
	Distance from track centre (m)	Height above track (m)	Distance from track centre (m)	Height above track (m)	
1	2.40	4.26	3.80	3.85	150
2	2.90	3.26	3.80	2.85	150
3	2.40	4.26	3.80	3.85	154
4	2.90	3.26	3.80	2.85	154
5	2.40	4.26	3.80	3.85	450
6	2.90	3.26	3.80	2.85	450

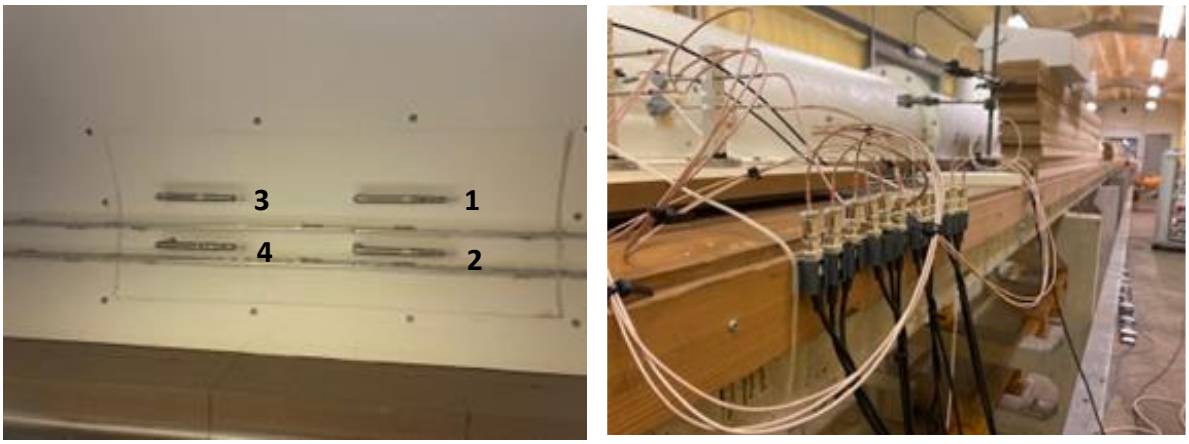


Figure 3: Sensor head inside the tunnel (left) and supports and connections outside the tunnel (right)

3. KEY RESULTS

For brevity, only key findings and results can be described. In terms of the influence of train type, the AGV train was observed to generate the greatest magnitude of air speeds, U_{res}, within the tunnels and the Class 373 the largest magnitude peak W speeds. The AGV train is physically larger than the Class 373 and thus resulted in a higher blockage ratio. In the open air, the Class 373 likely generated a more turbulent slipstream because of features around the train bogeys that were less aerodynamic than the AGV.

In terms of the influence of train configuration, the eight car trains, with the inter-car gaps, were observed to result in slightly lower peaks and troughs in air speeds, but with more velocity fluctuations caused by the expansion and contraction at the inter-car gap.

In terms of sensor locations, the lower sensors (typically Position 2) were observed to result in higher air speeds than the upper sensors. From open-air measurements it is known that the air speeds closer to the train wheels are larger than those higher up the train body and hence this is explicable. However, the differences between Position 1 and 2, for both positive and negative air speed directions were small.

The tunnel type was observed to result in a significant difference between measured air speeds. Figure 4 shows the difference between the HS1 and HS2 tunnels for the 8-car trains. The solid lines represent the average of 20 test runs. The averages have become smooth due to small offsets in peaks and troughs affecting the mean. The results are non-dimensionalized with respect to train position with 0 representing the nose passing the sensor and 1.0 representing the tail of the train passing the sensor.

The general pattern of a positive airflow in advance of the train, a rapid flow reversal as train passes the sensor, a large peak in the immediate wake of the train and then a gradual decay of the wake is observed. The wake is observed to pulse up and down which occurred because of the pressure pulses in the tunnel causing density changes as they travel up and down the tunnel and affect the wake.

The air speeds were higher in the HS1 tunnel for several reasons: (1) the HS1 tunnel was smaller and thus presented a higher blockage ratio than the HS2 tunnels; (2) the tunnel walls and thus sensors were closer to the train body in the HS1 tunnels, and hence exposed to higher air speeds; and (3) the sensors were lower in the HS1 tunnels (as is the cable management system) and thus closer to the lower portions of the trains where the train wake is generated.

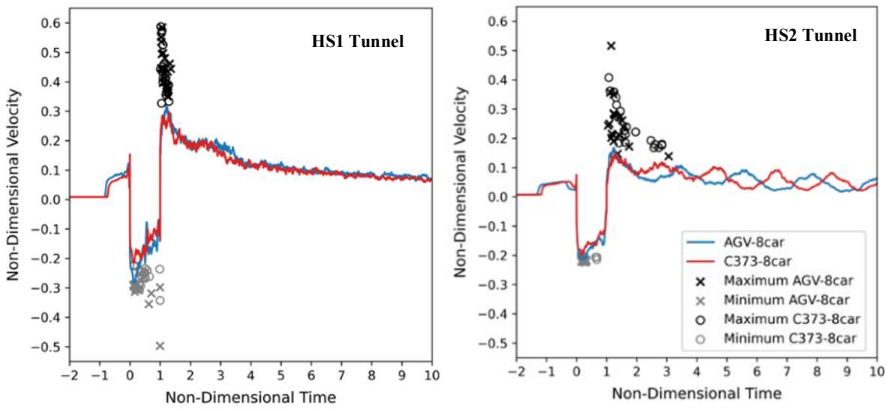


Figure 4: U_{res} (inc W component) comparison between tunnels

Figure 5 shows examples of the dimensionless U, V and W components for the AGV 8-car trains at Position 2 for the different tunnel types. The U direction air speeds are highest as they are coplanar with the wake. The U direction air speeds are important for features such as signal marker boards. The W direction components are important for features such as cable ladders, where the upwards/downwards air speeds will stagnate against the horizontal services and cause pressure differential loadings.

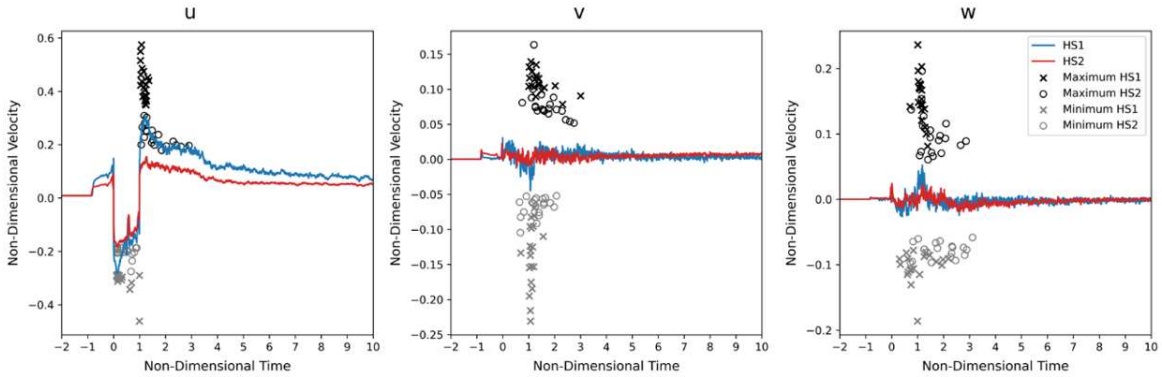


Figure 5: U, V and W dimensionless coefficients

4. FATIGUE

The maximum and minimum air speed results provided valuable information to determine the ultimate strength of the cable management systems. However, many smaller magnitude flow fluctuations were observed which may be more damaging to the systems in terms of fatigue.

A rainflow counting approach [18] was adopted to understand the fatigue loadings. The HS2 railway may ultimately operate at 20 trains per hour. Each of the 20 test runs therefore represented one equiprobable cycle of an hour of train operations. The 20 test run data were therefore conjugated to develop a single data file for one hour of train operations. The data was then passed through a rainflow counting algorithm to first extract the damaging cycles, which were then grouped into bins according to the mean value from the cycle and the range. The process was undertaken twice, once for the dimensionless coefficients and once for stagnation pressure, accounting for the train speeds that the tunnels will operate at. In this paper, for brevity, we present only the dimensionless velocity cycles. Figure 6 shows the fatigue cycles for the HS1 tunnels for the U, V and W components.

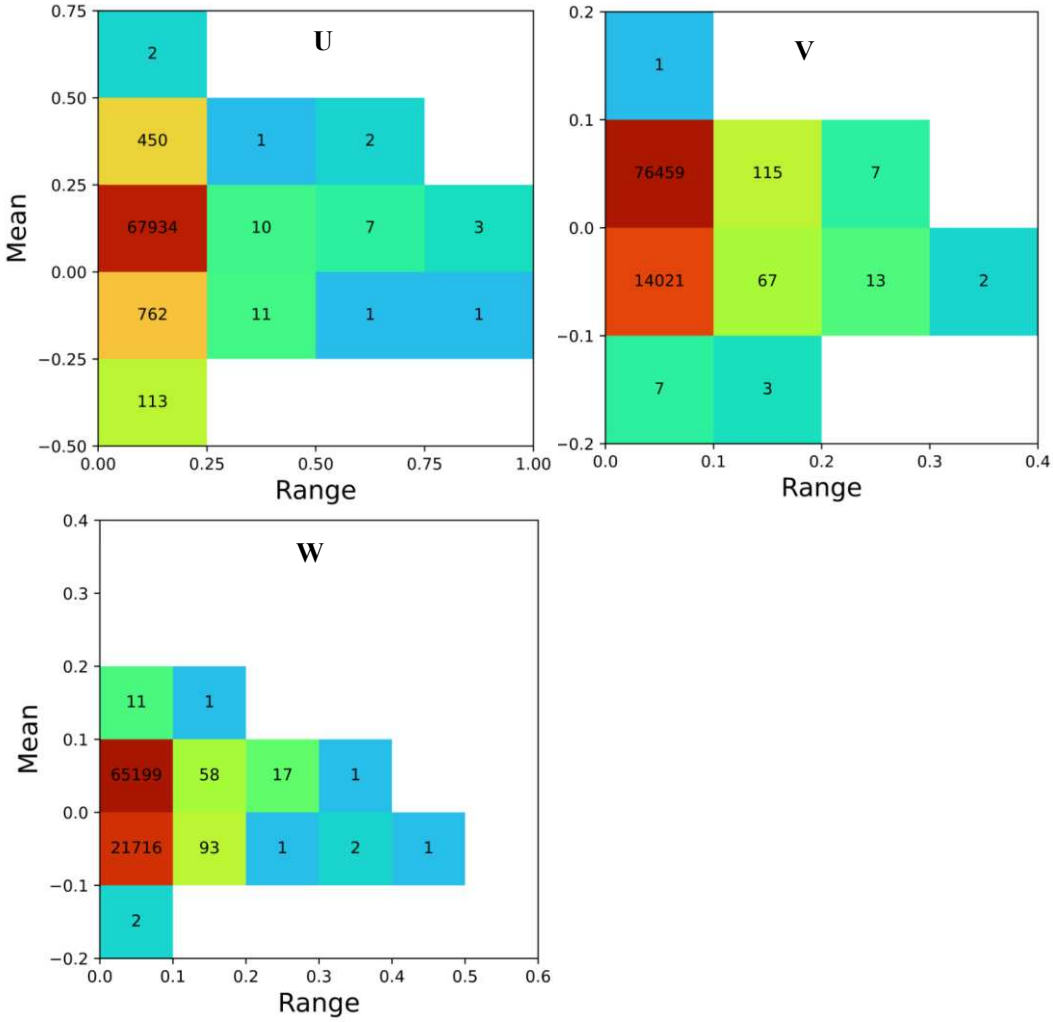


Figure 6: Fatigue cycles

The stagnation pressure calculated from the fatigue cycles can be converted into a force loading by multiplying it by a drag coefficient (typically around 2.0) and the projected area of the body perpendicular to the airflow direction. Each data bin will generate two load cases, a maximum load of the mean plus half the range and minimum of the mean minus half of the range. These two load cases can be used in a structural analysis to allow the stress range in any of the components to be predicted or measured. The stress range can then be interpreted on a material S-N diagram to determine the number of cycles that the component can tolerate before failure for each of the data bins. Based on Miner's rule [19] the damage for each data bin can be estimated by comparing the number of cycles in that range to the maximum permissible to give a damage assessment. The damage in each bin can be summated and if that sum exceeds 1.0 failure is likely.

The results indicate that there are substantially more lower magnitude cycles than higher. Given the extremely high cycle count of the smaller cycles, the component design must result in these being within the material's infinite fatigue life. The presented data relates to a discrete (small) object. Conversely, a 4m long span of cable ladder, for example, will be exposed to high-frequency fluctuations in speed due to small-scale turbulence and lower frequency fluctuations due to larger vortices. The forces due to the high-frequency fluctuations will cancel over the length of the span, resulting in a lower frequency, smoothed load compared to that experienced by a discrete object. The test data was further interpreted and smoothed using a Butterworth filter to account for this, resulting in fewer fatigue cycles for longer span objects. The peak fatigue cycles were considerably lower than originally expected and afford

the opportunity to optimize the tunnel services supports to save on both embodied carbon and costs, as well as develop and implement the design at lower risk.

5. SUMMARY AND CONCLUSION

Scale model testing has allowed for improved data and understanding of air speeds in tunnels to inform the design of tunnel services. Train speed, train to tunnel blockage ratio, proximity of the services to the train, height of the services in the tunnel, train aerodynamic characteristics and presence of an inter-car gap emerge as considerations that influence the slipstream and number of cycles within a tunnel.

The data has allowed for peak air speeds to be established, as well as interpretation of the overall pattern and nature of the wake to establish damaging fatigue cycles. Whilst the data is particularly important for high-speed tunnels due to their high train speeds, lower train-speed tunnels are normally smaller and thus have services closer to the train body. Industry would likely benefit from a series of air speed measurements being collected and published for a range of tunnel and train types.

6. REFERENCES

[1] C. Baker, T. Johnson, D. Flynn, H. Hemida, A. Quinn, D. Soper, M. Sterling. “Train aerodynamics: fundamentals and applications”. Butterworth-Heinemann, 2019.

[2] B. Schulte-Werning, C. Heine, G. Matschke, “Slipstream Development and Wake Flow Characteristics of modern High-Speed trains”, *Journal of Applied Mathmatics and Mechanics*, Volume 81, Issue 53, 2001.

[3] RAPIDE: Railway aerodynamics for passing and interactions with dynamic effects, EU project number: BE97-4089. 2001.

[4] D. Soper, M. Gallagher, C. Baker, A. Quinn,“A model-scale study to assess the influence of ground geometries on aerodynamic flow development around a train.” *Proceedings of the Institution of Mechanical Engineers*, Part F: Journal of Rail and Rapid Transit, 231(8), pp.916-933. 2017

[5] M. Sterling, C. Baker, S. Jordan, T. Johnson. “A study of the slipstreams of high-speed passenger trains and freight trains”. Proceedings of the Institution of Mechanical Engineers. Part F Journal of Rail and Rapid Transit 222 (2), 177-193. https://doi.org/10.1243/09544097JRRT133M. 2008

[6] C. Baker, S. Dalley, T. Johnson, A. Quinn, N. Wright. “The slipstream and wake of a high-speed train”. *Proceedings of the Institution of Mechanical Engineers*. Part F Journal of Rail and Rapid Transit 215 (2) 83-99. https://doi.org/10.1243/0954409011531422. 2001.

[7] M. Gallagher, J. Morden, C. Baker, D. Soper, A. Quinn, H. Hemida, M. Sterling. “Trains in crosswinds–comparison of full-scale on-train measurements, physical model tests and CFD calculations”. Journal of Wind Engineering and Industrial Aerodynamics, 175, pp.428-444. https://doi.org/10.1016/j.jweia.2018.03.002. 2018.

[8] W. Li, T. Liu, Z. Chen, Z. Guo, X. Huo. “Comparative study on the unsteady slipstream induced by a single train and two trains passing each other in a tunnel”. *Journal of Wind Engineering and Industrial Aerodynamics*, 198, p.104095. https://doi.org/10.1016/j.jweia.2020.104095. 2020.

[9] Z. Liu, D. Zhou, D. Soper, G. Chen, H. Hemida, Z. Guo, X. Li, X. "Numerical investigation of the slipstream characteristics of a maglev train in a tunnel". *Proceedings of the Institution of Mechanical Engineers*, Part F: Journal of Rail and Rapid Transit, 237(2), pp.179-192. https://doi.org/10.1177/09544097221100658. 2023

[10] S. Negri, G. Tomasini, P. Schito, D. Rocchi. "Full scale experimental tests to evaluate the train slipstream in tunnels". *Journal of Wind Engineering and Industrial Aerodynamics*, 240, p.105514. https://doi.org/10.1016/j.jweia.2023.105514S. 2023.

[11] S. Meng, D. Zhou, Z. Wang, "Moving model analysis on the transient pressure and slipstream caused by a metro train passing through a tunnel". *Plos one*, 14(9), p.e0222151. https://doi.org/10.1371/journal.pone.0222151. 2019

[12] T. Gilbert, C. Baker, A. Quinn. "Gusts caused by high-speed trains in confined spaces and tunnels". *Journal of wind engineering and industrial aerodynamics*, 121, pp.39-48. https://doi.org/10.1016/j.jweia.2013.07.015. 2013.

[13] M. Fu, P. Li, X.F. Liang. "Numerical analysis of the slipstream development around a high-speed train in a double-track tunnel". *PloS one*, 12(3), p.e0175044. https://doi.org/10.1371/journal.pone.0175044. 2017.

[14] S. Meng, X. Li, G. Chen, D. Zhou, Z. Chen, S. Krajnovic. "*Numerical simulation of slipstreams and wake flows of trains with different nose lengths passing through a tunnel".* Tunnelling and Underground Space Technology, 108, p.103701. https://doi.org/10.1016/j.tust.2020.103701. 2021.

[15] X. Xiong, R. Cong, X. Li, Y. Geng, M. Tang, S. Zhou, Y. Na, C. Jiang. *"Unsteady slipstream of a train passing through a high-speed railway tunnel with a cave".* Transportation Safety and Environment, 4(4). https://doi.org/10.1093/tse/tdac032. 2022.

[16] D. Soper, C. Baker, A. Jackson, D.R. Milne,L. Le Pen, G. Watson, W. Powrie. "Full scale measurements of train underbody flows and track forces". *Journal of Wind Engineering and Industrial Aerodynamics,* 169, pp.251-264. 2017.

[17] D. Soper, D. Flynn, C. Baker, A. Jackson, H. Hemida. "A comparative study of methods to simulate aerodynamic flow beneath a high-speed train". *Proceedings of the Institution of Mechanical Engineers,* Part F: Journal of Rail and Rapid Transit, 232(5), pp.1464-1482. 2018.

[18] ASTM. "Standard practices for cycle counting in fatigue analysis". ASTM E 1049-85. ASTM International. 2005.

[19] M. A. Miner. "Cumulative damage in fatigue". *Journal of Applied Mechanics*. 12: 149–164. 1945.

[20] British Standards (BS). Railway applications — Aerodynamics. Part 4: Requirements and assessments procedures for aerodynamics in tunnels. BS EN 14067-5:2021.

TRAIN-INDUCED AERODYNAMIC LOADS ACTING ON INSTALLATIONS OF GRANITZTAL TUNNEL

Michael Reiterer

REVOTEC, AT

DOI 10.3217/978-3-99161-087-8-041 (CC BY-NC 4.0)
https://creativecommons.org/licenses/by/4.0/deed.de
This CC license does not apply to third party material (attributed to other sources) and content noted otherwise.

ABSTRACT

In railway tunnels, highly dynamic pressure waves and flow-induced aerodynamic loads occur during train entry, passage, and exit. These loads act on all tunnel installations and must be considered in the design of the structural elements installed in tunnels. Due to the high number of daily train journeys and the associated high number of load cycles over the entire service life of the structural elements in tunnels, fatigue analyses, in addition to verifications of structural safety, are particularly important. During the planning phase, aerodynamic load assumptions were defined for the different installations in the Granitztal Tunnel, and these assumptions formed the basis for the design. The definition of these load assumptions was based on existing standards and regulations, as well as numerical simulation calculations and/or measurements of train-induced aerodynamic effects in comparable railway tunnels in Austria. During the commissioning runs of the Koralm railway line in 2025, the actual aerodynamic loads occurring during train journeys in the Granitztal Tunnel were measured and compared with the load assumptions defined for the design. This article describes and discusses the measurements carried out in the Granitztal Tunnel and the results obtained. It demonstrates that the aerodynamic load assumptions defined during the planning phase for the various tunnel installations are conservative, thus ensuring both the load-bearing capacity and fatigue resistance of the structures over their entire service life.

Keywords: aerodynamic loads, wake vortex, tunnel installations, dynamic amplification, fatigue.

1. INTRODUCTION

The dynamic loads resulting from train journeys in railway tunnels consist of pressure wave-induced and flow-induced aerodynamic loads (Figure 1) [1-3]. Pressure wave-induced loads (Figure 1a) arise immediately upon train entry and exit from the tunnel due to the sudden compression of air particles. The resulting pressure waves propagate at the speed of sound (343.2 m/s in dry air at 20°C) along the entire length of the tunnel. They alter the pressure field in the tunnel in a fraction of a second and, analogous to hydrostatic water pressure, act with the same magnitude in every direction on pressure-tight installations such as the tunnel emergency exit doors and ventilation flaps, which are tightly sealed towards the cross passages. For non-pressure-tight installations in tunnels such as signal signs, hectometer boards, suspension columns for the overhead conductor rail, ceiling power rail, and telecommunications cables, pressure compensation occurs due to the uniform impacts from all sides caused by pressure waves, resulting in no resulting stress or deformation reaction. Sudden pressure changes in the tunnel lead to shock loads on the tunnel installations, resulting in significantly greater deformation reactions compared to static loads. Therefore, a dynamic

shock factor (magnification factor) of φ_{dyn} = 1.40 must be applied when designing tunnel installations [2].

Flow-induced aerodynamic loads (Figure 1b) arise when trains pass through the tunnel due to the air displacement and vortex shedding effects [4]. In the immediate vicinity of the train traveling through the tunnel, changes in the flow field occur starting from the train's front, with the simultaneous formation of highly turbulent vortex trails at the rear of the train and in the wake behind it. The tunnel installations located near the train – regardless of whether they are pressure-tight or not – are hence subjected to sudden dynamic stresses due to the flow-induced aerodynamic loads.

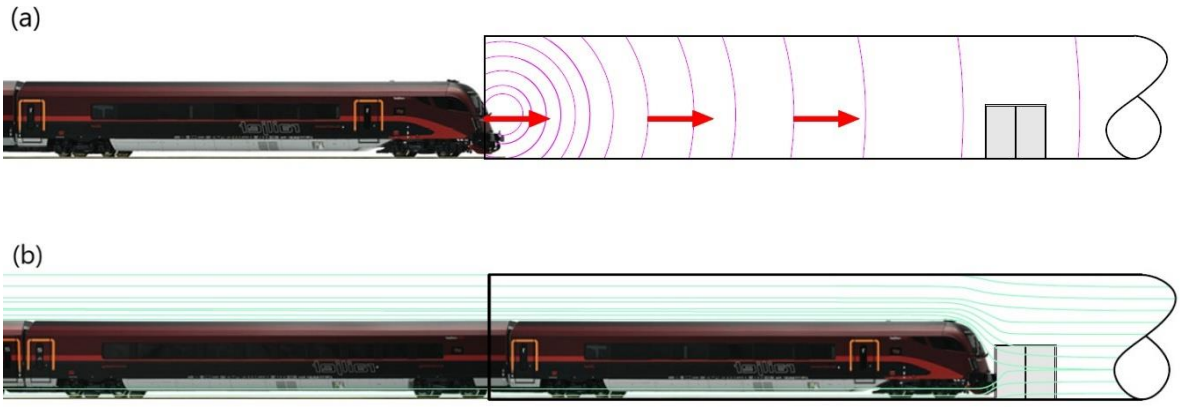


Figure 1: Pressure wave (a) and flow-induced (b) aerodynamic loads resulting from train journeys in railway tunnels

2. DESCRIPTION OF GRANITZ TUNNEL AND INSTALLED MEASUREMENT TECHNOLOGY

The Granitztal Tunnel is located at kilometer 75.812 (north portal, track 1) of the Austrian railway line 40101, west of St. Paul im Lavanttal. It is a double-tube, single-track railway tunnel with a total length of 6,106 m (Figure 2). The clear tunnel cross-section is 46 m² in the area of the ventilation center (constructed using the cut-and-cover method over a length of 606 m) and 41 m² in the remaining section (Langer Berg Tunnel and Deutsch Grutschen Tunnel). The tunnel was designed and built for a maximum train speed of 250 km/h.

To determine the actual aerodynamic loads occurring during train journeys, air pressure sensors were installed at five measurement cross-sections (MQi) in the southern tube of the tunnel (track 1, Graz direction) prior to the start of commissioning runs in February 2025 (Figure 2). Measurement cross-section MQ1 to MQ4 are located inside the tunnel tube, and for redundancy, two air pressure sensors were installed on the tunnel wall at each measurement point. Additionally, an autonomous train detection system was installed on the track at measurement point 1. This system allowed for the determination of the exact entry speeds of the trains and automated train type identification and classification, respectively. Measurement section 5 is located 25 m from the north portal of the Granitztal Tunnel, and in addition to the air pressure sensors, a sound level meter was also installed there to detect potential micropressure waves and sonic booms. This article focuses on investigating and assessing the actual magnitude of the train-induced aerodynamic loads within the tunnel, i.e., on analyzing the air pressure data recorded at measurement cross-sections 1 to 4.

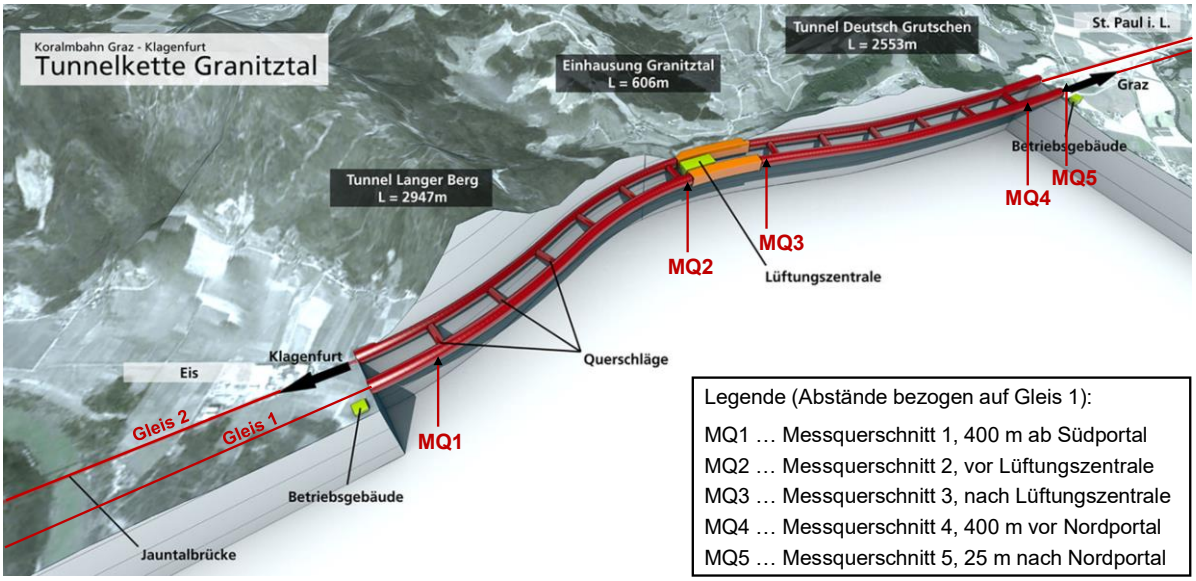


Figure 2: Twin-tube, single-track Granitztal Tunnel, measurement cross-sections MQ1 to MQ5

3. DEFINED DESIGN VALUES FOR AERODYNAMIC LOADING FOR TUNNEL INSTALLATIONS

The pressure wave and flow-induced aerodynamic loads resulting from train journeys in railway tunnels depend on the clear tunnel cross-section A_T, the train speed v_{ZUG}, the aerodynamic shape of the train, the train length, and the clearance dimension. The clearance dimension is defined as the ratio between the projected area of the train A_{ZUG} onto the vertical plane and the clear tunnel cross-sectional area A_T.

To determine the pressure wave-induced loads as a basis for the design of tunnel installations in new construction projects of ÖBB-Infrastruktur AG, extensive measurements of the actual pressure loads were carried out in 2014 in existing railway tunnels in Austria, such as the double-tube, single-track Wienerwald Tunnel. To generalize the measured pressure loads for different tunnel types (single-tube and double-tube), tunnel cross-sections, tunnel lengths, train types, and train speeds, as well as to investigate the relevant load case of "trains running in succession in long tunnels," numerical simulations of train operation in railway tunnels were performed using the software NUMSTA [5] in addition to the measurements. The computational models were then adapted to reality using the available measured values. To cover all possible (including future) operational trains, the TSI design train class 2 according to TSI LOC&PAS [6] was used in the simulation calculations. Finally, the characteristic aerodynamic pressure loads for different tunnel types, tunnel cross-sections, tunnel lengths, and train speeds were determined using the results of the extensive numerical simulation calculations [7]. The design values of characteristic aerodynamic loading for the structural safety and fatigue verification were defined differently for each of these scenarios. The increased dynamic deformation of the loaded structural element in railway tunnels resulting from the shock-like nature of the pressure loads, compared to a static load, was taken into account by adding the dynamic shock factor $\varphi_{dyn} = 1.40$ derived in [2]. Using formula (1), and after substituting the derived reference values for the minimum and maximum pressure (suction) for the reference tunnel cross-section $A_T = 40$ m², the maximum and minimum pressure wave-induced aerodynamic loads to be considered for the structural safety of tunnel installations can be determined as follow (Note: Equation (1) applies to train speeds 160 km/h $< V_{ZUG} \leq 250$ km/h):

$$p_{max,min} = p_{max,min,40m^2} \left(\frac{40}{A_T}\right)^{\frac{3}{2}} \cdot \varphi_{dyn} \quad (1)$$

p_{max} Maximum pressure wave-induced load (maximum pressure value) in Pascals
p_{min} Minimum pressure wave-induced load (maximum suction value) in Pascals
$p_{max,40m^2}$ Reference value for maximum pressure at A_T = 40m² in Pascal ($p_{max,40m^2}$ = 7215 Pa)
$p_{min,40m^2}$ Reference value for minimum pressure at A_T = 40m² in Pascal ($p_{min,40m^2}$ = -8460 Pa)
A_T clear tunnel cross-section in m²
φ_{dyn} Dynamic shock factor (φ_{dyn} = 1.4)

For the Granitztal Tunnel, applying equation (1) and using the clear tunnel cross-section A_T = 41 m², the following values are obtained for the pressure wave-induced loads to be considered in the design of the tunnel installations for proof of load-bearing capacity: p_{max} = 9,700 Pa and p_{min} = 11,400 Pa. For the determination of the pressure wave-induced aerodynamic loads to be considered in the proof of fatigue resistance, see [7].

The determination of the flow-induced loads occurring during train journeys in railway tunnels, in addition to the pressure wave-induced aerodynamic loads, was based on DB Guideline 853 [8]. To account for the impact load effect, the dynamic shock factor φ_{dyn} = 1.40 was also added here. The maximum flow-induced pressure load can be calculated using equation (2):

$$q_{max} = 0{,}04726 \cdot u^{*2} \cdot v_{ZUG}^2 \cdot \varphi_{dyn} \quad (2)$$

u^* Dimensionless air velocity as a function of the clear tunnel cross-section A_T according to DB guideline 853 [8]

v_{ZUG} Train speed in km/h

φ_{dyn} Dynamic shock factor (φ_{dyn} = 1.4)

For the Granitztal Tunnel, applying equation (2) and considering the clear tunnel cross-section A_T = 41 m², u^* = 1 according to DB guideline 853, and v_{ZUG} = 250 km/h, the following value is obtained for the maximum flow-induced pressure load to be used in the design of the tunnel installations: p_{max} = 4,135 Pa. This value was used in the design of all non-pressure-tight (flow-permeable) structural elements installed in the Granitztal Tunnel, such as signal signs, hectometer boards, suspension columns for the overhead conductor rail, ceiling power rail, and telecommunications cables. The pressure wave-induced loads do not need to be superimposed for these components, as pressure equalization occurs due to the pressure wave acting equally from all sides. Regarding fatigue design, it should be noted that the maximum pressure load must be determined according to equation (2) and the fatigue strength must be verified according to ÖNORM EN 1993-1-9 [9] with 5 million load cycles. Regarding the application limits of equation (2), it should be noted that it only calculates the flow-induced aerodynamic loads in the air gap between the moving train and the tunnel wall in the direction of travel. These load effects can therefore be used for the structural safety and fatigue design of all tunnel installations located in the air gap, which are subjected to airflow in or against the direction of travel of the train. However, practical experience has shown that the resulting aerodynamic load values for the design of tunnel installations subjected to airflow perpendicular to the direction of travel, such as telecommunications radiating cables, lead to a significant overestimation of the actual flow-induced loads occurring. In Austria, therefore, in 2021 a decision was made to carry out in-situ measurements on installations in existing railway tunnels to determine the actual flow-induced loads occurring perpendicular to the

direction of travel of the train. The results of these measurements are documented and presented in [4].

4. MEASUREMENT OF ACTUAL AERODYNAMIC LOADS IN THE GRANITZTAL TUNNEL

To measure the actual aerodynamic loads occurring during train journeys in the Granitztal Tunnel, air pressure sensors were installed at five measurement cross-sections in the tunnel prior to the start of the Koralm railway line commissioning runs in February 2025 (see the description of the installed measurement equipment in Section 2 and the position of the five measurement cross-sections in Figure 2). The aim of the measurements was to verify the aerodynamic load assumptions for pressure wave and flow-induced loads, which were primarily based on theoretical considerations and used in the design of the tunnel structures for all tunnels on the Koralm railway line (see Section 3). Furthermore, a comparison between the theoretical and measured aerodynamic load values was to be carried out in order to assess the conservatism and safety level of the aerodynamic load assumptions. During the commissioning runs of the Koralm railway line in June 2025, the relevant journeys with regard to aerodynamic loads in the Granitztal Tunnel were carried out at speeds of up to 233 km/h. In the southern tube of the Granitztal Tunnel, which was equipped with air pressure sensors, the journeys listed in Table 1 were recorded, and the highest-pressure values were recorded for train journey no. 12 for the DANI train.

Table 1: Overview of measured train journeys, Granitztal Tunnel track 1 (south tube)

Train journey	Type of train	Date, Time	Train Speed [km/h]
1	Railjet set 35 with locomotive 1216 / control car at the front	10. Juni 2025, 08:54:15	181
2		10. Juni 2025, 10:33:45	201
3		10. Juni 2025, 15:06:55	231
4	Railjet set 35 with locomotive 1116 / control car at the front	11. Juni 2025, 08:52:02	181
5		11. Juni 2025, 10:45:21	201
6		11. Juni 2025, 12:34:38	231
7	Railjet set 35 with power car 6193 / control car at the front	12. Juni 2025, 08:55:15	182
8		12. Juni 2025, 10:44:30	202
9		12. Juni 2025, 12:30:47	230
10		12. Juni 2025, 14:31:07	232
11	Tfz 1116.235 with DANI day train set / 9-piece	13. August 2025, 08:34:00	201
12		13. August 2025, 11:30:21	233
13		13. August 2025, 14:16:42	232
14	Tfz 1216.235 with CD-ComfortJet (9-piece set / 12-piece set)	21. August 2025, 09:06:52	199
15		21. August 2025, 11:39:08	230
16		21. August 2025, 14:07:21	233

Figure 3 shows the maximum and minimum pressure loads measured at the measurement cross-section MQ1 as a function of train speed. It can be seen that at MQ1, at the highest speed of 233 km/h (test run no. 12), a maximum value of approximately 3,600 Pa and a minimum value of approximately -1,800 Pa were measured. The speed dependence of the pressure loads is clearly visible in the diagram.

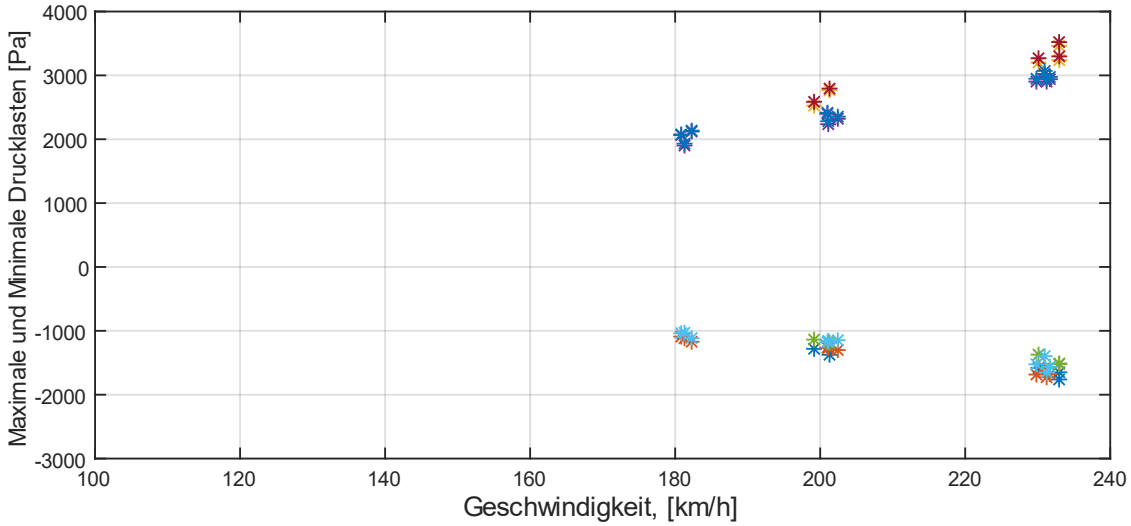


Figure 3: Measured maximum and minimum pressure loads as a function of the travel speed of the trains in the tunnel at measurement cross-section MQ1

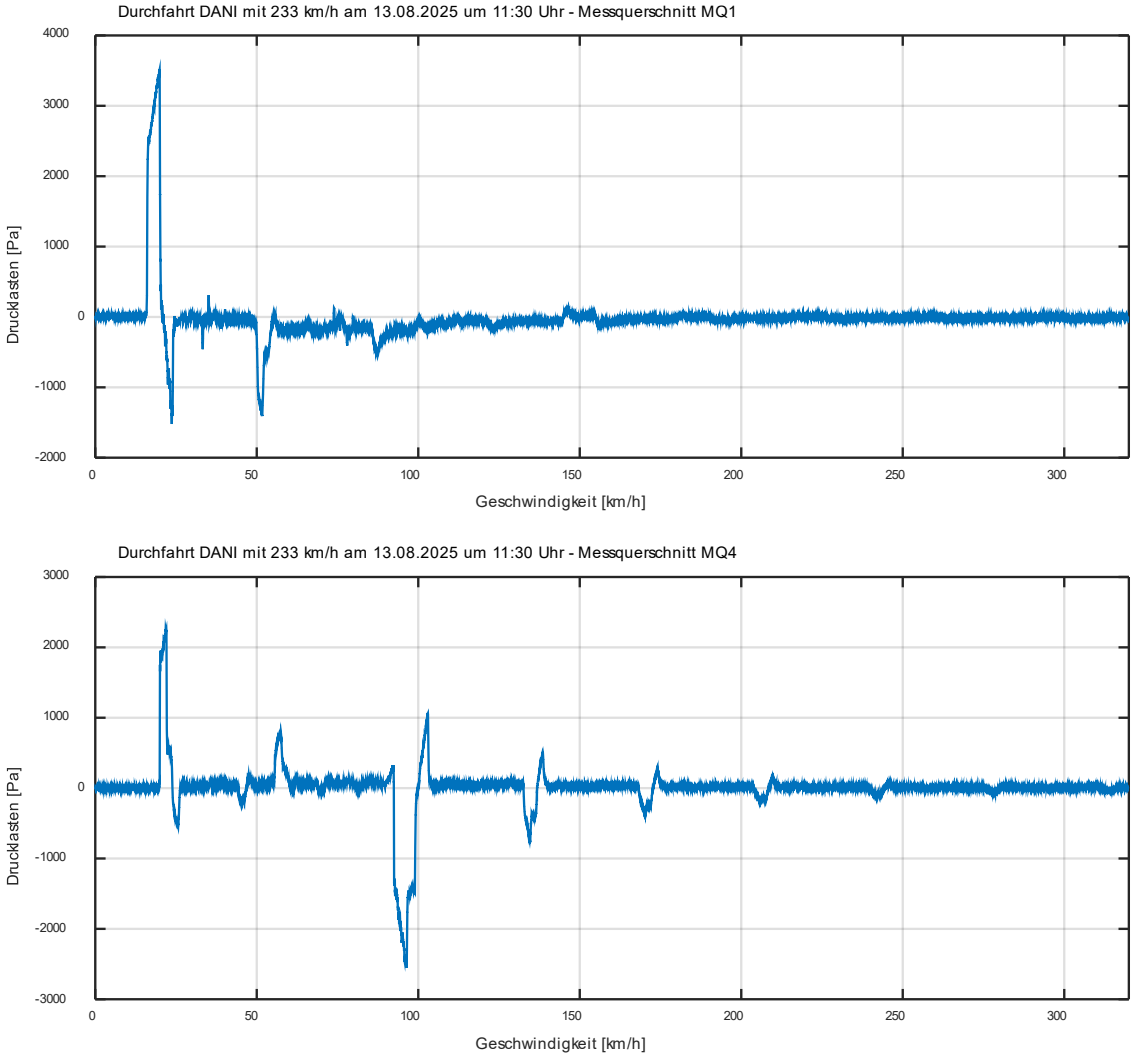


Figure 4: Pressure loads measured during passage of the DANI day train set at 233 km/h at measurement cross-section MQ1 (near the entrance portal) and MQ4 (near the exit portal).

Figure 4 shows the measured pressure load time histories for the train passage at 11:30:21 on August 13, 2025, at 233 km/h (DANI daytime train), which is decisive with regard to the highest-pressure values. The time histories displayed are taken at MQ1 (near the entrance portal) and MQ4 (near the exit portal). It is clearly evident that multiple reflections of the pressure waves occur and that the highest maximum values ($p_{max} \approx$ 3,600 Pa) are measured at measurement cross-section MQ1 (close to entry portal), while the highest minimum values ($p_{min} \approx$ -2,700 Pa) are measured at measurement cross-section MQ4 close to exit portal). The highest maximum pressure loads always occur close to the tunnel entry portal, while the highest minimum pressure loads always occur near the exit portal and depend on the tunnel length. For the comparison of the theoretical aerodynamic loads to the measurement results to be carried out in Section 5, the measured pressure loads must be multiplied by the dynamic shock factor φ_{dyn} = 1.40 due to their impact-like nature, resulting in the following comparative pressure loads: $p_{max,M,\varphi}$ = approx. 5,040 Pa and $p_{min,M,\varphi}$ = approx. -3,780 Pa.

5. SUMMARY AND CONCLUSION

For the Granitztal Tunnel and also for all other tunnels on the Koralm railway line, pressure wave-induced aerodynamic loads of p_{max} = 9,700 Pa and p_{min} = -11,400 Pa were specified during the planning phase for the design regarding proof of load bearing capacity of all pressure-tight tunnel installations, such as emergency exit doors and ventilation flaps to cross passages (see Section 3). In contrast, during the train runs carried out in 2025 among others with DANI daytime train set at the maximum speed of 233 km/h, taking into account the dynamic shock factor φ_{dyn} = 1.40, the measured pressure loads were determined to be $p_{max,M,\varphi}$ = approx. 5,040 Pa and $p_{min,M,\varphi}$ = approx. -3,780 Pa. Therefore, the measured train runs result in a utilization of 0.52 for $p_{max,M,\varphi} / p_{max}$ and 0.33 for $p_{max,M,\varphi} / p_{min}$. The load-bearing capacity of the installed pressure-tight tunnel installations in the Granitztal Tunnel is therefore fulfilled with a high degree of safety, and this can also be assumed for fatigue safety.

6. REFERENCES

[1] Hong-qi Tian, „Review of research on high-speed railway aerodynamics in China," in Transportation Safety and Environment, Vol. 1, No. 1, 2019, https://doi.org/10.1093/tse/tdz014.

[2] M. Reiterer und H. Kari, „Generalized shock spectrum of structures in tunnels due to aerodynamic loading," in Proceedings of the 13th International Railway Engineering Conference, 30th June – 1st July 2025, Radisson Blu Hotel, Edinburgh, Scotland, UK, ISBN 0.947644-80-6.

[3] ÖNORM EN 14067-5, „Bahnanwendungen – Aerodynamik, Teil 5: Anforderungen und Prüfverfahren für Aerodynamik im Tunnel," Austrian Standard Institute, 2011.

[4] M. Reiterer, „Aerodynamische Belastungen auf bahntechnischen Einbauten in schnell befahrenen Eisenbahntunnel," in Bautechnik 99, Heft 7, 2022, doi: https://doi.org/10.1002/bate.202100097.

[5] NUMSTA, "NUMerical Simulation of Tunnel Aerodynamics," 2019, available online: https://www.alexander-rudolf.de/NUMSTA/ (accessed on 12th December 2025).

[6] TSI LOC&PAS, „Fahrzeuge - Lokomotiven und Personenwagen," Verordnung (EU) Nr. 1302/2014, 12.12.2014.

[7] M. Reiterer, J. Schellander, H. Steiner, „Bahntechnische Einbauten in schnellbefahrenen Tunneln der ÖBB – Realitätsnahe Belastungsansätze in Theorie und Praxis,“ in Proceedings of STUVA Conference 2021, International Forum for Tunnels and Infrastructures, 24.-26.11.2021, Karlsruhe, Deutschland.

[8] Deutsche Bahn Richtlinie 853, „Eisenbahntunnel planen, bauen und instandhalten (Modul 853.2001A01: Aerodynamische Einwirkungen),“ DB Netz AG. Aktualisierung 1. Sept. 2018.

[9] ÖNORM EN 1993-1-9, „Eurocode 3: Bemessung und Konstruktion von Stahlbauten – Teil 1-9; Ermüdung“ Austrian Standard Institute, 2013.

REPORTS OF THE INSTITUTE OF THERMODYNAMICS AND SUSTAINABLE PROPULSION SYSTEMS

NR.	VERFASSER	TITEL	ERSCHIENEN
90	STURM P.J.	Sicherheit und Belüftung von Tunnelanlagen Tunnel Safety and Ventilation Tagung/Symposium 21.-23. April 2008	2008
91	HAUSBERGER St.et.al.	Verkehr und Umwelt Transport and Air Pollution Tagung/Symposium 16.-17. June 2008	2008
92	EICHLSEDER et.al.	Der Arbeitsprozess des Verbrennungsmotors The Working Process of the Internal Combustion Engine Tagung / Symposium 24. und 25. September 2009	2009
93	STURM P.J.	Sicherheit und Belüftung von Tunnelanlagen Tunnel Safety and Ventilation Tagung/Symposium 3.-4. Mai 2010	2010
94	EICHLSEDER et.al.	Der Arbeitsprozess des Verbrennungsmotors The Working Process of the Internal Combustion Engine Tagung / Symposium 22. und 23. September 2011	2011
95	STURM P.J.	Sicherheit und Belüftung von Tunnelanlagen Tunnel Safety and Ventilation Tagung/Symposium 23.-25. April 2012	2012
96	EICHLSEDER et.al.	Der Arbeitsprozess des Verbrennungsmotors The Working Process of the Internal Combustion Engine Tagung / Symposium 24. und 25. September 2013	2013
97	STURM P.J.	Sicherheit und Belüftung von Tunnelanlagen Tunnel Safety and Ventilation Tagung/Symposium 12.-13. Mai 2014	2014
98		Inter-Regional Air Quality Assessment Bridging the Gap between Regional and Kerbside PM Pollution Results of the PMinter Project Authors: U. Uhrner, B.C. Lackner, R. Reifeltshammer, M. Steiner, R. Forkel, P.J. Sturms	2014

99	EICHLSEDER et.al.	Der Arbeitsprozess des Verbrennungsmotors The Working Process of the Internal Combustion Engine Tagung / Symposium 24. und 25. September 2015	2015
100	STURM P.J.	Sicherheit und Belüftung von Tunnelanlagen Tunnel Safety and Ventilation Tagung/Symposium 25.-26. April 2016	2016
101	EICHLSEDER et.al.	Der Arbeitsprozess des Verbrennungsmotors The Working Process of the Internal Combustion Engine Tagung / Symposium 28. und 29. September 2017	2017
102	STURM P.J.	Sicherheit und Belüftung von Tunnelanlagen Tunnel Safety and Ventilation Tagung/Symposium 12.-14. Juni 2018	2018
103	EICHLSEDER et.al.	Der Arbeitsprozess des Verbrennungsmotors The Working Process of the Internal Combustion Engine Tagung / Symposium 26. und 27. September 2019	2019
104	EICHLSEDER et.al.	Nachhaltigkeit in Mobilität, Transport und Energieerzeugung (vormals: Der Arbeitsprozess des Verbrennungsmotors) Sustainable Mobility, Transport and Power Generation (formerly „The Working Process of the Internal Combustion Engine") Tagung / Symposium 23. und 24. September 2021	2021
105	STURM P.J.	Sicherheit und Belüftung von Tunnelanlagen Tunnel Safety and Ventilation Tagung/Symposium 09. & 10. Mai 2022	2022
106	EICHLSEDER et.al.	Nachhaltigkeit in Mobilität, Transport und Energieerzeugung Sustainable Mobility, Transport and Power Generation Tagung / Symposium 28. und 29. September 2023	2023
107	BACHER M.	Sicherheit und Belüftung von Tunnelanlagen Tunnel Safety and Ventilation Tagung/Symposium 16. & 17. April 2024	2024
108	EICHLSEDER et.al.	Nachhaltigkeit in Mobilität, Transport und Energieerzeugung Sustainable Mobility, Transport and Power Generation Tagung / Symposium 04. & 05. September 2025	2025
109	BACHER M.	Sicherheit und Belüftung von Tunnelanlagen Tunnel Safety and Ventilation Tagung/Symposium 21. & 22. April 2026	2026